

SIMON HAYKIN | MICHAEL MOHER

*Introduction to*  
**ANALOG & DIGITAL  
COMMUNICATIONS**

| Second Edition





# The first person to invent a car that runs on water...

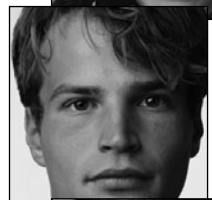
... may be sitting right in your classroom! Every one of your students has the potential to make a difference. And realizing that potential starts right here, in your course.

When students succeed in your course—when they stay on-task and make the breakthrough that turns confusion into confidence—they are empowered to realize the possibilities for greatness that lie within each of them. We know your goal is to create an environment where students reach their full potential and experience the exhilaration of academic success that will last them a lifetime. *WileyPLUS* can help you reach that goal.



**WileyPLUS** is an online suite of resources—including the complete text—that will help your students:

- come to class better prepared for your lectures
- get immediate feedback and context-sensitive help on assignments and quizzes
- track their progress throughout the course



---

"I just wanted to say how much this program helped me in studying... I was able to actually see my mistakes and correct them. ... I really think that other students should have the chance to use *WileyPLUS*."

Ashlee Krisko, *Oakland University*

---

[www.wiley.com/college/wileyplus](http://www.wiley.com/college/wileyplus)

**80%** of students surveyed said it improved their understanding of the material.\*

# FOR INSTRUCTORS

WileyPLUS is built around the activities you perform in your class each day. With WileyPLUS you can:

## Prepare & Present

Create outstanding class presentations using a wealth of resources such as PowerPoint™ slides, image galleries, interactive simulations, and more. You can even add materials you have created yourself.

## Create Assignments

Automate the assigning and grading of homework or quizzes by using the provided question banks, or by writing your own.

## Track Student Progress

Keep track of your students' progress and analyze individual and overall class results.

## Now Available with WebCT and Blackboard!

The screenshot shows a computer screen displaying the WileyPLUS software. A window titled "Chapter 8, Section 8.3, Question 8.3.19 - Mozilla Firefox" is open. The question asks: "The circuit shown in the figure below is at steady state before the switch closes. Find  $v(t)$  for  $t \geq 0$ .  
A circuit diagram shows a 24V DC voltage source in series with a 12Ω resistor. A switch labeled "t = 0" is closed, connecting the 12Ω resistor to a 6Ω resistor in parallel. Below the diagram is the equation:  $v(t) = (12/18)*24*(1-exp(-t/(6*0.2)))$  V for  $t \geq 0$ .  
A sidebar titled "References - Mozilla Firefox References" lists various chapters and sections from the textbook.  
A large text box titled "The Response of a First-Order Circuit to a Constant Input" contains a detailed explanation of the circuit analysis, mentioning the removal of a resistor after the switch closes, and the resulting Thevenin equivalent circuit.  
At the bottom of the window, there are buttons for "Text-Entry (Algorithm)", "Link", "Easy", "Wiley (Assessment)", and "Properties".

"It has been a great help, and I believe it has helped me to achieve a better grade."

Michael Morris,  
Columbia Basin College

# FOR STUDENTS

You have the potential to make a difference!

WileyPLUS is a powerful online system packed with features to help you make the most of your potential and get the best grade you can!

With WileyPLUS you get:

- A complete online version of your text and other study resources.
- Problem-solving help, instant grading, and feedback on your homework and quizzes.
- The ability to track your progress and grades throughout the term.

For more information on what WileyPLUS can do to help you and your students reach their potential, please visit [www.wiley.com/college/wileyplus](http://www.wiley.com/college/wileyplus).

76% of students surveyed said it made them better prepared for tests. \*



\*Based on a survey of 972 student users of WileyPLUS

# **Introduction to Analog and Digital Communications**

*This page intentionally left blank*

# **Introduction to Analog and Digital Communications**

## **Second Edition**

***Simon Haykin***

*McMaster University, Hamilton, Ontario, Canada*

***Michael Moher***

*Space-Time DSP, Ottawa, Ontario, Canada*



**JOHN WILEY & SONS, INC.**

ASSOCIATE PUBLISHER Dan Sayre  
SENIOR ACQUISITIONS EDITOR AND PROJECT MANAGER Catherine Shultz  
PROJECT EDITOR Gladys Soto  
MARKETING MANAGER Phyllis Diaz Cerys  
EDITORIAL ASSISTANT Dana Kellog  
SENIOR PRODUCTION EDITOR Lisa Wojcik  
MEDIA EDITOR Stefanie Liebman  
DESIGNER Hope Miller  
SENIOR ILLUSTRATION EDITOR Sigmund Malinowski  
COVER IMAGE © Photodisc/Getty Images

This book was set in Quark by Prepare Inc. and printed and bound by Hamilton Printing. The cover was printed by Phoenix Color Corp.

This book is printed on acid free paper. 

Copyright © 2007 John Wiley & Sons, Inc. All rights reserved. No part of this publication may be reproduced, stored in a retrieval system, or transmitted in any form or by any means, electronic, mechanical, photocopying, recording, scanning, or otherwise, except as permitted under Sections 107 or 108 of the 1976 United States Copyright Act, without either the prior written permission of the Publisher, or authorization through payment of the appropriate per-copy fee to the Copyright Clearance Center, Inc., 222 Rosewood Drive, Danvers, MA 01923, (978)750-8400, fax (978)646-8600, or on the web at [www.copyright.com](http://www.copyright.com). Requests to the Publisher for permission should be addressed to the Permissions Department, John Wiley & Sons, Inc., 111 River Street, Hoboken, NJ 07030-5774, (201)7486011, fax (201)748-6008, or online at <http://www.wiley.com/go/permissions>.

To order books or for customer service please, call 1-800-CALL WILEY (225-5945).

ISBN-13 978-0-471-43222-7  
ISBN-10 0-471-43222-9

Printed in the United States of America

10 9 8 7 6 5 4 3 2 1

To the 20<sup>th</sup> Century pioneers in communications who,  
through their mathematical theories and ingenious devices,  
have changed our planet into a global village

*This page intentionally left blank*

# PREFACE

An introductory course on analog and digital communications is fundamental to the undergraduate program in electrical engineering. This course is usually offered at the junior level. Typically, it is assumed that the student has a background in calculus, electronics, signals and systems, and possibly probability theory.

Bearing in mind the introductory nature of this course, a textbook recommended for the course must be easy to read, accurate, and contain an abundance of insightful examples, problems, and computer experiments. These objectives of the book are needed to expedite learning the fundamentals of communication systems at an introductory level and in an effective manner. This book has been written with all of these objectives in mind.

Given the mathematical nature of communication theory, it is rather easy for the reader to lose sight of the practical side of communication systems. Throughout the book, we have made a special effort not to fall into this trap. We have done this by moving through the treatment of the subject in an orderly manner, always trying to keep the mathematical treatment at an easy-to-grasp level and also pointing out practical relevance of the theory wherever it is appropriate to do so.

## ***Structural Philosophy of the Book***

To facilitate and reinforce learning, the layout and format of the book have been structured to do the following:

- Provide motivation to read the book and learn from it.
- Emphasize basic concepts from a “systems” perspective and do so in an orderly manner.
- Wherever appropriate, include examples and computer experiments in each chapter to illustrate application of the pertinent theory.
- Provide drill problems following the discussion of fundamental concepts to help the user of the book verify and master the concepts under discussion.
- Provide additional end-of-chapter problems, some of an advanced nature, to extend the theory covered in the text.

## ***Organization of the book***

1. *Motivation* Before getting deeply involved in the study of analog and digital communications, it is imperative that the user of the book be motivated to use the book and learn from it. To this end, Chapter 1 begins with a historical background of communication systems and important applications of the subject.
2. *Modulation Theory* Digital communication has overtaken analog communications as the dominant form of communications. Although, indeed, these two forms of communications work in different ways, modulation theory is basic to them both. Moreover, it is easiest to understand this important subject by first covering its fundamental concepts applied to analog communications and then moving on to digital communications. Moreover, amplitude modulation is simpler than angle modulation to present. One other highly relevant point is the fact that to understand modulation theory, it is important that Fourier theory be mastered first. With these points in mind, Chapters 2 through 7 are organized as follows:

**APPENDIX 1 ■ POWER RATIOS AND DECIBEL**

- Chapter 2 is devoted to reviewing the Fourier representation of signals and systems.
  - Chapters 3 and 4 are devoted to analog communications, with Chapter 3 covering amplitude modulation and Chapter 4 covering angle modulation.
  - Chapter 5 on pulse modulation covers the concepts pertaining to the transition from analog to digital communications.
  - Chapters 6 and 7 are devoted to digital communications, with Chapter 6 covering baseband data transmission and Chapter 7 covering band-pass data transmission.
- 3. Probability Theory and Signal Detection** Just as Fourier analysis is fundamental to modulation theory, probability theory is fundamental to signal detection and receiver performance evaluation in the presence of additive noise. Since probability theory is not critical to the understanding of modulation, we have purposely delayed the review of probability theory, random signals, and noise until Chapter 8. Then, with a good understanding of modulation theory applied to analog and digital communications and relevant concepts of probability theory and probabilistic models at hand, the stage is set to revisit analog and digital communication receivers, as summarized here:
- Chapter 9 discusses noise in analog communications.
  - Chapter 10 discusses noise in digital communications. Because analog and digital communications operate in different ways, it is natural to see some fundamental differences in treating the effects of noise in these two chapters.
- 4. Noise** The introductory study of analog and digital communications is completed in Chapter 11. This chapter illustrates the roles of modulation and noise in communication systems by doing four things:
- First, the physical sources of noise, principally, thermal noise and shot noise, are described.
  - Second, the metrics of noise figure and noise temperature are introduced.
  - Third, how propagation affects the signal strength in satellite and terrestrial wireless communications is explained.
  - Finally, we show how the signal strength and noise calculations may be combined to provide an estimate of the signal-to-noise ratio, the fundamental figure of merit for communication systems.
- 5. Theme Examples** In order to highlight important practical applications of communication theory, theme examples are included wherever appropriate. The examples are drawn from the worlds of both analog and digital communications.
- 6. Appendices** To provide back-up material for the text, eight appendices are included at the end of the book, which cover the following material in the order presented here:
- Power ratios and the decibel
  - Fourier series
  - Bessel functions
  - The Q-function and its relationship to the error function
  - Schwarz's inequality
  - Mathematical tables

- Matlab scripts for computer experiments to problems in Chapters 7–10
  - Answers to drill problems
7. *Footnotes*, included throughout the book, are provided to help the interested reader to pursue selected references for learning advanced material.
8. *Auxiliary Material* The book is essentially self-contained. A glossary of symbols and a bibliography are provided at the end of the book. As an aid to the teacher of the course using the book, a detailed *Solutions Manual* for all the problems, those within the text and those included at the end of chapters, will be made available through the publisher: John Wiley and Sons.

## How to Use the Book

The book can be used for an introductory course on analog and digital communications in different ways, depending on the background of the students and the teaching interests and responsibilities of the professors concerned. Here are two course models of how this may be done:

### COURSE MODEL A: FULL TWO-SEMESTER COURSE

- (A.1) The first semester course on modulation theory consists of Chapters 2 through 7, inclusive.
- (A.2) The second semester course on noise in communication systems consists of Chapters 8 through 11, inclusive.

### COURSE MODEL B: TWO SEMESTER COURSES, ONE ON ANALOG AND THE OTHER ON DIGITAL

- (B.1) The first course on analog communications begins with review material from Chapter 2 on Fourier analysis, followed by Chapter 3 on amplitude modulation and Chapter 4 on angle modulation, then proceeds with a review of relevant parts of Chapter 8 on noise, and finally finishes with Chapter 9 on noise in analog communications.
- (B.2) The second course on digital communications starts with Chapter 5 on pulse modulation, followed by Chapter 6 on baseband data transmission and Chapter 7 on digital modulation techniques, then proceeds with review of relevant aspects of probability theory in Chapter 8, and finally finishes with Chapter 10 on noise in digital communications.

Simon Haykin  
Ancaster, Ontario, Canada

Michael Moher  
Ottawa, Ontario, Canada

*This page intentionally left blank*

## **ACKNOWLEDGEMENTS**

The authors would like to express their deep gratitude to

- Lily Jiang, formerly of McMaster University for her help in performing many of the computer experiments included in the text.
- Wei Zhang, for all the help, corrections, and improvements she has made to the text.

They also wish to thank Dr. Stewart Crozier and Dr. Paul Guinand, both of the Communications Research Centre, Ottawa, for their inputs on different parts of the book.

They are also indebted to Catherine Fields Shultz, Senior Acquisitions Editor and Product Manager (Engineering and Computer Science) at John Wiley and Sons, Bill Zobrist formerly of Wiley, and Lisa Wojcik, Senior Production Editor at Wiley, for their guidance and dedication to the production of this book.

Last but by no means least, they are grateful to Lola Brooks, McMaster University, for her hard work on the preparation of the manuscript and related issues to the book.

*This page intentionally left blank*

# CONTENTS

## Chapter 1 *Introduction* 1

---

1.1	Historical Background	1
1.2	Applications	4
1.3	Primary Resources and Operational Requirements	13
1.4	Underpinning Theories of Communication Systems	14
1.5	Concluding Remarks	16

## Chapter 2 *Fourier Representation of Signals and Systems* 18

---

2.1	The Fourier Transform	19
2.2	Properties of the Fourier Transform	25
2.3	The Inverse Relationship Between Time and Frequency	39
2.4	Dirac Delta Function	42
2.5	Fourier Transforms of Periodic Signals	50
2.6	Transmission of Signals Through Linear Systems: Convolution Revisited	52
2.7	Ideal Low-pass Filters	60
2.8	Correlation and Spectral Density: Energy Signals	70
2.9	Power Spectral Density	79
2.10	Numerical Computation of the Fourier Transform	81
2.11	Theme Example: Twisted Pairs for Telephony	89
2.12	Summary and Discussion	90

*Additional Problems* 91

*Advanced Problems* 98

## Chapter 3 *Amplitude Modulation* 100

---

3.1	Amplitude Modulation	101
3.2	Virtues, Limitations, and Modifications of Amplitude Modulation	113
3.3	Double Sideband-Suppressed Carrier Modulation	114
3.4	Costas Receiver	120

3.5	Quadrature-Carrier Multiplexing	121
3.6	Single-Sideband Modulation	123
3.7	Vestigial Sideband Modulation	130
3.8	Baseband Representation of Modulated Waves and Band-Pass Filters	137
3.9	Theme Examples	142
3.10	Summary and Discussion	147

*Additional Problems* 148

*Advanced Problems* 150

## **Chapter 4 Angle Modulation**

**152**

4.1	Basic Definitions	153
4.2	Properties of Angle-Modulated Waves	154
4.3	Relationship between PM and FM Waves	159
4.4	Narrow-Band Frequency Modulation	160
4.5	Wide-Band Frequency Modulation	164
4.6	Transmission Bandwidth of FM Waves	170
4.7	Generation of FM Waves	172
4.8	Demodulation of FM Signals	174
4.9	Theme Example: FM Stereo Multiplexing	182
4.10	Summary and Discussion	184

*Additional Problems* 185

*Advanced Problems* 187

## **Chapter 5 Pulse Modulation: Transition from Analog to Digital Communications**

**190**

5.1	Sampling Process	191
5.2	Pulse-Amplitude Modulation	198
5.3	Pulse-Position Modulation	202
5.4	Completing the Transition from Analog to Digital	203
5.5	Quantization Process	205
5.6	Pulse-Code Modulation	206

5.7	Delta Modulation	211
5.8	Differential Pulse-Code Modulation	216
5.9	Line Codes	219
5.10	Theme Examples	220
5.11	Summary and Discussion	225

*Additional Problems* 226

*Advanced Problems* 228

---

## **Chapter 6 Baseband Data Transmission**

**231**

6.1	Baseband Transmission of Digital Data	232
6.2	The Intersymbol Interference Problem	233
6.3	The Nyquist Channel	235
6.4	Raised-Cosine Pulse Spectrum	238
6.5	Baseband Transmission of M-ary Data	245
6.6	The Eye Pattern	246
6.7	Computer Experiment: Eye Diagrams for Binary and Quaternary Systems	249
6.8	Theme Example: Equalization	251
6.9	Summary and Discussion	256

*Additional Problems* 257

*Advanced Problems* 259

---

## **Chapter 7 Digital Band-Pass Modulation Techniques**

**262**

7.1	Some Preliminaries	262
7.2	Binary Amplitude-Shift Keying	265
7.3	Phase-Shift Keying	270
7.4	Frequency-Shift Keying	281
7.5	Summary of Three Binary Signaling Schemes	289
7.6	Noncoherent Digital Modulation Schemes	291
7.7	M-ary Digital Modulation Schemes	295
7.8	Mapping of Digitally Modulated Waveforms onto Constellations of Signal Points	299

7.9	Theme Examples	302
7.10	Summary and Discussion	307
<i>Additional Problems</i>		309
<i>Advanced Problems</i>		310
<i>Computer Experiments</i>		312

**Chapter 8 Random Signals and Noise****313**

8.1	Probability and Random Variables	314
8.2	Expectation	326
8.3	Transformation of Random Variables	329
8.4	Gaussian Random Variables	330
8.5	The Central Limit Theorem	333
8.6	Random Processes	335
8.7	Correlation of Random Processes	338
8.8	Spectra of Random Signals	343
8.9	Gaussian Processes	347
8.10	White Noise	348
8.11	Narrowband Noise	352
8.12	Summary and Discussion	356
<i>Additional Problems</i>		357
<i>Advanced Problems</i>		361
<i>Computer Experiments</i>		363

**Chapter 9 Noise in Analog Communications****364**

9.1	Noise in Communication Systems	365
9.2	Signal-to-Noise Ratios	366
9.3	Band-Pass Receiver Structures	369
9.4	Noise in Linear Receivers Using Coherent Detection	370
9.5	Noise in AM Receivers Using Envelope Detection	373
9.6	Noise in SSB Receivers	377
9.7	Detection of Frequency Modulation (FM)	380

9.8	FM Pre-emphasis and De-emphasis	387
9.9	Summary and Discussion	390
<i>Additional Problems</i>		391
<i>Advanced Problems</i>		392
<i>Computer Experiments</i>		393

## **Chapter 10 Noise in Digital Communications**

**394**

10.1	Bit Error Rate	395
10.2	Detection of a Single Pulse in Noise	396
10.3	Optimum Detection of Binary PAM in Noise	399
10.4	Optimum Detection of BPSK	405
10.5	Detection of QPSK and QAM in Noise	408
10.6	Optimum Detection of Binary FSK	414
10.7	Differential Detection in Noise	416
10.8	Summary of Digital Performance	418
10.9	Error Detection and Correction	422
10.10	Summary and Discussion	433
<i>Additional Problems</i>		434
<i>Advanced Problems</i>		435
<i>Computer Experiments</i>		436

## **Chapter 11 System and Noise Calculations**

**437**

11.1	Electrical Noise	438
11.2	Noise Figure	442
11.3	Equivalent Noise Temperature	443
11.4	Cascade Connection of Two-Port Networks	445
11.5	Free-Space Link Calculations	446
11.6	Terrestrial Mobile Radio	451
11.7	Summary and Discussion	456

*Additional Problems* 457*Advanced Problems* 458

**APPENDIX 1 POWER RATIOS AND DECIBEL 459****APPENDIX 2 FOURIER SERIES 460****APPENDIX 3 BESSSEL FUNCTIONS 467****APPENDIX 4 THE Q-FUNCTION AND ITS RELATIONSHIP TO THE ERROR  
FUNCTION 470****APPENDIX 5 SCHWARZ'S INEQUALITY 473****APPENDIX 6 MATHEMATICAL TABLES 475****APPENDIX 7 MATLAB SCRIPTS FOR COMPUTER EXPERIMENTS TO  
PROBLEMS IN CHAPTERS 7-10 480****APPENDIX 8 ANSWERS TO DRILL PROBLEMS 488****GLOSSARY 495****BIBLIOGRAPHY 498****INDEX 501**

# CHAPTER 1

## INTRODUCTION

*“To understand a science it is necessary to know its history”*

—Auguste Comte (1798–1857)

### 1.1 ***Historical Background***

With this quotation from Auguste Comte in mind, we begin this introductory study of communication systems with a historical account of this discipline that touches our daily lives in one way or another.<sup>1</sup> Each subsection in this section focuses on some important and related events in the historical evolution of communication.

#### ***Telegraph***

The telegraph was perfected by Samuel Morse, a painter. With the words “What hath God wrought,” transmitted by Morse’s electric telegraph between Washington, D.C., and Baltimore, Maryland, in 1844, a completely revolutionary means of real-time, long-distance communications was triggered. The *telegraph*, ideally suited for manual keying, is the forerunner of digital communications. Specifically, the *Morse code* is a *variable-length* code using an alphabet of four symbols: a dot, a dash, a letter space, and a word space; short sequences represent frequent letters, whereas long sequences represent infrequent letters.

#### ***Radio***

In 1864, James Clerk Maxwell formulated the *electromagnetic theory* of light and predicted the existence of radio waves; the underlying set of equations bears his name. The existence of radio waves was confirmed experimentally by Heinrich Hertz in 1887. In 1894, Oliver Lodge demonstrated wireless communication over a relatively short distance (150 yards). Then, on December 12, 1901, Guglielmo Marconi received a *radio signal* at Signal Hill in Newfoundland; the radio signal had originated in Cornwall, England, 1700 miles away across the Atlantic. The way was thereby opened toward a tremendous broadening of the scope of communications. In 1906, Reginald Fessenden, a self-educated academic, made history by conducting the first radio broadcast.

In 1918, Edwin H. Armstrong invented the *superheterodyne radio* receiver; to this day, almost all radio receivers are of this type. In 1933, Armstrong demonstrated another revolutionary concept—namely, a modulation scheme that he called *frequency modulation* (FM). Armstrong’s paper making the case for FM radio was published in 1936.

---

<sup>1</sup>This historical background is adapted from Haykin’s book (2001).

### **Telephone**

In 1875, the *telephone* was invented by Alexander Graham Bell, a teacher of the deaf. The telephone made real-time transmission of speech by electrical encoding and replication of sound a practical reality. The first version of the telephone was crude and weak, enabling people to talk over short distances only. When telephone service was only a few years old, interest developed in automating it. Notably, in 1897, A. B. Strowger, an undertaker from Kansas City, Missouri, devised the automatic *step-by-step switch* that bears his name. Of all the electromechanical switches devised over the years, the Strowger switch was the most popular and widely used.

### **Electronics**

In 1904, John Ambrose Fleming invented the *vacuum-tube diode*, which paved the way for the invention of the *vacuum-tube triode* by Lee de Forest in 1906. The discovery of the triode was instrumental in the development of transcontinental telephony in 1913 and signaled the dawn of wireless voice communications. Indeed, until the invention and perfection of the transistor, the triode was the supreme device for the design of electronic amplifiers.

The *transistor* was invented in 1948 by Walter H. Brattain, John Bardeen, and William Shockley at Bell Laboratories. The first silicon integrated circuit (IC) was produced by Robert Noyce in 1958. These landmark innovations in solid-state devices and integrated circuits led to the development of *very-large-scale integrated* (VLSI) circuits and single-chip *microprocessors*, and with them the nature of signal processing and the telecommunications industry changed forever.

### **Television**

The first all-electronic *television* system was demonstrated by Philo T. Farnsworth in 1928, and then by Vladimir K. Zworykin in 1929. By 1939, the British Broadcasting Corporation (BBC) was broadcasting television on a commercial basis.

### **Digital Communications**

In 1928, Harry Nyquist published a classic paper on the theory of signal transmission in telegraphy. In particular, Nyquist developed criteria for the correct reception of telegraph signals transmitted over dispersive channels in the absence of noise. Much of Nyquist's early work was applied later to the transmission of digital data over dispersive channels.

In 1937, Alex Reeves invented *pulse-code modulation* (PCM) for the digital encoding of speech signals. The technique was developed during World War II to enable the encryption of speech signals; indeed, a full-scale, 24-channel system was used in the field by the United States military at the end of the war. However, PCM had to await the discovery of the transistor and the subsequent development of large-scale integration of circuits for its commercial exploitation.

The invention of the transistor in 1948 spurred the application of electronics to switching and digital communications. The motivation was to improve reliability, increase capacity, and reduce cost. The first call through a stored-program system was placed in March 1958 at Bell Laboratories, and the first commercial telephone service with digital switching began in Morris, Illinois, in June 1960. The first *T-1 carrier system* transmission was installed in 1962 by Bell Laboratories.

In 1943, D. O. North devised the *matched filter* for the optimum detection of a known signal in additive white noise. A similar result was obtained in 1946 independently by J. H. Van Vleck and D. Middleton, who coined the term *matched filter*.

In 1948, the theoretical foundations of digital communications were laid by Claude Shannon in a paper entitled “A Mathematical Theory of Communication.” Shannon’s paper was received with immediate and enthusiastic acclaim. It was perhaps this response that emboldened Shannon to amend the title of his paper to “The Mathematical Theory of Communications” when it was reprinted a year later in a book co-authored with Warren Weaver. It is noteworthy that prior to the publication of Shannon’s 1948 classic paper, it was believed that increasing the rate of information transmission over a channel would increase the probability of error. The communication theory community was taken by surprise when Shannon proved that this was not true, provided the transmission rate was below the channel capacity.

### **Computer Networks**

During the period 1943 to 1946, the first electronic digital computer, called the ENIAC, was built at the Moore School of Electrical Engineering of the University of Pennsylvania under the technical direction of J. Presper Eckert, Jr., and John W. Mauchly. However, John von Neumann’s contributions were among the earliest and most fundamental to the theory, design, and application of digital computers, which go back to the first draft of a report written in 1945. Computers and terminals started communicating with each other over long distances in the early 1950s. The links used were initially voice-grade telephone channels operating at low speeds (300 to 1200 b/s). Various factors have contributed to a dramatic increase in data transmission rates; notable among them are the idea of *adaptive equalization*, pioneered by Robert Lucky in 1965, and efficient modulation techniques, pioneered by G. Ungerboeck in 1982. Another idea widely employed in computer communications is that of *automatic repeat-request* (ARQ). The ARQ method was originally devised by H. C. A. van Duuren during World War II and published in 1946. It was used to improve radio-telephony for telex transmission over long distances.

From 1950 to 1970, various studies were made on *computer networks*. However, the most significant of them in terms of impact on computer communications was the Advanced Research Projects Agency Network (ARPANET), first put into service in 1971. The development of ARPANET was sponsored by the Advanced Research Projects Agency of the U. S. Department of Defense. The pioneering work in *packet switching* was done on ARPANET. In 1985, ARPANET was renamed the *Internet*. The turning point in the evolution of the Internet occurred in 1990 when Tim Berners-Lee proposed a hypermedia software interface to the Internet, which he named the *World Wide Web*. In the space of only about two years, the Web went from nonexistence to worldwide popularity, culminating in its commercialization in 1994. We may explain the explosive growth of the Internet by offering these reasons:

- ▶ Before the Web exploded into existence, the ingredients for its creation were already in place. In particular, thanks to VLSI, personal computers (PCs) had already become ubiquitous in homes throughout the world, and they were increasingly equipped with modems for interconnectivity to the outside world.
- ▶ For about two decades, the Internet had grown steadily (albeit within a confined community of users), reaching a critical threshold of electronic mail and file transfer.
- ▶ Standards for document description and transfer, hypertext markup language (HTML), and hypertext transfer protocol (HTTP) had been adopted.

Thus, everything needed for creating the Web was already in place except for two critical ingredients: a simple user interface and a brilliant service concept.

### **Satellite Communications**

In 1955, John R. Pierce proposed the use of satellites for communications. This proposal was preceded, however, by an earlier paper by Arthur C. Clark that was published in 1945, also proposing the idea of using an *Earth-orbiting* satellite as a relay point for communication between two Earth stations. In 1957, the Soviet Union launched Sputnik I, which transmitted telemetry signals for 21 days. This was followed shortly by the launching of Explorer I by the United States in 1958, which transmitted telemetry signals for about five months. A major experimental step in communications satellite technology was taken with the launching of Telstar I from Cape Canaveral on July 10, 1962. The Telstar satellite was built by Bell Laboratories, which had acquired considerable knowledge from pioneering work by Pierce. The satellite was capable of relaying TV programs across the Atlantic; this was made possible only through the use of maser receivers and large antennas.

### **Optical Communications**

The use of optical means (e.g., smoke and fire signals) for the transmission of information dates back to prehistoric times. However, no major breakthrough in optical communications was made until 1966, when K. C. Kao and G. A. Hockham of Standard Telephone Laboratories, U. K., proposed the use of a clad glass fiber as a dielectric waveguide. The *laser* (an acronym for light amplification by stimulated emission of radiation) had been invented and developed in 1959 and 1960. Kao and Hockham pointed out that (1) the attenuation in an optical fiber was due to impurities in the glass, and (2) the intrinsic loss, determined by Rayleigh scattering, is very low. Indeed, they predicted that a loss of 20 dB/km should be attainable. This remarkable prediction, made at a time when the power loss in a glass fiber was about 1000 dB/km, was to be demonstrated later. Nowadays, transmission losses as low as 0.1 dB/km are achievable.

The spectacular advances in microelectronics, digital computers, and lightwave systems that we have witnessed to date, and that will continue into the future, are all responsible for dramatic changes in the telecommunications environment. Many of these changes are already in place, and more changes will occur over time.

## **1.2 Applications**

The historical background of Section 1.1 touches many of the applications of communication systems, some of which are exemplified by the telegraph that has come and gone, while others exemplified by the Internet are of recent origin. In what follows, we will focus on radio, communication networks exemplified by the telephone, and the Internet, which dominate the means by which we communicate in one of two basic ways or both, as summarized here:

- ▶ *Broadcasting*, which involves the use of a single powerful transmitter and numerous receivers that are relatively inexpensive to build. In this class of communication systems, information-bearing signals flow only in one direction, from the transmitter to each of the receivers out there in the field.
- ▶ *Point-to-point communications*, in which the communication process takes place over a link between a single transmitter and a single receiver. In this second class of communication systems, there is usually a bidirectional flow of information-bearing

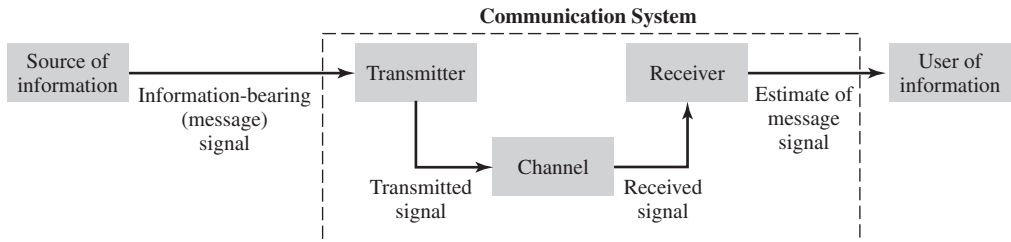


**FIGURE 1.1** Elements of a communication system.

signals, which, in effect, requires the use of a transmitter and receiver (i.e., transceiver) at each end of the link.

The block diagram of Fig. 1.1 highlights the basic composition of a communication system. The *transmitter*, at some location in space, converts the *message signal* produced by a *source of information* into a form suitable for transmission over the channel. The *channel*, in turn, transports the message signal and delivers it to the receiver at some other location in space. However, in the course of transmission over the channel, the signal is *distorted* due to channel imperfections. Moreover, noise and interfering signals (originating from other sources) are added to the channel output, with the result that the received signal is a corrupted version of the transmitted signal. The *receiver* has the task of operating on the received signal so as to produce an *estimate* of the original message signal for the *user of information*. We say an “estimate” here because of the unavoidable deviation, however small, of the receiver output compared to the transmitter input, the deviation being attributed to channel imperfections, noise, and interference.

## ■ RADIO

Speaking in a generic sense, the radio embodies the means for broadcasting as well as point-to-point communications, depending on how it is used.

The *AM radio* and *FM radio* are both so familiar to all of us. (AM stands for amplitude modulation, and FM stands for frequency modulation.) The two of them are built in an integrated form inside a single unit, and we find them in every household and installed in every car. Via radio we listen to news about local, national, and international events, commentaries, music, and weather forecasts, which are transmitted from broadcasting stations that operate in our neighborhood. Traditionally, AM radio and FM radio have been built using analog electronics. However, thanks to the ever-increasing improvements and cost-effectiveness of digital electronics, *digital radio* (in both AM and FM forms) is already in current use.

Radio transmits voice by electrical signals. *Television*, which operates on similar electromagnetic and communication-theoretic principles, also transmits visual images by electrical signals. A voice signal is naturally defined as a *one-dimensional function of time*, which therefore lends itself readily to signal-processing operations. In contrast, an image with motion is a *two-dimensional function of time*, and therefore requires more detailed attention. Specifically, each image at a particular instant of time is viewed as a frame subdivided into a number of small squares called *picture elements* or *pixels*; the larger the number of pixels used to represent an image, the better the resolution of that image will be. By *scanning* the pixels in an orderly sequence, the information contained in the image is converted into an electrical signal whose magnitude is proportional to the brightness level of the individual pixels. The electrical signal generated at the output of the scanner is

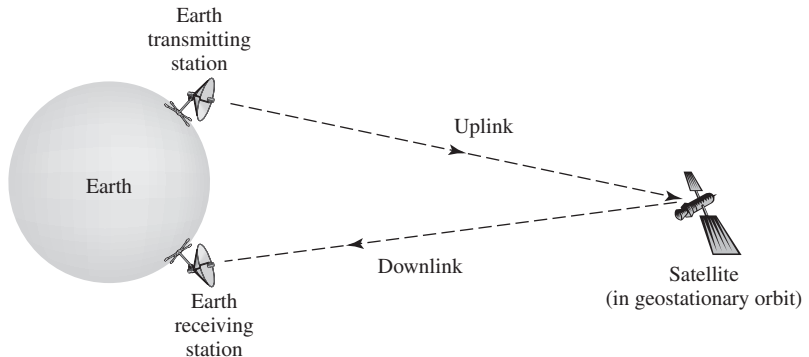


**FIGURE 1.2** Satellite communication system.

the *video signal* that is transmitted. Generation of the video signal is the result of a well-defined *mapping process* known to the receiver. Hence, given the video signal, the receiver is able to reconstruct the original image. As with digital radio, television is also the beneficiary of spectacular advances in digital electronics. These advances, coupled with the application of advanced digital signal processing techniques and the demands of consumers, have motivated the development of *high-definition television* (HDTV), which provides a significant improvement in the quality of reconstructed images at the receiver output.

We turn next to the point-to-point communication scene. The radio has also touched our daily lives in highly significant ways through two avenues: satellite communications and wireless communications. *Satellite communications*, built around a satellite in *geostationary orbit*, relies on *line-of-sight radio propagation* for the operation of an uplink and a downlink. The uplink connects an Earth terminal to a transponder (i.e., electronic circuitry) on board the satellite, while the downlink connects the transponder to another Earth terminal. Thus, an information-bearing signal is transmitted from the Earth terminal to the satellite via the uplink, amplified in the transponder, and then retransmitted from the satellite via the downlink to the other Earth terminal, as illustrated in Fig. 1.2. In so doing, a satellite communication system offers a unique capability: *global coverage*.

In a loose sense, *wireless communications* operates in a manner similar to satellite communications in that it also involves a downlink and an uplink. The *downlink* is responsible for forward-link radio transmission from a *base station* to its mobile users. The uplink is responsible for reverse-link radio transmission from the mobile users to their base stations. Unlike satellite communications, the operation of wireless communications is dominated by the *multipath phenomenon* due to reflections of the transmitted signal from objects (e.g., buildings, trees, etc.) that lie in the propagation path. This phenomenon tends to degrade the receiver performance, which makes the design of the receiver a challenging task. In any event, wireless communications offers a unique capability of its own: *mobility*. Moreover, through the use of the cellular concept, the wireless communication system is enabled to *reuse* the radio spectrum over a large area as many times as possible. Within a cell, the available communication resources can be shared by the mobile users operating within that cell.

## ■ COMMUNICATION NETWORKS

The *computer* was originally conceived as a machine working by itself to perform numerical calculations. However, given the natural ability of a computer to perform logical functions, it was soon recognized that the computer is ideally suited to the design of

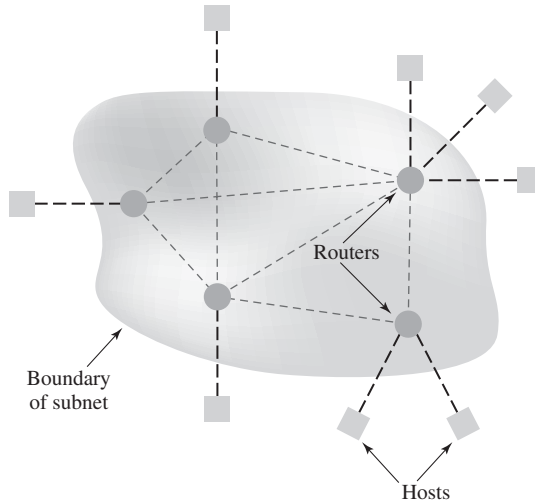


**FIGURE 1.3** Communication network.

communication networks. As illustrated in Fig. 1.3, a *communication network* consists of the interconnection of a number of *routers* that are made up of intelligent processors (e.g., microprocessors). The primary purpose of these processors is to route voice or data through the network, hence the name “routers.” Each router has one or more *hosts* attached to it; hosts refer to devices that communicate with one another. The purpose of a network is to provide for the delivery or exchange of voice, video, or data among its hosts, which is made possible through the use of *digital switching*. There are two principal forms of switching: circuit switching and packet switching.

In *circuit switching*, dedicated communication paths are established for the transmission of messages between two or more terminals, called *stations*. The communication path or *circuit* consists of a connected sequence of links from source to destination. For example, the links may consist of time slots (as in time-division multiplexed systems), for which a common channel is available for multiple users. The important point to note is that once it is in place, the circuit remains uninterrupted for the entire duration of transmission. Circuit switching is usually controlled by a centralized hierarchical control mechanism with knowledge of the network’s entire organization. To establish a circuit-switched connection, an available path through the telephone network is seized and then dedicated to the exclusive use of the two users wishing to communicate. In particular, a call-request signal propagates all the way to the destination, whereupon it is acknowledged before communication can begin. Then, the network is effectively transparent to the users, which means that during the entire connection time the resources allocated to the circuit are essentially “owned” by the two users. This state of affairs continues until the circuit is disconnected.

Circuit switching is well suited for telephone networks, where the transmission of voice constitutes the bulk of the network’s traffic. We say so because voice gives rise to a stream traffic, and voice conversations tend to be of long duration (about 2 minutes on the average) compared to the time required for setting up the circuit (about 0.1 to 0.5 seconds).

In *packet switching*,<sup>2</sup> on the other hand, the sharing of network resources is done on a *demand* basis. Hence, packet switching has an advantage over circuit switching in that

<sup>2</sup>Packet switching was invented by P. Baran in 1964 to satisfy a national defense need of the United States. The original need was to build a distributed network with different levels of redundant connections, which is *robust* in the sense that the network can withstand the destruction of many nodes due to a concerted attack, yet the surviving nodes are able to maintain intercommunication for carrying common and control information; see Baran (1990).

when a link has traffic to send, the link tends to be more fully utilized. Unlike voice signals, data tend to occur in the form of *bursts* on an occasional basis.

The network principle of packet switching is *store and forward*. Specifically, in a *packet-switched network*, any message longer than a specified size is subdivided prior to transmission into segments not exceeding the specified size. The segments so formed are called *packets*. After transporting the packets across different parts of the network, the original message is reassembled at the destination on a packet-by-packet basis. The network may thus be viewed as a pool of network resources (i.e., channel bandwidth, buffers, and switching processors), with the resources being *dynamically shared* by a community of competing hosts that wish to communicate. This dynamic sharing of network resources is in direct contrast to the circuit-switched network, where the resources are dedicated to a pair of hosts for the entire period they are in communication.

## ■ DATA NETWORKS

A communication network in which the hosts are all made up of computers and terminals is commonly referred to as a *data network*. The design of such a network proceeds in an orderly way by looking at the network in terms of a *layered architecture*, which is regarded as a hierarchy of nested layers. A *layer* refers to a process or device inside a computer system that is designed to perform a specific function. Naturally, the designers of a layer will be familiar with its internal details and operation. At the system level, however, a user views the layer in question merely as a “black box,” which is described in terms of inputs, outputs, and the functional relation between the outputs and inputs. In the layered architecture, each layer regards the next lower layer as one or more black boxes with some given functional specification to be used by the given higher layer. In this way, the highly complex communication problem in data networks is resolved as a manageable set of well-defined interlocking functions. It is this line of reasoning that has led to the development of the *open systems interconnection (OSI) reference model*.<sup>3</sup> The term “open” refers to the ability of any two systems to interconnect, provided they conform to the reference model and its associated standards.

In the OSI reference model, the communications and related-connection functions are organized as a series of *layers* with well-defined interfaces. Each layer is built on its predecessor. In particular, each layer performs a related subset of primitive functions, and it relies on the next lower layer to perform additional primitive functions. Moreover, each layer offers certain services to the next higher layer and shields that layer from the implementation details of those services. Between each pair of layers there is an *interface*, which defines the services offered by the lower layer to the upper layer.

As illustrated in Fig. 1.4, the OSI model is composed of seven layers. The figure also includes a description of the functions of the individual layers of the model. Layer  $k$  on system  $A$ , say, communicates with a layer  $R$  on some other system  $B$  in accordance with a set of rules and conventions, which collectively constitute layer  $k$  *protocol*, where  $k = 1, 2, \dots, 7$ . (The term “protocol” has been borrowed from common usage that describes conventional social behavior between human beings.) The entities that comprise the corresponding layers on different systems are referred to as *peer processes*. In other words, communication between system  $A$  and system  $B$  is achieved by having the peer processes in the two systems communicate via protocol. Physical connection between peer processes

---

<sup>3</sup>The OSI reference model was developed by a subcommittee of the International Organization for Standardization (ISO) in 1977. For a discussion of the principles involved in arriving at the original seven layers of the OSI model and a description of the layers themselves, see Tannenbaum (1996).

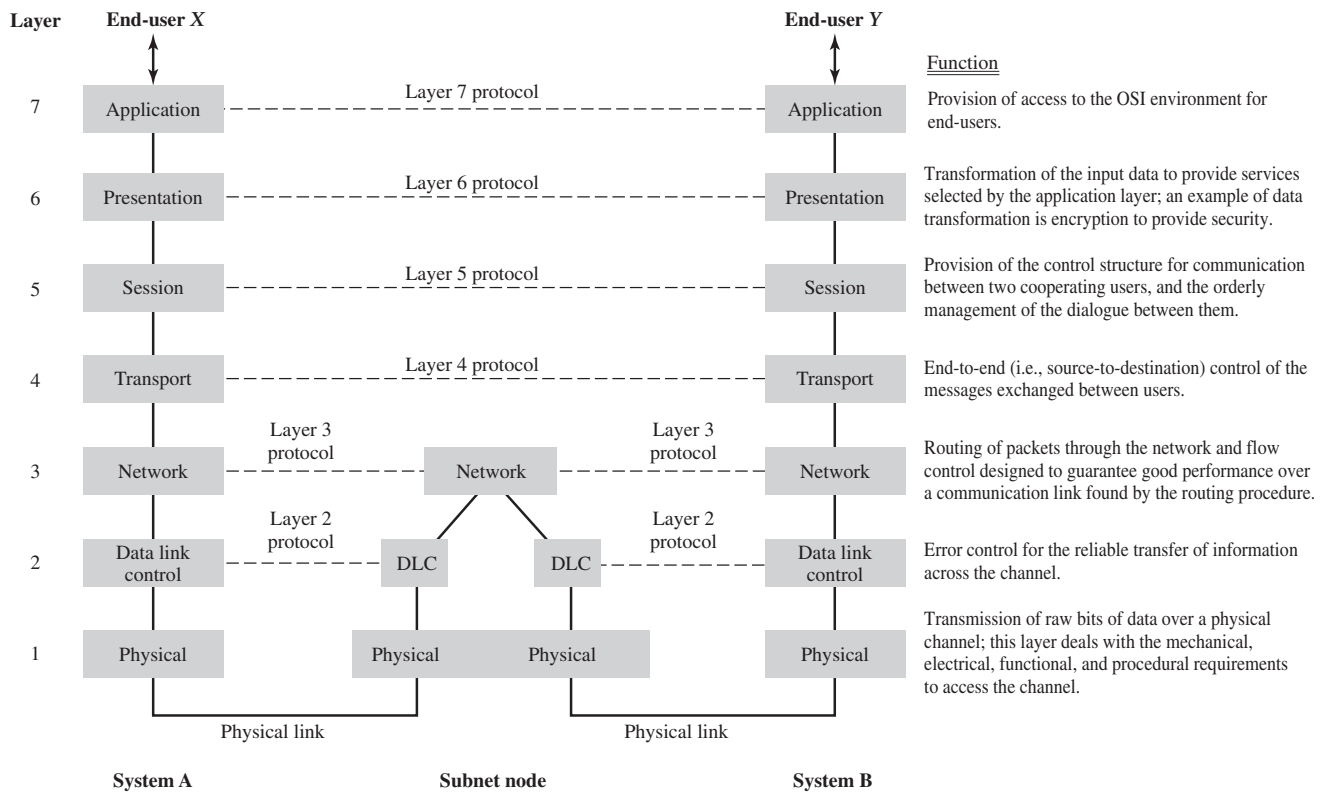


**FIGURE 1.4** OSI model; the acronym DLC in the middle of the figure stands for *data link control*.

exists only at layer 1—namely, the *physical layer*. The remaining layers, 2 through 7, are in *virtual communication* with their distant peers. Each of these latter six layers exchanges data and control information with its neighboring layers (lower and above) through layer-to-layer interfaces. In Fig. 1.4, physical communication is shown by solid lines, and virtual communications are shown by dashed lines.

## ■ INTERNET<sup>4</sup>

The discussion of data networks just presented leads to the *Internet*. In the Internet paradigm, the underlying network technology is decoupled from the applications at hand by adopting an abstract definition of network service. In more specific terms, we may say the following:

- ▶ The applications are carried out independently of the technology employed to construct the network.
- ▶ By the same token, the network technology is capable of evolving without affecting the applications.

<sup>4</sup>For a fascinating account of the Internet, its historical evolution from the ARPANET, and international standards, see Abbate (2000). For easy-to-read essays on the Internet, see Special Issue, IEEE Communications Magazine (2002); the articles presented therein are written by pioneering contributors to the development of the Internet.

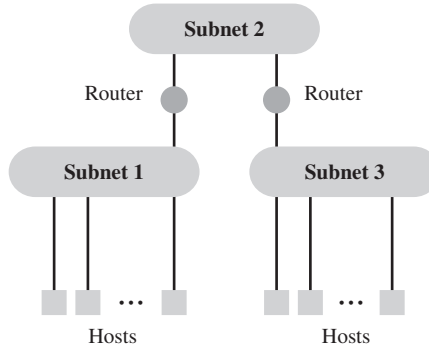
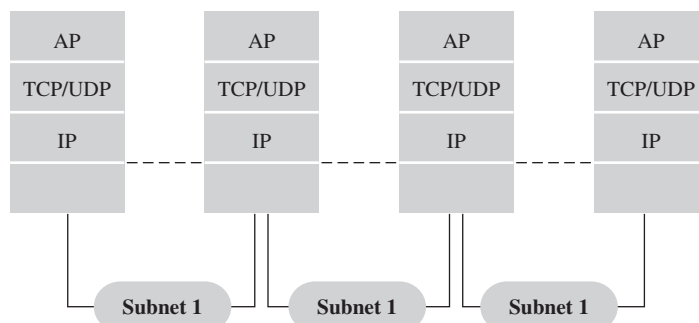


**FIGURE 1.5** An interconnected network of subnets.

The Internet application depicted in Fig. 1.5 has three functional blocks: hosts, subnets, and routers. The hosts constitute nodes of the network, where data originate or where they are delivered. The routers constitute intermediate nodes that are used to cross subnet boundaries. Within a subnet, all the hosts belonging to that subnet exchange data directly; see, for example, subnets 1 and 3 in Fig. 1.5. In basic terms, the internal operation of a subnet is organized in two different ways (Tanenbaum, 1996):

1. *Connected* manner, where the connections are called *virtual circuits*, in analogy with physical circuits set up in a telephone system.
2. *Connectionless* manner, where the independent packets are called *datagrams*, in analogy with telegrams.

Like other data networks, the Internet has a layered set of protocols. In particular, the exchange of data between the hosts and routers is accomplished by means of the *Internet protocol* (IP), as illustrated in Fig. 1.6. The IP is a universal protocol that resides in the network layer (i.e., layer 3 of the OSI reference model). It is simple, defining an addressing plan with a built-in capability to transport data in the form of packets from node to node. In crossing a subnetwork boundary, the routers make the decisions as to how the packets addressed for a specified destination should be routed. This is done on the basis of routing tables that are developed through the use of custom protocols for exchanging pertinent information with other routers. The net result of using the layered set of protocols is the provision of *best effort service*. That is, the Internet offers to deliver each packet of data,



AP: Application protocol  
TCP: Transmission control protocol  
IP: Internet protocol

UDP: User datagram protocol  
IP: Internet protocol

**FIGURE 1.6** Illustrating the network architecture of the Internet.

but there are no guarantees on the transit time experienced in delivery or even whether the packets will be delivered to the intended recipient.

The Internet has evolved into a worldwide system, placing computers at the heart of a communication medium that is changing our daily lives in the home and workplace in profound ways. We can send an *e-mail message* from a host in North America to another host in Australia at the other end of the globe, with the message arriving at its destination in a matter of seconds. This is all the more remarkable because the packets constituting the message are quite likely to have taken entirely different paths as they are transported across the network.

Another application that demonstrates the remarkable power of the Internet is our use of it to *surf the Web*. For example, we may use a *search engine* to identify the references pertaining to a particular subject of interest. A task that used to take hours and sometimes days searching through books and journals in the library now occupies a matter of seconds!

To fully utilize the computing power of the Internet from a host located at a remote site, we need a *wideband modem* (i.e., modulator-demodulator) to provide a fast communication link between that host and its subnet. When we say “fast,” we mean operating speeds on the order of megabits per second and higher. A device that satisfies this requirement is the so-called *digital subscriber line* (DSL). What makes the DSL all the more remarkable is the fact that it can operate over a linear wideband channel with an arbitrary frequency response. Such a channel is exemplified by an ordinary telephone channel built using twisted pairs for signal transmission. A *twisted pair* consists of two solid copper conductors, each of which is encased in a polyvinyl chloride (PVC) sheath. Twisted pairs are usually made up into cables, with each cable consisting of many twisted pairs in close proximity to each other. From a signal-transmission viewpoint, the DSL satisfies the challenging requirement described herein by following the well-known engineering principle of *divide and conquer*. Specifically, the given wideband channel is *approximated* by a set of narrowband channels, each of which can then be accommodated in a relatively straightforward manner.

One last comment is in order. Typically, access to the Internet is established via hosts in the form of computer terminals (i.e., servers). The access is expanded by using *hand-held devices* that act as hosts, which communicate with subnets of the Internet via wireless links. Thus, by adding mobility through the use of wireless communications to the computing power of the Internet to communicate, we have a new communication medium with enormous practical possibilities.

## ■ INTEGRATION OF TELEPHONE AND INTERNET

One of the important challenges facing the telecommunications industry is the transmission of *Voice over Internet Protocol* (VoIP), which would make it possible to integrate telephony services with the rapidly growing Internet-based applications. The challenge is all the more profound because the IP is designed to accommodate the exchange of data between the hosts and the routers, which makes it difficult to support quality of service for VoIP. *Quality of service* (QoS) is measured in terms of two parameters:

- ▶ *Packet loss ratio*, defined as the number of packets lost in transport across the network to the total number of packets pumped into the network.
- ▶ *Connection delay*, defined as the time taken for a packet of a particular host-to-host connection to transmit across the network.

Subjective tests performed on VoIP show that in order to provide voice-grade telephone service, the packet loss ratio must be held below 1 percent, and one-way connection delay

can accumulate up to 160 ms without significant degradation of quality. Well-designed and managed VoIP networks, satisfying these provisions, are being deployed. However, the issue of *initial-echo control* remains a challenge.<sup>5</sup> Initial echo refers to the echo experienced at the beginning of a call on the first word or couple of words out of a user's mouth. The echo arises due to an impedance mismatch somewhere in the network, whereupon the incident signal is reflected back to the source.

Looking into the future, we may make the following remarks on internet telephony:

1. VoIP will replace *private branch exchanges* (PBXs) and other office switches; PBXs are remote switching units that have their own independent controls.<sup>6</sup>
2. VoIP is also currently having success with longer distance calls, but this is mainly due to the excess capacity that is now available on long-haul networks. If the loading on these long-haul networks increases, the delays will increase and a real-time service such as VoIP will be degraded. Accordingly, if long-service providers keep adding capacity so that loading is always low and response time is fast, thereby ensuring quality of service, then VoIP telephony may become mainstream and widespread.

### ■ DATA STORAGE

When considering important applications of digital communication principles, it is natural to think in terms of broadcasting and point-to-point communication systems. Nevertheless, the very same principles are also applied to the digital storage of audio and video signals, exemplified by *compact disc* (CD) and *digital versatile disc* (DVD) players. DVDs are refinements of CDs in that their storage capacity (in the order of tens of gigabytes) are orders of magnitude higher than that of CDs, and they can also deliver data at a much higher rate.

The digital domain is preferred over the analog domain for the storage of audio and video signals for the following compelling reasons:

- (i) The quality of a digitized audio/video signal, measured in terms of frequency response, linearity, and noise, is determined by the digital-to-analog conversion (DAC) process, the parameterization of which is under the designer's control.
- (ii) Once the audio/video signal is digitized, we can make use of well-developed and powerful encoding techniques for data compression to reduce bandwidth, and error-control coding to provide protection against the possibility of making errors in the course of storage.
- (iii) For most practical applications, the digital storage of audio and video signals does not degrade with time.
- (iv) Continued improvements in the fabrication of integrated circuits used to build CDs and DVDs ensure the ever-increasing cost-effectiveness of these digital storage devices.

With the help of the powerful encoding techniques built into their design, DVDs can hold hours of high-quality audio-visual contents, which, in turn, makes them ideally suited for interactive multimedia applications.

---

<sup>5</sup>The limits on QoS measures mentioned herein are taken from the overview article by James, Chen, and Garrison (2004), which appears in a Special Issue of the *IEEE Communications Magazine* devoted to voice VoIP and quality of service.

<sup>6</sup>PBXs are discussed in McDonald (1990).

## 1.3 Primary Resources and Operational Requirements

The communication systems described in Section 1.2 cover many diverse fields. Nevertheless, in their own individual ways, the systems are designed to provide for the *efficient* utilization of two *primary communication resources*:

- ▶ *Transmitted power*, which is defined as the average power of the transmitted signal.
- ▶ *Channel bandwidth*, which is defined by the width of the passband of the channel.

Depending on which of these two resources is considered to be the limiting factor, we may classify communication channels as follows:

- (i) *Power-limited channels*, where transmitted power is at a premium. Examples of such channels include the following:
  - ▶ *Wireless channels*, where it is desirable to keep the transmitted power low so as to prolong battery life.
  - ▶ *Satellite channels*, where the available power on board the satellite transponder is limited, which, in turn, necessitates keeping the transmitted power on the down-link at a low level.
  - ▶ *Deep-space links*, where the available power on board a probe exploring outer space is extremely limited, which again requires that the average power of information-bearing signals sent by the probe to an Earth station be maintained as low as possible.
- (ii) *Band-limited channels*, where channel bandwidth is at a premium. Examples of this second category of communication channels include the following:
  - ▶ *Telephone channels*, where, in a multi-user environment, the requirement is to minimize the frequency band allocated to the transmission of each voice signal while making sure that the quality of service for each user is maintained.
  - ▶ *Television channels*, where the available channel bandwidth is limited by regulatory agencies and the quality of reception is assured by using a high enough transmitted power.

Another important point to keep in mind is the unavoidable presence of noise at the receiver input of a communication system. In a generic sense, *noise* refers to unwanted signals that tend to disturb the quality of the received signal in a communication system. The sources of noise may be internal or external to the system. An example of internal noise is the ubiquitous *channel noise* produced by thermal agitation of electrons in the front-end amplifier of the receiver. Examples of external noise include atmospheric noise and interference due to transmitted signals pertaining to other users.

A quantitative way to account for the beneficial effect of the transmitted power in relation to the degrading effect of noise (i.e., assess the quality of the received signal) is to think in terms of the *signal-to-noise ratio* (SNR), which is a dimensionless parameter. In particular, the SNR at the receiver input is formally defined as the ratio of the average power of the received signal (i.e., channel output) to the average power of noise measured at the receiver input. The customary practice is to express the SNR in *decibels* (dBs), which is defined as 10 times the logarithm (to base 10) of the power ratio.<sup>7</sup> For example, signal-to-noise ratios of 10, 100, and 1000 are 10, 20, and 30 dBs, respectively.

<sup>7</sup>For a discussion of the decibel, see Appendix 1.

In light of this discussion, it is now apparent that as far as performance evaluation is concerned, there are only two *system-design parameters*: signal-to-noise ratio and channel bandwidth. Stated in more concrete terms:

The design of a communication system boils down to a tradeoff between signal-to-noise ratio and channel bandwidth.

Thus, we may improve *system performance* by following one of two alternative design strategies, depending on system constraints:

1. Signal-to-noise ratio is increased to accommodate a limitation imposed on channel bandwidth.
2. Channel bandwidth is increased to accommodate a limitation imposed on signal-to-noise ratio.

Of these two possible design approaches, we ordinarily find that strategy 1 is simpler to implement than strategy 2, because increasing signal-to-noise ratio can be accomplished simply by raising the transmitted power. On the other hand, in order to exploit increased channel bandwidth, we need to increase the bandwidth of the transmitted signal, which, in turn, requires increasing the *complexity* of both the transmitter and receiver.

## 1.4 Underpinning Theories of Communication Systems

The study of communication systems is challenging not only in technical terms but also in theoretical terms. In this section, we highlight four theories, each of which is essential for understanding a specific aspect of communication systems.<sup>8</sup>

### ■ MODULATION THEORY

*Modulation* is a signal-processing operation that is basic to the transmission of an information-bearing signal over a communication channel, whether in the context of digital or analog communications. This operation is accomplished by changing some parameter of a *carrier wave* in accordance with the information-bearing (message) signal. The carrier wave may take one of two basic forms, depending on the application of interest:

- ▶ *Sinusoidal carrier wave*, whose amplitude, phase, or frequency is the parameter chosen for modification by the information-bearing signal.
- ▶ *Periodic sequence of pulses*, whose amplitude, width, or position is the parameter chosen for modification by the information-bearing signal.

Regardless of which particular approach is used to perform the modulation process, the issues in modulation theory that need to be addressed are:

- ▶ Time-domain description of the modulated signal.
- ▶ Frequency-domain description of the modulated signal.
- ▶ Detection of the original information-bearing signal and evaluation of the effect of noise on the receiver.

---

<sup>8</sup>One other theory—namely, Information Theory—is basic to the study of communication systems. We have not included this theory here because of its highly mathematical and therefore advanced nature, which makes it inappropriate for an introductory book.

## ■ FOURIER ANALYSIS

The *Fourier transform* is a *linear* mathematical operation that transforms the time-domain description of a signal into a frequency-domain description without loss of information, which means that the original signal can be recovered exactly from the frequency-domain description. However, for the signal to be Fourier transformable, certain conditions have to be satisfied. Fortunately, these conditions are satisfied by the kind of signals encountered in the study of communication systems.

Fourier analysis provides the mathematical basis for evaluating the following issues:

- ▶ Frequency-domain description of a modulated signal, including its transmission bandwidth.
- ▶ Transmission of a signal through a linear system exemplified by a communication channel or (frequency-selective) filter.
- ▶ Correlation (i.e., similarity) between a pair of signals.

These evaluations take on even greater importance by virtue of an algorithm known as the *fast Fourier transform*, which provides an efficient method for computing the Fourier transform.

## ■ DETECTION THEORY

Given a received signal, which is perturbed by additive channel noise, one of the tasks that the receiver has to tackle is how to *detect* the original information-bearing signal in a reliable manner. The *signal-detection problem* is complicated by two issues:

- ▶ The presence of noise.
- ▶ Factors such as the unknown phase-shift introduced into the carrier wave due to transmission of the sinusoidally modulated signal over the channel.

Dealing with these issues in analog communications is radically different from dealing with them in digital communications. In analog communications, the usual approach focuses on *output signal-to-noise ratio* and related calculations. In digital communications, on the other hand, the signal-detection problem is viewed as one of *hypothesis testing*. For example, in the specific case of binary data transmission, given that binary symbol 1 is transmitted, what is the probability that the symbol is correctly detected, and how is that probability affected by a change in the received signal-to-noise ratio at the receiver input?

Thus, in dealing with detection theory, we address the following issues in analog communications:

- ▶ The figure of merit for assessing the noise performance of a specific modulation strategy.
- ▶ The threshold phenomenon that arises when the transmitted signal-to-noise ratio drops below a critical value.
- ▶ Performance comparison of one modulation strategy against another.

In digital communications, on the other hand, we look at:

- ▶ The average probability of symbol error at the receiver output.
- ▶ The issue of dealing with uncontrollable factors.
- ▶ Comparison of one digital modulation scheme against another.

### ■ PROBABILITY THEORY AND RANDOM PROCESSES

From the brief discussion just presented on the role of detection theory in the study of communication systems, it is apparent that we need to develop a good understanding of the following:

- ▶ Probability theory for describing the behavior of randomly occurring events in mathematical terms.
- ▶ Statistical characterization of random signals and noise.

Unlike a deterministic signal, a *random signal* is a signal about which there is *uncertainty* before it occurs. Because of the uncertainty, a random signal may be viewed as belonging to an *ensemble*, or a *group*, of signals, with each signal in the ensemble having a different waveform from that of the others in the ensemble. Moreover, each signal within the ensemble has a certain probability of occurrence. The ensemble of signals is referred to as a *random process* or *stochastic process*. Examples of a random process include:

- ▶ Electrical noise generated in the front-end amplifier of a radio or television receiver.
- ▶ Speech signal produced by a male or female speaker.
- ▶ Video signal transmitted by the antenna of a TV broadcasting station.

In dealing with probability theory, random signals, and noise, we address the following issues:

- ▶ Basic concepts of probability theory and probabilistic models.
- ▶ Statistical description of a random process in terms of ensemble as well as temporal averages.
- ▶ Mathematical analysis and processing of random signals.

## 1.5 Concluding Remarks

In this chapter, we have given a historical account and applications of communications and a brief survey of underlying theories of communication systems. In addition, we presented the following points to support our view that the study of this discipline is both highly challenging and truly exciting:

- (i) Communication systems encompass many and highly diverse applications: radio, television, wireless communications, satellite communications, deep-space communications, telephony, data networks, Internet, and quite a few others.
- (ii) Digital communication has established itself as the dominant form of communication. Much of the progress that we have witnessed in the advancement of digital communication systems can be traced to certain enabling theories and technologies, as summarized here:
  - ▶ Abstract mathematical ideas that are highly relevant to a deep understanding of the processing of information-bearing signals and their transmission over physical media.
  - ▶ Digital signal-processing algorithms for the efficient computation of spectra, correlation, and filtering of signals.
  - ▶ Software development and novel architectures for designing microprocessors.
  - ▶ Spectacular advances in the physics of solid-state devices and the fabrication of very-large-scale integrated (VLSI) chips.

- (iii) The study of communication systems is a *dynamic discipline*, continually evolving by exploiting new technological innovations in other disciplines and responding to new societal needs.
- (iv) Last but by no means least, communication systems touch our daily lives both at home and in the workplace, and our lives would be much poorer without the wide availability of communication devices that we take for granted.

The remainder of the book, encompassing ten chapters, provides an introductory treatment of both analog and digital kinds of communication systems. The book should prepare the reader for going on to deepen his or her knowledge of a discipline that is best described as *almost limitless* in scope. This is especially the case given the trend toward the unification of wireline and wireless networks to accommodate the integrated transmission of voice, video, and data.

## CHAPTER 2

# FOURIER REPRESENTATION OF SIGNALS AND SYSTEMS

In mathematical terms, a signal is ordinarily described as a *function of time*, which is how we usually see the signal when its waveform is displayed on an oscilloscope. However, as pointed out in Chapter 1, from the perspective of a communication system it is important that we know the *frequency content* of the signal in question. The mathematical tool that relates the frequency-domain description of the signal to its time-domain description is the *Fourier transform*. There are in fact several versions of the Fourier transform available. In this chapter, we confine the discussion primarily to two specific versions:

- ▶ The *continuous Fourier transform*, or the Fourier transform (FT) for short, which works with continuous functions in both the time and frequency domains.
- ▶ The *discrete Fourier transform*, or DFT for short, which works with discrete data in both the time and frequency domains.

Much of the material presented in this chapter focuses on the Fourier transform, since the primary motivation of the chapter is to determine the frequency content of a continuous-time signal or to evaluate what happens to this frequency content when the signal is passed through a *linear time-invariant (LTI) system*. In contrast, the discrete Fourier transform, discussed toward the end of the chapter, comes into its own when the requirement is to evaluate the frequency content of the signal on a digital computer or to evaluate what happens to the signal when it is processed by a digital device as in digital communications.

The extensive material presented in this chapter teaches the following lessons:

- ▶ *Lesson 1: The Fourier transform of a signal specifies the complex amplitudes of the components that constitute the frequency-domain description or spectral content of the signal. The inverse Fourier transform uniquely recovers the signal, given its frequency-domain description.*
- ▶ *Lesson 2: The Fourier transform is endowed with several important properties, which, individually and collectively, provide invaluable insight into the relationship between a signal defined in the time domain and its frequency domain description.*
- ▶ *Lesson 3: A signal can only be strictly limited in the time domain or the frequency domain, but not both.*
- ▶ *Lesson 4: Bandwidth is an important parameter in describing the spectral content of a signal and the frequency response of a linear time-invariant filter.*

- **Lesson 5:** A widely used algorithm called the fast Fourier transform algorithm provides a powerful tool for computing the discrete Fourier transform; it is the mathematical tool for digital computations involving Fourier transformation.

## 2.1 The Fourier Transform<sup>1</sup>

### ■ DEFINITIONS

Let  $g(t)$  denote a *nonperiodic deterministic signal*, expressed as some function of *time*  $t$ . By definition, the *Fourier transform* of the signal  $g(t)$  is given by the integral

$$G(f) = \int_{-\infty}^{\infty} g(t) \exp(-j2\pi ft) dt \quad (2.1)$$

where  $j = \sqrt{-1}$ , and the variable  $f$  denotes *frequency*; the exponential function  $\exp(-j2\pi ft)$  is referred to as the *kernel* of the formula defining the Fourier transform. Given the Fourier transform  $G(f)$ , the original signal  $g(t)$  is recovered exactly using the formula for the *inverse Fourier transform*:

$$g(t) = \int_{-\infty}^{\infty} G(f) \exp(j2\pi ft) df \quad (2.2)$$

where the exponential  $\exp(j2\pi ft)$  is the *kernel* of the formula defining the inverse Fourier transform. The two kernels of Eqs. (2.1) and (2.2) are therefore the complex conjugate of each other.

Note also that in Eqs. (2.1) and (2.2) we have used a lowercase letter to denote the time function and an uppercase letter to denote the corresponding frequency function. The functions  $g(t)$  and  $G(f)$  are said to constitute a *Fourier-transform pair*. In Appendix 2, we derive the definitions of the Fourier transform and its inverse, starting from the Fourier series of a periodic waveform.

We refer to Eq. (2.1) as the *analysis equation*. Given the time-domain behavior of a system, we are enabled to analyze the frequency-domain behavior of a system. The basic advantage of transforming the time-domain behavior into the frequency domain is that *resolution into eternal sinusoids presents the behavior as the superposition of steady-state effects*. For systems whose time-domain behavior is described by linear differential equations, the separate steady-state solutions are usually simple to understand in theoretical as well as experimental terms.

Conversely, we refer to Eq. (2.2) as the *synthesis equation*. Given the superposition of steady-state effects in the frequency-domain, we can *reconstruct the original time-domain behavior of the system without any loss of information*. The analysis and synthesis equations, working side by side as depicted in Fig. 2.1, enrich the representation of signals and

---

<sup>1</sup>Joseph Fourier studied the flow of heat in the early 19th century. Understanding heat flow was a problem of both practical and scientific significance at that time and required solving a partial-differential equation called the heat equation. Fourier developed a technique for solving partial-differential equations that was based on the assumption that the solution was a weighted sum of harmonically related sinusoids with unknown coefficients, which we now term the *Fourier series*. Fourier's initial work on heat conduction was submitted as a paper to the Academy of Sciences of Paris in 1807 and rejected after review by Lagrange, Laplace, and Legendre. Fourier persisted in developing his ideas in spite of being criticized for a lack of rigor by his contemporaries. Eventually, in 1822, he published a book containing much of his work, *Theorie analytique de la chaleur*, which is now regarded as one of the classics of mathematics.

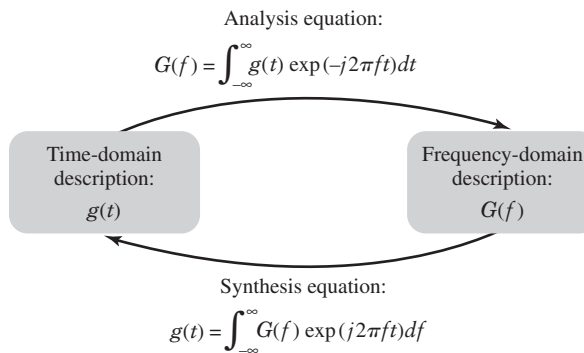


**FIGURE 2.1** Sketch of the interplay between the synthesis and analysis equations embodied in Fourier transformation.

systems by making it possible to view the representation in two interactive domains: the time domain and the frequency domain.

For the Fourier transform of a signal  $g(t)$  to exist, it is sufficient, but not necessary, that  $g(t)$  satisfies three conditions known collectively as *Dirichlet's conditions*:

1. The function  $g(t)$  is single-valued, with a finite number of maxima and minima in any finite time interval.
2. The function  $g(t)$  has a finite number of discontinuities in any finite time interval.
3. The function  $g(t)$  is absolutely integrable—that is,

$$\int_{-\infty}^{\infty} |g(t)| dt < \infty$$

We may safely ignore the question of the existence of the Fourier transform of a time function  $g(t)$  when it is an accurately specified description of a physically realizable signal (e.g., voice signal, video signal). In other words, physical realizability is a sufficient condition for the existence of a Fourier transform. For physical realizability of a signal  $g(t)$ , the energy of the signal defined by  $\int_{-\infty}^{\infty} |g(t)|^2 dt$  must satisfy the condition

$$\int_{-\infty}^{\infty} |g(t)|^2 dt < \infty$$

Such a signal is referred to as an energy-like signal or simply an *energy signal*. What we are therefore saying is that *all energy signals are Fourier transformable*.

### ■ NOTATIONS

The formulas for the Fourier transform and the inverse Fourier transform presented in Eqs. (2.1) and (2.2) are written in terms of two variables: *time t* measured in *seconds* (s) and frequency *f* measured in *hertz* (Hz). The frequency *f* is related to the *angular frequency*  $\omega$  as

$$\omega = 2\pi f$$

which is measured in *radians per second* (rad/s). We may simplify the expressions for the exponents in the integrands of Eqs. (2.1) and (2.2) by using  $\omega$  instead of  $f$ . However, the use of  $f$  is preferred over  $\omega$  for two reasons. First, the use of frequency results in mathematical *symmetry* of Eqs. (2.1) and (2.2) with respect to each other in a natural way. Second, the spectral contents of communication signals (i.e., voice and video signals) are usually expressed in hertz.

A convenient *shorthand* notation for the transform relations of Eqs. (2.1) and (2.2) is to write

$$G(f) = \mathbf{F}[g(t)] \quad (2.3)$$

and

$$g(t) = \mathbf{F}^{-1}[G(f)] \quad (2.4)$$

where  $\mathbf{F}[\cdot]$  and  $\mathbf{F}^{-1}[\cdot]$  play the roles of *linear operators*. Another convenient shorthand notation for the *Fourier-transform pair*, represented by  $g(t)$  and  $G(f)$ , is

$$g(t) \iff G(f) \quad (2.5)$$

The shorthand notations described in Eqs. (2.3) through (2.5) are used in the text where appropriate.

### ■ CONTINUOUS SPECTRUM

By using the Fourier transform operation, a pulse signal  $g(t)$  of finite energy is expressed as a continuous sum of exponential functions with frequencies in the interval  $-\infty$  to  $\infty$ . The amplitude of a component of frequency  $f$  is proportional to  $G(f)$ , where  $G(f)$  is the Fourier transform of  $g(t)$ . Specifically, at any frequency  $f$ , the exponential function  $\exp(j2\pi ft)$  is weighted by the factor  $G(f) df$ , which is the contribution of  $G(f)$  in an infinitesimal interval  $df$  centered on the frequency  $f$ . Thus we may express the function  $g(t)$  in terms of the continuous sum of such infinitesimal components, as shown by the integral

$$g(t) = \int_{-\infty}^{\infty} G(f) \exp(j2\pi ft) df$$

Restating what was mentioned previously, the Fourier transformation provides us with a tool to resolve a given signal  $g(t)$  into its complex exponential components occupying the entire frequency interval from  $-\infty$  to  $\infty$ . In particular, the Fourier transform  $G(f)$  of the signal defines the frequency-domain representation of the signal in that it specifies complex amplitudes of the various frequency components of the signal. We may equivalently define the signal in terms of its time-domain representation by specifying the function  $g(t)$  at each instant of *time*  $t$ . The signal is uniquely defined by either representation.

In general, the Fourier transform  $G(f)$  is a complex function of frequency  $f$ , so that we may express it in the form

$$G(f) = |G(f)| \exp[j\theta(f)] \quad (2.6)$$

where  $|G(f)|$  is called the *continuous amplitude spectrum* of  $g(t)$ , and  $\theta(f)$  is called the *continuous phase spectrum* of  $g(t)$ . Here, the spectrum is referred to as a *continuous spectrum* because both the amplitude and phase of  $G(f)$  are uniquely defined for all frequencies.

For the special case of a real-valued function  $g(t)$ , we have

$$G(-f) = G^*(f)$$

where the asterisk denotes complex conjugation. Therefore, it follows that if  $g(t)$  is a *real-valued function of time t*, then

$$|G(-f)| = |G(f)|$$

and

$$\theta(-f) = -\theta(f)$$

Accordingly, we may make the following statements on the spectrum of a real-valued signal:

1. The amplitude spectrum of the signal is an even function of the frequency; that is, the amplitude spectrum is *symmetric* with respect to the origin  $f = 0$ .
2. The phase spectrum of the signal is an odd function of the frequency; that is, the phase spectrum is *antisymmetric* with respect to the origin  $f = 0$ .

These two statements are summed up by saying that the spectrum of a real-valued signal exhibits *conjugate symmetry*.

**EXAMPLE 2.1** Rectangular Pulse

Consider a box function or *rectangular pulse* of duration  $T$  and amplitude  $A$ , as shown in Fig. 2.2(a). To define this pulse mathematically in a convenient form, we use the notation

$$\text{rect}(t) = \begin{cases} 1, & -\frac{1}{2} \leq t \leq \frac{1}{2} \\ 0, & t < -\frac{1}{2} \text{ or } t > \frac{1}{2} \end{cases} \quad (2.7)$$

which stands for a *rectangular function* of unit amplitude and unit duration centered at  $t = 0$ . Then, in terms of this “standard” function, we may express the rectangular pulse of Fig. 2.2(a) simply as

$$g(t) = A \text{ rect}\left(\frac{t}{T}\right)$$

The Fourier transform of the rectangular pulse  $g(t)$  is given by

$$\begin{aligned} G(f) &= \int_{-T/2}^{T/2} A \exp(-j2\pi f t) dt \\ &= AT \left( \frac{\sin(\pi f T)}{\pi f T} \right) \end{aligned} \quad (2.8)$$

To simplify the notation in the preceding and subsequent results, we introduce another standard function—namely, the *sinc function*—defined by

$$\text{sinc}(\lambda) = \frac{\sin(\pi\lambda)}{\pi\lambda} \quad (2.9)$$

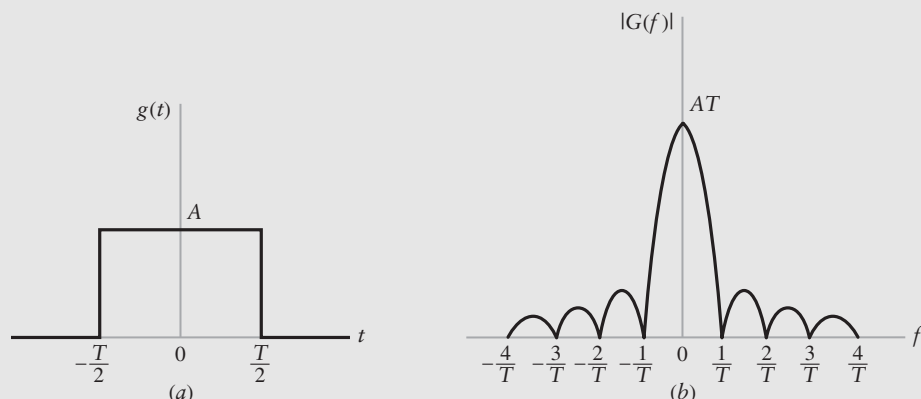


**FIGURE 2.2** (a) Rectangular pulse. (b) Amplitude spectrum.

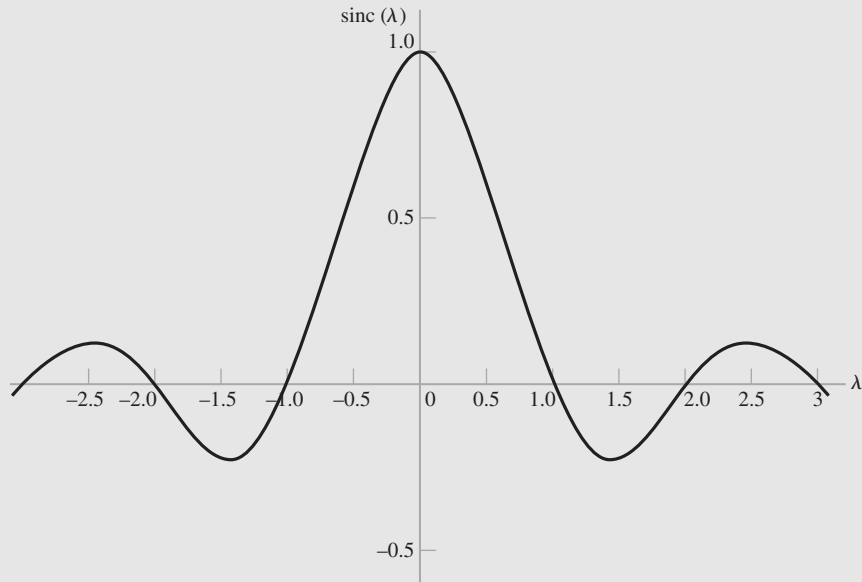


**FIGURE 2.3** The sinc function.

where  $\lambda$  is the independent variable. The sinc function plays an important role in communication theory. As shown in Fig. 2.3, it has its maximum value of unity at  $\lambda = 0$ , and approaches zero as  $\lambda$  approaches infinity, oscillating through positive and negative values. It goes through zero at  $\lambda = \pm 1, \pm 2, \dots$ , and so on.

Thus, in terms of the sinc function, we may rewrite Eq. (2.8) as

$$A \operatorname{rect}\left(\frac{t}{T}\right) \iff AT \operatorname{sinc}(fT) \quad (2.10)$$

The amplitude spectrum  $|G(f)|$  is shown plotted in Fig. 2.2(b). The first zero-crossing of the spectrum occurs at  $f = \pm 1/T$ . As the pulse duration  $T$  is decreased, this first zero-crossing moves up in frequency. Conversely, as the pulse duration  $T$  is increased, the first zero-crossing moves toward the origin.

This example shows that the relationship between the time-domain and frequency-domain descriptions of a signal is an *inverse* one. That is, a pulse narrow in time has a significant frequency description over a wide range of frequencies, and vice versa. We shall have more to say on the inverse relationship between time and frequency in Section 2.3.

Note also that in this example, the Fourier transform  $G(f)$  is a real-valued and symmetric function of frequency  $f$ . This is a direct consequence of the fact that the rectangular pulse  $g(t)$  shown in Fig. 2.2(a) is a symmetric function of *time*  $t$ .

### EXAMPLE 2.2 Exponential Pulse

A truncated decaying exponential pulse is shown in Fig. 2.4(a). We define this pulse mathematically in a convenient form using the unit step function:

$$u(t) = \begin{cases} 1, & t > 0 \\ \frac{1}{2}, & t = 0 \\ 0, & t < 0 \end{cases} \quad (2.11)$$

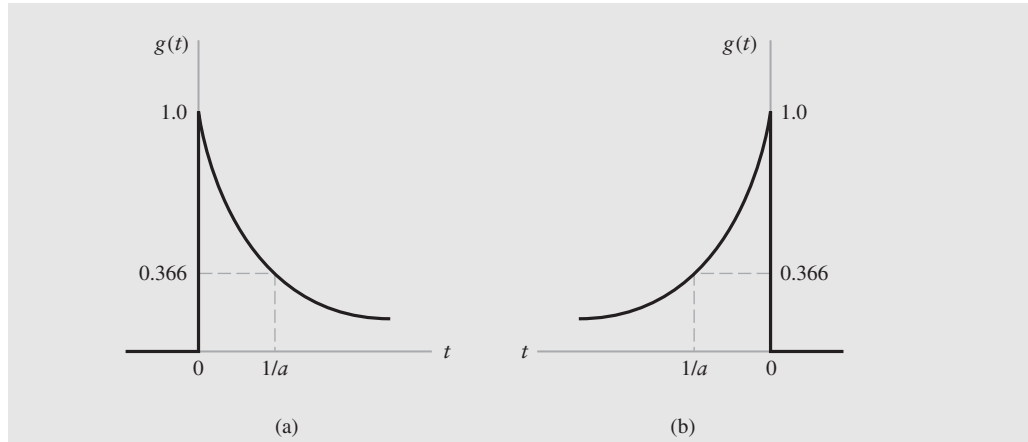


**FIGURE 2.4** (a) Decaying exponential pulse. (b) Rising exponential pulse.

We may then express the decaying exponential pulse of Fig. 2.4(a) as

$$g(t) = \exp(-at)u(t)$$

Recognizing that  $g(t)$  is zero for  $t < 0$ , the Fourier transform of this pulse is

$$\begin{aligned} G(f) &= \int_0^\infty \exp(-at) \exp(-j2\pi ft) dt \\ &= \int_0^\infty \exp[-t(a + j2\pi f)] dt \\ &= \frac{1}{a + j2\pi f} \end{aligned}$$

The Fourier-transform pair for the decaying exponential pulse of Fig. 2.4(a) is therefore

$$\exp(-at)u(t) \iff \frac{1}{a + j2\pi f} \quad (2.12)$$

A *truncated rising exponential pulse* is shown in Fig. 2.4(b), which is defined by

$$g(t) = \exp(at)u(-t)$$

Note that  $u(-t)$  is equal to unity for  $t < 0$ , one-half at  $t = 0$ , and zero for  $t > 0$ . With  $g(t)$  equal to zero for  $t > 0$ , the Fourier transform of this pulse is

$$G(f) = \int_{-\infty}^0 \exp(at) \exp(-j2\pi ft) dt$$

Replacing  $t$  with  $-t$ , we may next write

$$\begin{aligned} G(f) &= \int_0^\infty \exp[-t(a - j2\pi f)] dt \\ &= \frac{1}{a - j2\pi f} \end{aligned}$$

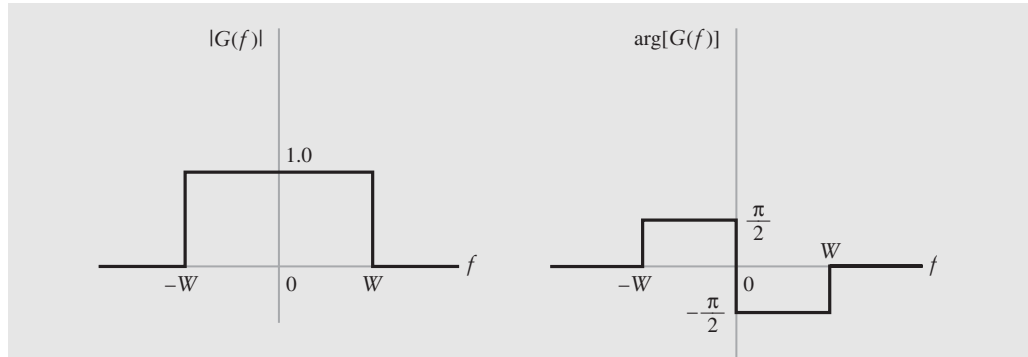


**FIGURE 2.5** Frequency function  $G(f)$  for Problem 2.2.

The Fourier-transform pair for the rising exponential pulse of Fig. 2.4(b) is therefore

$$\exp(-at)u(-t) \iff \frac{1}{a - j2\pi f} \quad (2.13)$$

The decaying and rising exponential pulses of Fig. 2.4 are both asymmetric functions of time  $t$ . Their Fourier transforms are therefore complex valued, as shown in Eqs. (2.12) and (2.13). Moreover, from these Fourier-transform pairs, we readily see that truncated decaying and rising exponential pulses have the same amplitude spectrum, but the phase spectrum of the one is the negative of the phase spectrum of the other.

► **Drill Problem 2.1** Evaluate the Fourier transform of the damped sinusoidal wave  $g(t) = \exp(-t) \sin(2\pi f_c t)u(t)$ , where  $u(t)$  is the unit step function. ◀

► **Drill Problem 2.2** Determine the inverse Fourier transform of the frequency function  $G(f)$  defined by the amplitude and phase spectra shown in Fig. 2.5. ◀

## 2.2 Properties of the Fourier Transform

It is useful to have insight into the relationship between a time function  $g(t)$  and its Fourier transform  $G(f)$ , and also into the effects that various operations on the function  $g(t)$  have on the transform  $G(f)$ . This may be achieved by examining certain properties of the Fourier transform. In this section, we describe fourteen properties, which we will prove, one by one. These properties are summarized in Table A8.1 of Appendix 8 at the end of the book.

**PROPERTY 1 Linearity (Superposition)** Let  $g_1(t) \iff G_1(f)$  and  $g_2(t) \iff G_2(f)$ . Then for all constants  $c_1$  and  $c_2$ , we have

$$c_1 g_1(t) + c_2 g_2(t) \iff c_1 G_1(f) + c_2 G_2(f) \quad (2.14)$$

The proof of this property follows simply from the linearity of the integrals defining  $G(f)$  and  $g(t)$ .

Property 1 permits us to find the Fourier transform  $G(f)$  of a function  $g(t)$  that is a linear combination of two other functions  $g_1(t)$  and  $g_2(t)$  whose Fourier transforms  $G_1(f)$  and  $G_2(f)$  are known, as illustrated in the following example.

**EXAMPLE 2.3** Combinations of Exponential Pulses

Consider a *double exponential pulse* (defined by (see Fig. 2.6(a)))

$$g(t) = \begin{cases} \exp(-at), & t > 0 \\ 1, & t = 0 \\ \exp(at), & t < 0 \end{cases}$$

$$= \exp(-a|t|) \quad (2.15)$$

This pulse may be viewed as the sum of a truncated decaying exponential pulse and a truncated rising exponential pulse. Therefore, using the linearity property and the Fourier-transform pairs of Eqs. (2.12) and (2.13), we find that the Fourier transform of the double exponential pulse of Fig. 2.6(a) is

$$G(f) = \frac{1}{a + j2\pi f} + \frac{1}{a - j2\pi f}$$

$$= \frac{2a}{a^2 + (2\pi f)^2}$$

We thus have the following Fourier-transform pair for the double exponential pulse of Fig. 2.6(a):

$$\exp(-a|t|) \iff \frac{2a}{a^2 + (2\pi f)^2} \quad (2.16)$$

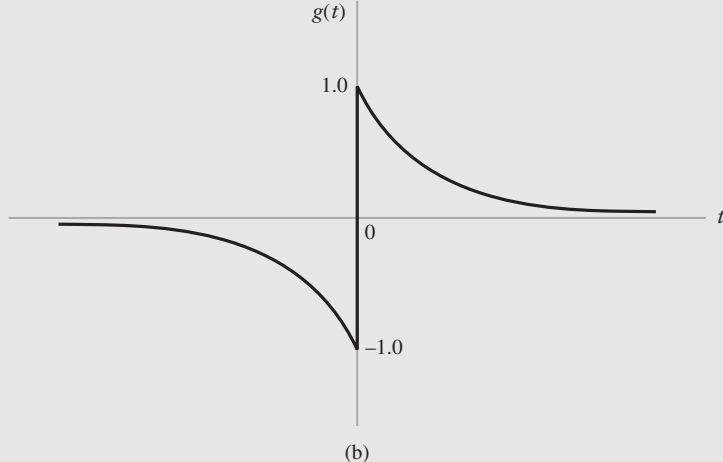
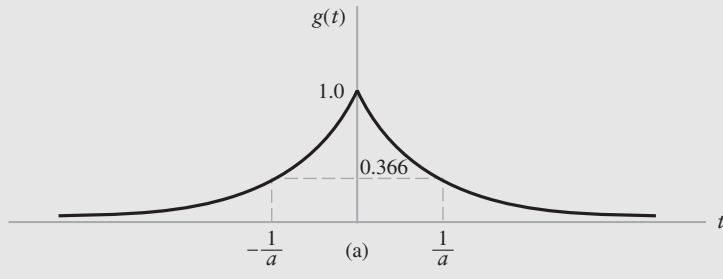


**FIGURE 2.6** (a) Double-exponential pulse (symmetric). (b) Another double-exponential pulse (odd-symmetric).

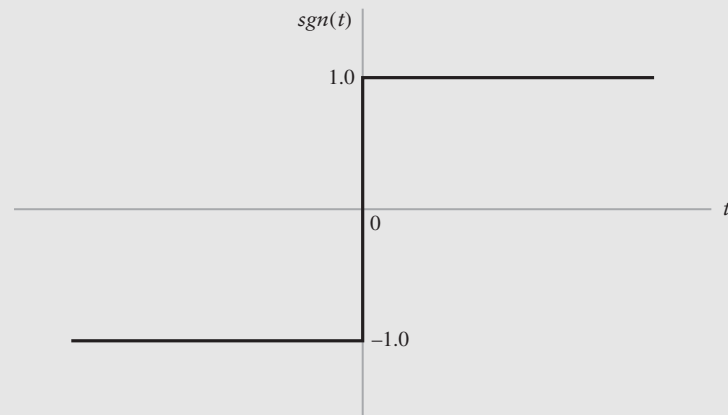


**FIGURE 2.7** Signum function.

Note that because of the symmetry in the time domain, as in Fig. 2.6(a), the spectrum is real and symmetric; this is a general property of such Fourier-transform pairs.

Another interesting combination is the difference between a truncated decaying exponential pulse and a truncated rising exponential pulse, as shown in Fig. 2.6(b). Here we have

$$g(t) = \begin{cases} \exp(-at), & t > 0 \\ 0, & t = 0 \\ -\exp(at), & t < 0 \end{cases} \quad (2.17)$$

We may formulate a compact notation for this composite signal by using the *signum function* that equals +1 for positive time and -1 for negative time, as shown by

$$\text{sgn}(t) = \begin{cases} +1, & t > 0 \\ 0, & t = 0 \\ -1, & t < 0 \end{cases} \quad (2.18)$$

The signum function is shown in Fig. 2.7. Accordingly, we may reformulate the composite signal  $g(t)$  defined in Eq. (2.17) simply as

$$g(t) = \exp(-a|t|) \text{sgn}(t)$$

Hence, applying the linearity property of the Fourier transform, we readily find that in light of Eqs. (2.12) and (2.13), the Fourier transform of the signal  $g(t)$  is given by

$$\begin{aligned} \mathbf{F}[\exp(-a|t|) \text{sgn}(t)] &= \frac{1}{a + j2\pi f} - \frac{1}{a - j2\pi f} \\ &= \frac{-j4\pi f}{a^2 + (2\pi f)^2} \end{aligned}$$

We thus have the Fourier-transform pair

$$\exp(-a|t|) \text{sgn}(t) \iff \frac{-j4\pi f}{a^2 + (2\pi f)^2} \quad (2.19)$$

In contrast to the Fourier-transform pair of Eq. (2.16), the Fourier transform in Eq. (2.19) is odd and purely imaginary. It is a general property of Fourier-transform pairs that apply to an *odd-symmetric* time function, which satisfies the condition  $g(-t) = -g(t)$ , as in Fig. 2.6(b); such a time function has an odd and purely imaginary function as its Fourier transform.

**PROPERTY 2 Dilation** Let  $g(t) \rightleftharpoons G(f)$ . Then, the dilation property or similarity property states that

$$g(at) \rightleftharpoons \frac{1}{|a|} G\left(\frac{f}{a}\right) \quad (2.20)$$

where the dilation factor—namely,  $a$ —is a real number.

To prove this property, we note that

$$\mathcal{F}[g(at)] = \int_{-\infty}^{\infty} g(at) \exp(-j2\pi ft) dt$$

Set  $\tau = at$ . There are two cases that can arise, depending on whether the dilation factor  $a$  is positive or negative. If  $a > 0$ , we get

$$\begin{aligned} \mathcal{F}[g(at)] &= \frac{1}{a} \int_{-\infty}^{\infty} g(\tau) \exp\left[-j2\pi\left(\frac{f}{a}\right)\tau\right] d\tau \\ &= \frac{1}{a} G\left(\frac{f}{a}\right) \end{aligned}$$

On the other hand, if  $a < 0$ , the limits of integration are interchanged so that we have the multiplying factor  $-(1/a)$  or, equivalently,  $1/|a|$ . This completes the proof of Eq. (2.20).

Note that the dilation factors  $a$  and  $1/a$  used in the time and frequency functions in Eq. (2.20) are reciprocals. In particular, the function  $g(at)$  represents  $g(t)$  compressed in time by the factor  $a$ , whereas the function  $G(f/a)$  represents  $G(f)$  expanded in frequency by the same factor  $a$ , assuming that  $0 < a < 1$ . Thus, the dilation rule states that the compression of a function  $g(t)$  in the time domain is equivalent to the expansion of its Fourier transform  $G(f)$  in the frequency domain by the same factor, or vice versa.

For the special case when  $a = -1$ , the dilation rule of Eq. (2.20) reduces to the *reflection property*, which states that if  $g(t) \rightleftharpoons G(f)$ , then

$$g(-t) \rightleftharpoons G(-f) \quad (2.21)$$

Referring to Fig. 2.4, we see that the rising exponential pulse shown in part (b) of the figure is the *reflection* of the decaying exponential pulse shown in part (a) with respect to the vertical axis. Hence, applying the reflection rule to Eq. (2.12) that pertains to the decaying exponential pulse, we readily see that the Fourier transform of the rising exponential pulse is  $1/(a - j2\pi f)$ , which is exactly what we have in Eq. (2.13).

**PROPERTY 3 Conjugation Rule** Let  $g(t) \rightleftharpoons G(f)$ . Then for a complex-valued time function  $g(t)$ , we have

$$g^*(t) \rightleftharpoons G^*(-f) \quad (2.22)$$

where the asterisk denotes the complex-conjugate operation.

To prove this property, we know from the inverse Fourier transform that

$$g(t) = \int_{-\infty}^{\infty} G(f) \exp(j2\pi ft) df$$

Taking the complex conjugates of both sides yields

$$g^*(t) = \int_{-\infty}^{\infty} G^*(f) \exp(-j2\pi ft) df$$

Next, replacing  $f$  with  $-f$  gives

$$\begin{aligned} g^*(t) &= - \int_{\infty}^{-\infty} G^*(-f) \exp(j2\pi ft) df \\ &= \int_{-\infty}^{\infty} G^*(-f) \exp(j2\pi ft) df \end{aligned}$$

That is,  $g^*(t)$  is the inverse Fourier transform of  $G^*(-f)$ , which is the desired result.

As a corollary to the conjugation rule of Eq. (2.22), we may state that if  $g(t) \rightleftharpoons G(f)$ , then

$$g^*(-t) \rightleftharpoons G^*(f) \quad (2.23)$$

This result follows directly from Eq. (2.22) by applying the reflection rule described in Eq. (2.21).

**PROPERTY 4 Duality** If  $g(t) \rightleftharpoons G(f)$ , then

$$G(t) \rightleftharpoons g(-f) \quad (2.24)$$

This property follows from the relation defining the inverse Fourier transform of Eq. (2.21) by first replacing  $t$  with  $-t$ , thereby writing it in the form

$$g(-t) = \int_{-\infty}^{\infty} G(f) \exp(-j2\pi ft) df$$

Finally, interchanging  $t$  and  $f$  (i.e., replacing  $t$  with  $f$  in the left-hand side of the equation and  $f$  with  $t$  in the right-hand side), we get

$$g(-f) = \int_{-\infty}^{\infty} G(t) \exp(-j2\pi ft) dt$$

which is the expanded part of Eq. (2.24) in going from the time domain to the frequency domain.

#### EXAMPLE 2.4 Sinc Pulse

Consider a signal  $g(t)$  in the form of a sinc function, as shown by

$$g(t) = A \operatorname{sinc}(2Wt)$$

To evaluate the Fourier transform of this function, we apply the duality and dilation properties to the Fourier-transform pair of Eq. (2.10). Then, recognizing that the rectangular function is an even function of time, we obtain the result

$$A \operatorname{sinc}(2Wt) \rightleftharpoons \frac{A}{2W} \operatorname{rect}\left(\frac{f}{2W}\right) \quad (2.25)$$

which is illustrated in Fig. 2.8. We thus see that the Fourier transform of a sinc pulse is zero for  $|f| > W$ . Note also that the sinc pulse itself is only asymptotically limited in time in the sense that it approaches zero as time  $t$  approaches infinity; it is this asymptotic characteristic that makes the sinc function into an energy signal and therefore Fourier transformable.

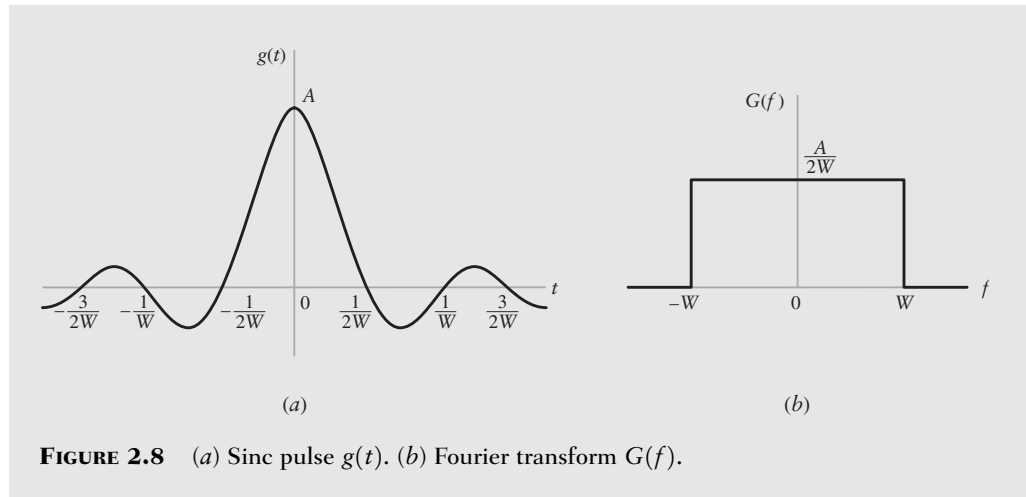


**FIGURE 2.8** (a) Sinc pulse  $g(t)$ . (b) Fourier transform  $G(f)$ .

**PROPERTY 5 Time Shifting** If  $g(t) \iff G(f)$ , then

$$g(t - t_0) \iff G(f) \exp(-j2\pi f t_0) \quad (2.26)$$

where  $t_0$  is a real constant time shift.

To prove this property, we take the Fourier transform of  $g(t - t_0)$  and then set  $\tau = (t - t_0)$  or, equivalently,  $t = \tau + t_0$ . We thus obtain

$$\begin{aligned} F[g(t - t_0)] &= \exp(-j2\pi f t_0) \int_{-\infty}^{\infty} g(\tau) \exp(-j2\pi \tau) d\tau \\ &= \exp(-j2\pi f t_0) G(f) \end{aligned}$$

The time-shifting property states that if a function  $g(t)$  is shifted along the time axis by an amount  $t_0$ , the effect is equivalent to multiplying its Fourier transform  $G(f)$  by the factor  $\exp(-j2\pi f t_0)$ . This means that the amplitude of  $G(f)$  is unaffected by the time shift, but its phase is changed by the linear factor  $-2\pi f t_0$ , which varies linearly with frequency  $f$ .

**PROPERTY 6 Frequency Shifting** If  $g(t) \iff G(f)$ , then

$$\exp(j2\pi f_c t) g(t) \iff G(f - f_c) \quad (2.27)$$

where  $f_c$  is a real constant frequency.

This property follows from the fact that

$$\begin{aligned} F[\exp(j2\pi f_c t) g(t)] &= \int_{-\infty}^{\infty} g(t) \exp[-j2\pi t(f - f_c)] dt \\ &= G(f - f_c) \end{aligned}$$

That is, multiplication of a function  $g(t)$  by the factor  $\exp(j2\pi f_c t)$  is equivalent to shifting its Fourier transform  $G(f)$  along the frequency axis by the amount  $f_c$ . This property is a special case of the *modulation theorem* discussed later under Property 11; basically, a shift of the range of frequencies in a signal is accomplished by using the process of modulation. Note the duality between the time-shifting and frequency-shifting operations described in Eqs. (2.26) and (2.27).

**EXAMPLE 2.5** Radio Frequency (RF) Pulse

Consider the pulse signal  $g(t)$  shown in Fig. 2.9(a), which consists of a sinusoidal wave of unit amplitude and frequency  $f_c$ , extending in duration from  $t = -T/2$  to  $t = T/2$ . This signal is sometimes referred to as an *RF pulse* when the frequency  $f_c$  falls in the radio-frequency band. The signal  $g(t)$  of Fig. 2.9(a) may be expressed mathematically as follows:

$$g(t) = \text{rect}\left(\frac{t}{T}\right) \cos(2\pi f_c t) \quad (2.28)$$

To find the Fourier transform of the RF signal, we first use *Euler's formula* to write

$$\cos(2\pi f_c t) = \frac{1}{2}[\exp(j2\pi f_c t) + \exp(-j2\pi f_c t)]$$

Therefore, applying the frequency-shifting property to the Fourier-transform pair of Eq. (2.10), and then invoking the linearity property of the Fourier transform, we get the desired result

$$\text{rect}\left(\frac{t}{T}\right) \cos(2\pi f_c t) \iff \frac{T}{2} \{\text{sinc}[T(f - f_c)] + \text{sinc}[T(f + f_c)]\} \quad (2.29)$$

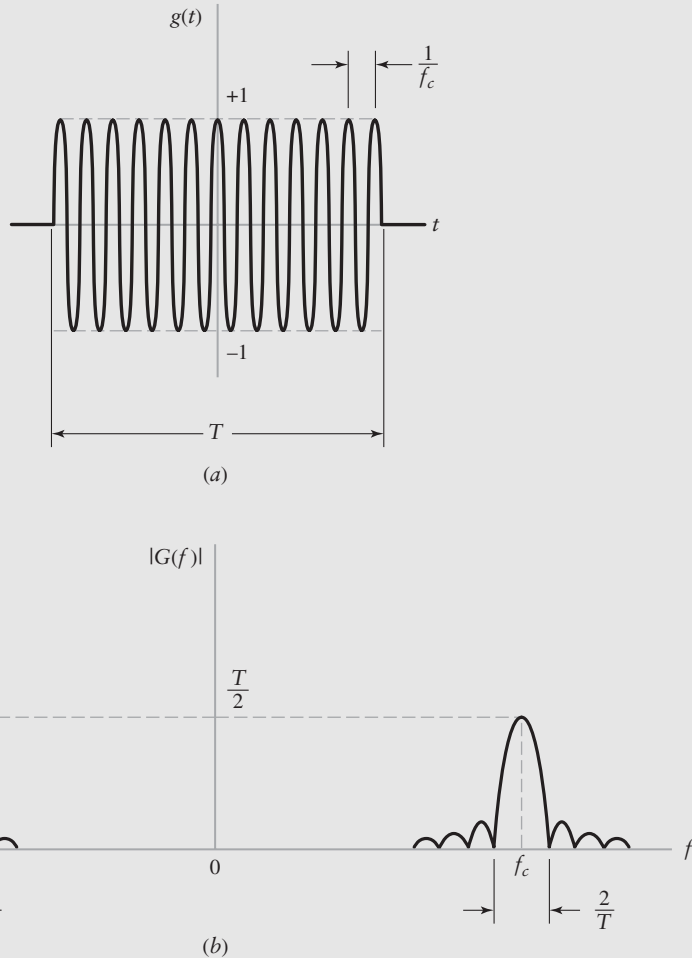


**FIGURE 2.9** (a) RF pulse of unit amplitude and duration  $T$ . (b) Amplitude spectrum.

In the special case of  $f_c T \gg 1$ —that is, the frequency  $f_c$  is large compared to the reciprocal of the pulse duration  $T$ —we may use the approximate result

$$G(f) \approx \begin{cases} \frac{T}{2} \operatorname{sinc}[T(f - f_c)], & f > 0 \\ 0, & f = 0 \\ \frac{T}{2} \operatorname{sinc}[T(f + f_c)], & f < 0 \end{cases} \quad (2.30)$$

Under the condition  $f_c T \gg 1$ , the amplitude spectrum of the RF pulse is shown in Fig. 2.9(b). This diagram, in relation to Fig. 2.2(b), clearly illustrates the frequency-shifting property of the Fourier transform.

**PROPERTY 7 Area Under  $g(t)$**  If  $g(t) \rightleftharpoons G(f)$ , then

$$\int_{-\infty}^{\infty} g(t) dt = G(0) \quad (2.31)$$

That is, the area under a function  $g(t)$  is equal to the value of its Fourier transform  $G(f)$  at  $f = 0$ .

This result is obtained simply by putting  $f = 0$  in Eq. (2.1) defining the Fourier transform of the function  $g(t)$ .

► **Drill Problem 2.3** Suppose  $g(t)$  is real valued with a complex-valued Fourier transform  $G(f)$ . Explain how the rule of Eq. (2.31) can be satisfied by such a signal. ◀

**PROPERTY 8 Area Under  $G(f)$**  If  $g(t) \rightleftharpoons G(f)$ , then

$$g(0) = \int_{-\infty}^{\infty} G(f) df \quad (2.32)$$

That is, the value of a function  $g(t)$  at  $t = 0$  is equal to the area under its Fourier transform  $G(f)$ .

The result is obtained simply by putting  $t = 0$  in Eq. (2.2) defining the inverse Fourier transform of  $G(f)$ .

► **Drill Problem 2.4** Continuing with Problem 2.3, explain how the rule of Eq. (2.32) can be satisfied by the signal  $g(t)$  described therein. ◀

**PROPERTY 9 Differentiation in the Time Domain** Let  $g(t) \rightleftharpoons G(f)$  and assume that the first derivative of  $g(t)$  with respect to time  $t$  is Fourier transformable. Then

$$\frac{d}{dt} g(t) \rightleftharpoons j2\pi f G(f) \quad (2.33)$$

That is, differentiation of a time function  $g(t)$  has the effect of multiplying its Fourier transform  $G(f)$  by the purely imaginary factor  $j2\pi f$ .

This result is obtained simply in two steps. In step 1, we take the first derivative of both sides of the integral in Eq. (2.2) defining the inverse Fourier transform of  $G(f)$ . In step 2, we interchange the operations of integration and differentiation.

We may generalize Eq. (2.33) for higher order derivatives of the time function  $g(t)$  as follows:

$$\frac{d^n}{dt^n}g(t) \iff (j2\pi f)^n G(f) \quad (2.34)$$

which includes Eq. (2.33) as a special case. Equation (2.34) assumes that the Fourier transform of the higher order derivative of  $g(t)$  exists.

#### EXAMPLE 2.6 Unit Gaussian Pulse

Typically, a pulse signal  $g(t)$  and its Fourier transform  $G(f)$  have different mathematical forms. This observation is illustrated by the Fourier-transform pairs studied in Examples 2.1 through 2.5. In this example, we consider an exception to this observation. In particular, we use the differentiation property of the Fourier transform to derive the particular form of a *pulse signal that has the same mathematical form as its own Fourier transform*.

Let  $g(t)$  denote the pulse signal expressed as a function of time  $t$ , and  $G(f)$  denote its Fourier transform. Differentiating the Fourier transform formula of Eq. (2.1) with respect to frequency  $f$ , we may write

$$-j2\pi t g(t) \iff \frac{d}{df}G(f)$$

or, equivalently,

$$2\pi t g(t) \iff j \frac{d}{df}G(f) \quad (2.35)$$

Suppose we now impose the following condition on the left-hand sides of Eqs. (2.33) and (2.35):

$$\frac{d}{dt}g(t) = -2\pi t g(t) \quad (2.36)$$

Then in a corresponding way, it follows that the right-hand sides of these two equations must (after cancelling the common multiplying factor  $j$ ) satisfy the condition

$$\frac{d}{df}G(f) = -2\pi f G(f) \quad (2.37)$$

Equations (2.36) and (2.37) show that the pulse signal  $g(t)$  and its Fourier transform  $G(f)$  have exactly the same mathematical form. In other words, provided that the pulse signal  $g(t)$  satisfies the differential equation (2.36), then  $G(f) = g(f)$ , where  $g(f)$  is obtained from  $g(t)$  by substituting  $f$  for  $t$ . Solving Eq. (2.36) for  $g(t)$ , we obtain

$$g(t) = \exp(-\pi t^2) \quad (2.38)$$

The pulse defined by Eq. (2.38) is called a *Gaussian pulse*, the name being derived from the similarity of the function to the Gaussian probability density function of probability theory (see Chapter 8). It is shown plotted in Fig. 2.10. By applying Eq. (2.31), we find that the area under

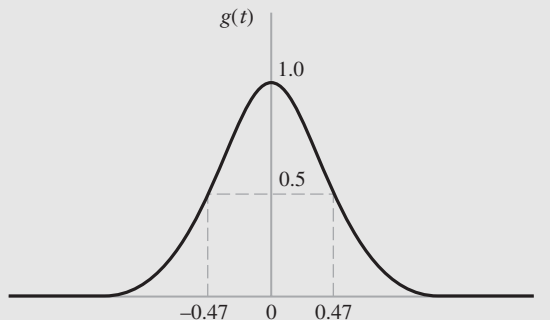


**FIGURE 2.10**  
Gaussian pulse.

this Gaussian pulse is unity, as shown by

$$\int_{-\infty}^{\infty} \exp(-\pi t^2) dt = 1 \quad (2.39)$$

When the central ordinate and the area under the curve of a pulse are both unity, as in Eqs. (2.38) and (2.39), we say that the Gaussian pulse is a *unit pulse*. We conclude therefore that the unit Gaussian pulse is its own Fourier transform, as shown by

$$\exp(-\pi t^2) \iff \exp(-\pi f^2) \quad (2.40)$$

**PROPERTY 10 Integration in the Time Domain** *Let  $g(t) \iff G(f)$ . Then provided that  $G(0) = 0$ , we have*

$$\int_{-\infty}^t g(\tau) d\tau \iff \frac{1}{j2\pi f} G(f) \quad (2.41)$$

*That is, integration of a time function  $g(t)$  has the effect of dividing its Fourier transform  $G(f)$  by the factor  $j2\pi f$ , provided that  $G(0)$  is zero.*

This property is verified by expressing  $g(t)$  as

$$g(t) = \frac{d}{dt} \left[ \int_{-\infty}^t g(\tau) d\tau \right]$$

and then applying the time-differentiation property of the Fourier transform to obtain

$$G(f) = (j2\pi f) \left\{ F \left[ \int_{-\infty}^t g(\tau) d\tau \right] \right\}$$

from which Eq. (2.41) follows immediately.

It is a straightforward matter to generalize Eq. (2.41) to multiple integration; however, the notation becomes rather cumbersome.

Equation (2.41) assumes that  $G(0)$ —that is, the area under  $g(t)$ —is zero. The more general case pertaining to  $G(0) \neq 0$  is deferred to Section 2.4.

### EXAMPLE 2.7 Triangular Pulse

Consider the *doublet pulse*  $g_1(t)$  shown in Fig. 2.11(a). By integrating this pulse with respect to time, we obtain the *triangular pulse*  $g_2(t)$  shown in Fig. 2.11(b). We note that the doublet pulse  $g_1(t)$  consists of two rectangular pulses: one of amplitude  $A$ , defined for the interval  $-T \leq t \leq 0$ ; and the other of amplitude  $-A$ , defined for the interval  $0 \leq t \leq T$ . Applying the time-shifting property of the Fourier transform to Eq. (2.10), we find that the Fourier transforms of these two rectangular pulses are equal to  $AT \operatorname{sinc}(fT) \exp(j\pi fT)$  and  $-AT \operatorname{sinc}(fT) \exp(-j\pi fT)$ , respectively. Hence, invoking the linearity property of the Fourier transform, we find that the Fourier transform  $G_1(f)$  of the doublet pulse  $g_1(t)$  of Fig. 2.11(a) is given by

$$\begin{aligned} G_1(f) &= AT \operatorname{sinc}(fT) [\exp(j\pi fT) - \exp(-j\pi fT)] \\ &= 2jAT \operatorname{sinc}(fT) \sin(\pi fT) \end{aligned} \quad (2.42)$$

We further note from Eq. (2.42) that  $G_1(0)$  is zero. Hence, using Eqs. (2.41) and (2.42), we find that the Fourier transform  $G_2(f)$  of the triangular pulse  $g_2(t)$  of Fig. 2.11(b) is given by

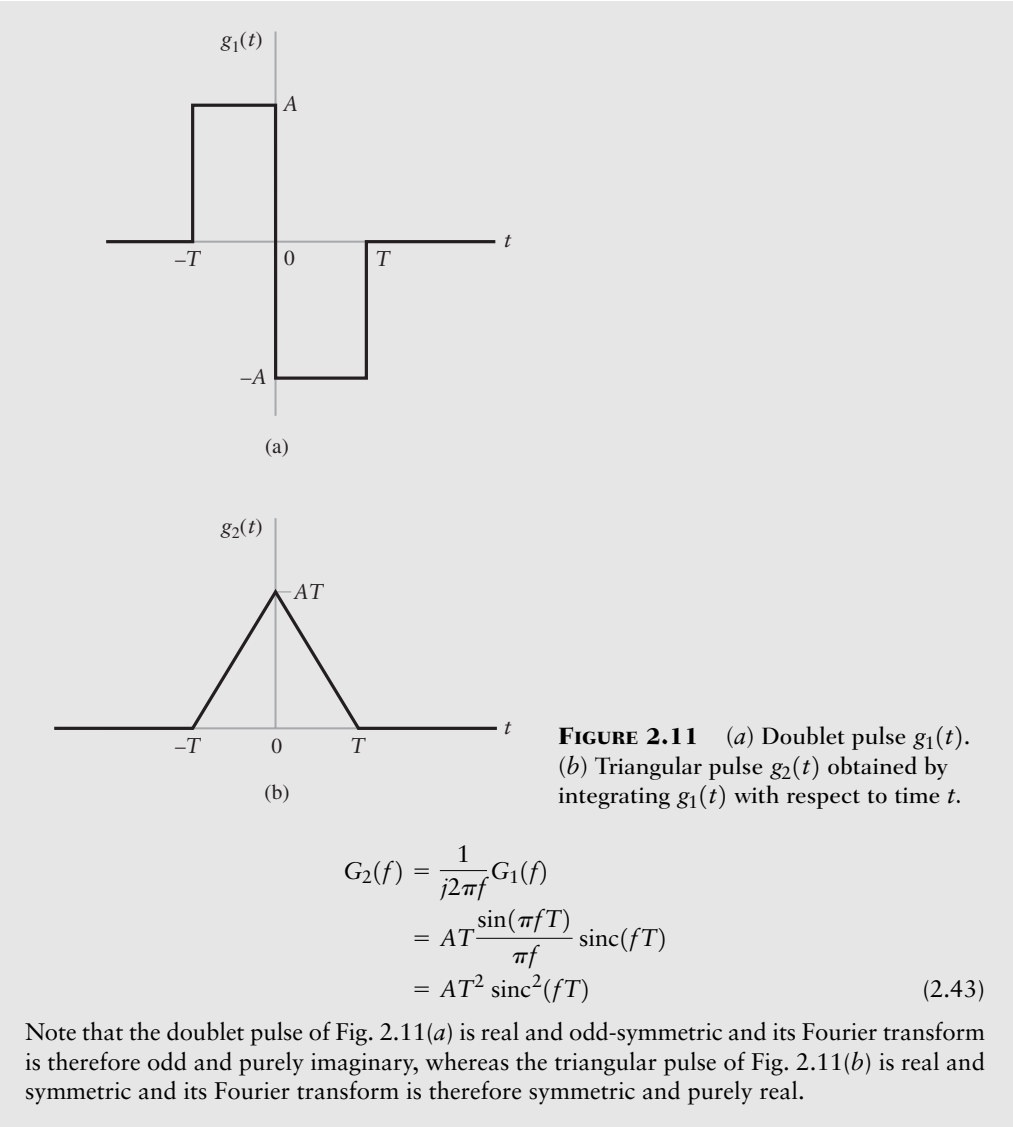


**FIGURE 2.11** (a) Doublet pulse  $g_1(t)$ .  
(b) Triangular pulse  $g_2(t)$  obtained by integrating  $g_1(t)$  with respect to time  $t$ .

$$\begin{aligned} G_2(f) &= \frac{1}{j2\pi f} G_1(f) \\ &= AT \frac{\sin(\pi f T)}{\pi f} \operatorname{sinc}(fT) \\ &= AT^2 \operatorname{sinc}^2(fT) \end{aligned} \quad (2.43)$$

Note that the doublet pulse of Fig. 2.11(a) is real and odd-symmetric and its Fourier transform is therefore odd and purely imaginary, whereas the triangular pulse of Fig. 2.11(b) is real and symmetric and its Fourier transform is therefore symmetric and purely real.

#### EXAMPLE 2.8 Real and Imaginary Parts of a Time Function

Thus far in the chapter, we have discussed the Fourier representation of various signals, some being purely real, others being purely imaginary, yet others being complex valued with real and imaginary parts. It is therefore apropos that at this stage in the Fourier analysis of signals, we use this example to develop a number of general formulas pertaining to complex signals and their spectra.

Expressing a complex-valued function  $g(t)$  in terms of its real and imaginary parts, we may write

$$g(t) = \operatorname{Re}[g(t)] + j\operatorname{Im}[g(t)] \quad (2.44)$$

where **Re** denotes “the real part of” and **Im** denotes the “imaginary part of.” The complex conjugate of  $g(t)$  is defined by

$$g^*(t) = \operatorname{Re}[g(t)] - j\operatorname{Im}[g(t)] \quad (2.45)$$

Adding Eqs. (2.44) and (2.45) gives

$$\text{Re}[g(t)] = \frac{1}{2}[g(t) + g^*(t)] \quad (2.46)$$

and subtracting them yields

$$\text{Im}[g(t)] = \frac{1}{2}[g(t) - g^*(t)] \quad (2.47)$$

Therefore, applying the conjugation rule of Eq. (2.22), we obtain the following two Fourier-transform pairs:

$$\left. \begin{aligned} \text{Re}[g(t)] &\iff \frac{1}{2}[G(f) + G^*(-f)] \\ \text{Im}[g(t)] &\iff \frac{1}{2}[G(f) - G^*(-f)] \end{aligned} \right\} \quad (2.48)$$

From the second line of Eq. (2.48), it is apparent that in the case of a real-valued time function  $g(t)$ , we have  $G(f) = G^*(-f)$ ; that is, the Fourier transform  $G(f)$  exhibits conjugate symmetry, confirming a result that we stated previously in Section 2.2.

**PROPERTY 11 Modulation Theorem** *Let  $g_1(t) \iff G_1(f)$  and  $g_2(t) \iff G_2(f)$ . Then*

$$g_1(t)g_2(t) \iff \int_{-\infty}^{\infty} G_1(\lambda)G_2(f - \lambda) d\lambda \quad (2.49)$$

To prove this property, we first denote the Fourier transform of the product  $g_1(t)g_2(t)$  by  $G_{12}(f)$ , so that we may write

$$g_1(t)g_2(t) \iff G_{12}(f)$$

where

$$G_{12}(f) = \int_{-\infty}^{\infty} g_1(t)g_2(t) \exp(-j2\pi ft) dt$$

For  $g_2(t)$ , we next substitute the inverse Fourier transform

$$g_2(t) = \int_{-\infty}^{\infty} G_2(f') \exp(j2\pi f' t) df'$$

in the integral defining  $G_{12}(f)$  to obtain

$$G_{12}(f) = \int_{-\infty}^{\infty} \int_{-\infty}^{\infty} g_1(t)G_2(f') \exp[-j2\pi(f - f')t] df' dt$$

Define  $\lambda = f - f'$ . Then, eliminating the variable  $f'$  and interchanging the order of integration, we obtain (after rearranging terms)

$$G_{12}(f) = \int_{-\infty}^{\infty} G_2(f - \lambda) \left[ \int_{-\infty}^{\infty} g_1(t) \exp(-j2\pi\lambda t) dt \right] d\lambda$$

assuming that  $f$  is fixed. The inner integral (inside the square brackets) is recognized simply as  $G_1(\lambda)$ ; we may therefore write

$$G_{12}(f) = \int_{-\infty}^{\infty} G_1(\lambda)G_2(f - \lambda) d\lambda$$

which is the desired result. This integral is known as the *convolution integral* expressed in the frequency domain, and the function  $G_{12}(f)$  is referred to as the *convolution* of  $G_1(f)$  and  $G_2(f)$ . We conclude that *the multiplication of two signals in the time domain is transformed into the convolution of their individual Fourier transforms in the frequency domain*. This property is also known as the *modulation theorem*. We have more to say on the practical implications of this property in subsequent chapters.

In a discussion of convolution, the following shorthand notation is frequently used:

$$G_{12}(f) = G_1(f) \star G_2(f)$$

Accordingly, we may reformulate Eq. (2.49) in the following symbolic form:

$$g_1(t)g_2(t) \rightleftharpoons G_1(f) \star G_2(f) \quad (2.50)$$

where the symbol  $\star$  denotes convolution. Note that convolution is *commutative*; that is,

$$G_1(f) \star G_2(f) = G_2(f) \star G_1(f)$$

which follows directly from Eq. (2.50).

**PROPERTY 12 Convolution Theorem** *Let  $g_1(t) \rightleftharpoons G_1(f)$  and  $g_2(t) \rightleftharpoons G_2(f)$ . Then*

$$\int_{-\infty}^{\infty} g_1(\tau)g_2(t - \tau) d\tau \rightleftharpoons G_1(f)G_2(f) \quad (2.51)$$

Equation (2.51) follows directly by combining Property 4 (duality) and Property 11 (modulation). We may thus state that *the convolution of two signals in the time domain is transformed into the multiplication of their individual Fourier transforms in the frequency domain*. This property is known as the *convolution theorem*. Its use permits us to exchange a convolution operation in the time domain for a multiplication of two Fourier transforms, an operation that is ordinarily easier to manipulate. We have more to say on convolution later in the chapter when the issue of filtering is discussed.

Using the shorthand notation for convolution, we may rewrite Eq. (2.51) in the simple form

$$g_1(t) \star g_2(t) \rightleftharpoons G_1(f)G_2(f) \quad (2.52)$$

Note that Properties 11 and 12, described by Eqs. (2.49) and (2.51), respectively, are the dual of each other.

► **Drill Problem 2.5** Develop the detailed steps that show that the modulation and convolution theorems are indeed the dual of each other. ◀

**PROPERTY 13 Correlation Theorem** *Let  $g_1(t) \rightleftharpoons G_1(f)$  and  $g_2(t) \rightleftharpoons G_2(f)$ . Then, assuming that  $g_1(t)$  and  $g_2(t)$  are complex valued,*

$$\int_{-\infty}^{\infty} g_1(t)g_2^*(t - \tau) dt \rightleftharpoons G_1(f)G_2^*(f) \quad (2.53)$$

where  $G_2^*(f)$  is the complex conjugate of  $G_2(f)$ , and  $\tau$  is the time variable involved in defining the inverse Fourier transform of the product  $G_1(f)G_2^*(f)$ .

To prove Eq. (2.53), we begin by reformulating the convolution integral with the roles of the time variables  $t$  and  $\tau$  interchanged, in which case we may simply rewrite Eq. (2.51) as

$$\int_{-\infty}^{\infty} g_1(t)g_2(\tau - t) dt \iff G_1(f)G_2(f) \quad (2.54)$$

As already pointed out in the statement of Property 13, the inverse Fourier transform of the product term  $G_1(f)G_2(f)$  has  $\tau$  as its time variable; that is,  $\exp(j2\pi f\tau)$  is its kernel. With the formula of Eq. (2.54) at hand, Eq. (2.53) follows directly by combining reflection rule (special case of the dilation property) and conjugation rule.

The integral on the left-hand side of Eq. (2.53) defines a measure of the *similarity* that may exist between a pair of complex-valued signals. This measure is called *correlation*, on which we have more to say later in the chapter.

► **Drill Problem 2.6** Develop the detailed steps involved in deriving Eq. (2.53), starting from Eq. (2.51). ◀

► **Drill Problem 2.7** Prove the following properties of the convolution process:

- (a) The commutative property:  $g_1(t) \star g_2(t) = g_2(t) \star g_1(t)$
- (b) The associative property:  $g_1(t) \star [g_2(t) \star g_3(t)] = [g_1(t) \star g_2(t)] \star g_3(t)$
- (c) The distributive property:  $g_1(t) \star [g_2(t) + g_3(t)] = g_1(t) \star g_2(t) + g_1(t) \star g_3(t)$

**PROPERTY 14 Rayleigh's Energy Theorem** Let  $g(t) \iff G(f)$ . Then

$$\int_{-\infty}^{\infty} |g(t)|^2 dt = \int_{-\infty}^{\infty} |G(f)|^2 df \quad (2.55)$$

To prove Eq. (2.55), we set  $g_1(t) = g_2(t) = g(t)$  in Eq. (2.53), in which case the correlation theorem reduces to

$$\int_{-\infty}^{\infty} g(t)g^*(t - \tau) dt \iff G(f)G^*(f) = |G(f)|^2$$

In expanded form, we may write

$$\int_{-\infty}^{\infty} g(t)g^*(t - \tau) dt = \int_{-\infty}^{\infty} |G(f)|^2 \exp(j2\pi f\tau) df \quad (2.56)$$

Finally, putting  $\tau = 0$  in Eq. (2.56) and recognizing that  $g(t)g^*(t) = |g(t)|^2$ , we get the desired result.

Equation (2.55), known as *Rayleigh's energy theorem*, states that the total energy of a Fourier-transformable signal equals the total area under the curve of squared amplitude spectrum of this signal. Determination of the energy is often simplified by invoking the Rayleigh energy theorem, as illustrated in the following example.

#### EXAMPLE 2.9 Sinc Pulse (continued)

Consider again the sinc pulse  $A \text{ sinc}(2Wt)$ . The energy of this pulse equals

$$E = A^2 \int_{-\infty}^{\infty} \text{sinc}^2(2Wt) dt$$

The integral in the right-hand side of this equation is rather difficult to evaluate. However, we note from Example 2.4 that the Fourier transform of the sinc pulse  $A \operatorname{sinc}(2Wt)$  is equal to  $(A/2W) \operatorname{rect}(f/2W)$ ; hence, applying Rayleigh's energy theorem to the problem at hand, we readily obtain the desired result:

$$\begin{aligned} E &= \left(\frac{A}{2W}\right)^2 \int_{-\infty}^{\infty} \operatorname{rect}^2\left(\frac{f}{2W}\right) df \\ &= \left(\frac{A}{2W}\right)^2 \int_{-W}^{W} df \\ &= \frac{A^2}{2W} \end{aligned} \quad (2.57)$$

This example clearly illustrates the usefulness of Rayleigh's energy theorem.

► **Drill Problem 2.8** Considering the pulse function  $\operatorname{sinc}(t)$ , show that

$$\int_{-\infty}^{\infty} \operatorname{sinc}^2(t) dt = 1.$$



## 2.3 The Inverse Relationship Between Time and Frequency

The properties of the Fourier transform discussed in Section 2.2 show that the time-domain and frequency-domain descriptions of a signal are *inversely* related to each other. In particular, we may make two important statements:

1. If the time-domain description of a signal is changed, the frequency-domain description of the signal is changed in an *inverse* manner, and vice versa. This inverse relationship prevents arbitrary specifications of a signal in both domains. In other words, *we may specify an arbitrary function of time or an arbitrary spectrum, but we cannot specify both of them together.*
2. If a signal is strictly limited in frequency, the time-domain description of the signal will trail on indefinitely, even though its amplitude may assume a progressively smaller value. We say a signal is *strictly limited in frequency* or *strictly band limited* if its Fourier transform is exactly zero outside a finite band of frequencies. The sinc pulse is an example of a strictly band-limited signal, as illustrated in Fig. 2.8. This figure also shows that the sinc pulse is only *asymptotically limited in time*. In an inverse manner, if a signal is *strictly limited in time* (i.e., the signal is exactly zero outside a finite time interval), then the spectrum of the signal is infinite in extent, even though the amplitude spectrum may assume a progressively smaller value. This behavior is exemplified by both the rectangular pulse (described in Fig. 2.2) and the triangular pulse (described in Fig. 2.11(b)). Accordingly, we may state that *a signal cannot be strictly limited in both time and frequency.*

### ■ BANDWIDTH

The *bandwidth* of a signal provides a measure of the *extent of the significant spectral content of the signal for positive frequencies*. When the signal is strictly band limited, the bandwidth is well defined. For example, the sinc pulse described in Fig. 2.8(a) has a bandwidth

equal to  $W$ . However, when the signal is not strictly band limited, which is generally the case, we encounter difficulty in defining the bandwidth of the signal. The difficulty arises because the meaning of the word “significant” attached to the spectral content of the signal is mathematically imprecise. Consequently, there is no universally accepted definition of bandwidth.

Nevertheless, there are some commonly used definitions for bandwidth. In this section, we consider three such definitions; the formulation of each definition depends on whether the signal is low-pass or band-pass. A signal is said to be *low-pass* if its significant spectral content is centered around the origin  $f = 0$ . A signal is said to be *band-pass* if its significant spectral content is centered around  $\pm f_c$ , where  $f_c$  is a constant frequency.

When the spectrum of a signal is symmetric with a *main lobe* bounded by well-defined *nulls* (i.e., frequencies at which the spectrum is zero), we may use the main lobe as the basis for defining the bandwidth of the signal. The rationale for doing so is that the main spectral lobe contains the significant portion of the signal energy. If the signal is low-pass, the bandwidth is defined as one half the total width of the main spectral lobe, since only one half of this lobe lies inside the positive frequency region. For example, a rectangular pulse of duration  $T$  seconds has a main spectral lobe of total width ( $2/T$ ) hertz centered at the origin, as depicted in Fig. 2.2(b). Accordingly, we may define the bandwidth of this rectangular pulse as ( $1/T$ ) hertz. If, on the other hand, the signal is band-pass with main spectral lobes centered around  $\pm f_c$ , where  $f_c$  is large, the bandwidth is defined as the width of the main lobe for positive frequencies. This definition of bandwidth is called the *null-to-null bandwidth*. For example, an RF pulse of duration  $T$  seconds and frequency  $f_c$  has main spectral lobes of width ( $2/T$ ) hertz centered around  $\pm f_c$ , as depicted in Fig. 2.9(b). Hence, we may define the null-to-null bandwidth of this RF pulse as ( $2/T$ ) hertz. On the basis of the definitions presented here, we may state that shifting the spectral content of a low-pass signal by a sufficiently large frequency has the effect of doubling the bandwidth of the signal. Such a frequency translation is attained by using the process of modulation, which is discussed in detail in Chapter 3.

Another popular definition of bandwidth is the *3-dB bandwidth*. Specifically, if the signal is low-pass, the 3-dB bandwidth is defined as the separation between zero frequency, where the amplitude spectrum attains its peak value, and the *positive frequency* at which the amplitude spectrum drops to  $1/\sqrt{2}$  of its peak value. For example, the decaying exponential and rising exponential pulses defined in Fig. 2.4 have a 3-dB bandwidth of  $(a/2\pi)$  hertz. If, on the other hand, the signal is band-pass, centered at  $\pm f_c$ , the 3-dB bandwidth is defined as the separation (along the positive frequency axis) between the two frequencies at which the amplitude spectrum of the signal drops to  $1/\sqrt{2}$  of the peak value at  $f_c$ . The 3-dB bandwidth has an advantage in that it can be read directly from a plot of the amplitude spectrum. However, it has a disadvantage in that it may be misleading if the amplitude spectrum has slowly decreasing tails.

Yet another measure for the bandwidth of a signal is the *root mean-square (rms) bandwidth*, defined as the square root of the second moment of a properly normalized form of the squared amplitude spectrum of the signal about a suitably chosen point. We assume that the signal is low-pass, so that the second moment may be taken about the origin. As for the normalized form of the squared amplitude spectrum, we use the nonnegative function  $|G(f)|^2 / \int_{-\infty}^{\infty} |G(f)|^2 df$ , in which the denominator applies the correct normalization in the sense that the integrated value of this ratio over the entire frequency axis is unity. We may thus formally define the rms bandwidth of a low-pass signal  $g(t)$  with Fourier transform  $G(f)$  as follows:

$$W_{\text{rms}} = \left( \frac{\int_{-\infty}^{\infty} f^2 |G(f)|^2 df}{\int_{-\infty}^{\infty} |G(f)|^2 df} \right)^{1/2} \quad (2.58)$$

An attractive feature of the rms bandwidth  $W_{\text{rms}}$  is that it lends itself more readily to mathematical evaluation than the other two definitions of bandwidth, although it is not as easily measured in the laboratory.

### ■ TIME-BANDWIDTH PRODUCT

For any family of pulse signals that differ by a time-scaling factor, the product of the signal's duration and its bandwidth is always a constant, as shown by

$$(\text{duration}) \times (\text{bandwidth}) = \text{constant}$$

The product is called the *time-bandwidth product* or *bandwidth-duration product*. The constancy of the time-bandwidth product is another manifestation of the inverse relationship that exists between the time-domain and frequency-domain descriptions of a signal. In particular, if the duration of a pulse signal is decreased by compressing the time scale by a factor  $a$ , say, the frequency scale of the signal's spectrum, and therefore the bandwidth of the signal, is expanded by the same factor  $a$ , by virtue of Property 2 (dilation), and the time-bandwidth product of the signal is thereby maintained constant. For example, a rectangular pulse of duration  $T$  seconds has a bandwidth (defined on the basis of the positive-frequency part of the main lobe) equal to  $(1/T)$  hertz, making the time-bandwidth product of the pulse equal unity. The important point to note here is that whatever definition we use for the bandwidth of a signal, the time-bandwidth product remains constant over certain classes of pulse signals. The choice of a particular definition for bandwidth merely changes the value of the constant.

To be more specific, consider the rms bandwidth defined in Eq. (2.58). The corresponding definition for the *rms duration* of the signal  $g(t)$  is

$$T_{\text{rms}} = \left( \frac{\int_{-\infty}^{\infty} t^2 |g(t)|^2 dt}{\int_{-\infty}^{\infty} |g(t)|^2 dt} \right)^{1/2} \quad (2.59)$$

where it is assumed that the signal  $g(t)$  is centered around the origin. It may be shown that using the rms definitions of Eqs. (2.58) and (2.59), the time-bandwidth product has the following form:

$$T_{\text{rms}} W_{\text{rms}} \geq \frac{1}{4\pi} \quad (2.60)$$

where the constant is  $(1/4\pi)$ . It may also be shown that the Gaussian pulse satisfies this condition with the equality sign. For the details of these calculations, the reader is referred to Problem 2.51.

## 2.4 Dirac Delta Function

Strictly speaking, the theory of the Fourier transform, as described in Sections 2.2 and 2.3, is applicable only to time functions that satisfy the Dirichlet conditions. Such functions include energy signals—that is, signals for which the condition

$$\int_{-\infty}^{\infty} |g(t)|^2 dt < \infty$$

holds. However, it would be highly desirable to extend the theory in two ways:

1. To combine the theory of Fourier series and Fourier transform into a unified framework, so that the Fourier series may be treated as a special case of the Fourier transform. (A review of the Fourier series is presented in Appendix 2.)
2. To expand applicability of the Fourier transform to include power signals—that is, signals for which the condition

$$\lim_{T \rightarrow \infty} \frac{1}{2T} \int_{-T}^{T} |g(t)|^2 dt < \infty$$

holds.

It turns out that both of these objectives are met through the “proper use” of the *Dirac delta function* or *unit impulse*.

The Dirac delta function, denoted by  $\delta(t)$ , is defined as having zero amplitude everywhere except at  $t = 0$ , where it is infinitely large in such a way that it contains unit area under its curve. Specifically,  $\delta(t)$  satisfies the pair of relations

$$\delta(t) = 0, \quad t \neq 0 \quad (2.61)$$

and

$$\int_{-\infty}^{\infty} \delta(t) dt = 1 \quad (2.62)$$

An implication of this pair of relations is that the delta function  $\delta(t)$  must be an even function of time  $t$ .

For the delta function to have meaning, however, it has to appear as a factor in the integrand of an integral with respect to time and then, strictly speaking, only when the other factor in the integrand is a continuous function of time. Let  $g(t)$  be such a function, and consider the product of  $g(t)$  and the time-shifted delta function  $\delta(t - t_0)$ . In light of the two defining equations (2.61) and (2.62), we may express the integral of the product  $g(t)\delta(t - t_0)$  with respect to time  $t$  as follows:

$$\int_{-\infty}^{\infty} g(t)\delta(t - t_0) dt = g(t_0) \quad (2.63)$$

The operation indicated on the left-hand side of this equation sifts out the value  $g(t_0)$  of the function  $g(t)$  at time  $t = t_0$ , where  $-\infty < t < \infty$ . Accordingly, Eq. (2.63) is referred to as the *sifting property* of the delta function. This property is sometimes used as the defining equation of a delta function; in effect, it incorporates Eqs. (2.61) and (2.62) into a single relation.

Noting that the delta function  $\delta(t)$  is an even function of  $t$ , we may rewrite Eq. (2.63) in a way that emphasizes its resemblance to the convolution integral, as shown by

$$\int_{-\infty}^{\infty} g(\tau)\delta(t - \tau) d\tau = g(t) \quad (2.64)$$

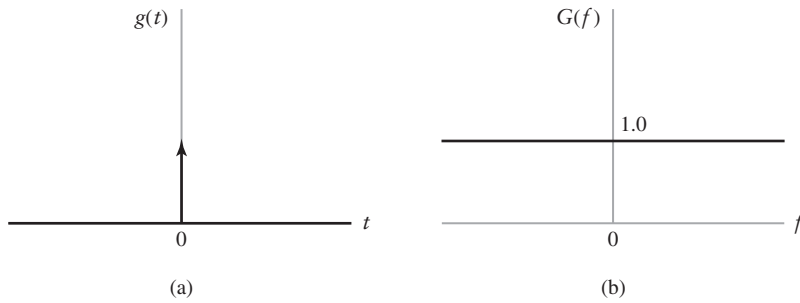


**FIGURE 2.12** (a) The Dirac delta function  $\delta(t)$ . (b) Spectrum of  $\delta(t)$ .

or, using the notation for convolution:

$$g(t) \star \delta(t) = g(t)$$

In words, the convolution of any time function  $g(t)$  with the delta function  $\delta(t)$  leaves that function completely unchanged. We refer to this statement as the *replication property* of the delta function.

By definition, the Fourier transform of the delta function is given by

$$\mathcal{F}[\delta(t)] = \int_{-\infty}^{\infty} \delta(t) \exp(-j2\pi ft) dt$$

Hence, using the sifting property of the delta function and noting that  $\exp(-j2\pi ft)$  is equal to unity at  $t = 0$ , we obtain

$$\mathcal{F}[\delta(t)] = 1$$

We thus have the Fourier-transform pair for the Dirac delta function:

$$\delta(t) \iff 1 \quad (2.65)$$

This relation states that the spectrum of the delta function  $\delta(t)$  extends uniformly over the entire frequency interval, as shown in Fig. 2.12.

It is important to realize that the Fourier-transform pair of Eq. (2.65) exists only in a limiting sense. The point is that no function in the ordinary sense has the two properties of Eqs. (2.61) and (2.62) or the equivalent sifting property of Eq. (2.63). However, we can imagine a sequence of functions that have progressively taller and thinner peaks at  $t = 0$ , with the area under the curve remaining equal to unity, whereas the value of the function tends to zero at every point except  $t = 0$ , where it tends to infinity. That is, we may view the delta function as *the limiting form of a pulse of unit area as the duration of the pulse approaches zero*. It is immaterial what sort of pulse shape is used.

In a rigorous sense, the Dirac delta function belongs to a special class of functions known as *generalized functions* or *distributions*. Indeed, in some situations its use requires that we exercise considerable care. Nevertheless, one beautiful aspect of the Dirac delta function lies precisely in the fact that a rather intuitive treatment of the function along the lines described herein often gives the correct answer.

#### EXAMPLE 2.10 The Delta Function as a Limiting Form of the Gaussian Pulse

Consider a Gaussian pulse of unit area, defined by

$$g(t) = \frac{1}{\tau} \exp\left(-\frac{\pi t^2}{\tau^2}\right) \quad (2.66)$$

where  $\tau$  is a variable parameter. The Gaussian function  $g(t)$  has two useful properties: (1) its derivatives are all continuous, and (2) it dies away more rapidly than any power of  $t$ . The delta function  $\delta(t)$  is obtained by taking the limit  $\tau \rightarrow 0$ . The Gaussian pulse then becomes infinitely narrow in duration and infinitely large in amplitude, yet its area remains finite and fixed at unity. Figure 2.13(a) illustrates the sequence of such pulses as the parameter  $\tau$  is permitted to decrease.

The Gaussian pulse  $g(t)$ , defined here, is the same as the unit Gaussian pulse  $\exp(-\pi t^2)$  derived in Example 2.6, except for the fact that it is now scaled in time by the factor  $\tau$  and scaled in amplitude by the factor  $1/\tau$ . Therefore, applying the linearity and dilation properties of the Fourier transform to the Fourier transform pair of Eq. (2.40), we find that the Fourier transform of the Gaussian pulse  $g(t)$  defined in Eq. (2.66) is also Gaussian, as shown by

$$G(f) = \exp(-\pi\tau^2 f^2)$$

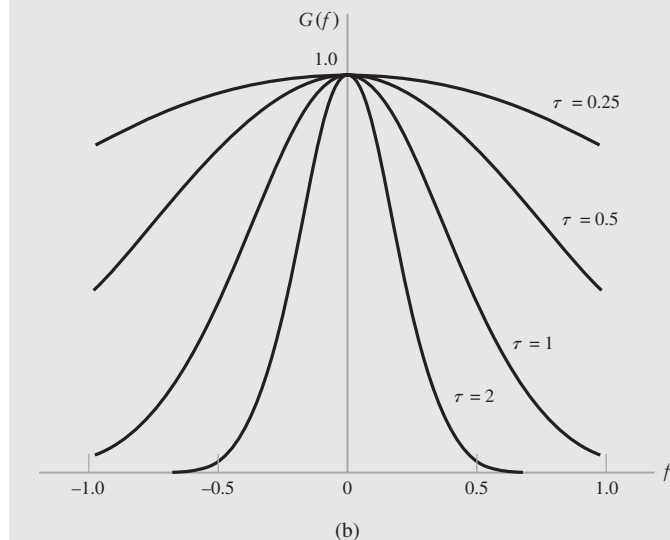
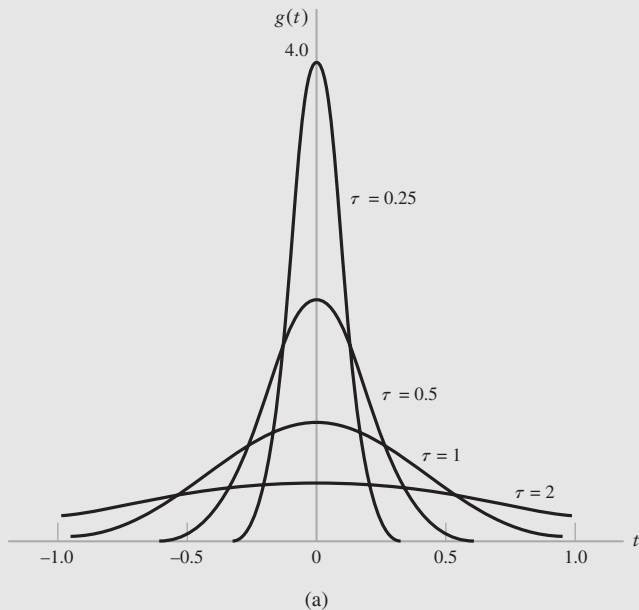


**FIGURE 2.13**  
 (a) Gaussian pulses of varying duration.  
 (b) Corresponding spectra.

Figure 2.13(b) illustrates the effect of varying the parameter  $\tau$  on the spectrum of the Gaussian pulse  $g(t)$ . Thus putting  $\tau = 0$ , we find, as expected, that the Fourier transform of the delta function is unity.

## ■ APPLICATIONS OF THE DELTA FUNCTION

### 1. dc Signal.

By applying the duality property to the Fourier-transform pair of Eq. (2.65) and noting that the delta function is an even function, we obtain

$$1 \rightleftharpoons \delta(f) \quad (2.67)$$

Equation (2.67) states that a *dc signal* is transformed in the frequency domain into a delta function  $\delta(f)$  occurring at zero frequency, as shown in Fig. 2.14. Of course, this result is intuitively satisfying.

Invoking the definition of Fourier transform, we readily deduce from Eq. (2.67) the useful relation

$$\int_{-\infty}^{\infty} \exp(-j2\pi ft) dt = \delta(f)$$

Recognizing that the delta function  $\delta(f)$  is real valued, we may simplify this relation as follows:

$$\int_{-\infty}^{\infty} \cos(2\pi ft) dt = \delta(f) \quad (2.68)$$

which provides yet another definition for the delta function, albeit in the frequency domain.

### 2. Complex Exponential Function.

Next, by applying the frequency-shifting property to Eq. (2.67), we obtain the Fourier-transform pair

$$\exp(j2\pi f_c t) \rightleftharpoons \delta(f - f_c) \quad (2.69)$$

for a complex exponential function of frequency  $f_c$ . Equation (2.69) states that the complex exponential function  $\exp(j2\pi f_c t)$  is transformed in the frequency domain into a delta function  $\delta(f - f_c)$  occurring at  $f = f_c$ .

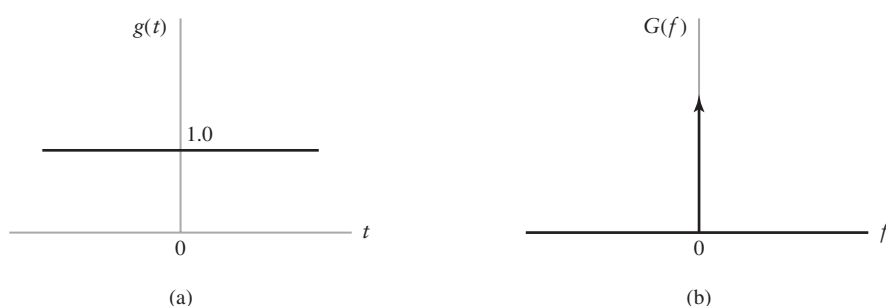


**FIGURE 2.14** (a) dc signal. (b) Spectrum.

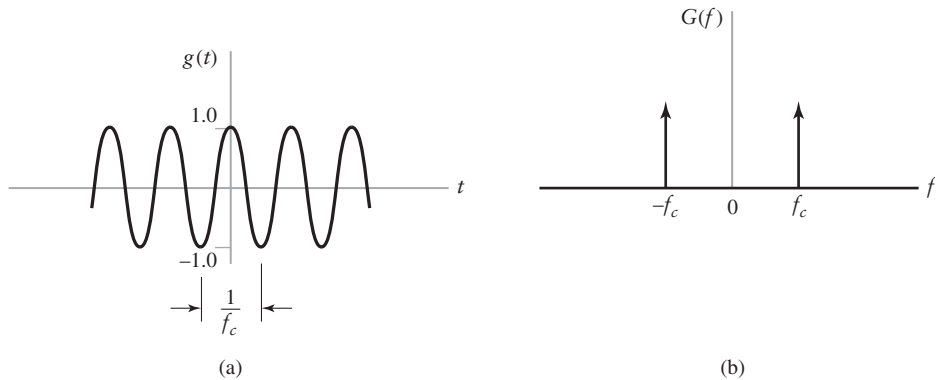


**FIGURE 2.15** (a) Cosine function. (b) Spectrum.

### 3. Sinusoidal Functions.

Consider next the problem of evaluating the Fourier transform of the cosine function  $\cos(2\pi f_c t)$ . We first use *Euler's formula* to write

$$\cos(2\pi f_c t) = \frac{1}{2}[\exp(j2\pi f_c t) + \exp(-j2\pi f_c t)] \quad (2.70)$$

Therefore, using Eq. (2.69), we find that the cosine function  $\cos(2\pi f_c t)$  is represented by the Fourier-transform pair

$$\cos(2\pi f_c t) \iff \frac{1}{2}[\delta(f - f_c) + \delta(f + f_c)] \quad (2.71)$$

In other words, the spectrum of the cosine function  $\cos(2\pi f_c t)$  consists of a pair of delta functions occurring at  $f = \pm f_c$ , each of which is weighted by the factor  $1/2$ , as shown in Fig. 2.15.

Similarly, we may show that the sine function  $\sin(2\pi f_c t)$  is represented by the Fourier-transform pair

$$\sin(2\pi f_c t) \iff \frac{1}{2j}[\delta(f - f_c) - \delta(f + f_c)] \quad (2.72)$$

which is illustrated in Fig. 2.16.

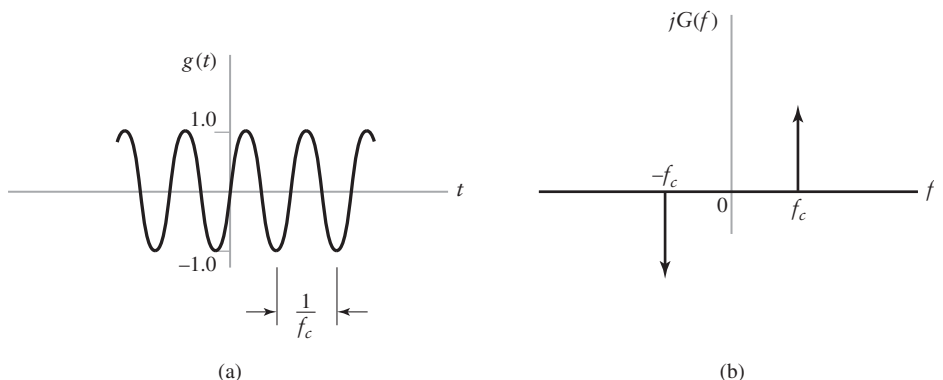


**FIGURE 2.16** (a) Sine function. (b) Spectrum.

► **Drill Problem 2.9** Determine the Fourier transform of the squared sinusoidal signals:

- (i)  $g(t) = \cos^2(2\pi f_c t)$
- (ii)  $g(t) = \sin^2(2\pi f_c t)$



#### 4. Signum Function.

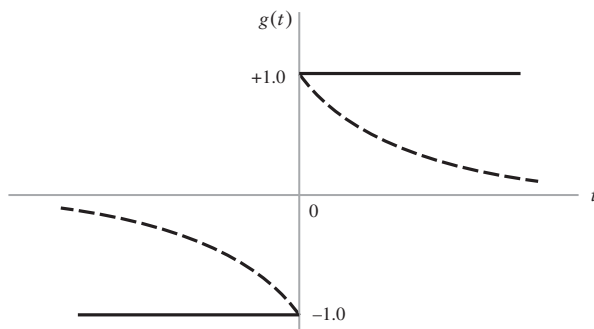
The *signum function*  $\text{sgn}(t)$  equals  $+1$  for positive time and  $-1$  for negative time, as shown by the solid curve in Fig. 2.17(a). The signum function was defined previously in Eq. (2.18); this definition is reproduced here for convenience of presentation:

$$\text{sgn}(t) = \begin{cases} +1, & t > 0 \\ 0, & t = 0 \\ -1, & t < 0 \end{cases}$$

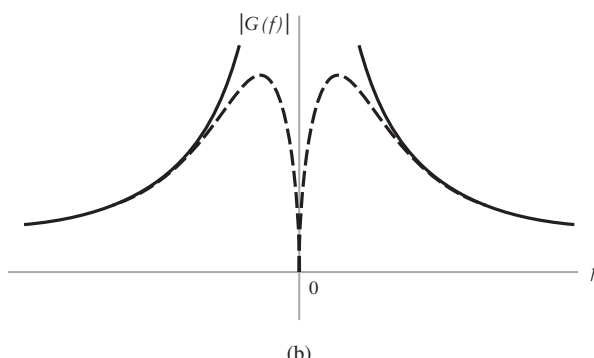
The signum function does not satisfy the Dirichlet conditions and therefore, strictly speaking, it does not have a Fourier transform. However, we may define a Fourier transform for the signum function by viewing it as the limiting form of the odd-symmetric double-exponential pulse

$$g(t) = \begin{cases} \exp(-at), & t > 0 \\ 0, & t = 0 \\ -\exp(at), & t < 0 \end{cases} \quad (2.73)$$

as the parameter  $a$  approaches zero. The signal  $g(t)$ , shown as the dashed curve in Fig. 2.17(a), does satisfy the Dirichlet conditions. Its Fourier transform was derived in



(a)



(b)

**FIGURE 2.17** (a) Signum function (continuous curve), and double-exponential pulse (dashed curve). (b) Amplitude spectrum of signum function (continuous curve), and that of double-exponential pulse (dashed curve).

Example 2.3; the result is given by [see Eq. (2.19)]:

$$G(f) = \frac{-j4\pi f}{a^2 + (2\pi f)^2}$$

The amplitude spectrum  $|G(f)|$  is shown as the dashed curve in Fig. 2.17(b). In the limit as  $a$  approaches zero, we have

$$\begin{aligned} F[\text{sgn}(t)] &= \lim_{a \rightarrow 0} \frac{-4j\pi f}{a^2 + (2\pi f)^2} \\ &= \frac{1}{j\pi f} \end{aligned}$$

That is,

$$\text{sgn}(t) \iff \frac{1}{j\pi f} \quad (2.74)$$

The amplitude spectrum of the signum function is shown as the continuous curve in Fig. 2.17(b). Here we see that for small  $a$ , the approximation is very good except near the origin on the frequency axis. At the origin, the spectrum of the approximating function  $g(t)$  is zero for  $a > 0$ , whereas the spectrum of the signum function goes to infinity.

### 5. Unit Step Function.

The *unit step function*  $u(t)$  equals +1 for positive time and zero for negative time. Previously defined in Eq. (2.11), it is reproduced here for convenience:

$$u(t) = \begin{cases} 1, & t > 0 \\ \frac{1}{2}, & t = 0 \\ 0, & t < 0 \end{cases}$$

The waveform of the unit step function is shown in Fig. 2.18(a). From this defining equation and that of the signum function, or from the waveforms of Figs. 2.17(a) and 2.18(a), we see that the unit step function and signum function are related by

$$u(t) = \frac{1}{2}[\text{sgn}(t) + 1] \quad (2.75)$$

Hence, using the linearity property of the Fourier transform and the Fourier-transform pairs of Eqs. (2.67) and (2.75), we find that the unit step function is represented by the Fourier-transform pair

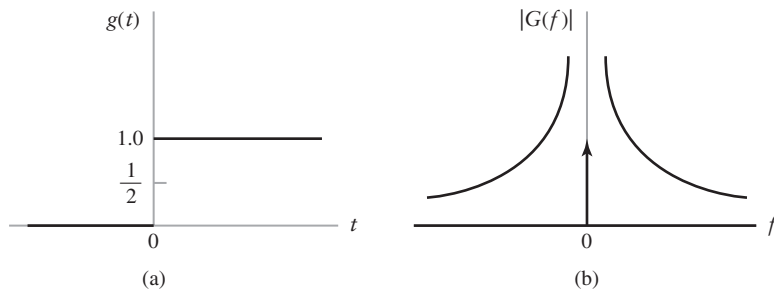


**FIGURE 2.18** (a) Unit step function. (b) Amplitude spectrum.

$$u(t) \iff \frac{1}{j2\pi f} + \frac{1}{2}\delta(f) \quad (2.76)$$

This means that the spectrum of the unit step function contains a delta function weighted by a factor of 1/2 and occurring at zero frequency, as shown in Fig. 2.18(b).

### 6. Integration in the Time Domain (Revisited).

The relation of Eq. (2.41) describes the effect of integration on the Fourier transform of a signal  $g(t)$ , assuming that  $G(0)$  is zero. We now consider the more general case, with no such assumption made.

Let

$$y(t) = \int_{-\infty}^t g(\tau) d\tau \quad (2.77)$$

The integrated signal  $y(t)$  can be viewed as the convolution of the original signal  $g(t)$  and the unit step function  $u(t)$ , as shown by

$$y(t) = \int_{-\infty}^{\infty} g(\tau)u(t - \tau) d\tau$$

where the time-shifted unit step function  $u(t - \tau)$  is itself defined by

$$u(t - \tau) = \begin{cases} 1, & \tau < t \\ \frac{1}{2}, & \tau = t \\ 0, & \tau > t \end{cases}$$

Recognizing that convolution in the time domain is transformed into multiplication in the frequency domain in accordance with Property 12, and using the Fourier-transform pair of Eq. (2.76) for the unit step function  $u(t)$ , we find that the Fourier transform of  $y(t)$  is

$$Y(f) = G(f) \left[ \frac{1}{j2\pi f} + \frac{1}{2}\delta(f) \right] \quad (2.78)$$

where  $G(f)$  is the Fourier transform of  $g(t)$ . According to the sifting property of a delta function formulated in the frequency domain, we have

$$G(f)\delta(f) = G(0)\delta(f)$$

Hence, we may rewrite Eq. (2.78) in the equivalent form:

$$Y(f) = \frac{1}{j2\pi f}G(f) + \frac{1}{2}G(0)\delta(f)$$

In general, the effect of integrating the signal  $g(t)$  is therefore described by the Fourier-transform pair

$$\int_{-\infty}^t g(\tau) d\tau \iff \frac{1}{j2\pi f}G(f) + \frac{1}{2}G(0)\delta(f) \quad (2.79)$$

This is the desired result, which includes Eq. (2.41) as a special case (i.e.,  $G(0) = 0$ ).

► **Drill Problem 2.10** Consider the function

$$g(t) = \delta\left(t + \frac{1}{2}\right) - \delta\left(t - \frac{1}{2}\right)$$

which consists of the difference between two delta functions at  $t = \pm \frac{1}{2}$ . The integration of  $g(t)$  with respect to time  $t$  yields the unit rectangular function  $\text{rect}(t)$ . Using Eq. (2.79), show that

$$\text{rect}(t) \iff \text{sinc}(f)$$

which is a special form of Eq. (2.10).  $\blacktriangleleft$

## 2.5 Fourier Transforms of Periodic Signals

It is well known that by using the Fourier series, a periodic signal can be represented as a sum of complex exponentials. (Appendix 2 presents a review of the Fourier series.) Also, in a limiting sense, Fourier transforms can be defined for complex exponentials, as demonstrated in Eqs. (2.69), (2.71), and (2.72). Therefore, it seems reasonable to represent a periodic signal in terms of a Fourier transform, provided that this transform is permitted to include delta functions.

Consider then a periodic signal  $g_{T_0}(t)$ , where the subscript  $T_0$  denotes the *period* of the signal. We know that  $g_{T_0}(t)$  can be represented in terms of the *complex exponential Fourier series* as (see Appendix 2)

$$g_{T_0}(t) = \sum_{n=-\infty}^{\infty} c_n \exp(j2\pi n f_0 t) \quad (2.80)$$

where  $c_n$  is the *complex Fourier coefficient*, defined by

$$c_n = \frac{1}{T_0} \int_{-T_0/2}^{T_0/2} g_{T_0}(t) \exp(-j2\pi n f_0 t) dt \quad (2.81)$$

and  $f_0$  is the *fundamental frequency* defined as the reciprocal of the period  $T_0$ ; that is,

$$f_0 = \frac{1}{T_0} \quad (2.82)$$

Let  $g(t)$  be a pulselike function, which equals  $g_{T_0}(t)$  over one period and is zero elsewhere; that is,

$$g(t) = \begin{cases} g_{T_0}(t), & -\frac{T_0}{2} \leq t \leq \frac{T_0}{2} \\ 0, & \text{elsewhere} \end{cases} \quad (2.83)$$

The periodic signal  $g_{T_0}(t)$  may now be expressed in terms of the function  $g(t)$  as the infinite summation

$$g_{T_0}(t) = \sum_{m=-\infty}^{\infty} g(t - mT_0) \quad (2.84)$$

Based on this representation, we may view  $g(t)$  as a *generating function*, in that it generates the periodic signal  $g_{T_0}(t)$ . Being pulselike with some finite energy, the function  $g(t)$  is Fourier transformable. Accordingly, in light of Eqs. (2.82) and (2.83), we may rewrite the formula for the complex Fourier coefficient  $c_n$  as follows:

$$\begin{aligned} c_n &= f_0 \int_{-\infty}^{\infty} g(t) \exp(-j2\pi n f_0 t) dt \\ &= f_0 G(n f_0) \end{aligned} \quad (2.85)$$

where  $G(nf_0)$  is the Fourier transform of  $g(t)$ , evaluated at the frequency  $f = nf_0$ . We may thus rewrite the formula of Eq. (2.80) for the reconstruction of the periodic signal  $g_{T_0}(t)$  as

$$g_{T_0}(t) = f_0 \sum_{n=-\infty}^{\infty} G(nf_0) \exp(j2\pi n f_0 t) \quad (2.86)$$

Therefore, eliminating  $g_{T_0}(t)$  between Eqs. (2.84) and (2.86), we may now write

$$\sum_{m=-\infty}^{\infty} g(t - mT_0) = f_0 \sum_{n=-\infty}^{\infty} G(nf_0) \exp(j2\pi n f_0 t) \quad (2.87)$$

which defines one form of *Poisson's sum formula*.

Finally, using Eq. (2.69), which defines the Fourier transform of a complex exponential function, in Eq. (2.87), we deduce the Fourier-transform pair:

$$\sum_{m=-\infty}^{\infty} g(t - mT_0) \iff f_0 \sum_{n=-\infty}^{\infty} G(nf_0) \delta(f - nf_0) \quad (2.88)$$

for the periodic signal  $g_{T_0}(t)$  whose fundamental frequency  $f_0 = (1/T_0)$ . Equation (2.88) simply states that the Fourier transform of a periodic signal consists of delta functions occurring at integer multiples of the fundamental frequency  $f_0$ , including the origin, and that each delta function is weighted by a factor equal to the corresponding value of  $G(nf_0)$ . Indeed, this relation merely provides a method to display the frequency content of the periodic signal  $g_{T_0}(t)$ .

It is of interest to observe that the pulselike function  $g(t)$ , constituting one period of the periodic signal  $g_{T_0}(t)$ , has a *continuous spectrum* defined by  $G(f)$ . On the other hand, the periodic signal  $g_{T_0}(t)$  itself has a *discrete spectrum*. In words, we may therefore sum up the transformation embodied in Eq. (2.88) as follows:

Periodicity in the time domain has the effect of changing the spectrum of a pulse-like signal into a discrete form defined at integer multiples of the fundamental frequency, and vice versa.

### EXAMPLE 2.11 Ideal Sampling Function

An *ideal sampling function*, or *Dirac comb*, consists of an infinite sequence of uniformly spaced delta functions, as shown in Fig. 2.19(a). We denote this waveform by

$$\delta_{T_0}(t) = \sum_{m=-\infty}^{\infty} \delta(t - mT_0) \quad (2.89)$$

We observe that the generating function  $g(t)$  for the ideal sampling function  $\delta_{T_0}(t)$  consists simply of the delta function  $\delta(t)$ . We therefore have  $G(f) = 1$ , and

$$G(nf_0) = 1 \quad \text{for all } n$$

Thus, the use of Eq. (2.88) yields the new result

$$\sum_{m=-\infty}^{\infty} \delta(t - mT_0) \iff f_0 \sum_{n=-\infty}^{\infty} \delta(f - nf_0) \quad (2.90)$$

Equation (2.90) states that the Fourier transform of a periodic train of delta functions, spaced  $T_0$  seconds apart, consists of another set of delta functions weighted by the factor  $f_0 = (1/T_0)$  and regularly spaced  $f_0$  Hz apart along the frequency axis as in Fig. 2.19(b). In the special case of  $T_0 = 1$ , a periodic train of delta functions is, like a Gaussian pulse, its own Fourier transform.

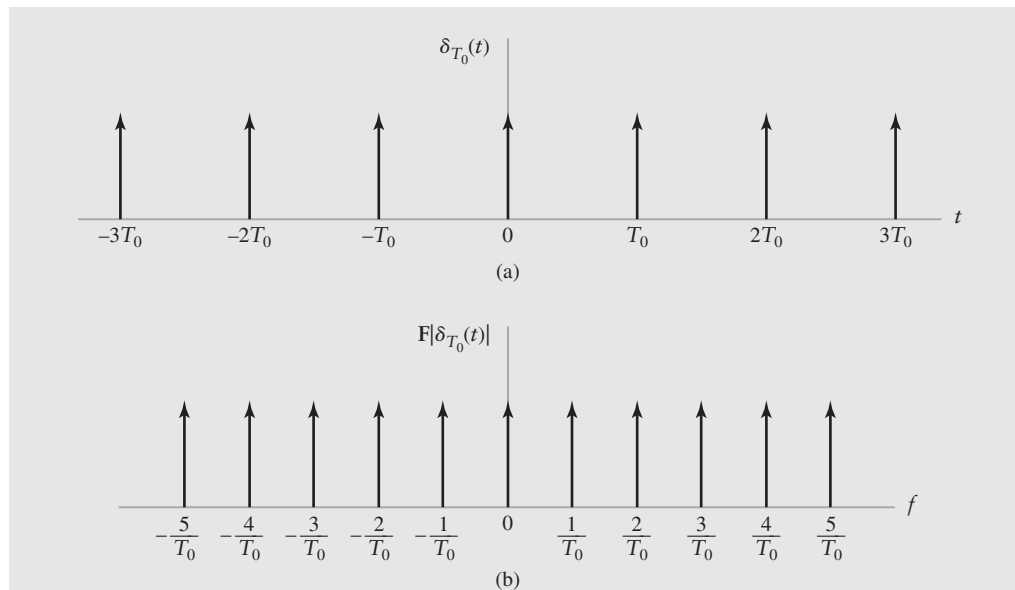


**FIGURE 2.19** (a) Dirac comb. (b) Spectrum.

Applying the inverse Fourier transform to the right-hand side of Eq. (2.90), we get the relationship

$$\sum_{m=-\infty}^{\infty} \delta(t - mT_0) = f_0 \sum_{n=-\infty}^{\infty} \exp(j2\pi n f_0 t) \quad (2.91)$$

On the other hand, applying the Fourier transform to the left-hand side of Eq. (2.90), we get the *dual* relationship:

$$T_0 \sum_{m=-\infty}^{\infty} \exp(j2\pi m f T_0) = \sum_{n=-\infty}^{\infty} \delta(f - n f_0) \quad (2.92)$$

where we have used the relation of Eq. (2.82) rewritten in the form  $T_0 = 1/f_0$ . Equations (2.91) and (2.92) are the *dual* of each other, in that in the delta functions show up in the time domain in Eq. (2.91) whereas in Eq. (2.92) the delta functions show up in the frequency domain.

► **Drill Problem 2.11** Using the Euler formula  $\cos x = \frac{1}{2} [\exp(jx) + \exp(-jx)]$ , reformulate Eqs. (2.91) and (2.92) in terms of sinusoidal functions. ◀

## 2.6 Transmission of Signals Through Linear Systems: Convolution Revisited

With the Fourier transform theory presented in the previous sections at our disposal, we are now ready to turn our attention to the study of a special class of systems known to be *linear*. A *system* refers to any physical device or phenomenon that produces an output signal in response to an input signal. It is customary to refer to the input signal as the *excitation* and to the output signal as the *response*. In a *linear system*, the *principle of superposition* holds; that is, *the response of a linear system to a number of excitations applied simultaneously is equal to the sum of the responses of the system when each excitation is applied individually*. Important examples of linear systems include *filters* and *communication channels* operating in their

linear region. A filter refers to a frequency-selective device that is used to limit the spectrum of a signal to some band of frequencies. A channel refers to a physical medium that connects the transmitter and receiver of a communication system. We wish to evaluate the effects of transmitting signals through linear filters and communication channels. This evaluation may be carried out in two ways, depending on the description adopted for the filter or channel. That is, we may use time-domain or frequency-domain ideas, as described below.

### ■ TIME RESPONSE

In the time domain, a linear system is described in terms of its *impulse response*, which is defined as *the response of the system (with zero initial conditions) to a unit impulse or delta function  $\delta(t)$  applied to the input of the system*. If the system is *time invariant*, then this property implies that a time-shifted unit impulse at the input of the system produces an impulse response at the output, shifted by exactly the same amount. In other words, the shape of the impulse response of a linear time-invariant system is the same no matter when the unit impulse is applied to the system. Thus, assuming that the unit impulse or delta function is applied at time  $t = 0$ , we may denote the impulse response of a linear time-invariant system by  $h(t)$ . Let this system be subjected to an arbitrary excitation  $x(t)$ , as in Fig. 2.20(a). To determine the response  $y(t)$  of the system, we begin by first approximating  $x(t)$  by a staircase function composed of narrow rectangular pulses, each of duration  $\Delta\tau$ , as shown in Fig. 2.20(b). Clearly the approximation becomes better for smaller  $\Delta\tau$ . As  $\Delta\tau$  approaches zero, each pulse approaches, in the limit, a delta function weighted by a factor equal to the height of the pulse times  $\Delta\tau$ . Consider a typical pulse, shown shaded in Fig. 2.20(b), which occurs at  $t = \tau$ . This pulse has an area equal to  $x(\tau)\Delta\tau$ . By definition, the response of the system to a unit impulse or delta function  $\delta(t)$ , occurring at  $t = 0$ , is  $h(t)$ . It follows therefore that the response of the system to a delta function, weighted by the factor  $x(\tau)\Delta\tau$  and occurring at  $t = \tau$ , must be  $x(\tau)h(t - \tau)\Delta\tau$ . To find the response  $y(t)$  at some time  $t$ , we

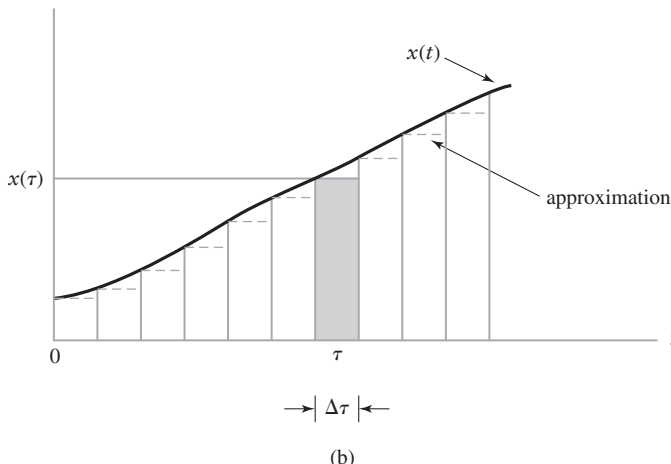
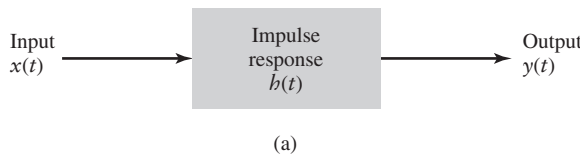


**FIGURE 2.20** (a) Linear system with input  $x(t)$  and output  $y(t)$ . (b) Staircase approximation of input  $x(t)$ .

apply the principle of superposition. Thus, summing the various infinitesimal responses due to the various input pulses, we obtain in the limit, as  $\Delta\tau$  approaches zero,

$$y(t) = \int_{-\infty}^{\infty} x(\tau)h(t - \tau) d\tau \quad (2.93)$$

This relation is called the *convolution integral*.

In Eq. (2.93), three different time scales are involved: *excitation time  $\tau$* , *response time  $t$* , and *system-memory time ( $t - \tau$ )*. This relation is the basis of time-domain analysis of linear time-invariant systems. It states that *the present value of the response of a linear time-invariant system is a weighted integral over the past history of the input signal, weighted according to the impulse response of the system*. Thus, the impulse response acts as a *memory function* for the system.

In Eq. (2.93), the excitation  $x(t)$  is convolved with the impulse response  $h(t)$  to produce the response  $y(t)$ . Since convolution is commutative, it follows that we may also write

$$y(t) = \int_{-\infty}^{\infty} h(\tau)x(t - \tau) d\tau \quad (2.94)$$

where  $h(t)$  is convolved with  $x(t)$ .

### EXAMPLE 2.12 Tapped-Delay-Line Filter

Consider a linear time-invariant filter with impulse response  $h(t)$ . We make two assumptions:

1. *Causality*, which means that the impulse response  $h(t)$  is zero for  $t < 0$ .
2. *Finite support*, which means that the impulse response of the filter is of some finite duration  $T_f$ , so that we may write  $h(t) = 0$  for  $t \geq T_f$ .

Under these two assumptions, we may express the filter output  $y(t)$  produced in response to the input  $x(t)$  as

$$y(t) = \int_0^{T_f} h(\tau)x(t - \tau) d\tau \quad (2.95)$$

Let the input  $x(t)$ , impulse response  $h(t)$ , and output  $y(t)$  be *uniformly sampled* at the rate  $(1/\Delta\tau)$  samples per second, so that we may put

$$t = n \Delta\tau$$

and

$$\tau = k \Delta\tau$$

where  $k$  and  $n$  are integers, and  $\Delta\tau$  is the *sampling period*. Assuming that  $\Delta\tau$  is small enough for the product  $h(\tau)x(t - \tau)$  to remain essentially constant for  $k \Delta\tau \leq \tau \leq (k + 1) \Delta\tau$  for all values of  $k$  and  $\tau$ , we may approximate Eq. (2.95) by a *convolution sum* as shown by

$$y(n \Delta\tau) = \sum_{k=0}^{N-1} h(k \Delta\tau)x(n \Delta\tau - k \Delta\tau) \Delta\tau$$

where  $N \Delta\tau = T_f$ . Define the *weight*

$$w_k = h(k \Delta\tau) \Delta\tau, \quad k = 0, 1, \dots, N - 1 \quad (2.96)$$

We may then rewrite the formula for  $y(n \Delta\tau)$  as

$$y(n \Delta\tau) = \sum_{k=0}^{N-1} w_k x(n \Delta\tau - k \Delta\tau) \quad (2.97)$$

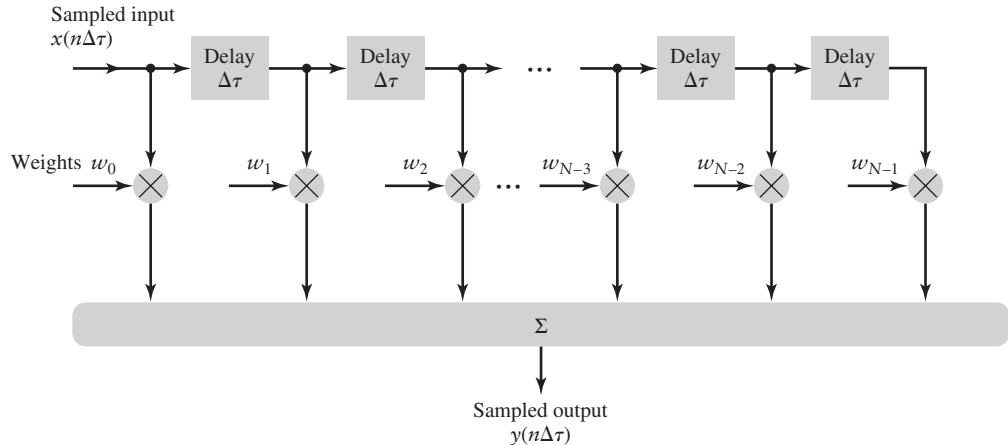


**FIGURE 2.21** Tapped-delay-line filter.

Equation (2.97) may be realized using the structure shown in Fig. 2.21, which consists of a set of *delay elements* (each producing a delay of  $\Delta\tau$  seconds), a set of *multipliers* connected to the *delay-line taps*, a corresponding set of *weights* supplied to the multipliers, and a *summer* for adding the multiplier outputs. This structure is known as a *tapped-delay-line filter* or *transversal filter*. Note that in Fig. 2.21 the tap-spacing or basic increment of delay is equal to the sampling period of the input sequence  $\{x(n\Delta\tau)\}$ .

### ■ CAUSALITY AND STABILITY

A system is said to be *causal* if it does not respond before the excitation is applied. For a linear time-invariant system to be causal, it is clear that the impulse response  $h(t)$  must vanish for negative time, as stated in Example 2.12. That is, we may formally state that the necessary and sufficient condition for a linear time-invariant system to be causal is

$$h(t) = 0, \quad t < 0 \quad (2.98)$$

Clearly, for a system operating in *real time* to be physically realizable, it must be causal. However, there are many applications in which the signal to be processed is only available in *stored form*; in these situations, the system can be noncausal and yet physically realizable.

The system is said to be *stable* if the output signal is bounded for all bounded input signals. We refer to this requirement as the *bounded input–bounded output* (BIBO) *stability criterion*, which is well suited for the analysis of linear time-invariant systems. Let the input signal  $x(t)$  be *bounded*, as shown by

$$|x(t)| < M \quad \text{for all } t$$

where  $M$  is a positive real finite number. Taking the absolute values of both sides of Eq. (2.94), we have

$$|y(t)| = \left| \int_{-\infty}^{\infty} h(\tau)x(t - \tau) d\tau \right| \quad (2.99)$$

Next, we recognize that the absolute value of an integral is *bounded* by the integral of the absolute value of the integrand, as shown by

$$\begin{aligned} \left| \int_{-\infty}^{\infty} h(\tau)x(t - \tau) d\tau \right| &\leq \int_{-\infty}^{\infty} |h(\tau)x(t - \tau)| d\tau \\ &= M \int_{-\infty}^{\infty} |h(\tau)| d\tau \end{aligned}$$

Hence, substituting this inequality into Eq. (2.99) yields the important result

$$|y(t)| \leq M \int_{-\infty}^{\infty} |h(\tau)| d\tau$$

It follows therefore that for a linear time-invariant system to be stable, the impulse response  $h(t)$  must be absolutely integrable. That is, *the necessary and sufficient condition for BIBO stability of a linear time-invariant system* is described by

$$\int_{-\infty}^{\infty} |h(t)| dt < \infty \quad (2.100)$$

where  $h(t)$  is the impulse response of the system.

### ■ FREQUENCY RESPONSE

Consider next a linear time-invariant system of impulse response  $h(t)$ , which is driven by a complex exponential input of unit amplitude and frequency  $f$ ; that is,

$$x(t) = \exp(j2\pi ft) \quad (2.101)$$

Using Eqs. (2.101) in (2.94), the response of the system is obtained as

$$\begin{aligned} y(t) &= \int_{-\infty}^{\infty} h(\tau) \exp[j2\pi f(t - \tau)] d\tau \\ &= \exp(j2\pi ft) \int_{-\infty}^{\infty} h(\tau) \exp(-j2\pi f\tau) d\tau \end{aligned} \quad (2.102)$$

Define the *transfer function* or *frequency response* of the system as the Fourier transform of its impulse response, as shown by

$$H(f) = \int_{-\infty}^{\infty} h(t) \exp(-j2\pi ft) dt \quad (2.103)$$

The terms transfer function and frequency response are used interchangably. The integral in the last line of Eq. (2.102) is the same as that of Eq. (2.103), except for the fact that  $\tau$  is used in place of  $t$ . Hence, we may rewrite Eq. (2.102) in the form

$$y(t) = H(f) \exp(j2\pi ft) \quad (2.104)$$

Equation (2.104) states that the response of a linear time-invariant system to a complex exponential function of frequency  $f$  is the same complex exponential function multiplied by a constant coefficient  $H(f)$ .

Equation (2.103) is one definition of the transfer function  $H(f)$ . An alternative definition of the transfer function may be deduced by dividing Eq. (2.104) by (2.101) to obtain

$$H(f) = \frac{y(t)}{x(t)} \Big|_{x(t) = \exp(j2\pi ft)} \quad (2.105)$$

Consider next an arbitrary signal  $x(t)$  applied to the system. The signal  $x(t)$  may be expressed in terms of its inverse Fourier transform as

$$x(t) = \int_{-\infty}^{\infty} X(f) \exp(j2\pi ft) df \quad (2.106)$$

Equivalently, we may express  $x(t)$  in the limiting form

$$x(t) = \lim_{\substack{\Delta f \rightarrow 0 \\ f = k \Delta f}} \sum_{k=-\infty}^{\infty} X(f) \exp(j2\pi ft) \Delta f \quad (2.107)$$

That is, the input signal  $x(t)$  may be viewed as a superposition of complex exponentials of incremental amplitude. Because the system is linear, the response to this superposition of complex exponential inputs is given by

$$\begin{aligned} y(t) &= \lim_{\substack{\Delta f \rightarrow 0 \\ f = k \Delta f}} \sum_{k=-\infty}^{\infty} H(f)X(f) \exp(j2\pi ft) \Delta f \\ &= \int_{-\infty}^{\infty} H(f)X(f) \exp(j2\pi ft) df \end{aligned} \quad (2.108)$$

The Fourier transform of the output signal  $y(t)$  is therefore readily obtained as

$$Y(f) = H(f)X(f) \quad (2.109)$$

According to Eq. (2.109), a linear time-invariant system may thus be described quite simply in the frequency domain by noting that *the Fourier transform of the output is equal to the product of the frequency response of the system and the Fourier transform of the input.*

Of course, we could have deduced the result of Eq. (2.109) directly by recognizing two facts:

1. The response  $y(t)$  of a linear time-invariant system of impulse response  $h(t)$  to an arbitrary input  $x(t)$  is obtained by convolving  $x(t)$  with  $h(t)$ , in accordance with Eq. (2.93).
2. The convolution of a pair of time functions is transformed into the multiplication of their Fourier transforms.

The alternative derivation of Eq. (2.109) above is presented primarily to develop an understanding of why the Fourier representation of a time function as a superposition of complex exponentials is so useful in analyzing the behavior of linear time-invariant systems.

The frequency response  $H(f)$  is a characteristic property of a linear time-invariant system. It is, in general, a complex quantity, so that we may express it in the form

$$H(f) = |H(f)| \exp[j\beta(f)] \quad (2.110)$$

where  $|H(f)|$  is called the *amplitude response* or *magnitude response*, and  $\beta(f)$  the *phase* or *phase response*. In the special case of a linear system with real-valued impulse response  $h(t)$ , the frequency response  $H(f)$  exhibits conjugate symmetry, which means that

$$|H(f)| = |H(-f)|$$

and

$$\beta(f) = -\beta(-f)$$

That is, the amplitude response  $|H(f)|$  of a linear system with real-valued impulse response is an even function of frequency, whereas the phase  $\beta(f)$  is an odd function of frequency.

In some applications it is preferable to work with the logarithm of  $H(f)$ , expressed in polar form, rather than with  $H(f)$  itself. Define the natural logarithm

$$\ln H(f) = \alpha(f) + j\beta(f) \quad (2.111)$$

where

$$\alpha(f) = \ln|H(f)| \quad (2.112)$$

The function  $\alpha(f)$  is one definition of the *gain* of the system. It is measured in *nepers*, whereas the phase  $\beta(f)$  is measured in radians. Equation (2.111) indicates that the gain  $\alpha(f)$  and phase  $\beta(f)$  are the real and imaginary parts of the natural logarithm of the frequency response  $H(f)$ , respectively. The gain may also be expressed in *decibels* (dB) by using the definition

$$\alpha'(f) = 20 \log_{10}|H(f)| \quad (2.113)$$

The two gain functions  $\alpha(f)$  and  $\alpha'(f)$  are related by

$$\alpha'(f) = 8.69\alpha(f) \quad (2.114)$$

That is, 1 neper is equal to 8.69 dB.

From the discussion presented Section 2.3, we note that the *bandwidth* of a system is specified by the constancy of its amplitude response. The bandwidth of a low-pass system is thus defined as the frequency at which the amplitude response  $|H(f)|$  is  $1/\sqrt{2}$  times its value of zero frequency or, equivalently, the frequency at which the gain  $\alpha'(f)$  drops by 3 dB below its value at zero frequency, as illustrated in Fig. 2.22(a). Correspondingly, the bandwidth of a band-pass system is defined as the range of frequencies over which the amplitude response  $|H(f)|$  remains within  $1/\sqrt{2}$  times its value at the mid-band frequency, as illustrated in Fig. 2.22(b).

### ■ PALEY–WIENER CRITERION

A necessary and sufficient condition for a function  $\alpha(f)$  to be the gain of a causal filter is the convergence of the integral.

$$\int_{-\infty}^{\infty} \left( \frac{|\alpha(f)|}{1 + f^2} \right) df < \infty \quad (2.115)$$

This condition is known as the *Paley–Wiener criterion*. It states that, provided the gain  $\alpha(f)$  satisfies the condition of Eq. (2.115), then we may associate with this gain a suitable phase  $\beta(f)$  such that the resulting filter has a causal impulse response that is zero for negative time. In other words, the Paley–Wiener criterion is the frequency-domain equivalent of the causality requirement. A system with a realizable gain characteristic may have infinite attenuation [i.e.,  $\alpha(f) = -\infty$ ] for a discrete set of frequencies, but it cannot have infinite attenuation over a band of frequencies; otherwise, the Paley–Wiener criterion is violated.

► **Drill Problem 2.12** Discuss the following two issues, citing examples for your answers:

- (a) Is it possible for a linear time-invariant system to be causal but unstable?
- (b) Is it possible for such a system to be noncausal but stable? ◀

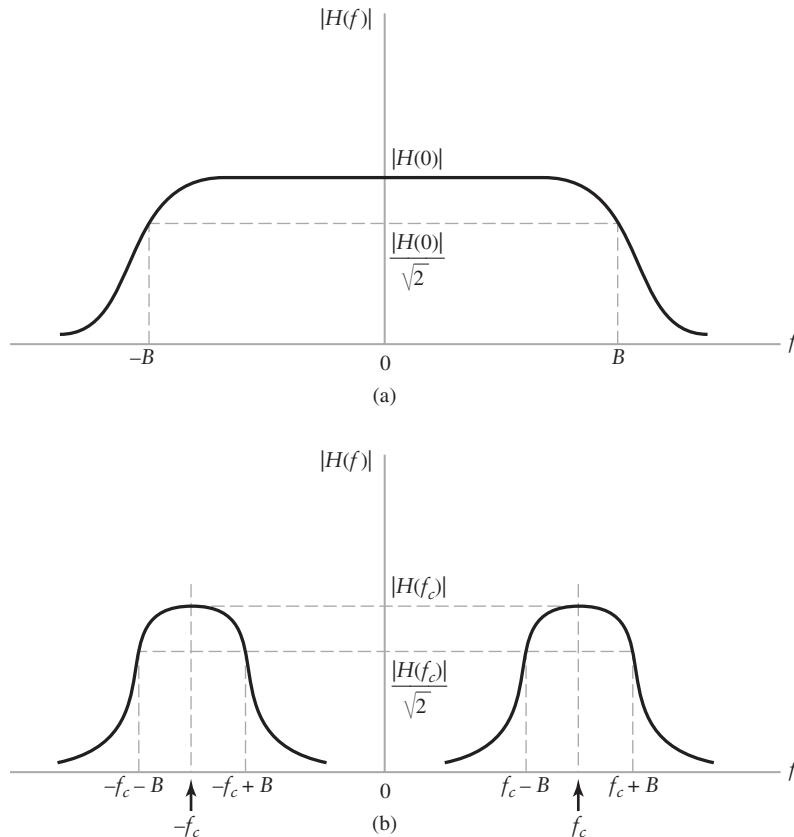


**FIGURE 2.22** Illustration of the definition of system bandwidth.  
(a) Low-pass system. (b) Band-pass system.

► **Drill Problem 2.13** The impulse response of a linear system is defined by the Gaussian function

$$h(t) = \exp\left(-\frac{t^2}{2\tau^2}\right)$$

where  $\tau$  is an adjustable parameter that defines pulse duration. Determine the frequency response of the system. ◀

► **Drill Problem 2.14** A tapped-delay-line filter consists of  $N$  weights, where  $N$  is odd. It is symmetric with respect to the center tap; that is, the weights satisfy the condition

$$w_n = w_{N-1-n}, \quad 0 \leq n \leq N-1$$

- (a) Find the amplitude response of the filter.
- (b) Show that this filter has a linear phase response. What is the implication of this property? ◀
- (c) What is the time delay produced by the filter? ◀

## 2.7 Ideal Low-Pass Filters

As previously mentioned, a *filter* is a frequency-selective system that is used to limit the spectrum of a signal to some specified band of frequencies. Its frequency response is characterized by a *passband* and a *stopband*. The frequencies inside the passband are transmitted with little or no distortion, whereas those in the stopband are rejected. The filter may be of the *low-pass*, *high-pass*, *band-pass*, or *band-stop* type, depending on whether it transmits low, high, intermediate, or all but intermediate frequencies, respectively. We have already encountered examples of low-pass and band-pass systems in Fig. 2.22.

Filters, in one form or another, represent an important functional block in building communication systems. In this book, we will be concerned with the use of high-pass, low-pass, and band-pass filters.

In this section, we study the time response of the *ideal low-pass filter*, which transmits, without any distortion, all frequencies inside the passband and completely rejects all frequencies inside the stopband, as illustrated in Fig. 2.23. According to this figure, the frequency response of an ideal low-pass filter satisfies two necessary conditions:

1. *The amplitude response of the filter is a constant inside the passband  $-B \leq f \leq B$ .*  
(The constant in Fig. 2.23 is set equal to unity for convenience of presentation.)
2. *The phase response varies linearly with frequency inside the passband of the filter.*  
(Outside the passband, the phase response may assume arbitrary values.)

In mathematical terms, the transfer function of an ideal low-pass filter is therefore defined by

$$H(f) = \begin{cases} \exp(-j2\pi ft_0), & -B \leq f \leq B \\ 0, & |f| > B \end{cases} \quad (2.116)$$

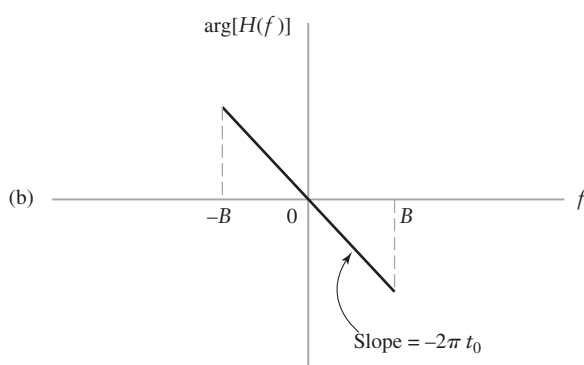
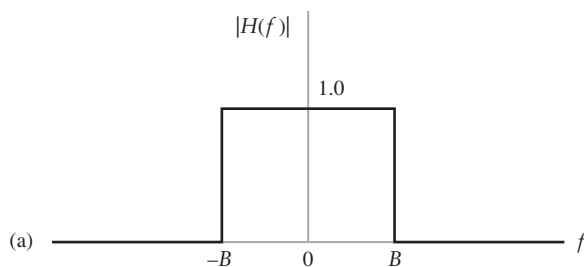


**FIGURE 2.23** Frequency response of ideal low-pass filter. (a) Amplitude response. (b) Phase response; outside the band  $-B \leq f \leq B$ , the phase response assumes an arbitrary form (not shown in the figure).

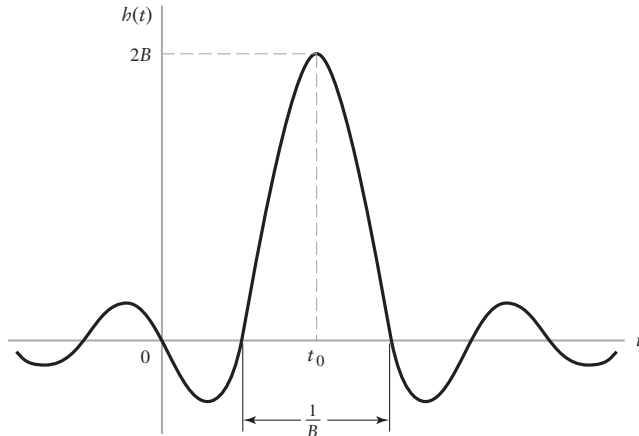


**FIGURE 2.24** Impulse response of ideal low-pass filter.

The parameter  $B$  defines the *bandwidth* of the filter. The ideal low-pass filter is, of course, noncausal because it violates the Paley–Wiener criterion. This observation may also be confirmed by examining the impulse response  $h(t)$ . Thus, by evaluating the inverse Fourier transform of the transfer function of Eq. (2.116), we get

$$h(t) = \int_{-B}^B \exp[j2\pi f(t - t_0)] df \quad (2.117)$$

where the limits of integration have been reduced to the frequency band inside which  $H(f)$  does not vanish. Equation (2.117) is readily integrated, yielding

$$\begin{aligned} h(t) &= \frac{\sin[2\pi B(t - t_0)]}{\pi(t - t_0)} \\ &= 2B \text{sinc}[2B(t - t_0)] \end{aligned} \quad (2.118)$$

The impulse response has a peak amplitude of  $2B$  centered on time  $t_0$ , as shown in Fig. 2.24 for  $t_0 = 1/B$ . The duration of the main lobe of the impulse response is  $1/B$ , and the build-up time from the zero at the beginning of the main lobe to the peak value is  $1/2B$ . We see from Fig. 2.24 that, for any finite value of  $t_0$ , there is some response from the filter before the time  $t = 0$  at which the unit impulse is applied to the input; this observation confirms that the ideal low-pass filter is noncausal. Note, however, that we can always make the delay  $t_0$  large enough for the condition

$$|\text{sinc}[2B(t - t_0)]| \ll 1, \quad \text{for } t < 0$$

to be satisfied. By so doing, we are able to build a causal filter that approximates an ideal low-pass filter, with the approximation improving with increasing delay  $t_0$ .

### ■ PULSE RESPONSE OF IDEAL LOW-PASS FILTERS

Consider a rectangular pulse  $x(t)$  of unit amplitude and duration  $T$ , which is applied to an ideal low-pass filter of bandwidth  $B$ . The problem is to determine the response  $y(t)$  of the filter.

The impulse response  $h(t)$  of the filter is defined by Eq. (2.118). Clearly, the delay  $t_0$  has no effect on the shape of the filter response  $y(t)$ . Without loss of generality, we may

therefore simplify the exposition by setting  $t_0 = 0$ , in which case the impulse response of Eq. (2.118) reduces to

$$h(t) = 2B \operatorname{sinc}(2Bt) \quad (2.119)$$

With the input  $x(t) = 1$  for  $-(T/2) \leq t \leq (T/2)$ , the resulting response of the filter is given by the convolution integral

$$\begin{aligned} y(t) &= \int_{-\infty}^{\infty} x(\tau)h(t - \tau) d\tau \\ &= 2B \int_{-T/2}^{T/2} \operatorname{sinc}[2B(t - \tau)] d\tau \\ &= 2B \int_{-T/2}^{T/2} \left( \frac{\sin[2\pi B(t - \tau)]}{2\pi B(t - \tau)} \right) d\tau \end{aligned} \quad (2.120)$$

Define a new dimensionless variable

$$\lambda = 2\pi B(t - \tau)$$

Then, changing the integration variable from  $\tau$  to  $\lambda$ , we may rewrite Eq. (2.120) as

$$\begin{aligned} y(t) &= \frac{1}{\pi} \int_{2\pi B(t-T/2)}^{2\pi B(t+T/2)} \left( \frac{\sin \lambda}{\lambda} \right) d\lambda \\ &= \frac{1}{\pi} \left[ \int_0^{2\pi B(t+T/2)} \left( \frac{\sin \lambda}{\lambda} \right) d\lambda - \int_0^{2\pi B(t-T/2)} \left( \frac{\sin \lambda}{\lambda} \right) d\lambda \right] \\ &= \frac{1}{\pi} \{ \operatorname{Si}[2\pi B(t + T/2)] - \operatorname{Si}[2\pi B(t - T/2)] \} \end{aligned} \quad (2.121)$$

In Eq. (2.121), we have introduced a new expression called the *sine integral*, which is defined by

$$\operatorname{Si}(u) = \int_0^u \frac{\sin x}{x} dx \quad (2.122)$$

Unfortunately, the sine integral  $\operatorname{Si}(u)$  cannot be evaluated in closed form in terms of elementary functions. However, it can be integrated in a power series, which, in turn, leads to the graph plotted in Fig. 2.25. From this figure we make three observations:

1. The sine integral  $\operatorname{Si}(u)$  is an oscillatory function of  $u$ , having odd symmetry about the origin  $u = 0$ .
2. It has its maxima and minima at multiples of  $\pi$ .
3. It approaches the limiting value  $(\pi/2)$  for large positive values of  $u$ .

In Fig. 2.25, we see that the sine integral  $\operatorname{Si}(u)$  oscillates at a frequency of  $1/2\pi$ . Correspondingly, the filter response  $y(t)$  will also oscillate at a frequency equal to the cutoff frequency (i.e., bandwidth)  $B$  of the low-pass filter, as indicated in Fig. 2.26. The maximum value of  $\operatorname{Si}(u)$  occurs at  $u_{\max} = \pi$  and is equal to

$$1.8519 = (1.179) \times \left( \frac{\pi}{2} \right)$$

We may show that the filter response  $y(t)$  has maxima and minima at

$$t_{\max} = \pm \frac{T}{2} \pm \frac{1}{2B}$$

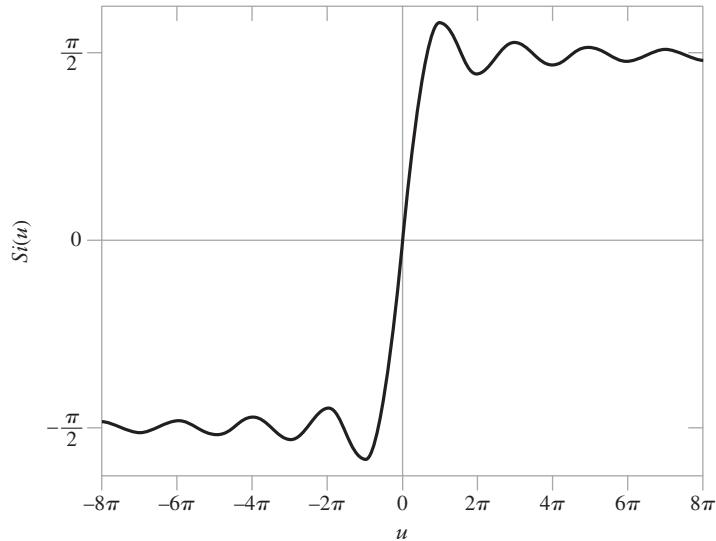


**FIGURE 2.25** The sine integral  $\text{Si}(u)$ .

with

$$\begin{aligned} y(t_{\max}) &= \frac{1}{\pi} [\text{Si}(\pi) - \text{Si}(\pi - 2\pi BT)] \\ &= \frac{1}{\pi} [\text{Si}(\pi) + \text{Si}(2\pi BT - \pi)] \end{aligned}$$

where, in the second line, we have used the odd symmetric property of the sine integral. Let

$$\text{Si}(2\pi BT - \pi) = \frac{\pi}{2}(1 \pm \Delta)$$

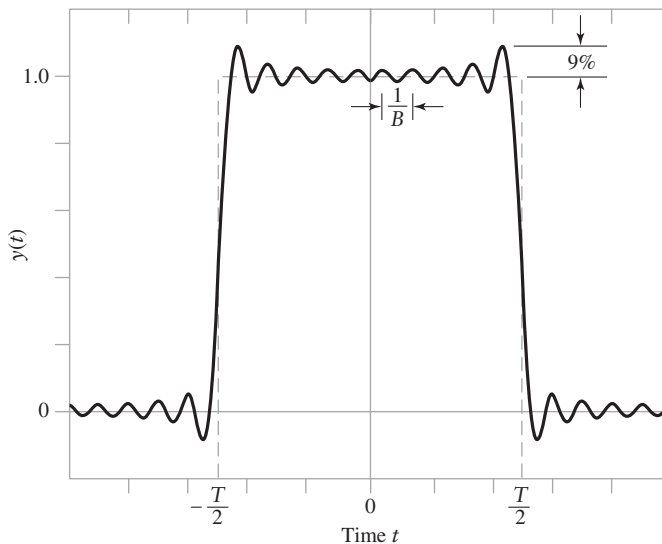


**FIGURE 2.26** Ideal low-pass filter response for a square pulse.

where  $\Delta$  is the absolute value of the deviation in the value of  $\text{Si}(2\pi BT - \pi)$  expressed as a fraction of the final value  $+\pi/2$ . Thus, recognizing that

$$\text{Si}(\pi) = (1.179)(\pi/2)$$

we may redefine  $y(t_{\max})$  as

$$\begin{aligned} y(t_{\max}) &= \frac{1}{2}(1.179 + 1 \pm \Delta) \\ &\approx 1.09 \pm \frac{1}{2}\Delta \end{aligned} \quad (2.123)$$

For a time-bandwidth product  $BT \gg 1$ , the fractional deviation  $\Delta$  has a very small value, in which case we may make two important observations from Eq. (2.123):

1. The percentage overshoot in the filter response is approximately 9 percent.
2. The overshoot is practically independent of the filter bandwidth  $B$ .

The basic phenomenon underlying these two observations is called the *Gibbs phenomenon*. Figure 2.26 shows the oscillatory nature of the filter response and the 9 percent overshoot characterizing the response, assuming that  $BT \gg 1$ .

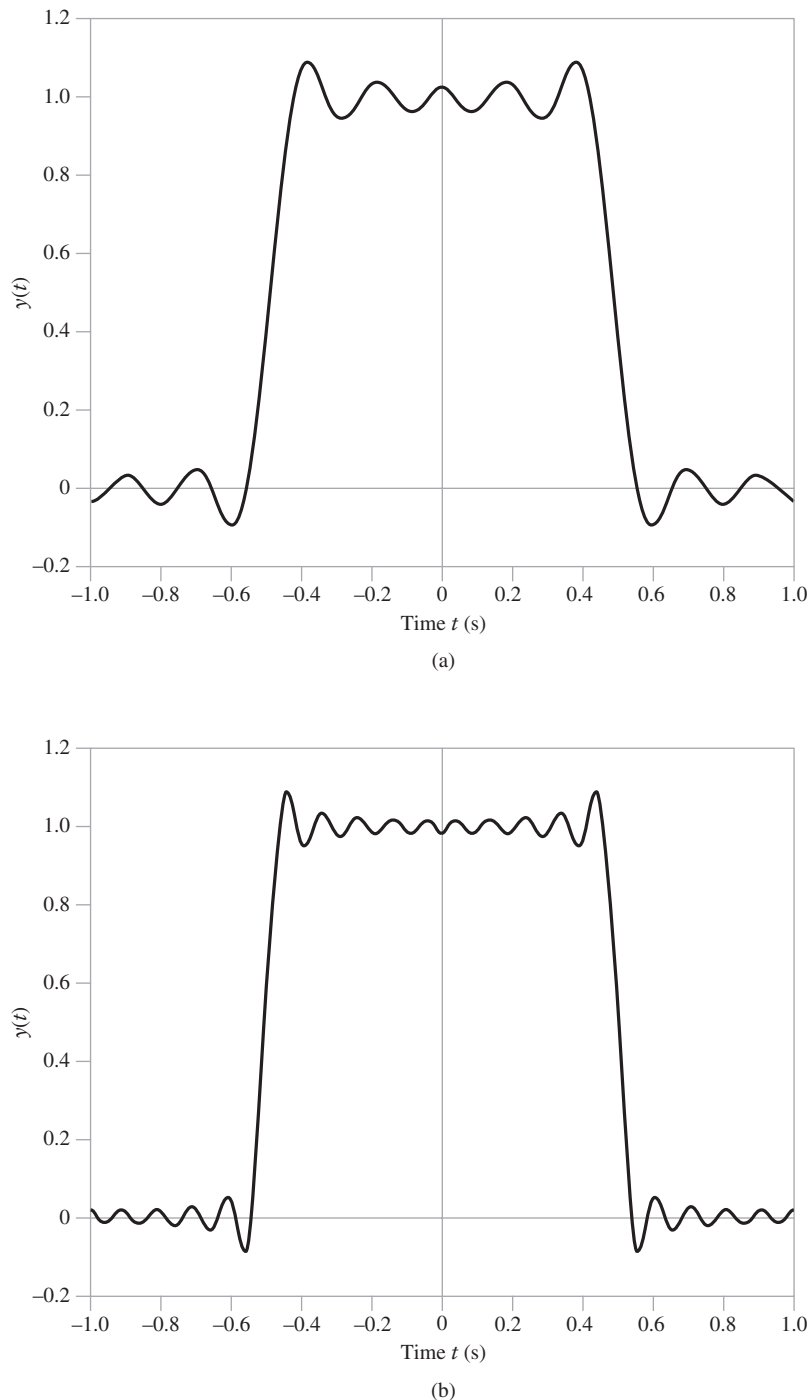
Figure 2.27, occupying pages 65 and 66, shows the filter response for four time-bandwidth products:  $BT = 5, 10, 20$ , and  $100$ , assuming that the pulse duration  $T$  is 1 second. Table 2.1 shows the corresponding frequencies of oscillations and percentage overshoots for these time-bandwidth products, confirming observations 1 and 2.

**TABLE 2.1 Oscillation Frequency and Percentage Overshoot for Varying Time-Bandwidth Product**

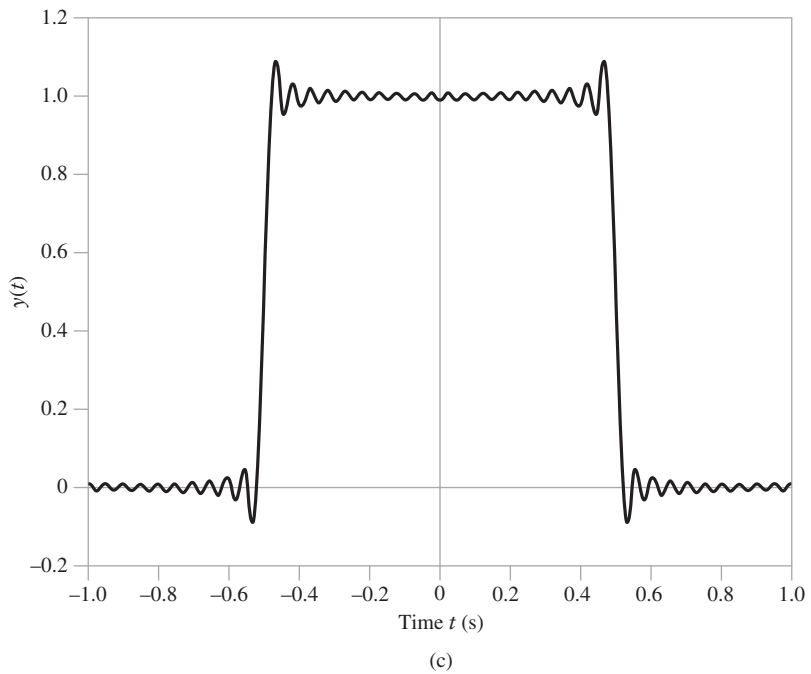
$BT$	Oscillation Frequency	Percentage Overshoot
5	5 Hz	9.11
10	10 Hz	8.98
20	20 Hz	8.99
100	100 Hz	9.63

Figure 2.28, occupying pages 67 and 68, shows the filter response for periodic square-wave inputs of different fundamental frequencies:  $f_0 = 0.1, 0.25, 0.5$ , and  $1$  Hz, and with the bandwidth of the low-pass filter being fixed at  $B = 1$  Hz. From Fig. 2.28 we may make the following observations:

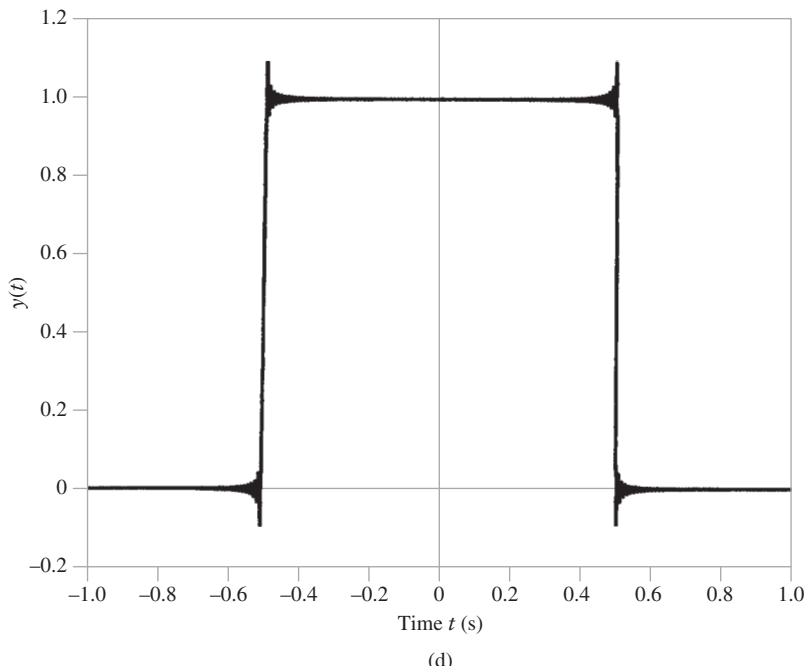
- For  $f_0 = 0.1$  Hz, corresponding to a time-bandwidth product  $BT = 5$ , the filter somewhat distorts the input square pulse, but the shape of the input is still evident at the filter output. Unlike the input, the filter output has nonzero rise and fall times that are inversely proportional to the filter bandwidth. Also, the output exhibits oscillations (ringing) at both the leading and trailing edges.
- As the fundamental frequency  $f_0$  of the input square wave increases, the low-pass filter cuts off more of the higher frequency components of the input. Thus, when  $f_0 = 0.25$  Hz, corresponding to  $BT = 2$ , only the fundamental frequency and the first harmonic component pass through the filter; the rise and fall times of the output are now significant compared with the input pulse duration  $T$ . When  $f_0 = 0.5$  Hz, corresponding to  $BT = 1$ , only the fundamental frequency component of the input square wave is preserved by the filter, resulting in an output that is essentially sinusoidal.



**FIGURE 2.27** Pulse response of ideal low-pass filter for pulse duration  $T = 1\text{s}$  and varying time-bandwidth ( $BT$ ) product. (a)  $BT = 5$ . (b)  $BT = 10$ .



(c)



(d)

**FIGURE 2.27** (continued) (c)  $BT = 20$ . (d)  $BT = 100$ .

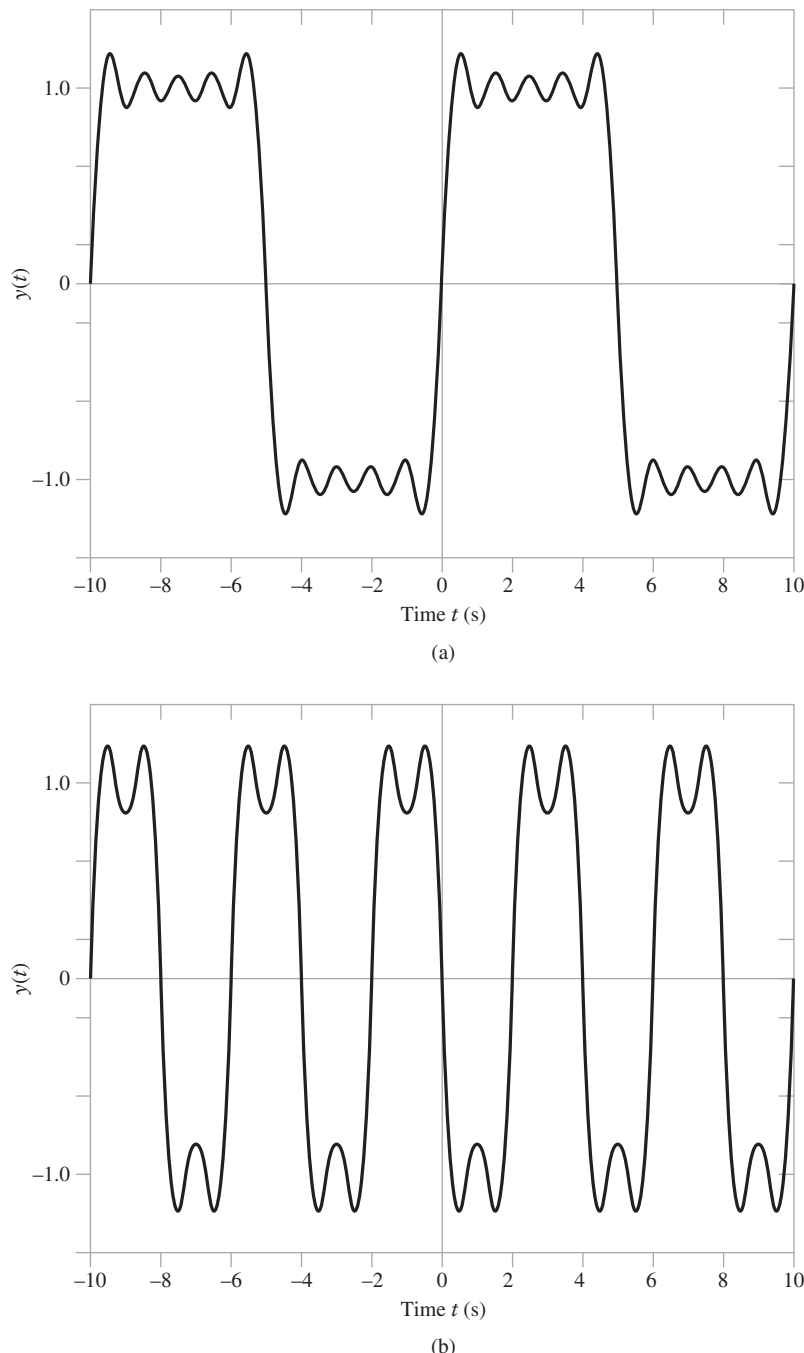


**FIGURE 2.28** Response of ideal low-pass filter to a square wave of varying frequency  $f_0$ .  
(a)  $f_0 = 0.1$  Hz. (b)  $f_0 = 0.25$  Hz.

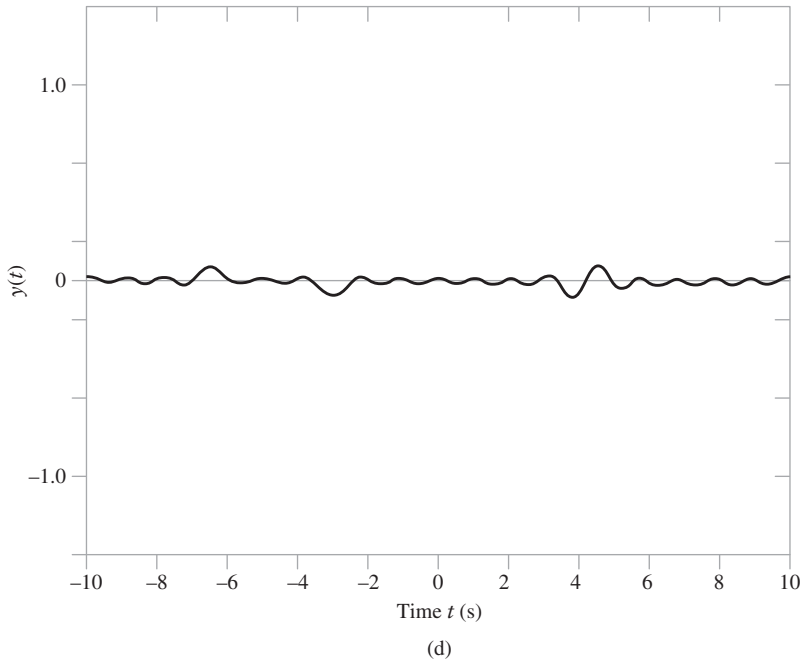
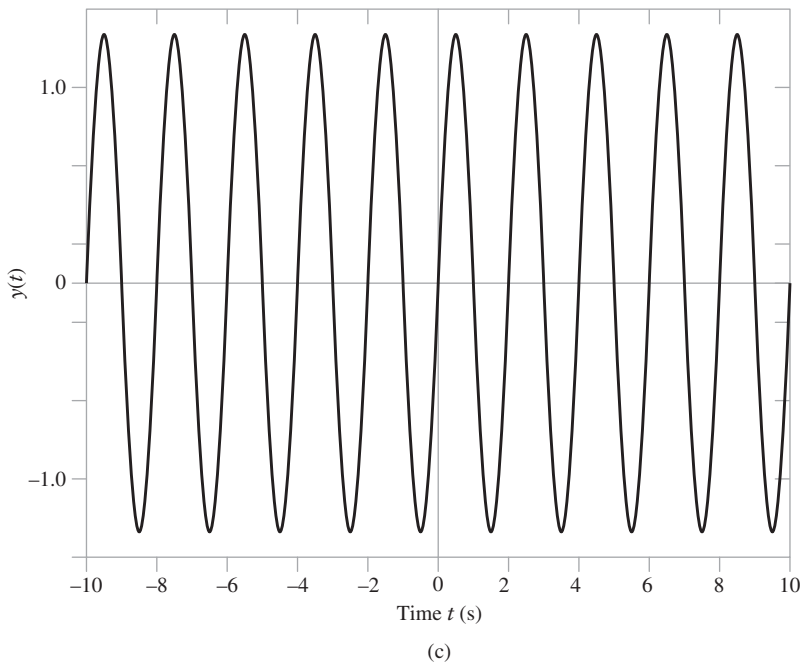


**FIGURE 2.28** (continued) (c)  $f_0 = 0.5$  Hz. (d)  $f_0 = 1$  Hz.

- When the fundamental frequency of the input square wave is increased further to the high value  $f_0 = 1\text{Hz}$ , which corresponds to a time-bandwidth product  $BT = 0.5$ , the dc component becomes the dominant output, and the shape of the input square wave is completely destroyed by the filter.

From these results, we draw an important conclusion: *When using an ideal low-pass filter, we must use a time-bandwidth product  $BT \geq 1$  to ensure that the waveform of the filter input is recognizable from the resulting output.* A value of  $BT$  greater than unity tends to reduce the rise time as well as decay time of the filter pulse response.

### ■ APPROXIMATION OF IDEAL LOW-PASS FILTERS

A filter may be characterized by specifying its impulse response  $h(t)$  or, equivalently, its transfer function  $H(f)$ . However, the application of a filter usually involves the separation of signals on the basis of their spectra (i.e., frequency contents). This, in turn, means that the design of filters is usually carried out in the frequency domain. There are two basic steps involved in the design of a filter:

1. The *approximation* of a prescribed frequency response (i.e., amplitude response, phase response, or both) by a realizable transfer function.
2. The *realization* of the approximating transfer function by a physical device.

For an approximating transfer function  $H(f)$  to be physically realizable, it must represent a *stable* system. Stability is defined here on the basis of the bounded input-bounded output criterion described in Eq. (2.100) that involves the impulse response  $h(t)$ . To specify the corresponding condition for stability in terms of the transfer function, the traditional approach is to replace  $j2\pi f$  with  $s$  and recast the transfer function in terms of  $s$ . The new variable  $s$  is permitted to have a real part as well as an imaginary part. Accordingly, we refer to  $s$  as the *complex frequency*. Let  $H'(s)$  denote the transfer function of the system, defined in the manner described herein. Ordinarily, the approximating transfer function  $H'(s)$  is a rational function, which may therefore be expressed in the *factored form*

$$\begin{aligned} H'(s) &= H(f)|_{j2\pi f=s} \\ &= K \frac{(s - z_1)(s - z_2) \cdots (s - z_m)}{(s - p_1)(s - p_2) \cdots (s - p_n)} \end{aligned}$$

where  $K$  is a scaling factor;  $z_1, z_2, \dots, z_m$  are called the *zeros* of the transfer function, and  $p_1, p_2, \dots, p_n$  are called its *poles*. For a low-pass transfer function, the number of zeros,  $m$ , is less than the number of poles,  $n$ . If the system is causal, then the bounded input-bounded output condition for stability of the system is satisfied by restricting all the poles of the transfer function  $H'(s)$  to be inside the left half of the  $s$ -plane; that is to say,

$$\operatorname{Re}([p_i]) < 0, \quad \text{for all } i$$

Note that the condition for stability involves only the poles of the transfer function  $H'(s)$ ; the zeros may indeed lie anywhere in the  $s$ -plane. Two types of systems may be distinguished, depending on locations of the  $m$  zeros in the  $s$ -plane:

- *Minimum-phase systems*, characterized by a transfer function whose poles and zeros are all restricted to lie inside the left hand of the  $s$ -plane.
- *Nonminimum-phase systems*, whose transfer functions are permitted to have zeros on the imaginary axis as well as the right half of the  $s$ -plane.

Minimum-phase systems distinguish themselves by the property that the phase response of this class of linear time-invariant systems is uniquely related to the gain response.

In the case of low-pass filters where the principal requirement is to approximate the ideal amplitude response shown in Fig. 2.23, we may mention two popular families of filters: *Butterworth filters* and *Chebyshev filters*, both of which have all their zeros at  $s = \infty$ . In a Butterworth filter, the poles of the transfer function  $H'(s)$  lie on a circle with origin as the center and  $2\pi B$  as the radius, where  $B$  is the 3-dB bandwidth of the filter. In a Chebyshev filter, on the other hand, the poles lie on an ellipse. In both cases, of course, the poles are confined to the left half of the  $s$ -plane.

Turning next to the issue of physical realization of the filter, we see that there are two basic options to do this realization, one analog and the other digital:

- ▶ *Analog filters*, built using (a) inductors and capacitors, or (b) capacitors, resistors, and operational amplifiers. The advantage of analog filters is the simplicity of implementation.
- ▶ *Digital filters*, for which the signals are sampled in time and their amplitude is also quantized. These filters are built using digital hardware; hence the name. An important feature of a digital filter is that it is *programmable*, thereby offering a high degree of flexibility in design. In effect, complexity is traded off for flexibility.

## 2.8 Correlation and Spectral Density: Energy Signals

In this section, we continue the characterization of signals and systems by considering the class of energy signals and therefore focusing on the notion of *energy*. (The characterization of signals and systems is completed in Section 2.9, where we consider the other class of signals, power signals.) In particular, we introduce a new parameter called *spectral density*, which is defined as the squared amplitude spectrum of the signal of interest. It turns out that the spectral density is the Fourier transform of the correlation function, which was first introduced under Property 13 in Section 2.2.

### ■ AUTOCORRELATION FUNCTION

Consider an energy signal  $x(t)$  that, for the purpose of generality, is assumed to be complex valued. Following the material presented under the correlation theorem (Property 13) in Section 2.2, we formally define the *autocorrelation function* of the energy signal  $x(t)$  for a *lag*  $\tau$  as

$$R_x(\tau) = \int_{-\infty}^{\infty} x(t)x^*(t - \tau) dt \quad (2.124)$$

According to this formula, the autocorrelation function  $R_x(\tau)$  provides a measure of the similarity between the signal  $x(t)$  and its delayed version  $x(t - \tau)$ . As such, it can be measured using the arrangement shown in Fig. 2.29. The time lag  $\tau$  plays the role of a *scanning* or *searching variable*. Note that  $R_x(\tau)$  is complex valued if  $x(t)$  is complex valued.

From Eq. (2.124) we readily see that the value of the autocorrelation function  $R_x(\tau)$  for  $\tau = 0$  is equal to the energy of the signal  $x(t)$ ; that is,

$$R_x(0) = \int_{-\infty}^{\infty} |x(t)|^2 dt$$

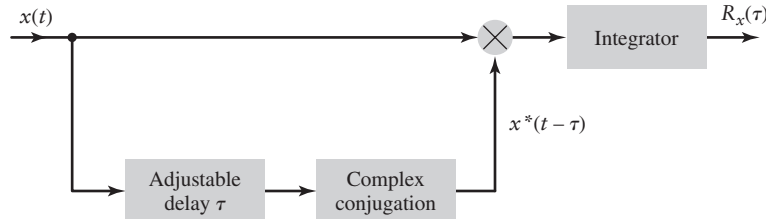


**FIGURE 2.29** Scheme for measuring the autocorrelation function  $R_x(\tau)$  of an energy signal  $x(t)$  for lag  $\tau$ .

## ■ ENERGY SPECTRAL DENSITY

The Rayleigh energy theorem, discussed under Property 14 in Section 2.2, is important because it not only provides a useful method for evaluating the energy of a pulse signal, but also it highlights the squared amplitude spectrum as the distribution of the energy of the signal measured in the frequency domain. It is in light of this theorem that we formally define the *energy spectral density* or *energy density spectrum* of an energy signal  $x(t)$  as

$$\psi_x(f) = |X(f)|^2 \quad (2.125)$$

where  $|X(f)|$  is the amplitude spectrum of  $x(t)$ . Clearly, the energy spectral density  $\psi_x(f)$  is a nonnegative real-valued quantity for all  $f$ , even though the signal  $x(t)$  may itself be complex valued.

## ■ WIENER-KHITCHINE RELATIONS FOR ENERGY SIGNALS

Referring to the correlation theorem described in Eq. (2.53), let  $g_1(t) = g_2(t) = x(t)$ , where  $x(t)$  is an energy signal and therefore Fourier transformable. Under this condition, the resulting left-hand side of Eq. (2.53) defines the autocorrelation function  $R_x(\tau)$  of the signal  $x(t)$ . Correspondingly, in the frequency domain, we have  $G_1(f) = G_2(f) = X(f)$ , in which case the right-hand side of Eq. (2.53) defines the energy spectral density  $\psi_x(f)$ . On this basis, we may therefore state that *given an energy signal  $x(t)$ , the autocorrelation function  $R_x(\tau)$  and energy spectral density  $\psi_x(f)$  form a Fourier-transform pair*. Specifically, we have the pair of relations:

$$\psi_x(f) = \int_{-\infty}^{\infty} R_x(\tau) \exp(-j2\pi f\tau) d\tau \quad (2.126)$$

and

$$R_x(\tau) = \int_{-\infty}^{\infty} \psi_x(f) \exp(j2\pi f\tau) df \quad (2.127)$$

Note, however, that the Fourier transformation in Eq. (2.126) is performed with respect to the adjustable lag  $\tau$ . The pair of equations (2.126) and (2.127) constitutes the *Wiener-Khinchine relations for energy signals*.

From Eqs. (2.126) and (2.127) we readily deduce the following two properties:

1. By setting  $f = 0$  in Eq. (2.126), we have

$$\int_{-\infty}^{\infty} R_x(\tau) d\tau = \psi_x(0)$$

which states that *the total area under the curve of the complex-valued autocorrelation function of a complex-valued energy signal is equal to the real-valued energy spectral  $\psi_x(0)$  at zero frequency.*

2. By setting  $\tau = 0$  in Eq. (2.127), we have

$$\int_{-\infty}^{\infty} \psi_x(f) df = R_x(0)$$

which states that *the total area under the curve of the real-valued energy spectral density of an energy signal is equal to the total energy of the signal.* This second result is merely another way of stating the Rayleigh energy theorem.

### EXAMPLE 2.13 Autocorrelation Function of Sinc Pulse

From Example 2.4, the Fourier transform of the sinc pulse

$$x(t) = A \operatorname{sinc}(2Wt)$$

is given by

$$X(f) = \frac{A}{2W} \operatorname{rect}\left(\frac{f}{2W}\right)$$

Since the rectangular function  $\operatorname{rect}(f/2W)$  is unaffected by squaring, the energy spectral density of  $x(t)$  is therefore

$$\psi_x(f) = \left(\frac{A}{2W}\right)^2 \operatorname{rect}\left(\frac{f}{2W}\right)$$

Taking the inverse Fourier transform of  $\psi_x(f)$ , we find that the autocorrelation function of the sinc pulse  $A \operatorname{sinc}(2Wt)$  is given by

$$R_x(\tau) = \frac{A^2}{2W} \operatorname{sinc}(2W\tau) \quad (2.128)$$

which has a similar waveform, plotted as a function of the lag  $\tau$ , as the sinc pulse itself.

This example teaches us that sometimes it is easier to use an indirect procedure based on the energy spectral density to determine the autocorrelation function of an energy signal rather than using the formula for the autocorrelation function.

### ■ EFFECT OF FILTERING ON ENERGY SPECTRAL DENSITY

Suppose now the energy signal  $x(t)$  is passed through a linear time-invariant system of transfer function  $H(f)$ , yielding the output signal  $y(t)$  as illustrated in Fig. 2.20(a). Then, according to Eq. (2.109), the Fourier transform of the output  $y(t)$  is related to the Fourier transform of the input  $x(t)$  as follows:

$$Y(f) = H(f)X(f)$$

Taking the squared amplitude of both sides of this equation, we readily get

$$\psi_y(f) = |H(f)|^2 \psi_x(f) \quad (2.129)$$

where, by definition,  $\psi_x(f) = |X(f)|^2$  and  $\psi_y(f) = |Y(f)|^2$ . Equation (2.129) states that *when an energy signal is transmitted through a linear time-invariant filter, the energy spectral density of the resulting output equals the energy spectral density of the input multiplied*

by the squared amplitude response of the filter. The simplicity of this statement emphasizes the importance of spectral density as a parameter for characterizing the distribution of the energy of a Fourier transformable signal in the frequency domain.

Moreover, on the basis of the Wiener–Khintchine equations (2.126) and (2.127) and the relationship of Eq. (2.129), we may describe an *indirect method* for evaluating the effect of linear time-invariant filtering on the autocorrelation function of an energy signal:

1. Determine the Fourier transforms of  $x(t)$  and  $h(t)$ , obtaining  $X(f)$  and  $H(f)$ , respectively.
2. Use Eq. (2.129) to determine the energy spectral density  $\psi_y(f)$  of the output  $y(t)$ .
3. Determine  $R_y(\tau)$  by applying the inverse Fourier transform to  $\psi_y(f)$  obtained under point 2.

#### EXAMPLE 2.14 Energy of Low-pass Filtered Version of Rectangular Pulse

A rectangular pulse of unit amplitude and unit duration is passed through an ideal low-pass filter of bandwidth  $B$ , as illustrated in Fig. 2.30(a). Part (b) of the figure depicts the waveform of the rectangular pulse. The amplitude response of the filter is defined by (see Fig. 2.30(c))

$$|H(f)| = \begin{cases} 1, & -B \leq f \leq B \\ 0, & \text{otherwise} \end{cases}$$

The rectangular pulse constituting the filter input has unit energy. We wish to evaluate the effect of varying the bandwidth  $B$  on the energy of the filter output.

We start with the Fourier transform pair:

$$\text{rect}(t) \iff \text{sinc}(f)$$

which represents the normalized version of the Fourier-transform pair given in Eq. (2.10). Hence, with the filter input defined by

$$x(t) = \text{rect}(t)$$

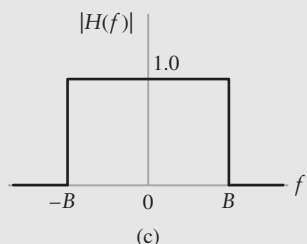
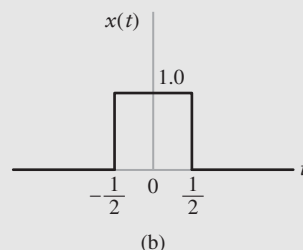
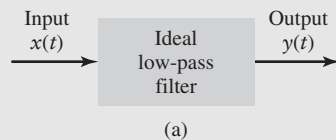


**FIGURE 2.30** (a) Ideal low-pass filtering. (b) Filter input. (c) Amplitude response of the filter.

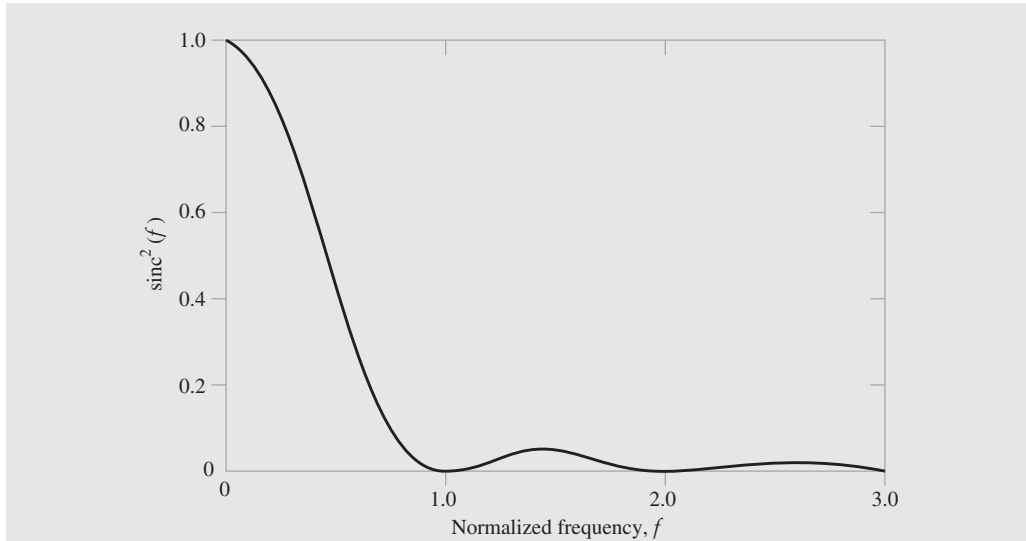


**FIGURE 2.31** Energy spectral density of the filter input  $x(t)$ ; only the values for positive frequencies are shown in the figure.

its Fourier transform equals

$$X(f) = \text{sinc}(f)$$

The energy spectral density of the filter input therefore equals

$$\begin{aligned} \psi_x(f) &= |X(f)|^2 \\ &= \text{sinc}^2(f) \end{aligned} \quad (2.130)$$

This normalized energy spectral density is plotted in Fig. 2.31.

To evaluate the energy spectral density  $\psi_y(f)$  of the filter output  $y(t)$ , we use Eq. (2.129), obtaining

$$\begin{aligned} \psi_y(f) &= |H(f)|^2 \psi_x(f) \\ &= \begin{cases} \psi_x(f), & -B \leq f \leq B \\ 0, & \text{otherwise} \end{cases} \end{aligned} \quad (2.131)$$

The energy of the filter output is therefore

$$\begin{aligned} E_y &= \int_{-\infty}^{\infty} \psi_y(f) df \\ &= \int_{-B}^{B} \psi_x(f) df \\ &= 2 \int_0^B \psi_x(f) df \\ &= 2 \int_0^B \text{sinc}^2(f) df \end{aligned} \quad (2.132)$$

Since the filter input has unit energy, we may also view the result given in Eq. (2.132) as *the ratio of the energy of the filter output to that of the filter input* for the general case of a rectangular pulse of arbitrary amplitude and arbitrary duration, processed by an ideal low-pass

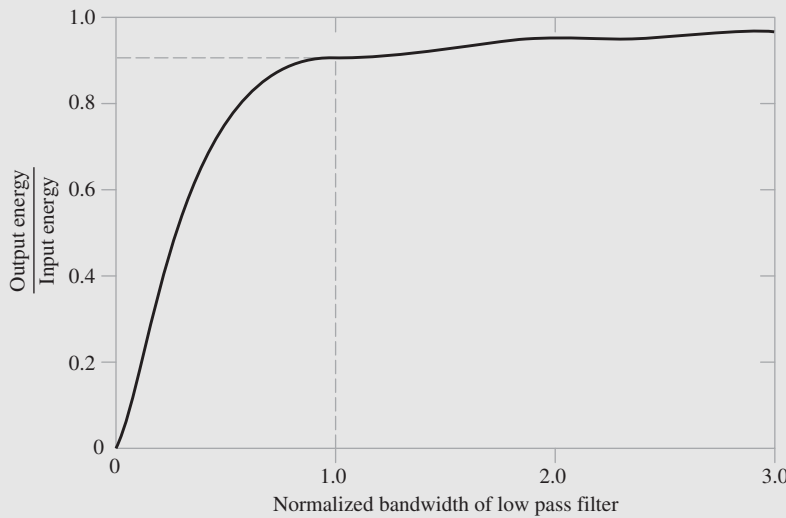


**FIGURE 2.32** Output energy-to-input energy ratio versus normalized bandwidth.

filter of bandwidth  $B$ . Accordingly, we may in general write

$$\begin{aligned} \rho &= \frac{\text{Energy of filter output}}{\text{Energy of filter input}} \\ &= 2 \int_0^B \text{sinc}^2(f) df \end{aligned} \quad (2.133)$$

According to Fig. 2.30(b), the rectangular pulse applied to the filter input has unit duration; hence, the variable  $f$  in Eq. (2.133) represents a *normalized frequency*. Equation (2.133) is plotted in Fig. 2.32. This figure shows that just over 90 percent of the total energy of a rectangular pulse lies inside the main spectral lobe of this pulse.

### ■ INTERPRETATION OF THE ENERGY SPECTRAL DENSITY

Equation (2.129) is important because it not only relates the output energy spectral density of a linear time-invariant system to the input energy spectral density, but it also provides a basis for the physical interpretation of the concept of energy spectral density itself. To be specific, consider the arrangement shown in Fig. 2.33(a), where an energy signal  $x(t)$  is passed through a narrow-band filter followed by an *energy meter*. Figure 2.33(b) shows the idealized amplitude response of the filter. That is, the filter is a band-pass filter whose amplitude response is defined by

$$|H(f)| = \begin{cases} 1, & f_c - \frac{\Delta f}{2} \leq |f| \leq f_c + \frac{\Delta f}{2} \\ 0, & \text{otherwise} \end{cases} \quad (2.134)$$

We assume that the *filter bandwidth*  $\Delta f$  is small enough for the amplitude response of the input signal  $x(t)$  to be essentially flat over the frequency interval covered by the passband

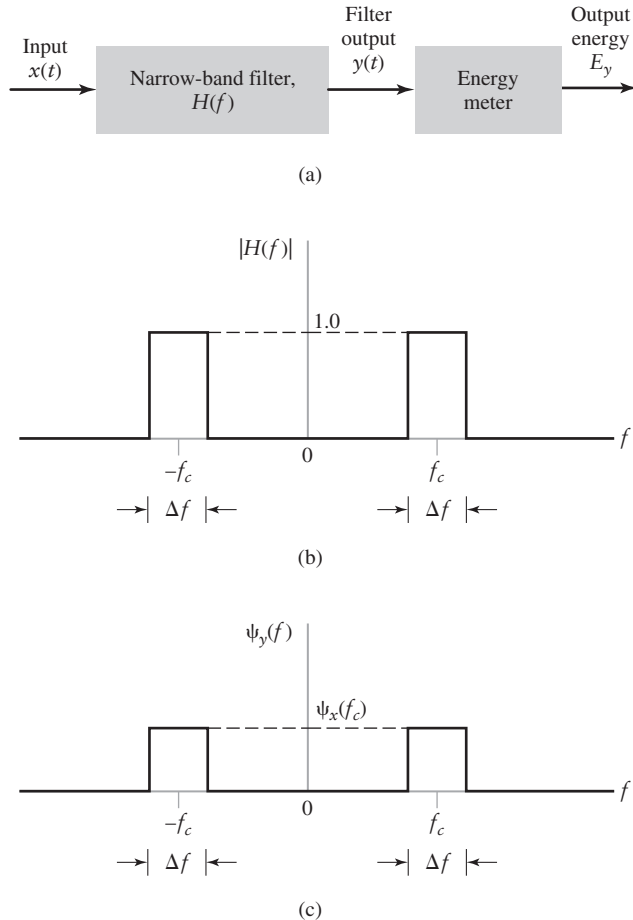


**FIGURE 2.33** (a) Block diagram of system for measuring energy spectral density. (b) Idealized amplitude response of the filter. (c) Energy spectral density of the filter output.

of the filter. Accordingly, we may express the amplitude spectrum of the filter output by the approximate formula

$$\begin{aligned} |Y(f)| &= |H(f)||X(f)| \\ &\approx \begin{cases} |X(f_c)|, & f_c - \frac{\Delta f}{2} \leq |f| \leq f_c + \frac{\Delta f}{2} \\ 0, & \text{otherwise} \end{cases} \end{aligned} \quad (2.135)$$

Correspondingly, the energy spectral density  $\psi_y(f)$  of the filter output  $y(t)$  is approximately related to the energy spectral density  $\psi_x(f)$  of the filter input  $x(t)$  as follows:

$$\psi_y(f) \approx \begin{cases} \psi_x(f_c), & f_c - \frac{\Delta f}{2} \leq |f| \leq f_c + \frac{\Delta f}{2} \\ 0, & \text{otherwise} \end{cases} \quad (2.136)$$

This relation is illustrated in Fig. 2.33(c), which shows that only the frequency components of the signal  $x(t)$  that lie inside the narrow passband of the ideal band-pass filter

reach the output. From Rayleigh's energy theorem, the energy of the filter output  $y(t)$  is given by

$$\begin{aligned} E_y &= \int_{-\infty}^{\infty} \psi_y(f) df \\ &= 2 \int_0^{\infty} \psi_y(f) df \end{aligned}$$

In light of Eq. (2.136), we may approximate  $E_y$  as

$$E_y \approx 2\psi_x(f_c) \Delta f \quad (2.137)$$

The multiplying factor 2 accounts for the contributions of negative as well as positive frequency components. We may rewrite Eq. (2.137) in the form

$$\psi_x(f_c) \approx \frac{E_y}{2\Delta f} \quad (2.138)$$

Equation (2.138) states that the energy spectral density of the filter input at some frequency  $f_c$  equals the energy of the filter output divided by  $2\Delta f$ , where  $\Delta f$  is the filter bandwidth centered on  $f_c$ . We may therefore interpret the energy spectral density of an energy signal for any frequency  $f$  as *the energy per unit bandwidth, which is contributed by frequency components of the signal around the frequency  $f$* .

The arrangement shown in the block diagram of Fig. 2.33(a) thus provides the basis for measuring the energy spectral density of an energy signal. Specifically, by using a *variable* band-pass filter to scan the frequency band of interest and determining the energy of the filter output for each midband frequency setting of the filter, a plot of the energy spectral density versus frequency is obtained. Note, however, for the formula of Eq. (2.138) to hold and therefore for the arrangement of Fig. 2.33(a) to work, the bandwidth  $\Delta f$  must remain fixed for varying  $f_c$ .

### ■ CROSS-CORRELATION OF ENERGY SIGNALS

The autocorrelation function provides a measure of the similarity between a signal and its own time-delayed version. In a similar way, we may use the *cross-correlation function* as a measure of the similarity between one signal and the time-delayed version of a second signal. Let  $x(t)$  and  $y(t)$  denote a pair of complex-valued energy signals. The cross-correlation function of this pair of signals is defined by

$$R_{xy}(\tau) = \int_{-\infty}^{\infty} x(t)y^*(t - \tau) dt \quad (2.139)$$

We see that if the two signals  $x(t)$  and  $y(t)$  are somewhat similar, then the cross-correlation function  $R_{xy}(\tau)$  will be finite over some range of  $\tau$ , thereby providing a quantitative measure of the similarity, or coherence, between them. The energy signals  $x(t)$  and  $y(t)$  are said to be *orthogonal* over the entire time interval if  $R_{xy}(0)$  is zero — that is, if

$$\int_{-\infty}^{\infty} x(t)y^*(t) dt = 0 \quad (2.140)$$

Equation (2.139) defines one possible value for the cross-correlation function for a specified value of the delay variable  $\tau$ . We may define a second cross-correlation function for

the energy signals  $x(t)$  and  $y(t)$  as

$$R_{yx}(\tau) = \int_{-\infty}^{\infty} y(t)x^*(t - \tau) dt \quad (2.141)$$

From the definitions of the cross-correlation functions  $R_{xy}(\tau)$  and  $R_{yx}(\tau)$  just given, we obtain the fundamental relationship

$$R_{xy}(\tau) = R_{yx}^*(-\tau) \quad (2.142)$$

Equation (2.142) indicates that unlike convolution, correlation is not in general commutative; that is,  $R_{xy}(\tau) \neq R_{yx}(\tau)$ .

To characterize the cross-correlation behavior of energy signals in the frequency domain, we introduce the notion of *cross-spectral density*. Specifically, given a pair of complex-valued energy signals  $x(t)$  and  $y(t)$ , we define their cross-spectral densities, denoted by  $\psi_{xy}(f)$  and  $\psi_{yx}(f)$ , as the respective Fourier transforms of the cross-correlation functions  $R_{xy}(\tau)$  and  $R_{yx}(\tau)$ , as shown by

$$\psi_{xy}(f) = \int_{-\infty}^{\infty} R_{xy}(\tau) \exp(-j2\pi f\tau) d\tau \quad (2.143)$$

and

$$\psi_{yx}(f) = \int_{-\infty}^{\infty} R_{yx}(\tau) \exp(-j2\pi f\tau) d\tau \quad (2.144)$$

In accordance with the correlation theorem (i.e., Property 13 of Section 2.2), we thus have

$$\psi_{xy}(f) = X(f)Y^*(f) \quad (2.145)$$

and

$$\psi_{yx}(f) = Y(f)X^*(f) \quad (2.146)$$

From this pair of relations, we readily see two properties of the cross-spectral density.

1. Unlike the energy spectral density, cross-spectral density is complex valued in general.
2.  $\psi_{xy}(f) = \psi_{yx}^*(f)$  from which it follows that, in general,  $\psi_{xy}(f) \neq \psi_{yx}(f)$ .

► **Drill Problem 2.15** Derive the relationship of Eq. (2.142) between the two cross-correlation functions  $R_{xy}(t)$  and  $R_{yx}(t)$ . ◀

► **Drill Problem 2.16** Consider the decaying exponential pulse

$$g(t) = \begin{cases} \exp(-at), & t > 0 \\ 1, & t = 0 \\ 0, & t < 0 \end{cases}$$

Determine the energy spectral density of the pulse  $g(t)$ . ◀

► **Drill Problem 2.17** Repeat Problem 2.16 for the double exponential pulse

$$g(t) = \begin{cases} \exp(-at), & t > 0 \\ 1, & t = 0 \\ \exp(at), & t < 0 \end{cases} \quad \blacktriangleleft$$

## 2.9 Power Spectral Density

In this section, we expand the important notion of spectral density to include the class of power signals. The *average power* of a signal  $x(t)$  is defined by

$$P = \lim_{T \rightarrow \infty} \frac{1}{2T} \int_{-T}^T |x(t)|^2 dt \quad (2.147)$$

The signal  $x(t)$  is said to be a *power signal* if the condition

$$P < \infty$$

holds. Examples of power signals include periodic signals and noise. We consider periodic signals in this section. (Noise is considered in Chapter 8.)

To develop a frequency-domain distribution of power, we need to know the Fourier transform of the signal  $x(t)$ . However, this may pose a problem, because power signals have infinite energy and may therefore not be Fourier transformable. To overcome the problem, we consider a *truncated* version of the signal  $x(t)$ . In particular, we define

$$\begin{aligned} x_T(t) &= x(t) \operatorname{rect}\left(\frac{t}{2T}\right) \\ &= \begin{cases} x(t), & -T \leq t \leq T \\ 0, & \text{otherwise} \end{cases} \end{aligned} \quad (2.148)$$

As long as the duration  $T$  is finite, the truncated signal  $x_T(t)$  has finite energy; hence  $x_T(t)$  is Fourier transformable. Let  $X_T(f)$  denote the Fourier transform of  $x_T(t)$ ; that is,

$$x_T(t) \iff X_T(f)$$

Using the truncated signal  $x_T(t)$ , we may rewrite Eq. (2.147) for the average power  $P$  in terms of  $x_T(t)$  as

$$P = \lim_{T \rightarrow \infty} \frac{1}{2T} \int_{-\infty}^{\infty} |x_T(t)|^2 dt \quad (2.149)$$

Since  $x_T(t)$  has finite energy, we may use the Rayleigh energy theorem to express the energy of  $x_T(t)$  in terms of its Fourier transform  $X_T(f)$  as

$$\int_{-\infty}^{\infty} |x_T(t)|^2 dt = \int_{-\infty}^{\infty} |X_T(f)|^2 df$$

where  $|X_T(f)|$  is the amplitude spectrum of  $x_T(t)$ . Accordingly, we may rewrite Eq. (2.149) in the equivalent form

$$P = \lim_{T \rightarrow \infty} \frac{1}{2T} \int_{-\infty}^{\infty} |X_T(f)|^2 df \quad (2.150)$$

As the duration  $T$  increases, the energy of  $x_T(t)$  increases. Correspondingly, the energy spectral density  $|X_T(f)|^2$  increases with  $T$ . Indeed as  $T$  approaches infinity, so will  $|X_T(f)|^2$ . However, for the average power  $P$  to be finite,  $|X_T(f)|^2$  must approach infinity at the same rate as  $T$ . This requirement ensures the *convergence* of the integral on the right-hand side of Eq. (2.150) in the limit as  $T$  approaches infinity. The convergence, in turn, permits us to *interchange the order in which the limiting operation and integration in Eq. (2.150) are performed*. We may then rewrite this equation as

$$P = \int_{-\infty}^{\infty} \left( \lim_{T \rightarrow \infty} \frac{1}{2T} |X_T(f)|^2 \right) df \quad (2.151)$$

Let the integrand in Eq. (2.151) be denoted by

$$S_x(f) = \lim_{T \rightarrow \infty} \frac{1}{2T} |X_T(f)|^2 \quad (2.152)$$

The frequency-dependent function  $S_x(f)$  is called the *power spectral density* or *power spectrum* of the power signal  $x(t)$ , and the quantity  $(|X_T(f)|^2/2T)$  is called the *periodogram* of the signal.

From Eq. (2.152), we readily see that the power spectral density is a nonnegative real-valued quantity for all frequencies. Moreover, from Eq. (2.152) we readily see that

$$P = \int_{-\infty}^{\infty} S_x(f) df \quad (2.153)$$

Equation (2.153) states: *the total area under the curve of the power spectral density of a power signal is equal to the average power of that signal*. The power spectral density of a power signal therefore plays a role similar to the energy spectral density of an energy signal.

► **Drill Problem 2.18** In an implicit sense, Eq. (2.153) embodies *Parseval's power theorem*, which states that for a *periodic signal*  $x(t)$  we have

$$\frac{1}{T} \int_{-T/2}^{T/2} |x(t)|^2 dt = \sum_{n=-\infty}^{\infty} |X(nf_0)|^2$$

where  $T$  is the period of the signal,  $f_0$  is the fundamental frequency, and  $X(nf_0)$  is the Fourier transform of  $x(t)$  evaluated at the frequency  $nf_0$ . Prove this theorem. ◀

### EXAMPLE 2.15 Modulated Wave

Consider the *modulated wave*

$$x(t) = g(t) \cos(2\pi f_c t) \quad (2.154)$$

where  $g(t)$  is a power signal that is band-limited to  $B$  hertz. We refer to  $x(t)$  as a “modulated wave” in the sense that the amplitude of the sinusoidal “carrier” of frequency  $f_c$  is varied linearly with the signal  $g(t)$ . (The subject of modulation is covered in detail in Chapter 3.) We wish to find the power spectral density of  $x(t)$  in terms of that of  $g(t)$ , given that the frequency  $f_c$  is larger than the bandwidth  $B$ .

Let  $g_T(t)$  denote the truncated version of  $g(t)$ , defined in a manner similar to that described in Eq. (2.148). Correspondingly, we may express the truncated version of  $x(t)$  as

$$x_T(t) = g_T(t) \cos(2\pi f_c t) \quad (2.155)$$

Since

$$\cos(2\pi f_c t) = \frac{1}{2} [\exp(j2\pi f_c t) + \exp(-j2\pi f_c t)], \quad (2.156)$$

it follows from the frequency-shifting property (i. e., Property 6) of the Fourier transform that

$$X_T(f) = \frac{1}{2} [G_T(f - f_c) + G_T(f + f_c)] \quad (2.157)$$

where  $G_T(f)$  is the Fourier transform of  $g_T(t)$ .

Given that  $f_c > B$ , we find that  $G_T(f - f_c)$  and  $G_T(f + f_c)$  represent nonoverlapping spectra; their product is therefore zero. Accordingly, using Eq. (2.157) to evaluate the squared amplitude of  $X_T(f)$ , we get

$$|X_T(f)|^2 = \frac{1}{4} [|G_T(f - f_c)|^2 + |G_T(f + f_c)|^2] \quad (2.158)$$

Finally, applying the definition of Eq. (2.152) for the power spectral density of the power signal  $g(t)$  to Eq (2.158), we get the desired result:

$$S_x(f) = \frac{1}{4} [S_g(f - f_c) + S_g(f + f_c)] \quad (2.159)$$

Except for the scaling factor 1/4, the power spectral density of the modulated wave  $x(t)$  is equal to the sum of the power spectral density  $S_g(f)$  shifted to the right by  $f_c$  and the  $S_g(f)$  shifted to the left by the same amount  $f_c$ .

## 2.10 Numerical Computation of the Fourier Transform

The material presented in this chapter clearly testifies to the importance of the Fourier transform as a theoretical tool for the representation of deterministic signals and linear time-invariant systems. The importance of the Fourier transform is further enhanced by the fact that there exists a class of algorithms called fast Fourier transform algorithms for the numerical computation of the Fourier transform in a highly efficient manner.

The fast Fourier transform algorithm is itself derived from the *discrete Fourier transform* in which, as the name implies, both time and frequency are represented in discrete form. The discrete Fourier transform provides an *approximation* to the Fourier transform. In order to properly represent the information content of the original signal, we have to take special care in performing the sampling operations involved in defining the discrete Fourier transform. A detailed treatment of the sampling process will be presented in Chapter 5. For the present, it suffices to say that given a band-limited signal, the sampling rate should be greater than twice the highest frequency component of the input signal. Moreover, if the samples are uniformly spaced by  $T_s$  seconds, the spectrum of the signal becomes periodic, repeating every  $f_s = (1/T_s)$  Hz. Let  $N$  denote the number of frequency samples contained in an interval  $f_s$ . Hence, the *frequency resolution* involved in the numerical computation of the Fourier transform is defined by

$$\Delta f = \frac{f_s}{N} = \frac{1}{NT_s} = \frac{1}{T} \quad (2.160)$$

where  $T = NT_s$  is the total duration of the signal.

Consider then a *finite data sequence*  $\{g_0, g_1, \dots, g_{N-1}\}$ . For brevity, we refer to this sequence as  $g_n$ , in which the subscript is the *time index*  $n = 0, 1, \dots, N - 1$ . Such a sequence may represent the result of sampling an analog signal  $g(t)$  at times  $t = 0, T_s, \dots, (N - 1)T_s$ , where  $T_s$  is the sampling interval. The ordering of the data sequence defines the sample time in that  $g_0, g_1, \dots, g_{N-1}$  denote samples of  $g(t)$  taken at times  $0, T_s, \dots, (N - 1)T_s$ , respectively. Thus we have

$$g_n = g(nT_s) \quad (2.161)$$

We formally define the *discrete Fourier transform* (DFT) of the sequence  $g_n$  as

$$G_k = \sum_{n=0}^{N-1} g_n \exp\left(-\frac{j2\pi}{N}kn\right), \quad k = 0, 1, \dots, N-1 \quad (2.162)$$

The sequence  $\{G_0, G_1, \dots, G_{N-1}\}$  is called the *transform sequence*. For brevity, we refer to this new sequence as  $G_k$ , in which the subscript is the *frequency index*  $k = 0, 1, \dots, N-1$ . Correspondingly, we define the *inverse discrete Fourier transform* (IDFT) of  $G_k$  as

$$g_n = \frac{1}{N} \sum_{k=0}^{N-1} G_k \exp\left(\frac{j2\pi}{N}kn\right), \quad n = 0, 1, \dots, N-1 \quad (2.163)$$

The DFT and the IDFT form a transform pair. Specifically, given the data sequence  $g_n$ , we may use the DFT to compute the transform sequence  $G_k$ ; and given the transform sequence  $G_k$ , we may use the IDFT to recover the original data sequence  $g_n$ . A distinctive feature of the DFT is that for the finite summations defined in Eqs. (2.162) and (2.163), there is no question of convergence.

When discussing the DFT (and algorithms for its computation), the words “sample” and “point” are used interchangeably to refer to a sequence value. Also, it is common practice to refer to a sequence of length  $N$  as an  *$N$ -point sequence*, and refer to the DFT of a data sequence of length  $N$  as an  *$N$ -point DFT*.

### ■ INTERPRETATIONS OF THE DFT AND THE IDFT

We may visualize the DFT process, described in Eq. (2.162), as a collection of  $N$  *complex heterodyning* and *averaging* operations, as shown in Fig. 2.34(a); in the picture depicted herein, heterodyning refers to the multiplication of data sequence  $g_n$  by a complex exponential. We say that the heterodyning is complex in that samples of the data sequence are multiplied by *complex exponential sequences*. There are a total of  $N$  complex exponential sequences to be considered, corresponding to the frequency index  $k = 0, 1, \dots, N-1$ . Their periods have been selected in such a way that each complex exponential sequence has precisely an integer number of cycles in the total interval 0 to  $N-1$ . The zero-frequency response, corresponding to  $k = 0$ , is the only exception.

For the interpretation of the IDFT process, described in Eq. (2.163), we may use the scheme shown in Fig. 2.34(b). Here we have a collection of  $N$  *complex signal generators*, each of which produces the *complex exponential sequence*

$$\begin{aligned} \exp\left(\frac{j2\pi}{N}kn\right) &= \cos\left(\frac{2\pi}{N}kn\right) + j \sin\left(\frac{2\pi}{N}kn\right) \\ &= \left\{ \cos\left(\frac{2\pi}{N}kn\right), \sin\left(\frac{2\pi}{N}kn\right) \right\}, \quad k = 0, 1, \dots, N-1 \end{aligned} \quad (2.164)$$

Thus, in reality, each complex signal generator consists of a pair of generators that output a cosinusoidal and a sinusoidal sequence of  $k$  cycles per observation interval. The output of each complex signal generator is weighted by the complex Fourier coefficient  $G_k$ . At each time index  $n$ , an output is formed by summing the weighted complex generator outputs.

It is noteworthy that although the DFT and the IDFT are similar in their mathematical formulations, as described in Eqs. (2.162) and (2.163), their interpretations, as depicted in Figs. 2.34(a) and 2.34(b), are so completely different.

Also, the addition of harmonically related periodic signals, as in Figs. 2.34(a) and 2.34(b), suggests that the sequences  $G_k$  and  $g_n$  must be both periodic. Moreover, the proce-

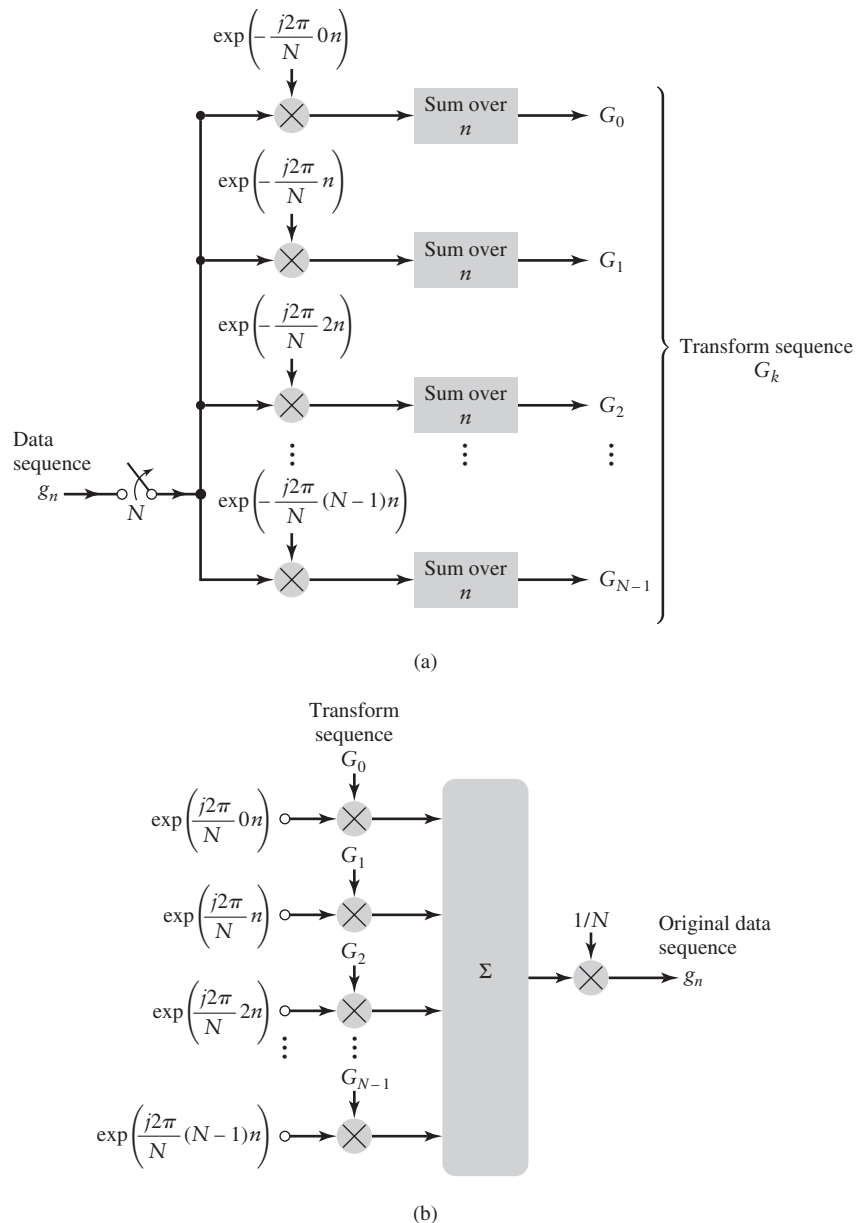


**FIGURE 2.34** Interpretations of (a) the DFT as an analyzer of the data sequence  $g_n$ , and (b) the IDFT as a synthesizer of  $g_n$ .

sors shown in Figs. 2.34(a) and 2.34(b) must be linear, suggesting that the DFT and IDFT are both linear operations. This important property is also obvious from the defining equations (2.162) and (2.163).

### ■ FAST FOURIER TRANSFORM ALGORITHMS

In the discrete Fourier transform (DFT), both the input and the output consist of sequences of numbers defined at uniformly spaced points in time and frequency, respectively. This feature makes the DFT ideally suited for direct numerical evaluation on a digital computer.

Moreover, the computation can be implemented most efficiently using a class of algorithms called *fast Fourier transform (FFT) algorithms*.<sup>2</sup> An algorithm refers to a “recipe” that can be written in the form of a computer program.

FFT algorithms are computationally efficient because they use a greatly reduced number of arithmetic operations as compared to the brute force computation of the DFT. Basically, an FFT algorithm attains its computational efficiency by following a *divide-and-conquer strategy*, whereby the original DFT computation is decomposed successively into smaller DFT computations. In this section, we describe one version of a popular FFT algorithm, the development of which is based on such a strategy.

To proceed with the development, we first rewrite Eq. (2.162), defining the DFT of  $g_n$ , in the simplified form

$$G_k = \sum_{n=0}^{N-1} g_n W^{nk}, \quad k = 0, 1, \dots, N-1 \quad (2.165)$$

where the new coefficient  $W$  is defined by

$$W = \exp\left(-\frac{j2\pi}{N}\right) \quad (2.166)$$

From this definition, we see that

$$\begin{aligned} W^N &= \exp(-j2\pi) = 1 \\ W^{N/2} &= \exp(-j\pi) = -1 \\ W^{(k+LN)(n+mN)} &= W^{kn}, \quad \text{for } m, l = 0, \pm 1, \pm 2, \dots \end{aligned}$$

That is,  $W^{kn}$  is periodic with period  $N$ . The *periodicity* of  $W^{kn}$  is a key feature in the development of FFT algorithms.

Let  $N$ , the number of points in the data sequence, be *an integer power of two*, as shown by

$$N = 2^L$$

where  $L$  is an integer. Since  $N$  is an even integer,  $N/2$  is an integer, and so we may divide the data sequence into the first half and the last half of the points. Thus, we may rewrite Eq. (2.165) in the equivalent form

$$\begin{aligned} G_k &= \sum_{n=0}^{(N/2)-1} g_n W^{nk} + \sum_{n=N/2}^{N-1} g_n W^{nk} \\ &= \sum_{n=0}^{(N/2)-1} g_n W^{nk} + \sum_{n=0}^{(N/2)-1} g_{n+N/2} W^{k(n+N/2)} \\ &= \sum_{n=0}^{(N/2)-1} (g_n + g_{n+N/2} W^{kN/2}) W^{kn}, \quad k = 0, 1, \dots, N-1 \quad (2.167) \end{aligned}$$

Note that in the second line of Eq. (2.167), we changed the index of the second summation term so that both summation terms cover the same range. Since  $W^{N/2} = -1$ , we have

$$W^{kN/2} = (-1)^k$$

---

<sup>2</sup>The fast Fourier transform (FFT) algorithm has a long history. Its modern discovery (or rediscovery to be more precise) is attributed to Cooley and Tukey in 1965; see the paper by Cooley (1992) for details.

For the evaluation of Eq. (2.167), we proceed by considering two cases, one corresponding to even values of  $k$  and the other corresponding to odd values of  $k$ . For the case of even  $k$ , let  $k = 2l$ , where  $l = 0, 1, \dots, (N/2)$ . Hence, we define

$$x_n = g_n + g_{n+N/2} \quad (2.168)$$

Then, for even  $k$  we may put Eq. (2.167) into the new form

$$G_{2l} = \sum_{n=0}^{(N/2)-1} x_n (W^2)^{ln}, \quad l = 0, 1, \dots, \frac{N}{2} - 1 \quad (2.169)$$

From the definition of  $W$  given in Eq. (2.166), we readily see that

$$\begin{aligned} W^2 &= \exp\left(-\frac{j4\pi}{N}\right) \\ &= \exp\left(-\frac{j2\pi}{N/2}\right) \end{aligned}$$

Hence, we recognize the sum on the right-hand side of Eq. (2.169) as the  $(N/2)$ -point DFT of the sequence  $x_n$ .

Consider next the remaining case of odd  $k$ , and let

$$k = 2l + 1, \quad l = 0, 1, \dots, \frac{N}{2} - 1$$

Then, recognizing that for odd  $k$ ,  $W^{kN/2} = -1$ , we may define

$$y_n = g_n - g_{n+N/2} \quad (2.170)$$

Hence, for the case of odd  $k$ , we may put Eq. (2.167) into the corresponding form

$$\begin{aligned} G_{2l+1} &= \sum_{n=0}^{(N/2)-1} y_n W^{(2l+1)n} \\ &= \sum_{n=0}^{(N/2)-1} [y_n W^n] (W^2)^{ln}, \quad l = 0, 1, \dots, \frac{N}{2} - 1 \end{aligned} \quad (2.171)$$

We recognize the sum on the right-hand side of Eq. (2.171) as the  $(N/2)$ -point DFT of the modified sequence  $y_n W^n$ . The coefficient  $W^n$  multiplying  $y_n$  is called a *twiddle factor*.

Equations (2.169) and (2.171) show that the even- and odd-valued samples of the transform sequence  $G_k$  can be obtained from the  $(N/2)$ -point DFTs of the sequences  $x_n$  and  $y_n W^n$ , respectively. The sequences  $x_n$  and  $y_n$  are themselves related to the original data sequence  $g_n$  by Eqs. (2.168) and (2.170), respectively. Thus, the problem of computing an  $N$ -point DFT is reduced to that of computing two  $(N/2)$ -point DFTs. This procedure is repeated a second time, whereby an  $(N/2)$ -point is decomposed into two  $(N/4)$ -point DFTs. The decomposition (or, more precisely, the divide-and-conquer procedure) is continued in this fashion until (after  $L = \log_2 N$  stages), we reach the trivial case of  $N$  single-point DFTs.

Figure 2.35 illustrates the computations involved in applying the formulas of Eqs. (2.169) and (2.171) to an 8-point data sequence; that is,  $N = 8$ . In constructing the left-hand portions of the figure, we have used signal-flow graph notation. A *signal-flow graph* consists of an interconnection of *nodes* and *branches*. The *direction* of signal transmission along a branch is indicated by an arrow. A branch multiplies the variable at a node (to which it is connected) by the branch *transmittance*. A node sums the outputs of all incoming branches. The convention used for branch transmittances in Fig. 2.35 is as follows.

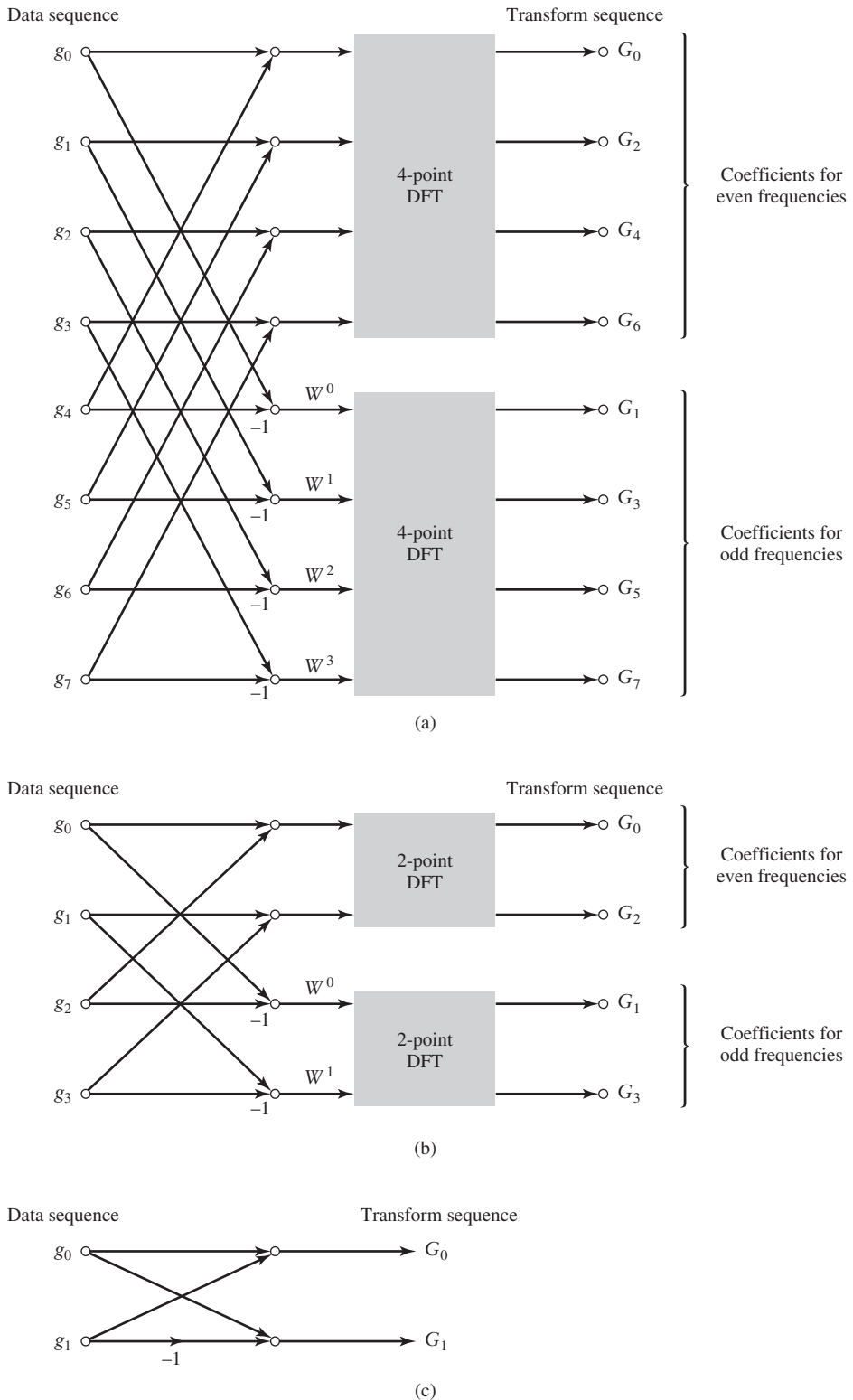


**FIGURE 2.35** (a) Reduction of 8-point DFT into two 4-point DFTs. (b) Reduction of 4-point DFT into two 2-point DFTs. (c) Trivial case of 2-point DFT.

When no coefficient is indicated on a branch, the transmittance of that branch is assumed to be unity. For other branches, the transmittance of a branch is indicated by  $-1$  or an integer power of  $W$ , placed alongside the arrow on the branch.

Thus, in Fig. 2.35(a), the computation of an 8-point DFT is reduced to that of two 4-point DFTs. The procedure for the 8-point DFT is mimicked to simplify the computation of the 4-point DFT. This is illustrated in Fig. 2.35(b), where the computation of a 4-point DFT is reduced to that of two 2-point DFTs. Finally, the computation of a 2-point DFT is shown in Fig. 2.35(c).

Combining the ideas described in Fig. 2.35, we obtain the complete signal-flow graph of Fig. 2.36 for the computation of the 8-point DFT. A repetitive structure, called a *butterfly*, can be discerned in the FFT algorithm of Fig. 2.36; a butterfly has two inputs and two outputs. Examples of butterflies (for the three stages of the algorithm) are illustrated by the bold-faced lines in Fig. 2.36.

For the general case of  $N = 2^L$ , the algorithm requires  $L = \log_2 N$  stages of computation. Each stage requires  $(N/2)$  butterflies. Each butterfly involves one complex multiplication and two complex additions (to be precise, one addition and one subtraction). Accordingly, the FFT structure described here requires  $(N/2) \log_2 N$  complex multiplications

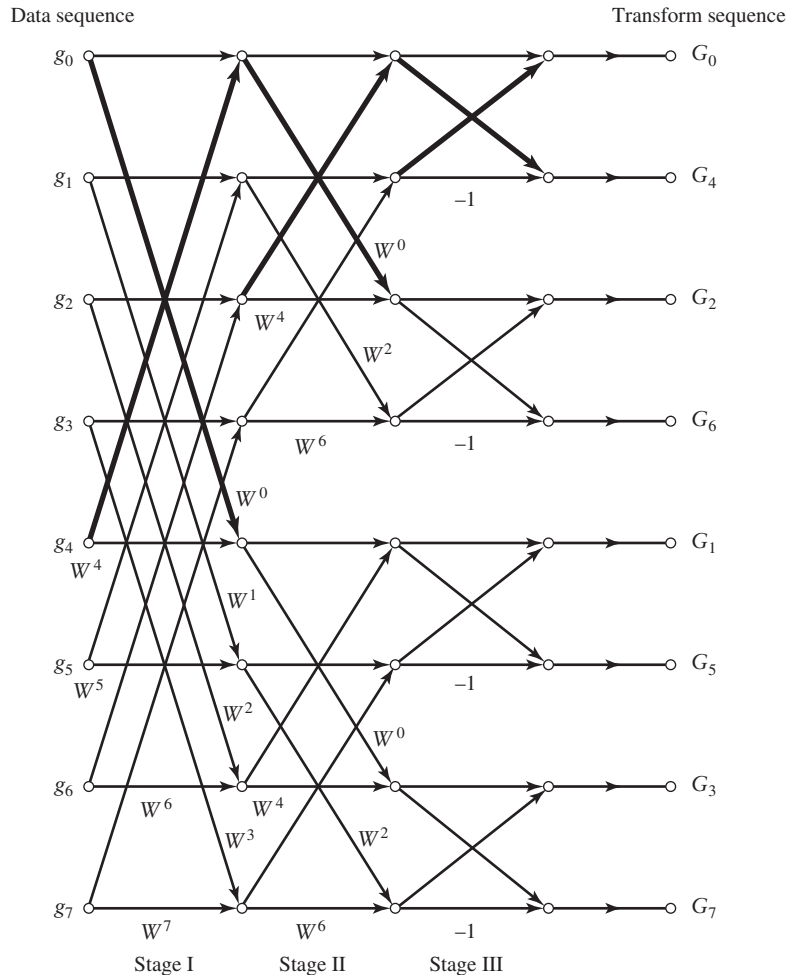


**FIGURE 2.36** Decimation-in-frequency FFT algorithm.

and  $N \log_2 N$  complex additions. (Actually, the number of multiplications quoted is pessimistic, because we may omit all twiddle factors  $W^0 = 1$  and  $W^{N/2} = -1$ ,  $W^{N/4} = -j$ ,  $W^{3N/4} = j$ .) This computational complexity is significantly smaller than that of the  $N^2$  complex multiplications and  $N(N - 1)$  complex additions required for the *direct* computation of the DFT. The computational savings made possible by the FFT algorithm become more substantial as we increase the data length  $N$ .

We may establish two other important features of the FFT algorithm by carefully examining the signal-flow graph shown in Fig. 2.36:

1. At each stage of the computation, the new set of  $N$  complex numbers resulting from the computation can be stored in the same memory locations used to store the previous set. This kind of computation is referred to as *in-place computation*.
2. The samples of the transform sequence  $G_k$  are stored in a *bit-reversed order*. To illustrate the meaning of this latter terminology, consider Table 2.2 constructed for the case of  $N = 8$ . At the left of the table, we show the eight possible values of the frequency index  $k$  (in their natural order) and their 3-bit binary representations. At the right of the table, we show the corresponding bit-reversed binary representations and indices. We observe that the bit-reversed indices in the right-most column of Table 2.2 appear in the same order as the indices at the output of the FFT algorithm in Fig. 2.36.

**TABLE 2.2 Illustrating Bit Reversal**

Frequency Index, $k$	Binary Representation	Bit-Reversed Binary Representation	Bit-Reversed Index
0	000	000	0
1	001	100	4
2	010	010	2
3	011	110	6
4	100	001	1
5	101	101	5
6	110	011	3
7	111	111	7

The FFT algorithm depicted in Fig. 2.36 is referred to as a *decimation-in-frequency algorithm*, because the transform (frequency) sequence  $G_k$  is divided successively into smaller subsequences. In another popular FFT algorithm, called a *decimation-in-time* algorithm, the data (time) sequence  $g_n$  is divided successively into smaller subsequences. Both algorithms have the same computational complexity. They differ from each other in two respects. First, for decimation-in-frequency, the input is in natural order, whereas the output is in bit-reversed order. The reverse is true for decimation-in-time. Second, the butterfly for decimation-in-time is slightly different from that for decimation-in-frequency. The reader is invited to derive the details of the decimation-in-time algorithm using the divide-and-conquer strategy that led to the development of the algorithm described in Fig. 2.36; See Problem 2.50.

### ■ COMPUTATION OF THE IDFT

The IDFT of the transform sequence  $G_k$  is defined by Eq. (2.163). We may rewrite this equation in terms of the complex parameter  $W$  as

$$g_n = \frac{1}{N} \sum_{k=0}^{N-1} G_k W^{-kn}, \quad n = 0, 1, \dots, N - 1 \quad (2.172)$$

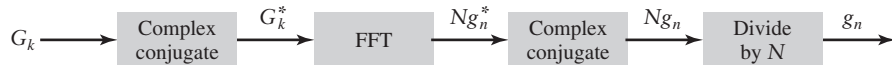


**FIGURE 2.37** Use of the FFT algorithm for computing the IDFT.

Taking the complex conjugate of Eq. (2.172), multiplying by  $N$ , and recognizing from the definition of Eq. (2.166) that  $W^* = W^{-1}$ , we get

$$Ng_n^* = \sum_{k=0}^{N-1} G_k^* W^{kn}, \quad 0, 1, \dots, N - 1 \quad (2.173)$$

The right-hand side of Eq. (2.173) is recognized as the  $N$ -point DFT of the complex-conjugated sequence  $G_k^*$ . Accordingly, Eq. (2.173) suggests that we may compute the desired sequence  $g_n$  using the scheme shown in Fig. 2.37, based on an  $N$ -point FFT algorithm. Thus, the same FFT algorithm can be used essentially to handle the computation of both the IDFT and the DFT.

## 2.11 Theme Example: Twisted Pairs for Telephony

The fundamental transmission medium for connecting homes to telephone central switching offices is the *twisted pair*. A twisted pair is usually a pair of solid copper wires with polyethylene sheathing. If the copper strand has a diameter of 0.4 mm, this cable size is referred to as #26 on the American Wire Gauge, or simply 26 AWG. A twisted pair is an example of a *transmission line*.

A transmission line consists of two conductors, each of which has its own inherent resistance and inductance. Since the two conductors are often in close proximity, there is also a capacitive effect between the two as well as potential conductance through the material that is used to insulate the two wires. A transmission line so constructed is often represented by the *lumped circuit* shown in Fig. 2.38. Although the impedances are shown as discrete elements in Fig. 2.38, it is more correct to consider them distributed through the length of the transmission line.

Depending upon the circuit element values in Fig. 2.38, it is clear that a transmission line will have a distorting effect on the transmitted signal. Furthermore, since the total impedance increases with the length of the line, so will the frequency response of the transmission line.

In Fig. 2.39, we show the typical response of a twisted pair with lengths of 2 to 8 kilometers. There are several observations to be made from the figure:

- ▶ Twisted pairs run directly from the central office to the home with one pair dedicated to each telephone line. Consequently, the transmission lines can be quite long.
- ▶ The results in Fig. 2.39 assume a continuous cable. In practice, there may be several splices in the cable, different gauge cables along different parts of the path, and so on. These discontinuities in the transmission medium will further affect the frequency response of the cable.

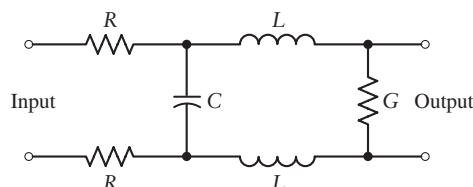


**FIGURE 2.38** Lumped circuit model of a transmission line.

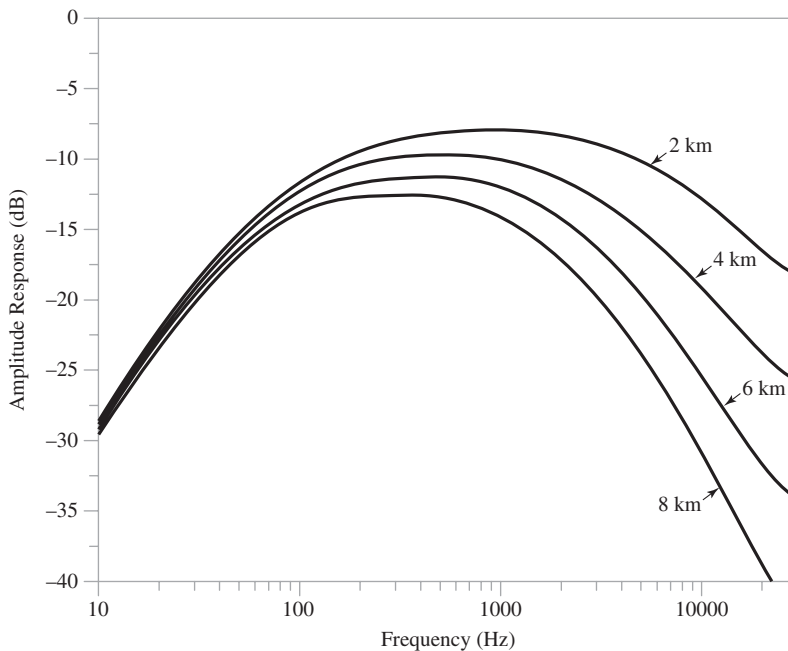


**FIGURE 2.39** Typical frequency response of a 26-AWG twisted-pair transmission line of different lengths with  $(600 \Omega + 2 \mu F)$  source and load impedances.

- ▶ We see that, for a 2-km cable, the frequency response is quite flat over the voice band from 300 to 3100 Hz for telephonic communication. However, for the 8-km cable, the frequency response starts to fall just above 1 kHz.
- ▶ The frequency response falls off at zero frequency because there is a capacitive connection at the load and the source. This capacitive connection is put to practical use by enabling dc power to be transported along the cable to power the remote telephone handset.

Analysis of the frequency response of longer cables indicates that it can be improved by adding some reactive loading. For this reason, we often hear of *loaded lines* that include lumped inductors at regular intervals (typically 66 milli-henry (mH) approximately every two kilometers). The loading improves the frequency response of the circuit in the range corresponding to voice signals without requiring additional power. The disadvantage of loaded lines, however, is their degraded performance at high frequency. Services such as digital subscriber line (DSL) (discussed later in Chapter 7), which rely on the high-frequency response of the twisted pairs, do not work well over loaded telephone lines.

In most of what follows, in the rest of the book, we will usually assume that the medium does not affect the transmission, except possibly through the addition of noise to the signal. In practice, the medium may affect the signal in a variety of ways as illustrated in the theme example just described.

## 2.12 Summary and Discussion

In this chapter, we have described the Fourier transform as a fundamental tool for relating the time-domain and frequency-domain descriptions of a deterministic signal. The signal of interest may be an energy signal or a power signal. The Fourier transform includes the exponential Fourier series as a special case, provided that we permit the use of the Dirac delta function.

An inverse relationship exists between the time-domain and frequency-domain descriptions of a signal. Whenever an operation is performed on the waveform of a signal in the time domain, a corresponding modification is applied to the spectrum of the signal in the frequency domain. An important consequence of this inverse relationship is the fact that the time-bandwidth product of an energy signal is a constant; the definitions of signal duration and bandwidth merely affect the value of the constant.

An important signal processing operation frequently encountered in communication systems is that of linear filtering. This operation involves the convolution of the input signal with the impulse response of the filter or, equivalently, the multiplication of the Fourier transform of the input signal by the transfer function (i.e., Fourier transform of the impulse response) of the filter. Note, however, that the material presented in the chapter on linear filtering assumes that the filter is *time-invariant* (i.e., the shape of the impulse response of the filter is invariant with respect to when the unit impulse or delta function is applied to the filter).

Another important signal processing operation encountered in communication systems is that of correlation. This operation may provide a measure of similarity between a signal and a delayed version of itself, in which case we speak of the autocorrelation function. When the measure of similarity involves a pair of different signals, however, we speak of the cross-correlation function. The Fourier transform of the autocorrelation function is called the spectral density. The Fourier transform of the cross-correlation function is called the cross-spectral density. Discussions of correlation and spectral density presented in the chapter were confined to energy signals and power signals exemplified by pulse-like signals and periodic signals respectively; the treatment of noise (another realization of power signal) is deferred to Chapter 8.

The final part of the chapter was concerned with the discrete Fourier transform and its numerical computation. Basically, the discrete Fourier transform is obtained from the standard Fourier transform by uniformly sampling both the input signal and the output spectrum. The fast Fourier transform algorithm provides a practical means for the efficient implementation of the discrete Fourier transform on a digital computer. This makes the fast Fourier transform algorithm a powerful computational tool for spectral analysis and linear filtering.

## ADDITIONAL PROBLEMS

- 2.19 (a) Find the Fourier transform of the half-cosine pulse shown in Fig. 2.40(a).

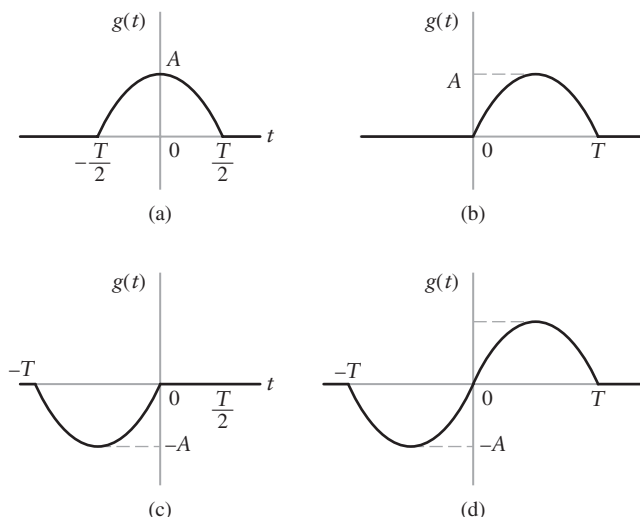


**FIGURE 2.40**  
Problem 2.19

- (b) Apply the time-shifting property to the result obtained in part (a) to evaluate the spectrum of the half-sine pulse shown in Fig. 2.40(b).
- (c) What is the spectrum of a half-sine pulse having a duration equal to  $aT$ ?
- (d) What is the spectrum of the negative half-sine pulse shown in Fig. 2.40(c)?
- (e) Find the spectrum of the single sine pulse shown in Fig. 2.40(d).
- 2.20 Any function  $g(t)$  can be split unambiguously into an *even part* and an *odd part*, as shown by

$$g(t) = g_e(t) + g_o(t)$$

The even part is defined by

$$g_e(t) = \frac{1}{2}[g(t) + g(-t)]$$

and the odd part is defined by

$$g_o(t) = \frac{1}{2}[g(t) - g(-t)]$$

- (a) Evaluate the even and odd parts of a rectangular pulse defined by

$$g(t) = A \operatorname{rect}\left(\frac{t}{T} - \frac{1}{2}\right)$$

- (b) What are the Fourier transforms of these two parts of the pulse?

- 2.21 The following expression may be viewed as an approximate representation of a pulse with finite rise time:

$$g(t) = \frac{1}{\tau} \int_{t-T}^{t+T} \exp\left(-\frac{\pi u^2}{\tau^2}\right) du$$

where it is assumed that  $T \gg \tau$ . Determine the Fourier transform of  $g(t)$ . What happens to this transform when we allow  $\tau$  to become zero?

- 2.22 The Fourier transform of a signal  $g(t)$  is denoted by  $G(f)$ . Prove the following properties of the Fourier transform:

- (a) If a real signal  $g(t)$  is an even function of time  $t$ , the Fourier transform  $G(f)$  is purely real. If the real signal  $g(t)$  is an odd function of time  $t$ , the Fourier transform  $G(f)$  is purely imaginary.

(b)  $t^n g(t) \iff \left(\frac{j}{2\pi}\right)^n G^{(n)}(f)$ , where  $G^{(n)}(f)$  is the  $n$ th derivative of  $G(f)$  with respect to  $f$ .

(c)  $\int_{-\infty}^{\infty} t^n g(t) dt = \left(\frac{j}{2\pi}\right)^n G^{(n)}(0)$

(d)  $\int_{-\infty}^{\infty} g_1(t) g_2^*(t) dt = \int_{-\infty}^{\infty} G_1(f) G_2^*(f) df$

- 2.23 The Fourier transform  $G(f)$  of a signal  $g(t)$  is bounded by the following three inequalities:

(a)  $|G(f)| \leq \int_{-\infty}^{\infty} |g(t)| dt$

(b)  $|j2\pi f G(f)| \leq \int_{-\infty}^{\infty} \left| \frac{dg(t)}{dt} \right| dt$

(c)  $|((j2\pi f)^2 G(f))| \leq \int_{-\infty}^{\infty} \left| \frac{d^2 g(t)}{dt^2} \right| dt$

It is assumed that the first and second derivatives of  $g(t)$  exist.

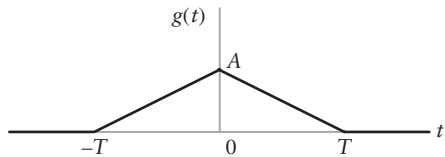


**FIGURE 2.41**  
Problem 2.23

Construct these three bounds for the triangular pulse shown in Fig. 2.41 and compare your results with the actual amplitude spectrum of the pulse.

- 2.24 Consider the convolution of two signals \$g\_1(t)\$ and \$g\_2(t)\$. Show that

$$(a) \frac{d}{dt}[g_1(t) \star g_2(t)] = \left[ \frac{d}{dt}g_1(t) \right] \star g_2(t)$$

$$(b) \int_{-\infty}^t [g_1(\tau) \star g_2(\tau)] d\tau = \left[ \int_{-\infty}^t g_1(\tau) d\tau \right] \star g_2(t)$$

- 2.25 A signal \$x(t)\$ of finite energy is applied to a square-law device whose output \$y(t)\$ is defined by

$$y(t) = x^2(t)$$

The spectrum of \$x(t)\$ is limited to the frequency interval \$-W \leq f \leq W\$. Hence, show that the spectrum of \$y(t)\$ is limited to \$-2W \leq f \leq 2W\$. Hint: Express \$y(t)\$ as \$x(t)\$ multiplied by itself.

- 2.26 Evaluate the Fourier transform of the delta function by considering it as the limiting form of (a) rectangular pulse of unit area, and (b) sinc pulse of unit area.

- 2.27 The Fourier transform \$G(f)\$ of a signal \$g(t)\$ is defined by

$$G(f) = \begin{cases} 1, & f > 0 \\ \frac{1}{2}, & f = 0 \\ 0, & f < 0 \end{cases}$$

Determine the signal \$g(t)\$.

- 2.28 Consider a pulselike function \$g(t)\$ that consists of a small number of straight-line segments. Suppose that this function is differentiated with respect to time \$t\$ twice so as to generate a sequence of weighted delta functions, as shown by

$$\frac{d^2g(t)}{dt^2} = \sum_i k_i \delta(t - t_i)$$

where the \$k\_i\$ are related to the slopes of the straight-line segments.

- (a) Given the values of the \$k\_i\$ and \$t\_i\$, show that the Fourier transform of \$g(t)\$ is given by

$$G(f) = -\frac{1}{4\pi^2 f^2} \sum_i k_i \exp(-j2\pi f t_i)$$

- (b) Using this procedure, show that the Fourier transform of the trapezoidal pulse shown in Fig. 2.42 is given by

$$G(f) = \frac{A}{\pi^2 f^2 (t_b - t_a)} \sin[\pi f(t_b - t_a)] \sin[\pi f(t_b + t_a)]$$

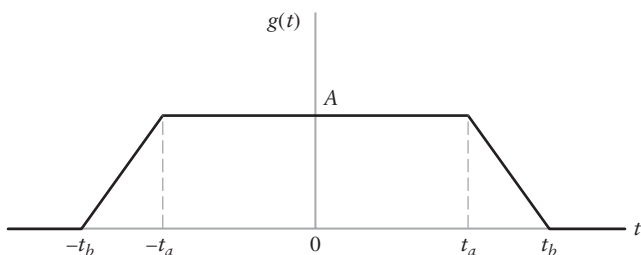


**FIGURE 2.42**  
Problem 2.28

- 2.29 A rectangular pulse of amplitude  $A$  and duration  $2t_a$  may be viewed as the limiting case of the trapezoidal pulse shown in Fig. 2.42 as  $t_b$  approaches  $t_a$ .
- Starting with the result given in part (b) of Problem 2.28, show that as  $t_b$  approaches  $t_a$ , this result approaches a sinc function.
  - Reconcile the result derived in part (a) with the Fourier-transform pair of Eq. (2.10).
- 2.30 Let  $x(t)$  and  $y(t)$  be the input and output signals of a linear time-invariant filter. Using Rayleigh's energy theorem, show that if the filter is stable and the input signal  $x(t)$  has finite energy, then the output signal  $y(t)$  also has finite energy. That is, if

$$\int_{-\infty}^{\infty} |x(t)|^2 dt < \infty$$

then

$$\int_{-\infty}^{\infty} |y(t)|^2 dt < \infty$$

- 2.31 (a) Determine the overall amplitude response of the cascade connection shown in Fig. 2.43 consisting of  $N$  identical stages, each with a time constant  $RC$  equal to  $\tau_0$ .
- (b) Show that as  $N$  approaches infinity, the amplitude response of the cascade connection approaches the Gaussian function  $\exp\left(-\frac{1}{2}f^2T^2\right)$ , where for each value of  $N$ , the time constant  $\tau_0$  is selected so that the condition

$$\tau_0^2 = \frac{T^2}{4\pi^2 N}$$

is satisfied.

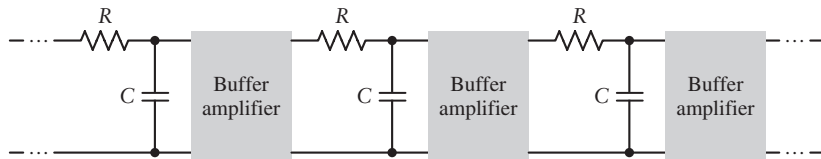


**FIGURE 2.43** Problem 2.31

- 2.32 Suppose that, for a given signal  $x(t)$ , the integrated value of the signal over an interval  $T$  is required, as shown by

$$y(t) = \int_{t-T}^t x(\tau) d\tau$$

- (a) Show that  $y(t)$  can be obtained by transmitting the signal  $x(t)$  through a filter with its transfer function given by

$$H(f) = T \operatorname{sinc}(fT) \exp(-j\pi fT)$$

- (b) An adequate approximation to this transfer function is obtained by using a low-pass filter with a bandwidth equal to  $1/T$ , passband amplitude response  $T$ , and delay  $T/2$ . Assuming this low-pass filter to be ideal, determine the filter output at time  $t = T$  due to a unit step function applied to the filter at  $t = 0$ , and compare the result with the corresponding output of the ideal integrator. Note that  $\operatorname{Si}(\pi) = 1.85$  and  $\operatorname{Si}(\infty) = \pi/2$ .

- 2.33 Show that the two different pulses defined in parts (a) and (b) of Fig. 2.44 have the same energy spectral density:

$$\Psi_g(f) = \frac{4A^2 T^2 \cos^2(\pi T f)}{\pi^2 (4T^2 f^2 - 1)^2}$$

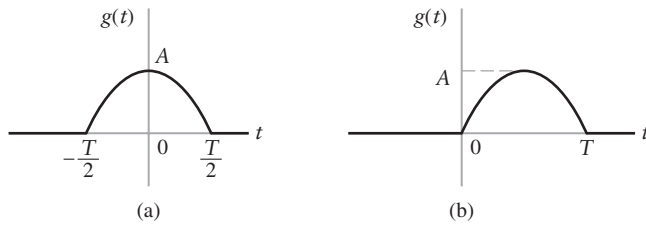


FIGURE 2.44 Problem 2.33

2.34 Determine and sketch the autocorrelation functions of the following exponential pulses:

- (a)  $g(t) = \exp(-at)u(t)$
- (b)  $g(t) = \exp(-a|t|)$
- (c)  $g(t) = \exp(-at)u(t) - \exp(at)u(-t)$

where  $u(t)$  is the unit step function, and  $u(-t)$  is its time-reversed version.

2.35 Determine and sketch the autocorrelation function of a Gaussian pulse defined by

$$g(t) = \frac{1}{t_0} \exp\left(-\frac{\pi t^2}{t_0^2}\right)$$

2.36 The Fourier transform of a signal is defined by  $\text{sinc}(f)$ . Show that the autocorrelation function of this signal is triangular in form.

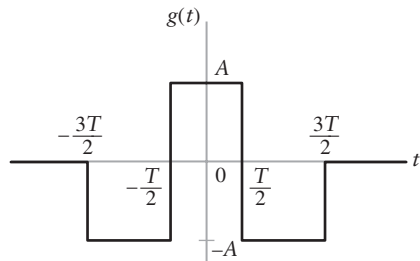
2.37 Specify two different pulse signals that have exactly the same autocorrelation function.

2.38 Consider a sinusoidal signal  $g(t)$  defined by

$$g(t) = A_0 + A_1 \cos(2\pi f_1 t + \theta_1) + A_2 \cos(2\pi f_2 t + \theta_2)$$

- (a) Determine the autocorrelation function  $R_g(\tau)$  of this signal.
- (b) What is the value of  $R_g(0)$ ?
- (c) Has any information about  $g(t)$  been lost in obtaining the autocorrelation function? Explain.

2.39 Determine the autocorrelation function of the triplet pulse shown in Fig. 2.45.

FIGURE 2.45  
Problem 2.39

2.40 Let  $G(f)$  denote the Fourier transform of a real-valued energy signal  $g(t)$ , and  $R_g(\tau)$  denote its autocorrelation function. Show that

$$\int_{-\infty}^{\infty} \left[ \frac{dR_g(\tau)}{d\tau} \right] d\tau = 4\pi^2 \int_{-\infty}^{\infty} f^2 |G(f)|^4 df$$

2.41 Determine the cross-correlation function  $R_{12}(\tau)$  of the rectangular pulse  $g_1(t)$  and triplet pulse  $g_2(t)$  shown in Fig. 2.46, and sketch it. What is  $R_{21}(\tau)$ ? Are these two signals orthogonal to each other? Why?

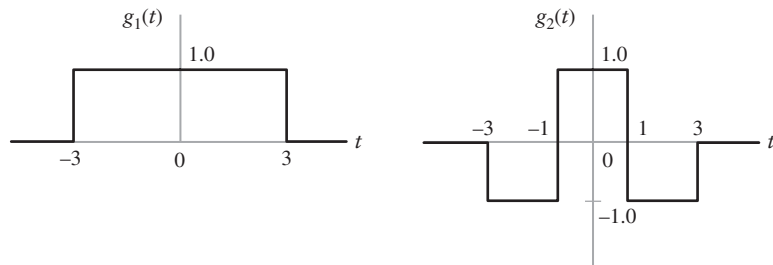
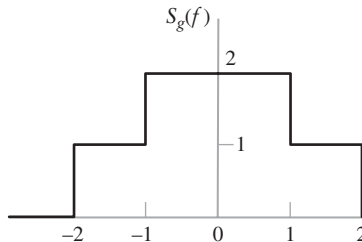


FIGURE 2.46 Problem 2.41

- 2.42 Consider two energy signals  $g_1(t)$  and  $g_2(t)$ . These two signals are delayed by amounts equal to  $t_1$  and  $t_2$  seconds, respectively. Show that the time delays are additive in convolving the pair of delayed signals, whereas they are subtractive in cross-correlating them.
- 2.43 (a) An energy signal  $x(t)$ , its Fourier transform  $X(f)$ , autocorrelation function  $R_x(\tau)$ , and energy spectral density  $\Psi_x(f)$  are all related, directly or indirectly. Construct a flow-graph that portrays all the possible direct relationships between them.  
 (b) If you are given the frequency-domain description  $X(f)$ , the autocorrelation function  $R_x(\tau)$  can be calculated from  $X(f)$ . Outline two ways in which this calculation can be performed.
- 2.44 Find the autocorrelation function of a power signal  $g(t)$  whose power spectral density is depicted in Fig. 2.47. What is the value of this autocorrelation function at the origin?

FIGURE 2.47  
Problem 2.44

- 2.45 Consider the square wave  $g(t)$  shown in Fig. 2.48. Find the power spectral density, average power, and autocorrelation function of this square wave. Does the wave have dc power? Explain your answer.

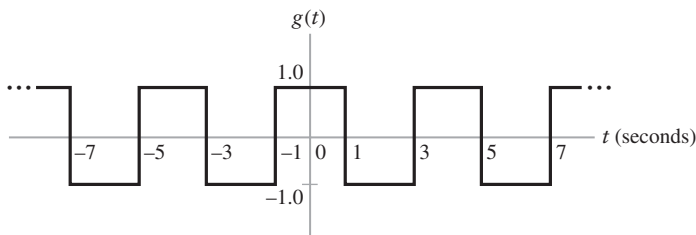


FIGURE 2.48 Problem 2.45

- 2.46 Consider two periodic signals  $g_{p1}(t)$  and  $g_{p2}(t)$  that have the following complex Fourier series representations:

$$g_{p1}(t) = \sum_{n=-\infty}^{\infty} c_{1,n} \exp\left(\frac{j2\pi nt}{T_0}\right)$$

and

$$g_{p2}(t) = \sum_{n=-\infty}^{\infty} c_{2,n} \exp\left(\frac{j2\pi nt}{T_0}\right)$$

The two signals have a common period equal to  $T_0$ .

Using the following definition of cross-correlation for a pair of periodic signals,

$$R_{12}(\tau) = \frac{1}{T_0} \int_{-T_0/2}^{T_0/2} g_{p1}(t)g_{p2}^*(t - \tau) dt$$

show that the prescribed pair of periodic signals satisfies the Fourier-transform pair

$$R_{12}(\tau) \iff \sum_{n=-\infty}^{\infty} c_{1,n} c_{2,n}^* \delta\left(f - \frac{n}{T_0}\right)$$

- 2.47** A periodic signal  $g_p(t)$  of period  $T_0$  is represented by the complex Fourier series

$$g_p(t) = \sum_{n=-\infty}^{\infty} c_n \exp(j2\pi nt/T_0)$$

where the  $c_n$  are the complex Fourier coefficients. The autocorrelation function of  $g_p(t)$  is defined by

$$R_{g_p}(\tau) = \frac{1}{T_0} \int_{-T_0/2}^{T_0/2} g_p(t)g_p^*(t - \tau) dt$$

- (a) Consider the sinusoidal wave

$$g_p(t) = A \cos(2\pi f_c t + \theta)$$

Determine the autocorrelation function  $R_{g_p}(\tau)$  and plot its waveform.

- (b) Show that  $R_{g_p}(0) = A^2/2$ .

- 2.48** Repeat parts (a) and (b) of Problem 2.47 for the square wave:

$$g_p(t) = \begin{cases} A, & -\frac{T_0}{4} \leq t \leq \frac{T_0}{4} \\ 0, & \text{for the remainder of period } T_0 \end{cases}$$

- 2.49** Determine the power spectral density of (a) the sinusoidal wave of Problem 2.47, and (b) the square wave of Problem 2.48.

- 2.50** Following a procedure similar to that described in Section 2.10 that led to the flow graph of Fig. 2.36 for the 8-point FFT algorithm based on decimation-in-frequency, do the following:

- (a) Develop the corresponding flow graph for the 8-point FFT algorithm based on decimation-in-time.
- (b) Compare the flow graph obtained in part (a) with that described in Fig. 2.36, stressing the similarities and differences between these two basic methods for deriving the FFT algorithm.

## | ADVANCED PROBLEMS

---

- 2.51 (a)** The *root mean-square (rms) bandwidth* of a low-pass signal  $g(t)$  of finite energy is defined by

$$W_{\text{rms}} = \left[ \frac{\int_{-\infty}^{\infty} f^2 |G(f)|^2 df}{\int_{-\infty}^{\infty} |G(f)|^2 df} \right]^{1/2}$$

where  $|G(f)|^2$  is the energy spectral density of the signal. Correspondingly, the *root mean-square (rms) duration* of the signal is defined by

$$T_{\text{rms}} = \left[ \frac{\int_{-\infty}^{\infty} t^2 |g(t)|^2 dt}{\int_{-\infty}^{\infty} |g(t)|^2 dt} \right]^{1/2}$$

Using these definitions, show that

$$T_{\text{rms}} W_{\text{rms}} \geq \frac{1}{4\pi}$$

Assume that  $|g(t)| \rightarrow 0$  faster than  $1/\sqrt{|t|}$  as  $|t| \rightarrow \infty$ .

- (b)** Consider a Gaussian pulse defined by

$$g(t) = \exp(-\pi t^2)$$

Show that, for this signal, the equality

$$T_{\text{rms}} W_{\text{rms}} = \frac{1}{4\pi}$$

can be reached.

*Hint:* Use Schwarz's inequality (see Appendix 5).

$$\left\{ \int_{-\infty}^{\infty} [g_1^*(t)g_2(t) + g_1(t)g_2^*(t)] dt \right\}^2 \leq 4 \int_{-\infty}^{\infty} |g_1(t)|^2 dt \int_{-\infty}^{\infty} |g_2(t)|^2 dt$$

in which we set

$$g_1(t) = tg(t)$$

and

$$g_2(t) = \frac{dg(t)}{dt}$$

- 2.52** The *Hilbert transform* of a Fourier transformable signal  $g(t)$  is defined by

$$\hat{g}(t) = \frac{1}{\pi} \int_{-\infty}^{\infty} \frac{g(\tau)}{t - \tau} d\tau$$

Correspondingly, the *inverse Hilbert transform* is defined by

$$g(t) = -\frac{1}{\pi} \int_{-\infty}^{\infty} \frac{\hat{g}(\tau)}{t - \tau} d\tau$$

Using these two formulas, derive the following set of Hilbert-transform pairs:

$g(t)$	$\hat{g}(t)$
$\frac{\sin t}{t}$	$\frac{1 - \cos t}{t}$
$\text{rect}(t)$	$-\frac{1}{\pi} \ln \left  \left( t - \frac{1}{2} \right) / \left( t + \frac{1}{2} \right) \right $
$\delta(t)$	$\frac{1}{\pi t}$
$\frac{1}{1 + t^2}$	$\frac{t}{1 + t^2}$

**2.53** Evaluate the inverse Fourier transform  $g(t)$  of the one-sided frequency function

$$G(f) = \begin{cases} \exp(-f), & f > 0 \\ \frac{1}{2}, & f = 0 \\ 0, & f < 0 \end{cases}$$

Hence, show that  $g(t)$  is complex, and that its real and imaginary parts constitute a Hilbert-transform pair.

- 2.54** A Hilbert transformer may be viewed as a device whose transfer function exhibits the following characteristics:
- (a) The amplitude response is unity for all positive and negative frequencies.
  - (b) The phase response is  $+90^\circ$  for negative frequencies and  $-90^\circ$  for positive frequencies.  
Starting with the definition of the Hilbert transform given in Problem 2.52, demonstrate the frequency-domain description embodied in parts (a) and (b).
  - (c) Is the Hilbert transformer physically realizable? Justify your answer.

## CHAPTER 3

# AMPLITUDE MODULATION

*Modulation* is defined as *the process by which some characteristic of a carrier wave is varied in accordance with an information-bearing signal*. The carrier is needed to facilitate the transportation of the modulated signal across a band-pass channel from the transmitter to the receiver. A commonly used carrier is a *sinusoidal wave*, the source of which is physically independent of the source of the information-bearing signal. When the information-bearing signal is of an analog kind, we speak of *continuous-wave modulation*, a term that stresses *continuity* of the modulated wave as a function of time.

In the context of communications, a primary motivation for modulation is to facilitate transmission of the information-bearing signal over a communication channel (e.g., radio channel) with a prescribed passband. In continuous-wave modulation, this is made possible by varying the amplitude or angle of the sinusoidal carrier wave. On this basis, we may classify continuous-wave modulation into two broadly defined families: amplitude modulation and angle modulation. These two families of modulation distinguish themselves by offering entirely different spectral characteristics and therefore different practical benefits. The classification is made on the basis of whether, on the one hand, the amplitude of the sinusoidal carrier wave, or, on the other hand, the phase or frequency (and therefore) the angle of the sinusoidal carrier wave, is varied in accordance with the information-bearing signal. The family of amplitude modulation is studied in this chapter, followed by the study of angle modulation in the next chapter.

In Chapter 1, we identified system complexity and the two primary communication resources—namely, transmitted power and channel bandwidth—as the central issues involved in the design of a communication system. With these issues in mind, in this chapter, we will study four *linear modulation strategies that constitute the amplitude modulation family*:

- ▶ amplitude modulation (AM)
- ▶ double sideband-suppressed carrier (DSB-SC)
- ▶ single sideband (SSB)
- ▶ vestigial sideband (VSB)

These four types of modulation differ from each other by virtue of their spectral characteristics. Their study will teach us the following lessons:

- ▶ *Lesson 1: Fourier analysis provides a powerful mathematical tool for developing mathematical as well as physical insight into the spectral characterization of linear modulation strategies.*

- **Lesson 2:** The implementation of analog communications is significantly simplified by using AM, at the expense of transmitted power and channel bandwidth.
- **Lesson 3:** The utilization of transmitted power and channel bandwidth is improved through well-defined modifications of an amplitude-modulated wave's spectral content at the expense of increased system complexity.

In short, we may make the statement:

There is no free lunch in designing a communication system: for every gain that is made, there is a price to be paid.

## 3.1 Amplitude Modulation

### ■ THEORY

Consider a *sinusoidal carrier wave*  $c(t)$  defined by

$$c(t) = A_c \cos(2\pi f_c t) \quad (3.1)$$

where  $A_c$  is the *carrier amplitude* and  $f_c$  is the *carrier frequency*. The *information-bearing signal* or *message signal* is denoted by  $m(t)$ ; the terms “information-bearing signal” and “message signal” are used interchangeably throughout the book. To simplify the exposition without affecting the results obtained and conclusions reached, we have assumed that the phase of the carrier wave is zero in Eq. (3.1). *Amplitude modulation*<sup>1</sup> (AM) is formally defined as a process in which the amplitude of the carrier wave  $c(t)$  is varied about a mean value, linearly with the message signal  $m(t)$ . An amplitude-modulated (AM) wave may thus be described as a function of time as follows:

$$s(t) = A_c[1 + k_a m(t)] \cos(2\pi f_c t) \quad (3.2)$$

where  $k_a$  is a constant called the *amplitude sensitivity* of the modulator responsible for the generation of the modulated signal  $s(t)$ . Typically, the carrier amplitude  $A_c$  and the message signal  $m(t)$  are measured in volts, in which case the amplitude sensitivity  $k_a$  is measured in volt<sup>-1</sup>. Notice that if the message signal  $m(t)$  is switched off, the sinusoidal carrier is left intact.

Figure 3.1(a) shows a message signal  $m(t)$ , and Figs. 3.1(b) and 3.1(c) show the corresponding AM wave  $s(t)$  for two values of amplitude sensitivity  $k_a$  and a carrier amplitude  $A_c = 1$  volt.

In amplitude modulation, information pertaining to the message signal  $m(t)$  resides solely in the *envelope*, which is defined as the amplitude of the modulated wave  $s(t)$ —that is,  $A_c|1 + k_a m(t)|$ . From this expression, we observe that the envelope of  $s(t)$  has essentially the same shape as the message signal  $m(t)$  provided that two conditions are satisfied:

1. The amplitude of  $k_a m(t)$  is always less than unity; that is,

$$|k_a m(t)| < 1, \quad \text{for all } t \quad (3.3)$$

This condition is illustrated in Fig. 3.1(b); it ensures that the function  $1 + k_a m(t)$  is always positive, in which case we may express the *envelope* of the AM wave  $s(t)$  of Eq. (3.2) simply as  $A_c[1 + k_a m(t)]$ . When the amplitude sensitivity  $k_a$  of the

---

<sup>1</sup>Throughout the book, the term “amplitude modulation” or AM, for short, is used to refer to that particular form of modulation in which the carrier wave and both sidebands are present.

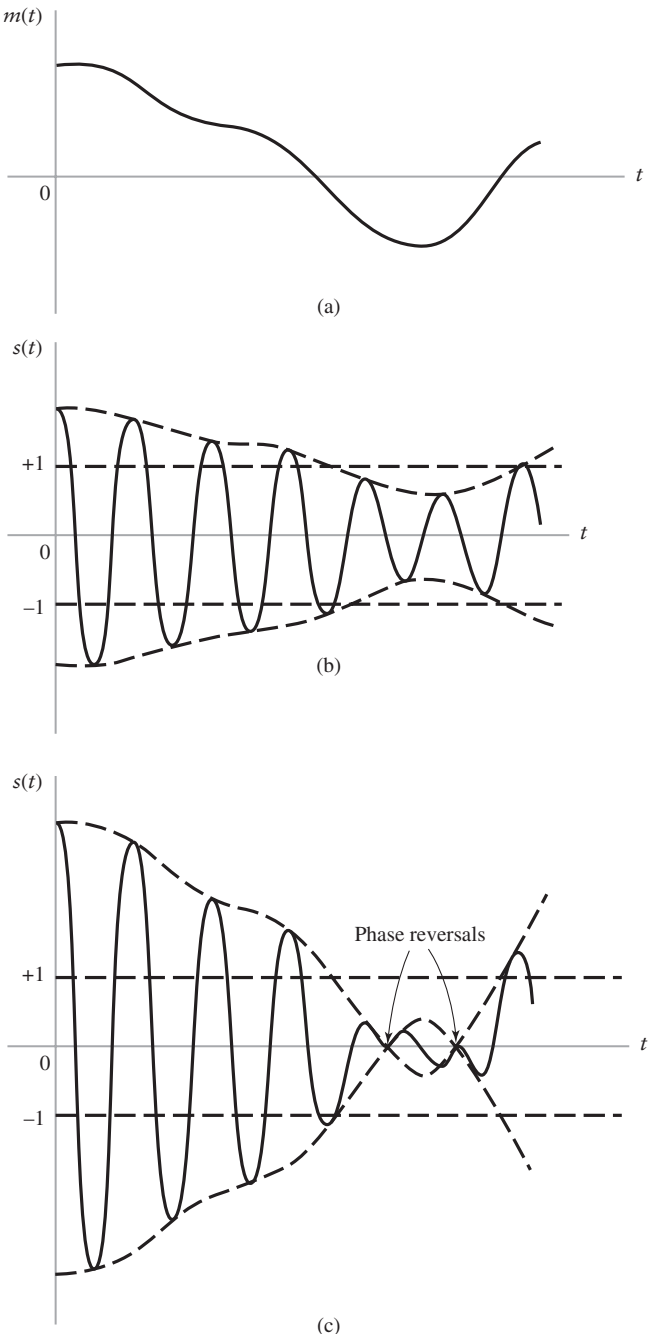


**FIGURE 3.1** Illustration of the amplitude modulation process. (a) Message signal  $m(t)$ . (b) AM wave for  $|k_a m(t)| < 1$  for all  $t$ . (c) AM wave for  $|k_a m(t)| > 1$  for some  $t$ .

modulator is large enough to make  $|k_a m(t)| > 1$  for any  $t$ , the carrier wave becomes *over modulated*, resulting in carrier phase reversals whenever the factor  $1 + k_a m(t)$  crosses zero. The modulated wave then exhibits *envelope distortion*, as in Fig. 3.1(c). It is therefore apparent that by avoiding overmodulation, a one-to-one relationship

is maintained between the envelope of the AM wave and the modulating wave for all values of time. The absolute maximum value of  $k_a m(t)$  multiplied by 100 is referred to as the *percentage modulation*.

2. The carrier frequency  $f_c$  is much greater than the highest frequency component  $W$  of the message signal  $m(t)$ —that is,

$$f_c \gg W \quad (3.4)$$

We call  $W$  the *message bandwidth*. If the condition of Eq. (3.4) is not satisfied, an envelope cannot be visualized (and therefore detected) satisfactorily.

Provided that the conditions of Eqs. (3.3) and (3.4) are satisfied, demodulation of the AM wave is achieved by using an *envelope detector*, which is defined as a *device whose output traces the envelope of the AM wave acting as the input signal*. The process of envelope detection is discussed later in the section.

The next issue for discussion is the frequency-domain description of AM. Let  $m(t) \rightleftharpoons M(f)$ , where the Fourier transform  $M(f)$  is called the *message spectrum*. From Eq. (3.2), we find that the Fourier transform or spectrum of the AM wave  $s(t)$  is given by

$$S(f) = \frac{A_c}{2} [\delta(f - f_c) + \delta(f + f_c)] + \frac{k_a A_c}{2} [M(f - f_c) + M(f + f_c)] \quad (3.5)$$

where we have used the relations:

$$\begin{aligned} \cos(2\pi f_c t) &= \frac{1}{2} [\exp(j2\pi f_c t) + \exp(-j2\pi f_c t)] \\ \exp(j2\pi f_c t) &\rightleftharpoons \delta(f - f_c) \end{aligned}$$

and

$$m(t) \exp(j2\pi f_c t) \rightleftharpoons M(f - f_c)$$

Following the terminology introduced in Chapter 2, the  $\delta(f)$  in Eq. (3.5) denotes the Dirac delta function in the frequency domain.

Suppose that the message signal  $m(t)$  is band-limited to the interval  $-W \leq f \leq W$ , as in Fig. 3.2(a). The shape of the spectrum shown in this figure is intended for the purpose of illustration only. We find from Eq. (3.5) that the spectrum  $S(f)$  of the AM wave is as shown in Fig. 3.2(b) for the case when  $f_c > W$ . This spectrum consists of two delta functions weighted by the factor  $A_c/2$  and occurring at  $\pm f_c$ , and two versions of the message spectrum translated in frequency by  $\pm f_c$  and scaled in amplitude by  $k_a A_c/2$ . From the spectrum of Fig. 3.2(b), we make three important observations:

1. As a result of the modulation process, the spectrum of the message signal  $m(t)$  for negative frequencies extending from  $-W$  to 0 becomes completely visible for positive (i.e., measurable) frequencies, provided that the carrier frequency satisfies the condition  $f_c > W$ ; herein lies the importance of the idea of “negative” frequencies, which was emphasized in Chapter 2.
2. For positive frequencies, the portion of the spectrum of an AM wave lying above the carrier frequency  $f_c$  is referred to as the *upper sideband*, whereas the symmetric portion below  $f_c$  is referred to as the *lower sideband*. The condition  $f_c > W$  ensures that the sidebands do not overlap. Moreover, with the upper sideband, lower sideband, and carrier fully represented in the spectrum of Fig. 3.2(b), the modulated wave is referred to as *AM*, in accordance with footnote 1 on page 101.

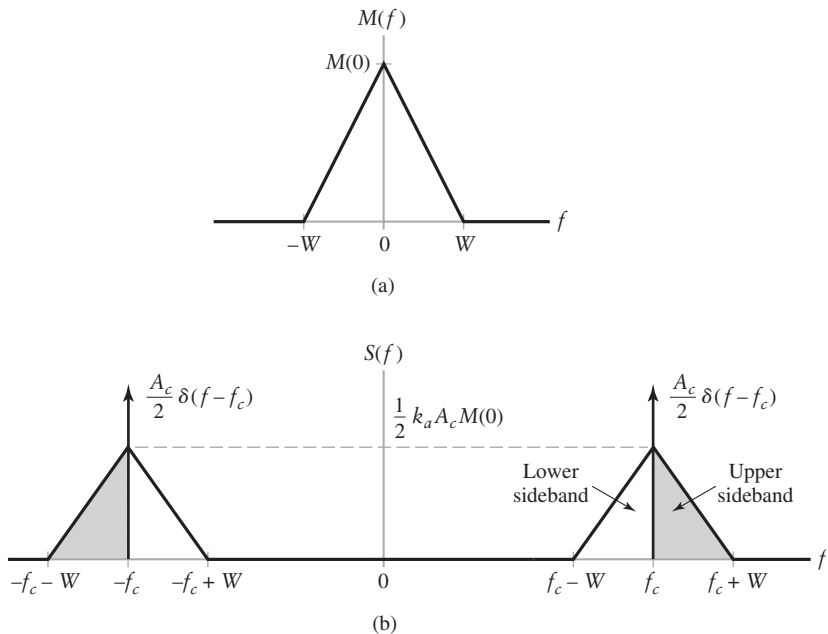


**FIGURE 3.2** (a) Spectrum of message signal  $m(t)$ . (b) Spectrum of AM wave  $s(t)$ .

- For positive frequencies, the highest frequency component of the AM wave equals  $f_c + W$ , and the lowest frequency component equals  $f_c - W$ . The difference between these two frequencies defines the *transmission bandwidth*  $B_T$  of the AM wave, which is exactly twice the message bandwidth  $W$ ; that is,

$$B_T = 2W \quad (3.6)$$

#### EXAMPLE 3.1 Single-Tone Modulation

Consider a modulating wave  $m(t)$  that consists of a single tone or frequency component; that is,

$$m(t) = A_m \cos(2\pi f_m t)$$

where  $A_m$  is the amplitude of the sinusoidal modulating wave and  $f_m$  is its frequency (see Fig. 3.3(a)). The sinusoidal carrier wave has amplitude  $A_c$  and frequency  $f_c$  (see Fig. 3.3(b)). The corresponding AM wave is therefore given by

$$s(t) = A_c[1 + \mu \cos(2\pi f_m t)] \cos(2\pi f_c t) \quad (3.7)$$

where

$$\mu = k_a A_m$$

The dimensionless constant  $\mu$  is called the *modulation factor*, or the *percentage modulation* when it is expressed numerically as a percentage. To avoid envelope distortion due to over-modulation, the modulation factor  $\mu$  must be kept below unity, as explained previously.

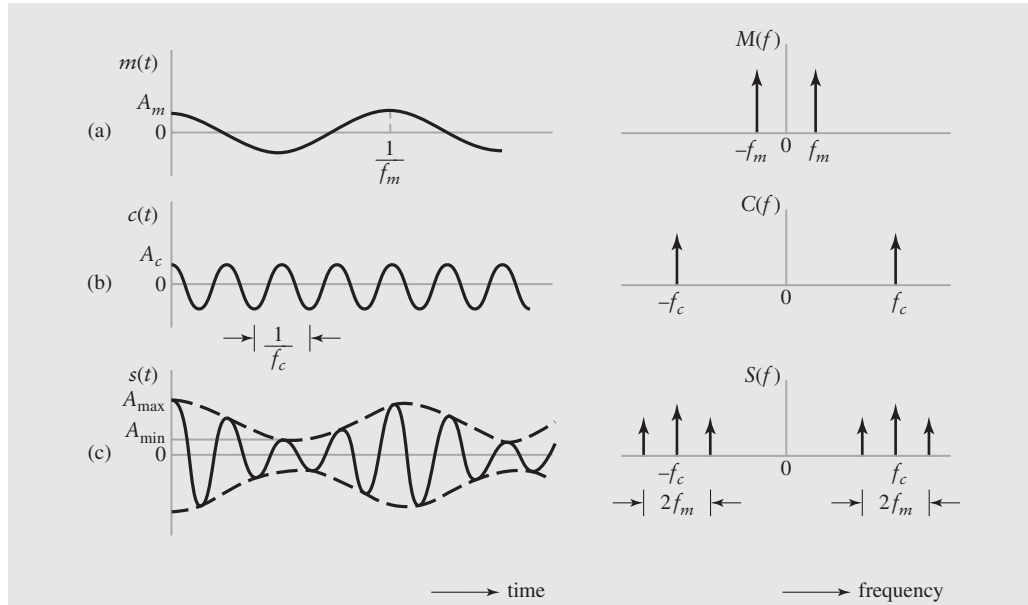


**FIGURE 3.3** Illustration of the time-domain (on the left) and frequency-domain (on the right) characteristics of amplitude modulation produced by a single tone. (a) Modulating wave. (b) Carrier wave. (c) AM wave.

Figure 3.3(c) shows a sketch of  $s(t)$  for  $\mu$  less than unity. Let  $A_{\max}$  and  $A_{\min}$  denote the maximum and minimum values of the envelope of the modulated wave, respectively. Then, from Eq. (3.7) we get

$$\frac{A_{\max}}{A_{\min}} = \frac{A_c(1 + \mu)}{A_c(1 - \mu)}$$

Rearranging this equation, we may express the modulation factor as

$$\mu = \frac{A_{\max} - A_{\min}}{A_{\max} + A_{\min}}$$

Expressing the product of the two cosines in Eq. (3.7) as the sum of two sinusoidal waves, one having frequency  $f_c + f_m$  and the other having frequency  $f_c - f_m$ , we get

$$s(t) = A_c \cos(2\pi f_c t) + \frac{1}{2}\mu A_c \cos[2\pi(f_c + f_m)t] + \frac{1}{2}\mu A_c \cos[2\pi(f_c - f_m)t]$$

The Fourier transform of  $s(t)$  is therefore

$$\begin{aligned} S(f) &= \frac{1}{2}A_c[\delta(f - f_c) + \delta(f + f_c)] \\ &\quad + \frac{1}{4}\mu A_c[\delta(f - f_c - f_m) + \delta(f + f_c + f_m)] \\ &\quad + \frac{1}{4}\mu A_c[\delta(f - f_c + f_m) + \delta(f + f_c - f_m)] \end{aligned}$$

Thus the spectrum of an AM wave, for the special case of sinusoidal modulation, consists of delta functions at  $\pm f_c$ ,  $f_c \pm f_m$ , and  $-f_c \pm f_m$ , as shown in Fig. 3.3(c).

In practice, the AM wave  $s(t)$  is a voltage or current wave. In either case, the average power delivered to a 1-ohm resistor by  $s(t)$  is comprised of three components:

$$\text{Carrier power} = \frac{1}{2}A_c^2$$

$$\text{Upper side-frequency power} = \frac{1}{8}\mu^2 A_c^2$$

$$\text{Lower side-frequency power} = \frac{1}{8}\mu^2 A_c^2$$

For a load resistor  $R$  different from 1 ohm, which is usually the case in practice, the expressions for carrier power, upper side-frequency power, and lower side-frequency power are merely scaled by the factor  $1/R$  or  $R$ , depending on whether the modulated wave  $s(t)$  is a voltage or a current, respectively. In any case, the ratio of the total sideband power to the total power in the modulated wave is equal to  $\mu^2/(2 + \mu^2)$ , which depends only on the modulation factor  $\mu$ . If  $\mu = 1$ —that is, 100 percent modulation is used—the total power in the two side frequencies of the resulting AM wave is only one-third of the total power in the modulated wave.

Figure 3.4 shows the percentage of total power in both side frequencies and in the carrier plotted versus the percentage modulation. Notice that when the percentage modulation is less than 20 percent, the power in one side frequency is less than 1 percent of the total power in the AM wave.

### ■ COMPUTER EXPERIMENT: AM

For the AM experiment, we will study sinusoidal modulation based on the following parameters:

$$\text{Carrier amplitude, } A_c = 1$$

$$\text{Carrier frequency, } f_c = 0.4 \text{ Hz}$$

$$\text{Modulation frequency, } f_m = 0.05 \text{ Hz}$$

We wish to display and analyze 10 full cycles of the modulated wave, corresponding to a total duration of 200 seconds. To perform the experiment on a digital computer, the modulated wave is sampled at the rate  $f_s = 10$  Hz, obtaining a total of  $200 \times f_s = 2000$  Hz data points. The frequency band occupied by the modulated wave is  $-5 \text{ Hz} \leq f \leq 5 \text{ Hz}$ . Since the separation between the carrier frequency and either side frequency is equal to the modulation frequency  $f_m = 0.05 \text{ Hz}$ , we would like to have a frequency resolution  $f_r = 0.005 \text{ Hz}$ . To achieve this frequency resolution, it is recommended that the number of frequency samples satisfies the condition:

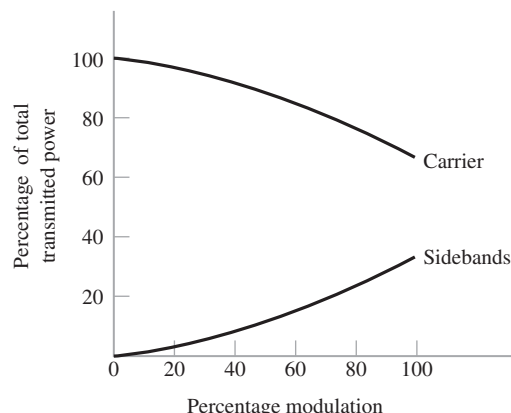


**FIGURE 3.4** Variations of carrier power and total sideband power with percentage modulation in amplitude modulation.

$$M \geq \frac{f_s}{f_r} = \frac{10}{0.005} = 2000$$

We therefore choose  $M = 2000$ . To approximate the Fourier transform of the modulated wave, we use a 2000-point FFT algorithm; the FFT algorithm was described in Chapter 2.

The only variable parameter in the full AM experiment is the modulation factor  $\mu$ , with respect to which three different situations are investigated:

- $\mu = 0.5$ , corresponding to undermodulation
- $\mu = 1.0$ , corresponding to 100 percent modulation
- $\mu = 2.0$ , corresponding to overmodulation

The results of the investigations are displayed in Figs. 3.5 through 3.7, details of which are described next.

### 1. Modulation factor $\mu = 0.5$

Figure 3.5(a) displays 10 cycles of the AM wave, corresponding to  $\mu = 0.5$ . The

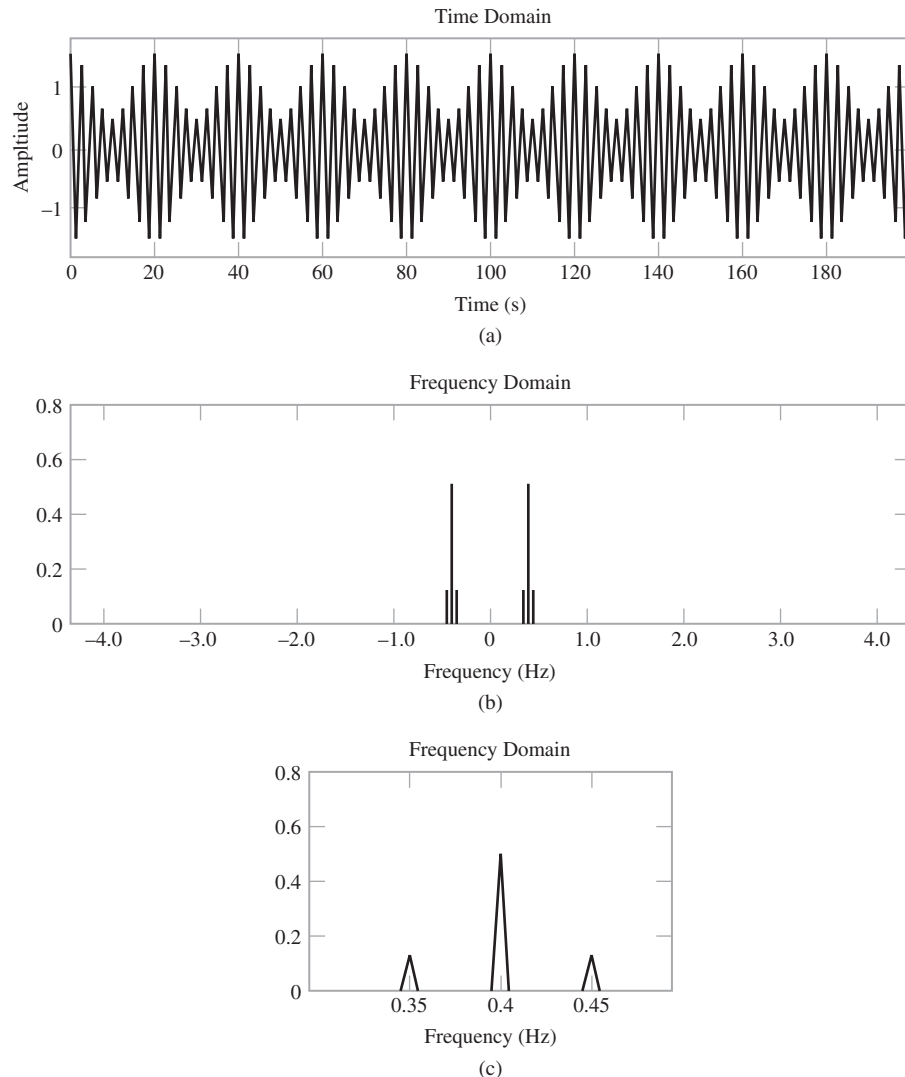


**FIGURE 3.5** Amplitude modulation with 50 percent modulation: (a) AM wave, (b) magnitude spectrum of the AM wave, and (c) expanded spectrum around the carrier frequency.

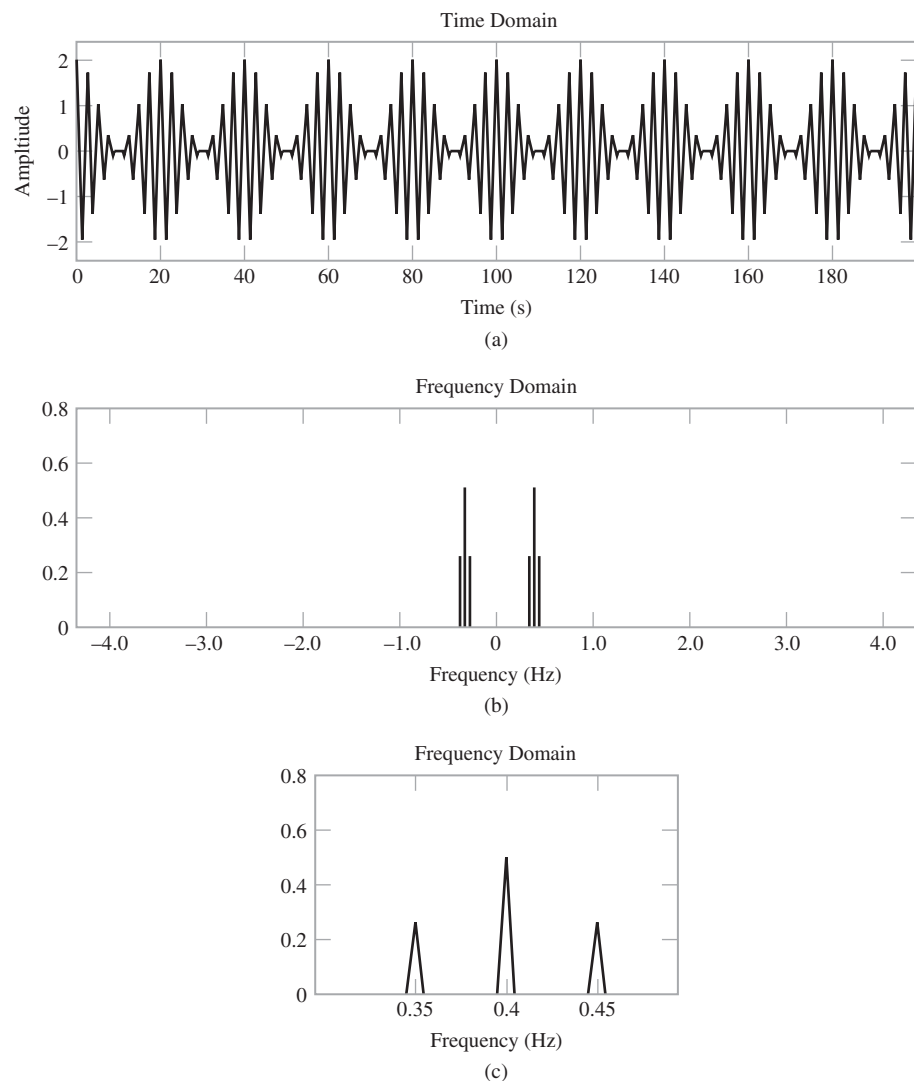
envelope of the modulated wave is clearly seen to follow the sinusoidal modulating wave faithfully. This means that we can use an envelope detector for demodulation.

Figure 3.5(b) displays the magnitude (amplitude) spectrum of the modulated wave. In Fig. 3.5(c), we have zoomed in on the fine structure of the modulated wave around the carrier frequency. The two figures clearly display the exact relationships between the two side frequencies and the carrier, in accordance with amplitude modulation theory, as summarized here:

- ▶ The lower side frequency, the carrier, and the upper side frequency are located at  $(f_c - f_m) = \pm 0.35$  Hz,  $f_c = \pm 0.4$  Hz, and  $(f_c + f_m) = \pm 0.45$  Hz.
- ▶ The amplitude of both side frequencies is  $(\mu/2) = 0.25$  times the amplitude of the carrier.

## 2. Modulation factor $\mu = 1.0$

Figure 3.6(a) shows 10 cycles of the modulated wave with the same parameters as in



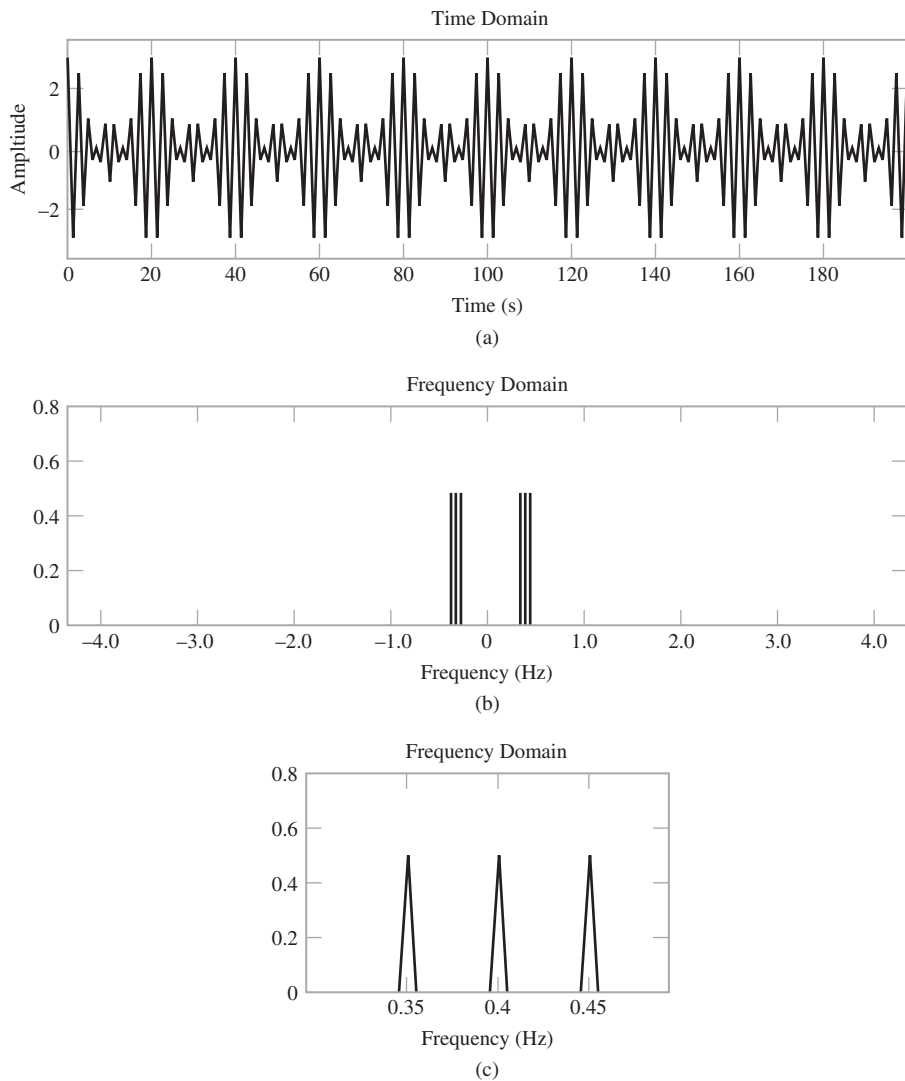
**FIGURE 3.6** Amplitude modulation with 100 percent modulation: (a) AM wave, (b) magnitude spectrum of the AM wave, and (c) expanded spectrum around the carrier frequency.

Fig. 3.5(a), except for the fact that  $\mu = 1.0$ . This new figure shows that the modulated wave is now on the verge of overmodulation.

The magnitude spectrum of the modulated wave is shown in Fig. 3.6(b), and its zoomed version (around the carrier frequency) is shown in Fig. 3.6(c). Here again, we see that the basic structure of the modulated wave's magnitude spectrum is in perfect agreement with amplitude modulation theory.

### 3. Modulation factor $\mu = 2.0$

Figure 3.7(a) demonstrates the effect of overmodulation by using a modulation factor  $\mu = 2.0$ . Here we see that there is no clear relationship between the envelope of the overmodulated wave and the sinusoidal modulating wave. As expected, the result implies that an envelope detector will not work for  $\mu = 2.0$ .



**FIGURE 3.7** Amplitude modulation with 200 percent modulation: (a) AM wave, (b) magnitude spectrum of the AM wave, and (c) expanded spectrum around the carrier frequency.

Nevertheless, the spectral content of the overmodulated wave displayed in Figs. 3.7(b) and 3.7(c) follows exactly what the amplitude modulation theory predicts.

► **Drill Problem 3.1** For 100 percent modulation, is it possible for the envelope of AM to become zero for some time  $t$ ? Justify your answer. ◀

► **Drill Problem 3.2** For a particular case of AM using sinusoidal modulating wave, the percentage modulation is 20 percent. Calculate the average power in (a) the carrier and (b) each side frequency. ◀

► **Drill Problem 3.3** In AM, *spectral overlap* is said to occur if the lower sideband for positive frequencies overlaps with its *image* for negative frequencies. What condition must the modulated wave satisfy if we are to avoid spectral overlap? Assume that the message signal  $m(t)$  is of a low-pass kind with bandwidth  $W$ . ◀

► **Drill Problem 3.4** A *square-law modulator* for generating an AM wave relies on the use of a nonlinear device (e.g., diode); Fig. 3.8 depicts the simplest form of such a modulator. Ignoring higher order terms, the input-output characteristic of the diode-load resistor combination in this figure is represented by the *square law*:

$$v_2(t) = a_1 v_1(t) + a_2 v_1^2(t)$$

where

$$v_1(t) = A_c \cos(2\pi f_c t) + m(t)$$

is the input signal,  $v_2(t)$  is the output signal developed across the load resistor, and  $a_1$  and  $a_2$  are constants.

- (a) Determine the spectral content of the output signal  $v_2(t)$ .
- (b) To extract the desired AM wave from  $v_2(t)$ , we need a band-pass filter (not shown in Fig. 3.8). Determine the cutoff frequencies of the required filter, assuming that the message signal is limited to the band  $-W \leq f \leq W$ .
- (c) To avoid *spectral distortion* by the presence of undesired modulation products in  $v_2(t)$ , the condition  $W < f_c > 3W$  must be satisfied; validate this condition. ◀

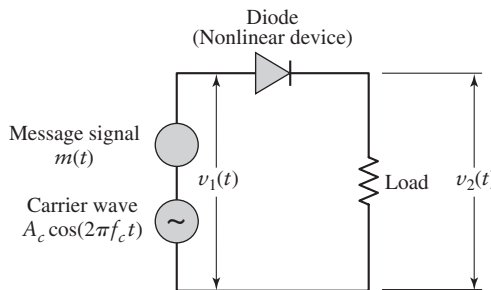


**FIGURE 3.8** Nonlinear circuit using a diode.

### ■ ENVELOPE DETECTION

The square-law modulator addressed in Problem 3.4 is testimony to the implementational simplicity involved in building an AM transmitter. The implementational simplicity of AM is further reinforced when we consider the demodulation of an AM wave, which is the inverse of modulation. In particular, the demodulation of an AM wave can be accomplished by means of a simple and yet highly effective circuit called the *envelope detector*<sup>2</sup>, provided two practical conditions are satisfied:

1. The AM wave is *narrowband*, which means that the carrier frequency is large compared to the message bandwidth.
2. The percentage modulation in the AM wave is less than 100 percent.

An envelope detector of the series type is shown in Fig. 3.9(a), which consists of a diode and resistor-capacitor (RC) filter. The operation of this envelope detector is as follows. On a positive half-cycle of the input signal, the diode is forward-biased and the capacitor C charges up rapidly to the peak value of the input signal. When the input signal falls below this value, the diode becomes reverse-biased and the capacitor C discharges slowly through the load resistor  $R_L$ . The discharging process continues until the next positive half-cycle. When the input signal becomes greater than the voltage across the capacitor, the diode conducts again and the process is repeated. We assume that the diode is ideal, presenting resistance  $r_f$  to current flow in the forward-biased region and infinite resistance in the reverse-biased region. We further assume that the AM wave applied to the envelope detector is supplied by a voltage source of internal impedance  $R_s$ . The charging time constant  $(r_f + R_s)C$  must be short compared with the carrier period  $1/f_c$ —that is,

$$(r_f + R_s)C \ll \frac{1}{f_c}$$

so that the capacitor C charges rapidly and thereby follows the applied voltage up to the positive peak when the diode is conducting. On the other hand, the discharging time constant  $R_L C$  must be long enough to ensure that the capacitor discharges slowly through the load resistor  $R_L$  between positive peaks of the carrier wave, but not so long that the capacitor voltage will not discharge at the maximum rate of change of the modulating wave—that is,

$$\frac{1}{f_c} \ll R_L C \ll \frac{1}{W}$$

where W is the message bandwidth. The result is that the capacitor voltage or detector output is nearly the same as the envelope of the AM wave, as demonstrated next.

---

<sup>2</sup>In the Preface, we pointed out that the approach taken in this book is from a systems perspective. In describing the envelope detector in detail, we are clearly making an exception to this approach. The reason for doing so is in recognition of the fact that the envelope detector, by virtue of its simplicity, is used in almost all commercial AM receivers. Indeed, the simplicity of building AM transmitters and receivers is such a compelling economic factor that, despite the ever-increasing dominance of digital communications, amplitude modulation will continue to find practical use in one form or another.

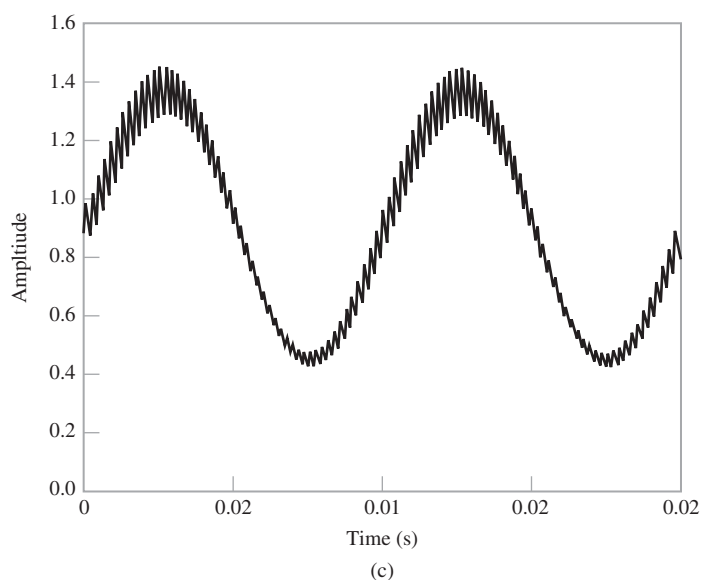
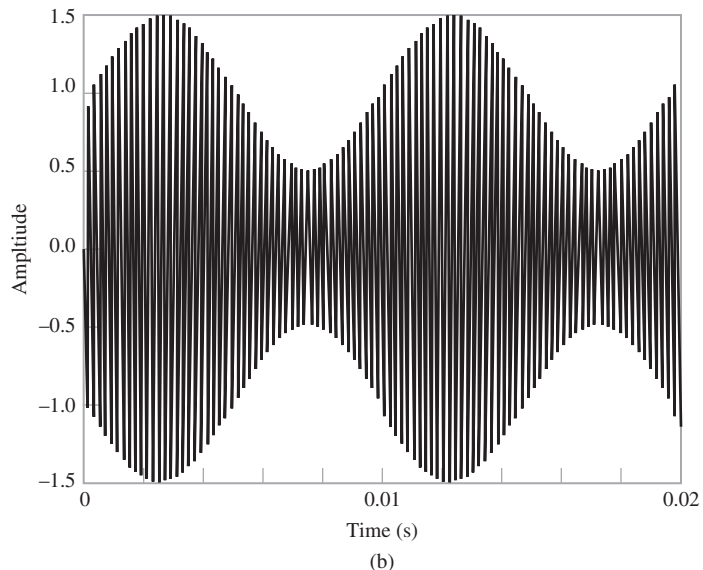
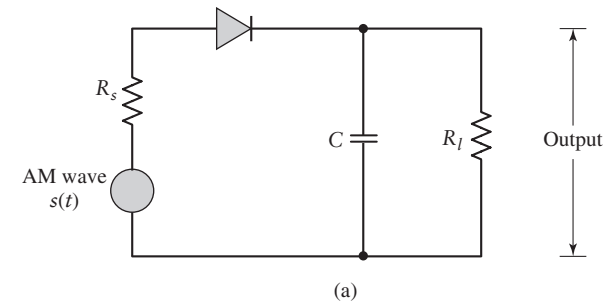


**FIGURE 3.9** Envelope detector. (a) Circuit diagram. (b) AM wave input. (c) Envelope detector output

### ■ COMPUTER EXPERIMENT: ENVELOPE DETECTION FOR SINUSOIDAL AM

Consider the sinusoidal AM wave shown in Fig. 3.9(b), assuming 50 percent modulation. The envelope detector output is shown in Fig. 3.9(c). This latter waveform is computed assuming that the diode is ideal, having a constant resistance  $r_f$  when forward-biased and infinite resistance when reverse-biased. The numerical values used in the computation of Fig. 3.9(c) are as follows:

Source resistance	$R_s = 75 \Omega$
Forward resistance	$r_f = 25 \Omega$
Load resistance	$R_L = 10 k\Omega$
Capacitance	$C = 0.01 \mu F$
Message bandwidth	$W = 1 \text{ kHz}$
Carrier frequency	$f_c = 20 \text{ kHz}$

Notice that the envelope detector output includes a high-frequency ripple; this ripple can be removed by using a low-pass filter (not shown in Fig. 3.9 (a))

## 3.2 Virtues, Limitations, and Modifications of Amplitude Modulation

Amplitude modulation is the oldest method of performing modulation. As already remarked in Section 3.1, its biggest virtue is the ease with which it is generated and reversed. The net result is that an amplitude modulation system is relatively inexpensive to build.

However, from Chapter 1 we recall that transmitted power and channel bandwidth are our two primary communication resources and they should be used efficiently. In this context, we find that the amplitude modulation defined in Eq. (3.2) suffers from two major practical limitations:

1. *Amplitude modulation is wasteful of transmitted power.* The carrier wave  $c(t)$  is completely independent of the information-bearing signal  $m(t)$ . The transmission of the carrier wave therefore represents a waste of power, which means that in amplitude modulation only a fraction of the total transmitted power is actually affected by  $m(t)$ .
2. *Amplitude modulation is wasteful of channel bandwidth.* The upper and lower sidebands of an AM wave are uniquely related to each other by virtue of their symmetry about the carrier frequency; hence, given the amplitude and phase spectra of either sideband, we can uniquely determine the other. This means that insofar as the transmission of information is concerned, only one sideband is necessary, and the communication channel therefore needs to provide only the same bandwidth as the message signal. In light of this observation, amplitude modulation is wasteful of channel bandwidth as it requires a transmission bandwidth equal to twice the message bandwidth.

To overcome these two limitations of AM, we must make certain changes that result in increased system complexity of the amplitude modulation process. In effect, we trade off system complexity for improved utilization of communication resources. Starting with amplitude modulation, we can distinguish three modifications of amplitude modulation:

1. *Double sideband-suppressed carrier (DSB-SC) modulation*, in which the transmitted wave consists of only the upper and lower sidebands. Transmitted power is saved here through the suppression of the carrier wave, but the channel bandwidth requirement is the same as before (i.e., twice the message bandwidth).
2. *Single sideband (SSB) modulation*, in which the modulated wave consists only of the upper sideband or the lower sideband. The essential function of SSB modulation is therefore to translate the spectrum of the modulating signal (with or without inversion)

to a new location in the frequency domain. Single sideband modulation is particularly suited for the transmission of voice signals by virtue of the *energy gap* that exists in the spectrum of voice signals between zero and a few hundred hertz. SSB is the optimum form of continuous-wave modulation in that it requires the minimum transmitted power and minimum channel bandwidth; its principal disadvantages are increased complexity and limited applicability.

3. *Vestigial sideband (VSB) modulation*, in which one sideband is passed almost completely and just a trace, or *vestige*, of the other sideband is retained. The required channel bandwidth is therefore slightly in excess of the message bandwidth by an amount equal to the width of the vestigial sideband. This form of modulation is well suited for the transmission of wideband signals such as television signals that contain significant components at extremely low frequencies. In commercial television broadcasting, a sizable carrier is transmitted together with the modulated wave, which makes it possible to demodulate the incoming modulated signal by an envelope detector in the receiver and thereby simplify the receiver design.

In Section 3.3 we discuss DSB-SC modulation, followed by discussions of SSB and VSB forms of modulation in subsequent sections and in that order.

### 3.3 Double Sideband-Suppressed Carrier Modulation

#### ■ THEORY

Basically, *double sideband-suppressed carrier (DSB-SC) modulation* consists of the product of the message signal  $m(t)$  and the carrier wave  $c(t)$ , as shown in the equation

$$\begin{aligned} s(t) &= c(t)m(t) \\ &= A_c \cos(2\pi f_c t)m(t) \end{aligned} \quad (3.8)$$

Accordingly, the device used to generate the DSB-SC modulated wave is referred to as a *product modulator*. From Eq. (3.8) we also note that unlike amplitude modulation, DSB-SC modulation is reduced to zero whenever the message signal  $m(t)$  is switched off.

Most noticeably, however, is the fact that the modulated signal  $s(t)$  undergoes a *phase reversal* whenever the message signal  $m(t)$  crosses zero, as indicated in Fig. 3.10(b) for the message signal  $m(t)$  depicted in part (a) of the figure. The envelope of a DSB-SC modulated signal is therefore different from the message signal, which means that simple demodulation using an envelope detection is not a viable option for DSB-SC modulation.

From Eq. (3.8), the Fourier transform of  $s(t)$  is obtained as

$$S(f) = \frac{1}{2}A_c[M(f - f_c) + M(f + f_c)] \quad (3.9)$$

where  $m(t) \iff M(f)$ . For the case when the message signal  $m(t)$  is limited to the interval  $-W \leq f \leq W$ , as in Fig. 3.11(a), we find that the spectrum  $S(f)$  of the DSB-SC wave  $s(t)$  is as illustrated in Fig. 3.11(b). Except for a change in scale factor, the modulation process simply *translates* the spectrum of the message signal by  $f_c$  to the right and by  $-f_c$  to the left. Of course, the transmission bandwidth required by DSB-SC modulation is the same as that for amplitude modulation—namely,  $2W$ .

In short, insofar as bandwidth occupancy is concerned, DSB-SC offers no advantage over AM. Its only advantage lies in saving transmitted power, which is important enough when the available transmitted power is at a premium.

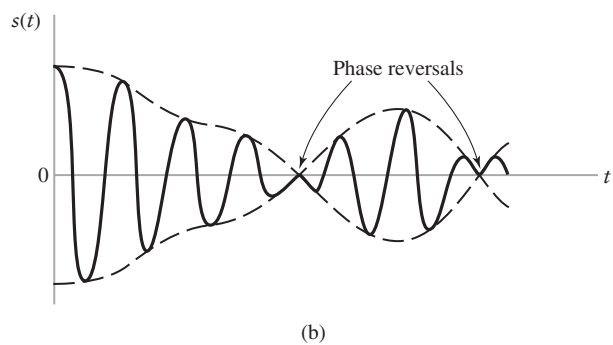
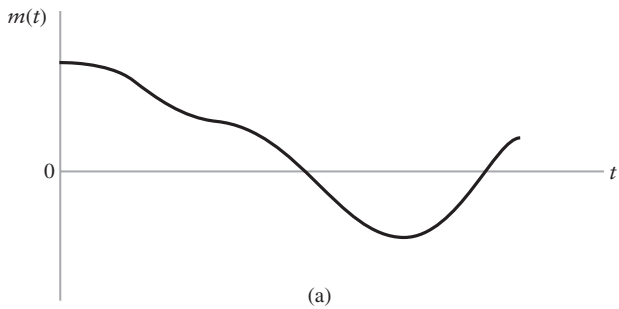


**FIGURE 3.10** (a) Message signal  $m(t)$ . (b) DSB-SC modulated wave  $s(t)$ .

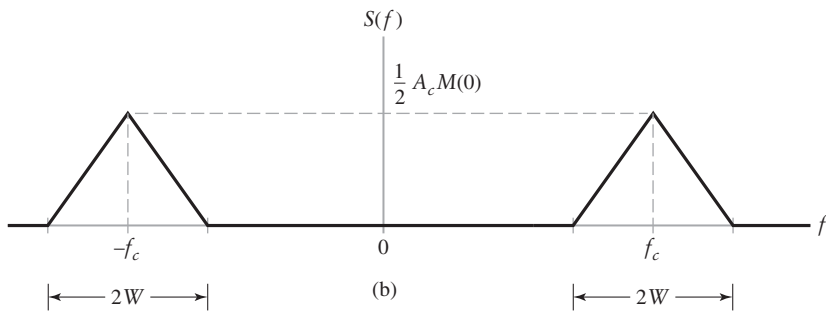
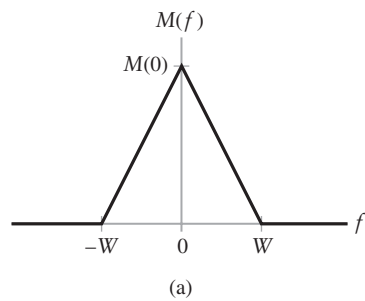


**FIGURE 3.11** (a) Spectrum of message signal  $m(t)$ . (b) Spectrum of DSB-SC modulated wave  $s(t)$ .

**EXAMPLE 3.2** Sinusoidal DSB-SC spectrum

Consider DSB-SC modulation using a sinusoidal modulating wave of amplitude  $A_m$  and frequency  $f_m$  and operating on a carrier of amplitude  $A_c$  and frequency  $f_c$ . The message spectrum is

$$M(f) = \frac{1}{2}A_m\delta(f - f_m) + \frac{1}{2}A_m\delta(f + f_m)$$

Invoking Eq. (3.9), the shifted spectrum  $\frac{1}{2}A_cM(f - f_c)$  defines the two side-frequencies for positive frequencies:

$$\frac{1}{4}A_cA_m\delta(f - (f_c + f_m)); \quad \frac{1}{4}A_cA_m\delta(f - (f_c - f_m))$$

The other shifted spectrum of Eq. (3.9)—namely,  $\frac{1}{2}A_cM(f + f_c)$ ,—defines the remaining two side-frequencies for negative frequencies:

$$\frac{1}{4}A_cA_m\delta(f + (f_c - f_m)); \quad \frac{1}{4}A_cA_m\delta(f + (f_c + f_m))$$

which are the *images* of the first two side-frequencies with respect to the origin, in reverse order.

► **Drill Problem 3.5** For the sinusoidal DSB-SC modulation considered in Example 3.2, what is the average power in the lower or upper side-frequency, expressed as a percentage of the average power in the DSB-SC modulated wave? ◀

**■ COHERENT DETECTION**

Since the envelope of the DSB-SC modulated wave  $s(t)$  is different from the message signal  $m(t)$ , we have to find some other means for recovering  $m(t)$  from  $s(t)$ . To this end, we recognize that  $\cos^2(2\pi f_c t)$  contains a constant term, as shown by the trigonometric identity

$$\cos^2(\theta) = \frac{1}{2} + \frac{1}{2}\cos(2\theta)$$

In light of this relation rewritten for  $\theta = 2\pi f_c t$ , we see from Eq. (3.8) that the recovery of the message signal  $m(t)$  can be accomplished by first multiplying  $s(t)$  with a locally generated sinusoidal wave and then low-pass filtering the product. It is assumed that the local oscillator signal is exactly coherent or synchronized, in both frequency and phase, with the carrier wave  $c(t)$  used in the product modulator to generate  $s(t)$ . This method of demodulation is known as *coherent detection* or *synchronous demodulation*.

It is instructive to derive coherent detection as a special case of the more general demodulation process using a local oscillator signal of the same frequency but arbitrary phase difference  $\phi$ , measured with respect to the carrier wave  $c(t)$ . Thus, denoting the local oscillator signal by  $A'_c \cos(2\pi f_c t + \phi)$  and using Eq. (3.8) for the DSB-SC wave  $s(t)$ , we find that the product modulator output in Fig. 3.12 is

$$\begin{aligned} v(t) &= A'_c \cos(2\pi f_c t + \phi)s(t) \\ &= A_c A'_c \cos(2\pi f_c t) \cos(2\pi f_c t + \phi)m(t) \\ &= \frac{1}{2}A_c A'_c \cos(4\pi f_c t + \phi)m(t) + \frac{1}{2}A_c A'_c \cos(\phi)m(t) \end{aligned} \quad (3.10)$$

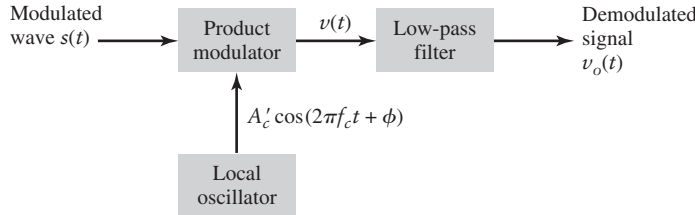


**FIGURE 3.12** Block diagram of coherent detector, assuming that the local oscillator is out of phase by  $\phi$  with respect to the sinusoidal carrier oscillator in the transmitter.

where we have used the trigonometric identity

$$\cos(\theta_1) \cos(\theta_2) = \frac{1}{2} \cos(\theta_1 + \theta_2) + \frac{1}{2} \cos(\theta_1 - \theta_2)$$

where, for the application at hand, we have  $\theta_1 = 2\pi f_c t$  and  $\theta_2 = 2\pi f_c t + \phi$ .

The first term in Eq. (3.10) represents a new DSB-SC modulated signal with carrier frequency  $2f_c$ , whereas the second term is proportional to the message signal  $m(t)$ . This is further illustrated by the spectrum  $V(f)$  shown in Fig. 3.13, where it is assumed that the message signal  $m(t)$  is limited to the interval  $-W \leq f \leq W$ . It is therefore apparent that the first term in Eq. (3.10) is removed by the low-pass filter in Fig. 3.12, provided that the cut-off frequency of this filter is greater than  $W$  but less than  $2f_c - W$ . This is satisfied by choosing  $f_c > W$ . At the filter output we then obtain a signal given by

$$v_o(t) = \frac{1}{2} A_c A'_c \cos(\phi) m(t) \quad (3.11)$$

The demodulated signal  $v_o(t)$  is therefore proportional to  $m(t)$  when the phase error  $\phi$  is a constant. The amplitude of this demodulated signal is maximum when  $\phi = 0$ , and it is minimum (zero) when  $\phi = \pm\pi/2$ . The zero demodulated signal, which occurs for  $\phi = \pm\pi/2$ , represents the *quadrature null effect*, which is an inherent property of coherent detection. Thus the phase error  $\phi$  in the local oscillator causes the detector output to be attenuated by a factor equal to  $\cos \phi$ . As long as the phase error  $\phi$  is constant, the detector output provides an undistorted version of the message signal  $m(t)$ . In practice, however, we usually find that the phase error  $\phi$  varies randomly with time, due to random variations in the communication channel. The result is that at the detector output, the multiplying factor  $\cos \phi$  would also vary randomly with time, which is obviously undesirable. Therefore, provision must be made in the system to maintain the local oscillator in the receiver in *synchronism, in both frequency and phase*, with the carrier wave used to generate the DSB-SC modulated signal in the transmitter. The resulting system complexity is the price that must be paid for suppressing the carrier wave to save transmitted power.

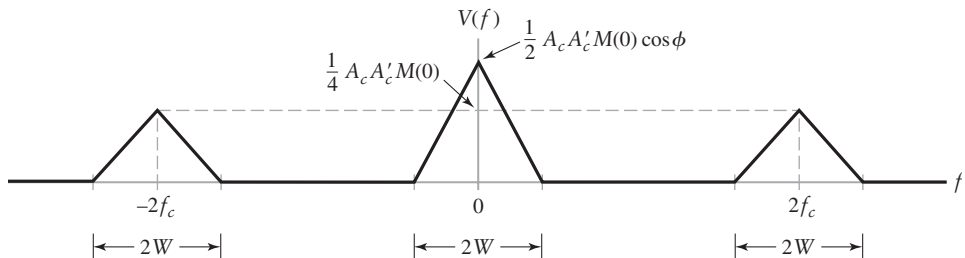


**FIGURE 3.13** Illustration of the spectrum of product modulator output  $v(t)$  in the coherent detector of Fig. 3.12, which is produced in response to a DSB-SC modulated wave as the detector input.

► **Drill Problem 3.6** The sinusoidally modulated DSB-SC wave of Example 3.2 is applied to a product modulator using a locally generated sinusoid of unit amplitude, and which is synchronous with the carrier used in the modulator.

- Determine the output of the product modulator, denoted by  $v(t)$ .
- Identify the two sinusoidal terms in  $v(t)$  that are produced by the DSB-SC modulated wave for positive frequencies, and the remaining two sinusoidal terms produced by the DSB-SC modulated wave for negative frequencies.

► **Drill Problem 3.7** The coherent detector for the demodulation of DSB-SC fails to operate satisfactorily if the modulator experiences spectral overlap. Explain the reason for this failure. ◀

### ■ COMPUTER EXPERIMENT: DSB-SC

For the experimental study of DSB-SC modulation, we follow the same setup described in Section 3.1, except for the changes brought on by the use of DSB-SC in place of AM. Results of the experiment are described under two points:

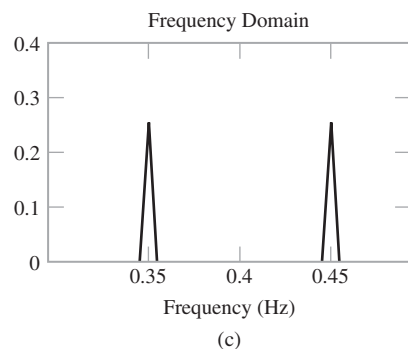
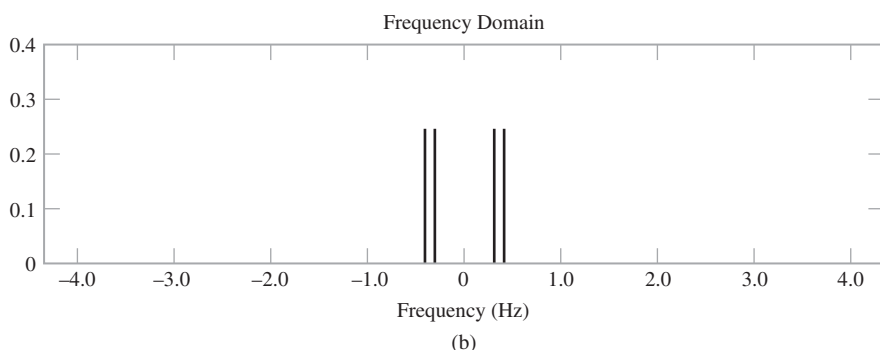
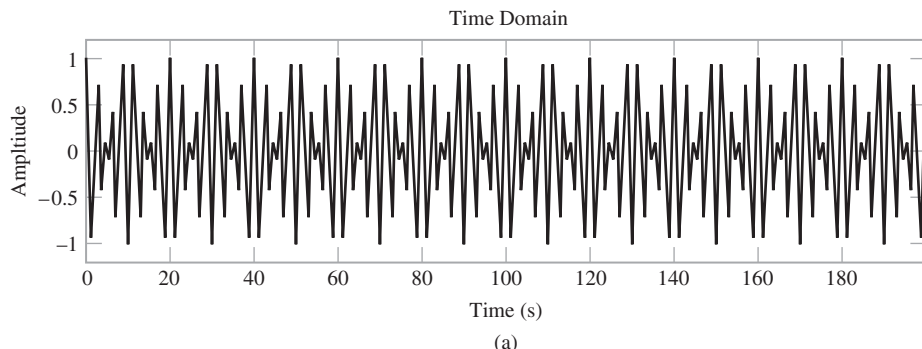


**FIGURE 3.14** DSB-SC modulation: (a) DSB-SC modulated wave, (b) magnitude spectrum of the modulated wave, and (c) expanded spectrum around the carrier frequency.

- Figure 3.14(a) displays 10 cycles of the DSB-SC modulated wave produced by the sinusoidal modulating wave of frequency 0.05 Hz. As expected, the envelope of the modulated wave bears no clear relationship to the sinusoidal modulating wave. Accordingly, we must use coherent detection for demodulation, which is discussed under point 2.

Figure 3.14(b) shows the magnitude spectrum of the modulated wave. An expanded view of the spectrum around the carrier frequency of frequency 0.4 Hz is shown in Fig. 3.14(c). These two figures clearly show that the carrier is indeed suppressed, and that the upper and lower side frequencies are located exactly where they should be—namely, at  $\pm 0.45$  and  $\pm 0.35$  Hz, respectively.

- To perform coherent detection, we proceed in two stages: (i) multiply the DSB-SC modulated wave by an exact replica of the carrier, and (ii) pass the product through a low-pass filter, as described under coherent detection in this section. With two operational stages involved in the coherent detection process, the results of this part of the experiment are presented as follows:
- (i) Figure 3.15(a) displays the waveform of the product modulator's output in the coherent detector. The magnitude spectrum of this waveform is shown in

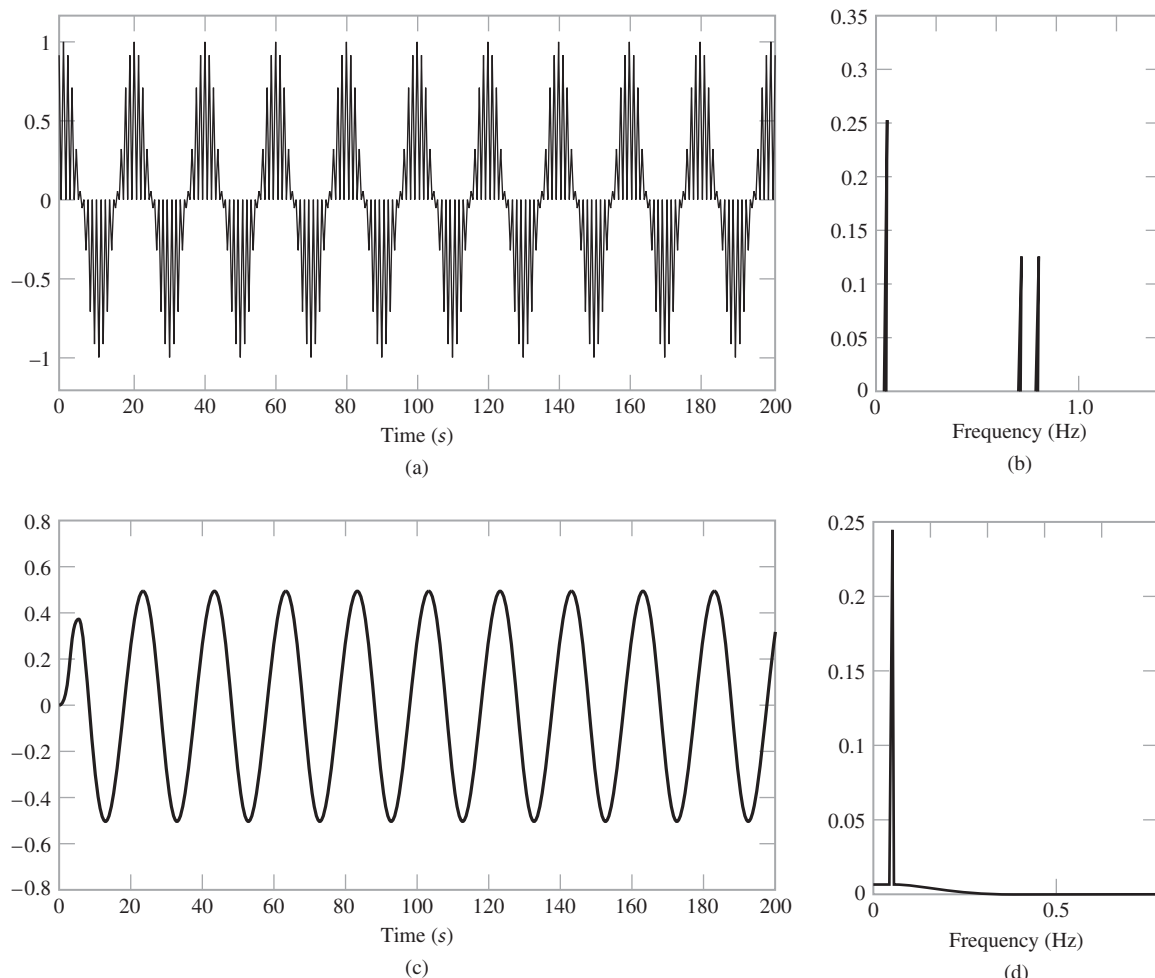


**FIGURE 3.15** Coherent detection of DSB-SC modulated wave: (a) Waveform of signal produced at the output of product modulator, (b) amplitude spectrum of the signal in part (a); (c) waveform of low-pass filter output; and (d) amplitude spectrum of signal in part (c).

Fig. 3.15(b), which readily shows that the waveform consists of the following components:

- ▶ A sinusoidal component with frequency 0.05 Hz, representing the sinusoidal modulating wave.

- ▶ A new DSB-SC modulated wave with double carrier frequency of 0.8 Hz; in actuality, the two side-frequencies of this modulated wave are located at 0.75 and 0.85 Hz, exactly where they should be.

- (ii) Figure 3.15(c) shows the waveform of the coherent detector's overall output, which results after passing the product modulator's output through the low-pass filter. Except for transient effects experienced early on in the detection process, the waveform is recognized to be the desired sinusoidal modulating wave of frequency 0.05 Hz. This result is further confirmed in the amplitude spectrum displayed in Fig. 3.15(d); the pedestal on which the line frequency component at 0.05 Hz sits is due to the transient effects just described.

## 3.4 Costas Receiver

Coherent detection of a DSB-SC modulated wave requires that the locally generated carrier in the receiver be *synchronous in both frequency and phase* with the oscillator responsible for generating the carrier in the transmitter. This is a rather demanding requirement, all the more so since the carrier is suppressed from the transmitted DSB-SC signal. One method of satisfying this requirement is to use the *Costas receiver* shown in Fig. 3.16. This receiver consists of two coherent detectors supplied with the same input signal—namely, the incoming DSB-SC wave  $A_c \cos(2\pi f_c t)m(t)$ , but with two local oscillator signals that are in phase quadrature with respect to each other. The frequency of the local oscillator is adjusted to be the same as the carrier frequency  $f_c$ ; it is assumed known *a priori*. This assumption is reasonable since the system designer has access to the detailed specifications of both the transmitter and receiver. The detector in the upper path is referred to as the *in-phase coherent detector* or *I-channel*, and the detector in the lower path is referred to as

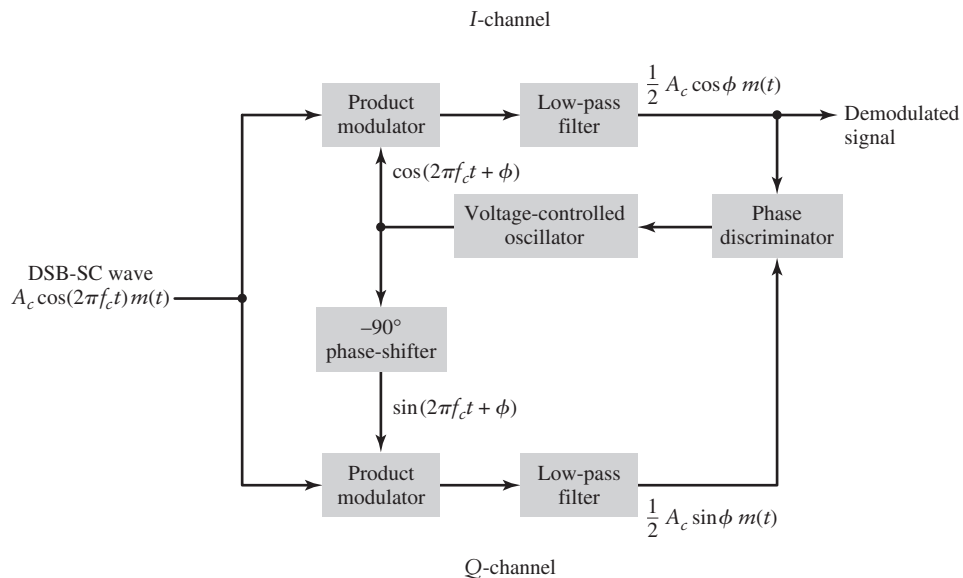


**FIGURE 3.16** Costas receiver for the demodulation of a DSB-SC modulated wave.

the *quadrature-phase coherent detector or Q-channel*. These two detectors are coupled together to form a *negative feedback* system designed in such a way as to maintain the local oscillator in synchronism with the carrier wave.

To understand the operation of this receiver, suppose that the local oscillator signal is of the same phase as the carrier wave  $A_c \cos(2\pi f_{ct})$  used to generate the incoming DSB-SC wave. Under these conditions, we find that the *I*-channel output contains the desired demodulated signal  $m(t)$ , whereas the *Q*-channel output is zero due to the quadrature null effect of the *Q*-channel. Next suppose that the local oscillator phase drifts from its proper value by a small angle  $\phi$  radians. From the discussion on coherent detection in Section 3.3 we know that the *I*-channel output is proportional to  $\cos \phi$  and  $\cos \phi \approx 1$  for small  $\phi$ ; hence, the *I*-channel output remains essentially unchanged so long as  $\phi$  is small. But there will now be some signal, albeit small, appearing at the *Q*-channel output, which is proportional to  $\sin \phi \approx \phi$  for small  $\phi$ . This *Q*-channel output will have the same polarity as the *I*-channel output for one direction of local oscillator phase drift  $\phi$  and the opposite polarity for the opposite direction of  $\phi$ . Thus, by combining the *I*- and *Q*-channel outputs in a *phase discriminator* (which consists of a multiplier followed by a time-averaging unit), a dc control signal proportional to the phase drift  $\phi$  is generated. With negative feedback acting around the Costas receiver, the control signal tends to automatically correct for the local phase error  $\phi$  in the *voltage-controlled oscillator*.

It is apparent that phase control in the Costas receiver ceases with modulation, which means that phase-lock would have to be re-established with the reappearance of modulation. This is not a serious problem, because the lock-up process normally occurs so rapidly that no distortion is perceptible.

**► Drill Problem 3.8** As just mentioned, the phase discriminators in the Costas receiver of Fig. 3.16 consist of a multiplier followed by a time-averaging unit. Referring to this figure, do the following:

- Assuming that the phase error  $\phi$  is small compared to one radian, show that the output  $g(t)$  of the multiplier component is approximately  $\frac{1}{4}\phi m^2(t)$ .
- Furthermore, passing  $g(t)$  through the time-averaging unit defined by

$$\frac{1}{2T} \int_{-T}^{T} g(t) dt$$

where the averaging interval  $2T$  is long enough compared to the reciprocal of the bandwidth of  $g(t)$ , show that the output of the phase discriminator is proportional to the phase-error  $\phi$  multiplied by the dc (direct current) component of  $m^2(t)$ . The amplitude of this signal (acting as the control signal applied to the voltage-controlled oscillator in Fig. 3.16) will therefore always have the same algebraic sign as that of the phase error  $\phi$ , which is how it should be. ◀

## 3.5 Quadrature-Carrier Multiplexing

The quadrature null effect of the coherent detector may also be put to good use in the construction of the so-called *quadrature-carrier multiplexing* or *quadrature-amplitude modulation* (QAM). This scheme enables two DSB-SC modulated waves (resulting from the application of two physically *independent* message signals) to occupy the same channel bandwidth. Yet it allows for the separation of the two message signals at the receiver output. Quadrature-carrier multiplexer is therefore a *bandwidth-conservation system*.

A block diagram of this system is shown in Fig. 3.17. The transmitter part of the system, shown in Fig. 3.17(a), involves the use of two separate product modulators that are supplied with two carrier waves of the same frequency but differing in phase by

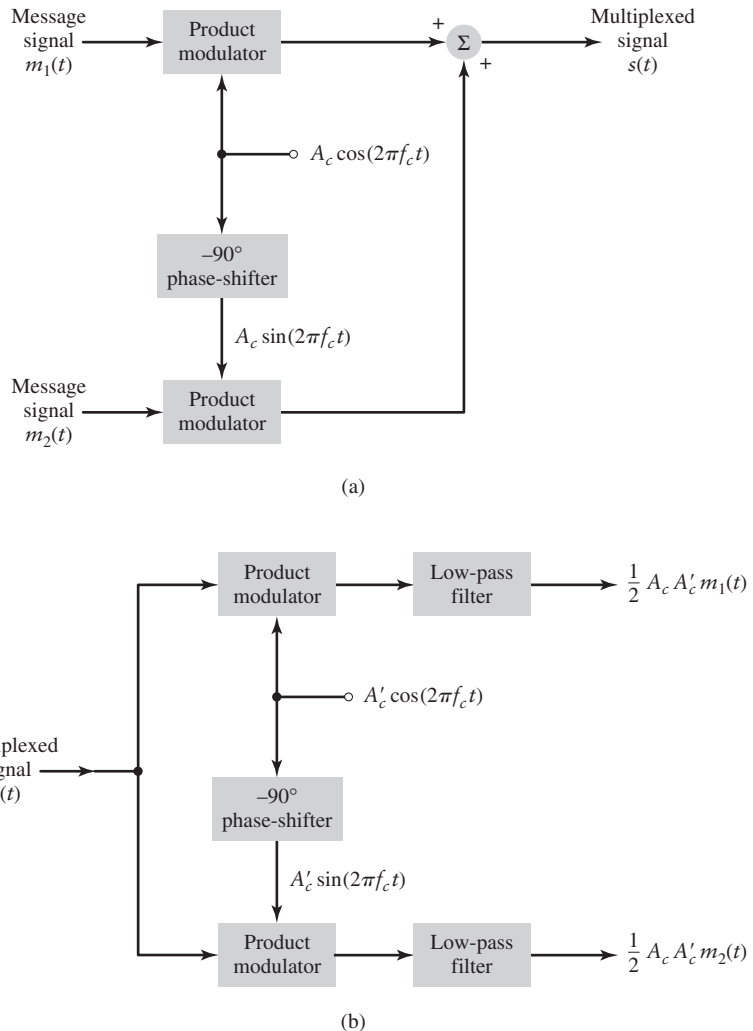


**FIGURE 3.17** Quadrature-carrier multiplexing system: (a) Transmitter, (b) receiver.

-90 degrees. The transmitted signal  $s(t)$  consists of the sum of these two product modulator outputs, as shown by

$$s(t) = A_c m_1(t) \cos(2\pi f_c t) + A_c m_2(t) \sin(2\pi f_c t) \quad (3.12)$$

where  $m_1(t)$  and  $m_2(t)$  denote the two different message signals applied to the product modulators. The multiplexed signal  $s(t)$  occupies a channel bandwidth of  $2W$  centered on the carrier frequency  $f_c$ , where  $W$  is the message bandwidth, assumed to be common to both  $m_1(t)$  and  $m_2(t)$ . According to Eq. (3.12), we may view  $A_c m_1(t)$  as the in-phase component of the multiplexed band-pass signal  $s(t)$  and  $-A_c m_2(t)$  as its quadrature component.

The receiver part of the system is shown in Fig. 3.17(b). Specifically, the multiplexed signal  $s(t)$  is applied simultaneously to two separate coherent detectors that are supplied with two local carriers of the same frequency, but differing in phase by -90 degrees. The output of the top detector is  $\frac{1}{2} A_c A'_c m_1(t)$ , whereas the output of the bottom detector is  $\frac{1}{2} A_c A'_c m_2(t)$ . For the system to operate satisfactorily, it is important to maintain the correct phase and frequency relationships between the oscillator used to generate the carriers in the transmitter and the corresponding local oscillator used in the receiver.

To maintain this synchronization, we may use a Costas receiver described in Section 3.4. Another commonly used method is to send a *pilot signal* outside the passband of the modulated signal. In the latter method, the pilot signal typically consists of a low-power sinusoidal tone whose frequency and phase are related to the carrier wave  $c(t) = A_c(2\pi f_c t)$ . At the receiver, the pilot signal is extracted by means of a suitably tuned circuit and then translated to the correct frequency for use in the coherent detector.

► **Drill Problem 3.9** Verify that the outputs of the receiver in Fig. 3.17(b) are as indicated in the figure, assuming perfect synchronism between the receiver and transmitter. ◀

## 3.6 Single-Sideband Modulation

In suppressing the carrier, DSB-SC modulation takes care of a major limitation of AM that pertains to the wastage of transmitted power. To take care of the other major limitation of AM that pertains to channel bandwidth, we need to suppress one of the two sidebands in the DSB-SC modulated wave. This modification of DSB-SC modulation is precisely what is done in *single sideband (SSB) modulation*. In effect, SSB modulation relies solely on the lower sideband or upper sideband to transmit the message signal across a communication channel. Depending on which particular sideband is actually transmitted, we speak of *lower SSB* or *upper SSB* modulation.

### ■ THEORY

A rigorous derivation of SSB modulation theory that applies to an arbitrary message signal is rather demanding and therefore beyond the scope of this book. To simplify matters, we will take an approach different from that used in Section 3.1 on AM and Section 3.3 on DSB-SC. Specifically, we start the study of SSB modulation by first considering the simple case of a *sinusoidal modulating wave*, and then we generalize the results to an arbitrary modulating signal in a step-by-step manner.

To proceed then, consider a DSB-SC modulator using the sinusoidal modulating wave

$$m(t) = A_m \cos(2\pi f_m t)$$

With the carrier  $c(t) = A_c \cos(2\pi f_c t)$ , the resulting DSB-SC modulated wave is defined by

$$\begin{aligned} S_{\text{DSB}}(t) &= c(t)m(t) \\ &= A_c A_m \cos(2\pi f_c t) \cos(2\pi f_m t) \\ &= \frac{1}{2} A_c A_m \cos[2\pi(f_c + f_m)t] + \frac{1}{2} A_c A_m \cos[2\pi(f_c - f_m)t] \end{aligned} \quad (3.13)$$

which is characterized by two *side-frequencies*, one at  $f_c + f_m$  and the other at  $f_c - f_m$ . Suppose that we would like to generate a sinusoidal SSB modulated wave that retains the upper side-frequency at  $f_c + f_m$ . Then, suppressing the second term in Eq. (3.13), we may express the upper SSB modulated wave as

$$S_{\text{USSB}}(t) = \frac{1}{2} A_c A_m \cos[2\pi(f_c + f_m)t] \quad (3.14)$$

The cosine term in Eq. (3.14) includes the sum of two angles—namely,  $2\pi f_c t$  and  $2\pi f_m t$ . Therefore, expanding the cosine term in Eq. (3.14) using a well-known trigonometric identity, we have

$$S_{\text{USSB}}(t) = \frac{1}{2} A_c A_m \cos(2\pi f_c t) \cos(2\pi f_m t) - \frac{1}{2} A_c A_m \sin(2\pi f_c t) \sin(2\pi f_m t) \quad (3.15)$$

If, on the other hand, we were to retain the lower side-frequency at  $f_c - f_m$  in the DSB-SC modulated wave of Eq. (3.13), then we would have a lower SSB modulated wave defined by

$$S_{\text{LSSB}}(t) = \frac{1}{2}A_c A_m \cos(2\pi f_c t) \cos(2\pi f_m t) + \frac{1}{2}A_c A_m \sin(2\pi f_c t) \sin(2\pi f_m t) \quad (3.16)$$

Examining Eqs. (3.15) and (3.16), we see that they differ from each other in only one respect: the minus sign in Eq. (3.15) is replaced with the plus sign in Eq. (3.16). Accordingly, we may combine these two equations and thereby define a sinusoidal SSB modulated wave as follows:

$$S_{\text{SSB}}(t) = \frac{1}{2}A_c A_m \cos(2\pi f_c t) \cos(2\pi f_m t) \mp \frac{1}{2}A_c A_m \sin(2\pi f_c t) \sin(2\pi f_m t) \quad (3.17)$$

where the plus sign applies to lower SSB and the minus sign applies to upper SSB.

With the generalization of Eq. (3.17) as the goal, we next proceed in two stages. In stage 1, we let the message signal be periodic; and in stage 2, we let it be nonperiodic. Consider then a *periodic message signal* defined by the Fourier series

$$m(t) = \sum_n a_n \cos(2\pi f_n t) \quad (3.18)$$

which consists of a mixture of sinusoidal waves with harmonically related frequencies. Recognizing that the carrier  $c(t)$  is common to all the sinusoidal components of  $m(t)$ , we may therefore immediately infer from Eq. (3.17) the expression

$$S_{\text{SSB}}(t) = \frac{1}{2}A_c \cos(2\pi f_c t) \sum_n a_n \cos(2\pi f_n t) \mp \frac{1}{2}A_c \sin(2\pi f_c t) \sum_n a_n \sin(2\pi f_n t) \quad (3.19)$$

as the corresponding formula for the SSB modulated wave.

Next, let us consider another periodic signal defined by the Fourier series

$$\hat{m}(t) = \sum_n a_n \sin(2\pi f_n t) \quad (3.20)$$

which is of a form similar to that of Eq. (3.18) except for the fact that the cosine term  $\cos(2\pi f_c t)$  is replaced by the sine term  $\sin(2\pi f_c t)$ . Then, in light of the definitions in Eqs. (3.19) and (3.20), we may reformulate the SSB modulated wave of Eq. (3.17) as

$$S_{\text{SSB}}(t) = \frac{A_c}{2}m(t) \cos(2\pi f_c t) \mp \frac{A_c}{2}\hat{m}(t) \sin(2\pi f_c t) \quad (3.21)$$

Comparing Eq. (3.20) with Eq. (3.18), we observe that the periodic signal  $\hat{m}(t)$  can be derived from the periodic modulating signal  $m(t)$  simply by shifting the phase of each cosine term in Eq. (3.18) by  $-90^\circ$ .

In both technical and practical terms, the observation we have just made is very important for two reasons:

1. We know from Fourier analysis that *under appropriate conditions, the Fourier series representation of a periodic signal converges to the Fourier transform of a nonperiodic signal*; see Appendix 2 for details.
2. *The signal  $\hat{m}(t)$  is the Hilbert transform of the signal  $m(t)$ .* Basically, a *Hilbert transformer* is a system whose transfer function is defined by

$$H(f) = -j \operatorname{sgn}(f) \quad (3.22)$$

where  $\operatorname{sgn}(f)$  is the signum function; for the definition of the signum function see Section 2.4. In words, the Hilbert transformer is a *wide-band phase-shifter* whose frequency response is characterized in two parts as follows (see Problem 2.52):

- The magnitude response is unity for all frequencies, both positive and negative.

- The phase response is  $+90^\circ$  for negative frequencies and  $-90^\circ$  for positive frequencies.

Equipped analytically in the manner described under points 1 and 2, we may finally generalize Eq. (3.21) as the formula for a single-sideband modulated wave produced by a message signal, regardless of whether it is periodic or nonperiodic. Specifically, given a Fourier transformable message signal  $m(t)$  with its Hilbert transform denoted by  $\hat{m}(t)$ , the SSB modulated wave produced by  $m(t)$  is defined by

$$s(t) = \frac{A_c}{2} m(t) \cos(2\pi f_c t) \mp \frac{A_c}{2} \hat{m}(t) \sin(2\pi f_c t) \quad (3.23)$$

where  $A_c \cos(2\pi f_c t)$  is the carrier,  $A_c \sin(2\pi f_c t)$  is its  $-90^\circ$  phase-shifted version; the plus and minus signs apply to the lower SSB and upper SSB, respectively. In Eq. (3.23), we have omitted the use of SSB as a subscript for  $s(t)$ , with it being understood that this equation refers to SSB modulation in its most generic form.

- **Drill Problem 3.10** Using Eqs. (3.22) and (3.23), show that for positive frequencies the spectra of the two kinds of SSB modulated waves are defined as follows:

(a) For the upper SSB,

$$S(f) = \begin{cases} \frac{A_c}{2} M(f - f_c), & \text{for } f \geq f_c \\ 0, & \text{for } 0 < f \leq f_c \end{cases} \quad (3.24)$$

(b) For the lower SSB,

$$S(f) = \begin{cases} 0, & \text{for } f > f_c \\ \frac{A_c}{2} M(f - f_c), & \text{for } 0 < f \leq f_c \end{cases} \quad (3.25)$$

- **Drill Problem 3.11** Show that if the message signal  $m(t)$  is low-pass, then the Hilbert transform  $\hat{m}(t)$  is also low-pass with exactly the same bandwidth as  $m(t)$ . ◀

The two spectral formulas defined in parts (a) and (b) of Problem 3.10 are intuitively satisfying. In particular, they are both in perfect accord with the two pictures displayed in parts (b) and (c) of Fig. 3.18, respectively. Figure 3.18(b) describes an SSB modulated wave that has retained the upper sideband, whereas Fig. 3.18(c) describes the other kind of SSB modulation that has retained the lower sideband. From a practical perspective, the only issue that distinguishes one kind of SSB modulation from the other is that of bandwidth occupancy.

## ■ MODULATORS FOR SSB

In light of the theory presented in this section, we may develop two methods for generating SSB-modulated waves, as described next.

### **Frequency Discrimination Method**

One straightforward method for SSB generation, called the *frequency discrimination method*, is depicted in Fig. 3.19; this discriminator follows directly from Eqs. (3.24) and (3.25) presented in Problem 3.10. The SSB modulator of Fig. 3.19 consists of two components: product modulator followed by band-pass filter. The product modulator produces a DSB-SC modulated wave with an upper sideband and a lower sideband. The band-pass

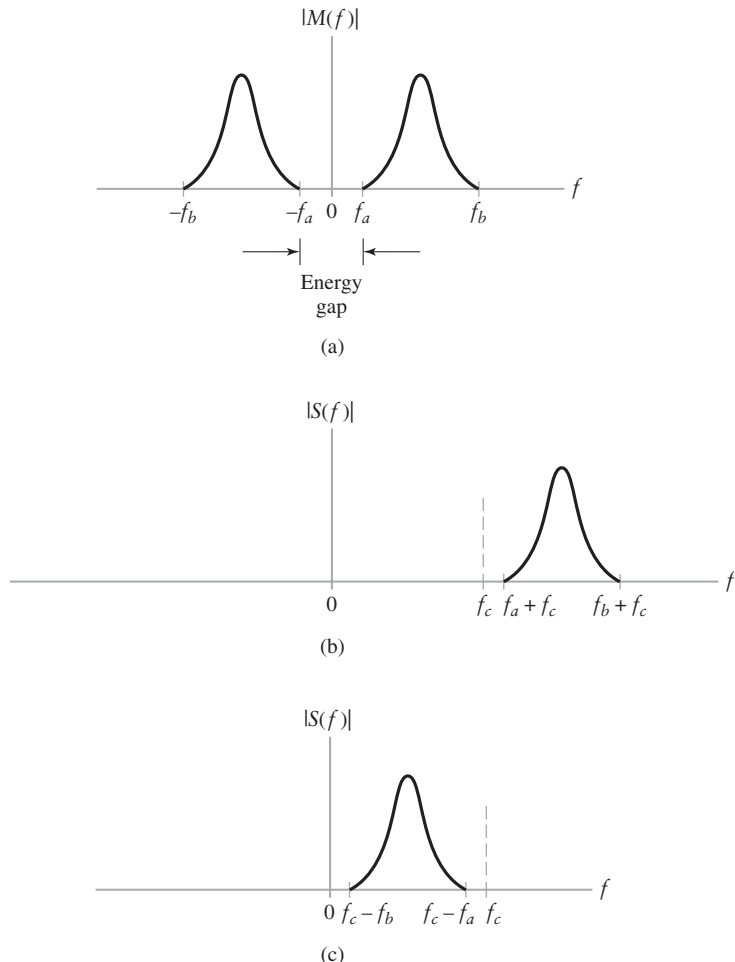


**FIGURE 3.18** (a) Spectrum of a message signal  $m(t)$  with energy gap centered around zero frequency. Corresponding spectra of SSB-modulated waves using (b) upper sideband, and (c) lower sideband. In parts (b) and (c), the spectra are only shown for positive frequencies.

filter is designed to transmit one of these two sidebands, depending on whether the upper SSB or lower SSB is the desired modulation. For the design of the band-pass filter to be practically feasible, there must be a certain separation between the two sidebands that is wide enough to accommodate the transition band of the band-pass filter. This separation is equal to  $2f_a$ , where  $f_a$  is the lowest frequency component of the message signal, as illustrated in Fig. 3.18. This requirement limits the applicability of SSB modulation to speech signals for

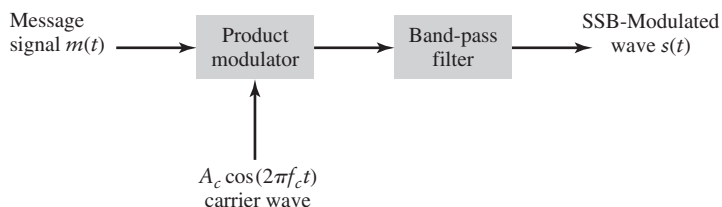


**FIGURE 3.19** Frequency-discrimination scheme for the generation of a SSB modulated wave.

which  $f_a \approx 100$  Hz, but rules it out for video signals and computer data whose spectral content extends down to almost zero frequency.

### Phase Discrimination Method

The second method for SSB generation, called the *phase discrimination* method, is depicted in Fig. 3.20; its implementation follows from the time-domain description of SSB waves defined in Eq. (3.23). This second SSB modulator consists of two parallel paths, one called the *in-phase path* and the other called the *quadrature path*. Each path involves a product modulator. The sinusoidal carrier waves applied to the two product modulators are in *phase-quadrature*, which is taken care of by simply using a  $-90^\circ$  phase-shifter as shown in Fig. 3.20. However, the one functional block in Fig. 3.20 that requires special attention is the *wide-band phase-shifter*, which is designed to produce the Hilbert transform  $\hat{m}(t)$  in response to the incoming message signal  $m(t)$ . The role of the quadrature path embodying the wide-band phase shifter is merely to interfere with the in-phase path so as to eliminate power in one of the two sidebands, depending on whether upper SSB or lower SSB is the requirement.

The two modulators of Figs. 3.19 and 3.20 are clearly quite different in their structures. In terms of design challenge, the band-pass filter in the frequency discriminator of Fig. 3.19 stands out as the functional block that requires special attention. On the other hand, in the phase discriminator of Fig. 3.20, it is the wide-band phase shifter that requires special attention.

### ■ COHERENT DETECTION OF SSB

The demodulation of DSB-SC is complicated by the suppression of the carrier in the transmitted signal. To make up for the absence of the carrier in the received signal, the receiver resorts to the use of *coherent detection*, which requires synchronization of a local oscillator in the receiver with the oscillator responsible for generating the carrier in the transmitter. The synchronization requirement has to be in both phase and frequency. Although the carrier is suppressed, information on the carrier phase and frequency is embedded into the sidebands of the modulated wave, which is exploited in the receiver. However, the demodulation of SSB is further complicated by the additional suppression of the upper or lower sideband. In actuality, however, the two sidebands share an important property: they

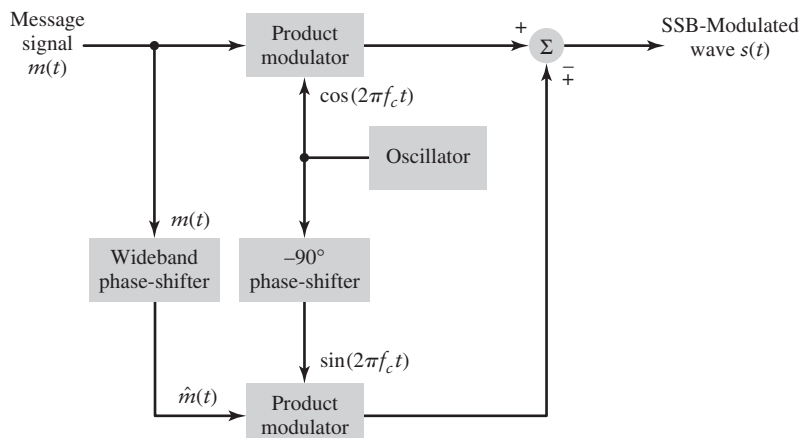


**FIGURE 3.20** Phase discrimination method for generating a SSB-modulated wave.

Note: The plus sign at the summing junction pertains to transmission of the lower sideband and the minus sign pertains to transmission of the upper sideband.

are the *images* of each other with respect to the carrier. Here again, coherent detection comes to the rescue of SSB demodulation.

The coherent detector of Fig. 3.12 applies equally well to the demodulation of both DSB-SC and SSB; the only difference between these two applications is how the modulated wave  $s(t)$  is defined.

► **Drill Problem 3.12** For the low-pass filter in Fig. 3.12 (assuming perfect synchronism) to suppress the undesired SSB wave, the following condition must be satisfied

$$f_c > W, \quad f_c = \text{carrier frequency, and } W = \text{message bandwidth}$$

Justify this condition. ◀

► **Drill Problem 3.13** Starting with Eq. (3.23) for a SSB modulated wave, show that the output produced by the coherent detector of Fig. 3.12 in response to this modulated wave is defined by

$$\nu_o(t) = \frac{A_c A'_c}{4} m(t)$$

Assume that the phase error  $\phi = 0$  in Fig. 3.12. ◀

### ■ FREQUENCY TRANSLATION

The basic operation performed in single sideband modulation is in fact a form of *frequency translation*, which is why single sideband modulation is sometimes referred to as *frequency changing, mixing, or heterodyning*.

The idea of single sideband modulation has thus far been presented in the context of a raw message signal. This idea may be generalized to encompass frequency translation as follows. Suppose that we have a modulated wave  $s_1(t)$  whose spectrum is centered on a carrier frequency  $f_1$ , and the requirement is to translate it upward or downward in frequency, such that the carrier frequency is changed from  $f_1$  to a new value  $f_2$ . This requirement is accomplished by using a *mixer*. As depicted in Fig. 3.21, the mixer is a functional block that consists of a product modulator followed by a band-pass filter, as it is in a conventional SSB modulator but with an important difference: the band-pass filter is now straightforward to design, as explained in what follows.

Specifically, to explain the action of the mixer, consider the spectral situation depicted in Fig. 3.22(a), where, for the purpose of illustration, it is assumed that the mixer input  $s_1(t)$  is a wave with carrier frequency  $f_1$  and bandwidth  $2W$ . Figure 3.21(b) displays the spectrum  $S'(f)$  of the resulting signal  $s'(t)$  produced at the output of the product modulator in Fig. 3.21.

The signal  $s'(t)$  may be viewed as the sum of two modulated components: one component represented by the shaded spectrum in Fig. 3.22(b), and the other component represented by the unshaded spectrum in this figure. Depending on whether the incoming

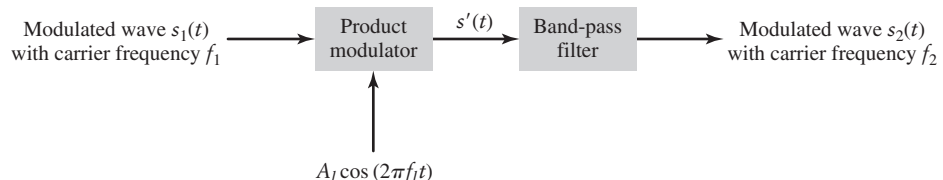


**FIGURE 3.21** Block diagram of mixer.

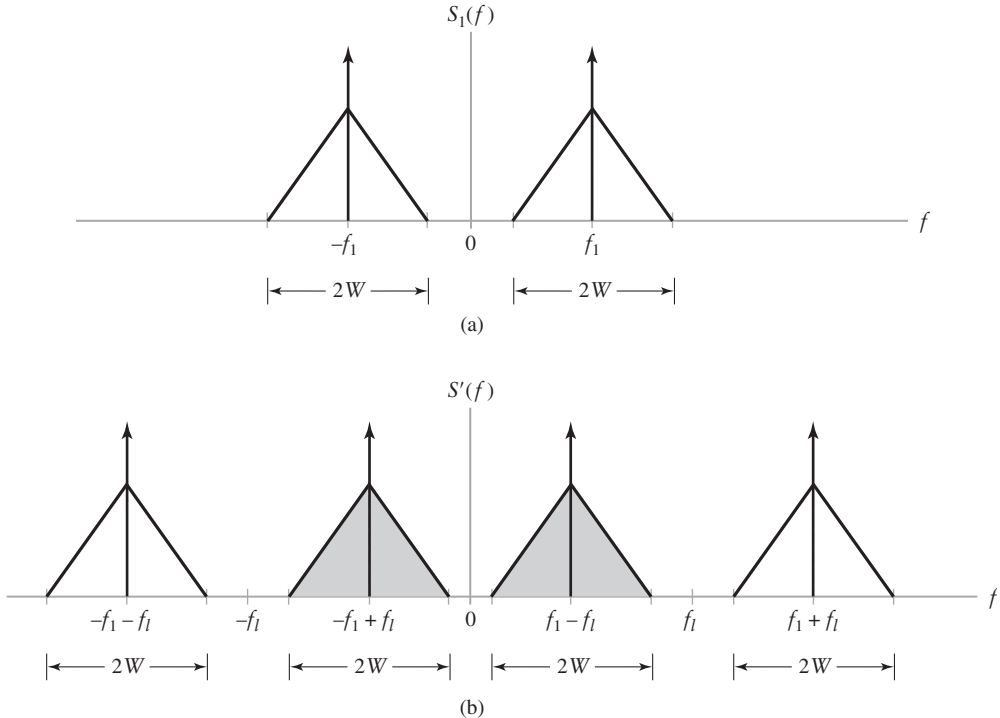


**FIGURE 3.22** (a) Spectrum of modulated signal  $s_1(t)$  at the mixer input. (b) Spectrum of the corresponding signal  $s'(t)$  at the output of the product modulator in the mixer.

carrier frequency  $f_1$  is to be translated upward or downward, we may now identify two different situations:

- (i) *Up conversion.* In this form of mixing, the translated carrier frequency, denoted by  $f_2$ , is greater than the incoming carrier frequency  $f_1$ . The required local oscillator frequency  $f_l$  is therefore defined by

$$f_2 = f_1 + f_l$$

Solving for  $f_l$ , we therefore have

$$f_l = f_2 - f_1$$

In this situation, the unshaded part of the spectrum in Fig. 3.22(b) defines the up-converted signal  $s_2(t)$ , and the shaded part of this spectrum defines the *image signal* associated with  $s_2(t)$ , which is removed by the band-pass filter in Fig. 3.21. For obvious reasons, the mixer in this case is referred to as a *frequency-up converter*.

- (ii) *Down conversion.* In this second form of mixing, the translated carrier frequency  $f_2$  is smaller than the incoming carrier frequency  $f_1$ , as shown by

$$f_2 = f_1 - f_l$$

The required local oscillator frequency is therefore

$$f_l = f_1 - f_2$$

The picture we have this time is the reverse of that pertaining to up conversion. In particular, the shaded part of the spectrum in Fig. 3.22(b) defines the down-converted

signal  $s_2(t)$ , and the unshaded part of this spectrum defines the associated image signal. Accordingly, this second mixer is referred to as a *frequency-down converter*. Note that in this case, the translated carrier frequency  $f_2$  has to be larger than  $W$  (i.e., one half of the bandwidth of the incoming modulated signal  $s_2(t)$ ) to avoid sideband overlap.

The purpose of the band-pass filter in the mixer of Fig. 3.21 is now clear: pass the signal  $s_2(t)$  and eliminate the associated image signal. This objective is achieved by aligning the midband frequency of the filter with the translated carrier frequency  $f_2$  and assigning it a bandwidth equal to that of the incoming modulated signal  $s_1(t)$ . Regardless of whether the frequency conversion is up or down, the transition band of the filter is permitted to occupy the gap from  $f_1 - f_l + W$  to  $f_1 + f_l - W$ ; that is, the permissible width of the transition band is  $2(f_l - W)$ , which, in effect, requires that the local oscillator frequency  $f_l$  be greater than  $W$ . Moreover, to avoid spectral overlap in down conversion, we also require that  $f_1 - f_l - W$  be greater than zero; that is,  $f_l > f_1 - W$ .

It is important to note that mixing is a *linear* operation. Accordingly, the relation of the sidebands of the incoming modulated wave to the original carrier existing at the mixer input is completely preserved at the mixer output.

## 3.7 Vestigial Sideband Modulation

### MOTIVATION

Single-sideband modulation works satisfactorily for an information-bearing signal (e.g., speech signal) with an energy gap centered around zero frequency. However, for the spectrally efficient transmission of *wideband signals*, we have to look to a new method of modulation for two reasons:

1. Typically, the spectra of wideband signals (exemplified by television video signals and computer data) contain significant low frequencies, which make it impractical to use SSB modulation.
2. The spectral characteristics of wideband data befit the use of DSB-SC. However, DSB-SC requires a transmission bandwidth equal to twice the message bandwidth, which violates the bandwidth conservation requirement.

To overcome these two practical limitations, we need a *compromise* method of modulation that lies somewhere between SSB and DSB-SC in its spectral characteristics. *Vestigial sideband*, the remaining modulation scheme to be considered in this section, is that compromise scheme.

Vestigial sideband (VSB) modulation distinguishes itself from SSB modulation in two practical respects:

1. Instead of completely removing a sideband, a trace or *vestige* of that sideband is transmitted; hence, the name “vestigial sideband.”
2. Instead of transmitting the other sideband in full, *almost* the whole of this second band is also transmitted.

Accordingly, the transmission bandwidth of a VSB modulated signal is defined by

$$B_T = f_v + W$$

where  $f_v$  is the *vestige bandwidth* and  $W$  is the *message bandwidth*. Typically,  $f_v$  is 25 percent of  $W$ , which means that the VSB bandwidth  $B_T$  lies between the SSB bandwidth,  $W$ , and DSB-SC bandwidth,  $2W$ .

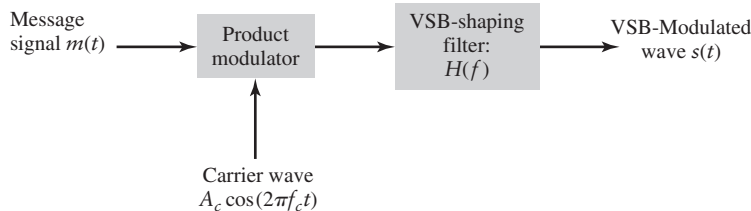


**FIGURE 3.23** VSB modulator using frequency discrimination.

### ■ SIDEBAND SHAPING FILTER

To produce VSB modulation, we may use the modulator depicted in Fig. 3.23, which consists of a product modulator followed by a band-pass filter. For VSB modulation, the band-pass filter is referred to as a *sideband shaping filter*. Assuming that the vestige of the VSB lies in the lower sideband of the DSB-SC modulated wave, the VSB spectrum at the modulator output is shaped in a manner depicted in Fig. 3.24(a). The spectrum shaping is defined by the transfer function of the filter, which is denoted by  $H(f)$ . The only requirement that the sideband shaping performed by  $H(f)$  must satisfy is that the transmitted vestige *compensates* for the spectral portion missing from the other sideband. This requirement ensures that coherent detection of the VSB modulated wave recovers a replica of the message signal, except for amplitude scaling.

By imposing this requirement on the VSB demodulation process, it turns out that the sideband shaping filter must itself satisfy the following condition:

$$H(f + f_c) + H(f - f_c) = 1, \quad \text{for } -W \leq f \leq W \quad (3.26)$$

where  $f_c$  is the carrier frequency. The term  $H(f + f_c)$  is the positive-frequency part of the band-pass transfer function  $H(f)$  shifted to the left by  $f_c$ , and  $H(f - f_c)$  is the negative-frequency part of  $H(f)$  shifted to the right by  $f_c$ . A proof of Eq. (3.26) dealing with an arbitrary Fourier transformable message signal is presented later in this section on the coherent detection of VSB.

Two properties of the sideband shaping filter follow from Eq. (3.26):

1. *The transfer function of the sideband shaping filter exhibits odd symmetry about the carrier frequency  $f_c$ .* To explain this property, we first express  $H(f)$  as the difference between two frequency-shifted functions as follows:

$$H(f) = u(f - f_c) - H_v(f - f_c), \quad \text{for } f_c - f_v < |f| < f_c + W \quad (3.27)$$

The first term  $u(f - f_c)$  denotes the frequency-shifted version of the *unit-step frequency function*  $u(f)$ , which is depicted in Fig. 3.24(b). That is,

$$u(f) = \begin{cases} 1, & \text{for } f > 0 \\ 0, & \text{for } f < 0 \end{cases} \quad (3.28)$$

The second term  $H_v(f - f_c)$  denotes the frequency-shifted version of a new *low-pass transfer function*  $H_v(f)$ , which, as depicted in Fig. 3.24(c), is completely determined by the vestige of the modulated wave  $s(t)$ . The relationship defined in Eq. (3.27) follows readily from the three example parts of Fig. 3.24. The important point to note

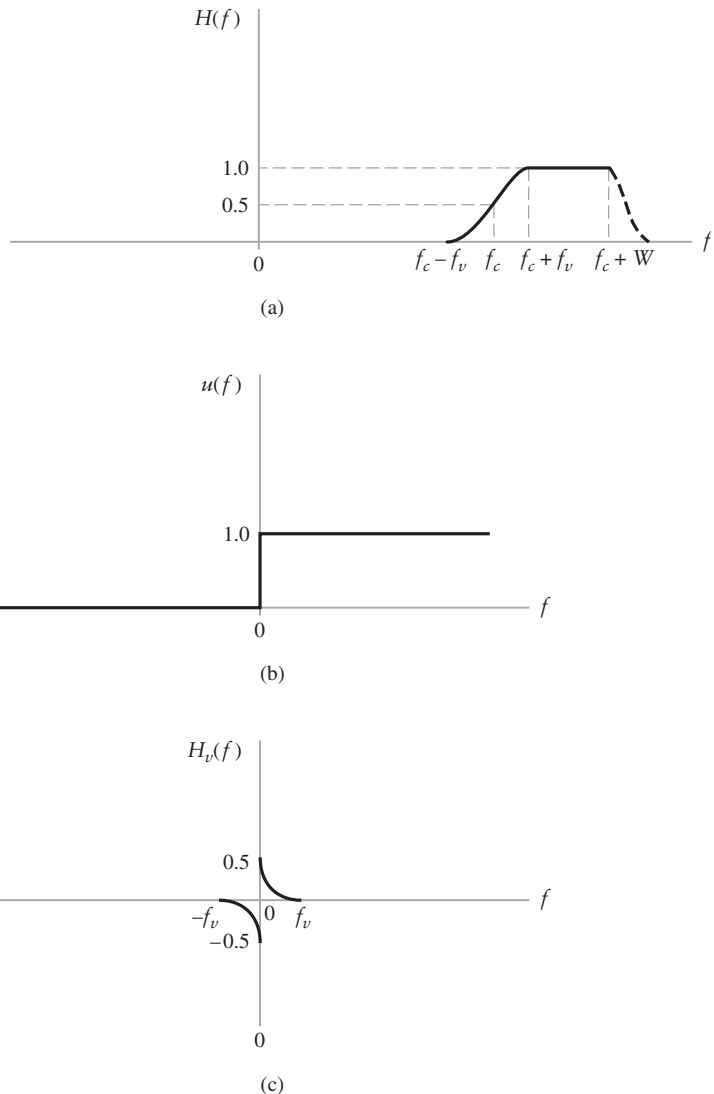


**FIGURE 3.24** (a) Amplitude response of sideband-shaping filter; only the positive-frequency portion is shown, the dashed part of the amplitude response is arbitrary. (b) Unit-step function defined in the frequency domain. (c) Low-pass transfer function  $H_v(f)$ .

from part (c) of the figure is that  $H_v(f)$  satisfies the property of *odd symmetry* about zero frequency, as shown by

$$H_v(-f) = -H_v(f) \quad (3.29)$$

It is therefore in this sense that Property 1 is stated.

2. The transfer function  $H_v(f)$  is required to satisfy the condition of Eq. (3.26) only for the frequency interval  $-W \leq f \leq W$ , where  $W$  is the message bandwidth. The practical implication of this second property is that, for the case of VSB depicted in Fig. 3.24(a), the transfer function of the sideband shaping filter can have an arbitrary specification for  $|f| > f_c + W$ ; it is for this reason that the part of the spectrum lying above  $f_c + W$  is shown dashed in Fig. 3.24(a).

**EXAMPLE 3.3 Sinusoidal VSB**

Consider the simple example of sinusoidal VSB modulation produced by the sinusoidal modulating wave

$$m(t) = A_m \cos(2\pi f_m t)$$

and carrier wave

$$c(t) = A_c \cos(2\pi f_c t)$$

Let the upper side-frequency at  $f_c + f_m$  as well as its image at  $-(f_c + f_m)$  be attenuated by the factor  $k$ . To satisfy the condition of Eq. (3.26), the lower side-frequency at  $f_c - f_m$  and its image  $-(f_c - f_m)$  must be attenuated by the factor  $(1 - k)$ . The VSB spectrum is therefore

$$\begin{aligned} S(f) = & \frac{1}{4} k A_c A_m [\delta(f - (f_c + f_m)) + \delta(f + (f_c + f_m))] \\ & + \frac{1}{4} (1 - k) A_c A_m [\delta(f - (f_c - f_m)) + \delta(f + (f_c - f_m))] \end{aligned}$$

Correspondingly, the sinusoidal VSB modulated wave is defined by

$$\begin{aligned} s(t) = & \frac{1}{4} k A_c A_m [\exp(j2\pi(f_c + f_m)t) + \exp(-j2\pi(f_c + f_m)t)] \\ & + \frac{1}{4} (1 - k) A_c A_m [\exp(j2\pi(f_c - f_m)t) + \exp(-j2\pi(f_c - f_m)t)] \\ = & \frac{1}{2} k A_c A_m \cos(2\pi(f_c + f_m)t) + \frac{1}{2} (1 - k) A_c A_m \cos(2\pi(f_c - f_m)t) \quad (3.30) \end{aligned}$$

Using well-known trigonometric identities to expand the cosine terms  $\cos(2\pi(f_c + f_m)t)$  and  $\cos(2\pi(f_c - f_m)t)$ , we may reformulate Eq. (3.30) as the linear combination of two sinusoidal DSB-SC modulated waves.

$$\begin{aligned} s(t) = & \frac{1}{2} A_c A_m \cos(2\pi f_c t) \cos(2\pi f_m t) \\ & + \frac{1}{2} A_c A_m (1 - 2k) \sin((2\pi f_c t) \sin(2\pi f_m t)) \quad (3.31) \end{aligned}$$

where the first term on the right-hand side is the in-phase component of  $s(t)$  and the second term is the quadrature component.

To summarize, depending on how the attenuation factor  $k$  in Eq. (3.31) is defined in the interval  $(0, 1)$ , we may identify all the different sinusoidal forms of linear modulated waves studied in Sections 3.3, 3.6, and 3.7 as follows:

1.  $k = \frac{1}{2}$ , for which  $s(t)$  reduces to DSB-SC
2.  $k = 0$ , for which  $s(t)$  reduces to lower SSB  
 $k = 1$ , for which  $s(t)$  reduces to upper SSB
3.  $0 < k < \frac{1}{2}$ , for which the attenuated version of the upper side-frequency defines the vestige of  $s(t)$   
 $\frac{1}{2} < k < 1$ , for which the attenuated version of the lower side frequency defines the vestige of  $s(t)$

### ■ COHERENT DETECTION OF VSB

For an exact recovery of the message signal  $m(t)$  from the VSB modulated wave  $s(t)$ , except for some amplitude scaling, we may use the *coherent detector* shown in Fig. 3.12. As with the DSB-SC and SSB demodulations studied previously, the demodulation of VSB consists of multiplying  $s(t)$  with a locally generated sinusoid and then low-pass filtering the resulting product signal  $v(t)$ . It is assumed that the local sinusoid in the coherent detector of Fig. 3.12 is in *perfect synchronism* with the carrier in the modulator responsible for generating the VSB-modulated wave. Then setting the phase  $\phi$  in the local sinusoid in Fig. 3.12 equal to zero, we express the Fourier transform of the product signal

$$v(t) = A'_c s(t) \cos(2\pi f_c t)$$

as follows

$$V(f) = \frac{1}{2} A'_c [S(f - f_c) + S(f + f_c)] \quad (3.32)$$

where

$$s(t) \iff S(f)$$

Next, we express the Fourier transform of the VSB modulated wave  $s(t)$  as

$$S(f) = \frac{1}{2} A_c [M(f - f_c) + M(f + f_c)] H(f) \quad (3.33)$$

which follows from Fig. 3.23 depicting the VSB modulator;  $M(f)$  is the message spectrum and  $H(f)$  is the transfer function of the sideband shaping filter. Shifting the VSB spectrum  $S(f)$  to the right by  $f_c$  yields

$$S(f - f_c) = \frac{1}{2} A_c [M(f - 2f_c) + M(f)] H(f - f_c) \quad (3.34)$$

and shifting it to the left by  $f_c$  yields

$$S(f + f_c) = \frac{1}{2} A_c [M(f) + M(f + 2f_c)] H(f + f_c) \quad (3.35)$$

Hence, substituting Eqs. (3.34) and (3.35) into Eq. (3.32) and then combining terms, we obtain

$$\begin{aligned} V(f) &= \frac{1}{4} A_c A'_c M(f) [H(f - f_c) + H(f + f_c)] \\ &\quad + \frac{1}{4} A_c A'_c [M(f - 2f_c) H(f - f_c) + M(f + 2f_c) H(f + f_c)] \end{aligned}$$

which, in light of the condition imposed on  $H(f)$  in Eq. (3.26), reduces to

$$\begin{aligned} V(f) &= \frac{1}{4} A_c A'_c M(f) \\ &\quad + \frac{1}{4} A_c A'_c [M(f - 2f_c) H(f - f_c) + M(f + 2f_c) H(f + f_c)] \end{aligned} \quad (3.36)$$

The first term on the right-hand side of Eq. (3.36) is a scaled version of the message spectrum  $M(f)$ . The second term of Eq. (3.36) is the Fourier transform of high-frequency components, representing a new VSB wave modulated onto a carrier of frequency  $2f_c$ . Provided that the low-pass filter in the coherent detector of Fig. 3.12 has a cutoff frequency just slightly greater than the message bandwidth, the high-frequency components of  $v(t)$  are removed by the low-pass filter. The resulting demodulated signal is a scaled version of the desired message signal  $m(t)$ .

► **Drill Problem 3.14** Validate the statement that the high-frequency components in Eq. (3.36) represent a VSB wave modulated onto a carrier of frequency  $2f_c$ . ◀

#### EXAMPLE 3.4 Coherent detection of sinusoidal VSB

Recall from Eq. (3.31) of Example 3.3, that the sinusoidal VSB modulated signal is defined by

$$\begin{aligned} s(t) &= \frac{1}{2} A_c A_m \cos(2\pi f_m t) \cos(2\pi f_c t) \\ &\quad + \frac{1}{2} A_c A_m (1 - 2k) \sin(2\pi f_c t) \sin(2\pi f_m t) \end{aligned}$$

Multiplying  $s(t)$  by  $A'_c \cos(2\pi f_c t)$  in accordance with perfect coherent detection yields the product signal

$$\begin{aligned} v(t) &= A'_c s(t) \cos(2\pi f_c t) \\ &= \frac{1}{2} A_c A'_c A_m \cos(2\pi f_m t) \cos^2(2\pi f_c t) \\ &\quad + \frac{1}{2} A_c A'_c A_m (1 - 2k) \sin(2\pi f_m t) \sin(2\pi f_c t) \cos(2\pi f_c t) \end{aligned}$$

Next, using the trigonometric identities

$$\cos^2(2\pi f_c t) = \frac{1}{2} [1 + \cos(4\pi f_c t)]$$

and

$$\sin(2\pi f_c t) \cos(2\pi f_c t) = \frac{1}{2} \sin(4\pi f_c t)$$

we may redefine  $\nu(t)$  as

$$\begin{aligned}\nu(t) &= \frac{1}{4} A_c A'_c A_m \cos(2\pi f_m t) \\ &\quad + \frac{1}{4} A_c A'_c A_m [\cos(2\pi f_m t) \cos(4\pi f_c t) + (1 - 2k) \sin(2\pi f_m t) \sin(4\pi f_c t)]\end{aligned}\quad (3.37)$$

The first term on the right-hand side of Eq. (3.37) is a scaled version of the message signal  $A_m \cos(2\pi f_m t)$ . The second term of the equation is a new sinusoidal VSB wave modulated onto a carrier of frequency  $2f_c$ , which represents the high-frequency components of  $\nu(t)$ . This second term is removed by the low-pass filter in the detector of Fig. 3.12, provided that the cut-off frequency of the filter is just slightly greater than the message frequency  $f_m$ .

### EXAMPLE 3.5 Envelope detection of VSB plus carrier

The coherent detection of VSB requires synchronism of the receiver to the transmitter, which increases system complexity. To simplify the demodulation process, we may purposely add the carrier to the VSB signal (scaled by the factor  $k_a$ ) prior to transmission and then use envelope detection in the receiver.<sup>3</sup> Assuming sinusoidal modulation, the “VSB-plus-carrier” signal is defined [see Eq. (3.31) of Example 3.3] as

$$\begin{aligned}s_{\text{VSB+C}}(t) &= A_c \cos(2\pi f_c t) + k_a s(t), \quad k_a = \text{amplitude sensitivity factor} \\ &= A_c \cos(2\pi f_c t) + \frac{k_a}{2} A_c A_m \cos(2\pi f_m t) \cos(2\pi f_c t) \\ &\quad + \frac{k_a}{2} A_c A_m (1 - 2k) \sin(2\pi f_m t) \sin(2\pi f_c t) \\ &= A_c \left[ 1 + \frac{k_a}{2} A_m \cos(2\pi f_m t) \right] \cos(2\pi f_c t) \\ &\quad + \frac{k_a}{2} A_c A_m (1 - 2k) \sin(2\pi f_m t) \sin(2\pi f_c t)\end{aligned}$$

The envelope of  $s_{\text{VSB+C}}(t)$  is therefore

$$\begin{aligned}a(t) &= \left\{ A_c^2 \left[ 1 + \frac{k_a}{2} A_m \cos(2\pi f_m t) \right]^2 + A_c^2 \left[ \frac{k_a}{2} A_m (1 - 2k) \sin(2\pi f_m t) \right]^2 \right\}^{1/2} \\ &= A_c \left[ 1 + \frac{k_a}{2} A_m \cos(2\pi f_m t) \right] \left\{ 1 + \left[ \frac{\frac{k_a}{2} A_m (1 - 2k) \sin(2\pi f_m t)}{1 + \frac{k_a}{2} A_m \cos(2\pi f_m t)} \right]^2 \right\}^{1/2}\end{aligned}\quad (3.38)$$

<sup>3</sup> Another procedure used for the detection of a VSB modulated wave is to add a *pilot* to the modulated wave at the transmitter. The pilot would be a frequency-translated version of the carrier used in the generation of the modulated wave, but it lies outside the band of frequencies occupied by the modulated wave. At the receiver, the pilot is extracted by means of a band-pass filter and then translated (upward or downward) to produce a replica of the original carrier. With this replica of the carrier available to the receiver, coherent detection may be used to recover the original message signal.

A similar procedure can be used for the coherent detection of SSB modulated waves.

Equation (3.38) shows that *distortion* in the envelope detection performed on the envelope  $a(t)$  is contributed by the quadrature component of the sinusoidal VSB signal. This distortion can be reduced by using a combination of two methods:

- ▶ The amplitude sensitivity factor  $k_a$  is reduced, which has the effect of reducing the percentage modulation.
- ▶ The width of the vestigial sideband is reduced, which has the effect of reducing the factor  $(1 - 2k)$ .

Both of these methods are intuitively satisfying in light of what we see inside the square brackets in Eq. (3.38).

## 3.8 Baseband Representation of Modulated Waves and Band-Pass Filters

From the discussion of different modulation strategies presented in this chapter, we see that a modulated wave using a sinusoidal wave as the carrier is actually a *band-pass signal centered on the carrier frequency*. By virtue of this very fact, the carrier wave imprints itself into the structure of the modulated wave. In an explicit sense, it does so when the carrier wave is contained as a separate component in the transmitted signal. When the carrier wave is suppressed, it makes its presence known to the receiver in an *implicit* sense by positioning the sidebands of the transmitted spectrum around the carrier frequency in one form or another, depending on the type of modulation used.

Typically, the carrier frequency is large compared to the message bandwidth, which makes the processing of a modulated wave on a digital computer a difficult proposition. However, from the modulation theory presented in this chapter, we do know that all the information content of a message signal resides completely in the sidebands of the modulated wave. Accordingly, when the objective is to process a modulated wave on a computer, the *efficient* procedure is to do the processing on the *baseband* version of the modulated wave rather than directly on the modulated wave itself. The term “baseband” is used to designate the *band of frequencies representing the original signal as delivered by a source of information*.

### ■ BASEBAND REPRESENTATION OF MODULATED WAVES

Consider then a *generic, linear modulated wave*, which is defined by

$$s(t) = s_I(t) \cos(2\pi f_c t) - s_Q(t) \sin(2\pi f_c t) \quad (3.39)$$

Let

$$c(t) = \cos(2\pi f_c t)$$

be the carrier wave with frequency  $f_c$ , and

$$\hat{c}(t) = \sin(2\pi f_c t)$$

be the *quadrature-phase* version of the carrier. To simplify matters, without loss of generality we have set the carrier amplitude equal to unity. We now express the modulated wave in the compact form

$$s(t) = s_I(t)c(t) - s_Q(t)\hat{c}(t) \quad (3.40)$$

The term  $s_I(t)$  is called the *in-phase component* of the modulated wave  $s(t)$ , so called because it is multiplied by the carrier  $c(t)$ . By the same token, the term  $s_Q(t)$  is called the *quadrature-phase component* or simply the *quadrature component* of  $s(t)$ , so called because it is multiplied by the quadrature carrier  $\hat{c}(t)$ . The carriers  $c(t)$  and  $\hat{c}(t)$  are *orthogonal* to each other.

Equation (3.39) or (3.40) is itself referred to as the *canonical representation of linear modulated waves*. Most important, this representation includes all the members of the amplitude modulation family discussed in this chapter, as shown in Table 3.1.

From this table, it is clearly apparent that the information content of the message signal  $m(t)$  and the way in which the modulation strategy is implemented are fully described by the in-phase component  $s_I(t)$  in both AM and DSB-SC, or in the combination of the in-phase component  $s_I(t)$  and the quadrature component  $s_Q(t)$  in both SSB and VSB. Moreover, the orthogonality of  $s_I(t)$  and  $s_Q(t)$  with respect to each other prompts us to introduce a new signal called the *complex envelope* of the modulated wave  $s(t)$ , which is formally defined by

$$\tilde{s}(t) = s_I(t) + j s_Q(t) \quad (3.41)$$

This definition is motivated by the way in which we deal with complex numbers. In any event, the important point to take from Eq. (3.41) is the fact that the complex envelope  $\tilde{s}(t)$  accounts fully for the information contents of both  $s_I(t)$  and  $s_Q(t)$ . Note, however, that the complex envelope  $\tilde{s}(t)$  is a fictitious signal, the use of which is intended merely to simplify signal processing operations on band-pass signals, which are exemplified by modulated waves based on a sinusoidal carrier.

In a manner corresponding to Eq. (3.41), we may define the *complex carrier wave*

$$\begin{aligned} \tilde{c}(t) &= c(t) + j \hat{c}(t) \\ &= \cos(2\pi f_c t) + j \sin(2\pi f_c t) \\ &= \exp(j2\pi f_c t) \end{aligned} \quad (3.42)$$

Accordingly, the modulated wave  $s(t)$  is itself defined by

$$\begin{aligned} s(t) &= \text{Re}[\tilde{s}(t)\tilde{c}(t)] \\ &= \text{Re}[\tilde{s}(t) \exp(j2\pi f_c t)] \end{aligned} \quad (3.43)$$

where  $\text{Re}[\cdot]$  extracts the real part of the complex quantity enclosed inside the square brackets.

Now we can see the practical advantage of the complex envelope  $\tilde{s}(t)$  over the real-valued modulated wave  $s(t)$ :

1. The highest frequency component of  $s(t)$  may be as large as  $f_c + W$ , where  $f_c$  is the carrier frequency and  $W$  is the message bandwidth.
2. On the other hand, the highest frequency component of  $\tilde{s}(t)$  is considerably smaller, being limited by the message bandwidth  $W$ .

Yet, in using Eq. (3.43) as the representation of the modulated wave  $s(t)$ , there is nothing lost whatsoever.

Given an arbitrary modulated wave  $s(t)$ , we may derive the in-phase compound  $s_I(t)$  and quadrature component  $s_Q(t)$  using the scheme shown in Fig. 3.25(a). Conversely, given

**TABLE 3.1 Different Forms of Linear Modulation as Special Cases of Eq. (3.39), assuming unit carrier amplitude**

Type of modulation	In-phase component $s_I(t)$	Quadrature component $s_Q(t)$	Comments
AM	$1 + k_a m(t)$	0	$k_a$ = amplitude sensitivity $m(t)$ = message signal
DSB-SC	$m(t)$	0	
SSB:			
(a) Upper sideband transmitted	$\frac{1}{2}m(t)$	$\frac{1}{2}\hat{m}(t)$	$\hat{m}(t)$ = Hilbert transform of $m(t)$ (see part (i) of footnote 4) <sup>4</sup>
(b) Lower sideband transmitted	$\frac{1}{2}m(t)$	$-\frac{1}{2}\hat{m}(t)$	
VSB:			
(a) Vestige of lower sideband transmitted	$\frac{1}{2}m(t)$	$\frac{1}{2}m'(t)$	$m'(t)$ = response of filter with transfer function $H_Q(f)$ due to message signal $m(t)$ . The $H_Q(f)$ is defined by the formula (see part (ii) of footnote 4)
(b) Vestige of upper sideband transmitted	$\frac{1}{2}m(t)$	$-\frac{1}{2}m'(t)$	$H_Q(f) = -j[H(f + f_c) - H(f - f_c)]$ where $H(f)$ is the transfer function of the VSB sideband shaping filter.

<sup>4</sup>Two additional comments on Table 3.1 are in order:

(i) In SSB modulation, the *Hilbert transform*

$$\hat{m}(t) = \frac{1}{\pi} \int_{-\infty}^{\infty} \frac{m(\tau)}{t - \tau} d\tau$$

defines the quadrature component of the modulated wave  $s(t)$ ; that is,

$$s_Q(t) = \hat{m}(t)$$

In the frequency domain, the Hilbert transformation is described by

$$\hat{M}(f) = -j \operatorname{sgn}(f) M(f)$$

where

$$\operatorname{sgn}(f) = \begin{cases} 1, & \text{for } f > 0 \\ 0, & \text{for } f = 0 \\ -1, & \text{for } f < 0 \end{cases}$$

is the signum function.

(ii) In VSB modulation, the quadrature component  $S_Q(t) = m'(t)$  is obtained by passing the message signal  $m(t)$  through a linear time-invariant filter whose transfer function is denoted by  $H_Q(t)$ . The  $H_Q(t)$  is itself defined by

$$H_Q(f) = -j[H(f + f_c) - H(f - f_c)]$$

where  $H(f)$  is the transfer function of the VSB sideband shaping filter. In the limit, as the vestige sideband  $f_v$  approaches zero, we have

$$\lim_{f_v \rightarrow 0} H_Q(f) = -j \operatorname{sgn}(f)$$

and with it the VSB reduces to SSB, which is exactly how it should be.

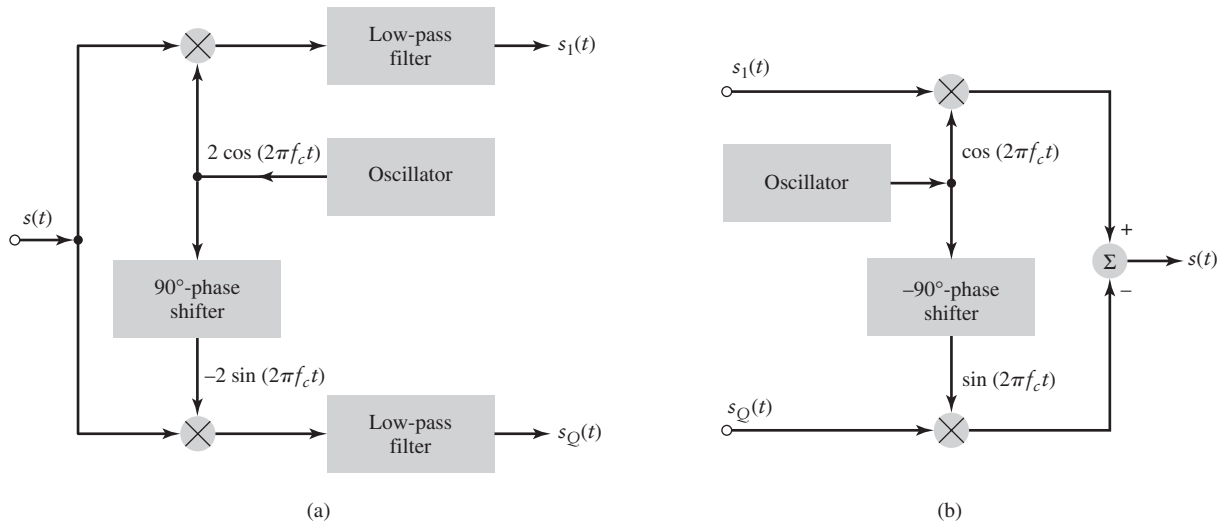


**FIGURE 3.25** (a) Scheme for deriving the in-phase and quadrature components of a linearly modulated (i.e., band-pass) signal. (b) Scheme for reconstructing the modulated signal from its in-phase and quadrature components.

the pair of in-phase component  $s_I(t)$  and quadrature component  $s_Q(t)$ , we may generate the modulated wave  $s(t)$  using the complementary scheme shown in Fig. 3.25(b). For obvious reasons, these two schemes are respectively called the *analyzer* and *synthesizer* of modulated waves.

► **Drill Problem 3.15** Derivation of the synthesizer depicted in Fig. 3.25(b) follows directly from Eq. (3.39). However, derivation of the analyzer depicted in Fig. 3.25(a) requires more detailed consideration. Given that  $f_c > W$  and the trigonometric identities:

$$\begin{aligned}\cos^2(2\pi f_c t) &= \frac{1}{2}[1 + \cos(4\pi f_c t)], \\ \sin^2(2\pi f_c t) &= \frac{1}{2}[1 - \cos(4\pi f_c t)],\end{aligned}$$

and

$$\sin(2\pi f_c t) \cos(2\pi f_c t) = \frac{1}{2}\sin(4\pi f_c t),$$

show that the analyzer of Fig. 3.25(a) yields  $s_I(t)$  and  $s_Q(t)$  as its two outputs. ◀

### ■ BASEBAND REPRESENTATION OF BAND-PASS FILTERS

The baseband representation of a band-pass signal (exemplified by a modulated wave) developed in this section prompts the desire to develop the corresponding representation for band-pass filters, including band-pass communication channels.

To this end, consider a linear band-pass filter whose input–output behavior is defined by the transfer function  $H(f)$ , which is limited to frequencies within  $\pm B$  of the mid-band frequency  $f_c$ ; in effect,  $2B$  defines the bandwidth of the filter. Suppose a modulated wave  $s(t)$  is applied to this filter, producing the output  $y(t)$ , as shown in Fig. 3.26(a). We assume that the transmission bandwidth of the modulated wave is  $2W$ , centered on a carrier fre-

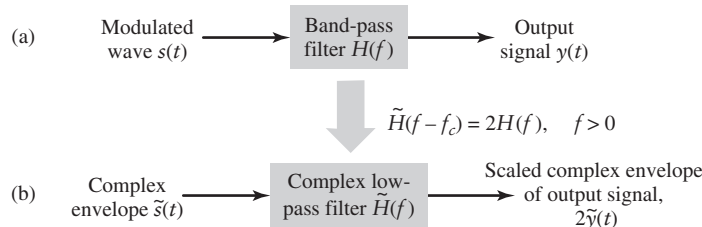


**FIGURE 3.26** Band-pass filter to complex low-pass system transformation: (a) Real-valued band-pass configuration, and (b) corresponding complex-valued low-pass configuration.

quency  $f_c$ . In other words, the spectrum of the modulated wave and the frequency response of the band-pass filter are aligned, with  $B \leq W$ . (The reason for ignoring the case  $B > W$  is that in such a situation the modulated wave  $s(t)$  passes through the filter completely unaffected, which is therefore of no practical importance.) Obviously, we may determine the output signal  $y(t)$  by evaluating the inverse Fourier transform of the product  $H(f)S(f)$ . A simpler procedure, however, is to use a *band-pass to low-pass (i.e., baseband) transformation*,<sup>5</sup> which eliminates the carrier frequency  $f_c$  from the analysis. Specifically, this transformation is defined by

$$\tilde{H}(f - f_c) = 2H(f), \quad \text{for } f > 0 \quad (3.44)$$

The new frequency function  $\tilde{H}(f)$  is the transfer function of the *complex low-pass filter*, which results from the transformation defined in Eq. (3.44). The scaling factor 2 in this equation is required to make sure that the transformation yields the exact result when we come to evaluate the output  $y(t)$ .

According to Eq. (3.44), we may determine  $\tilde{H}(f)$  by proceeding as follows:

- Given the transfer function  $H(f)$  of a band-pass filter, which is defined for both positive and negative frequencies, keep the part of  $H(f)$  that corresponds to positive frequencies; let  $H_+(f)$  denote this part.
- Shift  $H_+(f)$  to the left along the frequency axis by an amount equal to  $f_c$ , and scale it by the factor 2. The result so obtained defines the desired  $\tilde{H}(f)$ .

Having determined the complex low-pass filter characterized by  $\tilde{H}(f)$ , we may then proceed onto the next stage of *complex signal processing*. Specifically, we input into this filter the complex envelope  $\tilde{s}(t)$  of the modulated wave  $s(t)$ ; the  $\tilde{s}(t)$  is derived from  $s(t)$  in accordance with Eq. (3.41). Then, applying  $\tilde{s}(t)$  to  $\tilde{H}(f)$  as depicted in Fig. 3.26(b), we determine the complex envelope  $\tilde{y}(t)$  of the output signal  $y(t)$ . Finally, the actual output  $y(t)$  is determined from the formula

$$y(t) = \operatorname{Re}[\tilde{y}(t) \exp(j2\pi f_c t)] \quad (3.45)$$

which is simply a rewrite of Eq. (3.43).

► **Drill Problem 3.16** Starting with the complex low-pass system depicted in Fig. 3.26(b), show that the  $y(t)$  derived from Eq. (3.45) is identical to the actual output  $y(t)$  in Fig. 3.26 (a). ◀

<sup>5</sup>For a derivation of the transformation defined by Eq. (3.44), see Haykin (2000), p. 731.

## 3.9 Theme Examples

In this section, we describe three theme examples, which build on the continuous-wave modulation theory described in previous sections of the chapter. The presentations emphasize insight into the operational aspects of analog communication systems rather than mathematical equations or design details.

### SUPERHETERODYNE RECEIVER

In a *broadcasting* system, irrespective of whether it is based on amplitude modulation or frequency modulation, the receiver not only has the task of demodulating the incoming modulated signal, but also it is required to perform some other system functions:

- ▶ *Carrier-frequency tuning*, the purpose of which is to select the desired signal (i.e., desired radio or TV station).
- ▶ *Filtering*, which is required to separate the desired signal from other modulated signals that may be picked up along the way.
- ▶ *Amplification*, which is intended to compensate for the loss of signal power incurred in the course of transmission.

The *superheterodyne receiver*, or *superhet* as it is often referred to, is a special type of receiver that fulfills all three functions, particularly the first two, in an elegant and practical fashion. Specifically, it overcomes the difficulty of having to build a tunable highly frequency-selective and variable filter. Indeed, practically all radio and TV receivers now being made are of the superheterodyne type.

Basically, the receiver consists of a radio-frequency (RF) section, a mixer and local oscillator, an intermediate frequency (IF) section, demodulator, and power amplifier. Typical frequency parameters of commercial AM radio receivers are listed in Table 3.2. (For the sake of completeness, the table also includes the corresponding frequency parameters of commercial FM receivers; frequency modulation (FM) theory is covered in Chapter 4.) Figure 3.27 shows the block diagram of a superheterodyne receiver for amplitude modulation using an envelope detector for demodulation.

The incoming amplitude-modulated wave is picked up by the receiving antenna and amplified in the RF section that is tuned to the carrier frequency of the incoming wave. The combination of mixer and local oscillator (of adjustable frequency) provides a *heterodyning* function, whereby the incoming signal is converted to a predetermined fixed *intermediate frequency*, usually lower than the incoming carrier frequency. This frequency

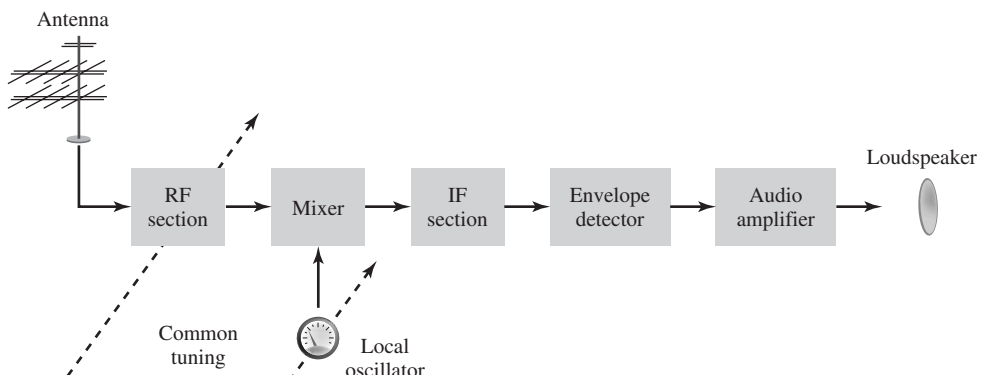


**FIGURE 3.27** Basic elements of an AM radio receiver of the superheterodyne type.

**TABLE 3.2 Typical Frequency Parameters of AM and FM Radio Receivers**

	AM Radio	FM Radio
RF carrier range	0.535–1.605 MHz	88–108 MHz
Mid-band frequency of IF section	0.455 MHz	10.7 MHz
IF bandwidth	10 kHz	200 kHz

translation is achieved without disturbing the relation of the sidebands to the carrier. The result of the heterodyning is to produce an intermediate-frequency carrier defined by

$$f_{\text{IF}} = f_{\text{RF}} - f_{\text{LO}} \quad (3.46)$$

where  $f_{\text{LO}}$  is the frequency of the local oscillator and  $f_{\text{RF}}$  is the carrier frequency of the incoming RF signal. We refer to  $f_{\text{IF}}$  as the intermediate frequency (IF), because the signal is neither at the original input frequency nor at the final baseband frequency. The mixer-local oscillator combination is sometimes referred to as the *first detector*, in which case the demodulator (envelope detector in Fig. 3.27) is called the *second detector*.

The IF section consists of one or more stages of tuned amplification, with a bandwidth as required for the particular type of signal that the receiver is intended to handle. This section provides most of the amplification and selectivity in the receiver. The output of the IF section is applied to a demodulator, the purpose of which is to recover the baseband signal. If coherent detection is used, then a coherent signal source must be provided in the receiver. The final operation in the receiver is the power amplification of the recovered message signal.

In a superheterodyne receiver, the mixer will develop an intermediate frequency output when the input signal frequency is greater or less than the local oscillator frequency by an amount equal to the intermediate frequency. That is, there are two input frequencies—namely,  $|f_{\text{LO}} \pm f_{\text{IF}}|$ , that will result in  $f_{\text{IF}}$  at the mixer output. This introduces the possibility of simultaneous reception of two signals differing in frequency by twice the intermediate frequency. For example, a receiver tuned to 1 MHz and having an IF of 0.455 MHz is subject to an *image interference* at 1.910 MHz. Indeed, any receiver with this value of IF, when tuned to any station, is subject to image interference at a frequency of 0.910 MHz higher than the desired station. Since the function of the mixer is to produce the difference between two applied frequencies, it is incapable of distinguishing between the desired signal and its image in that it produces an IF output from either one of them. The only practical cure for the suppression of image interference is to employ highly selective stages in the RF section (i.e., between the antenna and the mixer) in order to favor the desired signal and discriminate against the undesired or *image signal*. The effectiveness of suppressing unwanted image signals increases as the number of selective stages in the radio-frequency section increases and as the ratio of intermediate to signal frequency increases.

## ■ TELEVISION SIGNALS

Vestigial sideband modulation, discussed in Section 3.7, plays a key role in commercial television. The exact details of the modulation format used to transmit the video signal characterizing a TV system are influenced by two factors:

1. The video signal exhibits a large bandwidth and significant low-frequency content, which suggest the use of vestigial sideband modulation.
2. The circuitry used for demodulation in the receiver should be simple and therefore inexpensive. This suggests the use of envelope detection, which requires the addition of a carrier to the VSB modulated wave.

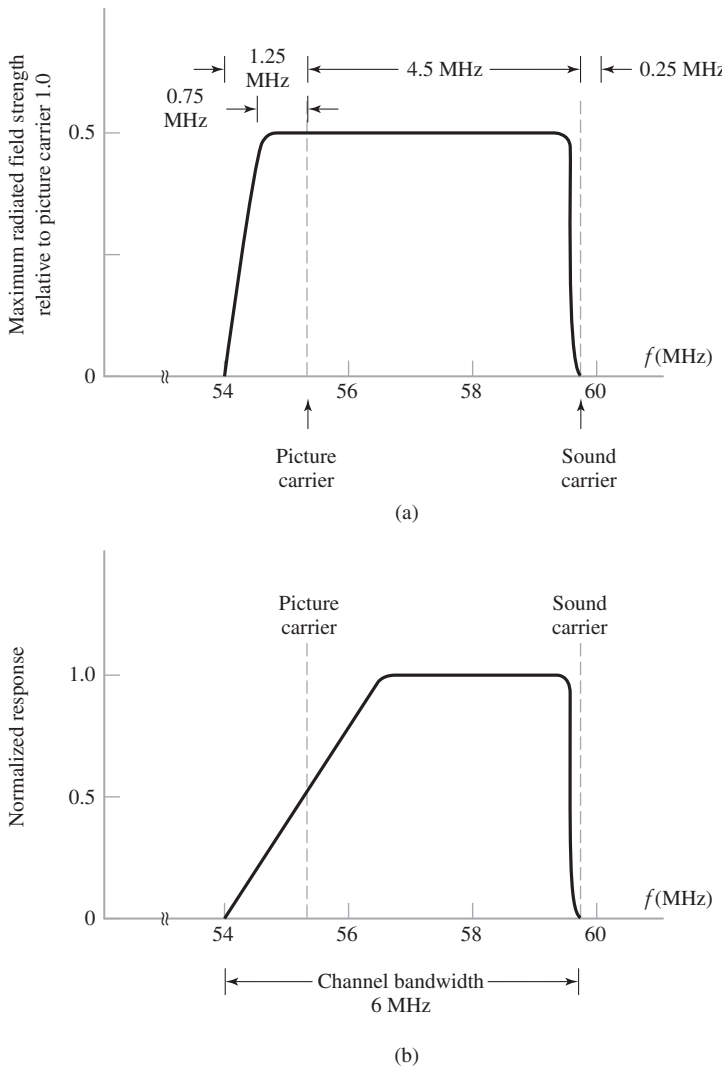


**FIGURE 3.28** (a) Idealized amplitude spectrum of a transmitted TV signal. (b) Amplitude response of a VSB shaping filter in the receiver.

With regard to point 1, however, it should be stressed that although there is indeed a basic desire to conserve bandwidth, in commercial TV broadcasting the transmitted signal is not quite VSB modulated. The reason is that at the transmitter the power levels are high, with the result that it would be expensive to rigidly control the filtering of sidebands. Instead, a *VSB filter* is inserted in each receiver where the power levels are low. The overall performance is the same as conventional vestigial-sideband modulation, except for some wasted power and bandwidth. These remarks are illustrated in Fig. 3.28. In particular, Fig. 3.28(a) shows the idealized spectrum of a transmitted TV signal. The upper sideband, 25 percent of the lower sideband, and the picture carrier are transmitted. The frequency response of the VSB filter used to do the required spectrum shaping in the receiver is shown in Fig. 3.28(b).

The channel bandwidth used for TV broadcasting in North America is 6 MHz, as indicated in Fig. 3.28(b). This channel bandwidth not only accommodates the bandwidth requirement of the VSB modulated video signal but also provides for the accompanying sound signal that modulates a carrier of its own. The values presented on the frequency axis

in Figs. 3.28(a) and 3.28(b) pertain to a specific TV channel. According to this figure, the picture carrier frequency is at 55.25 MHz, and the sound carrier frequency is at 59.75 MHz. Note, however, that the information content of the TV signal lies in a *baseband spectrum* extending from 1.25 MHz below the picture carrier to 4.5 MHz above it.

With regard to point 2, on page 143, the use of envelope detection (applied to a VSB modulated wave plus carrier) produces *waveform distortion* in the video signal recovered at the detector output. As discussed in Example 3.5, the waveform distortion is produced by the quadrature component of the VSB modulated wave. As pointed out in that example, we may reduce the extent of waveform distortion by reducing the percentage modulation and minimizing the width of the vestigial sideband.

### ■ FREQUENCY-DIVISION MULTIPLEXING

Another important signal processing operation in analog communications is *multiplexing*, whereby a number of independent signals can be combined into a composite signal suitable for transmission over a common channel. Voice frequencies transmitted over telephone systems, for example, range from 300 to 3100 Hz. To transmit a number of these signals over the same channel (e.g. cable), the signals must be kept apart so that they do not interfere with each other, and thus they can be separated at the receiving end. This is accomplished by separating the signals either in frequency or in time. The technique of separating the signals in frequency is referred to as *frequency-division multiplexing* (FDM), whereas the technique of separating the signals in time is called *time-division multiplexing* (TDM). In this subsection, we discuss FDM; the discussion of TDM is deferred to Chapter 5.

A block diagram of an FDM system is shown in Fig. 3.29. The incoming message signals are assumed to be of the low-pass type, but their spectra do not necessarily have nonzero

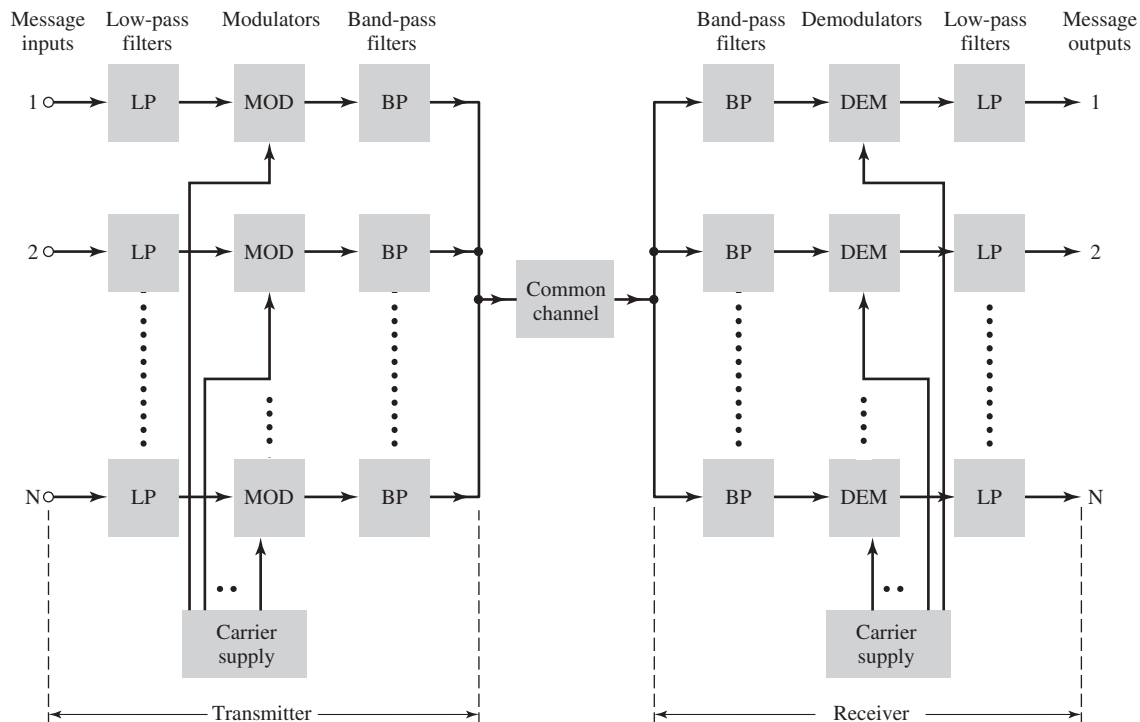


**FIGURE 3.29** Block diagram of frequency-division multiplexing (FDM) system.

values all the way down to zero frequency. Following each signal input, we have shown a low-pass filter, which is designed to remove high-frequency components that do not contribute significantly to signal representation but are capable of disturbing other message signals that share the common channel. These low-pass filters may be omitted only if the input signals are sufficiently band-limited initially. The filtered signals are applied to modulators that shift the frequency ranges of the signals so as to occupy mutually exclusive frequency intervals. The necessary carrier frequencies needed to perform these frequency translations are obtained from a carrier supply. For the modulation, we may use any one of the methods described in previous sections of this chapter. However, in telephony, the most widely used method of modulation in frequency-division multiplexing is single sideband modulation, which, in the case of voice signals, requires a bandwidth that is approximately equal to that of the original voice signal. In practice, each voice input is usually assigned a bandwidth of 4 kHz. The band-pass filters following the modulators are used to restrict the band of each modulated wave to its prescribed range. The resulting band-pass filter outputs are next combined in parallel to form the input to the common channel. At the receiving terminal, a bank of band-pass filters, with their inputs connected in parallel, is used to separate the message signals on a frequency-occupancy basis. Finally, the original message signals are recovered by individual demodulators. Note that the FDM system shown in Fig. 3.29 operates in only one direction. To provide for two-way transmission, as in telephony for example, we have to completely duplicate the multiplexing facilities, with the components connected in reverse order and with the signal waves proceeding from right to left.

#### EXAMPLE 3.6 Modulation steps in a 60-channel FDM system

The practical implementation of an FDM system usually involves many steps of modulation and demodulation, as illustrated in Fig. 3.30. The first multiplexing step combines 12 voice

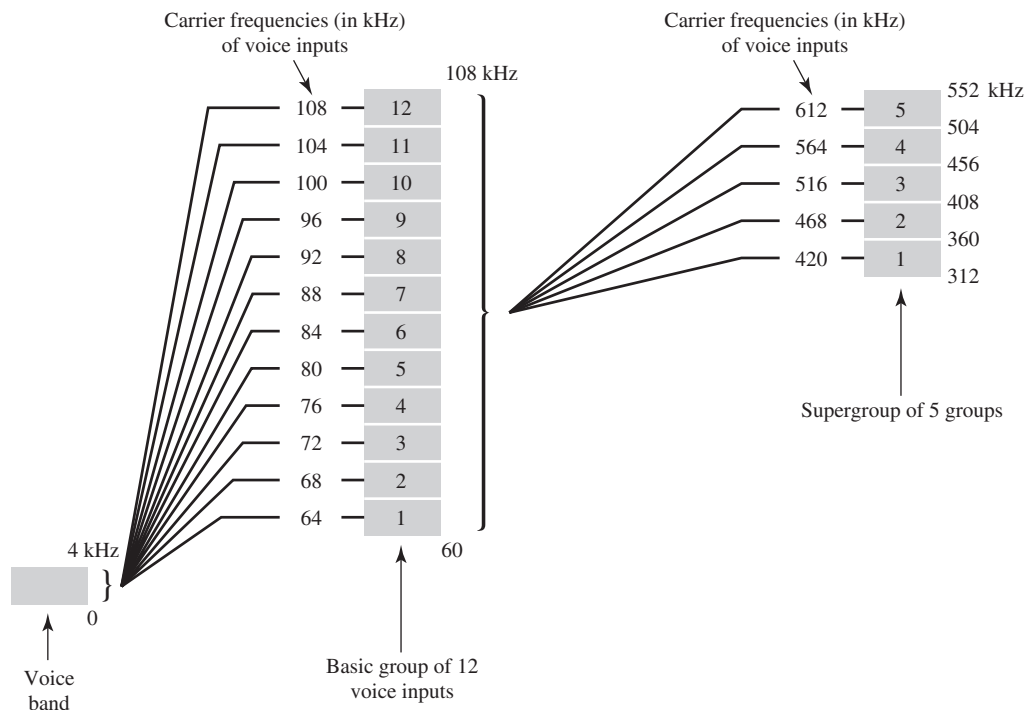


FIGURE 3.30 Illustration of the modulation steps in an FDM system.

inputs into a *basic group*, which is formed by having the  $n$ th input modulate a carrier at frequency  $f_c = 60 + 4n$  kHz, where  $n = 1, 2, \dots, 12$ . The lower sidebands are then selected by band-pass filtering and combined to form a group of 12 lower sidebands (one for each voice input). Thus the basic group occupies the frequency band 60–108 kHz. The next step in the FDM hierarchy involves the combination of five basic groups into a *supergroup*. This is accomplished by using the  $n$ th group to modulate a carrier of frequency  $f_c = 372 + 48n$  kHz, where  $n = 1, 2, \dots, 5$ . Here again the lower sidebands are selected by filtering and then combined to form a supergroup occupying the band 312–552 kHz. Thus, a supergroup is designed to accommodate 60 independent voice inputs. The reason for forming the supergroup in this manner is that economical filters of the required characteristics are available only over a limited frequency range. In a similar manner, supergroups are combined into *mastergroups*, and master-groups are combined into *very large groups*.

## 3.10 Summary and Discussion

In this chapter, we studied the family of amplitude modulation, in which the carrier is a sine wave whose amplitude is varied in accordance with a message signal. The format of this analog modulation family is typified by the example modulated wave

$$s(t) = A_c m(t) \cos(2\pi f_c t) \quad (3.47)$$

where  $m(t)$  is the message signal and  $A_c \cos(2\pi f_c t)$  is the carrier. The amplitude modulation family encompasses four types of continuous wave modulation, depending on the spectral content of the modulated wave. The four types of modulation and their practical merits are summarized here:

1. Amplitude modulation (AM), in which the upper and lower sidebands are transmitted in full, accompanied by the carrier wave. Generation of an AM wave can be accomplished simply by using a nonlinear device (e.g., diode) in a square-law modulator, for example. By the same token, demodulation of the AM wave is accomplished equally simply in the receiver by using an envelope detector, for example. It is for these two reasons, simple generation and simple detection, that amplitude modulation is commonly used in commercial AM radio *broadcasting*, which involves a single powerful transmitter and numerous receivers that are relatively inexpensive to build.
2. Double sideband-suppressed carrier (DSB-SC) modulation, defined by Eq. (3.47), in which only the upper and lower sidebands are transmitted. The suppression of the carrier wave means that DSB-SC modulation requires less power than AM to transmit the same message signal. This advantage of DSB-SC modulation over AM is, however, attained at the expense of increased receiver complexity. DSB-SC modulation is therefore well suited for *point-to-point communication* involving one transmitter and one receiver. In this form of analog communication, transmitted power is at a premium and the use of a complex receiver is therefore justifiable.
3. Single sideband (SSB) modulation, in which only the upper sideband or lower sideband is transmitted. It is optimum in the sense that it requires the minimum transmitted power and the minimum channel bandwidth for conveying a message signal from one point to another. However, implementation of the SSB transmitter imposes several constraints on the spectral content of the incoming message signal. Specifically, it requires the presence of a low-frequency gap around zero frequency, which for example, is satisfied by voice signals for telephonic communication.

4. Vestigial sideband modulation, in which “almost” the whole of one sideband and a “vestige” of the other sideband are transmitted in a prescribed complementary fashion. VSB modulation requires a channel bandwidth that is intermediate between that required for SSB and DSB-SC systems, and the saving in bandwidth can be significant if modulating signals with large bandwidths are being handled, as in the case of television signals and high-speed digital data.

One final comment is in order. Although the development of the amplitude modulation family has been motivated by its direct relevance to analog communications, many aspects of this branch of modulation theory are equally applicable to digital communications. If, for example, the message signal in Eq. (3.47) for the modulated wave  $s(t)$  is restricted to levels of  $-1$  or  $+1$  representing a binary “0” and “1” respectively, then we have a basic form of digital modulation known as binary phase-shift-keying (BPSK) that is discussed further in Chapter 7.

### ADDITIONAL PROBLEMS

---

- 3.17** Throughout the chapter we focused on

$$c(t) = A_c \cos(2\pi f_c t)$$

as the sinusoidal carrier wave. Suppose we choose

$$c(t) = A_c \sin(2\pi f_c t)$$

as the sinusoidal carrier wave. To be consistent, suppose we also define

$$m(t) = A_m \sin(2\pi f_m t)$$

- (a) Evaluate the spectrum of the new definition of AM:

$$s(t) = A_c [1 + k_a m(t)] \sin(2\pi f_c t)$$

where  $k_a$  is the amplitude sensitivity.

- (b) Compare the result derived in part (a) with that studied in Example 3.1.  
(c) What difference does the formulation in this problem make to the formulation of modulation theory illustrated in Example 3.1?

- 3.18.** Consider the message signal

$$m(t) = 20 \cos(2\pi t) \text{ volts}$$

and the carrier wave

$$c(t) = 50 \cos(100\pi t) \text{ volts}$$

- (a) Sketch (to scale) the resulting AM wave for 75 percent modulation.  
(b) Find the power developed across a load of 100 ohms due to this AM wave.

- 3.19.** Using the message signal

$$m(t) = \frac{t}{1 + t^2}$$

determine and sketch the modulated wave for amplitude modulation whose percentage modulation equals the following values:

- (a) 50 percent  
(b) 100 percent  
(c) 125 percent

- 3.20 Suppose a nonlinear device is available for which the output current  $i_o$  and input voltage  $v_i$  are related by

$$i_o = a_1 v_i + a_3 v_i^3$$

where  $a_1$  and  $a_3$  are constants. Explain how such a device could be used to provide amplitude modulation. Could such a device also be used for demodulation? Justify your answer.

- 3.21 Consider the DSB-SC modulated wave obtained by using the sinusoidal modulating wave

$$m(t) = A_m \cos(2\pi f_m t)$$

and the carrier wave

$$c(t) = A_c \cos(2\pi f_c t + \phi)$$

The phase angle  $\phi$ , denoting the phase difference between  $c(t)$  and  $m(t)$  at time  $t = 0$ , is variable. Sketch this modulated wave for the following values of  $\phi$ :

- (a)  $\phi = 0$
- (b)  $\phi = 45^\circ$
- (c)  $\phi = 90^\circ$
- (d)  $\phi = 135^\circ$

Comment on your results.

- 3.22 Given the nonlinear device described in Problem 3.20, explain how it could be used to provide a product modulator.

- 3.23 Consider a message signal  $m(t)$  with the spectrum shown in Fig. 3.31. The message bandwidth  $W = 1$  kHz. This signal is applied to a product modulator, together with a carrier wave  $A_c \cos(2\pi f_c t)$ , producing the DSB-SC modulated wave  $s(t)$ . This modulated wave is next applied to a coherent detector. Assuming perfect synchronism between the carrier waves in the modulator and detector, determine the spectrum of the detector output when: (a) the carrier frequency  $f_c = 1.25$  kHz and (b) the carrier frequency  $f_c = 0.75$  kHz. What is the lowest carrier frequency for which each component of the modulated wave  $s(t)$  is uniquely determined by  $m(t)$ ?

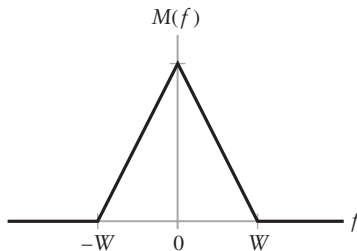


**FIGURE 3.31** Problem 3.23

- 3.24 Consider a composite wave obtained by adding a noncoherent carrier  $A_c \cos(2\pi f_c t + \phi)$  to a DSB-SC wave  $\cos(2\pi f_c t)m(t)$ . This composite wave is applied to an ideal envelope detector. Find the resulting detector output for

- (a)  $\phi = 0$
- (b)  $\phi \neq 0$  and  $|m(t)| \ll A_c/2$

- 3.25 A DSB-SC wave is demodulated by applying it to a coherent detector.

- (a) Evaluate the effect of a frequency error  $\Delta f$  in the local carrier frequency of the detector, measured with respect to the carrier frequency of the incoming DSB-SC wave.
- (b) For the case of a sinusoidal modulating wave, show that because of this frequency error, the demodulated wave exhibits beats at the error frequency. Illustrate your answer with a sketch of this demodulated wave. (A *beat* refers to a signal whose frequency is the difference between the frequencies of two input signals.)

- 3.26 Consider a pulse of amplitude  $A$  and duration  $T$ . This pulse is applied to a SSB modulator, producing the modulated wave  $s(t)$ . Determine the envelope of  $s(t)$ , and show that this envelope exhibits peaks at the beginning and end of the pulse.
- 3.27 (a) Consider a message signal  $m(t)$  containing frequency components at 100, 200, and 400 Hz. This signal is applied to a SSB modulator together with a carrier at 100 kHz, with only the upper sideband retained. In the coherent detector used to recover  $m(t)$ , the local oscillator supplies a sinusoidal wave of frequency 100.02 kHz. Determine the frequency components of the detector output.  
 (b) Repeat your analysis, assuming that only the lower sideband is transmitted.
- 3.28 Throughout this chapter, we have expressed the sinusoidal carrier wave in the form

$$c(t) = A_c \cos(2\pi f_c t)$$

where  $A_c$  is the carrier amplitude and  $f_c$  is the carrier frequency. In Chapter 7 dealing with digital band-pass modulation techniques, we find it more convenient to express the carrier in the form

$$c(t) = \sqrt{\frac{2}{T_b}} \cos(2\pi f_c t)$$

where  $T_b$  is the duration allotted to the transmission of symbol 1 or symbol 0. Determine the value of carrier amplitude  $A_c$  for the energy in  $c(t)$  per symbol to equal unity.

### ADVANCED PROBLEMS

---

- 3.29 For a p-n junction diode, the current  $i$  through the diode and the voltage  $v$  across it are related by

$$i = I_0 \left[ \exp\left(-\frac{v}{V_T}\right) - 1 \right]$$

where  $I_0$  is the reverse saturation current and  $V_T$  is the thermal voltage defined by

$$V_T = \frac{kT}{e}$$

where  $k$  is Boltzmann's constant in joules per degree Kelvin,  $T$  is the absolute temperature in degrees Kelvin, and  $e$  is the charge of an electron. At room temperature,  $V_T = 0.026$  volt.

- (a) Expand  $i$  as a power series in  $v$ , retaining terms up to  $v^3$ .  
 (b) Let
- $$v = 0.01 \cos(2\pi f_m t) + 0.01 \cos(2\pi f_c t) \text{ volts}$$
- where  $f_m = 1$  kHz and  $f_c = 100$  kHz. Determine the spectrum of the resulting diode current  $i$ .  
 (c) Specify the bandpass filter required to extract from the diode current an AM wave with carrier frequency  $f_c$ .  
 (d) What is the percentage modulation of this AM wave?
- 3.30 Consider the quadrature-carrier multiplex system of Fig. 3.17. The multiplexed signal  $s(t)$  produced at the transmitter output in part (a) of this figure is applied to a communication channel of transfer function  $H(f)$ . The output of this channel is, in turn, applied to the receiver input in part (b) of Fig. 3.17. Prove that the condition

$$H(f_c + f) = H^*(f_c - f), \quad \text{for } 0 \leq f \leq W$$

is necessary for recovery of the message signals  $m_1(t)$  and  $m_2(t)$  at the receiver outputs;  $f_c$  is the carrier frequency,  $W$  is the message bandwidth. The asterisk in  $H^*(f_c - f)$  denotes complex conjugation.

*Hint:* Evaluate the spectra of the two receiver outputs.

- 3.31 (a) Let  $s_u(t)$  denote the SSB wave obtained by transmitting only the upper sideband, and  $\hat{s}_u(t)$  its Hilbert transform. Show that

$$m(t) = \frac{2}{A_c} [s_u(t) \cos(2\pi f_c t) + \hat{s}_u(t) \sin(2\pi f_c t)]$$

and

$$\hat{m}(t) = \frac{2}{A_c} [\hat{s}_u(t) \cos(2\pi f_c t) - s_u(t) \sin(2\pi f_c t)]$$

where  $m(t)$  is the message signal,  $\hat{m}(t)$  is its Hilbert transform,  $f_c$  the carrier frequency, and  $A_c$  is the carrier amplitude.

- (b) Show that the corresponding equations in terms of the SSB wave  $s_l(t)$  obtained by transmitting only the lower sideband are

$$m(t) = \frac{2}{A_c} [s_l(t) \cos(2\pi f_c t) + \hat{s}_l(t) \sin(2\pi f_c t)]$$

and

$$\hat{m}(t) = \frac{2}{A_c} [s_l(t) \cos(2\pi f_c t) - \hat{s}_l(t) \sin(2\pi f_c t)]$$

- (c) Using the results of (a) and (b), set up the block diagrams of a receiver for demodulating an SSB wave.

*Note:* The Hilbert transform is defined in Problem 2.52; see also footnote 4 of this chapter.

- 3.32 In this problem, we continue the discussion on VSB modulation for the case when a vestige of the lower sideband is transmitted; Fig. 3.24 depicts the frequency response  $H(f)$  of the sideband shaping filter used to generate such a modulated wave. In particular, we wish to examine the complex representation of this filter, denoted by  $\tilde{H}(f)$ .

Let  $H_I(f)$  and  $H_Q(f)$  denote the in-phase and quadrature components of  $\tilde{H}(f)$ , respectively. Show that over the interval  $-W \leq f \leq W$ , we have

- (a)  $H_I(f)$  represents an all-pass filter; that is, the frequency response of the filter is constant as shown by

$$H_I(f) = 1, \quad \text{for } -W \leq f \leq W$$

where  $W$  is the message bandwidth.

- (b)  $H_Q(f)$  represents a low-pass filter with an odd-symmetric frequency response, described by the following three relations

$$1. H_Q(-f) = -H_Q(f), \quad -W \leq f \leq W$$

$$2. H_Q(0) = 0$$

$$3. H_Q(f) = 1 \quad \text{for } f_v \leq f \leq W$$

where  $f_v$  is the width of the vestigial sideband.

## CHAPTER 4

# ANGLE MODULATION

In the previous chapter, we investigated the effect of slowly varying the amplitude of a sinusoidal carrier wave in accordance with an information-bearing signal, keeping the carrier frequency fixed. There is another way of modulating a sinusoidal carrier wave—namely, *angle modulation*, in which the angle of the carrier wave is varied according to the information-bearing signal. In this second family of modulation techniques, the amplitude of the carrier wave is maintained constant.

An important feature of angle modulation is that it can provide better discrimination against noise and interference than amplitude modulation. As will be shown in Chapter 9, however, this improvement in performance is achieved at the expense of increased transmission bandwidth; that is, angle modulation provides us with a practical means of exchanging channel bandwidth for improved noise performance. Such a tradeoff is *not* possible with amplitude modulation. Moreover, the improvement in noise performance in angle modulation is achieved at the cost of increased system complexity in both the transmitter and receiver.

The material presented in this chapter on angle modulation will teach us three lessons:

- *Lesson 1: Angle modulation is a nonlinear process, which testifies to its sophisticated nature. In the context of analog communications, this distinctive property of angle modulation has two implications:*

- *In analytic terms, the spectral analysis of angle modulation is complicated.*
  - *In practical terms, the implementation of angle modulation is demanding.*

*Both of these statements are made with amplitude modulation as the frame of reference.*

- *Lesson 2: Whereas the transmission bandwidth of an amplitude-modulated wave (or any of its variants) is of limited extent, the transmission bandwidth of an angle-modulated wave may assume an infinite extent, at least in theory.*
- *Lesson 3: Given that the amplitude of the carrier wave is maintained constant, we would intuitively expect that additive noise would affect the performance of angle modulation to a lesser extent than amplitude modulation.*

## 4.1 Basic Definitions

Let  $\theta_i(t)$  denote the *angle* of a modulated sinusoidal carrier at time  $t$ ; it is assumed to be a function of the information-bearing signal or message signal. We express the resulting *angle-modulated wave* as

$$s(t) = A_c \cos[\theta_i(t)] \quad (4.1)$$

where  $A_c$  is the carrier amplitude. A complete oscillation occurs whenever the angle  $\theta_i(t)$  changes by  $2\pi$  radians. If  $\theta_i(t)$  increases monotonically with time, then the average frequency in hertz, over a small interval from  $t$  to  $t + \Delta t$ , is given by

$$f_{\Delta t}(t) = \frac{\theta_t(t + \Delta t) - \theta_i(t)}{2\pi\Delta t}$$

Allowing the time interval  $\Delta t$  to approach zero leads to the following definition for the *instantaneous frequency* of the angle-modulated signal  $s(t)$ :

$$\begin{aligned} f_i(t) &= \lim_{\Delta t \rightarrow 0} f_{\Delta t}(t) \\ &= \lim_{\Delta t \rightarrow 0} \left[ \frac{\theta_t(t + \Delta t) - \theta_i(t)}{2\pi\Delta t} \right] \\ &= \frac{1}{2\pi} \frac{d\theta_i(t)}{dt} \end{aligned} \quad (4.2)$$

where, in the last line, we have invoked the definition for the derivative of the angle  $\theta_i(t)$  with respect to time  $t$ .

Thus according to Eq. (4.1), we may interpret the angle-modulated signal  $s(t)$  as a rotating phasor of length  $A_c$  and angle  $\theta_i(t)$ . The angular velocity of such a phasor is  $d\theta_i(t)/dt$ , measured in radians per second. In the simple case of an unmodulated carrier, the angle  $\theta_i(t)$  is

$$\theta_i(t) = 2\pi f_c t + \phi_c, \quad \text{for } m(t) = 0$$

and the corresponding phasor rotates with a constant angular velocity equal to  $2\pi f_c$  radians per second. The constant  $\phi_c$  defines the angle of the unmodulated carrier at time  $t = 0$ .

There are an infinite number of ways in which the angle  $\theta_i(t)$  may be varied in some manner with the message signal. However, we shall consider only two commonly used methods, phase modulation and frequency modulation, as defined below:

1. *Phase modulation (PM) is that form of angle modulation in which the instantaneous angle  $\theta_i(t)$  is varied linearly with the message signal  $m(t)$* , as shown by

$$\theta_i(t) = 2\pi f_c t + k_p m(t) \quad (4.3)$$

The term  $2\pi f_c t$  represents the *angle of the unmodulated carrier* with the constant  $\phi_c$  set equal to zero for convenience of presentation; the constant  $k_p$  represents the *phase sensitivity factor* of the modulator, expressed in radians per volt on the assumption that  $m(t)$  is a voltage waveform. The phase-modulated wave  $s(t)$  is correspondingly described in the time domain by

$$s(t) = A_c \cos[2\pi f_c t + k_p m(t)] \quad (4.4)$$

2. Frequency modulation (FM) is that form of angle modulation in which the instantaneous frequency  $f_i(t)$  is varied linearly with the message signal  $m(t)$ , as shown by

$$f_i(t) = f_c + k_f m(t) \quad (4.5)$$

The constant term  $f_c$  represents the frequency of the unmodulated carrier; the constant  $k_f$  represents the frequency-sensitivity factor of the modulator, expressed in hertz per volt on the assumption that  $m(t)$  is a voltage waveform. Integrating Eq. (4.5) with respect to time and multiplying the result by  $2\pi$ , we get

$$\begin{aligned} \theta_i(t) &= 2\pi \int_0^t f_i(\tau) d\tau \\ &= 2\pi f_c t + 2\pi k_f \int_0^t m(\tau) d\tau \end{aligned} \quad (4.6)$$

where the second term accounts for the increase or decrease in the instantaneous phase  $\theta_i(t)$  due to the message signal  $m(t)$ . The frequency-modulated wave is therefore

$$s(t) = A_c \cos \left[ 2\pi f_c t + 2\pi k_f \int_0^t m(\tau) d\tau \right] \quad (4.7)$$

Table 4.1 summarizes the basic definitions embodied in the generation of angle-modulated waves. These definitions apply to all kinds of message signals, be they of the analog or digital kind.

**TABLE 4.1 Summary of Basic Definitions in Angle Modulation**

	Phase modulation	Frequency modulation	Comments
Instantaneous phase $\theta_i(t)$	$2\pi f_c t + k_p m(t)$	$2\pi f_c t + 2\pi k_f \int_0^t m(\tau) d\tau$	$A_c$ : carrier amplitude $f_c$ : carrier frequency $m(t)$ : message signal $k_p$ : phase-sensitivity factor $k_f$ : frequency-sensitivity factor
Instantaneous frequency $f_i(t)$	$f_c + \frac{k_p}{2\pi} \frac{d}{dt} m(t)$	$f_c + k_f m(t)$	
Modulated wave $s(t)$	$A_c \cos[2\pi f_c t + k_p m(t)]$	$A_c \cos \left[ 2\pi f_c t + 2\pi k_f \int_0^t m(\tau) d\tau \right]$	

## 4.2 Properties of Angle-Modulated Waves

Angle-modulated waves are characterized by some important properties, which follow from the basic definitions summarized in Table 4.1. Indeed, it is these properties that put angle-modulated waves in a family of their own, and distinguish them from the family of amplitude-modulated waves, as illustrated by the waveforms shown in Fig. 4.1 for the example of sinusoidal modulation. Figures 4.1(a) and 4.1(b) are the sinusoidal carrier and modulating waves, respectively. Figures 4.1(c), 4.1(d), and 4.1(e) display the corresponding amplitude-modulated (AM), phase-modulated (PM), and frequency-modulated (FM) waves, respectively.

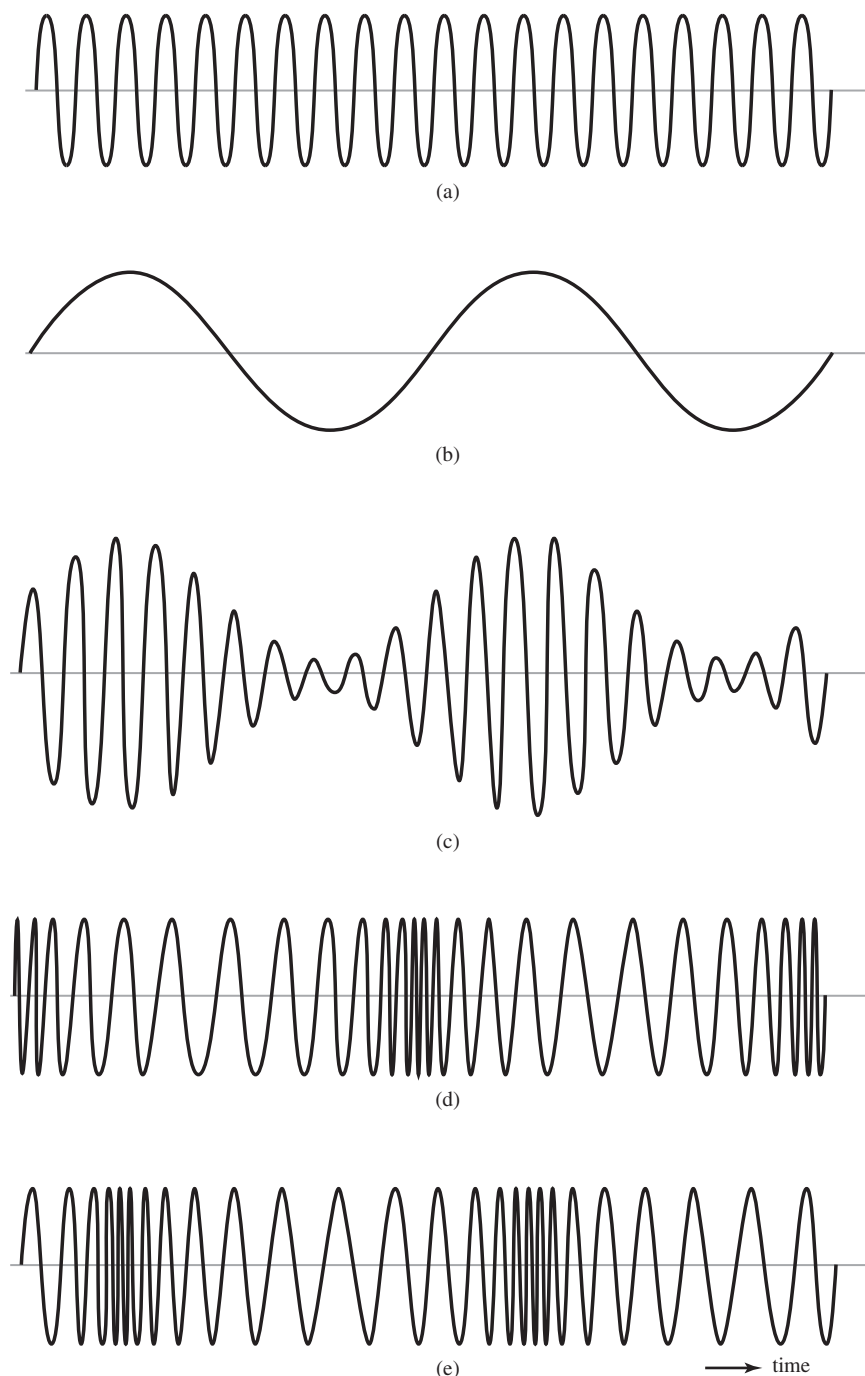


**FIGURE 4.1** Illustration of AM, PM, and FM waves produced by a single tone.  
(a) Carrier wave. (b) Sinusoidal modulating signal. (c) Amplitude-modulated  
signal. (d) Phase-modulated signal. (e) Frequency modulated signal.

**PROPERTY 1 Constancy of transmitted power** From both Eqs. (4.4) and (4.7), we readily see that the amplitude of PM and FM waves is maintained at a constant value equal to the carrier amplitude  $A_c$  for all time  $t$ , irrespective of the sensitivity factors  $k_p$  and  $k_f$ . This property is well demonstrated by the PM wave of Fig. 4.1(d) and FM wave of Fig. 4.1(e). Consequently, the average transmitted power of angle-modulated waves is a constant, as shown by

$$P_{av} = \frac{1}{2} A_c^2 \quad (4.8)$$

where it is assumed that the load resistor is 1 ohm.

**PROPERTY 2 Nonlinearity of the modulation process** Another distinctive property of angle modulation is its nonlinear character. We say so because both PM and FM waves violate the principle of superposition. Suppose, for example, that the message signal  $m(t)$  is made up of two different components  $m_1(t)$  and  $m_2(t)$ , as shown by

$$m(t) = m_1(t) + m_2(t)$$

Let  $s(t)$ ,  $s_1(t)$ , and  $s_2(t)$  denote the PM waves produced by  $m(t)$ ,  $m_1(t)$ , and  $m_2(t)$  in accordance with Eq. (4.4), respectively. In light of this equation, we may express these PM waves as follows:

$$\begin{aligned} s(t) &= A_c \cos[2\pi f_c t + k_p(m_1(t) + m_2(t))] \\ s_1(t) &= A_c \cos[2\pi f_c t + k_p m_1(t)] \end{aligned}$$

and

$$s_2(t) = A_c \cos[2\pi f_c t + k_p m_2(t)]$$

From these expressions, despite the fact that  $m(t) = m_1(t) + m_2(t)$ , we readily see that the principle of superposition is violated because

$$s(t) \neq s_1(t) + s_2(t)$$

► **Drill Problem 4.1** Using Eq. (4.7), show that FM waves also violate the principle of superposition. ◀

The fact that the angle-modulation process is nonlinear complicates the spectral analysis and noise analysis of PM and FM waves, compared to amplitude modulation. By the same token, the angle-modulation process has practical benefits of its own. For example, frequency modulation offers a superior noise performance compared to amplitude modulation, which is attributed to the nonlinear character of frequency modulation.

**PROPERTY 3 Irregularity of zero-crossings** A consequence of allowing the instantaneous angle  $\theta_i(t)$  to become dependent on the message signal  $m(t)$  as in Eq. (4.3) or its integral  $\int_0^t m(\tau) d\tau$  as in Eq. (4.6) is that, in general, the zero-crossings of a PM or FM wave no longer have a perfect regularity in their spacing across the time-scale. Zero-crossings are defined as the instants of time at which a waveform changes its amplitude from a positive to negative value or the other way around. In a way, the irregularity of zero-crossings in angle-modulated waves is also attributed to the nonlinear character of the modulation process. To illustrate this property, we may contrast the PM wave of Fig. 4.1(d) and the FM wave of Fig. 4.1(e) to Fig. 4.1(c) for the corresponding AM wave.

However, we may cite two special cases where regularity is maintained in angle modulation:

1. The message signal  $m(t)$  increases or decreases linearly with time  $t$ , in which case the instantaneous frequency  $f_i(t)$  of the PM wave changes from the unmodulated carrier frequency  $f_c$  to a new constant value dependent on the slope of  $m(t)$ .
2. The message signal  $m(t)$  is maintained at some constant value, positive or negative, in which case the instantaneous frequency  $f_i(t)$  of the FM wave changes from the unmodulated carrier frequency  $f_c$  to a new constant value dependent on the constant value of  $m(t)$ .

In any event, it is important to note that in angle modulation, the information content of the message signal  $m(t)$  resides in the zero-crossings of the modulated wave. This statement holds provided the carrier frequency  $f_c$  is large compared to the highest frequency component of the message signal  $m(t)$ .

**PROPERTY 4 Visualization difficulty of message waveform** In AM, we see the message waveform as the envelope of the modulated wave, provided, of course, the percentage modulation is less than 100 percent, as illustrated in Fig. 4.1(c) for sinusoidal modulation. This is not so in angle modulation, as illustrated by the corresponding waveforms of Figs. 4.1(d) and 4.1(e) for PM and FM, respectively. In general, the difficulty in visualizing the message waveform in angle-modulated waves is also attributed to the nonlinear character of angle-modulated waves.

**PROPERTY 5 Tradeoff of increased transmission bandwidth for improved noise performance** An important advantage of angle modulation over amplitude modulation is the realization of improved noise performance. This advantage is attributed to the fact that the transmission of a message signal by modulating the angle of a sinusoidal carrier wave is less sensitive to the presence of additive noise than transmission by modulating the amplitude of the carrier. The improvement in noise performance is, however, attained at the expense of a corresponding increase in the transmission bandwidth requirement of angle modulation. In other words, the use of angle modulation offers the possibility of exchanging an increase in transmission bandwidth for an improvement in noise performance. Such a tradeoff is not possible with amplitude modulation since the transmission bandwidth of an amplitude-modulated wave is fixed somewhere between the message bandwidth  $W$  and  $2W$ , depending on the type of modulation employed. The effect of noise on angle modulation is discussed in Chapter 9.

#### EXAMPLE 4.1 Zero-crossings

Consider a modulating wave  $m(t)$  that increases linearly with time  $t$ , starting at  $t = 0$ , as shown by

$$m(t) = \begin{cases} at, & t \geq 0 \\ 0, & t < 0 \end{cases}$$

where  $a$  is the slope parameter; see Fig. 4.2(a). In what follows, we study the zero-crossings of the PM and FM waves produced by  $m(t)$  for the following set of parameters:

$$f_c = \frac{1}{4} \text{ Hz}$$

$$a = 1 \text{ volt/s}$$

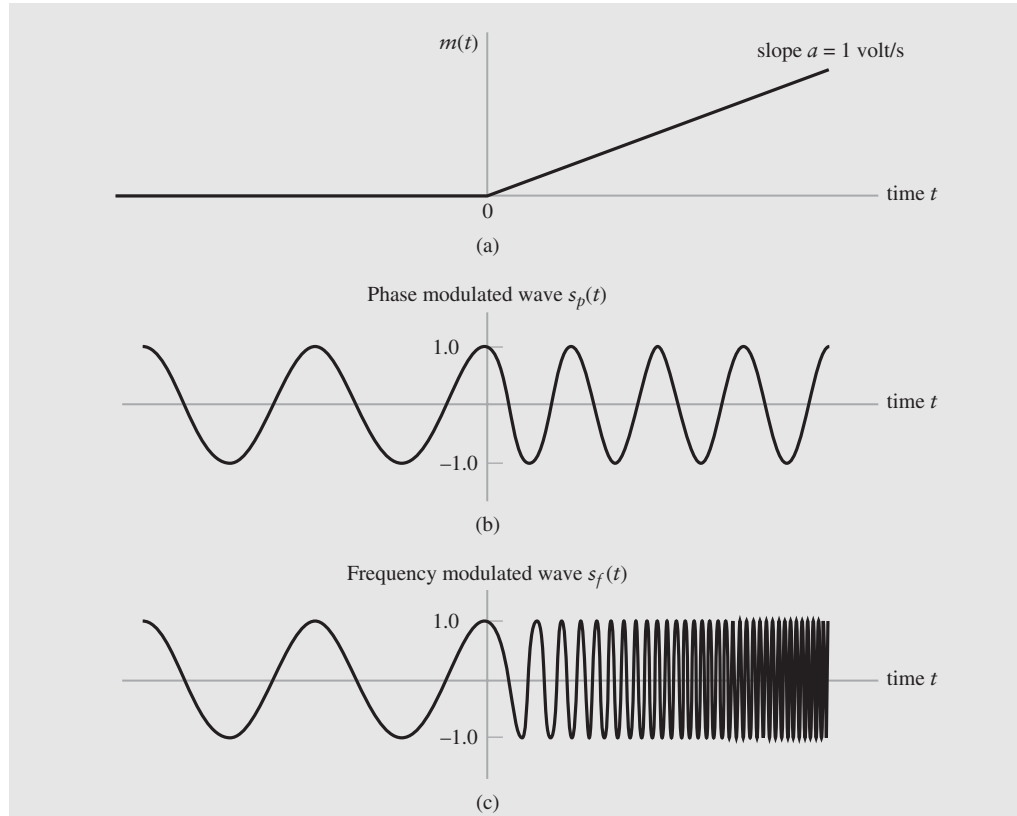


**FIGURE 4.2** Starting at time  $t = 0$ , the figure displays (a) linearly increasing message signal  $m(t)$ , (b) phase-modulated wave, and (c) frequency-modulated wave.

1. *Phase modulation:* phase-sensitivity factor  $k_p = \frac{\pi}{2}$  radians/volt. Applying Eq. (4.4) to the given  $m(t)$  yields the PM wave

$$s(t) = \begin{cases} A_c \cos(2\pi f_{ct} + k_p a t), & t \geq 0 \\ A_c \cos(2\pi f_{ct}), & t < 0 \end{cases}$$

which is plotted in Fig. 4.2(b) for  $A_c = 1$  volt.

Let  $t_n$  denote the instant of time at which the PM wave experiences a zero-crossing; this occurs whenever the angle of the PM wave is an odd multiple of  $\pi/2$ . Then, we may set up

$$2\pi f_c t_n + k_p a t_n = \frac{\pi}{2} + n\pi, \quad n = 0, 1, 2, \dots$$

as the *linear* equation for  $t_n$ . Solving this equation for  $t_n$ , we get the linear formula

$$t_n = \frac{\frac{1}{2} + n}{2f_c + \frac{k_p}{\pi} a}$$

Substituting the given values for  $f_c$ ,  $a$ , and  $k_p$  into this linear formula, we get

$$t_n = \frac{1}{2} + n, \quad n = 0, 1, 2, \dots$$

where  $t_n$  is measured in seconds.

2. *Frequency modulation:* frequency-sensitivity factor,  $k_f = 1 \text{ Hz/volt}$ . Applying Eq. (4.7) yields the FM wave

$$s(t) = \begin{cases} A_c \cos(2\pi f_c t + \pi k_f a t^2), & t \geq 0 \\ A_c \cos(2\pi f_c t), & t < 0 \end{cases}$$

which is plotted in Fig. 4.2(c).

Invoking the definition of a zero-crossing, we may set up

$$2\pi f_c t_n + \pi k_f a t_n^2 = \frac{\pi}{2} + n\pi, \quad n = 0, 1, 2, \dots$$

as the *quadratic* equation for  $t_n$ . The positive root of this equation—namely,

$$t_n = \frac{1}{ak_f} \left( -f_c + \sqrt{f_c^2 + ak_f \left( \frac{1}{2} + n \right)} \right), \quad n = 0, 1, 2, \dots$$

defines the formula for  $t_n$ . Substituting the given values of  $f_c$ ,  $a$ , and  $k_f$  into this quadratic formula, we get

$$t_n = \frac{1}{4} (-1 + \sqrt{9 + 16n}), \quad n = 0, 1, 2, \dots$$

where  $t_n$  is again measured in seconds.

Comparing the zero-crossing results derived for PM and FM waves, we may make the following observations once the linear modulating wave begins to act on the sinusoidal carrier wave:

1. For PM, regularity of the zero-crossings is maintained; the instantaneous frequency changes from the unmodulated value of  $f_c = 1/4 \text{ Hz}$  to the new constant value of  $f_c + k_p(a/2\pi) = \frac{1}{2} \text{ Hz}$ .
2. For FM, the zero-crossings assume an irregular form; as expected, the instantaneous frequency increases linearly with time  $t$ .

The angle-modulated waveforms of Fig. 4.2 should be contrasted with the corresponding ones of Fig. 4.1. Whereas in the case of sinusoidal modulation depicted in Fig. 4.1 it is difficult to discern the difference between PM and FM, this is not so in the case of Fig. 4.2. In other words, depending on the modulating wave, it is possible for PM and FM to exhibit entirely different waveforms.

## 4.3 Relationship Between PM and FM Waves

Examining the definitions of Eqs. (4.4) and (4.7), we see that an FM wave may be viewed as a PM wave produced by the modulating wave  $\int_0^t m(\tau) d\tau$  in place of  $m(t)$ . This means that an FM wave can be generated by first integrating the message signal  $m(t)$  with respect to time  $t$  and then using the resulting signal as the input to a phase modulator, as shown in Fig. 4.3(a).

Conversely, a PM wave can be viewed as an FM wave produced by the modulating wave  $dm(t)/dt$ . Hence, a PM wave can be generated by first differentiating  $m(t)$  with respect to time  $t$  and then using the resulting signal as the input to a frequency modulator, as shown in Fig. 4.3(b).

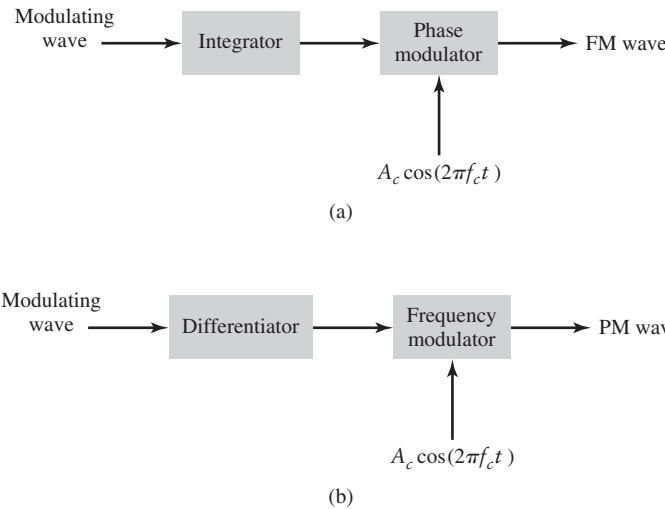


**FIGURE 4.3** Illustration of the relationship between frequency modulation and phase modulation. (a) Scheme for generating an FM wave by using a phase modulator. (b) Scheme for generating a PM wave by using a frequency modulator.

It follows therefore that phase modulation and frequency modulation are uniquely related to each other. This relationship, in turn, means that we may deduce the properties of phase modulation from those of frequency modulation and vice versa. For this reason, in this chapter we will be focusing much of the discussion on frequency modulation.

► **Drill Problem 4.2** The scheme shown in Fig. 4.3(a) provides the basis for the indirect generation of an FM wave. The phase modulator is defined by Eq. (4.4). Show that if the resulting FM wave is to have exactly the form as that defined in Eq. (4.7), then the phase-sensitivity factor  $k_p$  of the phase modulator is related to the frequency sensitivity factor  $k_f$  in Eq. (4.7) by the formula

$$k_p = 2\pi k_f T$$

where  $T$  is the interval over which the integration in Fig. 4.3(a) is performed. Justify the dimensionality of this expression. ◀

## 4.4 Narrow-Band Frequency Modulation

In Section 4.2, we stressed the fact that an FM wave is a nonlinear function of the modulating wave. This property makes the spectral analysis of the FM wave a much more difficult task than that of the corresponding AM wave.

How then can we tackle the spectral analysis of an FM wave? We propose to provide an empirical answer to this important question by proceeding in the following manner:

- We first consider the simple case of a single-tone modulation that produces a narrow-band FM wave.
- We next consider the more general case also involving a single-tone modulation, but this time the FM wave is wide-band.

We could, of course, go on and consider the more elaborate case of a multitone FM wave. However, we propose not to do so, because our immediate objective is to establish an empirical relationship between the transmission bandwidth of an FM wave and the

message bandwidth. As we shall subsequently see, the two-stage spectral analysis described above provides us with enough insight to propose a useful solution to the problem.

Consider then a sinusoidal modulating wave defined by

$$m(t) = A_m \cos(2\pi f_m t) \quad (4.9)$$

The instantaneous frequency of the resulting FM wave is

$$\begin{aligned} f_i(t) &= f_c + k_f A_m \cos(2\pi f_m t) \\ &= f_c + \Delta f \cos(2\pi f_m t) \end{aligned} \quad (4.10)$$

where

$$\Delta f = k_f A_m \quad (4.11)$$

The quantity  $\Delta f$  is called the *frequency deviation*, representing the maximum departure of the instantaneous frequency of the FM wave from the carrier frequency  $f_c$ . A fundamental characteristic of sinusoidal frequency modulation is that the frequency deviation  $\Delta f$  is proportional to the amplitude of the modulating signal and is independent of the modulating frequency.

Using Eq. (4.10) in the first line of Eq. (4.6), the angle  $\theta_i(t)$  of the FM wave is obtained as

$$\theta_i(t) = 2\pi f_c t + \frac{\Delta f}{f_m} \sin(2\pi f_m t) \quad (4.12)$$

The ratio of the frequency deviation  $\Delta f$  to the modulation frequency  $f_m$  is commonly called the *modulation index* of the FM wave. We denote this new parameter by  $\beta$ , so we write

$$\beta = \frac{\Delta f}{f_m} \quad (4.13)$$

and

$$\theta_i(t) = 2\pi f_c t + \beta \sin(2\pi f_m t) \quad (4.14)$$

From Eq. (4.14) we see that, in a physical sense, the parameter  $\beta$  represents the phase deviation of the FM wave—that is, the maximum departure of the angle  $\theta_i(t)$  from the angle  $2\pi f_c t$  of the unmodulated carrier. Hence,  $\beta$  is measured in radians.

The FM wave itself is given by

$$s(t) = A_c \cos[2\pi f_c t + \beta \sin(2\pi f_m t)] \quad (4.15)$$

For the FM wave  $s(t)$  of Eq. (4.15) to be narrow-band the modulation index  $\beta$  must be small compared to one radian. To proceed further, we use the trigonometric identity

$$\cos(A + B) = \cos A \cos B - \sin A \sin B$$

to expand Eq. (4.15) as

$$s(t) = A_c \cos(2\pi f_c t) \cos[\beta \sin(2\pi f_m t)] - A_c \sin(2\pi f_c t) \sin[\beta \sin(2\pi f_m t)] \quad (4.16)$$

Then under the condition that the modulation index  $\beta$  is small compared to one radian, we may use the following two approximations for all times  $t$ :

$$\cos[\beta \sin(2\pi f_m t)] \approx 1$$

and

$$\sin[\beta \sin(2\pi f_m t)] \approx \beta \sin(2\pi f_m t)$$

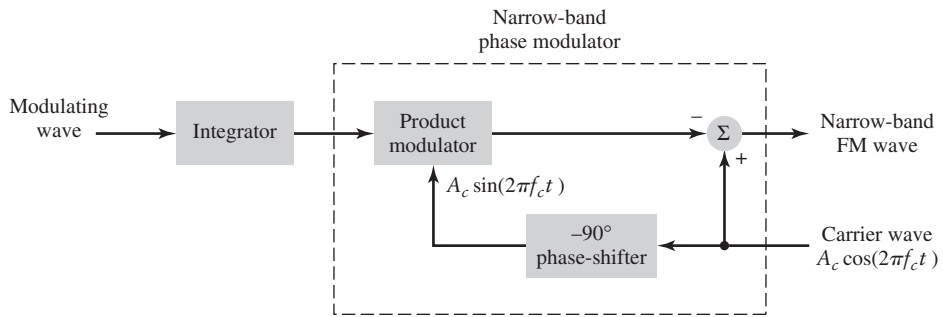


**FIGURE 4.4** Block diagram of an indirect method for generating a narrow-band FM wave.

Accordingly, Eq. (4.16) simplifies to

$$s(t) \approx A_c \cos(2\pi f_c t) - \beta A_c \sin(2\pi f_c t) \sin(2\pi f_m t) \quad (4.17)$$

Equation (4.17) defines the *approximate form* of a narrow-band FM wave produced by the sinusoidal modulating wave  $A_m \cos(2\pi f_m t)$ . From this approximate representation, we deduce the modulator shown in block diagram form in Fig. 4.4. This modulator involves splitting the carrier wave  $A_c \cos(2\pi f_c t)$  into two paths. One path is direct; the other path contains a  $-90^\circ$  degree phase-shifting network and a product modulator, the combination of which generates a DSB-SC modulated wave. The difference between these two signals produces a narrow-band FM wave, but with some *amplitude distortion*, as discussed next.

Ideally, an FM wave has a constant envelope and, for the case of a sinusoidal modulating signal of frequency  $f_m$ , the angle  $\theta_i(t)$  is also sinusoidal with the same frequency. But the modulated wave produced by the narrow-band modulator of Fig. 4.4 differs from this ideal condition in two fundamental respects:

1. The envelope contains a *residual amplitude modulation* that varies with time.
2. The angle  $\theta_i(t)$  contains *harmonic distortion* in the form of third- and higher order harmonics of the modulation frequency  $f_m$ .

► **Drill Problem 4.3** The *Cartesian representation* of band-pass signals discussed in Section 3.8 is well-suited for linear modulation schemes exemplified by the amplitude modulation family. On the other hand, the *polar representation*

$$s(t) = a(t) \cos[2\pi f_c t + \phi(t)]$$

is well-suited for nonlinear modulation schemes exemplified by the angle modulation family. The  $a(t)$  in this new representation is the envelope of  $s(t)$  and  $\phi(t)$  is its phase.

Starting with the representation [see Eq. (3.39)]

$$s(t) = s_I(t) \cos(2\pi f_c t) - s_Q(t) \sin(2\pi f_c t)$$

where  $s_I(t)$  is the in-phase component and  $s_Q(t)$  is the quadrature component, we may write

$$a(t) = [s_I^2(t) + s_Q^2(t)]^{1/2}$$

and

$$\phi(t) = \tan^{-1} \left[ \frac{s_Q(t)}{s_I(t)} \right]$$

Show that the polar representation of  $s(t)$  in terms of  $a(t)$  and  $\phi(t)$  is exactly equivalent to its Cartesian representation in terms of  $s_I(t)$  and  $s_Q(t)$ . ◀

► **Drill Problem 4.4** Consider the narrow-band FM wave approximately defined by Eq. (4.17). Building on Problem 4.3, do the following:

- Determine the envelope of this modulated wave. What is the ratio of the maximum to the minimum value of this envelope?
- Determine the average power of the narrow-band FM wave, expressed as a percentage of the average power of the unmodulated carrier wave.
- By expanding the angular argument  $\theta(t) = 2\pi f_c t + \phi(t)$  of the narrow-band FM wave  $s(t)$  in the form of a power series, and restricting the modulation index  $\beta$  to a maximum value of 0.3 radian, show that

$$\theta(t) \approx 2\pi f_c t + \beta \sin(2\pi f_m t) - \frac{\beta^3}{3} \sin^3(2\pi f_m t)$$

What is the value of the harmonic distortion for  $\beta = 0.3$  radian?

*Hint:* For small  $x$ , the following power series approximation

$$\tan^{-1}(x) \approx x - \frac{1}{3}x^3$$

holds. In this approximation, terms involving  $x^5$  and higher order ones are ignored, which is justified when  $x$  is small compared to unity. ◀

The important point to note from Problem 4.4 is that by restricting the modulation index to  $\beta \leq 0.3$  radian, the effects of residual amplitude modulation and harmonic distortion are limited to negligible levels. We are therefore emboldened to proceed further with the use of Eq. (4.17), provided  $\beta \leq 0.3$  radian. In particular, we may expand the modulated wave further into three frequency components:

$$s(t) \approx A_c \cos(2\pi f_c t) + \frac{1}{2} \beta A_c \{ \cos[2\pi(f_c + f_m)t] - \cos[2\pi(f_c - f_m)t] \} \quad (4.18)$$

This expression is somewhat similar to the corresponding one defining an AM wave, which is reproduced from Example 3.1 of Chapter 3 as follows:

$$s_{\text{AM}}(t) = A_c \cos(2\pi f_c t) + \frac{1}{2} \mu A_c \{ \cos[2\pi(f_c + f_m)t] + \cos[2\pi(f_c - f_m)t] \} \quad (4.19)$$

where  $\mu$  is the modulation factor of the AM signal. Comparing Eqs. (4.18) and (4.19) and putting aside the respective constants  $\beta$  and  $\mu$ , we see that in the case of sinusoidal modulation, the basic difference between an AM wave and a narrow-band FM wave is that the algebraic sign of the lower side-frequency in the narrow-band FM is reversed. Nevertheless, a narrow-band FM wave requires essentially the same transmission bandwidth (i.e.,  $2f_m$  for sinusoidal modulation) as the AM wave.

### ■ PHASOR INTERPRETATION

We may represent the narrow-band FM wave with a phasor diagram as shown in Fig. 4.5(a), where we have used the carrier phasor as reference. We see that the resultant of the two side-frequency phasors is always at right angles to the carrier phasor. The effect of this geometry is to produce a resultant phasor representing the narrow-band FM wave that is approximately of the same amplitude as the carrier phasor, but out of phase with respect to it.

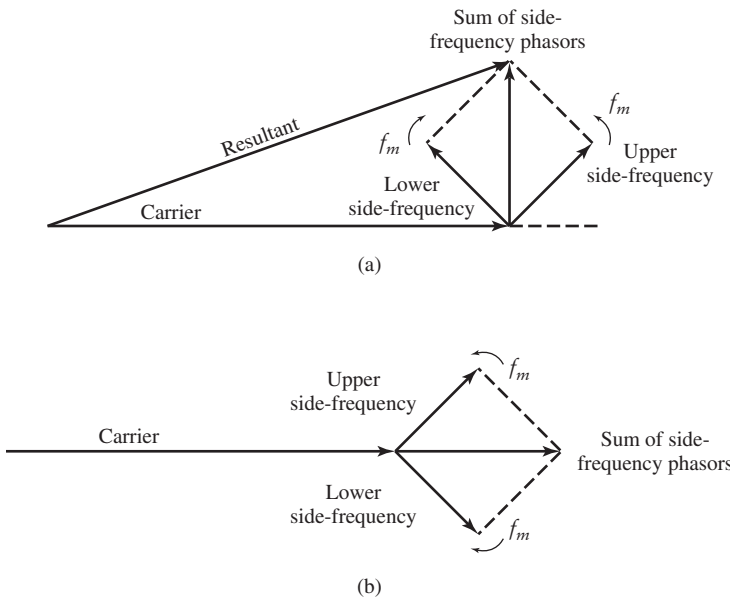


**FIGURE 4.5** Phasor comparison of narrow-band FM and AM waves for sinusoidal modulation. (a) Narrow-band FM wave. (b) AM wave.

The phasor diagram for the FM wave should be contrasted with that of Fig. 4.5(b), representing the corresponding AM wave. In this latter case, we see that the resultant phasor representing the AM wave has a different amplitude from that of the carrier phasor, but always in phase with it.

Despite the fact that both the narrow-band FM of Eq. (4.18) and the AM wave of Eq. (4.19) have three sinusoidal components, the two parts of Fig. 4.5 clearly illustrate the major differences between these two modulated waves; the differences are attributed to the ways in which these two modulated waves are generated.

## 4.5 Wide-Band Frequency Modulation

We next wish to determine the spectrum of the single-tone FM wave defined by the exact formula in Eq. (4.15) for an arbitrary value of the modulation index  $\beta$ . In general, such an FM wave produced by a sinusoidal modulating wave is a periodic function of time  $t$  only when the carrier frequency  $f_c$  is an integral multiple of the modulation frequency  $f_m$ .

► **Drill Problem 4.5** Strictly speaking, the FM wave of Eq. (4.15) produced by a sinusoidal modulating wave is a nonperiodic function of time  $t$ . Demonstrate this property of frequency modulation. ◀

In light of this problem, how can we simplify the spectral analysis of the wide-band FM wave defined in Eq. (4.15)? The answer lies in using the complex baseband representation of a modulated (i.e., bandpass) signal, which was discussed in Section 3.8. Specifically, assume that the carrier frequency  $f_c$  is large enough (compared to the bandwidth of the FM wave) to justify rewriting Eq. (4.15) in the form

$$\begin{aligned} s(t) &= \operatorname{Re}[A_c \exp(j2\pi f_c t + j\beta \sin(2\pi f_m t))] \\ &= \operatorname{Re}[\tilde{s}(t) \exp(j2\pi f_c t)] \end{aligned} \quad (4.20)$$

where the operator  $\text{Re}[\cdot]$  extracts the real part of the complex quantity contained inside the square brackets. The new term

$$\tilde{s}(t) = A_c \exp[j\beta \sin(2\pi f_m t)] \quad (4.21)$$

introduced in Eq. (4.21) is the *complex envelope* of the FM wave  $s(t)$ . The important point to note from Eq. (4.21) is that unlike the original FM wave  $s(t)$ , the complex envelope  $\tilde{s}(t)$  is a periodic function of time with a fundamental frequency equal to the modulation frequency  $f_m$ . Specifically, replacing time  $t$  in Eq. (4.21) with  $t + k/f_m$  for some integer  $k$ , we have

$$\begin{aligned}\tilde{s}(t) &= A_c \exp[j\beta \sin(2\pi f_m(t + k/f_m))] \\ &= A_c \exp[j\beta \sin(2\pi f_m t + 2k\pi)] \\ &= A_c \exp[j\beta \sin(2\pi f_m t)]\end{aligned}$$

which confirms  $f_m$  as the fundamental frequency of  $\tilde{s}(t)$ . We may therefore expand  $\tilde{s}(t)$  in the form of a complex Fourier series as follows:

$$\tilde{s}(t) = \sum_{n=-\infty}^{\infty} c_n \exp(j2\pi n f_m t) \quad (4.22)$$

where the complex Fourier coefficient

$$\begin{aligned}c_n &= f_m \int_{-1/(2f_m)}^{1/(2f_m)} \tilde{s}(t) \exp(-j2\pi n f_m t) dt \\ &= f_m A_c \int_{-1/(2f_m)}^{1/(2f_m)} \exp[j\beta \sin(2\pi f_m t) - j2\pi n f_m t] dt\end{aligned} \quad (4.23)$$

Define the new variable:

$$x = 2\pi f_m t \quad (4.24)$$

Hence, we may redefine the complex Fourier coefficient  $c_n$  in Eq. (4.23) in the new form

$$c_n = \frac{A_c}{2\pi} \int_{-\pi}^{\pi} \exp[j(\beta \sin x - nx)] dx \quad (4.25)$$

The integral on the right-hand side of Eq. (4.25), except for the carrier amplitude  $A_c$ , is referred to as the *nth order Bessel function* of the first kind and argument  $\beta$ . This function is commonly denoted by the symbol  $J_n(\beta)$ , so we may write

$$J_n(\beta) = \frac{1}{2\pi} \int_{-\pi}^{\pi} \exp[j(\beta \sin x - nx)] dx \quad (4.26)$$

Accordingly, we may rewrite Eq. (4.25) in the compact form

$$c_n = A_c J_n(\beta) \quad (4.27)$$

Substituting Eq. (4.27) into (4.22), we get, in terms of the Bessel function  $J_n(\beta)$ , the following expansion for the complex envelope of the FM wave:

$$\tilde{s}(t) = A_c \sum_{n=-\infty}^{\infty} J_n(\beta) \exp(j2\pi n f_m t) \quad (4.28)$$

Next, substituting Eq. (4.28) into (4.20), we get

$$s(t) = \text{Re} \left[ A_c \sum_{n=-\infty}^{\infty} J_n(\beta) \exp[j2\pi(f_c + n f_m)t] \right] \quad (4.29)$$

The carrier amplitude  $A_c$  is a constant and may therefore be taken outside the real-time operator  $\text{Re}[\cdot]$ . Moreover, we may interchange the order of summation and real-part operation, as they are both linear operators. Accordingly, we may rewrite Eq. (4.29) in the simplified form

$$s(t) = A_c \sum_{n=-\infty}^{\infty} J_n(\beta) \cos[2\pi(f_c + nf_m)t] \quad (4.30)$$

Equation (4.30) is the desired form for the Fourier series expansion of the single-tone FM signal  $s(t)$  for an arbitrary value of modulation index  $\beta$ .

The discrete spectrum of  $s(t)$  is obtained by taking the Fourier transforms of both sides of Eq. (4.30), which yields

$$S(f) = \frac{A_c}{2} \sum_{n=-\infty}^{\infty} J_n(\beta) [\delta(f - f_c - nf_m) + \delta(f + f_c + nf_m)] \quad (4.31)$$

where  $s(t) \Leftrightarrow S(f)$  and  $\cos(2\pi f_i t) \Leftrightarrow \frac{1}{2} [\delta(f - f_i) + \delta(f + f_i)]$  for an arbitrary  $f_i$ . Equation (4.31) shows that the spectrum of  $s(t)$  consists of an infinite number of delta functions spaced at  $f = f_c \pm nf_m$  for  $n = 0, +1, +2, \dots$

### ■ PROPERTIES OF SINGLE-TONE FM FOR ARBITRARY MODULATION INDEX $\beta$

In Fig. 4.6, we have plotted the Bessel function  $J_n(\beta)$  versus the modulation index  $\beta$  for different positive integer values of  $n$ . We can develop further insight into the behavior of the Bessel function  $J_n(\beta)$  by making use of the following properties (see Appendix 3 for more details):

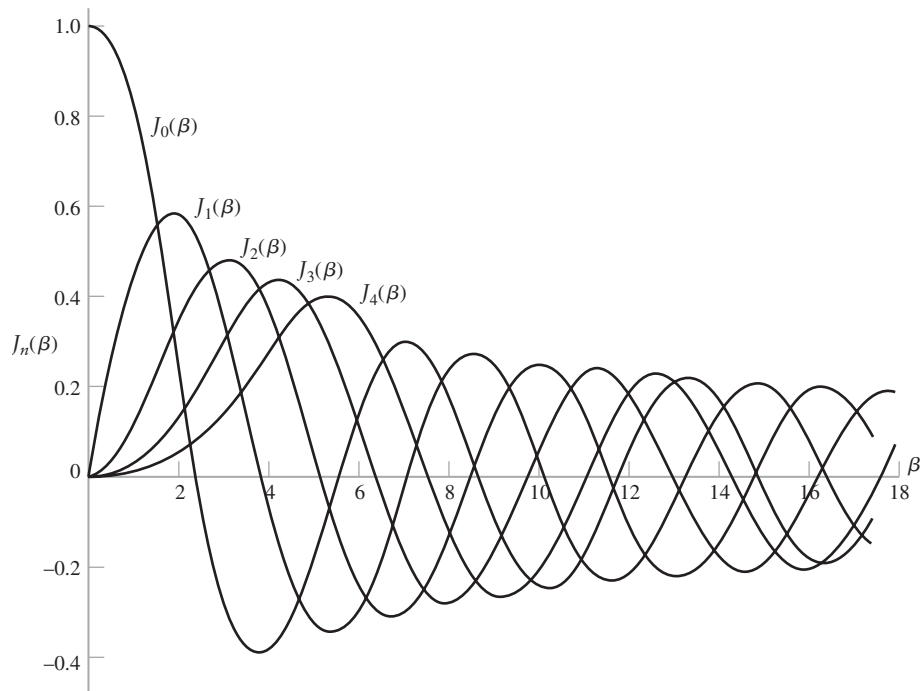


**FIGURE 4.6** Plots of the Bessel function of the first kind,  $J_n(\beta)$ , for varying order  $n$ .

- For different integer (positive and negative) values of  $n$ , we have

$$J_n(\beta) = J_{-n}(\beta), \quad \text{for } n \text{ even} \quad (4.32)$$

and

$$J_n(\beta) = -J_{-n}(\beta), \quad \text{for } n \text{ odd} \quad (4.33)$$

- For small values of the modulation index  $\beta$ , we have

$$\left. \begin{array}{l} J_0(\beta) \approx 1, \\ J_1(\beta) \approx \frac{\beta}{2}, \\ J_n(\beta) \approx 0, \quad n > 2 \end{array} \right\} \quad (4.34)$$

- The equality

$$\sum_{n=-\infty}^{\infty} J_n^2(\beta) = 1 \quad (4.35)$$

holds exactly for arbitrary  $\beta$ .

Thus using Eqs. (4.31) through (4.35) and the curves of Fig. 4.6, we may make the following observations:

- The spectrum of an FM wave contains a carrier component and an infinite set of side frequencies located symmetrically on either side of the carrier at frequency separations of  $f_m, 2f_m, 3f_m, \dots$ . In this respect, the result is unlike the picture that prevails in AM, since in the latter case a sinusoidal modulating wave gives rise to only one pair of side frequencies.
- For the special case of  $\beta$  small compared with unity, only the Bessel coefficients  $J_0(\beta)$  and  $J_1(\beta)$  have significant values, so that the FM wave is effectively composed of a carrier and a single pair of side-frequencies at  $f_c \pm f_m$ . This situation corresponds to the special case of narrow-band FM that was considered in Section 4.4.
- The amplitude of the carrier component varies with  $\beta$  according to  $J_0(\beta)$ . That is, unlike an AM wave, the amplitude of the carrier component of an FM wave is dependent on the modulation index  $\beta$ . The physical explanation for this property is that the envelope of an FM wave is constant, so that the average power of such a signal developed across a 1-ohm resistor is also constant, as in Eq. (4.8), which is reproduced here for convenience of presentation:

$$P_{av} = \frac{1}{2} A_c^2$$

When the carrier is modulated to generate the FM wave, the power in the side-frequencies may appear only at the expense of the power originally in the carrier, thereby making the amplitude of the carrier component dependent on  $\beta$ . Note that the average power of an FM wave may also be determined from Eq. (4.30), as shown by

$$P = \frac{1}{2} A_c^2 \sum_{n=-\infty}^{\infty} J_n^2(\beta) \quad (4.36)$$

Substituting Eq. (4.35) into (4.36), the expression for the average power  $P_{av}$  reduces to Eq. (4.8), and so it should.

**EXAMPLE 4.2** FM Spectrum for Varying Amplitude and Frequency of Sinusoidal Modulating Wave

In this example, we wish to investigate the ways in which variations in the amplitude and frequency of a sinusoidal modulating wave affect the spectrum of the FM wave. Consider first the case when the frequency of the modulating wave is fixed, but its amplitude is varied, producing a corresponding variation in the frequency deviation  $\Delta f$ . Thus, keeping the modulation frequency  $f_m$  fixed, we find that the amplitude spectrum of the resulting FM wave is as shown plotted in Fig. 4.7 for  $\beta = 1, 2$ , and  $5$ . In this diagram, we have normalized the spectrum with respect to the unmodulated carrier amplitude.

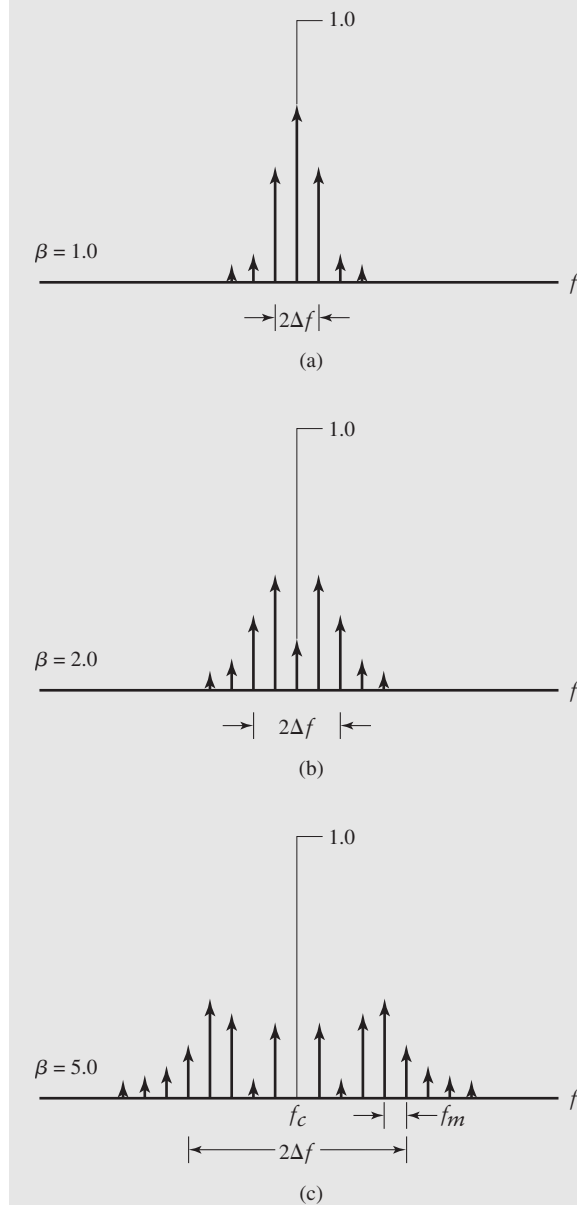


**FIGURE 4.7** Discrete amplitude spectra of an FM wave, normalized with respect to the unmodulated carrier amplitude, for the case of sinusoidal modulation of fixed frequency and varying amplitude. Only the spectra for positive frequencies are shown.

Consider next the case when the amplitude of the modulating wave is fixed; that is, the frequency deviation  $\Delta f$  is maintained constant, and the modulation frequency  $f_m$  is varied. In this second case, we find that the amplitude spectrum of the resulting FM wave is as shown plotted in Fig. 4.8 for  $\beta = 1, 2$ , and  $5$ . We now see that when  $\Delta f$  is fixed and  $\beta$  is increased, we have an increasing number of spectral lines crowding into the fixed frequency interval  $f_c - \Delta f < |f| < f_c + \Delta f$ . That is, when  $\beta$  approaches infinity, the bandwidth of the FM wave approaches the limiting value of  $2\Delta f$ , which is an important point to keep in mind.

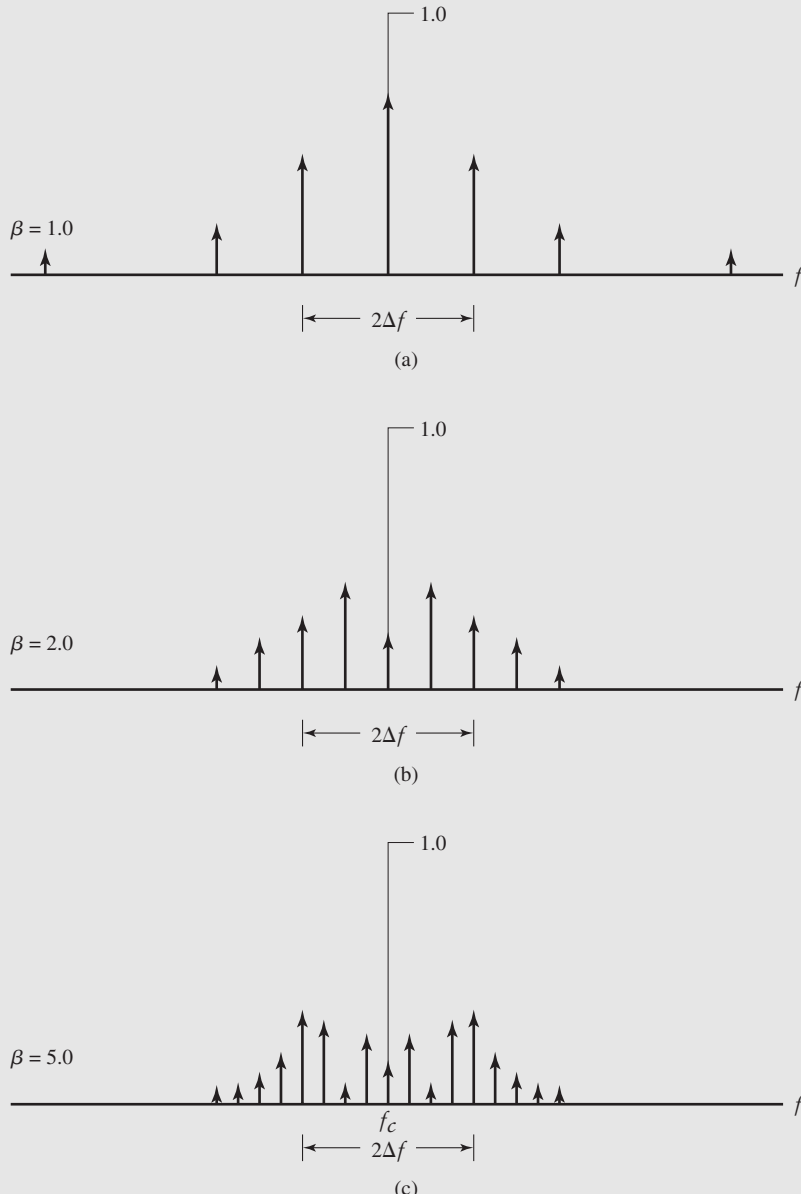


**FIGURE 4.8** Discrete amplitude spectra of an FM wave, normalized with respect to the unmodulated carrier amplitude, for the case of sinusoidal modulation of varying frequency and fixed amplitude. Only the spectra for positive frequencies are shown.

## 4.6 Transmission Bandwidth of FM Waves

### ■ CARSON'S RULE

In theory, an FM wave contains an infinite number of side-frequencies so that the bandwidth required to transmit such a modulated wave is similarly infinite in extent. In practice, however, we find that the FM wave is *effectively limited to a finite number of significant side-frequencies compatible with a specified amount of distortion*. We may therefore build on this idea to specify an effective bandwidth required for the transmission of an FM wave. Consider first the case of an FM wave generated by a single-tone modulating wave of frequency  $f_m$ . In such an FM wave, the side-frequencies that are separated from the carrier frequency  $f_c$  by an amount greater than the frequency deviation  $\Delta f$  decrease rapidly toward zero, so that the bandwidth always exceeds the total frequency excursion, but nevertheless is limited. Specifically, we may identify two limiting cases:

1. For large values of the modulation index  $\beta$ , the bandwidth approaches, and is only slightly greater than the total frequency excursion  $2\Delta f$ , as illustrated in Fig. 4.8(c).
2. For small values of the modulation index  $\beta$ , the spectrum of the FM wave is effectively limited to the carrier frequency  $f_c$  and one pair of side-frequencies at  $f_c \pm f_m$ , so that the bandwidth approaches  $2f_m$ , as illustrated in Section 4.4.

In light of these two limiting scenarios, we may define an approximate rule for the transmission bandwidth of an FM wave generated by a single-tone modulating wave of frequency  $f_m$  as

$$B_T \approx 2\Delta f + 2f_m = 2\Delta f \left(1 + \frac{1}{\beta}\right) \quad (4.37)$$

This simple empirical relation is known as *Carson's rule*.

### ■ UNIVERSAL CURVE FOR FM TRANSMISSION BANDWIDTH

Carson's rule is simple to use, but, unfortunately, it does not always provide a good estimate of the bandwidth requirements of communication systems using wideband frequency modulation. For a more accurate assessment of FM bandwidth, we may use a definition based on retaining the maximum number of significant side frequencies whose amplitudes are all greater than some selected value. A convenient choice for this value is one percent of the unmodulated carrier amplitude. We may thus define *the transmission bandwidth of an FM wave as the separation between the two frequencies beyond which none of the side frequencies is greater than one percent of the carrier amplitude obtained when the modulation is removed*. That is, we define the transmission bandwidth as  $2n_{\max}f_m$ , where  $f_m$  is the modulation frequency and  $n_{\max}$  is the largest value of the integer  $n$  that satisfies the requirement  $|J_n(\beta)| > 0.01$ . The value of  $n_{\max}$  varies with the modulation index  $\beta$  and can be determined readily from tabulated values of the Bessel function  $J_n(\beta)$ . Table 4.2 shows the total number of significant side-frequencies (including both the upper and lower side-frequencies) for different values of  $\beta$ , calculated on the one percent basis. The transmission bandwidth  $B_T$  calculated using this procedure can be presented in the form of a universal curve by normalizing it with respect to the frequency deviation  $\Delta f$  and then plotting it versus  $\beta$ . This curve is shown in Fig. 4.9, which is drawn as a best fit through the set of points obtained by using Table 4.2. In Fig. 4.9, we note that as the modulation index  $\beta$  is increased, the bandwidth occupied by the significant side-frequencies drops toward that

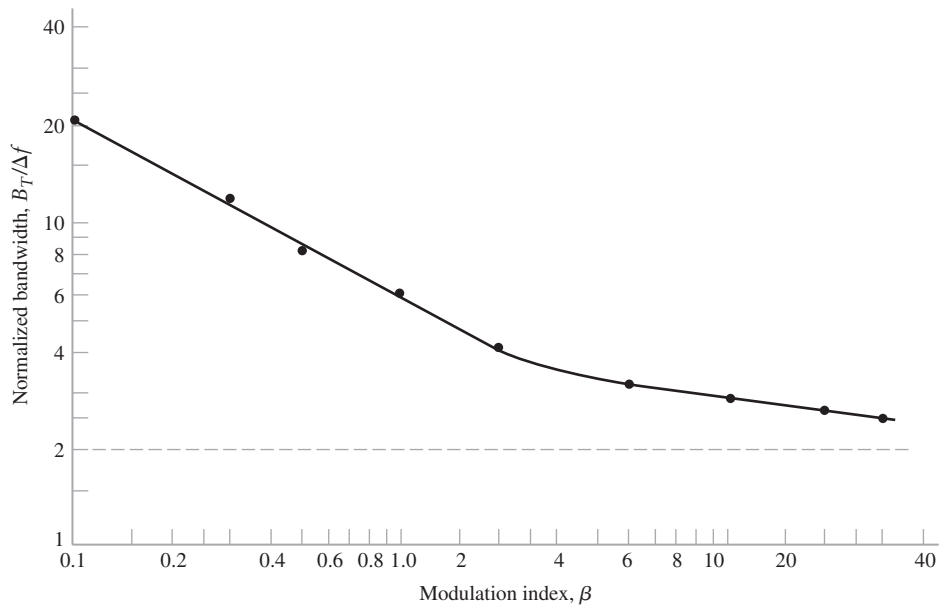


**FIGURE 4.9** Universal curve for evaluating the one percent bandwidth of an FM wave.

value over which the carrier frequency actually deviates. This means that the small values of modulation index  $\beta$  are relatively more extravagant in transmission bandwidth than the larger values of  $\beta$ .

### ■ ARBITRARY MODULATING WAVE

Consider next the more general case of an arbitrary modulating wave  $m(t)$  with its highest frequency component denoted by  $W$ ; that is,  $W$  denotes the message bandwidth. We now have a more difficult situation to deal with. One way of tackling it is to seek a *worst-case* evaluation of the transmission bandwidth. Specifically, the bandwidth required to transmit an FM wave generated by an arbitrary modulating wave is based on a worst-case tone-modulation analysis. We first determine the so-called *deviation ratio*  $D$ , defined as the ratio of the frequency deviation  $\Delta f$ , which corresponds to the maximum possible amplitude of

**TABLE 4.2 Number of Significant Side-Frequencies of a Wide-Band FM Signal for Varying Modulation Index**

Modulation Index $\beta$	Number of Significant Side-Frequencies $2n_{\max}$
0.1	2
0.3	4
0.5	4
1.0	6
2.0	8
5.0	16
10.0	28
20.0	50
30.0	70

the modulation wave  $m(t)$ , to the highest modulation frequency  $W$ . These conditions represent the extreme cases possible. We may thus formally write

$$D = \frac{\Delta f}{W} \quad (4.38)$$

The deviation ratio  $D$  plays the same role for nonsinusoidal modulation that the modulation index  $\beta$  plays for the case of sinusoidal modulation. Hence, replacing  $\beta$  by  $D$  and replacing  $f_m$  with  $W$ , we may generalize Eq. (4.37) as follows:

$$B_T = 2(\Delta f + W) \quad (4.39)$$

Hereafter, we refer to Eq. (4.39) as the *generalized Carson rule* for the transmission bandwidth of an arbitrary FM signal. In a similar way, we may generalize the universal curve of Fig. 4.9 to obtain a value for the transmission bandwidth of the FM signal. From a practical viewpoint, the generalized Carson rule somewhat underestimates the bandwidth requirement of an FM system, whereas, in a corresponding way, using the universal curve of Fig. 4.9 yields a somewhat conservative result. Thus, the choice of a transmission bandwidth that lies between the bounds provided by these two rules of thumb is acceptable for most practical purposes.

#### EXAMPLE 4.3 Commercial FM Broadcasting

In North America, the maximum value of frequency deviation  $\Delta f$  is fixed at 75 kHz for commercial FM broadcasting by radio. If we take the modulation frequency  $W = 15$  kHz, which is typically the “maximum” audio frequency of interest in FM transmission, we find that the corresponding value of the deviation ratio is [using Eq. (4.38)]

$$D = \frac{75}{15} = 5$$

Using the values  $\Delta f = 75$  kHz and  $D = 5$  in the generalized Carson rule of Eq. (4.39), we find that the approximate value of the transmission bandwidth of the FM signal is obtained as

$$B_T = 2(75 + 15) = 180 \text{ kHz}$$

On the other hand, use of the universal curve of Fig. 4.9 gives the transmission bandwidth of the FM signal to be

$$B_T = 3.2 \Delta f = 3.2 \times 75 = 240 \text{ kHz}$$

In this example, Carson’s rule underestimates the transmission bandwidth by 25 percent compared with the result of using the universal curve of Fig. 4.9.

## 4.7 Generation of FM Waves

According to Eq. (4.5), the instantaneous frequency  $f_i(t)$  of an FM wave varies linearly with the message signal  $m(t)$ . For the design of a *frequency modulator*, we therefore need a device that produces an output signal whose instantaneous frequency is sensitive to variations in the amplitude of an input signal in a linear manner.

There are two basic methods of generating frequency-modulated waves, one direct and the other indirect.

#### ■ DIRECT METHOD

The *direct method* uses a sinusoidal oscillator, with one of the reactive elements (e.g., capacitive element) in the tank circuit of the oscillator being directly controllable by the message

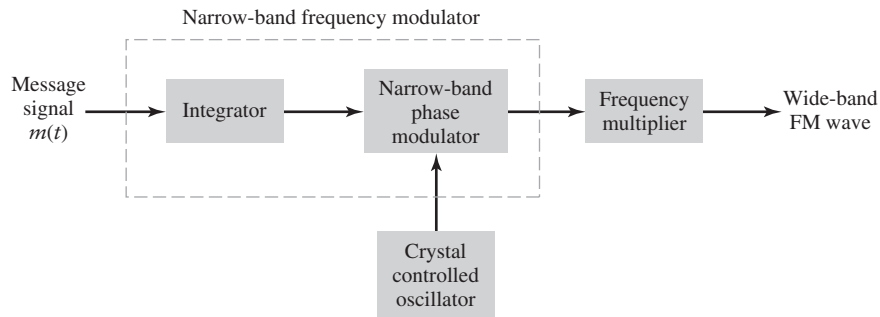


**FIGURE 4.10** Block diagram of the indirect method of generating a wide-band FM wave.

signal. In conceptual terms, the direct method is therefore straightforward to implement. Moreover, it is capable of providing large frequency deviations. However, a serious limitation of the direct method is the tendency for the carrier frequency to drift, which is usually unacceptable for commercial radio applications. To overcome this limitation, frequency stabilization of the FM generator is required, which is realized through the use of *feedback* around the oscillator; see Problem 4.15 for the description of one such procedure. Although the oscillator may itself be simple to build, the use of frequency stabilization adds system complexity to the design of the frequency modulator.

### ■ INDIRECT METHOD: ARMSTRONG MODULATOR

In the *indirect method*, on the other hand, the message signal is first used to produce a *narrow-band FM*, which is followed by *frequency multiplication* to increase the frequency deviation to the desired level. In this second method, the carrier-frequency stability problem is alleviated by using a highly stable oscillator (e.g., crystal oscillator) in the narrow-band FM generation; this modulation scheme is called the *Armstrong wide-band frequency modulator*, in recognition of its inventor.

A simplified block diagram of this indirect FM system is shown in Fig. 4.10. The message signal  $m(t)$  is first integrated and then used to phase-modulate a crystal-controlled oscillator; the use of crystal control provides *frequency stability*. In order to minimize the distortion inherent in the phase modulator, the maximum phase deviation or modulation index  $\beta$  is purposely kept small, thereby resulting in a narrow-band FM wave; for the implementation of the narrow-band phase modulator, we may use the arrangement described in Fig. 4.4. The narrow-band FM wave is next multiplied in frequency by means of a frequency multiplier so as to produce the desired wide-band FM wave.

A *frequency multiplier* consists of a *memoryless* nonlinear device followed by a band-pass filter, as shown in Fig. 4.11. The implication of the nonlinear device being memoryless is that it has no energy-storage elements. The input-output relation of such a device may be expressed in the general form

$$v(t) = a_1 s(t) + a_1 s^2(t) + \cdots + a_n s^n(t) \quad (4.40)$$

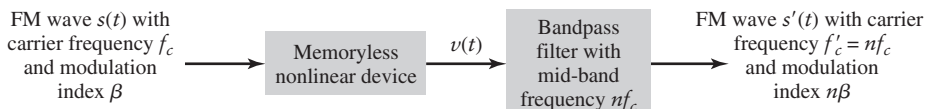


**FIGURE 4.11** Block diagram of frequency multiplier.

where  $a_1, a_2, \dots, a_n$  are coefficients determined by the operating point of the device, and  $n$  is the *highest order of nonlinearity*. In other words, the memoryless nonlinear device is an  $n$ th power-law device.

The input  $s(t)$  is an FM wave defined by

$$s(t) = A_c \cos \left[ 2\pi f_c t + 2\pi k_f \int_0^t m(\tau) d\tau \right] \quad (4.41)$$

where the instantaneous frequency is

$$f_i(t) = f_c + k_f m(t) \quad (4.42)$$

Suppose that (1) the mid-band frequency of the bandpass filter in Fig. 4.11 is set equal to  $nf_c$ , where  $f_c$  is the carrier frequency of the incoming FM wave  $s(t)$ , and (2) the bandpass filter is designed to have a bandwidth equal to  $n$  times the transmission bandwidth of  $s(t)$ . In Problem 4.24 dealing with nonlinear effects in FM systems, we address the spectral contributions of such nonlinear terms as the second- and third-order terms in the input-output relation of Eq. (4.40). For now it suffices to say that after bandpass filtering of the nonlinear device's output  $v(t)$ , we have a new FM wave defined by

$$s'(t) = A_c \cos \left[ 2\pi f'_c t + 2\pi k'_f \int_0^t m(\tau) d\tau \right] \quad (4.43)$$

whose instantaneous frequency is

$$f'_i(t) = nf_c + nk_f m(t) \quad (4.44)$$

Thus, comparing Eq. (4.44) with (4.42), we see that the nonlinear subsystem of Fig. 4.11 acts as a frequency multiplier with  $f'_c = nf_c$  and  $k'_f = nk_f$ . The frequency multiplication ratio  $n$  is determined by the highest power  $n$  in the input-output relation of Eq. (4.40), characterizing the memoryless nonlinear device.

## 4.8 Demodulation of FM Signals

*Frequency demodulation* is the process by means of which the original message signal is recovered from an incoming FM wave. In other words, frequency demodulation is the *inverse* of frequency modulation. With the frequency modulator being a device that produces an output signal whose instantaneous frequency varies linearly with the amplitude of the input message signal, it follows that for frequency demodulation we need a device whose output amplitude is sensitive to variations in the instantaneous frequency of the input FM wave in a linear manner too.

In what follows, we describe two devices for frequency demodulation. One device, called a frequency discriminator, relies on slope detection followed by envelope detection. The other device, called a phase-locked loop, performs frequency demodulation in a somewhat indirect manner.

### ■ FREQUENCY DISCRIMINATOR

Recall that the FM signal is given by

$$s(t) = A_c \cos \left( 2\pi f_c t + 2\pi k_f \int_0^t m(\tau) d\tau \right)$$

which is Eq. (4.41), reproduced here for convenience of presentation. The question to be addressed is: how do we recover the message signal  $m(t)$  from the modulated signal  $s(t)$ ? We can motivate the formulation of a receiver for doing this recovery by noting that if we take the derivative of Eq. (4.44) with respect to time, then we obtain

$$\frac{ds(t)}{dt} = -2\pi A_c [f_c + k_f m(t)] \sin\left(2\pi f_c t + 2\pi k_f \int_0^t m(\tau) d\tau\right) \quad (4.45)$$

Inspecting Eq. (4.45), we observe that the derivative is a band-pass signal with amplitude modulation defined by the multiplying term  $[f_c + k_f m(t)]$ . Consequently, if  $f_c$  is large enough such that the carrier is not overmodulated, then we can recover the message signal  $m(t)$  with an envelope detector in a manner similar to that described for AM signals in Chapter 3. This idea provides the motivation for the *frequency discriminator*, which is basically a demodulator that consists of a differentiator followed by an envelope detector.

However, there are practical issues related to implementation of the discriminator as just described—particularly, the differentiator. In Chapter 2, we showed that differentiation corresponds to a linear transfer function in the frequency domain; that is,

$$\frac{d}{dt} \rightleftharpoons j2\pi f \quad (4.46)$$

where, as usual,  $\rightleftharpoons$  implies a Fourier-transform relationship. In practical terms, it is difficult to construct a circuit that has a transfer function equivalent to the right-hand side of Eq. (4.46) for all frequencies. Instead, we construct a circuit that approximates this transfer function over the band-pass signal bandwidth—in particular, for  $f_c - (B_T/2) \leq |f| \leq f_c + (B_T/2)$ , where  $B_T$  is the transmission bandwidth of the incoming FM signal  $s(t)$ . A typical transfer characteristic that satisfies this requirement is described by

$$H_1(f) = \begin{cases} j2\pi[f - (f_c - B_T/2)], & f_c - (B_T/2) \leq |f| \leq f_c + (B_T/2) \\ 0, & \text{otherwise} \end{cases} \quad (4.47)$$

The transfer characteristic of this so-called *slope circuit* is illustrated in Fig. 4.12 for positive frequencies. A practical slope circuit would have a nonunity gain associated with the slope; but, to simplify matters, we assume that it has unity gain without loss of generality. The circuit is also not required to have zero response outside the transmission bandwidth, provided that the circuit is preceded by a band-pass filter centered on  $f_c$  with bandwidth  $B_T$ .

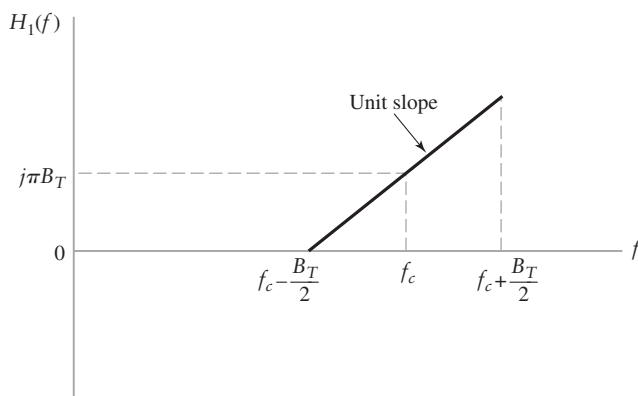


**FIGURE 4.12** Frequency response of an ideal slope circuit.

It is simplest to proceed with a *complex baseband representation* of the signal processing performed by the discriminator. Specifically, following the theory of this representation developed in Chapter 3, we find that the complex envelope of the FM signal  $s(t)$  (reproduced at the bottom of page 174) is

$$\tilde{s}(t) = A_c \exp\left(j2\pi k_f \int_0^t m(\tau) d\tau\right) \quad (4.48)$$

the applicability of which requires that the carrier frequency  $f_c$  be large compared to  $B_T$ . Correspondingly, we may express the complex baseband filter (i.e., slope circuit) corresponding to Eq. (4.48) as

$$\tilde{H}_1(f) = \begin{cases} j2\pi[f + (B_T/2)], & -B_T/2 \leq f \leq B_T/2 \\ 0, & \text{otherwise} \end{cases} \quad (4.49)$$

Let  $\tilde{s}_1(t)$  denote the complex envelope of the response of the slope circuit due to  $\tilde{s}(t)$ . Then, according to the band-pass to low-pass transformation described in Chapter 3, we may express the Fourier transform of  $\tilde{s}_1(t)$  as

$$\begin{aligned} \tilde{S}_1(f) &= \frac{1}{2} \tilde{H}_1(f) \tilde{S}(f) \\ &= \begin{cases} j\pi\left(f + \frac{1}{2}B_T\right)\tilde{S}(f), & -\frac{1}{2}B_T \leq f \leq \frac{1}{2}B_T \\ 0, & \text{elsewhere} \end{cases} \end{aligned} \quad (4.50)$$

where  $\tilde{S}(f)$  is the Fourier transform of  $\tilde{s}(t)$ . The reason for introducing the multiplying factor 1/2 in the first line of Eq. (4.50) was delineated in Chapter 3. To determine  $\tilde{s}_1(t)$ , which is the inverse of  $\tilde{S}_1(f)$ , we invoke two pertinent properties of the Fourier transform, as outlined here (see Chapter 2):

1. Multiplication of the Fourier transform  $\tilde{S}(f)$  by  $j2\pi f$  is equivalent to differentiating the inverse Fourier transform  $\tilde{s}(t)$  in accordance with Property 9 described in Eq. (2.33), as shown by

$$\frac{d}{dt}\tilde{s}(t) \iff j2\pi f\tilde{S}(f)$$

2. Application of the linearity property (i.e., Eq. (2.14)) to the nonzero part of  $\tilde{S}_1(f)$  yields

$$\tilde{s}_1(t) = \frac{1}{2} \frac{d}{dt}\tilde{s}(t) + \frac{1}{2}j\pi B_T \tilde{s}(t) \quad (4.51)$$

Substituting Eq. (4.48) into (4.51), we get

$$\tilde{s}_1(t) = \frac{1}{2}j\pi A_c B_T \left[ 1 + \left( \frac{2k_f}{B_T} \right) m(t) \right] \exp\left(j2\pi k_f \int_0^t m(\tau) d\tau\right) \quad (4.52)$$

Finally, the actual response of the slope circuit due to the FM wave  $s(t)$  is given by<sup>1</sup>

---

<sup>1</sup>Note that the first line of Eq. (4.53) on page 177 is a repeat of Eq. (3.43) in Chapter 3, which deals with the relationship between a modulated signal  $s(t)$  and its complex representation  $\tilde{s}(t)$ .

$$\begin{aligned}s_1(t) &= \operatorname{Re}[\tilde{s}_1(t) \exp(j2\pi f_c t)] \\ &= \frac{1}{2}\pi A_c B_T \left[ 1 + \left( \frac{2k_f}{B_T} \right) m(t) \right] \cos \left( 2\pi f_c t + 2\pi k_f \int_0^t m(\tau) d\tau + \frac{\pi}{2} \right)\end{aligned}\quad (4.53)$$

The next functional block to be considered is the envelope detector, which is fed by  $s_1(t)$ . From Eq. (4.53), we see that  $s_1(t)$  is a *hybrid modulated wave*, exhibiting both amplitude modulation and frequency modulation of the message signal  $m(t)$ . Provided that we maintain the extent of amplitude modulation, namely,

$$\left( \frac{2k_f}{B_T} \right) |m(t)|_{\max} < 1, \quad \text{for all } t$$

then the envelope detector recovers the message signal  $m(t)$ , except for a bias. Specifically, under ideal conditions, the output of the envelope detector is given by

$$v_1(t) = \frac{1}{2}\pi A_c B_T \left[ 1 + \left( \frac{2k_f}{B_T} \right) m(t) \right] \quad (4.54)$$

The bias in  $v_1(t)$  is defined by the constant term in Eq. (4.54)—namely,  $\pi A_c B_T / 2$ .

To remove the bias, we may use a second slope circuit followed by an envelope detector of its own. This time, however, we design the slope circuit so as to have a negative slope. On this basis, we infer from Eq. (4.54) that the output of this second configuration is given by

$$v_2(t) = \frac{1}{2}\pi A_c B_T \left[ 1 - \left( \frac{2k_f}{B_T} \right) m(t) \right] \quad (4.55)$$

Accordingly, subtracting Eq. (4.55) from Eq. (4.54), we obtain an overall output that is *bias-free*, as shown by

$$\begin{aligned}\nu(t) &= v_1(t) - v_2(t) \\ &= cm(t)\end{aligned}\quad (4.56)$$

where  $c$  is a constant.

In light of Eqs. (4.54) to (4.56), we may now construct the block diagram of Fig. 4.13 for the ideal frequency discriminator whose composition is as follows:

- The upper path of the figure pertains to Eq. (4.54).
- The lower path pertains to Eq. (4.55)
- The summing junction accounts for Eq. (4.56).

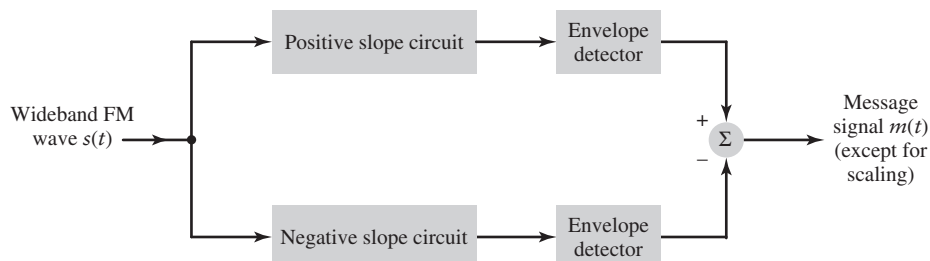


**FIGURE 4.13** Block diagram of balanced frequency discriminator.

This particular detection system is called a *balanced frequency discriminator*, where the term “balanced” refers to the fact that the two slope circuits of the system are related to each other in the manner described in Eqs. (4.54) and (4.55).

From a practical perspective, the challenge in implementing the balanced frequency discriminator<sup>2</sup> of Fig. 4.13 is how to build the two slope circuits so as to satisfy the design requirements of Eqs. (4.54) and (4.55).

### ■ PHASE-LOCKED LOOP

The *phase-locked loop* is a feedback system whose operation is closely linked to frequency modulation. It is commonly used for carrier synchronization, and indirect frequency demodulation. The latter application is the subject of interest here.

Basically, the phase-locked loop consists of three major components:

- ▶ *Voltage-controlled oscillator* (VCO), which performs frequency modulation on its own control signal.
- ▶ *Multiplier*, which multiplies an incoming FM wave by the output of the voltage-controlled oscillator.
- ▶ *Loop filter* of a low-pass kind, the function of which is to remove the high-frequency components contained in the multiplier’s output signal and thereby shape the overall frequency response of the system.

As shown in the block diagram of Fig. 4.14, these three components are connected together to form a *closed-loop feedback system*.

To demonstrate the operation of the phase-locked loop as a frequency demodulator, we assume that the VCO has been adjusted so that when the control signal (i.e., input) is zero, two conditions are satisfied:

1. The frequency of the VCO is set precisely at the unmodulated carrier frequency  $f_c$  of the incoming FM wave  $s(t)$ .
2. The VCO output has a 90-degree phase-shift with respect to the unmodulated carrier wave.

Suppose then that the incoming FM wave is defined by

$$s(t) = A_c \sin[2\pi f_c t + \phi_1(t)] \quad (4.57)$$

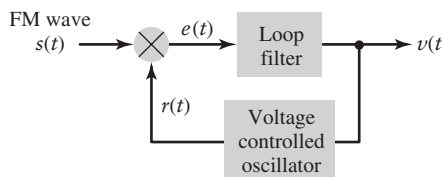


**FIGURE 4.14** Block diagram of the phase-locked loop.

<sup>2</sup>In Haykin (1994), pp. 178–180, a practical realization of the balanced frequency discriminator is described, using a pair of highly resonant RLC filters. The two filters are designed to have a high *Q-factor*. The *quality factor* or *Q-factor* of a resonant filter is a measure of how sharp the frequency response of the filter is; it is formally defined as  $2\pi$  times the ratio of the maximum energy stored in the filter to the energy dissipated in the filter, both being measured on a per cycle basis. For the application at hand, one filter is tuned to a frequency above the unmodulated carrier frequency  $f_c$  and the other filter is correspondingly tuned to a frequency below  $f_c$ . By making the *Q-factor* high, the linearity pertaining to the required portion of the total frequency response, centered on  $f_c$ , is determined by the separation of the two resonant frequencies.

where  $A_c$  is the carrier amplitude. By definition, the angle  $\phi_1(t)$  is related to the message signal  $m(t)$  by the integral

$$\phi_1(t) = 2\pi k_f \int_0^t m(\tau) d\tau \quad (4.58)$$

where  $k_f$  is the frequency-sensitivity factor of the frequency modulator responsible for the generation of  $s(t)$ . Correspondingly, in accordance with points (1) and (2) on page 178, we define the FM wave produced by the VCO as

$$r(t) = A_v \cos[2\pi f_c t + \phi_2(t)] \quad (4.59)$$

where  $A_v$  is the amplitude. The angle  $\phi_2(t)$  is related to the control signal  $v(t)$  of the VCO by the integral

$$\phi_2(t) = 2\pi k_v \int_0^t v(\tau) d\tau \quad (4.60)$$

where  $k_v$  is the frequency-sensitivity factor of the VCO.

The function of the feedback loop acting around the VCO is to adjust the angle  $\phi_2(t)$  so that it equals  $\phi_1(t)$ , thereby setting the stage for frequency demodulation. To delve more deeply into this function and how it can arise, we need to develop a model for the phase-locked loop, as described next.

To this end, we first note that multiplication of the incoming FM wave  $s(t)$  by the locally generated FM wave  $r(t)$  produces two components (except for the scaling factor 1/2):

1. A high-frequency component, which is defined by the *double-frequency term*—namely,

$$k_m A_c A_v \sin[4\pi f_c t + \phi_1(t) + \phi_2(t)]$$

where  $k_m$  is the *multiplier gain*.

2. A low-frequency component, which is defined by the *difference-frequency term*—namely,

$$k_m A_c A_v \sin[\phi_1(t) - \phi_2(t)]$$

► **Drill Problem 4.6** Using a well-known trigonometric identity involving the product of the sine of an angle and the cosine of another angle, demonstrate the two results just described under points 1 and 2. ◀

With the loop-filter designed to suppress the high-frequency components in the multiplier's output, we may henceforth discard the double-frequency term. Doing this, we may reduce the signal applied to the loop filter to

$$e(t) = k_m A_c A_v \sin[\phi_e(t)] \quad (4.61)$$

where  $\phi_e(t)$  is the *phase error* defined by

$$\begin{aligned} \phi_e(t) &= \phi_1(t) - \phi_2(t) \\ &= \phi_1(t) - 2\pi k_v \int_0^t v(\tau) d\tau \end{aligned} \quad (4.62)$$

When the phase error  $\phi_e(t)$  is zero, the phase-locked loop is said to be in *phase-lock*. It is said to be *near-phase-lock* when the phase error  $\phi_e(t)$  is small compared with one radian, under which condition we may use the approximation

$$\sin[\phi_e(t)] \approx \phi_e(t)$$

This approximation is accurate to within four percent provided that  $\phi_e(t)$  is less than 0.5 radian. Correspondingly, we may approximate the error signal of Eq. (4.61) as

$$\begin{aligned} e(t) &\approx k_m A_c A_v \phi_e(t) \\ &= \frac{K_0}{k_v} \phi_e(t) \end{aligned} \quad (4.63)$$

where the new parameter

$$K_0 = k_m k_v A_c A_v \quad (4.64)$$

is called the *loop-gain parameter* of the phase-lock loop.

The error signal  $e(t)$  acts on the loop filter to produce the overall output  $v(t)$ . Let  $h(t)$  denote the impulse response of the loop filter. We may then relate  $v(t)$  to  $e(t)$  by the convolution integral

$$v(t) = \int_{-\infty}^{\infty} e(\tau) h(t - \tau) d\tau \quad (4.65)$$

Equations (4.62), (4.63), (4.65), and (4.60), in that order, constitute a *linearized feedback model* of the phase-locked loop. The model is depicted in Fig. 4.15(a) with the angle  $\phi_1(t)$  of the incoming FM wave  $s(t)$  acting as input and the loop filter's output  $v(t)$  acting as the overall output of the phase-locked loop.

From linear feedback theory, we recall the following important theorem:<sup>3</sup>

When the open-loop transfer function of a linear feedback system has a large magnitude compared with unity for all frequencies, the closed-loop transfer function of the system is effectively determined by the inverse of the transfer function of the feedback path.

Stated in another way, the closed-loop transfer function of the feedback system becomes essentially independent of the forward path.

From the linearized feedback model of Fig. 4.15(a), we observe three points pertinent to the problem at hand:

1. The feedback path is defined solely by the scaled integrator described in Eq. (4.60), which is the VCO's contribution to the model. Correspondingly, the inverse of this feedback path is described in the time domain by the *scaled differentiator*:

$$v(t) = \frac{1}{2\pi k_v} \left( \frac{d\phi_2(t)}{dt} \right) \quad (4.66)$$

2. The closed-loop time-domain behavior of the phase-locked loop is described by the overall output  $v(t)$  produced in response to the angle  $\phi_1(t)$  in the incoming FM wave  $s(t)$ .

---

<sup>3</sup>Consider the classic example of a *negative feedback amplifier*, which is made up of two components: an amplifier of gain  $\mu$  in the forward path and a network of gain  $\beta$  in the feedback path. The *closed-loop gain* of the amplifier is defined by

$$A = \frac{\mu}{1 + \mu\beta}$$

The product term  $\mu\beta$  in the denominator is the *open-loop gain* of the feedback amplifier. When  $\mu\beta$  is large compared with unity, the formula for  $A$  is effectively determined by the inverse of  $\beta$ , as shown by

$$A \approx \frac{1}{\beta}$$

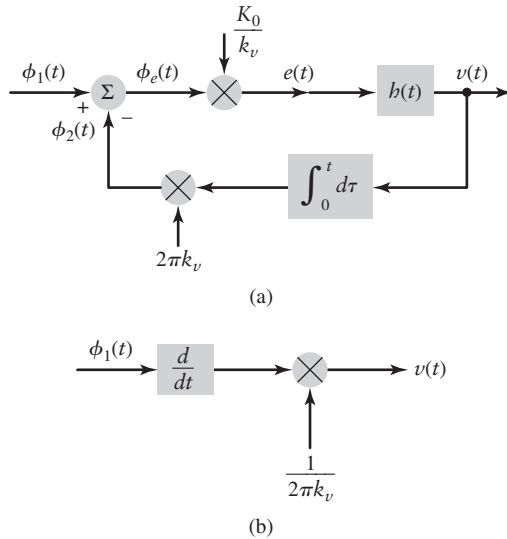


**FIGURE 4.15** (a) Linearized model of the phase-locked loop. (b) Approximate form of the model, assuming that the loop gain  $K_0$  is large compared with unity.

3. The magnitude of the open-loop transfer function of the phase-locked loop is controlled by the loop-gain parameter  $K_0$  of Eq. (4.64).

Assuming that the loop-gain parameter  $K_0$  is large compared with unity, application of the linear feedback theorem to the model of Fig. 4.15(a) teaches us that the closed-loop transfer function (i.e., closed-loop time-domain behavior) of the phase-locked loop is effectively determined by the inverse of the transfer function (i.e., time-domain behavior) of the feedback path. Accordingly, in light of the feedback theorem stated on page 180 and Eq. (4.66), we may relate the overall output  $v(t)$  to the input angle  $\phi_1(t)$  by the approximate formula

$$v(t) \approx \frac{1}{2\pi k_v} \left( \frac{d\phi_1(t)}{dt} \right) \quad (4.67)$$

Permitting  $K_0$  to assume a large value has the effect of making the phase error  $\phi_e(t)$  approach zero. Under this condition, we have  $\phi_1(t) \approx \phi_2(t)$  in accordance with the first line of Eq. (4.62). This condition of approximate equality provides the rationale for replacing  $\phi_2(t)$  with  $\phi_1(t)$  in Eq. (4.67).

In light of the approximate relationship described in Eq. (4.67), we may now simplify the linearized feedback model of Fig. 4.15(a) to the form shown in part (b) of the figure. Hence, substituting Eq. (4.58) into (4.67), we obtain

$$\begin{aligned} v(t) &\approx \frac{1}{2\pi k_v} \cdot \frac{d}{dt} \left( 2\pi k_f \int_0^t m(\tau) d\tau \right) \\ &= \frac{k_f}{k_v} m(t) \end{aligned} \quad (4.68)$$

Equation (4.68) states that when the system operates in the phase-lock mode or near phase lock and the loop-gain parameter  $K_0$  is large compared with unity, *frequency demodulation of the incoming FM wave  $s(t)$  is accomplished*; that is, the original message signal  $m(t)$  is recovered from  $s(t)$ , except for the scaling factor  $(k_f/k_v)$ .

An important feature of the phase-locked loop, acting as a frequency demodulator, is that the bandwidth of the incoming FM wave  $s(t)$  can be much wider than that of the

loop filter characterized by the transfer function  $H(f)$ —that is, the Fourier transform of the loop filter's impulse response  $h(t)$ . *The transfer function  $H(f)$  of the loop filter can and therefore should be restricted to the baseband* (i.e., the original frequency band occupied by the message signal). Then the control signal of the VCO—namely,  $v(t)$ —has the bandwidth of the baseband (message) signal  $m(t)$ , whereas the VCO output  $r(t)$  is a wide-band frequency-modulated wave whose instantaneous frequency *tracks* the variations in the instantaneous frequency of the incoming FM wave  $s(t)$  due to  $m(t)$ . Here we are merely restating the fact that the bandwidth of a wide-band FM wave is much larger than the bandwidth of the message signal responsible for its generation.

The *complexity* of the phase-locked loop is determined by the transfer function  $H(f)$  of the loop filter. The simplest form of a phase-locked loop is obtained by setting  $H(f) = 1$ ; that is, there is no loop filter, in which case the phase-locked loop is referred to as a *first-order phase-locked loop*. For higher order loops, the transfer function  $H(f)$  assumes a more complex frequency-dependent form.

A major limitation of a first-order phase-locked loop is that the loop-gain parameter  $K_0$  controls both the loop bandwidth as well as the hold-in frequency range of the loop. The *hold-in frequency range* refers to the range of frequencies for which the loop remains in a phase-locked condition with respect to the incoming FM wave. It is for this reason that despite its simplicity, a first-order phase-locked loop is seldom used in practice. Rather, the recommended procedure is to use a second-order phase-locked loop, the realization of which is satisfied by using a first-order loop filter; See Problem 4.25.

► **Drill Problem 4.7** Using the linearized model of Fig. 4.15(a), show that the model is approximately governed by the integro-differential equation

$$\frac{d\phi_e(t)}{dt} + 2\pi K_0 \int_{-\infty}^{\infty} \phi_e(\tau) h(t - \tau) d\tau \approx \frac{d\phi_1(t)}{dt}$$

Hence, derive the following two approximate results in the frequency domain:

$$(a) \Phi_e(f) \approx \frac{1}{1 + L(f)} \Phi_1(f)$$

$$(b) V(f) \approx \frac{jf}{k_v} \frac{L(f)}{1 + L(f)} \Phi_1(f)$$

where

$$L(f) = K_0 \frac{H(f)}{jf}$$

is the open-loop transfer function. Finally, show that when  $L(f)$  is large compared with unity for all frequencies inside the message band, the time-domain version of the formula in part (b) reduces to the approximate form in Eq. (4.68). ◀

## 4.9 Theme Example: FM Stereo Multiplexing

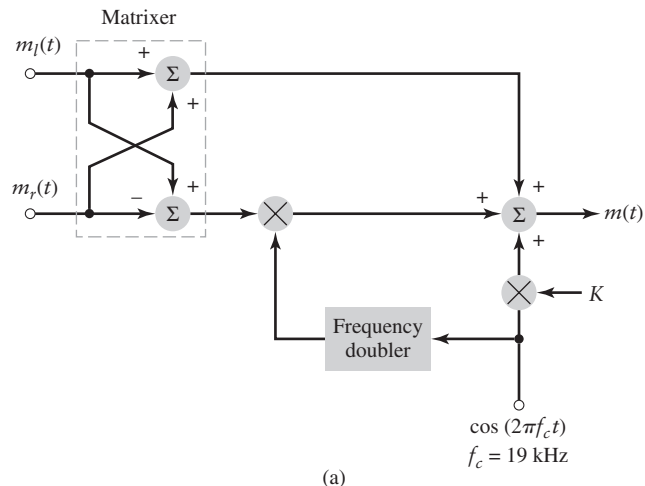
*Stereo multiplexing* is a form of frequency-division multiplexing (FDM) designed to transmit two separate signals via the same carrier. It is widely used in FM radio broadcasting to send two different elements of a program (e.g., two different sections of an orchestra, a vocalist and an accompanist) so as to give a *spatial* dimension to its perception by a listener at the receiving end.

The specification of standards for FM stereo transmission is influenced by two factors:

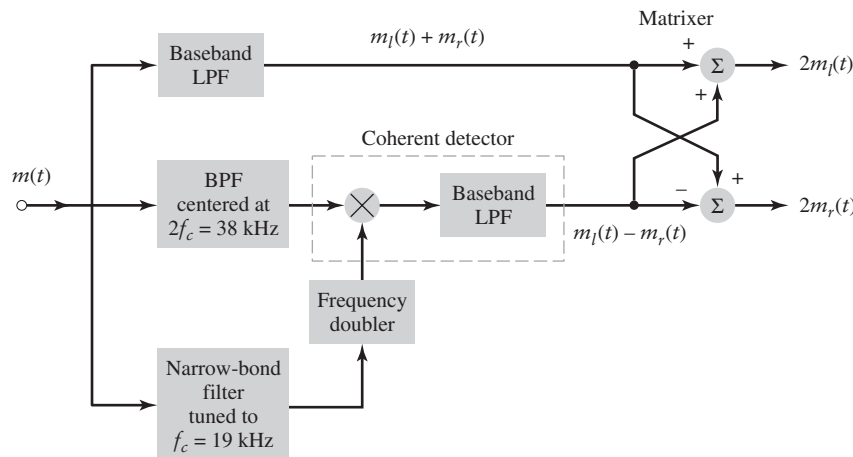
1. The transmission has to operate within the allocated FM broadcast channels.
2. It has to be compatible with monophonic radio receivers.

The first requirement sets the permissible frequency parameters, including frequency deviation. The second requirement constrains the way in which the transmitted signal is configured.

Figure 4.16(a) shows the block diagram of the multiplexing system used in an FM stereo transmitter. Let  $m_l(t)$  and  $m_r(t)$  denote the signals picked up by left-hand and right-hand microphones at the transmitting end of the system. They are applied to a simple *matrixer* that generates the *sum signal*,  $m_l(t) + m_r(t)$ , and the *difference signal*,  $m_l(t) - m_r(t)$ . The sum signal is left unprocessed in its baseband form; it is available for monophonic reception. The difference signal and a 38-kHz subcarrier (derived from a 19-kHz crystal oscillator by frequency doubling) are applied to a product modulator, thereby producing a DSB-SC modulated wave. In addition to the sum signal and this DSB-SC modulated wave, the multiplexed signal  $m(t)$  also includes a 19-kHz pilot to provide a reference



(a)



(b)

**FIGURE 4.16** (a) Multiplexer in transmitter of FM stereo. (b) Demultiplexer in receiver of FM stereo.

for the coherent detection of the difference signal at the stereo receiver. Thus in accordance with Fig. 4.16(a), the multiplexed signal is described by

$$m(t) = [m_l(t) + m_r(t)] + [m_l - m_r(t)] \cos(4\pi f_c t) + K \cos(2\pi f_c t) \quad (4.69)$$

where  $f_c = 19$  kHz, and  $K$  is the amplitude of the pilot tone. The multiplexed signal  $m(t)$  then frequency-modulates the main carrier to produce the transmitted signal, this frequency modulation is not shown in Fig. 4.16(a). The pilot is allotted between 8 and 10 percent of the peak frequency deviation; the amplitude  $K$  in Eq. (4.69) is chosen to satisfy this requirement.

At a stereo receiver, first of all the multiplexed signal  $m(t)$  is recovered by frequency demodulating the incoming FM wave. Then  $m(t)$  is applied to the *demultiplexing system* shown in Fig. 4.16(b). The individual components of the multiplexed signal  $m(t)$  are separated by the use of three appropriate filters. The recovered pilot (using a narrow-band filter tuned to 19 kHz) is frequency-doubled to produce the desired 38-kHz subcarrier. The availability of this subcarrier enables the *coherent detection* of the DSB-SC modulated wave, see the part of Fig. 4.16(b) inside the dashed rectangle. The difference signal  $m_l(t) - m_r(t)$  is thereby recovered. The baseband low-pass filter in the top path of Fig. 4.16(b) is designed to pass the sum signal,  $m_l(t) + m_r(t)$ . Finally, the simple *matrixer* reconstructs the original left-hand signal  $m_l(t)$  and right-hand signal  $m_r(t)$ , except for the scaling factor 2, and applies them to their respective speakers. FM stereophonic reception is thereby accomplished.

## 4.10 Summary and Discussion

In Chapter 3, we studied the underlying principles of the first family of continuous-wave (CW) modulation, based on amplitude modulation and its variants. In this chapter, we completed the study of the underlying principles of CW modulation, based on angle modulation.

Fundamentally, there are two kinds of angle modulation:

- ▶ Phase modulation (PM), where the instantaneous phase of the sinusoidal carrier wave is varied linearly with the message signal.
- ▶ Frequency modulation (FM), where the instantaneous frequency of the sinusoidal carrier wave is varied linearly with the message signal.

These two methods of modulation are closely related in that if we are given one of them, we can derive the other one. For this reason we focused much of the discussion on frequency modulation.

Frequency modulation (FM) is typified by the equation

$$s(t) = A_c \cos\left(2\pi f_c t + 2\pi k_f \int_0^t m(\tau) d\tau\right) \quad (4.70)$$

where  $m(t)$  is the message signal,  $A_c \cos(2\pi f_c t)$  is the sinusoidal carrier wave, and  $k_f$  is the frequency sensitivity of the modulator. Equation (4.70) is a repeat of Eq. (4.7), reproduced at this point merely for convenience of presentation.

Unlike amplitude modulation, from Eq. (4.70) we see that FM is a nonlinear modulation process. Accordingly, the spectral analysis of FM is more difficult than for AM. Nevertheless, by studying single-tone FM, we were able to develop a great deal of insight into the spectral properties of FM. In particular, we derived an empirical rule known as the generalized Carson rule for an approximate evaluation of the transmission bandwidth  $B_T$  of FM. According to this rule,  $B_T$  is controlled by a single parameter: the modulation index  $\beta$  for sinusoidal FM or the deviation ratio  $D$  for nonsinusoidal FM.

In FM, the carrier amplitude and therefore the transmitted average power is maintained constant. Herein lies the important advantage of FM over AM in combating the effects of noise

or interference at reception, an issue that we study in Chapter 9, after familiarizing ourselves with probability theory and random processes in Chapter 8. This advantage becomes increasingly more pronounced as the modulation index (deviation ratio) is increased, which has the effect of increasing the transmission bandwidth in a corresponding way. Thus, frequency modulation provides a practical method for the tradeoff of channel bandwidth for improved noise performance, which is not feasible with amplitude modulation.

One final comment is in order. Just as with amplitude modulation, the development of the angle modulation family has been motivated by its direct relevance to analog communications, but many aspects of this branch of modulation theory are equally applicable to digital communications. For example, if the message signal in Eq. (4.70) is restricted to levels of  $-1$  or  $+1$  representing binary 0 and binary symbol 1, respectively, then we have a basic form of digital modulation known as binary frequency-shift-keying (BFSK), discussed in Chapter 7.

## ADDITIONAL PROBLEMS

- 4.8 Sketch the PM and FM waves produced by the sawtooth wave shown in Fig. 4.17 as the source of modulation.

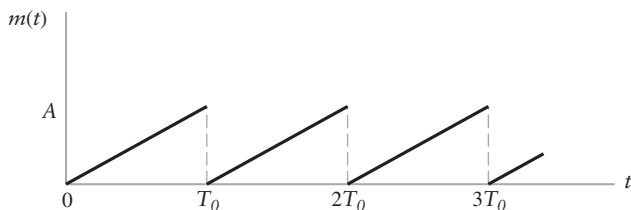


**FIGURE 4.17** Problem 4.8

- 4.9 In a *frequency-modulated radar* the instantaneous frequency of the transmitted carrier is varied as in Fig. 4.18. Such a signal is generated by frequency modulation with a periodic triangular modulating wave. The instantaneous frequency of the received echo signal is shown dashed in Fig. 4.18 where  $\tau$  is the round-trip delay time. The transmitted and received echo signals are applied to a mixer, and the difference frequency component is retained. Assuming that  $f_0\tau \ll 1$  for all  $\tau$ , determine the number of beat cycles at the mixer output, averaged over one second, in terms of the peak deviation  $\Delta f$  of the carrier frequency, the delay  $\tau$ , and the repetition frequency  $f_0$  of the transmitted signal. (The *beat* refers to a signal whose frequency is the difference between the frequencies of the two input signals.)

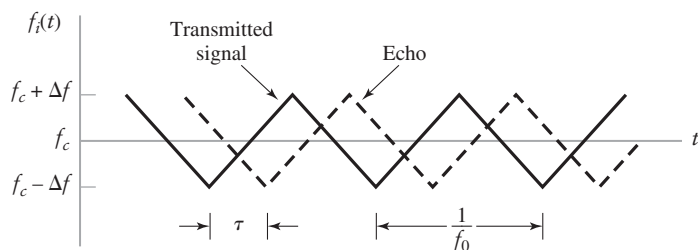


**FIGURE 4.18** Problem 4.9

- 4.10 Consider an interval  $\Delta t$  of an FM wave  $s(t) = A_c \cos[\theta(t)]$  such that  $\theta(t)$  satisfies the condition
- $$\theta(t + \Delta t) - \theta(t) = \pi$$

Hence, show that if  $\Delta t$  is sufficiently small, the instantaneous frequency of the FM wave inside this interval is approximately given by

$$f_i \approx \frac{1}{2\Delta t}$$

- 4.11 The sinusoidal modulating wave

$$m(t) = A_m \cos(2\pi f_m t)$$

is applied to a phase modulator with phase sensitivity  $k_p$ . The unmodulated carrier wave has frequency  $f_c$  and amplitude  $A_c$ . Determine the spectrum of the resulting phase-modulated wave, assuming that the maximum phase deviation  $\beta = k_p A_m$  does not exceed 0.3 radian.

- 4.12 A carrier wave is frequency-modulated using a sinusoidal signal of frequency  $f_m$  and amplitude  $A_m$ .
- (a) Determine the values of the modulation index  $\beta$  for which the carrier component of the FM wave is reduced to zero. For this calculation you may use the values of  $J_0(\beta)$  given in Appendix 3.
  - (b) In a certain experiment conducted with  $f_m = 1$  kHz and increasing  $A_m$  (starting from zero volt), it is found that the carrier component of the FM wave is reduced to zero for the first time when  $A_m = 2$  volts. What is the frequency sensitivity of the modulator? What is the value of  $A_m$  for which the carrier component is reduced to zero for the second time?
- 4.13 A carrier wave of frequency 100 MHz is frequency-modulated by a sinusoidal wave of amplitude 20 V and frequency 100 kHz. The frequency sensitivity of the modulator is 25 kHz/V.
- (a) Determine the approximate bandwidth of the FM wave, using Carson's rule.
  - (b) Determine the bandwidth obtained by transmitting only those side-frequencies with amplitudes that exceed one percent of the unmodulated carrier amplitude. Use the universal curve of Fig. 4.9 for this calculation.
  - (c) Repeat your calculations, assuming that the amplitude of the modulating wave is doubled.
  - (d) Repeat your calculations, assuming that the modulation frequency is doubled.
- 4.14 Consider a wide-band PM wave produced by the sinusoidal modulating wave  $A_m \cos(2\pi f_m t)$ , using a modulator with a phase sensitivity equal to  $k_p$  radians per volt.
- (a) Show that if the maximum phase deviation of the PM wave is large compared with one radian, the bandwidth of the PM wave varies linearly with the modulation frequency  $f_m$ .
  - (b) Compare this characteristic of a wide-band PM wave with that of a wide-band FM wave.
- 4.15 Figure 4.19 shows the block diagram of a closed-loop feedback system for the carrier-frequency stabilization of a wide-band frequency modulator. The voltage-controlled oscillator shown in the figure constitutes the frequency modulator. Using the ideas of mixing (i.e., frequency translation) (described in Chapter 3) and frequency discrimination (described in this chapter), discuss how the feedback system of Fig. 4.19 is capable of exploiting the frequency accuracy of the crystal oscillator to stabilize the voltage-controlled oscillator.

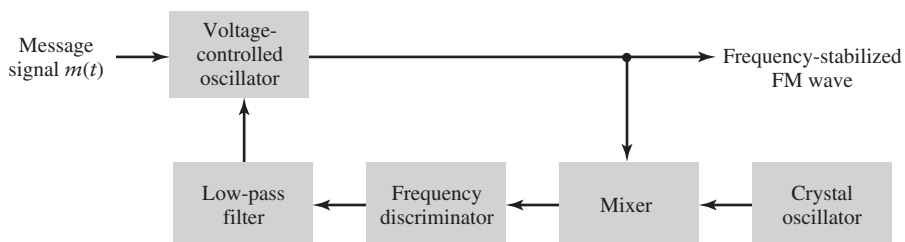


FIGURE 4.19 Problem 4.15

- 4.16 Consider the frequency demodulation scheme shown in Fig. 4.20 in which the incoming FM wave  $s(t)$  is passed through a delay line that produces a phase shift of  $-\pi/2$  radians at the carrier frequency  $f_c$ . The delay-line output is subtracted from  $s(t)$ , and the resulting composite wave is then envelope-detected. This demodulator finds application in demodulating FM waves at microwave frequencies. Assuming that

$$s(t) = A_c \cos[2\pi f_c t + \beta \sin(2\pi f_m t)]$$

analyze the operation of this demodulator when the modulation index  $\beta$  is less than unity and the delay  $T$  produced by the delay line is sufficiently small to justify making the approximations:

$$\cos(2\pi f_m T) \approx 1$$

and

$$\sin(2\pi f_m T) \approx 2\pi f_m T$$

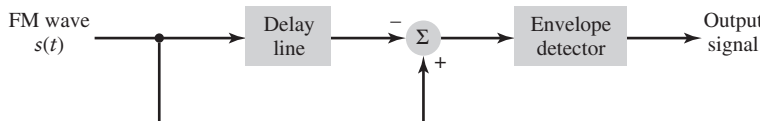


**FIGURE 4.20** Problem 4.16

- 4.17 Consider the following pair of modulating signals:

$$1. m_1(t) = \begin{cases} a_1 t + a_0, & t \geq 0 \\ 0, & t = 0 \end{cases}$$

$$2. m_2(t) = \begin{cases} b_2 t^2 + b_1 t + b_0, & t \geq 0 \\ 0, & t = 0 \end{cases}$$

where the  $as$  and the  $bs$  are constant parameters.

Signal 1 is applied to a frequency modulator, while signal 2 is applied to a phase modulator. Determine the conditions for which the outputs of these two angle modulators are exactly the same.

- 4.18 In this problem, we work on the specifications of a superheterodyne FM receiver listed in Table 3.2. In particular, given those specifications, do the following work:
- Determine the range of frequencies provided by the local oscillator of the receiver in order to accommodate the RF carrier range 88-108 MHz.
  - Determine the corresponding range of image frequencies.

## ADVANCED PROBLEMS

- 4.19 The instantaneous frequency of a sinusoidal wave is equal to  $f_c + \Delta f$  for  $|t| < T/2$  and  $f_c$  for  $|t| > T/2$ . Determine the spectrum of this frequency-modulated wave. Hint: Divide up the time interval of interest into three nonoverlapping regions:

$$(i) -\infty < t < -T/2$$

$$(ii) -T/2 \leq t \leq T/2$$

$$(iii) T/2 < t < \infty$$

- 4.20 Figure 4.21 shows the block diagram of a *real-time spectrum analyzer* working on the principle of frequency modulation. The given signal  $g(t)$  and a frequency-modulated signal  $s(t)$  are applied to a multiplier and the output  $g(t)s(t)$  is fed into a filter of impulse  $h(t)$ . The  $s(t)$  and  $h(t)$  are linear FM signals whose instantaneous frequencies vary at opposite rates, as shown by

$$s(t) = \cos(2\pi f_c t + \pi k t^2)$$

and

$$h(t) = \cos(2\pi f_c t - \pi k t^2)$$

where  $k$  is a constant. Show that the envelope of the filter output is proportional to the amplitude spectrum of the input signal  $g(t)$  with the product term  $kt$  playing the role of frequency  $f$ . *Hint:* Use the complex notations described in Section 3.8 for band-pass transmission.

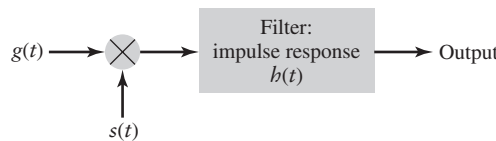


**FIGURE 4.21** Problem 4.20

- 4.21 Consider the modulated wave

$$s_1(t) = a(t) \cos \left[ 2\pi f_c t + 2\pi k_f \int_0^t m(\tau) d\tau \right]$$

where  $a(t)$  is a slowly varying envelope function,  $f_c$  is the carrier frequency,  $k_f$  is the frequency sensitivity, and  $m(t)$  is a message signal. The modulated wave  $s(t)$  is processed by a *band-pass limiter*, which consists of a hard limiter followed by a band-pass filter. The function of the band-pass limiter is to remove amplitude fluctuations due to  $a(t)$ . Specify the parameters of the band-pass filter component so as to produce the FM wave

$$s_2(t) = A \cos \left[ 2\pi f_c t + 2\pi k_f \int_0^t m(\tau) d\tau \right]$$

where  $A$  is a constant amplitude.

- 4.22 The analysis of distortion produced in an FM wave applied to a linear communication channel is of important practical interest. In this problem, we explore this analysis for the special case of a wide-band FM wave produced by a sinusoidal modulating wave. Let  $H(f)$  denote the transfer function of the channel. Starting with Eq. (4.15), do the following:
- (a) Derive an expression for the modulated signal produced at the channel output.
  - (b) Using the expression derived in part (a), discuss the distortion produced by the channel.
- 4.23 In Section 4.1, we pointed out that the instantaneous angle  $\theta_i(t)$  in angle-modulated waves can be varied in accordance with a message signal  $m(t)$  in an infinite number of ways. The treatment of angle modulation presented in this chapter focused on phase modulation and frequency modulation as two important candidates. The purpose of this problem is to explore other methods of producing angle-modulated waves.
- (a) Do this exploration by considering derivatives and integrals of the message signal  $m(t)$  as possible functions response for the modulation process.
  - (b) Would there be any practical benefits in these new methods of angle modulation? Elaborate on your answer.
- 4.24 In this problem, we explore how the use of FM can overcome nonlinear distortion. Consider a memoryless channel characterized by the nonlinear input-output relationship:

$$v_o(t) = a_1 v_i(t) + a_2 v_i^2(t) + a_3 v_i^3(t)$$

where  $v_i(t)$  is the input and  $v_o(t)$  is the output;  $a_1$ ,  $a_2$ , and  $a_3$  are fixed coefficients. The input is defined by the frequency-modulated signal

$$v_i(t) = A_c \cos \left( 2\pi f_c t + 2\pi k_f \int_0^t m(\tau) d\tau \right)$$

The message bandwidth is denoted by  $W$ , and the frequency deviation of the FM signal is  $\Delta f$ .

- (a) Evaluate the output  $v_o(t)$ .
- (b) Using the generalized Carson rule, show that if the carrier frequency satisfies the condition

$$f_c > 3 \Delta f + 2W$$

then the effect of nonlinear distortion can be removed by band-pass filtering.

- (c) Specify the mid-band frequency and bandwidth of the filter in part (b).

**4.25** Consider a *second-order phase-locked loop* using a loop filter with the transfer function

$$H(f) = 1 + \frac{a}{jf}$$

where  $a$  is a filter parameter.

- (a) Using this loop filter in the following formula (see part a of Drill Problem 4.7)

$$\Phi_e(f) = \frac{1}{1 + L(f)} \Phi_1(f)$$

show that the resulting Fourier transform of phase error  $\Phi_e(t)$  is expressed as

$$\Phi_e(f) = \left( \frac{(jf/f_n)^2}{1 + 2\zeta(jf/f_n) + (jf/f_n)^2} \right) \Phi_1(f)$$

where  $f_n$  is the *natural frequency* of the loop, and

$$\zeta = \sqrt{K_0/4a}$$

is its *damping factor*.

- (b) Hence, justify the statement that by appropriately choosing the parameters  $f_n$  and  $\zeta$ , it is possible for this phase-locked loop to overcome the limitations of the first-order version of the loop.

## CHAPTER 5

# PULSE MODULATION: TRANSITION FROM ANALOG TO DIGITAL COMMUNICATIONS

In *continuous-wave (CW) modulation*, which we studied in Chapters 3 and 4, some parameter of a sinusoidal carrier wave is varied continuously in accordance with the message signal. This is in direct contrast to pulse modulation, which we study in the present chapter. In *pulse modulation*, some parameter of a *pulse train* is varied in accordance with the message signal. In this context, we may distinguish two families of pulse modulation, *analog pulse modulation* and *digital pulse modulation*, depending on how the modulation is performed. In analog pulse modulation, a periodic pulse train is used as the carrier wave, and some characteristic feature of each pulse (e.g., amplitude, duration, or position) is varied in a continuous manner in accordance with the corresponding *sample* value of the message signal. Thus, in analog pulse modulation, information is transmitted basically in analog form, but the transmission takes place at discrete times. In digital pulse modulation, on the other hand, the message signal is represented in a form that is *discrete in both time and amplitude*, thereby permitting its transmission in digital form as a sequence of *coded pulses*. Simply put, digital pulse modulation has *no CW counterpart*.

The use of coded pulses for the transmission of analog information-bearing signals represents a basic ingredient in the application of digital communications. This chapter may therefore be viewed as the transition from analog to digital communications in our study of the principles of communication systems.

We begin the chapter by describing the sampling process, which is basic to all pulse modulation systems. This is followed by a discussion of pulse-amplitude modulation, which is the simplest form of analog pulse modulation. We then move on to describe the quantization process, the use of which distinguishes digital pulse modulation from analog pulse modulation. In particular, we describe three widely used forms of digital pulse modulation—namely, pulse-code modulation, delta modulation and differential pulse-code modulation.

The material presented in this chapter on pulse modulation teaches us the following two lessons:

- *Lesson 1: Given a strictly band-limited message signal, the sampling theorem embodies the conditions for a uniformly sampled version of the signal to preserve its information content.*

- **Lesson 2:** Analog pulse-modulation systems rely on the sampling process to maintain continuous amplitude representation of the message signal. In contrast, digital pulse-modulation systems use not only the sampling process but also the quantization process, which is non-reversible. Quantization provides a representation of the message signal that is discrete in both time and amplitude. In so doing, digital pulse modulation makes it possible to exploit the full power of digital signal-processing techniques.

## 5.1 Sampling Process

Much of the material on the representation of signals and systems covered up to this stage in the book has been devoted to signals and systems that are continuous in both time and frequency. At various points in Chapter 2, however, we did consider the representation of periodic signals. In particular, recall that the Fourier transform of a periodic signal with period  $T_0$  consists of an infinite sequence of delta functions occurring at integer multiples of the fundamental frequency  $f_0 = 1/T_0$ . We may therefore state that *making a signal periodic in the time domain has the effect of sampling the spectrum of the signal in the frequency domain*. We may go one step further by invoking the duality property of the Fourier transform, and state that *sampling a signal in the time domain has the effect of making the spectrum of the signal periodic in the frequency domain*. This latter issue is the subject of this section.

The *sampling process* is usually, but not exclusively, described in the time domain. As such, it is an operation that is basic to digital signal processing and digital communications. Through use of the sampling process, an analog signal is converted into a corresponding sequence of samples that are usually spaced uniformly in time. Clearly, for such a procedure to have practical utility, it is necessary that we choose the sampling rate properly, so that the sequence of samples uniquely defines the original analog signal. This is the essence of the sampling theorem, which is derived in what follows.

### ■ INSTANTANEOUS SAMPLING AND FREQUENCY-DOMAIN CONSEQUENCES

Consider an arbitrary signal  $g(t)$  of finite energy, which is specified for all time  $t$ . A segment of the signal  $g(t)$  is shown in Fig. 5.1(a). Suppose that we sample the signal  $g(t)$  instantaneously and at a uniform rate, once every  $T_s$  seconds. Consequently, we obtain an infinite sequence of samples spaced  $T_s$  seconds apart and denoted by  $\{g(nT_s)\}$ , where  $n$  takes on all possible integer values, both positive and negative. We refer to  $T_s$  as the *sampling period* or *sampling interval* and to its reciprocal  $f_s = 1/T_s$  as the *sampling rate*. This ideal form of sampling is called *instantaneous sampling*.

Let  $g_\delta(t)$  denote the signal obtained by individually weighting the elements of a periodic sequence of Dirac delta functions spaced  $T_s$  seconds apart by the sequence of numbers  $\{g(nT_s)\}$ , as shown by (see Fig. 5.1(b))

$$g_\delta(t) = \sum_{n=-\infty}^{\infty} g(nT_s) \delta(t - nT_s) \quad (5.1)$$

We refer to  $g_\delta(t)$  as the *instantaneously (ideal) sampled signal*. The term  $\delta(t - nT_s)$  represents a delta function positioned at time  $t = nT_s$ . From the definition of the delta function presented in Section 2.4, recall that such an idealized function has unit area. We may therefore view the multiplying factor  $g(nT_s)$  in Eq. (5.1) as a “mass” assigned to the delta function  $\delta(t - nT_s)$ . A delta function weighted in this manner is closely approximated by a rectangular pulse of duration  $\Delta t$  and amplitude  $g(nT_s)/\Delta t$ ; the smaller we make  $\Delta t$ , the better the approximation will be.

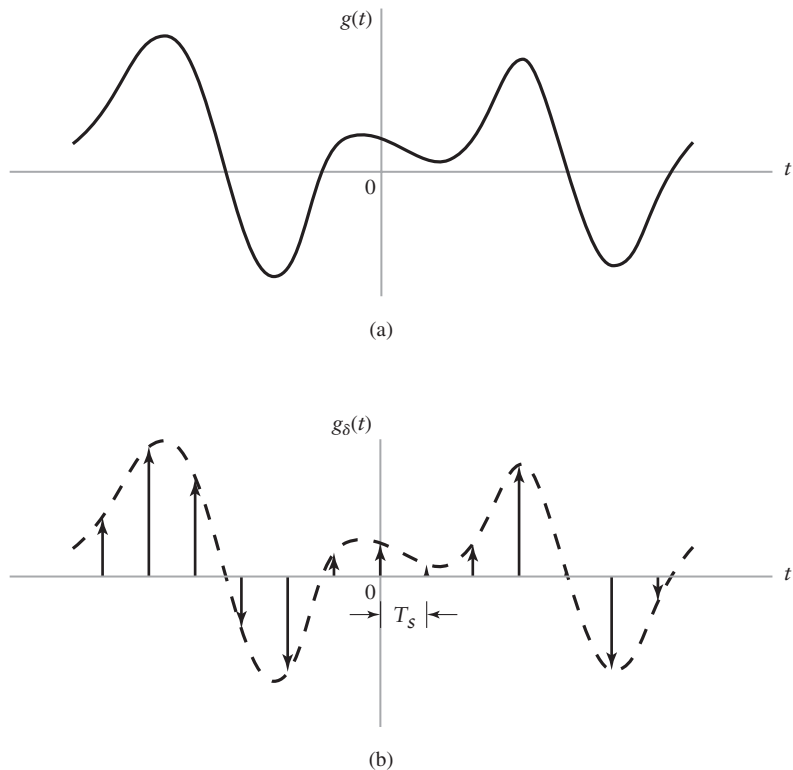


**FIGURE 5.1** Illustration of the sampling process. (a) Analog waveform  $g(t)$ . (b) Instantaneously sampled representation of  $g(t)$ .

The instantaneously sampled signal  $g_\delta(t)$  has a mathematical form similar to that of the Fourier transform of a periodic signal. This is readily established by comparing Eq. (5.1) for  $g_\delta(t)$  with the Fourier transform of a periodic signal given by the right-hand side of Eq. (2.88). This correspondence suggests that we may determine the Fourier transform of the sampled signal  $g_\delta(t)$  by invoking the duality property of the Fourier transform, the essence of which is embodied in Eq. (2.24). Indeed, by applying this property to the Fourier transform of Eq. (2.88) and the related Eq. (2.87), we may develop Table 5.1. The entries listed in the table describe the duality relationships between sampling in the time domain and its counterpart, sampling in the frequency domain.

#### ► Drill Problem 5.1

- Using the material presented in Section 2.5, justify the mathematical relationships listed at the bottom of the left-hand side of Table 5.1, which pertain to ideal sampling in the frequency domain.
- Applying the duality property of the Fourier transform to part (a), justify the mathematical relationships listed at the bottom of the right-hand side of this table, which pertain to ideal sampling in the time-domain. ◀

The motivation for formulating table 5.1 is to lay the mathematical groundwork for formulating the sampling theorem in the time-domain. To this end, we reproduce the relationships listed at the bottom of the right-hand side of the table in the form

$$\sum_{n=-\infty}^{\infty} g(nT_s)\delta(t - nT_s) \iff f_s \sum_{m=-\infty}^{\infty} G(f - mf_s) = \sum_{n=-\infty}^{\infty} g(nT_s) \exp(-j2\pi nT_s f) = G_\delta(f) \quad (5.2)$$

**TABLE 5.1 Time-Frequency Sampling-Duality Relationships**

<i>Ideal sampling in the frequency domain (Discrete spectrum); see Chapter 2</i>	<i>Ideal sampling in the time domain (Discrete-time function); see this chapter</i>
Fundamental period $T_0 = 1/f_0$	Sampling rate $f_s = 1/T_s$
Delta function $\delta(f - mf_0)$ , where $m = 0, \pm 1, \pm 2, \dots$	Delta function $\delta(t - nT_s)$ where $n = 0, \pm 1, \pm 2, \dots$
Periodicity in the time-domain	Periodicity in the frequency domain
Time-limited function	Band-limited spectrum
$T_0 \sum_{m=-\infty}^{\infty} g(t - mT_0) = \sum_{n=-\infty}^{\infty} G(nf_0) e^{j2\pi nf_0 t}$ $\Downarrow$ $\sum_{n=-\infty}^{\infty} G(nf_0) \delta(f - nf_0)$	$\sum_{n=-\infty}^{\infty} g(nT_s) \delta(t - nT_s)$ $\Downarrow$ $\sum_{n=-\infty}^{\infty} g(nT_s) e^{-j2\pi nT_s f} = f_s \sum_{m=-\infty}^{\infty} G(f - mf_s)$

where  $G(f)$  is the Fourier transform of the original signal  $g(t)$ , and  $f_s = 1/T_s$  is the sampling rate. In words, Eq. (5.2) states that *the process of uniformly sampling a continuous-time signal of finite energy results in a periodic spectrum with a repetition frequency equal to the sampling rate*.

## ■ SAMPLING THEOREM

The relations of Eq. (5.2) apply to any continuous-time signal  $g(t)$  of finite energy. Suppose, however, that the signal  $g(t)$  is *strictly band-limited*, with no frequency components higher than  $W$  hertz. That is, the Fourier transform  $G(f)$  of the signal  $g(t)$  has the property that  $G(f) = 0$  for  $|f| \geq W$ , as illustrated in Fig. 5.2(a); the shape of the spectrum shown in this figure is intended for the purpose of illustration only. Suppose also that we choose the sampling period  $T_s = 1/2W$ , which, as we shall see, is the maximum permissible value. Then the corresponding spectrum  $G_\delta(f)$  of the sampled signal  $g_\delta(t)$  is as shown in Fig. 5.2(b). Putting  $T_s = 1/2W$  in Eq. (5.2) and using  $G_\delta(f)$  to denote the Fourier transform of  $g_\delta(t)$ , we may write

$$G_\delta(f) = \sum_{n=-\infty}^{\infty} g\left(\frac{n}{2W}\right) \exp\left(-j\frac{\pi n f}{W}\right) \quad (5.3)$$

Equation (5.3) defines the Fourier transform  $G_\delta(f)$  of the sequence  $\{g(n/2W)\}_{n=-\infty}^{\infty}$ , which is obtained by uniform sampling of a continuous-time signal  $g(t)$  at the special rate  $(1/T_s) = f_s = 2W$ . The formula obtained by using the sampling period  $T_s = 1/2W$ , shown in Eq. (5.3), is called the *discrete-time Fourier transform*<sup>1</sup> of the sequence  $\{g(nT_s)\}_{n=-\infty}^{\infty}$ .

<sup>1</sup>In the Fourier formula of Eq. (5.3), time  $t$  is implicitly discretized. If we go one step further and discretize the frequency  $f$  too by setting  $f = k \times 2W$ , we get the discrete Fourier transform, which is periodic in both time and frequency; specifically,

$$G_k = \sum_{n=0}^{N-1} g_n \exp(-j2\pi nk), \quad k = 0, 1, \dots, N-1$$

where

$$g_n = g\left(\frac{n}{2W}\right) = g(nT_s)$$

and

$$G_k = G_\delta(2kW) = G_\delta\left(\frac{k}{T_s}\right)$$

The parameter  $N$  is the number of samples in each period, whether in the time or frequency domain. The discrete Fourier transform was discussed in Chapter 2.

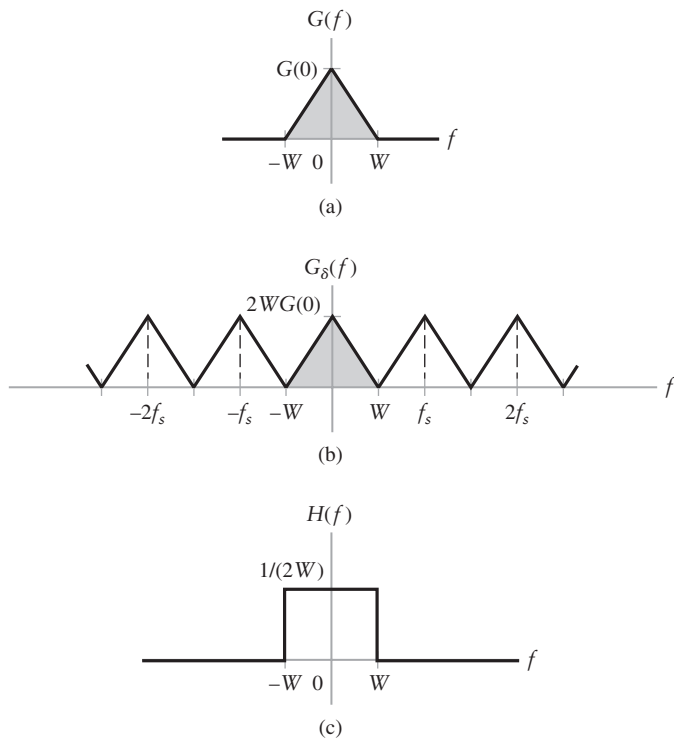


**FIGURE 5.2** (a) Spectrum of a strictly band-limited signal  $g(t)$ . (b) Spectrum of instantaneously sampled version of  $g(t)$  for a sampling period  $T_s = 1/2W$ . (c) Frequency response of ideal low-pass filter aimed at recovering the original message signal  $g(t)$  from its uniformly sampled version.

► **Drill Problem 5.2** Show that as the sampling period  $T_s$  approaches zero, the formula for the discrete-time Fourier transform  $G_\delta(f)$  given in Eq. (5.3) approaches the formula for the Fourier transform  $G(f)$ . ◀

Returning to Eq. (5.2), suppose we isolate the term corresponding to  $m = 0$  in the summation term and thus write

$$G_\delta(f) = f_s G(f) + f_s \sum_{\substack{m=-\infty \\ m \neq 0}}^{\infty} G(f - mf_s)$$

From this expression we find that, for a strictly band-limited signal, under the two conditions

1.  $G(f) = 0$  for  $|f| \geq W$
2.  $f_s = 2W$

the summation term is constrained to be zero. Then, solving the simplified expression for  $G(f)$ , we obtain

$$G(f) = \frac{1}{2W} G_\delta(f), \quad -W < f < W \quad (5.4)$$

Eliminating  $G_\delta(f)$  between Eq. (5.3) and Eq. (5.4) yields

$$G(f) = \frac{1}{2W} \sum_{n=-\infty}^{\infty} g\left(\frac{n}{2W}\right) \exp\left(-j\frac{\pi n f}{W}\right), \quad -W < f < W \quad (5.5)$$

Therefore, if the sample values  $g(n/2W)$  of a signal  $g(t)$  are specified for all time, then the Fourier transform  $G(f)$  of the signal  $g(t)$  is uniquely determined, except for the scaling fac-

tor  $1/2W$ , by the *discrete-time Fourier transform* of Eq. (5.3) for the spectrum  $G_\delta(f)$  limited to the interval  $-W \leq f \leq W$ . Because  $g(t)$  is related to  $G(f)$  by the inverse Fourier transform, it follows that the signal  $g(t)$  is itself uniquely determined by the sample values  $g(n/2W)$  for  $-\infty < n < \infty$ . In other words, the sequence  $\{g(n/2W)\}$  has all the information contained in  $g(t)$ .

Consider next the problem of reconstructing the signal  $g(t)$  from the sequence of sample values  $\{g(n/2W)\}$ . Substituting Eq. (5.5) into the formula for the inverse Fourier transform defining  $g(t)$  in terms of  $G(f)$ , we get

$$\begin{aligned} g(t) &= \int_{-\infty}^{\infty} G(f) \exp(j2\pi ft) df \\ &= \int_{-W}^{W} \frac{1}{2W} \sum_{n=-\infty}^{\infty} g\left(\frac{n}{2W}\right) \exp\left(-\frac{j\pi nf}{W}\right) \exp(j2\pi ft) df \end{aligned}$$

We are permitted to interchange the order of summation and integration, as they are both linear operations. Accordingly, we may go on to redefine the desired signal  $g(t)$  as

$$g(t) = \sum_{n=-\infty}^{\infty} g\left(\frac{n}{2W}\right) \frac{1}{2W} \int_{-W}^{W} \exp\left[j2\pi f\left(t - \frac{n}{2W}\right)\right] df \quad (5.6)$$

► **Drill Problem 5.3** Show that

$$\begin{aligned} \frac{1}{2W} \int_{-W}^{W} \exp\left[j2\pi f\left(t - \frac{n}{2W}\right)\right] df &= \frac{\sin(2\pi Wt - n\pi)}{(2\pi Wt - n\pi)} \\ &= \text{sinc}(2Wt - n) \end{aligned} \quad \blacktriangleleft$$

In light of Problem 5.3, the formula of Eq. (5.6) reduces to

$$g(t) = \sum_{n=-\infty}^{\infty} g\left(\frac{n}{2W}\right) \text{sinc}(2Wt - n), \quad -\infty < t < \infty \quad (5.7)$$

Equation (5.7) is the *interpolation formula* for reconstructing the original signal  $g(t)$  from the sequence of sample values  $\{g(n/2W)\}$ , with the sinc function  $\text{sinc}(2Wt)$  playing the role of an *interpolation function*. Each sample is multiplied by a delayed version of the interpolation function, and all the resulting waveforms are added to obtain  $g(t)$ .

► **Drill Problem 5.4** This problem is intended to identify a linear filter for satisfying the interpolation formula of Eq. (5.7), albeit in a non-physically realizable manner. Equation (5.7) is based on the premise that the signal  $g(t)$  is strictly limited to the band  $-W \leq f \leq W$ . With this specification in mind, consider an ideal low-pass filter whose frequency response  $H(f)$  is as depicted in Fig. 5.2(c). The impulse response of this filter is defined by (see Eq. (2.25))

$$h(t) = \text{sinc}(2Wt), \quad -\infty < t < \infty$$

Suppose that the correspondingly instantaneously sampled signal  $g_\delta(t)$  defined in Eq. (5.1) is applied to this ideal low-pass filter. With this background, use the convolution integral to show that the resulting output of the filter is defined exactly by the interpolation formula of Eq. (5.7). ◀

In light of Problem 5.4, we may now formally say that the *synthesis filter* or *reconstruction filter* aimed at recovering the original strictly band-limited signal  $g(t)$  from its instantaneously sampled version  $g_\delta(t)$  in accordance with Eq. (5.7) consists of an ideal low-pass whose frequency response is limited exactly to the same band as the signal  $g(t)$

itself—namely,  $-W \leq f \leq W$ . This reconstruction filter is non-causal and therefore non-physically realizable. Later on in this section, we will describe how by relaxing the specification of the signal  $g(t)$ , physical realization of the reconstruction filter can be assured.

The discrete-time Fourier transform of Eq. (5.5) defines the message spectrum  $G(f)$  in terms of the uniformly spaced samples values  $g(n/2W)$  for  $\infty < n < \infty$ . The interpolation formula of Eq. (5.7) defines the message signal  $g(t)$  in terms of these same sample values. On the basis of these two formulas, we may now state the *sampling theorem* for strictly band-limited signals of finite energy in two equivalent parts:

1. **Analysis.** A band-limited signal of finite energy that has no frequency components higher than  $W$  hertz is completely described by specifying the values of the signal at instants of time separated by  $1/2W$  seconds.
2. **Synthesis.** A band-limited signal of finite energy that has no frequency components higher than  $W$  hertz is completely recovered from knowledge of its samples taken at the rate of  $2W$  samples per second.

The sampling rate of  $2W$  samples per second for a signal bandwidth of  $W$  hertz is called the *Nyquist rate*; its reciprocal  $1/2W$  (measured in seconds) is called the *Nyquist interval*. The analysis part of the sampling theorem applies to the transmitter. The synthesis part of the theorem, on the other hand applies to the receiver. Note also that the Nyquist rate is the minimum sampling rate permissible.

► **Drill Problem 5.5** Specify the Nyquist rate and the Nyquist interval for each of the following signals:

- (a)  $g(t) = \text{sinc}(200t)$
- (b)  $g(t) = \text{sinc}^2(200t)$
- (c)  $g(t) = \text{sinc}(200t) + \text{sinc}^2(200t)$

► **Drill Problem 5.6** Consider uniform sampling of the sinusoidal wave

$$g(t) = \cos(\pi t)$$

Determine the Fourier transform of the sampled waveform for each of the following sampling periods:

- (a)  $T_s = 0.25\text{s}$
- (b)  $T_s = 1\text{s}$
- (c)  $T_s = 1.5\text{s}$

► **Drill Problem 5.7** Consider a continuous-time signal defined by

$$g(t) = \frac{\sin(\pi t)}{\pi t}$$

The signal  $g(t)$  is uniformly sampled to produce the infinite sequence  $\{g(nT_s)\}_{n=-\infty}^{\infty}$ . Determine the condition that the sampling period  $T_s$  must satisfy so that the signal  $g(t)$  is uniquely recovered from the sequence  $\{g(nT_s)\}$ .

### ■ ALIASING PHENOMENON

Derivation of the sampling theorem, as described herein, is based on the assumption that the signal  $g(t)$  is strictly band-limited. In practice, however, no information-bearing signal of physical origin is strictly band-limited, with the result that some degree of undersampling

is always encountered. Consequently, *aliasing* is produced by the sampling process. Aliasing refers to the phenomenon of a high-frequency component in the spectrum of the signal seemingly taking on the identity of a lower frequency in the spectrum of its sampled version, as illustrated in Fig. 5.3. The aliased spectrum shown by the solid curve in Fig. 5.3(b) pertains to an “undersampled” version of the message signal represented by the spectrum of Fig. 5.3(a).

To combat the effects of aliasing in practice, we may use two *corrective measures*:

1. Prior to sampling, a low-pass *anti-alias filter* is used to attenuate those high-frequency components of a message signal that are not essential to the information being conveyed by the signal.
2. The filtered signal is sampled at a rate slightly higher than the Nyquist rate.

The use of a sampling rate higher than the Nyquist rate also has the beneficial effect of easing the design of the *synthesis filter* used to recover the original signal from its sampled version. Consider the example of a message signal that has been anti-alias (low-pass) filtered, resulting in the spectrum shown in Fig. 5.4(a). The corresponding spectrum of the instantaneously sampled version of the signal is shown in Fig. 5.4(b), assuming a sampling rate higher than the Nyquist rate. According to the picture depicted in Fig. 5.4(b), we now readily see that the design of a *physically realizable reconstruction filter* aimed at recovering the original signal from its uniformly sampled version may be achieved as follows (see Fig. 5.4(c)):

- The reconstruction filter is of a low-pass kind with a passband extending from  $-W$  to  $W$ , which is itself determined by the anti-alias filter.
- The filter has a non-zero transition band extending (for positive frequencies) from  $W$  to  $f_s - W$ , where  $f_s$  is the sampling rate.

The non-zero transition band of the filter assures physical realizability, it is shown dashed to emphasize the arbitrary way of actually realizing it.

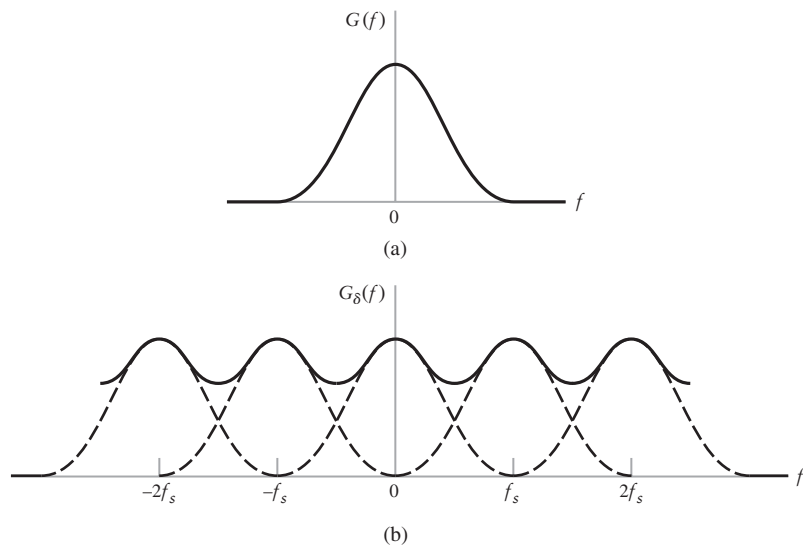


**FIGURE 5.3** (a) Spectrum of a signal. (b) Spectrum of an undersampled version of the signal, exhibiting the aliasing phenomenon.

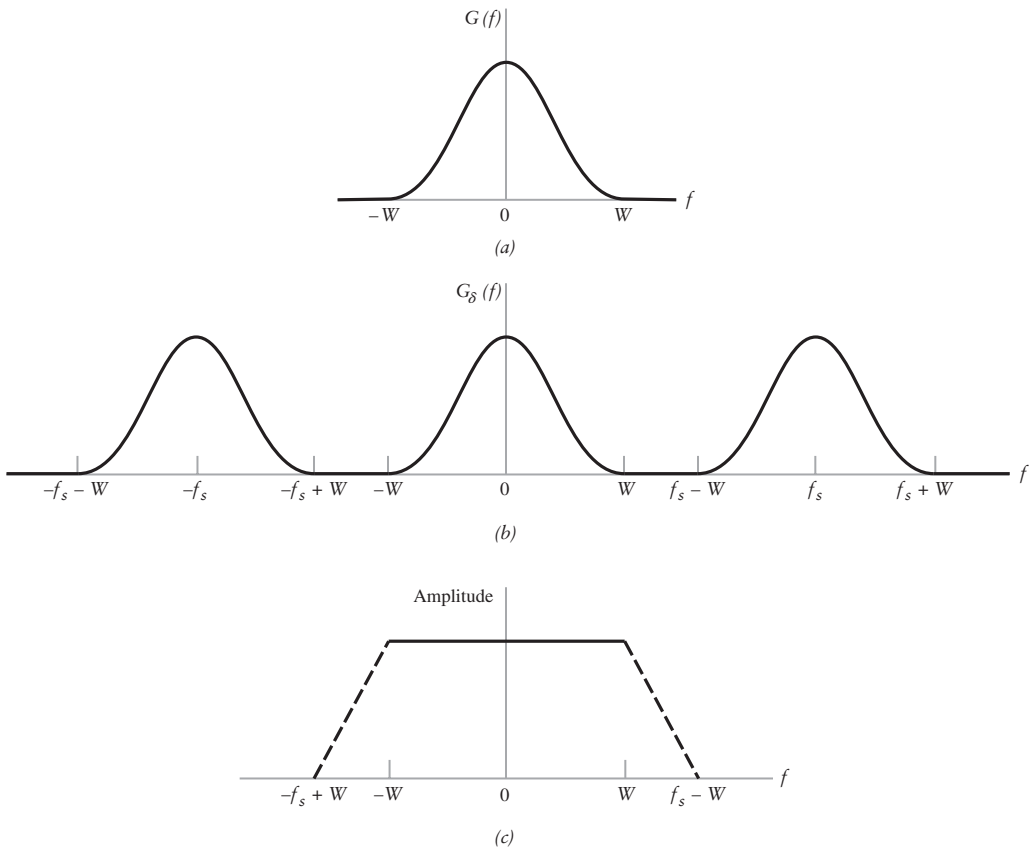


**FIGURE 5.4** (a) Anti-alias filtered spectrum of an information-bearing signal. (b) Spectrum of instantaneously sampled version of the signal, assuming the use of a sampling rate greater than the Nyquist rate. (c) Idealized amplitude response of the reconstruction filter.

## 5.2 Pulse-Amplitude Modulation

Now that we understand the essence of the sampling process, we are ready to formally define pulse-amplitude modulation, which is the simplest and most basic form of analog pulse modulation techniques. In *pulse-amplitude modulation* (PAM), the amplitudes of regularly spaced pulses are varied in proportion to the corresponding sample values of a continuous message signal; the pulses can be of a rectangular form or some other appropriate shape. Pulse-amplitude modulation as defined here is somewhat similar to *natural sampling*, where the message signal is multiplied by a periodic train of rectangular pulses. In natural sampling, however, the top of each modulated rectangular pulse is permitted to vary with the message signal, whereas in PAM it is maintained flat. (Natural sampling is explored further in Problem 5.26.)

The waveform of a PAM signal is illustrated in Fig. 5.5. The dashed curve in this figure depicts the waveform of the message signal  $m(t)$ , and the sequence of amplitude-modulated rectangular pulses shown as solid lines represents the corresponding PAM signal  $s(t)$ . There are two operations involved in the generation of the PAM signal:

1. *Instantaneous sampling* of the message signal  $m(t)$  every  $T_s$  seconds, where the sampling rate  $f_s = 1/T_s$  is chosen in accordance with the sampling theorem.
2. *Lengthening* the duration of each sample, so that it occupies some finite value  $T$ .

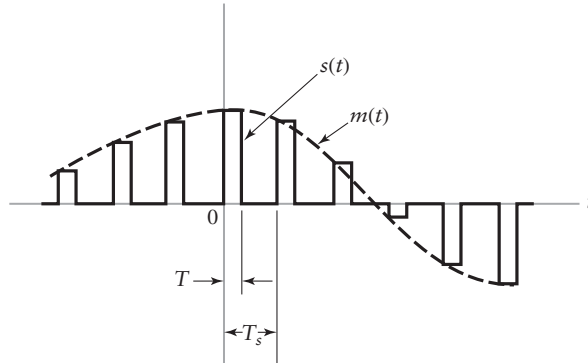


**FIGURE 5.5** Flat-top sampling of a message signal.

In digital circuit technology, these two operations are jointly referred to as “sample and hold.” One important reason for intentionally lengthening the duration of each sample is to avoid the use of an excessive channel bandwidth, since bandwidth is inversely proportional to pulse duration. However, care has to be exercised in how long we make the sample duration  $T$ , as the following analysis reveals.

### ■ SAMPLE-AND-HOLD FILTER: ANALYSIS

Let  $s(t)$  denote the sequence of flat-top pulses generated in the manner described in Fig. 5.5. Hence, we may express the PAM signal as

$$s(t) = \sum_{n=-\infty}^{\infty} m(nT_s)h(t - nT_s) \quad (5.8)$$

where  $T_s$  is the sampling period and  $m(nT_s)$  is the sample value of  $m(t)$  obtained at time  $t = nT_s$ . The  $h(t)$  is a standard rectangular pulse of unit amplitude and duration  $T$ , defined as follows (see Fig. 5.6(a)):

$$h(t) = \text{rect}\left(\frac{t - \frac{T}{2}}{T}\right) = \begin{cases} 1, & 0 < t < T \\ \frac{1}{2}, & t = 0, t = T \\ 0, & \text{otherwise} \end{cases} \quad (5.9)$$

By definition, the instantaneously sampled version of  $m(t)$  is given by [see Eq. (5.1)]

$$m_\delta(t) = \sum_{n=-\infty}^{\infty} m(nT_s)\delta(t - nT_s) \quad (5.10)$$

where  $\delta(t - nT_s)$  is a time-shifted delta function. To modify  $m_\delta(t)$  so as to assume the same form as the PAM signal  $s(t)$ , we convolve  $m_\delta(t)$  with the pulse  $h(t)$ , obtaining

$$\begin{aligned} m_\delta(t) \star h(t) &= \int_{-\infty}^{\infty} m_\delta(\tau)h(t - \tau) d\tau \\ &= \int_{-\infty}^{\infty} \sum_{n=-\infty}^{\infty} m(nT_s)\delta(\tau - nT_s)h(t - \tau) d\tau \\ &= \sum_{n=-\infty}^{\infty} m(nT_s) \int_{-\infty}^{\infty} \delta(\tau - nT_s)h(t - \tau) d\tau \end{aligned} \quad (5.11)$$

where, in the last line, we have interchanged the order of summation and integration, both of which are linear operations. Using the sifting property of the delta function—namely,

$$\int_{-\infty}^{\infty} \delta(\tau - nT_s) h(t - \tau) d\tau = h(t - nT_s)$$

we find that Eq. (5.11) reduces to

$$m_\delta(t) \star h(t) = \sum_{n=-\infty}^{\infty} m(nT_s) h(t - nT_s) \quad (5.12)$$

The summation terms in Eqs. (5.8) and (5.12) are identical. It follows therefore that *the PAM signal  $s(t)$  is mathematically equivalent to the convolution of  $m_\delta(t)$ , the instantaneously sampled version of  $m(t)$ , and the pulse  $h(t)$* , as shown by

$$s(t) = m_\delta(t) \star h(t) \quad (5.13)$$

Taking the Fourier transform of both sides of Eq. (5.13) and recognizing that the convolution of two time functions is transformed into the multiplication of their respective Fourier transforms, we get

$$S(f) = M_\delta(f)H(f) \quad (5.14)$$

where  $S(f) = F[s(t)]$ ,  $M_\delta(f) = F[m_\delta(t)]$ , and  $H(f) = F[h(t)]$ . From Eq. (5.2) we find that the Fourier transform  $M_\delta(f)$  is related to the original message spectrum  $m(t)$  as follows:

$$M_\delta(f) = f_s \sum_{k=-\infty}^{\infty} M(f - kf_s) \quad (5.15)$$

where  $f_s = 1/T_s$  is the sampling rate. Therefore, substitution of Eq. (5.15) into (5.14) yields

$$S(f) = f_s \sum_{k=-\infty}^{\infty} M(f - kf_s)H(f) \quad (5.16)$$

► **Drill Problem 5.8** Starting with Eq. (5.9), show that the Fourier transform of the rectangular pulse  $h(t)$  is given by

$$H(f) = T \operatorname{sinc}(fT) \exp(-j\pi fT) \quad (5.17)$$

What happens to  $H(f)/T$  as the pulse duration  $T$  approaches zero? ◀

Given a PAM signal  $s(t)$  whose Fourier transform  $S(f)$  is defined in Eq. (5.16), how do we recover the original message signal  $m(t)$ ? As a first step in this recovery, we may pass  $s(t)$  through a low-pass filter whose frequency response is defined in Fig. 5.2(c); here it is assumed that the message signal  $m(t)$  is limited to bandwidth  $W$  and the sampling rate  $f_s$  is larger than the Nyquist rate  $2W$ . Then from Eq. (5.16) we find that the spectrum of the resulting filter output is equal to  $M(f)H(f)$ . This output is equivalent to passing the message signal  $m(t)$  through another low-pass filter of transfer function  $H(f)$ . The next step in recovering the message signal  $m(t)$  requires the use of *equalization*, as discussed next.

### ■ APERTURE EFFECT AND ITS EQUALIZATION

Figure 5.6(b) shows plots of the magnitude and phase of the Fourier transform  $H(f)$  versus frequency  $f$ . From this figure we see that by using flat-top samples to generate a PAM signal, we have introduced *amplitude distortion* as well as a *delay* of  $T/2$ . This effect is rather similar to the variation in transmission with frequency that is caused by the finite size of the scanning aperture in television. For this reason, the distortion caused by the use

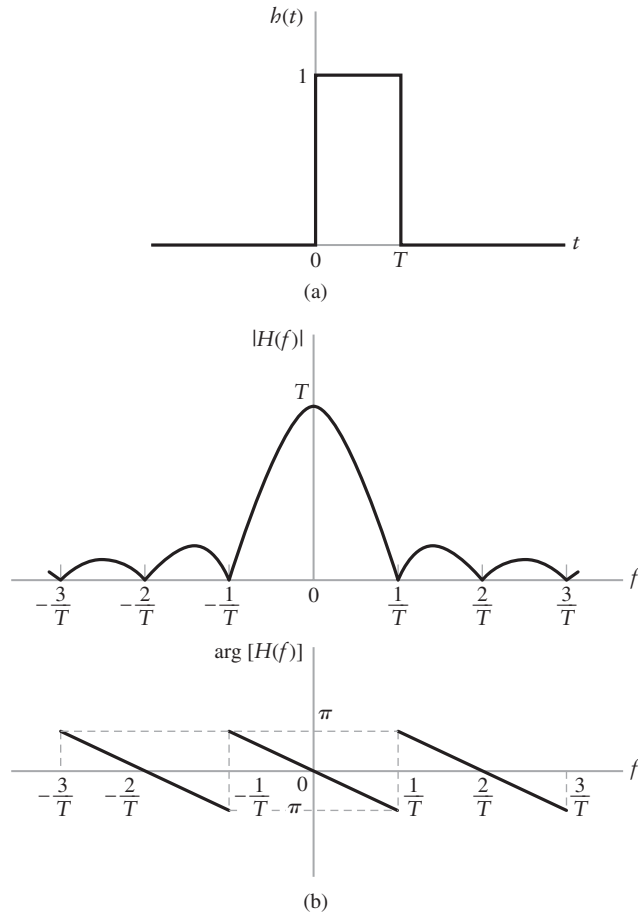


**FIGURE 5.6** (a) Rectangular pulse  $h(t)$ . (b) Spectrum  $H(f)$ , defined in terms of its magnitude and phase.

of pulse-amplitude modulation (based on flat-top sampling) to transmit an analog information-bearing signal is referred to as the *aperture effect*.

This distortion may be corrected by connecting an *equalizer* in cascade with the low-pass reconstruction filter, as shown in Fig. 5.7. The equalizer has the effect of decreasing the in-band loss of the reconstruction filter as the frequency increases in such a manner as to compensate for the aperture effect. Ideally, the amplitude response of the equalizer is given by

$$\frac{1}{|H(f)|} = \frac{1}{T \operatorname{sinc}(fT)} = \frac{\pi f}{\sin(\pi fT)}$$

The amount of equalization needed in practice is usually small. Indeed, for a duty cycle  $(T/T_s) \leq 0.1$ , the amplitude distortion is less than 0.5 percent, in which case the need for equalization may be omitted altogether.



**FIGURE 5.7** Recovering the message signal  $m(t)$  from the PAM signal  $s(t)$ .

The transmission of a PAM signal imposes rather stringent requirements on the amplitude and phase responses of the channel, because of the relatively short duration of the transmitted pulses. Furthermore, it may be shown that the noise performance of a PAM system can never be better than direct transmission of the message signal. Accordingly, we find that for transmission over long distances, PAM would be used only as a means of message processing for time-division multiplexing. The concept of time-division multiplexing is discussed later in this chapter.

### 5.3 Pulse-Position Modulation

In pulse-amplitude modulation, pulse amplitude is the variable parameter. Pulse duration is the next logical parameter available for modulation. *In pulse-duration modulation (PDM), the samples of the message signal are used to vary the duration of the individual pulses.* This form of modulation is also referred to as *pulse-width modulation* or *pulse-length modulation*. The modulating signal may vary the time of occurrence of the leading edge, the trailing edge, or both edges of the pulse. In Fig. 5.8(c) the trailing edge of each pulse is varied in accordance with the message signal, assumed to be sinusoidal as shown in Fig. 5.8(a). The periodic pulse carrier is shown in Fig. 5.8(b).

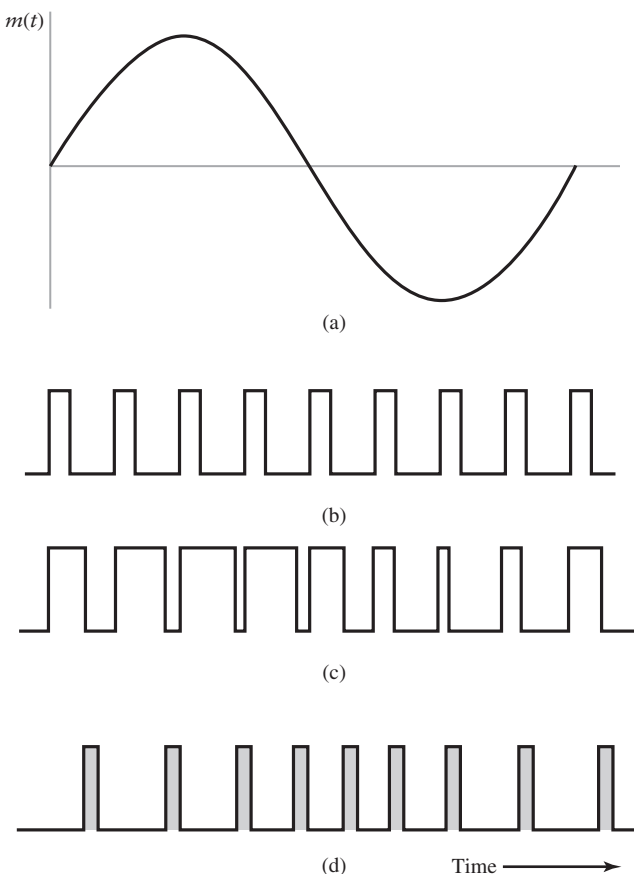


**FIGURE 5.8** Illustration of two different forms of pulse-time modulation for the case of a sinusoidal modulating wave. (a) Modulating wave. (b) Pulse carrier. (c) PDM wave. (d) PPM wave.

PDM is wasteful of power, in that long pulses expend considerable power during the pulse while bearing no additional information. If this unused power is subtracted from PDM, so that only time transitions are essentially preserved, we obtain a more efficient type of pulse modulation known as *pulse-position modulation* (PPM). In PPM, the position of a pulse relative to its unmodulated time of occurrence is varied in accordance with the message signal, as illustrated in Fig. 5.8(d) for the case of sinusoidal modulation.

Let  $T_s$  denote the sample duration. Using the sample  $m(nT_s)$  of a message signal  $m(t)$  to modulate the position of the  $n$ th pulse, we obtain the PPM signal

$$s(t) = \sum_{n=-\infty}^{\infty} g(t - nT_s - k_p m(nT_s)) \quad (5.18)$$

where  $k_p$  is the sensitivity factor of the pulse-position modulator (in seconds per volt) and  $g(t)$  denotes a standard pulse of interest. Clearly, the different pulses constituting the PPM signal  $s(t)$  must be *strictly nonoverlapping*; a sufficient condition for this requirement to be satisfied is to have

$$g(t) = 0, \quad |t| > (T_s/2) - k_p |m(t)|_{\max} \quad (5.19)$$

which, in turn, requires that

$$k_p |m(t)|_{\max} < (T_s/2) \quad (5.20)$$

The closer  $k_p |m(t)|_{\max}$  is to one half the sampling duration  $T_s$ , the narrower must the standard pulse  $g(t)$  be to ensure that the individual pulses of the PPM signal  $s(t)$  do not interfere with each other, and the wider will the bandwidth occupied by the PPM signal be. Assuming that Eq. (5.19) is satisfied and that there is no interference between adjacent pulses of the PPM signal  $s(t)$ , then the signal samples  $m(nT_s)$  can be recovered perfectly.<sup>2</sup> Furthermore, if the message signal  $m(t)$  is strictly band-limited, it follows from the sampling theorem that the original message signal  $m(t)$  can be recovered from the PPM signal  $s(t)$  without distortion.

## 5.4 Completing the Transition from Analog to Digital

At this point in the book, it is instructive that we look at the modulation techniques that we have studied thus far, for transmitting analog information-bearing signals (i.e., voice and video signals) over a communication channel, and look at those that are yet to be considered. The techniques studied thus far are continuous-wave modulation and analog pulse modulation. Although, these two families of modulation techniques are indeed different, they share similar attributes and limitations.

First, it is natural to think of pulse-amplitude modulation as the counterpart of amplitude modulation studied in Chapter 3. What do we have as a pulse-modulation counterpart to frequency modulation studied in Chapter 4? In frequency modulation, the zero-crossings of the modulated wave vary with time in accordance with the message signal. In pulse-position modulation, the positions of transmitted pulses vary with time in accordance with the message signal. In a loose sense, we may therefore think of pulse-position modulation as the counterpart of frequency modulation.

An intuitive conclusion to draw from this loose analogy between members of analog pulse modulation and those of continuous-wave modulation is that these two families of modulation techniques offer the same order of performance when they are applied to the transmission of analog signals over communication channels. In the context of performance, we are thinking in terms of transmission bandwidth requirement and receiver noise behavior.

<sup>2</sup>Generation and detection of PPM waves are discussed in Haykin (1994), pp. 365–369.

The operational feature that distinguishes the two families is that continuous-wave modulation techniques operate in continuous time, whereas analog pulse modulation techniques operate in discrete time.

In going from continuous-wave modulation to analog pulse modulation, we have moved ourselves into *discrete-time signal processing*. Why not go one step further and also incorporate *amplitude discretization*? Indeed, this is precisely what is done in *digital pulse modulation*. In so doing, we have a new family of modulation techniques for the transmission of analog signals over communication channels. The advantages offered by digital pulse modulation techniques include the following:

1. *Performance.* In an analog communication system, using either a continuous-wave modulation or analog pulse modulation technique, the effects of signal distortion and channel noise (incurred along the transmission path) are *cumulative*. These sources of impairments therefore tend to become progressively stronger, ultimately overwhelming the ability of the communication system to offer an acceptable level of performance from source to destination. Unfortunately, the use of repeaters in the form of amplifiers, placed at different points along the transmission path, offers little help because the message signal and noise are amplified to the same extent. In sharp contrast, digital pulse modulation permits the use of *regenerative repeaters*, which, when placed along the transmission path at short enough distances, can practically eliminate the degrading effects of channel noise and signal distortion.
2. *Ruggedness.* Unlike an analog communication system, a digital communication system can be designed to withstand the effects of channel noise and signal distortion, provided the noise and distortion are kept under certain limits.
3. *Reliability.* Digital communication systems can be made highly reliable by exploiting powerful error-control coding techniques in such a way that the estimate of a message signal delivered to a user is almost indistinguishable from the message signal delivered by a source of information at the other end of the system. (Error-control coding is discussed in Chapter 10.)
4. *Security.* By the same token, digital communication systems can be made highly secure by exploiting powerful encryption algorithms that rely on digital processing for their implementation.
5. *Efficiency.* Digital communication systems are inherently more efficient than analog communication systems in the tradeoff between transmission bandwidth and signal-to-noise ratio.
6. *System integration.* The use of digital communications makes it possible to integrate digitized analog signals (i.e., voice and video signals) with digital computer data, which is not possible with analog communications.

This impressive list of advantages has made the use of digital pulse modulation techniques the method of choice for the transmission of voice and video signals over communication channels.

The benefits of using digital pulse modulation, however, are attained at the expense of increased system complexity. Nevertheless, by exploiting the computing power of digital signal processors in hardware and/or software form and the flexibility these processors offer, digital communication systems can be designed in a cost-effective manner, thanks to the continuing improvements in very-large-scale integrated (VLSI) silicon chips.

Now that we have identified the digital pulse modulation family as the method of choice for communications, our next task in this chapter is to describe three family members—namely, pulse-code modulation, delta modulation, and differential pulse-code modulation. The study

of pulse-code modulation occupies Sections 5.5 and 5.6, followed by the other two in Sections 5.7 and 5.8, respectively. Pulse-code modulation is the standard against which delta modulation and differential pulse-code modulation are usually compared.

## 5.5 Quantization Process

A continuous signal, such as voice, has a continuous range of amplitudes and therefore its samples have a continuous amplitude range. In other words, within the finite amplitude range of the signal, we find an infinite number of amplitude levels. In actual fact, however, it is not necessary to transmit the exact amplitudes of the samples. We say so because any human sense (the ear or the eye) as the ultimate receiver can detect only finite intensity differences. This means that the original continuous signal may be *approximated* by a signal constructed of discrete amplitudes selected on a minimum-error basis from an available set. The existence of a finite number of discrete amplitude levels is a basic condition of digital-pulse modulation. Clearly, if we assign the discrete amplitude levels with sufficiently close spacing, we can make the approximated signal indistinguishable from the original continuous signal for all practical purposes. Note also that quantization is non-reversible.

Amplitude *quantization* is defined as *the process of transforming the sample amplitude  $m(nT_s)$  of a baseband signal  $m(t)$  at time  $t = nT_s$  into a discrete amplitude  $v(nT_s)$  taken from a finite set of possible levels*. We confine attention to a quantization process that is *memoryless* and *instantaneous*, which means that the transformation at time  $t = nT_s$  is not affected by earlier or later samples of the message signal. This form of quantization, though not optimal, is commonly used in practice because of its simplicity.

When dealing with a memoryless quantizer, we may simplify the notation by dropping the time index. That is, we use the symbol  $m$  in place of the sample  $m(nT_s)$ , as indicated in Fig. 5.9(a). Then, as shown in Fig. 5.9(b), the signal amplitude  $m$  is specified by the index  $k$  if it lies inside the interval

$$I_k: \{m_k < m \leq m_{k+1}\}, \quad k = 1, 2, \dots, L \quad (5.21)$$

where  $L$  is the total number of amplitude levels used in the *quantizer*, which refers to the subsystem that performs the quantization process. The amplitudes,  $m_k$ ,  $k = 1, 2, \dots, L$ , are called *decision levels* or *decision thresholds*. At the quantizer output, the index  $k$  is transformed into an amplitude  $v_k$  that represents all amplitudes that lie inside the interval  $I_k$ . The amplitudes  $v_k$ ,  $k = 1, 2, \dots, L$ , are called *representation levels* or *reconstruction levels*, and the spacing between two adjacent representation levels is called a *quantum* or *step-size*. Thus, the quantizer output  $v$  equals  $v_k$  if the input signal sample  $m$  belongs to the interval  $I_k$ . The mapping

$$v = g(m) \quad (5.22)$$

is the *quantizer characteristic*. This characteristic is described by a staircase function.

Quantizers can be of a *uniform* or *nonuniform* type. In a uniform quantizer, the representation levels are uniformly spaced; otherwise, the quantizer is nonuniform. The quantizers considered in this section are of the uniform variety; nonuniform quantizers are

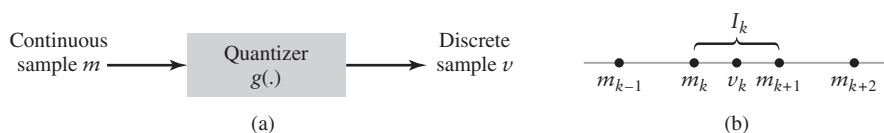


**FIGURE 5.9** Description of a memoryless quantizer.

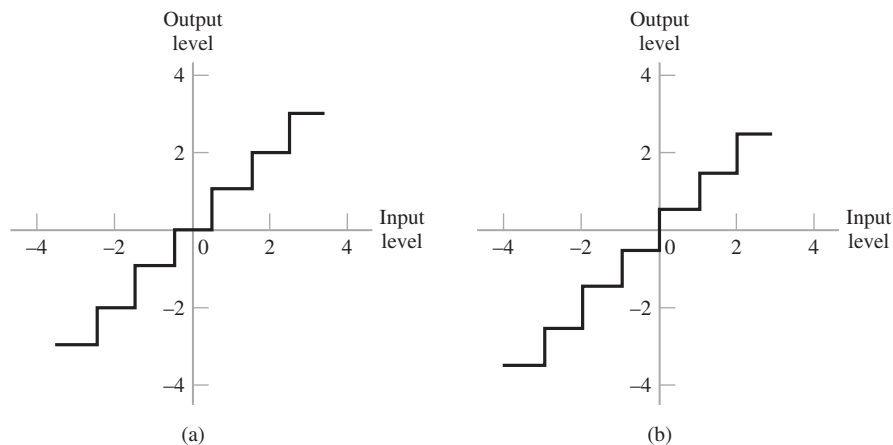


**FIGURE 5.10** Two types of quantization: (a) midtread and (b) midrise.

considered in Section 5.6. The quantizer characteristic can also be of a *midtread* or *midrise* type. Figure 5.10(a) shows the input–output characteristic of a uniform quantizer of the midtread type, which is so called because the origin lies in the middle of a tread of the staircaselike graph. Figure 5.10(b) shows the corresponding input–output characteristic of a uniform quantizer of the midrise type, in which the origin lies in the middle of a rising part of the staircaselike graph. Note that both the midtread and midrise types of uniform quantizers, illustrated in Fig. 5.10, are *symmetric* about the origin.

## 5.6 Pulse-Code Modulation

With the sampling and quantization processes at our disposal, we are now ready to describe pulse-code modulation, which is the most basic form of digital pulse modulation. In *pulse-code modulation (PCM)*, a message signal is represented by a sequence of coded pulses, which is accomplished by representing the signal in discrete form in both time and amplitude.

The basic operations performed in the transmitter of a PCM system are *sampling*, *quantization*, and *encoding*, as shown in Fig. 5.11(a); the low-pass filter prior to sampling is included merely to prevent aliasing of the message signal. The quantizing and encoding operations are usually performed in the same circuit, which is called an *analog-to-digital converter*.

The basic operations in the receiver are *regeneration* of impaired signals, *decoding*, and *reconstruction* of the train of quantized samples, as shown in Fig. 5.11(c). Regeneration also occurs at intermediate points along the transmission path as necessary, as indicated in Fig. 5.11(b). When time-division multiplexing (discussed later in the chapter) is used, it becomes necessary to synchronize the receiver to the transmitter for the overall system to operate satisfactorily. In what follows we describe the operations of sampling, quantizing, and encoding that are basic to a PCM system.

### ■ OPERATIONS IN THE TRANSMITTER

#### (i) Sampling

The incoming message (baseband) signal is sampled with a train of rectangular pulses, narrow enough to closely approximate the instantaneous sampling process. To ensure perfect reconstruction of the message signal at the receiver, the sampling rate must be greater than twice the highest frequency component  $W$  of the message signal in accordance with the sampling theorem. In practice, an anti-alias (low-pass) filter is used at

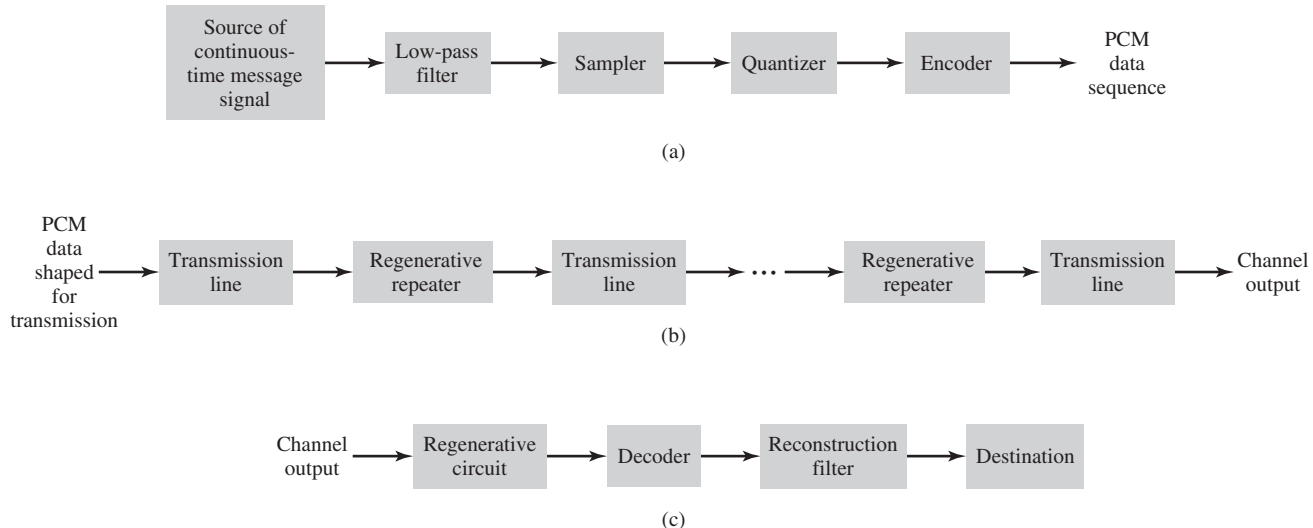


**FIGURE 5.11** The basic elements of a PCM system: (a) Transmitter, (b) transmission path, connecting the transmitter to the receiver, and (c) receiver.

the front end of the sampler in order to exclude frequencies greater than  $W$  before sampling, as shown in Fig. 5.11(a). Thus the application of sampling permits the reduction of the continuously varying message signal (of some finite duration) to a limited number of discrete values per second.

### (ii) Nonuniform Quantization

The sampled version of the message signal is then quantized, thereby providing a new representation of the signal that is discrete in both time and amplitude. The quantization process may follow a uniform law as described in Section 5.5. In certain applications, however, it is preferable to use a variable separation between the representation levels. For example, the range of voltages covered by voice signals, from the peaks of loud talk to the weak passages of weak talk, is on the order of 1000 to 1. By using a *nonuniform quantizer* with the feature that the step size increases as the separation from the origin of the input-output amplitude characteristic is increased, the large end-step of the quantizer can take care of possible excursions of the voice signal into the large amplitude ranges that occur relatively infrequently. In other words, the weak passages that need more protection are favored at the expense of the loud passages. In this way, a nearly uniform percentage precision is achieved throughout the greater part of the amplitude range of the input signal, with the result that fewer steps are needed than would be the case if a uniform quantizer were used.

The use of a nonuniform quantizer is equivalent to passing the message signal through a *compressor* and then applying the compressed signal to a uniform quantizer. A particular form of compression law that is used in practice is the so called  $\mu$ -*law*<sup>3</sup> defined by

$$|v| = \frac{\log(1 + \mu|m|)}{\log(1 + \mu)} \quad (5.23)$$

<sup>3</sup>The  $\mu$ -*law* used for signal compression is described in Smith (1957); this compression law is used in the United States, Canada, and Japan. In Europe, the *A*-*law* is used for signal compression; this second compression law is described in Cattermole (1969, pp. 133–140). For discussion of the  $\mu$ -*law* and *A*-*law*, see also the paper by Kaneko (1970).

where the logarithm is the natural logarithm;  $m$  and  $v$  are respectively the normalized input and output voltages, and  $\mu$  is a positive constant. For convenience of presentation, the input to the quantizer and its output are both *normalized* so as to occupy a dimensionless range of values from zero to one, as shown in Fig. 5.12(a); here we have plotted the  $\mu$ -law for varying  $\mu$ . Practical values of  $\mu$  tend to be in the vicinity of 255. The case of uniform quantization corresponds to  $\mu = 0$ . For a given value of  $\mu$ , the reciprocal slope of the compression curve, which defines the quantum steps, is given by the derivative of  $|m|$  with respect to  $|v|$ ; that is,

$$\frac{d|m|}{d|v|} = \frac{\log(1 + \mu)}{\mu} (1 + \mu|m|) \quad (5.24)$$

We see therefore that the  $\mu$ -law is neither strictly linear nor strictly logarithmic, but it is approximately linear at low input levels corresponding to  $\mu|m| \ll 1$ , and approximately logarithmic at high input levels corresponding to  $\mu|m| \gg 1$ .

Another compression law that is used in practice is the so-called *A-law*, defined by

$$|v| = \begin{cases} \frac{A|m|}{1 + \log A}, & 0 \leq |m| \leq \frac{1}{A} \\ \frac{1 + \log(A|m|)}{1 + \log A}, & \frac{1}{A} \leq |m| \leq 1 \end{cases} \quad (5.25)$$

which is shown plotted in Fig. 5.12(b). Typical values of  $A$  used in practice tend to be in the vicinity of 100. The case of uniform quantization corresponds to  $A = 1$ . The reciprocal slope of this second compression curve is given by the derivative of  $|m|$  with respect to  $|v|$ , as shown by

$$\frac{d|m|}{d|v|} = \begin{cases} \frac{1 + \log A}{A}, & 0 \leq |m| \leq \frac{1}{A} \\ (1 + \log A)|m|, & \frac{1}{A} \leq |m| \leq 1 \end{cases} \quad (5.26)$$

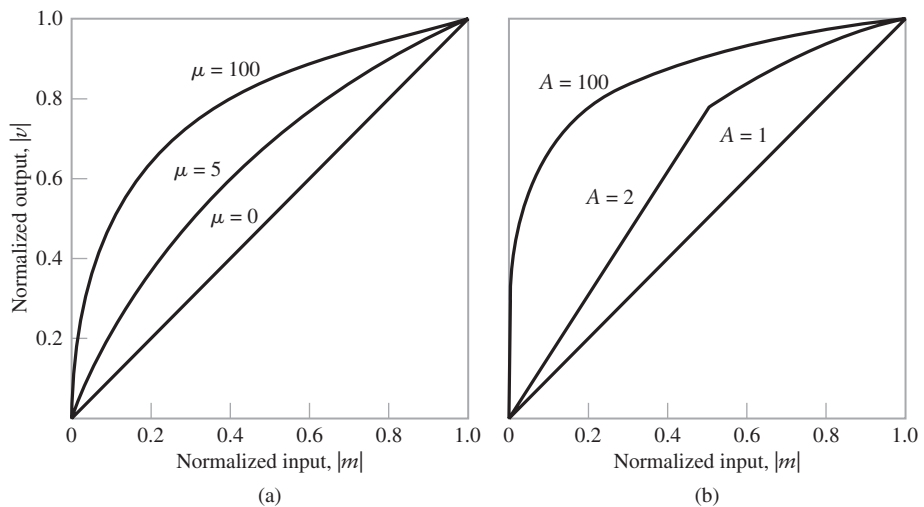


**FIGURE 5.12** Compression laws. (a)  $\mu$ -law. (b)  $A$ -law.

From the first line of Eq. (5.26) we may infer that the quantum steps over the central linear segment, which have the dominant effect on small signals, are diminished by the factor  $A/(1 + \log A)$ . This is typically about 25 dB in practice, as compared with uniform quantization.

- **Drill Problem 5.9** Using Eqs. (5.23) and (5.25), respectively, derive the slope characteristics of Eqs. (5.24) and (5.26). ◀

### (iii) Encoding

In combining the processes of sampling and quantization, the specification of a continuous message (baseband) signal becomes limited to a discrete set of values, but not in the form best suited to transmission over a wire line or radio path. To exploit the advantages of sampling and quantization for the purpose of making the transmitted signal more robust to noise, interference and other channel degradations, we require the use of an *encoding process* to translate the discrete set of sample values to a more appropriate form of signal. Any plan for representing this discrete set of values as a particular arrangement of discrete events is called a *code*. One of the discrete events in a code is called a *code element* or *symbol*. For example, the presence or absence of a pulse is a symbol. A particular arrangement of symbols used in a code to represent a single value of the discrete set is called a *code word* or *character*.

In a *binary code*, each symbol may be either of two distinct values, such as a negative pulse or positive pulse. The two symbols of the binary code are customarily denoted as 0 and 1. In practice, a binary code is preferred over other codes (e.g., ternary code) for two reasons:

1. The maximum advantage over the effects of noise in a transmission medium is obtained by using a binary code, because a binary symbol withstands a relatively high level of noise.
2. The binary code is easy to generate and regenerate.

Suppose that, in a binary code, each code word consists of  $R$  bits: the bit is an acronym for *binary digit*. Then  $R$  denotes the number of *bits per sample*. Hence, by using such a code, we represent a total of  $2^R$  distinct numbers. For example, a sample quantized into one of 256 levels may be represented by an 8-bit code word.

There are several ways of establishing a one-to-one correspondence between representation levels and code words. A convenient method is to express the ordinal number of the representation level as a binary number. In the binary number system, each digit has a place-value that is a power of 2, as illustrated in Table 5.2 for the case of four bits per sample (i.e.,  $R = 4$ ).

## ■ REGENERATION ALONG THE TRANSMISSION PATH

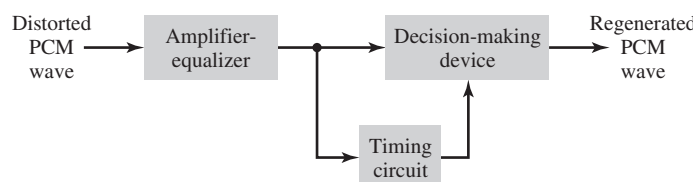
The most important feature of a PCM system lies in the ability to *control* the effects of distortion and noise produced by transmitting a PCM signal over a channel. This capability is accomplished by reconstructing the PCM signal by means of a chain of *regenerative repeaters* located at sufficiently close spacing along the transmission route. As illustrated in Fig. 5.13, three basic functions are performed by a regenerative repeater: *equalization*, *timing*, and *decision making*. The equalizer shapes the received pulses so as to compensate for the effects of amplitude and phase distortions produced by the transmission characteristics of the channel. The timing circuitry provides a periodic pulse train, derived from the received pulses; this is done for renewed sampling of the equalized pulses at the instants

**TABLE 5.2** *Binary Number System for R = 4*

<i>Ordinal Number of Representation Level</i>	<i>Level Number Expressed as Sum of Powers of 2</i>	<i>Binary Number</i>
0		0000
1	$2^0$	0001
2	$2^1$	0010
3	$2^1 + 2^0$	0011
4	$2^2$	0100
5	$2^2 + 2^0$	0101
6	$2^2 + 2^1$	0110
7	$2^2 + 2^1 + 2^0$	0111
8	$2^3$	1000
9	$2^3 + 2^0$	1001
10	$2^3 + 2^1$	1010
11	$2^3 + 2^1 + 2^0$	1011
12	$2^3 + 2^2$	1100
13	$2^3 + 2^2 + 2^0$	1101
14	$2^3 + 2^2 + 2^1$	1110
15	$2^3 + 2^2 + 2^1 + 2^0$	1111

of time where the signal-to-noise ratio is a maximum. The sample so extracted is compared to a predetermined *threshold* in the decision-making device. In each bit interval, a decision is then made on whether the received symbol is a 1 or 0 on the basis of whether the threshold is exceeded or not. If the threshold is exceeded, a clean new pulse representing symbol 1 is transmitted to the next repeater. Otherwise, another clean new pulse representing symbol 0 is transmitted. In this way, the accumulation of distortion and noise in a repeater span is removed, provided the disturbance is not too large to cause an error in the decision-making process. Ideally, except for delay, the regenerated signal is exactly the same as the information-bearing signal that was originally transmitted. In practice, however, the regenerated signal departs from the original signal for two main reasons:

1. The unavoidable presence of channel noise and interference causes the repeater to make wrong decisions occasionally, thereby introducing *bit errors* into the regenerated signal.
2. If the spacing between received pulses deviates from its assigned value, a *jitter* is introduced into the regenerated pulse position, thereby causing distortion.

**FIGURE 5.13** Block diagram of a regenerative repeater.

**■ OPERATIONS IN THE RECEIVER****(i) Decoding and Expanding**

The first operation in the receiver is to *regenerate* (i.e., reshape and clean up) the received pulses one last time. These clean pulses are then regrouped into code words and decoded (i.e., mapped back) into a quantized PAM signal. The *decoding* process involves generating a pulse whose amplitude is the linear sum of all the pulses in the code word; each pulse is weighted by its place value ( $2^0, 2^1, 2^2, 2^3, \dots, 2^{R-1}$ ) in the code, where  $R$  is the number of bits per sample.

The sequence of decoded samples represents an *estimate* of the sequence of compressed samples produced by the quantizer in the transmitter. We use the term “estimate” here to emphasize the fact that there is no way for the receiver to compensate for the approximation introduced into the transmitted signal by the quantizer. Moreover, other sources of noise include bit errors and jitter produced along the transmission path. In order to restore the sequence of decoded samples to their correct relative level, we must, of course, use a subsystem in the receiver with a characteristic complementary to the compressor, used in the transmitter. Such a subsystem is called an *expander*. Ideally, the compression and expansion laws are exactly *inverse* so that, except for the effect of quantization, the expander output is equal to the compressor input if these two devices were connected directly. The combination of a compressor and an expander is referred to as a *compander*.

**(ii) Reconstruction**

The final operation in the receiver is to recover the message signal. This operation is achieved by passing the expander output through a *low-pass reconstruction filter* whose cutoff frequency is equal to the message bandwidth. Recovery of the message signal is intended to signify estimation rather than exact reconstruction.

One last comment is in order. The term “modulation” in pulse-code modulation is a misnomer. In reality, pulse-code modulation is a *source-encoding strategy*, by means of which an analog signal emitted by a source is converted into digital form. Transmission of the digital data so produced is another topic, the treatment of which is deferred to Chapter 6.

## 5.7 Delta Modulation

From the discussion presented in Section 5.6, it is apparent that the design of a pulse-code modulation system involves many operations, which tend to make its practical implementation rather costly. To simplify the system design, we may use another digital pulse modulation technique known as delta modulation, which is considered in this section.

**■ BASIC CONSIDERATIONS**

In *delta modulation* (DM), an incoming message signal is oversampled (i.e., at a rate much higher than the Nyquist rate) to purposely increase the *correlation* between adjacent samples of the signal. The increased correlation is done so as to permit the use of a simple quantizing strategy for constructing the encoded signal.

In its basic form, DM provides a *staircase approximation* to the oversampled version of the message signal. Unlike PCM, the difference between the input signal and its approximation is quantized into only two levels—namely,  $\pm\Delta$ , corresponding to positive and negative *differences*. Thus, if the approximation falls below the input signal at any sampling epoch, it is increased by  $\Delta$ . If, on the other hand, the approximation lies above the signal, it is diminished

by  $\Delta$ . Provided the input signal does not change too rapidly from sample to sample, we find that the staircase approximation remains within  $\pm\Delta$  of the input signal.

We denote the input signal by  $m(t)$  and its staircase approximation by  $m_q(t)$ . The basic principle of delta modulation may then be formalized in the following set of three discrete-time relations:

$$e(nT_s) = m(nT_s) - m_q(nT_s - T_s) \quad (5.27)$$

$$e_q(nT_s) = \Delta \text{sgn}[e(nT_s)] \quad (5.28)$$

$$m_q(nT_s) = m_q(nT_s - T_s) + e_q(nT_s) \quad (5.29)$$

where  $T_s$  is the sampling period;  $e(nT_s)$  is an *error signal* representing the difference between the present sample value  $m(nT_s)$  of the input signal and the latest approximation to it—that is,  $m(nT_s) - m_q(nT_s - T_s)$ ; and  $e_q(nT_s)$  is the quantized version of  $e(nT_s)$ ; and  $\text{sgn}[\cdot]$  is the signum function, assuming the value +1 or -1. The quantizer output  $e_q(nT_s)$  is finally encoded to produce the desired DM data.

Figure 5.14(a) illustrates the way in which the staircase approximately follows variations in the input signal  $m(t)$  in accordance with Eqs. (5.27) to (5.29), and Fig. 5.19(b) displays the corresponding binary sequence at the delta modulator output. It is apparent that in a delta modulation system, the rate of information transmission is simply equal to the sampling rate  $f_s = 1/T_s$ .

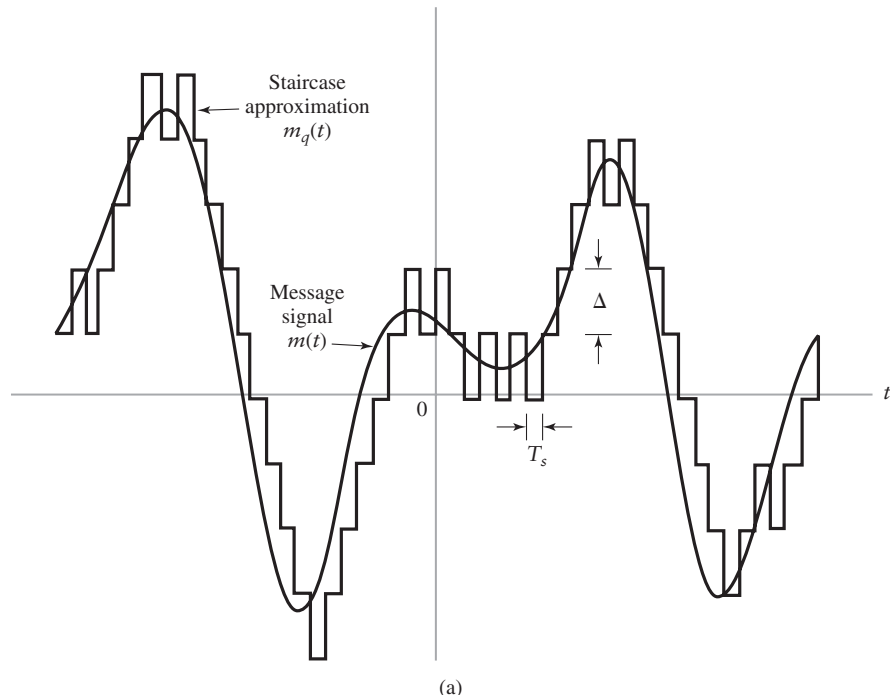


**FIGURE 5.14** Illustration of delta modulation. (a) Analog waveform  $m(t)$  and its staircase approximation  $m_q(t)$ . (b) Binary sequence at the modulator output.

### ■ SYSTEM DETAILS

The principal virtue of delta modulation is its *simplicity*. It may be implemented by applying a sampled version of the incoming message signal to a transmitter that consists of a *comparator*, *quantizer*, and *accumulator* connected together as shown in Fig. 5.15(a). Details of the transmitter follow directly from Eqs. (5.27) to (5.29). The comparator computes the difference between its two inputs. The quantizer consists of a *hard limiter* with an input–output characteristic that is a scaled version of the signum function. The accumulator operates on the quantizer output so as to produce an approximation to the message signal.

Equation (5.29) is a *difference equation of order one*; the order refers to the fact the present sample  $m_q(nT_s)$  differs from the past sample  $m_q(nT_s - T_s)$  by an amount equal to the quantization error  $e_q(nT_s)$ . Assuming that the accumulation process starts at zero time, the solution to this equation yields the approximate result

$$\begin{aligned} m_q(nT_s) &= m_q(nT_s - T_s) + e_q(nT_s) \\ &= m_q(nT_s - 2T_s) + e_q(nT_s - T_s) + e_q(nT_s) \\ &\quad \vdots \\ &= \sum_{i=1}^n e_q(iT_s) \end{aligned} \quad (5.30)$$

where  $e_q(nT_s)$  is itself related to the message sample  $m(nT_s)$  by Eqs. (5.27) and (5.28).

Thus, at the sampling instant  $nT_s$ , the accumulator increments the approximation by the increment  $\Delta$  in a positive or negative direction, depending on the algebraic sign of the error signal  $e(nT_s)$ . If the input signal  $m(nT_s)$  is greater than the most recent approximation  $m_q(nT_s)$ , a positive increment  $+\Delta$  is applied to the approximation. If, on the other hand, the input signal is smaller, a negative increment  $-\Delta$  is applied to the approximation.

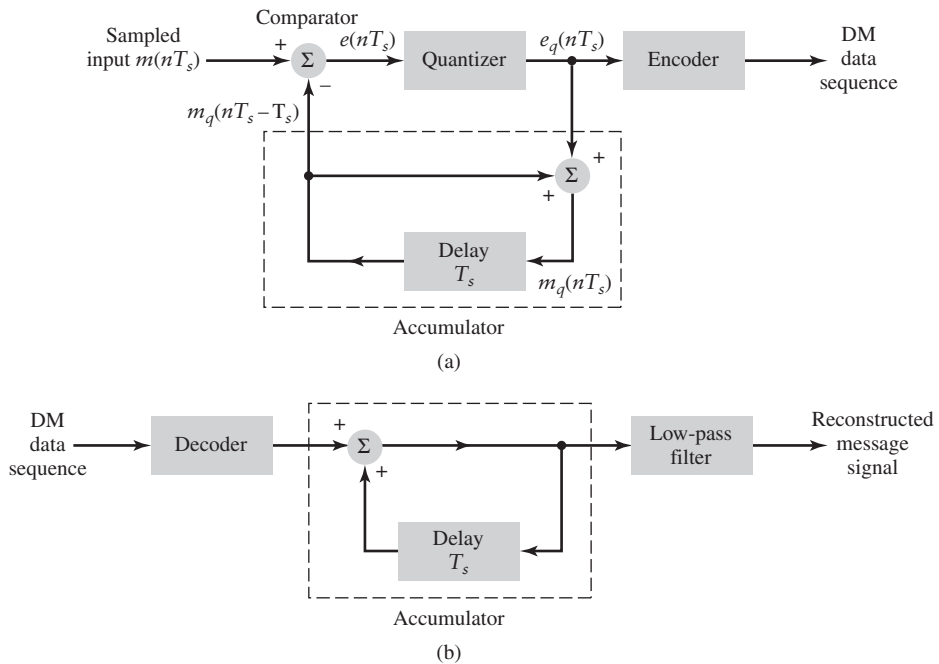


FIGURE 5.15 DM system: (a) Transmitter and (b) receiver.

In this way, the accumulator does the best it can to *track* the input samples one step (of amplitude  $+\Delta$  or  $-\Delta$ ) at a time.

In the receiver shown in Fig. 5.15(b), the staircase approximation  $m_q(t)$  is reconstructed by passing the sequence of positive and negative pulses, produced at the decoder output, through an accumulator in a manner similar to that used in the transmitter. The out-of-band quantization noise present in the high-frequency staircase waveform  $m_q(t)$  is rejected by passing  $m_q(t)$  through a filter, as in Fig. 5.15(b). The filter is of a low-pass kind, with a bandwidth equal to the original message bandwidth.

### ■ QUANTIZATION ERRORS

Delta modulation is subject to two types of quantization error: (1) slope overload distortion and (2) granular noise. We first discuss the cause of slope overload distortion and then granular noise.

We observe that Eq. (5.29) is the *digital equivalent of integration* in the sense that it represents the accumulation of positive and negative increments of magnitude  $\Delta$ . Also, denoting the quantization error by  $q(nT_s)$ , as shown by

$$m_q(nT_s) = m(nT_s) + q(nT_s) \quad (5.31)$$

we observe from Eq. (5.27) that the input to the quantizer is

$$e(nT_s) = m(nT_s) - m(nT_s - T_s) - q(nT_s - T_s) \quad (5.32)$$

Thus, except for the delayed quantization error  $q(nT_s - T_s)$ , the quantizer input is a first *backward difference* of the input signal, which may be viewed as a digital approximation to the derivative of the input signal or, equivalently, as the inverse of the digital integration process. If we now consider the maximum slope of the original message signal  $m(t)$ , it is clear that in order for the sequence of quantized samples  $\{m_q(nT_s)\}$  to increase as fast as the sequence of input samples  $\{m(nT_s)\}$  in a region of maximum slope of  $m(t)$ , we require that the condition

$$\frac{\Delta}{T_s} \geq \max \left| \frac{dm(t)}{dt} \right| \quad (5.33)$$

be satisfied. Otherwise, we find that the step size  $\Delta$  is too small for the staircase approximation  $m_q(t)$  to follow a steep segment of the original message signal  $m(t)$ , with the result that  $m_q(t)$  falls behind  $m(t)$ , as illustrated in Fig. 5.16. This condition is called *slope overload*. Correspondingly, the resulting quantization error is called *slope-overload distortion* (noise). Note that since the maximum slope of the staircase approximation  $m_q(t)$  is fixed by the step size  $\Delta$ , increases and decreases in  $m_q(t)$  tend to occur along straight lines, as illustrated in the front end of Fig. 5.16. For this reason, a delta modulator using a fixed value for the step size  $\Delta$  is often referred to as a *linear delta modulator*.

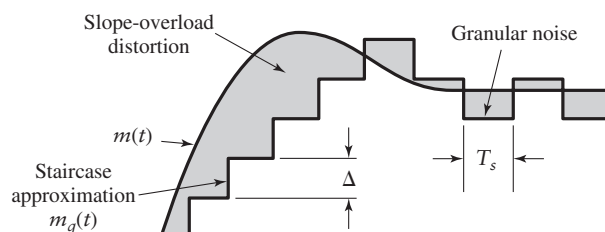


**FIGURE 5.16** Illustration of quantization errors, slope-overload distortion and granular noise, in delta modulation.

In contrast to slope-overload distortion, *granular noise* occurs when the step size  $\Delta$  is too large relative to the local slope characteristic of the original message signal  $m(t)$ . This second situation causes the staircase approximation  $m_q(t)$  to hunt around a relatively flat segment of  $m(t)$ , which is illustrated in the back end of Fig. 5.16. Granular noise in delta modulation may be viewed as the analog of quantization noise in pulse-code modulation.

► **Drill Problem 5.10** The best that a linear DM system can do is to provide a compromise between slope-overload distortion and granular noise. Justify this statement. ◀

From this discussion we see that there is a need to have a large step size to accommodate a wide dynamic range, whereas a small step size is required for the accurate representation of relatively low-level signals. It is therefore clear that if we are to choose an optimum step size that minimizes the average power<sup>4</sup> of the quantization error in a delta modulator, we need to make the DM system *adaptive*. This requirement, in turn, means that the step size has to vary in accordance with the incoming message signal.

### ■ DELTA-SIGMA MODULATION

As mentioned previously, the quantizer input in the conventional form of delta modulation may be viewed as an approximation to the *derivative* of the incoming message signal. This behavior leads to a drawback of delta modulation in that transmission disturbances such as noise result in an accumulative error in the demodulated signal. This drawback can be overcome by *integrating* the message signal prior to delta modulation. The use of integration also has other beneficial effects:

- The low-frequency content of the input signal is pre-emphasized.
- Correlation between adjacent samples of the delta modulator input is increased, which tends to improve overall system performance by reducing the average power of the error signal at the quantizer input.
- Design of the receiver is simplified.

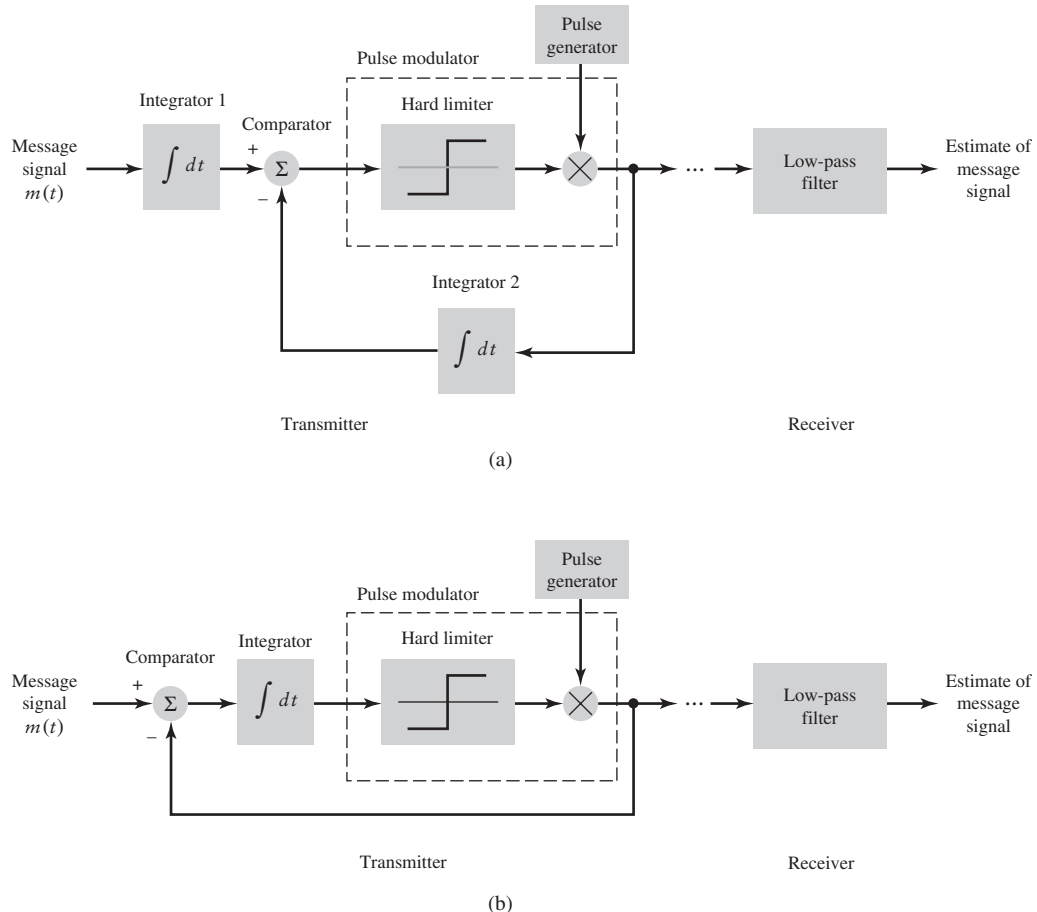
A delta modulation system that incorporates integration at its input is called *delta-sigma modulation* (D- $\Sigma$ M). To be more precise, however, it should be called *sigma-delta modulation*, because the integration is in fact performed before the delta modulation. Nevertheless, the former terminology is the one commonly used in the literature.

Figure 5.17(a) shows the block diagram of a delta-sigma modulation system. In this diagram, the message signal  $m(t)$  is defined in its continuous-time form, which means that the pulse modulator now consists of a hard-limiter followed by a multiplier; the latter component is also fed from an external pulse generator (clock) to produce a 1-bit encoded signal. The use of integration at the transmitter input clearly requires an inverse signal emphasis—namely, differentiation—at the receiver. The need for this differentiation is, however, eliminated because of its cancellation by integration in the conventional DM receiver. Thus, the receiver of a delta-sigma modulation system consists simply of a low-pass filter, as indicated in Fig. 5.17(a).

Moreover, we note that integration is basically a linear operation. Accordingly, we may simplify the design of the transmitter by combining the two integrators 1 and 2 of Fig. 5.17(a) into a single integrator placed after the comparator, as shown in Fig. 5.17(b).

---

<sup>4</sup>In statistical terms, the average power of a random process (exemplified by quantization error) is equal to the mean-square value of that process; this issue is discussed in Chapter 8.



**FIGURE 5.17** Two equivalent versions of delta-sigma modulation system: the system shown in part (b) of the figure is a simplified version of the system in part (a).

This latter form of implementing delta-sigma modulation is not only simpler than that of Fig. 5.17(a), but also it provides an interesting interpretation of delta-sigma modulation as a “smoothed” version of 1-bit pulse-code modulation. In this context, smoothing refers to the fact that the comparator output is integrated prior to quantization, and the term 1-bit pulse-code modulation merely restates the fact that the quantizer consists of a hard-limiter with only two representation levels.

## 5.8 Differential Pulse-Code Modulation

For yet another form of digital pulse modulation, we recognize that when a voice or video signal is sampled at a rate slightly higher than the Nyquist rate, the resulting sampled signal is found to exhibit a high degree of correlation between adjacent samples. The meaning of this high correlation is that, in an average sense, the signal does not change rapidly from one sample to the next, with the result that the difference between adjacent samples has an average power that is smaller than the average power of the signal itself. When

these highly correlated samples are encoded as in a standard PCM system, the resulting encoded signal contains *redundant information*. Redundancy means that symbols that are not absolutely essential to the transmission of information are generated as a result of the encoding process. By removing this redundancy before encoding, we obtain a more *efficient* encoded signal, compared to PCM.

Now, if we know a sufficient part of a redundant signal, we may *infer* the rest, or at least make the most probable estimate. In particular, if we know the past behavior of a signal up to a certain point in time, it is possible to make some inference about its future values; such a process is commonly called *prediction*. Suppose then a message signal  $m(t)$  is sampled at the rate  $f_s = 1/T_s$  to produce a sequence of correlated samples  $T_s$  seconds apart; this sequence is denoted by  $\{m(nT_s)\}$ . The fact that it is possible to predict future values of the signal  $m(t)$  provides motivation for the *differential quantization* scheme shown in Fig. 5.18(a). In this scheme, the input signal to the quantizer is defined by

$$e(nT_s) = m(nT_s) - \hat{m}(nT_s) \quad (5.34)$$

which is the difference between the input sample  $m(nT_s)$  and a prediction of it, denoted by  $\hat{m}(nT_s)$ . This predicted value is produced by using a *prediction filter* whose input, as we will see, consists of a quantized version of  $m(nT_s)$ . The difference signal  $e(nT_s)$  is called the *prediction error*, since it is the amount by which the prediction filter fails to predict the incoming message signal exactly. A simple and yet effective approach to implement the prediction filter is to use a *tapped-delay-line filter* or *discrete-time filter*, with the basic delay set equal to the sampling period. The block diagram of this filter is shown in Fig. 5.19, according to which the prediction  $\hat{m}(nT_s)$  is modeled as a linear combination of  $p$  past sample values of the quantized version of  $m(nT_s)$ , where  $p$  is the *prediction order*.

By encoding the quantizer output in Fig. 5.18(a), we obtain a variation of PCM, which is known as *differential pulse-code modulation* (DPCM). It is this encoded signal that is used for transmission.

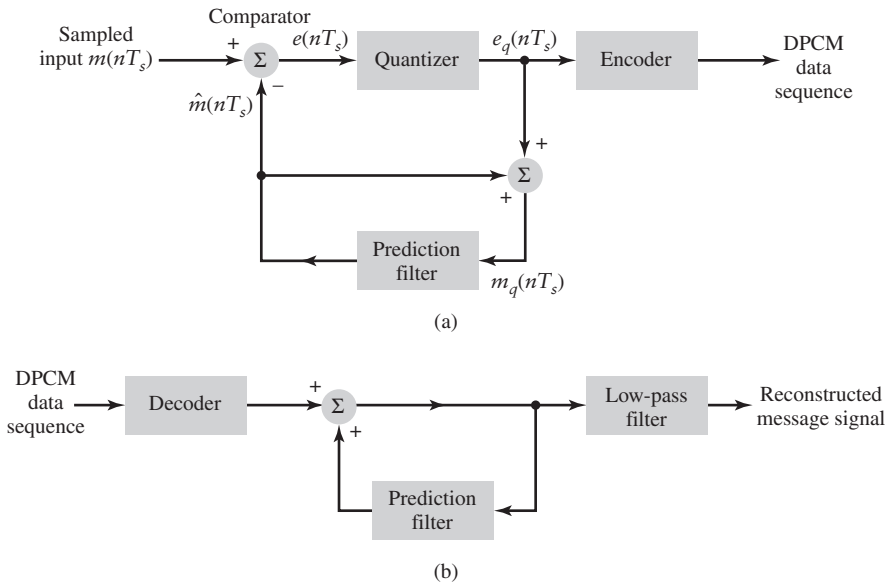
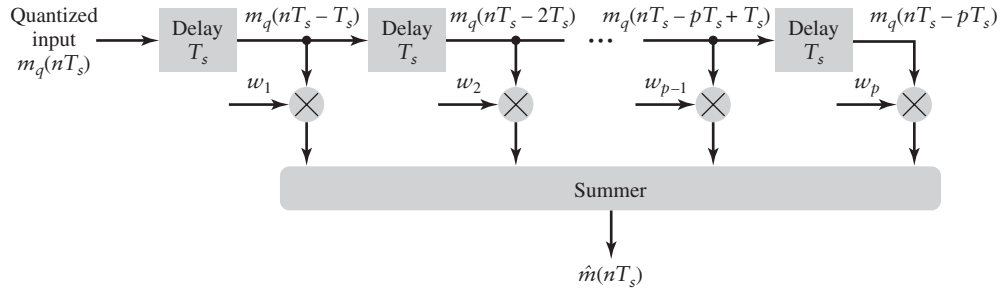


FIGURE 5.18 DPCM system: (a) Transmitter and (b) receiver.



**FIGURE 5.19** Tapped-delay line filter used as prediction filter.

The quantizer output may be expressed as

$$e_q(nT_s) = e(nT_s) + q(nT_s) \quad (5.35)$$

where  $q(nT_s)$  is the quantization error. According to Fig. 5.18(a), the quantizer output  $e_q(nT_s)$  is added to the predicted value  $\hat{m}(nT_s)$  to produce the prediction-filter input

$$m_q(nT_s) = \hat{m}(nT_s) + e_q(nT_s) \quad (5.36)$$

Substituting Eq. (5.35) into (5.36), we get

$$m_q(nT_s) = \hat{m}(nT_s) + e(nT_s) + q(nT_s) \quad (5.37)$$

However, from Eq. (5.34) we observe that the sum term  $\hat{m}(nT_s) + e(nT_s)$  is equal to the sampled message signal  $m(nT_s)$ . Therefore, we may rewrite Eq. (5.37) as

$$m_q(nT_s) = m(nT_s) + q(nT_s) \quad (5.38)$$

which represents a quantized version of the message sample  $m(nT_s)$ . That is, irrespective of the properties of the prediction filter, the quantized signal  $m_q(nT_s)$  at the prediction filter input differs from the sampled message signal  $m(nT_s)$  by the quantization error  $q(nT_s)$ . Accordingly, if the prediction is good, the average power of the prediction error  $e(nT_s)$  will be smaller than the average power of  $m(nT_s)$ , so that a quantizer with a given number of levels can be adjusted to produce a quantization error with a smaller average power than would be possible if  $m(nT_s)$  were quantized directly using PCM.

The receiver for reconstructing the quantized version of the message signal is shown in Fig. 5.18(b). It consists of a decoder to reconstruct the quantized error signal. The quantized version of the original input is reconstructed from the decoder output using the same prediction filter in the transmitter of Fig. 5.18(a). In the absence of channel noise, we find that the encoded signal at the receiver input is identical to the encoded signal at the transmitter output. Accordingly, the corresponding receiver output is equal to  $m_q(nT_s)$ , which differs from the original input  $m(nT_s)$  only by the quantization error  $q(nT_s)$  incurred as a result of quantizing the prediction error  $e(nT_s)$ . Finally, an estimate of the original message signal  $m(t)$  is obtained by passing the sequence  $m_q(nT_s)$  through a low-pass reconstruction filter.

From the foregoing analysis we thus observe that in a noise-free environment, the prediction filters in the transmitter and receiver operate on the same sequence of samples,  $\{m_q(nT_s)\}$ . With this very purpose in mind, a feedback path is added to the quantizer in the transmitter, as shown in Fig. 5.18(a).

Differential pulse-code modulation includes delta modulation as a special case. In particular, comparing the DPCM system of Fig. 5.18 with the DM system of Fig. 5.15, we see that they are basically similar, except for two important differences:

- ▶ The use of a one-bit (two-level) quantizer in the DM system.
- ▶ Replacement of the prediction filter in the DPCM by a single delay element (i.e., zero prediction order).

In other words, DM is the 1-bit version of DPCM. Note, however, that unlike a PCM system, the transmitters of both the DPCM and DM involve the use of *feedback*.

Insofar as noise is concerned, we may finally make the following two statements:

1. DPCM, like DM, is subject to slope-overload distortion whenever the input signal changes too rapidly for the prediction filter to track it.
2. Like PCM, DPCM suffers from quantization noise.

► **Drill Problem 5.11** Justify the two statements just made on sources of noise in a DPCM system. ◀

## 5.9 Line Codes

In reality, PCM, DM, and DPCM represent different strategies for source encoding, whereby an analog signal is converted into digital form. However, all three of them share a common feature: once a binary sequence of 1s and 0s is produced, a *line code* is needed for electrical representation of that binary sequence. There are several line codes that can be used for this representation, as summarized here:

1. *On-off signaling*, in which symbol 1 is represented by transmitting a pulse of constant amplitude for the duration of the symbol, and symbol 0 is represented by switching off the pulse, as in Fig. 5.20(a).
2. *Nonreturn-to-zero (NRZ) signaling*, in which symbols 1 and 0 are represented by pulses of equal positive and negative amplitudes, as illustrated in Fig. 5.20(b).
3. *Return-to-zero (RZ) signaling*, in which symbol 1 is represented by a positive rectangular pulse of half-symbol width, and symbol 0 is represented by transmitting *no* pulse, as illustrated in Fig. 5.20(c).
4. *Bipolar return-to-zero (BRZ) signaling*, which uses three amplitude levels as indicated in Fig. 5.20(d). Specifically, positive and negative pulses of equal amplitude are used alternately for symbol 1, and no pulse is always used for symbol 0. A useful property of BRZ signaling is that the power spectrum of the transmitted signal has no dc component and relatively insignificant low-frequency components for the case when symbols 1 and 0 occur with equal probability.
5. *Split-phase (Manchester code)*, which is illustrated in Fig. 5.20(e). In this method of signaling, symbol 1 is represented by a positive pulse followed by a negative pulse, with both pulses being of equal amplitude and half-symbol width. For symbol 0, the polarities of these two pulses are reversed. The Manchester code suppresses the dc component and has relatively insignificant low-frequency components, regardless of the signal statistics.
6. *Differential encoding*, in which the information is encoded in terms of signal transitions, as illustrated in Fig. 5.20(f). In the example of the binary PCM signal shown in the figure, a transition is used to designate symbol 0, whereas no transition is used to designate symbol 1. It is apparent that a differentially encoded signal may be inverted without affecting its interpretation. The original binary information is recovered by comparing the polarity of adjacent symbols to establish whether or not a transition has occurred. Note that differential encoding requires the use of a *reference bit*, as indicated in Fig. 5.20 (f).

The waveforms shown in parts (a) to (f) of Fig. 5.20 are drawn for the binary data stream 01101001. It is important, to note that rectangular pulse-shaping is used to draw these waveforms, largely to simplify the electrical representation. The benefits of using other pulse shapes for the transmission of PCM data are discussed in Chapter 6.

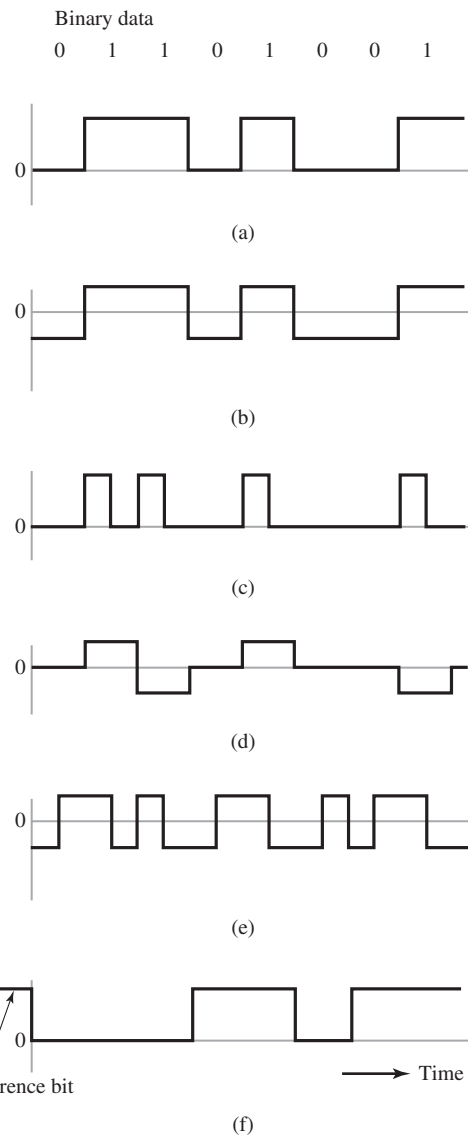


**FIGURE 5.20** Line codes. (a) On-off signaling, (b) Nonreturn-to-zero signaling, (c) Return-to-zero signaling, (d) Bipolar return-to-zero signaling, (e) Split-phase or Manchester encoding, (f) Differential encoding.

## 5.10 Theme Examples

### ■ TIME-DIVISION MULTIPLEXING

The sampling theorem provides the basis for transmitting the information contained in a band-limited message signal  $m(t)$  as a sequence of samples of  $m(t)$  taken uniformly at a rate that is usually slightly higher than the Nyquist rate. An important feature of the sampling process is a *conservation of time*. That is, the transmission of the message samples engages the communication channel for only a fraction of the sampling interval on a peri-

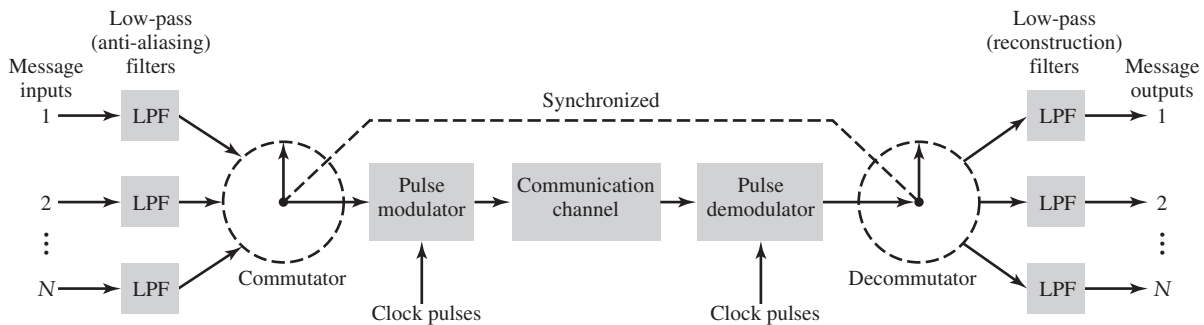


FIGURE 5.21 Block diagram of TDM system.

odic basis, and in this way some of the time interval between adjacent samples is cleared for use by other independent message sources on a time-shared basis. We thereby obtain a *time-division multiplex* (TDM) system, which enables the joint utilization of a common communication channel by a plurality of independent message sources without mutual interference among them.

The concept of TDM is illustrated by the block diagram shown in Fig. 5.21. Each input message signal is first restricted in bandwidth by a low-pass anti-aliasing filter to remove the frequencies that are nonessential to an adequate signal representation. The low-pass filter outputs are then applied to a *commutator*, which is usually implemented using electronic switching circuitry. The function of the commutator is twofold: (1) to take a narrow sample of each of the  $N$  input messages at a rate  $f_s$  that is slightly higher than  $2W$ , where  $W$  is the cutoff frequency of the anti-aliasing filter, and (2) to sequentially interleave these  $N$  samples inside the sampling interval  $T_s$ . Indeed, this latter function is the essence of the time-division multiplexing operation.

Following the commutation process, the multiplexed signal is applied to a *pulse modulator*, the purpose of which is to transform the multiplexed signal into a form suitable for transmission over the common channel. It is clear that the use of time-division multiplexing introduces a bandwidth expansion factor  $N$ , because the scheme must squeeze  $N$  samples derived from  $N$  independent message sources into a time slot equal to one sampling interval. At the receiving end of the system, the received signal is applied to a *pulse demodulator*, which performs the reverse operation of the pulse modulator. The narrow samples produced at the pulse demodulator output are distributed to the appropriate low-pass reconstruction filters by means of a *decommutator*, which operates in *synchronism* with the commutator in the transmitter. This synchronization is essential for a satisfactory operation of the system. The way this synchronization is implemented depends naturally on the method of pulse modulation used to transmit the multiplexed sequence of samples.

The TDM system is highly sensitive to dispersion in the common channel—that is, a non-constant magnitude response of the channel and a nonlinear phase response, both being measured with respect to frequency. Accordingly, *equalization* of both magnitude and phase responses of the channel is necessary so as to ensure a satisfactory operation of the system; in effect, equalization compensates for dispersion in the channel. (The subject of channel equalization is discussed in Chapter 6.) However, unlike frequency-division multiplexing (FDM) considered in Chapter 3, to a first-order approximation TDM is immune to nonlinearities in the channel as a source of cross-talk. The reason for this behavior is that different message signals are not simultaneously applied to the channel.

### Synchronization

In applications using PCM, for example, it is natural to multiplex different message sources by time division, whereby each source keeps its distinction from all other sources throughout the journey from the transmitter to the receiver. This individuality accounts for the comparative ease with which message sources may be dropped or reinserted in a time-division multiplex system. As the number of independent message sources is increased, the time interval that may be allotted to each source has to be reduced, since all of them must be accommodated into a time interval equal to the reciprocal of the sampling rate. This, in turn, means that the allowable duration of a codeword representing a single sample is reduced. However, pulses tend to become more difficult to generate and to transmit as their duration is reduced. Furthermore, if the pulses become too short, impairments in the transmission medium begin to interfere with the proper operation of the system. Accordingly, in practice, it is necessary to restrict the number of independent message sources that can be included within a time-division group.

In any event, for a PCM system with time-division multiplexing to operate satisfactorily, it is necessary that the timing operations at the receiver, except for the time lost in transmission and regenerative repeating, follow closely the corresponding operations at the transmitter. In a general way, this amounts to requiring a local clock at the receiver to keep the same time as a distant standard clock at the transmitter, except that the local clock is delayed by an amount equal to the time required to transport the message signals from the transmitter to the receiver. This delay, in turn, gives rise to a phase difference between the two clocks. One possible procedure to synchronize the transmitter and receiver clocks is to set aside a code element or pulse at the end of a *frame* (consisting of a code word derived from each of the independent message sources in succession) and to transmit this pulse every other frame only. In such a case, the receiver includes a circuit that would search for the pattern of 1s and 0s alternating at half the frame rate, and thereby establish synchronization between the transmitter and receiver.

When the transmission path is interrupted, it is highly unlikely that the transmitter and receiver clocks will continue to indicate the same time for long. Accordingly, in carrying out a synchronization process, we must set up an orderly procedure for detecting the synchronizing pulse. The procedure consists of observing the code elements one by one until the synchronizing pulse is detected. That is, after observing a particular code element long enough to establish the absence of the synchronizing pulse, the receiver clock is set back by one code element and the next code element is observed. This *searching process* is repeated until the synchronizing pulse is detected. Clearly, the time required for synchronization depends on the epoch at which proper transmission is re-established.

#### EXAMPLE 5.1 The T1 System

In this example, we describe the important characteristics of a PCM system known as the *T1 system*, which carries 24 voice channels over pairs of wires with regenerative repeaters spaced at approximately 2-km intervals. The T1 carrier system is basic to the North American digital switching hierarchy<sup>5</sup> for telephonic communication.

A voice signal (male or female) is essentially limited to a band from 300 to 3100 Hz in that frequencies outside this band do not contribute much to voice recognition and comprehension. Indeed, telephone circuits that respond to this range of frequencies give

<sup>5</sup>For a description of the digital switching hierarchy used in North America, see Haykin (2001), pp. 214–217.

quite satisfactory service. Accordingly, it is customary to pass the voice signal through a low-pass filter with a cutoff frequency of about 3.1 kHz prior to sampling. Hence, with  $W = 3.1$  kHz, the nominal value of the Nyquist rate is 6.2 kHz. The filtered voice signal is usually sampled at a slightly higher rate—namely, 8 kHz—which is the *standard* sampling rate in telephone systems.

For companding, the T1 system uses a *piecewise-linear* characteristic (consisting of 15 linear segments) to approximate the logarithmic  $\mu$ -law of Eq. (5.23) with the constant  $\mu = 255$ . This approximation is constructed in such a way that the segment end points lie on the compression curve computed from Eq. (5.23), and their projections onto the vertical axis are spaced uniformly.

There are a total of 255 representation levels associated with the 15-segment companding law. To accommodate this number of representation levels, each of the 24 voice channels uses a binary code with an 8-bit word. The first bit indicates whether the input voice sample is positive or negative; this bit is a 1 if positive and a 0 if negative. The next three bits of the code word identify the particular segment inside which the amplitude of the input voice sample lies, and the last four bits identify the actual representation level inside that segment.

With a sampling rate of 8 kHz, each frame of the T1 multiplexed signal occupies a period of 125  $\mu$ s. In particular, it consists of twenty-four 8-bit words, plus a single bit that is added at the end of the frame for the purpose of synchronization. Hence, each frame consists of a total of  $(24 \times 8) + 1 = 193$  bits. Correspondingly, the duration of each bit equals 0.647  $\mu$ s, and the resulting transmission rate is 1.544 megabits per second (Mb/s).

## ■ IMPULSE RADIO

Traditional digital transmission systems attempt to minimize the bandwidth of the transmitted signal. Hence, filtering is often applied to rectangular pulses to reduce the occupied bandwidth. However, a method that does not follow this philosophy and has captured attention recently is known as *impulse radio*. With this technique, information is sent by means of very narrow pulses that are widely separated in time. Since the pulse widths are very narrow, the spectrum of the resulting signal is very broad; consequently, this technique is a form of *ultra-wideband (UWB) radio transmission*, which forms the subject of our third and last theme example.

Specifically, one type of pulse used for impulse radio is the *Gaussian monocycle*. This pulse shape is the derivative of the scaled Gaussian pulse  $g(t) = \exp(-\pi t^2)$  discussed in Chapter 2. The waveform of the Gaussian monocycle is given by

$$\nu(t) = A \left( \frac{t}{\tau} \right) \exp \left\{ -\pi \left( \frac{t}{\tau} \right)^2 \right\} \quad (5.39)$$

where  $A$  is an amplitude scale factor and  $\tau$  is the time constant of the pulse. This signal is depicted in Fig. 5.22. It consists of a positive lobe followed by a negative lobe, with a pulse width of approximately  $\tau$ . For impulse radio applications, the pulse width  $\tau$  is typically between 0.20 and 1.50 nanoseconds.

The spectrum of a sequence of these pulses can be obtained from the Fourier transform of an individual pulse and this spectrum is shown in Fig. 5.23. The frequency axis in Fig. 5.23 has been normalized in terms of the time constant  $\tau$ ; for  $\tau = 1.0$  nanosecond, this frequency axis ranges from 0 to 4 GHz.

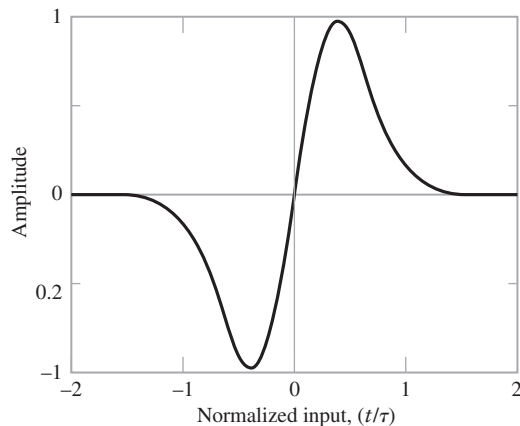


**FIGURE 5.22** Time-domain plot of Gaussian monocycle used for impulse radio.

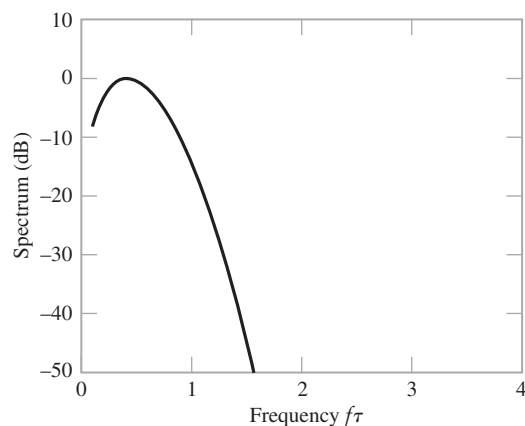


**FIGURE 5.23** Spectrum of Gaussian monocycle.

There are several methods for digitally modulating such an impulse wave. One method is pulse-position modulation as depicted in Fig. 5.24. (Pulse-position modulation was considered in Section 5.3.) With this method, there is a nominal time separation  $T_p$  between successive pulses. To transmit binary signal 0, the pulse is transmitted slightly early, at time  $t = -T_c$ . To transmit binary signal 1, the pulse is transmitted slightly late at time  $t = +T_c$ . The receiver detects this *early/late timing* and demodulates the data accordingly. Typical separations between pulses (i.e.,  $T_p$ ) range from 25 nanoseconds to 1000 nanoseconds, resulting in a range of data rates from 40 Mbit/s to 1 Mbit/s.

The ultra-wideband nature of the modulated signal has both good and bad aspects. Since the signal power is spread over a large bandwidth, the amount of power that falls in any particular narrowband channel is small, which is good. However, the power falls in all such narrowband channels, which is bad. In particular, there is the concern that ultra-wideband radios will cause harmful interference into existing narrowband radio services occupying the same radio spectrum. As a consequence, although ultra-wideband radio has been allowed in various jurisdictions, there are strict limits on the power spectra that may be transmitted. Due to this limitation on transmit power, ultra-wideband radio is restricted to short-range applications, typically less than a few hundred meters.<sup>6</sup>

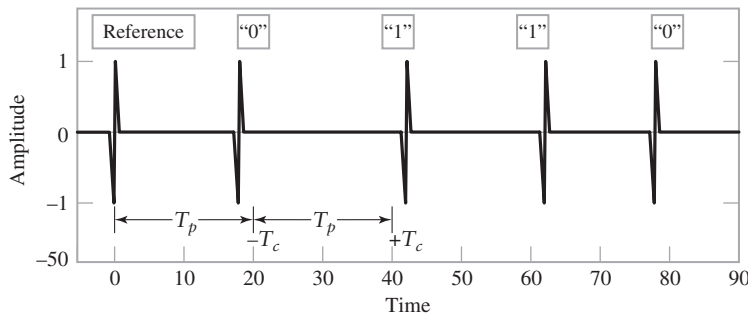


**FIGURE 5.24** Pulse-position modulation of impulse radio.

<sup>6</sup>For more detailed discussions of ultra-wideband radio, see the following two references: Win and Scholtz (1998) and Cassioli, Win, and Molisch (2002).

## 5.11 Summary and Discussion

In this chapter, we introduced two fundamental and complementary processes:

- ▶ *Sampling*, which operates in the time domain; the sampling process is the link between an analog waveform and its discrete-time representation.
- ▶ *Quantization*, which operates in the amplitude domain; the quantization process is the link between an analog waveform and its discrete-amplitude representation.

The sampling process builds on the *sampling theorem*, which states that a strictly band-limited signal with no frequency components higher than  $W$  Hz is represented uniquely by a sequence of samples taken at a uniform rate equal to or greater than the Nyquist rate of  $2W$  samples per second. As for the quantization process it exploits the fact that any human sense, as ultimate receiver, can only detect finite intensity differences.

The sampling process is basic to the operation of all pulse modulation systems, which may be classified into analog pulse modulation and digital pulse modulation. The distinguishing feature between them is that analog pulse modulation systems maintain a continuous amplitude representation of the message signal, whereas digital pulse modulation systems employ quantization to provide a representation of the message signal that is discrete in both time and amplitude.

Analog pulse modulation results from varying some parameter of the transmitted pulses, such as amplitude, duration, or position, in which case we speak of pulse-amplitude modulation (PAM), pulse-duration modulation (PDM), or pulse-position modulation (PPM), respectively.

Digital pulse modulation systems, on the other hand, transmit analog message signals as a sequence of coded pulses, which is made possible through the combined use of sampling and quantization. Pulse-code modulation is a form of digital pulse modulation that is endowed with some unique system advantages, which, in turn, have made it the preferred *method of encoding* for the transmission of such analog signals as voice and video signals. The advantages of pulse-code modulation include robustness to noise and interference, efficient regeneration of the encoded pulses along the transmission path, and a uniform format for different kinds of message signals. (i.e. voice, video, and data).

Delta modulation and differential pulse-code modulation are two other useful forms of digital pulse modulation. The principal advantage of delta modulation is simplified circuitry. However, this advantage is gained at the expense of increased data transmission rate. In contrast, differential pulse-code modulation employs increased circuit complexity to improve system performance. The improvement is achieved at the expense of increased system complexity, which facilitates the idea of prediction to remove redundant symbols from the incoming data stream, and thereby permit the use of reduced channel bandwidth compared to PCM.

Further improvements in the operations of delta modulation and differential pulse-code modulation can be made through the use of adaptivity to account for statistical variations in the input data. Specifically, adaptivity is used in delta modulation to improve noise performance. On the other hand, adaptivity is used in differential pulse-code modulation to reduce bandwidth requirement.

It is important to recognize that pulse modulation techniques are *lossy* in the sense that some information is lost as a result of the signal representation that they perform. For example, in pulse-amplitude modulation, the customary practice is to use anti-alias (low-pass) filtering prior to sampling; in so doing, information is lost by virtue of the fact that high-frequency components considered to be unessential are removed by the filter. The lossy nature of pulse modulation is most vividly seen in pulse-code modulation that is impaired by quantization

noise (i.e., distortion), which arises because the transmitted sequence of encoded pulses does not have the infinite precision needed to represent continuous samples exactly. Nevertheless, the loss of information incurred by the use of a pulse modulation process is *under the designer's control*, in that it can be made small enough for it to be nondiscernible by the end user.

A point that needs to be stressed one last time: In reality, PCM, DM, and DPCM are *source-encoding strategies*, whose purpose is to convert analog signals into digital form. For actual transmission of the encoded data over a communication channel, the discrete form of pulse-amplitude modulation (PAM) is typically used. (Details of this application of PAM are presented in the next chapter).

In the chapter, we also included three theme examples, addressing important applications summarized here:

- ▶ Time-division multiplexing, which enables the joint utilization of a communication channel by a multitude of independent message sources by building on an important feature of the sampling process—namely, the conservation of time.
- ▶ The T1 system, which accommodates the PCM transmission of 24 voice channels over pairs of wires with regenerative repeaters spaced at approximately 2-km intervals.
- ▶ Impulse radio, by means of which information is sent across a wireless channel at baseband, using very narrow pulses.

### ADDITIONAL PROBLEMS

---

- 5.12 (a)** Plot the spectrum of a PAM wave produced by the modulating signal

$$m(t) = A_m \cos(2\pi f_m t)$$

assuming the modulation frequency  $f_m = 0.2$  Hz, sampling period  $T_s = 1$  s, and pulse duration

$$T = 0.45 \text{ s}$$

- (b)** Using an ideal reconstruction filter, plot the spectrum of the filter output. Compare this result with the output that would be obtained if there were no aperture effect.

- 5.13** In this problem, we evaluate the equalization needed for the aperture effect in a PAM system. The operating frequency  $f = f_s/2$ , which corresponds to the highest frequency component of the message signal for a sampling rate equal to the Nyquist rate. Plot  $1/\text{sinc}(0.5T/T_s)$  versus  $T/T_s$ , and hence find the equalization needed when  $T/T_s = 0.25$ .

- 5.14** A PAM *telemetry* system involves the multiplexing of four input signals:  $s_i(t)$ ,  $i = 1, 2, 3, 4$ . Two of the signals  $s_1(t)$  and  $s_2(t)$  have bandwidths of 80 Hz each, whereas the remaining two signals  $s_3(t)$  and  $s_4(t)$  have bandwidths of 1 kHz each. The signals  $s_3(t)$  and  $s_4(t)$  are each sampled at the rate of 2400 samples per second. This sampling rate is divided by  $2^R$  (i.e., an integer power of 2) in order to derive the sampling rate for  $s_1(t)$  and  $s_2(t)$ .

- (a) Find the maximum value of  $R$ .
- (b) Using the value of  $R$  found in part (a), design a multiplexing system that first multiplexes  $s_1(t)$  and  $s_2(t)$  into a new sequence,  $s_5(t)$ , and then multiplexes  $s_3(t)$ ,  $s_4(t)$ , and  $s_5(t)$ .

- 5.15 (a)** A sinusoidal signal with an amplitude of 3.25 volts is applied to a uniform quantizer of the midtread type whose output takes on the values  $0, \pm 1, \pm 2, \pm 3$  volts. Sketch the waveform of the resulting quantizer output for one complete cycle of the input.

- (b)** Repeat this evaluation for the case when the quantizer is of the midrise type whose output takes on the values  $\pm 0.5, \pm 1.5, \pm 2.5, \pm 3.5$  volts.

- 5.16 Consider the following sequences of 1s and 0s:

- (a) An alternating sequence of 1s and 0s.
  - (b) A long sequence of 1s followed by a long sequence of 0s.
  - (c) A long sequence of 1s followed by a single 0 and then a long sequence of 1s.
- Sketch the waveform for each of these sequences using the following methods of representing symbols 1 and 0:
- (a) On-off signaling.
  - (b) Bipolar return-to-zero signaling.

- 5.17 The sinusoidal wave

$$m(t) = 6 \sin(2\pi t) \text{ volts}$$

is transmitted using a 4-bit binary PCM system. The quantizer is of the midrise type, with a step size of 1 volt. Sketch the resulting PCM wave for one complete cycle of the input. Assume a sampling rate of four samples per second, with samples taken at  $t = \pm 1/8, \pm 3/8, \pm 5/8, \dots$ , seconds.

- 5.18 Consider a compact disc that uses pulse-code modulation to record audio signals whose bandwidth  $W = 15$  kHz. Specifications of the modulator include the following:

- Quantization: uniform with 512 levels  
Encoding: binary

Determine (a) the Nyquist rate, and (b) the minimum permissible bit rate.

- 5.19 This problem addresses the digitization of a television signal using pulse-code modulation. The signal bandwidth is 4.5 MHz. Specifications of the modulator include the following:

- Sampling: 15% in excess of the Nyquist rate  
Quantization: uniform with 1024 levels  
Encoding: binary

Determine (a) the Nyquist rate, and (b) the minimum permissible bit rate.

- 5.20 Figure 5.25 shows a PCM signal in which the amplitude levels of +1 volt and -1 volt are used to represent binary symbols 1 and 0, respectively. The code word used consists of three bits. Find the sampled version of an analog signal from which this PCM signal is derived.

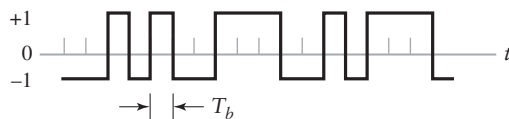


**FIGURE 5.25** Problem 5.20

- 5.21 Consider a sinusoidal wave of frequency  $f_m$  and amplitude  $A_m$ , applied to a delta modulator of step size  $\Delta$ . Show that slope-overload distortion will occur if

$$A_m > \frac{\Delta}{2\pi f_m T_s}$$

where  $T_s$  is the sampling period. What is the maximum power that may be transmitted without slope-overload distortion?

- 5.22 Consider a delta modulation (DM) system used to transmit a voice signal, which is uniformly sampled at the rate of 64 kHz. Assume the following specifications:

$$\begin{aligned} \text{Voice signal bandwidth} &= 3.1 \text{ kHz} \\ \text{Maximum signal amplitude} &= 10 \text{ volts} \end{aligned}$$

- (a) To avoid slope overload distortion, what is the minimum permissible value of the step size  $\Delta$  used in the system?
- (b) Determine the average power of granular noise.
- (c) Determine the minimum-channel bandwidth needed to transmit the DM encoded data.
- 5.23 Repeat Problem 5.22, this time using a sinusoidal wave of frequency = 3.1 kHz and peak amplitude = 10 volts.
- 5.24 In the DPCM system depicted in Fig. 5.26, show that in the absence of channel noise, the transmitting and receiving prediction filters operate on slightly different input signals.

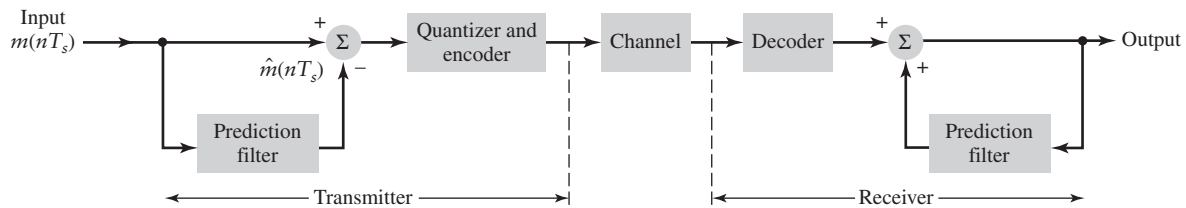


FIGURE 5.26 Problem 5.24

### ADVANCED PROBLEMS

- 5.25 (a) Given any physical signal, it is not possible to sample the signal without impairment due to the aliasing phenomenon.
- (b) The best that a designer can do is to manage the aliasing problem in such a way that the impairment is not discernible by a human user.  
Justify the validity of these two statements.
- 5.26 In *natural sampling*, an analog signal  $g(t)$  is multiplied by a periodic train of rectangular pulses  $c(t)$ . Given that the pulse-repetition frequency of this periodic train is  $f_s$  and the duration of each rectangular pulse is  $T$  (with  $f_s T \gg 1$ ), do the following:
- Find the spectrum of the signal  $s(t)$  that results from the use of natural sampling; you may assume that  $t = 0$  corresponds to the midpoint of a rectangular pulse in  $c(t)$ .
  - Show that the original signal  $g(t)$  may be recovered exactly from its naturally sampled version, provided that the conditions embodied in the sampling theorem are satisfied.
- 5.27 Figure 5.27 shows the block diagram of a *bipolar chopper*. The chopper has two parallel paths, one direct and the other inverting. The commutator at the output switches back and forth between these two paths at a frequency denoted by  $f_s$ . The chopper produces an output signal  $y(t)$  in response to the input signal  $x(t)$ .

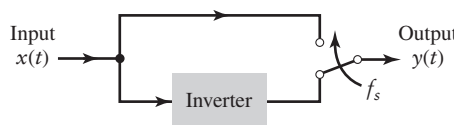
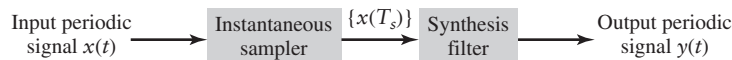


FIGURE 5.27 Problem 5.27

- Determine  $y(t)$  in terms of  $x(t)$ .
- Given that  $X(f)$  is the Fourier transform of  $x(t)$ , determine the Fourier transform of  $y(t)$ . Use graphical displays to illustrate your answers.

- 5.28 Figure 5.28 shows a subsystem consisting of an instantaneous sampler followed by a synthesis filter, which is used in a *sampling oscilloscope*. The subsystem is designed to exploit the aliasing phenomenon for the expanded display of arbitrary periodic signals. Assume that the input periodic signal  $x(t)$  has been prefiltered (not shown in Fig. 5.28) to suppress all frequency components higher than the  $m$ th harmonic.



**FIGURE 5.28** Problem 5.28

Specifically, the input periodic signal  $x(t)$  is sampled at a rate  $f_s$  slightly smaller than its fundamental frequency  $f_0$ , as shown by

$$f_s = (1 - a)f_0$$

where the factor  $a$  lies in the interval  $0 < a < 1$ . In so doing, aliasing is purposely introduced into the composition of the sample sequence  $\{x(nT_s)\}$ , where  $n = 0, \pm 1, \pm 2, \dots$ , and  $T_s = 1/f_s$ . The sequence  $\{x(nT_s)\}$  is next processed by the low-pass synthesis filter of cutoff frequency  $B = f_s/2$ , thereby producing the output periodic signal  $y(t)$ .

Use graphical plots to illustrate the relationships between  $x(t)$  and  $y(t)$  and their respective spectra  $X(f)$  and  $Y(f)$ , and include the following:

- (a) Show that the output signal is an *expanded* version of the input signal, as shown by

$$y(t) = x(at)$$

- (b) To prevent spectral overlap, the expansion factor  $a$  must satisfy the condition

$$a < \frac{1}{2m + 1}$$

- (c) The spectrum  $Y(f)$  contains a *compressed* image of the spectrum  $X(f)$ .

- 5.29 In a television set, the video signal is produced by capturing 60 still frames of a scene per second; hence, the sampling period of the video signal is  $T_s = 1/60$  second. This means that a given point on the television screen is actually dark most of the time; the point is lit periodically every  $1/60$  second. The light emitted by the television set makes for an interesting experiment on the aliasing phenomenon experienced in uniform sampling of the complex sinusoid  $\exp(j2\pi ft)$ .

Suppose that the television screen is masked off, except for a narrow horizontal strip, and we sit with our back to the television. To see what is happening on the television, we use a mirror that rotates counterclockwise about the horizontal axis. Demonstrate the following two possible results:

- (a) The horizontal strip will appear still if the rotation speed of the mirror matches the sampling rate of the video signal.  
 (b) Otherwise, the horizontal strip on the television screen will appear in the mirror as though it is rotating backwards.

(Note: The experiment described in Problem 5.29 shows how a television set can be used to demonstrate the way in which a device called the *stroboscope* works.)

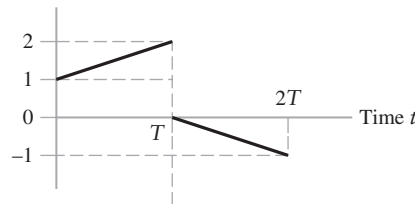
- 5.30 In Section 5.2, we discussed the interpolation of a sample sequence based on the sample-and-hold filter. In the control literature, this interpolation filter is referred to as the *zero-order hold*. A more complex interpolation filter called the *first-order hold* may be preferred to the zero-order hold. As the name implies, the first-order hold performs interpolation between data points by a first-order polynomial—namely, a straight line.

Figure 5.29 depicts the impulse response  $h(t)$  of a first-order hold filter to a pulse of unit amplitude and duration  $T$ .

- (a) Show that the frequency response of the first-order hold filter is given by

$$H(f) = T \left( \frac{1 - \exp(-j2\pi fT)}{j2\pi fT} \right)^2 (1 + j2\pi fT)$$

- (b) Plot the magnitude and phase responses of the first-order hold filter, and compare them to the sample-and-hold filter.
- (c) Determine the transfer function of the equalizer that needs to be cascaded with the first-order hold filter for perfect reconstruction of the message signal. Compare your result with the equalization needed for the sample-and-hold filter for a duty cycle  $(T/T_s) \leq 0.1$ . Comment on your results.
- (d) Plot the response of the first-order hold filter to the sinusoidal input  $\cos(50t)$ , assuming  $f_s = 100$  Hz and  $T = 0.01$ . Compare your result with that produced by the sample-and-hold filter. Here again, comment on what the comparison teaches us.



**FIGURE 5.29** Problem 5.30

- 5.31 In this problem, we address derivation of the Gaussian monocycle  $v(t)$  of Eq. (5.39) and its spectrum plotted in Fig. 5.23.

To be specific, consider the unit Gaussian pulse

$$g(t) = \exp(-\pi t^2)$$

which is its own Fourier transform, as shown by

$$G(f) = \exp(-\pi f^2)$$

(For details of this Fourier-transform pair, see Example 2.6).

Differentiating  $g(t)$  with respect to time  $t$ , we get the corresponding Gaussian monocycle

$$g'(t) = -2\pi t \exp(-\pi t^2)$$

where the prime signifies differentiation.

- (a) Applying the linearity and dilation properties of the Fourier transform to  $g'(t)$ , derive the  $v(t)$  of Eq. (5.39). What is the value of parameter  $A$  of the pulse in Fig. 5.22?
- (b) Building on the results of part (a) and making use of the differentiation property of the Fourier transform, derive the formula used to plot the spectrum of  $v(t)$  shown in Fig. 5.23.

The properties of the Fourier transform referred to in parts (a) and (b) are discussed in Chapter 2.

## CHAPTER 6

# BASEBAND DATA TRANSMISSION

The transmission of digital data (regardless of their origin) over a physical communication channel is limited by two unavoidable factors:

1. *Intersymbol interference*, which arises due to imperfections in the frequency response of the channel.
2. *Channel noise*, which refers to unwanted electric signals that arise at the channel output due to random and unpredictable physical phenomena.

In this chapter, we focus attention on the intersymbol interference problem. The discussion of noise in digital communication receivers is deferred to the latter part of the book.

As the name implies, intersymbol interference refers to interference caused by the time response of the channel spilling over from one symbol into adjacent symbols. Intersymbol interference is troublesome because it has the effect of introducing deviations (i.e., errors) between the data sequence reconstructed at the receiver output and the original data sequence applied to the transmitter input. Hence, unless corrective measures are taken, intersymbol interference could impose a limit on the attainable rate of data transmission across the channel, which is below the physical capability of the channel.

With intersymbol interference acting as an issue of practical concern, we will study an important corrective measure to deal with it—namely, *baseband pulse shaping*. This measure involves the use of band-limited pulses that are shaped in a special manner so as to mitigate the intersymbol interference problem; this corrective measure builds on prior knowledge about the channel.

The chapter will teach us three lessons:

- *Lesson 1: Understanding of the intersymbol interference problem and how to cure it is of fundamental importance to the design of digital communication systems.*
- *Lesson 2: The raised cosine spectrum provides a powerful mathematical tool for baseband pulse-shaping designed to mitigate the intersymbol interference problem.*
- *Lesson 3: The eye pattern is a visual indicator of performance, displaying the physical limitations of a digital data transmission system in an insightful manner.*

## 6.1 Baseband Transmission of Digital Data

From Chapter 1, we recall that the term “baseband” is used to designate the band of frequencies representing the original signal delivered by a source of information. The source of information, for example, could be a computer that produces a stream of binary data made up of the symbols 0 and 1. The task of a digital communication system is to transport the data stream from the source to its destination over a channel and do so in a reliable manner. To accomplish this task, we need to use a modulation technique that involves varying the amplitude, phase or frequency of transmitted pulses in accordance with the raw data in some discrete manner. In this chapter, we emphasize the use of *discrete pulse-amplitude modulation*, which is a form of pulse-amplitude modulation (previously discussed in Chapter 5) with the amplitude being quantized into a set of discrete levels. There are three reasons for this emphasis:

1. Discrete pulse-amplitude modulation is simple to analyze.
2. It is the most efficient form of discrete pulse modulation in terms of both power and bandwidth use.
3. The analytic techniques developed for handling discrete pulse-amplitude modulation may be extended to other discrete-pulse modulation techniques using phase or frequency.

In *discrete pulse-amplitude modulation (PAM)*, the amplitude of transmitted pulses is varied in a discrete manner in accordance with an input stream of digital data. Figure 6.1(a) depicts the basic functional blocks of a *baseband PAM system*. The input binary data stream is denoted by  $\{b_k\}$ . At time  $t = kT_b$ , where  $T_b$  is the *bit duration* and  $k = 0, \pm 1, \pm 2, \dots$ ; the element  $b_k$ , representing binary symbol 1 or 0, is emitted by the *source of information*. The binary data stream  $\{b_k\}$  is applied to a *line encoder*, the purpose of which is to produce a level-encoded signal denoted by  $\{a_k\}$ . (Line codes were described

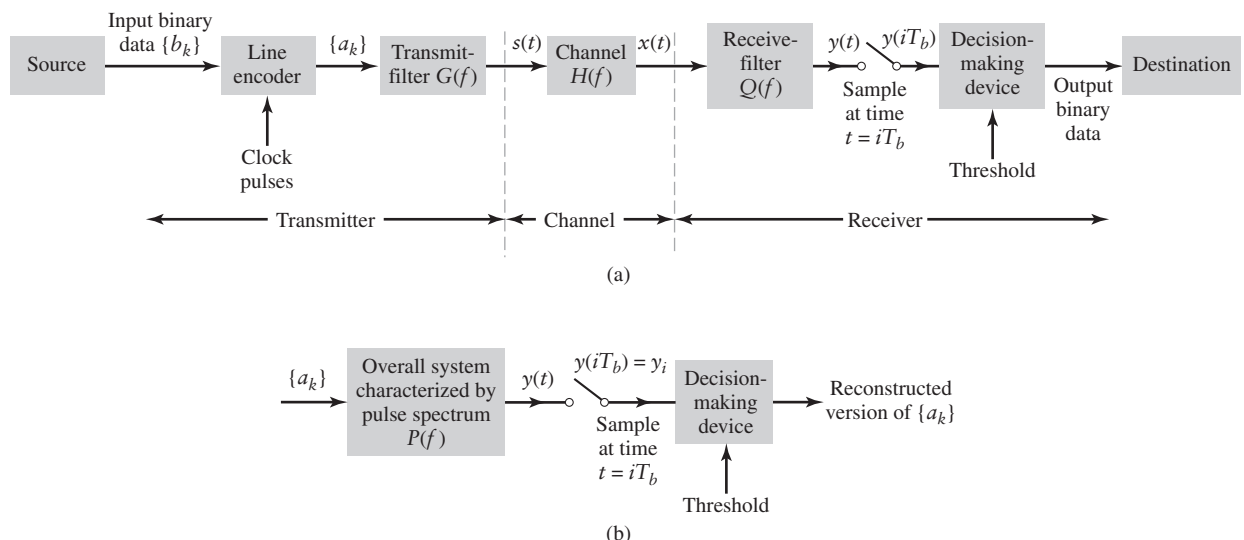


**FIGURE 6.1** Baseband binary data transmission. (a) Block diagram of the system, depicting its constituent components all the way from the source to destination. (b) Simplified representation of the system.

in Chapter 5.) For example, we may define level-encoded signal  $\{a_k\}$  in terms of positive and negative pulses of fixed amplitude and short duration (short enough for the two pulses to be viewed as unit impulses of opposite polarities). Specifically, we write

$$a_k = \begin{cases} +1 & \text{if the input } b_k \text{ is symbol 1} \\ -1 & \text{if the input } b_k \text{ is symbol 0} \end{cases} \quad (6.1)$$

The level-encoded signal  $\{a_k\}$  is applied to a *transmit filter* to produce a sequence of pulses, whose basic shape is denoted in the time and frequency domains by  $g(t)$  and  $G(f)$ , respectively. In effect, the level-encoded signal  $\{a_k\}$  plays the role of a modulating signal, with the result that the discrete PAM signal is defined by

$$s(t) = \sum_{k=-\infty}^{\infty} a_k g(t - kT_b) \quad (6.2)$$

The PAM signal  $s(t)$  is transmitted across a *linear communication channel*, which is described in the time and frequency domains by the impulse response  $h(t)$  and transfer function  $H(f)$ , respectively. Putting aside the effect of additive channel noise, we may express the channel output as

$$x(t) = s(t) \star h(t) \quad (6.3)$$

where the symbol  $\star$  denotes convolution in the time domain.

The channel output  $x(t)$  is processed by a *receive-filter*, which is described in the time and frequency domains by the impulse response  $q(t)$  and transfer function  $Q(f)$ , respectively. The resulting output is therefore defined by the convolution of  $x(t)$  and  $q(t)$  —namely,

$$y(t) = x(t) \star q(t) \quad (6.4)$$

The filter output  $y(t)$  is next *sampled synchronously* with the *generator of clock pulses* in the transmitter; synchronization is commonly established by extracting a *clock* or *timing signal* from the receive-filter output. Finally, the sequence of samples thus obtained is used to reconstruct the original binary data stream by means of a *decision-making device*. Specifically, the amplitude of each sample is compared to a *threshold*. If the threshold is exceeded, a decision is made in favor of symbol 1, say. If the threshold is not exceeded, a decision is made in favor of symbol 0. If the sample amplitude equals the threshold exactly, the symbol may be chosen as 0 or 1 through the flip of a fair coin without affecting overall performance. For the case when symbols 0 and 1 are equiprobable, it is reasonable to set the threshold at the zero amplitude level.

The model shown in Fig. 6.1(a) represents not only a data transmission system inherently baseband in nature (e.g., data transmission over a coaxial cable) but also the *baseband equivalent* of a linear modulation system used to transmit data over a band-pass channel (e.g., telephone channel). In the latter case, the baseband equivalent model of the data transmission system is developed by using the ideas presented in Section 3.8.

## 6.2 The Intersymbol Interference Problem

As already mentioned, for the present discussion we ignore the effect of additive channel noise. We do so in order to focus attention on the effects of imperfections in the frequency response of the channel (i.e., dispersion of the pulse shape by the channel) on data transmission through the channel.

Using Eqs. (6.2) through (6.4), except for a scaling factor, we may express the *receive-filter output* as the modified PAM signal

$$y(t) = \sum_{k=-\infty}^{\infty} a_k p(t - kT_b) \quad (6.5)$$

Linearity of the data transmission depicted in Fig. 6.1 leads us to express the *overall pulse shape*  $p(t)$  in Eq. (6.5) by the multiple convolution product

$$p(t) = g(t) \star h(t) \star q(t) \quad (6.6)$$

Naturally, the received pulse  $p(t)$  has a shape different from that of the transmitted signal  $s(t)$  of Eq. (6.2). Let the spectrum  $P(f)$  denote the Fourier transform of the pulse  $p(t)$ . Then, in the frequency domain, we may equivalently write

$$P(f) = G(f)H(f)\mathcal{Q}(f) \quad (6.7)$$

As remarked previously, the receive-filter output  $y(t)$  of Eq. (6.5) is sampled synchronously with the transmitter. Let<sup>1</sup>

$$y(iT_b) = \sum_{k=-\infty}^{\infty} a_k p[(i - k)T_b], \quad i = 0, \pm 1, \pm 2, \dots$$

denote the sample of  $y(t)$  produced at time  $t = iT_b$ . To simplify the presentation, we introduce the discrete-time shorthand notation:

$$y_i = y(iT_b)$$

and, correspondingly,

$$p_i = p(iT_b)$$

We thus rewrite the sample of  $y(t)$  at time  $t = iT_b$  compactly as the *discrete convolution sum*

$$y_i = \sum_{k=-\infty}^{\infty} a_k p_{i-k}, \quad i = 0, \pm 1, \pm 2, \dots \quad (6.8)$$

Referring to Fig. 6.1(a), we see that  $y_i = y(iT_b)$  is the input to the decision-making device. Define

$$p_0 = p(0) = \sqrt{E} \quad (6.9)$$

where  $E$  is the *transmitted signal energy per bit (symbol)*. The index  $i$  refers to the instant at which the receive-filter output is sampled in the receiver, whereas the index  $k$  refers to a symbol in the data stream produced by the source of information at the transmitted input. Thus, isolating the term representing  $k = i$  in Eq. (6.8), we may equivalently write

$$y_i = \sqrt{E}a_i + \sum_{\substack{k=-\infty \\ k \neq i}}^{\infty} a_k p_{i-k}, \quad i = 0, \pm 1, \pm 2, \dots \quad (6.10)$$

In Eq. (6.10), the first term  $a_i$  represents the transmitted binary symbol, except for the scaling factor  $\sqrt{E}$ . The second term, involving the combined effect of all other transmitted

---

<sup>1</sup>In practice, it may be preferable to sample the receive-filter output  $y(t)$  at times  $t = iT_b + t_0$  rather than  $t = iT_b$ . The reason for doing so is the unavoidable presence of delay and distortion in the overall pulse response  $p(t)$ . To simplify the presentation, we have ignored this effect.

binary symbols before and after  $a_i$ , represents a residual phenomenon called the *intersymbol interference* (ISI). In the absence of ISI (and the assumed absence of channel noise), Eq. (6.10) reduces to the ideal condition

$$y_i = \sqrt{E}a_i, \quad \text{for all } i$$

which, of course, represents perfect decoding.

The *pulse-shaping problem* involved in designing the PAM system of Fig. 6.1(a) may now be stated as follows (ignoring the effect of channel noise):

*Given the channel transfer function  $H(f)$ , determine the transmit-pulse spectrum  $G(f)$  and receive-filter transfer function  $Q(f)$  so as to satisfy two basic requirements:*

- (i) *Intersymbol interference is reduced to zero.*
- (ii) *Transmission bandwidth is conserved.*

To satisfy both of these requirements, we have to exercise control over the overall pulse shape  $p(t)$  in the time domain or, equivalently, the overall pulse spectrum  $P(f)$  in the frequency domain. The key question is how this control is actually exercised.

## 6.3 The Nyquist Channel

In light of Eqs. (6.5) and (6.7), we may replace the PAM system of Fig. 6.1(a) with the simpler PAM configuration depicted in part (b) of the figure. The distinctive feature of Fig. 6.1(b) is its focus on the overall pulse spectrum  $P(f)$ .

For the *optimum solution* to the pulse-shaping problem, the condition for zero intersymbol interference would have to be satisfied at the *minimum* transmission bandwidth possible. With  $y_i = a_i$  for all  $i$  defining the condition for zero intersymbol interference, we infer from Eq. (6.10) that it is necessary for the overall pulse shape  $p(t)$ , the inverse Fourier transform of the pulse spectrum  $P(f)$  in Fig. 6.1(b), to satisfy the condition

$$p_i = p(iT_b) = \begin{cases} \sqrt{E}, & \text{for } i = 0 \\ 0, & \text{for all } i \neq 0 \end{cases} \quad (6.11)$$

Equation (6.11) implies sampling  $p(t)$  at a uniform rate equal to the *bit rate*  $1/T_b$ . Suppose that  $p(t)$  is band-limited to frequencies in the interval  $-B_0 < f < B_0$ , where  $B_0$  is to be defined. Then, invoking the *interpolation formula* of Eq. (5.7) that is embodied in the *sampling theorem*, we may express the pulse shape  $p(t)$  in terms of its sample values as

$$p(t) = \sum_{i=-\infty}^{\infty} p\left(\frac{i}{2B_0}\right) \operatorname{sinc}(2B_0t - i) \quad (6.12)$$

Suppose the bandwidth  $B_0$  is related to the bit rate  $1/T_b$  as

$$B_0 = \frac{1}{2T_b} \quad (6.13)$$

Then substituting Eq. (6.11) into Eq. (6.12), we obtain the *sinc function*

$$\begin{aligned} p_{\text{opt}}(t) &= \sqrt{E} \operatorname{sinc}(2B_0t) \\ &= \frac{\sqrt{E} \sin(2\pi B_0 t)}{2\pi B_0 t} \end{aligned} \quad (6.14)$$

as the *optimum pulse shape*.

► **Drill Problem 6.1** The pulse shape  $p(t)$  of a baseband binary PAM system is defined by

$$p(t) = \text{sinc}\left(\frac{t}{T_b}\right)$$

where  $T_b$  is the bit duration of the input binary data. The amplitude levels at the pulse generator output are  $+1$  or  $-1$ , depending on whether the binary symbol at the input is  $1$  or  $0$ , respectively. Describe the waveform at the output of the receiving filter in response to the input data sequence  $001101001$ . ◀

The overall pulse spectrum is defined by the *optimum brick-wall function*

$$P_{\text{opt}}(f) = \begin{cases} \frac{\sqrt{E}}{2B_0}, & \text{for } -B_0 < f < B_0 \\ 0, & \text{otherwise} \end{cases} \quad (6.15)$$

Parts (a) and (b) of Fig. 6.2, respectively, plot the optimum spectrum  $P_{\text{opt}}(f)$  and its inverse  $p_{\text{opt}}(t)$ .

The important points to take from the idealized plots of Fig. 6.2 are twofold:

1. The brick-wall spectrum  $P_{\text{opt}}(f)$  defines  $B_0$  as the *minimum transmission bandwidth for zero intersymbol interference*. That is, the optimum solution for the pulse-shaping problem involves no frequencies of absolute value exceeding half the bit rate. The parameter  $B_0$  defined in accordance with Eq. (6.13) is called the *Nyquist bandwidth*. Correspondingly, the PAM system of Fig. 6.1(b) with the optimum pulse spectrum  $P_{\text{opt}}(f)$  defined by Eq. (6.15) is called the *Nyquist channel*.
2. The optimum pulse shape  $p_{\text{opt}}(t)$  is the impulse response of an ideal low-pass channel with an amplitude response of  $P_{\text{opt}}(f)$  in the passband and a bandwidth  $B_0$ . Being defined as a sinc function,  $p_{\text{opt}}(t)$  has its peak value at the origin and goes through zero at integer multiples of the bit duration  $T_b$ . On this basis, the pulses defined by  $p_{\text{opt}}(t - kT_b)$  in Eq. (6.5) with  $k = 0, \pm 1, \pm 2, \dots$ , will not interfere with each other.

In short, the Nyquist channel defined by the overall pulse spectrum  $P(f)$  of Eq. (6.15) is the *optimum solution for zero intersymbol interference at the minimum transmission bandwidth possible* in a noise-free environment.

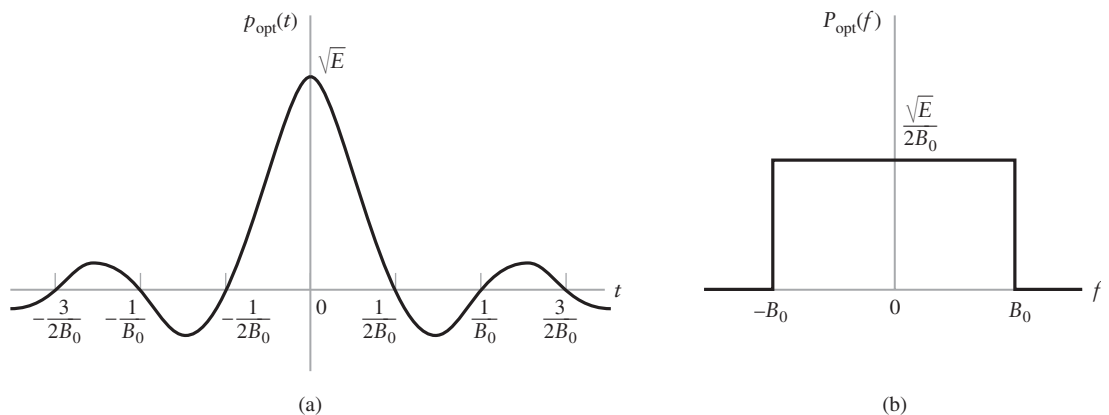


**FIGURE 6.2** (a) Sinc function  $p(t)$  as the optimum pulse shape. (b) Optimum pulse spectrum.

Although the Nyquist channel is indeed the optimum solution to the pulse-shaping problem, there are two difficulties that make its use for a PAM system impractical:

1. The system requires that the spectrum  $P(f)$  be flat from  $-B_0$  to  $B_0$ , and zero elsewhere. This is physically unrealizable, and very difficult to approximate in practice because of the abrupt transitions at  $\pm B_0$ .
2. The time function  $p(t)$  decreases as  $1/|t|$  for large  $|t|$ , resulting in a slow rate of decay. This is caused by the discontinuity of  $P(f)$  at  $\pm B_0$ . Accordingly, there is practically *no margin of error* in sampling times in the receiver.

To pursue the *timing error problem* under point 2, consider Eq. (6.5) and sample the  $y(t)$  at  $t = \Delta t$ , where  $\Delta t$  is the timing error. To simplify the analysis, we shall put the correct sampling time  $iT_b$  equal to zero. We thus obtain (in the absence of channel noise)

$$y(\Delta t) = \sqrt{E} \sum_{k=-\infty}^{\infty} a_k p(\Delta t - kT_b), \quad \text{for } iT_b = 0$$

Setting  $p(t)$  equal to the optimum value defined in the first line of Eq. (6.14) yields

$$y(\Delta t) = \sum_{k=-\infty}^{\infty} a_k \operatorname{sinc}[2B_0(\Delta t - kT_b)]$$

With  $2B_0 T_b = 1$  in accordance with Eq. (6.13), we may simplify the expression for  $y(\Delta t)$  into

$$\begin{aligned} y(\Delta t) &= \sqrt{E} \sum_{k=-\infty}^{\infty} a_k \operatorname{sinc}(2B_0 \Delta t - k) \\ &= \sqrt{E} a_0 \operatorname{sinc}(2B_0 \Delta t) + \sqrt{E} \sum_{\substack{k=-\infty \\ k \neq 0}}^{\infty} a_k \frac{\sin(2\pi B_0 \Delta t - \pi k)}{2\pi B_0 \Delta t - \pi k} \end{aligned}$$

where, in the second line, we have done two things: isolate the term corresponding to  $k = 0$ , and use the formula for the sinc function. Next, using the trigonometric identity

$$\sin(2\pi B_0 \Delta t - \pi k) = \sin(2\pi B_0 \Delta t) \cos(\pi k) - \cos(2\pi B_0 \Delta t) \sin(\pi k)$$

with  $\cos(\pi k) = (-1)^k$  and  $\sin(\pi k) = 0$  for all  $k$ , we may go one step further and write

$$y(\Delta t) = \sqrt{E} a_0 \operatorname{sinc}(2B_0 \Delta t) + \sqrt{E} \left( \frac{\sin(2\pi B_0 \Delta t)}{\pi} \right) \sum_{\substack{k=-\infty \\ k \neq 0}}^{\infty} \frac{(-1)^k a_k}{2B_0 \Delta t - k} \quad (6.16)$$

The first term on the right-hand side of Eq. (6.16) defines the desired binary symbol, whereas the remaining series represents the *intersymbol interference caused by the timing error*  $\Delta t$  in sampling the signal  $y(t)$ . The intersymbol interference so caused decays at the rate  $1/\Delta t$ . Moreover, depending on the value of  $\Delta t$ , it is possible for this series to diverge, thereby causing erroneous decisions in the receiver.

To mitigate the problems due to physical realizability of the Nyquist channel and zero timing error, we therefore have to look to other pulse shapes. In the next section, we present one such solution that relaxes the minimum-bandwidth (ideal) solution embodied in the Nyquist channel.

## 6.4 Raised-Cosine Pulse Spectrum

To ensure physical realizability of the overall pulse spectrum  $P(f)$ , we need a solution that differs from the Nyquist channel in one important respect: *the modified  $P(f)$  decreases toward zero gradually rather than abruptly*. In more specific terms,  $P(f)$  is proposed to consist of two portions:

1. *Flat portion*, which occupies the frequency band  $0 \leq |f| \leq f_1$  for some parameter  $f_1$  to be defined.
2. *Roll-off portion*, which occupies the frequency band  $f_1 < |f| < 2B_0 - f_1$ .

The parameter  $f_1$  is *adjustable* under the designer's control. The flat portion may thus retain part of the ideal brick-wall solution. As for the roll-off portion, it provides for the gradual decrease of  $P(f)$  toward zero. The key question is how to formulate this gradual roll-off characteristic. For the answer, we first look to *one full cycle of the cosine function defined in the frequency domain, which is raised up by an amount equal to its amplitude*. The next thing we do is to split this function at the origin into two equal halves, separate them by an amount equal to the width  $2f_1$  of the flat portion under point 1, and finally use them to account for the roll-off portion under point 2. This new figure constitutes the desired shape for the modified pulse spectrum  $P(f)$ . For obvious reasons, the  $P(f)$  constructed in this manner is called the *raised-cosine pulse spectrum*.

To cast the raised-cosine pulse spectrum in mathematical terms, we write

$$P(f) = \begin{cases} \frac{\sqrt{E}}{2B_0}, & 0 \leq |f| < f_1 \\ \frac{\sqrt{E}}{4B_0} \left\{ 1 + \cos \left[ \frac{\pi(|f| - f_1)}{2(B_0 - f_1)} \right] \right\}, & f_1 \leq |f| < 2B_0 - f_1 \\ 0, & 2B_0 - f_1 \leq |f| \end{cases} \quad (6.17)$$

The frequency  $f_1$  and the Nyquist bandwidth  $B_0$  are related by the new parameter

$$\alpha = 1 - \frac{f_1}{B_0} \quad (6.18)$$

which is called the *roll-off factor*. For  $\alpha = 0$ —that is,  $f_1 = B_0$ —we get the Nyquist channel described in Section 6.3.

The spectrum  $P(f)$ , normalized by multiplying it by  $2B_0/\sqrt{E}$ , is plotted in Fig. 6.3(a) versus the normalized frequency  $f/B_0$  for three values of  $\alpha$ : namely, 0, 0.5, and 1. We see that for  $\alpha = 0.5$  or 1, the function  $P(f)$  cuts off gradually as compared with the ideal brick-wall solution (corresponding to  $\alpha = 0$ ).

The modified pulse shape  $p(t)$ —that is, the inverse Fourier transform of the raised-cosine pulse spectrum  $P(f)$ —is defined by

$$p(t) = \sqrt{E} \operatorname{sinc}(2B_0 t) \left( \frac{\cos(2\pi\alpha B_0 t)}{1 - 16\alpha^2 B_0^2 t^2} \right) \quad (6.19)$$

The time function of Eq. (6.19) consists of the product of two factors: the factor  $\sqrt{E} \operatorname{sinc}(2B_0 t)$  that defines the Nyquist channel, and a second factor that decreases as  $1/|t|^2$  for large  $|t|$ . The first factor ensures zero crossings of  $p(t)$  at the desired sampling instants of time  $t = iT_b$  with  $i$  an integer (positive and negative). The second factor reduces the tails of the pulse considerably below the Nyquist channel, so that the transmission of

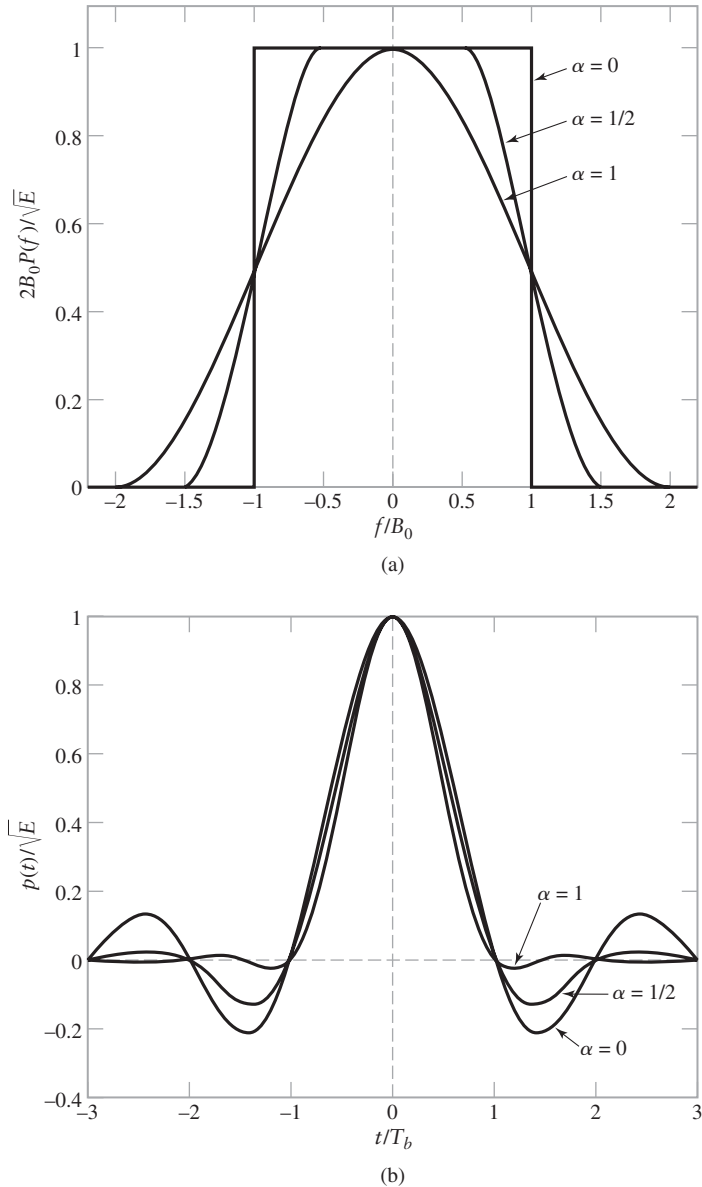


**FIGURE 6.3** (a) Raised-cosine pulse spectrum for varying roll-off rates. (b) Pulse response  $p(t)$  (i.e., inverse Fourier transform of  $P(f)$  for varying roll-off rates).

binary waves using such pulses is relatively insensitive to sampling time errors. In fact, *the amount of intersymbol interference resulting from a timing error  $\Delta t$  decreases as the roll-off factor  $\alpha$  is increased from zero to unity.*

The modified pulse shape  $p(t)$  is plotted in Fig. 6.3(b) for  $\alpha = 0, 0.5$ , and  $1$ . For the special case of  $\alpha = 1$ , the function  $p(t)$  simplifies as

$$p(t) = \sqrt{E} \left( \frac{\text{sinc}(4B_0 t)}{1 - 16B_0^2 t^2} \right) \quad (6.20)$$

The function  $p(t)$  of Eq. (6.20) exhibits two interesting properties:

1. At  $t = \pm T_b/2 = \pm 1/(4B_0)$ , we have  $p(t) = 0.5\sqrt{E}$ ; that is, the pulse width measured at half amplitude is exactly equal to the bit duration  $T_b$ .
2. There are zero crossings at  $t = \pm 3T_b/2, \pm 5T_b/2, \dots$ , in addition to the usual zero crossings at the sampling times  $t = \pm T_b, \pm 2T_b, \dots$

These two properties are particularly useful in the provision of a basis for extracting a timing signal from the receive-filter output  $y(t)$ , which is used to synchronize the receiver to the transmitter.

► **Drill Problem 6.2** Show that for positive frequencies, the area under the normalized raised-cosine curve of  $P(f)/(\sqrt{E}/2B_0)$  versus  $f/B_0$  is equal to unity for all values of the roll-off factor in the range  $0 \leq \alpha \leq 1$ . A similar statement holds for negative frequencies. ◀

► **Drill Problem 6.3** Given that  $P(f)$  is the Fourier transform of a pulse-like function  $p(t)$ , we may state the following theorem:<sup>2</sup>

The pulse  $p(t)$  decreases asymptotically with time as  $1/t^{k+1}$  provided that the following two conditions hold:

1. The first  $k - 1$  derivatives of the Fourier transform  $P(f)$  with respect to frequency  $f$  are all continuous.
2. The  $k$ th derivative of  $P(f)$  is discontinuous.

Demonstrate the validity of this theorem for the three different values of  $\alpha$  plotted in Fig. 6.3(a). ◀

► **Drill Problem 6.4** Equation (6.17) defines the raised-cosine pulse spectrum  $P(f)$  as real-valued and therefore zero delay. In practice, every transmission system experiences some finite delay. To accommodate this practicality, we may associate with  $P(f)$  a linear phase characteristic over the frequency band  $0 \leq |f| \leq 2B_0 - f_1$ .

- (a) Show that this modification of  $P(f)$  introduces a finite delay into its inverse Fourier transform, namely, the pulse shape  $p(t)$ .
- (b) According to Eq. (6.19),  $p(t)$  represents a non-causal time response. The delay introduced into  $p(t)$  through the modification of  $P(f)$  has also a beneficial effect, tending to make  $p(t)$  essentially causal. For this to happen, however, the delay must not be less than a certain value dependent on the roll-off factor  $\alpha$ . Suggest suitable values for the delay for  $\alpha = 0, 1/2$ , and  $1$ . ◀

### ■ TRANSMISSION-BANDWIDTH REQUIREMENT

From Eq. (6.17) we see that the nonzero portion of the raised-cosine pulse spectrum  $P(f)$  is limited to the interval  $(0, 2B_0 - f_1)$  for positive frequencies. Accordingly, the transmission bandwidth required by using the raised-cosine pulse spectrum is given by

$$B_T = 2B_0 - f_1$$

Eliminating  $f_1$  between Eq. (6.18) and this formula for  $B_T$ , we obtain

$$B_T = B_0(1 + \alpha) \quad (6.21)$$

where  $B_0$  is the Nyquist bandwidth and  $\alpha$  is the roll-off factor. Thus, the transmission bandwidth requirement of the raised-cosine spectrum exceeds that of the optimum Nyquist channel by the amount

$$f_\nu = \alpha B_0 \quad (6.22)$$

---

<sup>2</sup>For detailed discussion of this theorem, see Gitlin, Hayes and Weinstein (1992), p. 258.

which is called the *excess bandwidth*. From this definition, we readily see that the ratio of the excess bandwidth  $f_v$  (resulting from the use of raised-cosine pulse spectrum) to the Nyquist bandwidth  $B_0$  (required by the Nyquist channel) is equal to the roll-off factor  $\alpha$ ; this is why the roll-off factor is also sometimes called the *excess-bandwidth factor*. In any event, the need for accommodating the excess bandwidth  $f_v$  is the price we have to pay for transmitting binary data over the channel at a bit rate equal to  $1/T_b$  and doing so with zero intersymbol interference in a physically realizable manner.

The following two cases, one ideal and the other practical, are of particular interest:

1. When the roll-off factor  $\alpha$  is zero, the excess bandwidth  $f_v$  is reduced to zero, thereby permitting the transmission bandwidth  $B_T$  to assume its minimum possible value  $B_0 = 1/(2T_b)$ .
2. When the roll-off factor  $\alpha$  is unity, the excess bandwidth is increased to  $B_0$ . Correspondingly, the transmission bandwidth  $B_T$  is doubled, compared to the (ideal) case 1. As pointed out previously, the choice of  $\alpha = 1$  provides a basis for synchronizing the receiver to the transmitter.

#### EXAMPLE 6.1 Bandwidth Requirements of the T1 System

In Chapter 5, we described the signal format for the *T1 carrier system* that is used to multiplex 24 independent voice inputs, which is based on an 8-bit PCM word. The bit duration of the resulting time-division multiplexed signal (including a framing bit) is

$$T_b = 0.647 \mu\text{s}$$

The bit rate of the T1 system is

$$R_b = \frac{1}{T_b} = 1.544 \text{ Mb/s}$$

For  $\alpha = 0$ , the Nyquist bandwidth of the T1 system is

$$B_0 = \frac{1}{2T_b} = 772 \text{ kHz}$$

which is the minimum transmission bandwidth of the T1 system for zero intersymbol interference. However, a more realistic value for the transmission bandwidth is obtained by using a raised-cosine pulse spectrum with roll-off factor  $\alpha = 1$ . In this case, the use of Eq. (6.21) yields

$$B_T = 0.772(1 + 1) = 1.544 \text{ MHz}$$

which is double the Nyquist bandwidth  $B_0$ .

#### ■ TWO ADDITIONAL PROPERTIES OF THE RAISED-COSINE PULSE SPECTRUM

From the definition of the raised-cosine pulse spectrum  $P(f)$  given in Eq. (6.17), we find that it exhibits two other interesting properties, as described in the material that follows.

**PROPERTY 1** *The roll-off portion of the spectrum  $P(f)$  exhibits odd symmetry about the midpoints  $f = \pm B_0$*

To prove this property, define the frequency function

$$P_v(f) = P_{\text{opt}}(f) - P(f) \quad (6.23)$$

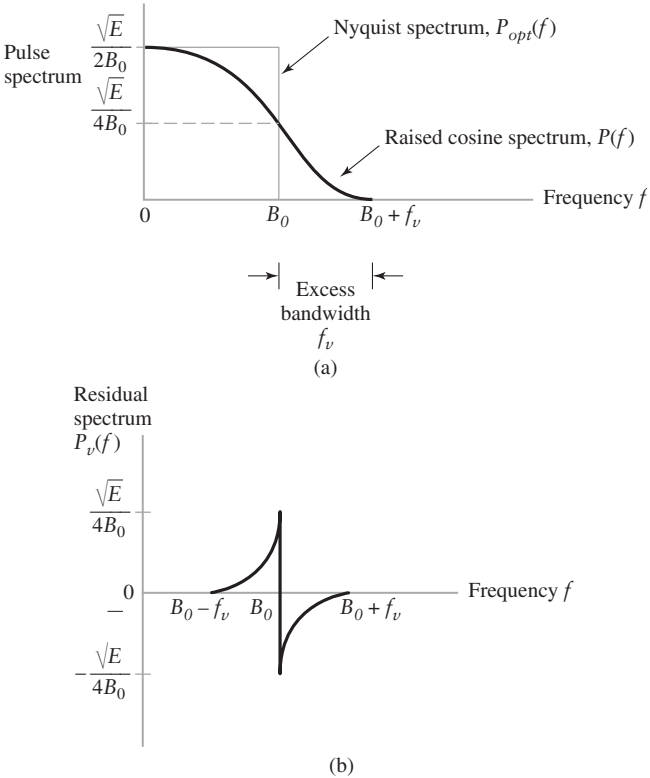


**FIGURE 6.4** (a) Nyquist and raised-cosine pulse spectra for positive frequencies.  
(b) Residual spectrum \$P\_v(f)\$.

which is a unique characterization of the roll-off portion of the raised-cosine spectrum. Using Eqs. (6.15) and (6.17) in this definition yields

$$P_v(f) = \begin{cases} 0, & \text{for } 0 \leq |f| \leq f_1 \\ \frac{\sqrt{E}}{4B_0} \left\{ 1 - \cos \left[ \frac{\pi(|f| - f_1)}{2(B_0 - f_1)} \right] \right\}, & \text{for } f_1 \leq |f| \leq B_0 \\ -\frac{\sqrt{E}}{4B_0} \left\{ 1 + \cos \left[ \frac{\pi(|f| - f_1)}{2(B_0 - f_1)} \right] \right\}, & \text{for } B_0 \leq |f| \leq 2B_0 - f_1 \\ 0, & \text{for } 2B_0 - f_1 < |f| \leq 2B_0 \end{cases} \quad (6.24)$$

Figure 6.4(a) plots \$P\_{opt}(f)\$ and \$P(f)\$ for roll-off factor \$\alpha = 1/2\$; only plots for positive frequencies are shown in the figure. The corresponding *residual function* \$P\_v(f)\$ is plotted in Fig. 6.4(b). From this figure we immediately see that

$$P_v(-f') = -P_v(f') \quad (6.25)$$

where

$$f' = f - B_0 \quad (6.26)$$

Equation (6.25) confirms the odd-property of the roll-off portion about the midpoint \$f = B\_0\$ for positive frequencies. Similarly, this property also holds at the other midpoint \$f = -B\_0\$ for negative frequencies.

► **Drill Problem 6.5** Starting with the formula of Eq. (6.24) and using the definition of Eq. (6.26), demonstrate the property of Eq. (6.25). ◀

The spectral characteristic portrayed in Fig. 6.4(a) reminds us of a similar situation pertaining to vestigial sideband modulation, which was studied in Chapter 3. Specifically, comparing Figs. 3.24(a) and 6.4(a), we readily see that although these two spectral characteristics refer to entirely different applications, they are basically of an identical mathematical form, except for two minor differences:

1. The baseband raised-cosine pulse spectrum  $P(f)$  of Fig. 6.4(a) is centered on the origin at  $f = 0$ , whereas the vestigial sideband spectrum of Fig. 3.24(a) is centered on the sinusoidal carrier frequency  $f_c$ .
2. The parameter  $f_v$  in Fig. 6.4(a) refers to the excess bandwidth measured with respect to the ideal brick-wall solution for zero intersymbol interference, whereas the parameter  $f_v$  in Fig. 3.24(a) refers to the excess bandwidth measured with respect to the optimum bandwidth attainable with single sideband modulation.

Difference 1 is of a technical nature, and difference 2 merely pertains to terminology. What is really important to note is that in both applications, where the raised-cosine pulse spectrum is intended for baseband digital data transmission and the vestigial sideband spectrum is usually (but not always) intended for analog modulation, the motivation is to ensure physical realizability.<sup>3</sup> (The Theme Example on digital television to be presented in Chapter 7 uses vestigial sideband modulation.)

**PROPERTY 2** *The infinite summation of replicas of the raised-cosine pulse spectrum, spaced by  $2B_0$  hertz, equals a constant, as shown by*

$$\sum_{m=-\infty}^{\infty} P(f - 2mB_0) = \frac{\sqrt{E}}{2B_0} \quad (6.27)$$

To prove this property, recall from Chapter 2 that *sampling of a Fourier transformable function in the time domain is transformed into periodicity in the frequency domain*, as described in Eq. (2.88). Adapting this equation to the situation at hand, we may write

$$\sum_{n=-\infty}^{\infty} p\left(\frac{n}{2B_0}\right) \delta\left(t - \frac{n}{2B_0}\right) \Longleftrightarrow 2B_0 \sum_{m=-\infty}^{\infty} P(f - 2mB_0) \quad (6.28)$$

The raised-cosine pulse spectrum  $P(f)$  and its inverse  $p(t)$  are respectively defined in Eqs. (6.17) and (6.19). In particular, sampling the modified pulse response  $p(t)$  at the rate  $1/2B_0$ , we may write

$$p\left(\frac{n}{2B_0}\right) = \sqrt{E} \operatorname{sinc}(n) \left( \frac{\cos(\pi n \alpha)}{1 - 4n^2 \alpha^2} \right)$$

---

<sup>3</sup>It is even more interesting to note, that Harry Nyquist is the originator of both vestigial sideband modulation and raised-cosine pulse spectrum:

The spectral shaping for vestigial sideband modulation appeared in the paper, H. Nyquist and K. W. Pfeifer, "Effect of the quadrature component in single-sideband transmission," *The Bell System Technical Journal*, vol. 19, pp. 63–73, January 1940.

The raised-cosine pulse spectrum was described in the earlier classic paper: H. Nyquist, "Certain topics in telegraph transmission theory", *Transactions of the American Institute of Electrical Engineers*, vol. 47, pp. 617–644, April 1928.

where  $n = 0, \pm 1, \pm 2, \dots$ . Noting the two points:

$$\begin{aligned} 1. \quad \text{sinc}(n) &= \frac{\sin(n\pi)}{n\pi} \\ &= \begin{cases} 1, & \text{for } n = 0 \\ 0, & \text{for } n = \pm 1, \pm 2, \dots \end{cases} \end{aligned}$$

$$2. \quad \cos(\pi n \alpha) = 1 \text{ for } n = 0,$$

it follows that

$$p\left(\frac{n}{2B_0}\right) = \begin{cases} \sqrt{E}, & \text{for } n = 0 \\ 0, & \text{for } n = \pm 1, \pm 2, \dots \end{cases}$$

Accordingly, Eq. (6.28) reduces to

$$\sqrt{E}\delta(t) \iff 2B_0 \sum_{m=-\infty}^{\infty} P(f - 2mB_0)$$

or, equivalently,

$$\frac{\sqrt{E}}{2B_0}\delta(t) \iff \sum_{m=-\infty}^{\infty} P(f - 2mB_0) \quad (6.29)$$

Finally, noting that the Fourier transform of the delta function  $\delta(t)$  is unity, Eq. (6.29) is merely another way of describing the desired form shown in Eq. (6.27).

Having proved the validity of Property 2, we may turn it around. Specifically, the *pulse-shaping criterion for zero intersymbol interference* is embodied in the following general statement:

Given the modified pulse shape  $p(t)$  for transmitting data over an imperfect channel using discrete pulse-amplitude modulation at the data rate  $1/T$ , the pulse shape  $p(t)$  eliminates intersymbol interference if, and only if, its spectrum  $P(f)$  satisfies the condition

$$\sum_{m=-\infty}^{\infty} P\left(f - \frac{m}{T}\right) = \text{constant}, \quad |f| \leq \frac{1}{2T} \quad (6.30)$$

This statement includes binary PAM as a special case, for which the data rate  $1/T_b$  equals  $2B_0$  in accordance with Eq. (6.13). Moreover, the raised-cosine pulse spectrum is one example, albeit an important one, that satisfies Eq. (6.30).

### ■ ROOT RAISED-COSINE PULSE SPECTRUM

A more sophisticated form of pulse shaping for baseband digital data transmission is to use the *root raised-cosine pulse spectrum* rather than the regular pulse-shaping spectrum of Eq. (6.17). Specifically, we write

$$G(f)H(f) = P^{1/2}(f) \quad (6.31)$$

where, as before,  $G(f)$  is the transmit-filter's frequency response and  $H(f)$  is the channel's frequency response. Correspondingly, the receive-filter's frequency response is defined by

$$Q(f) = P^{1/2}(f) \quad (6.32)$$

Multiplying Eq. (6.31) by (6.32) yields

$$G(f)H(f)Q(f) = P(f)$$

which is a repeat of Eq. (6.7). On this basis, the pulse shaping is partitioned equally between two entities:

- ▶ The combination of transmit-filter and channel constitutes one entity. With  $H(f)$  known and  $P(f)$  defined by Eq. (6.17) for a prescribed roll-off factor  $\alpha$ , we may use Eq. (6.31) to determine the frequency response of the transmit filter.
- ▶ The receive filter constitutes the other entity. Hence, for the same roll-off factor  $\alpha$  we may use Eqs. (6.17) and (6.32) to determine the frequency response of the receive-filter.

If the channel is affected by additive noise and the pulse-shaping is partitioned equally between the transmitter and receiver in the manner described herein, then the receiver would maximize the output signal-to-noise ratio at the sampling instants. Further discussion of this issue is deferred to Chapter 10, which is devoted to noise in digital communication receivers.

## 6.5 Baseband Transmission of M-ary Data

In the baseband binary PAM system of Fig. 6.1(a), the sequence  $\{b_k\}$  emitted by the source of information consists of binary symbols that are represented by one of two possible amplitude levels,  $-1$  for symbol 0 and  $+1$  for symbol 1. On the other hand, in a *baseband M-ary* version of the system, the output of the line encoder takes on one of  $M$  possible amplitude levels with  $M > 2$ . In an  $M$ -ary system, the information source emits a sequence of symbols from an alphabet that consists of  $M$  symbols. Each amplitude level at the line-encoder output corresponds to a distinct symbol, so that there are  $M$  distinct amplitude levels to be transmitted.

Consider then an  $M$ -ary PAM system with a signal alphabet that contains  $M$  symbols, with the *symbol duration* denoted by  $T$  seconds. We refer to  $1/T$  as the *signaling rate* or *symbol rate* of the system, which is expressed in *symbols per second* or simply *bauds*. It is informative to relate the signaling rate of this system to that of an equivalent binary PAM system for which the value of  $M$  is 2 and the bit duration is  $T_b$  seconds. The binary PAM system transmits data at the rate of  $1/T_b$  *bits per second*. We also observe that in the case of a *quaternary* PAM system, for example, the four possible symbols may be identified with the dubits 00, 10, 11, and 01; a *dabit* refers to a word consisting of two bits. We thus see that each symbol represents 2 bits of data and 1 baud is equal to 2 bits per second. We may generalize this result by stating that in an  $M$ -ary PAM system, 1 baud is equal to  $\log_2 M$  bits per second, and the symbol duration  $T$  of the  $M$ -ary PAM system is related to the bit duration  $T_b$  of a binary PAM system with the equivalent bit rate as follows:

$$T = T_b \log_2 M \quad (6.33)$$

Therefore, in a given channel bandwidth, we find that by using an  $M$ -ary PAM system we are able to transmit data at a rate that is  $\log_2 M$  faster than the corresponding binary PAM system.

However, this improvement in bandwidth utilization is attained at a price. Specifically, the transmitted power must be increased by a factor equal to  $M^2/\log_2 M$ , compared to a binary PAM system, if we are to realize the same performance in the presence of channel noise; this issue is discussed in Chapter 10. Also, system complexity is increased.

## 6.6 The Eye Pattern

Up to this point in the chapter, we have discussed the intersymbol interference problem and how to mitigate it. In this section, we describe a tool called the eye pattern for its experimental evaluation.

The *eye pattern* is produced by the *synchronized superposition of (as many as possible) successive symbol intervals of the distorted waveform appearing at the output of the receive-filter prior to thresholding*. As an illustrative example, consider the distorted, but noise-free, waveform shown in Fig. 6.5(a). Part (b) of the figure displays the corresponding synchronized superposition of the waveform's eight binary symbol intervals. The resulting display is called an “eye pattern” because of its resemblance to a human eye. By the same token, the interior of the eye pattern is called the *eye opening*.

As long as the additive channel noise is not large, then the eye pattern is well defined and may therefore be studied experimentally on an oscilloscope. The waveform under study is applied to the deflection plates of the oscilloscope with its time-base circuit operating in a synchronized condition. From an experimental perspective, the eye pattern offers two compelling virtues:

- ▶ The simplicity of generation.
- ▶ The provision of a great deal of insightful information about the characteristics of the data transmission system, hence its wide use as a visual indicator<sup>4</sup> of how well or poorly a data transmission system performs the task of transporting a data sequence across a physical channel.

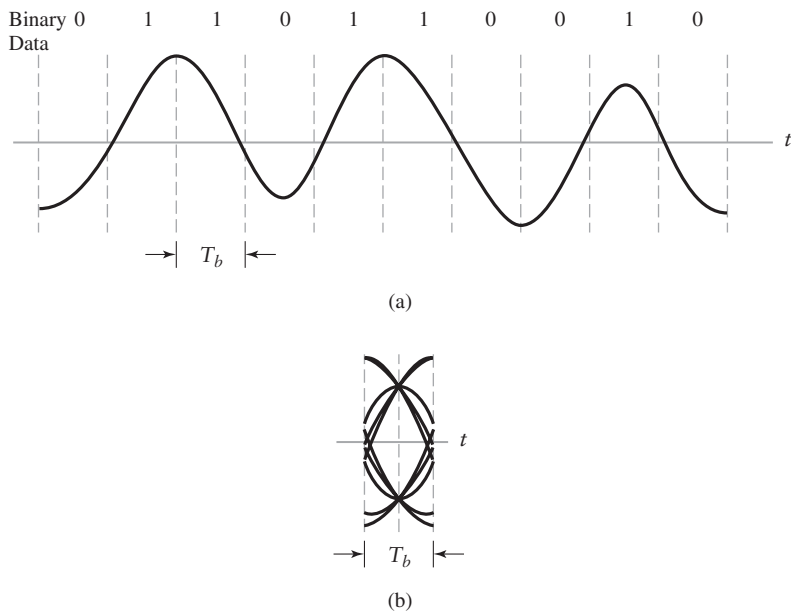


**FIGURE 6.5** (a) Binary data sequence and its waveform. (b) Corresponding eye pattern.

<sup>4</sup>Another visual indicator of system performance is the so-called *scatter diagram*, which is obtained by plotting the imaginary part versus the real part of the complex signal appearing at the output of the receiver filter; for more details, see the book by Jeruchim, Balaban, and Shanmugan (2000), pp. 666–667.

### ■ TIMING FEATURES

Figure 6.6 depicts a *generic* eye pattern for distorted, but noise-free, binary data. The horizontal axis, representing time, spans the symbol interval from  $-T_b/2$  to  $+T_b/2$ , where  $T_b$  is the bit duration.

From this diagram, we may infer three timing features pertaining to a binary data transmission system, exemplified by the PAM system of Fig. 6.1(a):

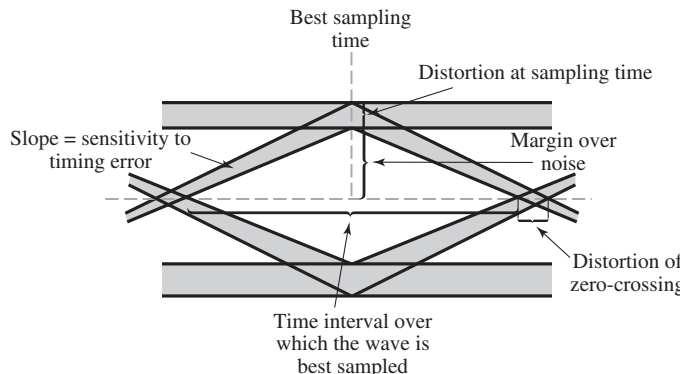
- (i) *Optimum sampling time*. The width of the eye opening defines the time interval over which the distorted binary waveform appearing at the output of the receive-filter in Fig. 6.1(a) can be uniformly sampled without decision errors. Clearly, the *optimum sampling time* is the time at which the eye opening is at its widest.
- (ii) *Zero-crossing jitter*. In practice, the timing signal (for synchronizing the receiver to the transmitter) is extracted from the *zero-crossings* of the waveform that appears at the receive-filter output. In such a form of synchronization, there will always be irregularities in the zero-crossings, which, in turn, give rise to *jitter* and therefore non-optimum sampling times.
- (iii) *Timing sensitivity*. Another timing-related feature is that of sensitivity of the system to *timing errors*. This sensitivity is determined by the rate at which the eye pattern is closed as the sampling time is varied.

Figure 6.6 indicates how these three timing features of the system can be measured from the eye pattern.

### ■ THE PEAK DISTORTION FOR INTERSYMBOL INTERFERENCE

Hereafter, we assume that the ideal signal amplitude is scaled to occupy the range from  $-1$  to  $+1$ . We then find that in the absence of channel noise, the eye opening assumes two extreme values:

- (i) *An eye opening of unity*<sup>5</sup>, which corresponds to zero intersymbol interference.
- (ii) *An eye opening of zero*, which corresponds to a completely closed eye pattern; this second extreme case occurs when the effect of intersymbol interference is severe enough for some upper traces in the eye pattern to cross with its lower traces.



**FIGURE 6.6** Interpretation of the eye pattern for a baseband binary data transmission system.

<sup>5</sup>In a strict sense, an eye pattern that is completely open occupies the range from  $-1$  to  $+1$ . On this basis, zero-intersymbol interference would correspond to an ideal eye opening of two. However, for two reasons, convenience of presentation and consistency with the literature, we have chosen an eye opening of unity to refer to the ideal condition of zero-intersymbol interference.

In situation (ii), it is indeed possible for the receiver to make decision errors even when the channel is noise-free. Typically, *an eye opening of 0.5 or better is considered to yield reliable data transmission*.

In a noisy environment, the extent of eye opening at the optimum sampling time provides a measure of the operating margin over additive channel noise. This measure, as illustrated in Fig. 6.6, is referred to as the *noise margin*.

From this discussion, it is apparent that the eye opening plays an important role in assessing system performance, hence the need for a formal definition of the eye opening. To this end, we offer the following definition:

$$(\text{Eye opening}) = 1 - D_{\text{peak}} \quad (6.34)$$

where  $D_{\text{peak}}$  denotes a new criterion called the *peak distortion*. The point to note here is that peak distortion is a *worst-case* criterion for assessing the effect of intersymbol interference on the performance (i.e., error rate) of a data-transmission system. The relationship between the eye opening and peak distortion is illustrated in Fig. 6.7. With the eye opening being dimensionless, the peak distortion is dimensionless too. To emphasize this statement, the two extreme eye-opening values defined on the previous page translate as follows:

- (i) *Zero peak distortion*, which occurs when the eye opening is unity.
- (ii) *Unity peak distortion*, which occurs when the eye pattern is completely closed.

With this background, the *peak distortion* is formally defined as *the maximum value assumed by the intersymbol interference over all possible transmitted sequences, with this evaluation divided by a normalization factor equal to the absolute value of the corresponding signal level idealized for zero intersymbol interference*. Referring to Eq. (6.10), the two components embodied in this definition are themselves defined as follows:

- (i) The idealized signal component of the receive-filter output  $y_i = y(iT_b)$  is defined by the first term in Eq. (6.10)—namely,  $a_i$ , where  $a_i$  is the  $i$ th encoded symbol and unit transmitted signal energy per bit.
- (ii) The intersymbol interference is defined by the second term—namely,

$$\sum_{\substack{k=-\infty \\ k \neq i}}^{\infty} a_k p_{i-k}$$

The maximum value of this summation occurs when each encoded symbol  $a_k$  has the same algebraic sign as  $p_{i-k}$ . Therefore,

$$(\text{Maximum ISI}) = \sum_{\substack{k=-\infty \\ k \neq i}}^{\infty} |p_{i-k}|$$

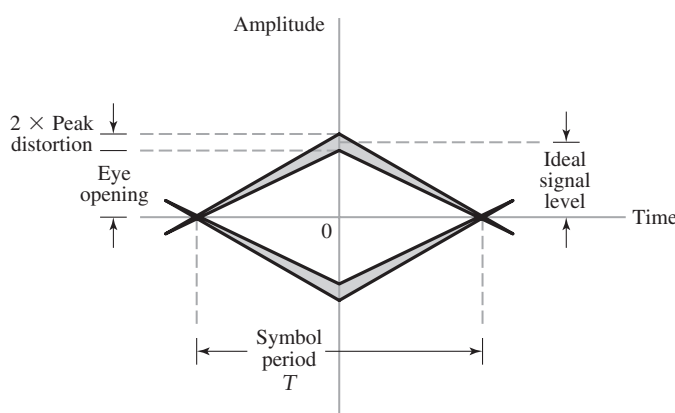


**FIGURE 6.7** Illustrating the relationship between peak distortion and eye opening. Note: The ideal signal level is scaled to lie inside the range  $-1$  to  $+1$ .

Hence, invoking the definition of peak distortion, we get the desired formula:

$$\begin{aligned} D_{\text{peak}} &= \sum_{k=-\infty}^{\infty} |p_{i-k}| \\ &= \sum_{\substack{k=-\infty \\ k \neq i}}^{\infty} |p[(i-k)T_b]| \end{aligned} \quad (6.35)$$

where for all  $i = k$ ,  $p_0 = p(0) = 1$ . Note that by involving the assumption of a signal amplitude from  $-1$  to  $+1$ , we have scaled the transmitted signal energy for symbol to  $E = 1$ .

By its very nature, the peak distortion is a *worst-case criterion for data transmission over a noisy channel*. The eye opening specifies the smallest possible noise margin.<sup>6</sup>

### ■ EYE PATTERNS FOR M-ARY TRANSMISSION

As pointed out previously in Section 6.5, an  $M$ -ary data transmission system uses  $M$  encoded symbols in the transmitter and  $M - 1$  thresholds in the receiver. Correspondingly, the eye pattern for an  $M$ -ary data transmission system contains  $(M - 1)$  eye openings stacked vertically one on top of the other. The thresholds are defined by the amplitude-transition levels as we move up from one eye opening to the adjacent eye opening. When the encoded symbols are all equiprobable, the thresholds will be equidistant from each other.

In a strictly linear data-transmission system with truly transmitted random data sequences, all the  $M - 1$  eye openings would be identical. In practice, however, it is often possible to find asymmetries in the eye pattern of an  $M$ -ary data-transmission system, which are caused by nonlinearities in the communication channel or other parts of the system.

## 6.7 Computer Experiment: Eye Diagrams for Binary and Quaternary Systems

Figures 6.8(a) and 6.8(b) show the eye diagrams for a baseband PAM transmission system using  $M = 2$  and  $M = 4$ , respectively. The channel has no bandwidth limitation, and the source symbols used are randomly generated on a computer. A raised cosine pulse is used in both cases. The system parameters used for the generation of these eye diagrams are as follows: bit rate = 1 Hz, and roll-off factor  $\alpha = 0.5$ . For the binary case of  $M = 2$  displayed in Fig. 6.8(a), the symbol duration  $T$  and the bit duration  $T_b$  are the same, with  $T_b = 1$ s. For the case of  $M = 4$  displayed in Fig. 6.8(b), we have  $T = T_b \log_2 M = 2T_b$ . In both cases, we see that the eyes are open, indicating perfectly reliable operation of the system, perfect in the sense that the intersymbol interference is zero.

Figures 6.9(a) and 6.9(b) show the eye diagrams for these two baseband-pulse transmission systems using the same system parameters as before, but this time under a bandwidth-limited condition. Specifically, the channel is now modeled by a low-pass *Butterworth filter*, whose frequency response is defined by

$$|H(f)| = \frac{1}{1 + (f/f_0)^{2N}}$$

where  $N$  is the order of the filter, and  $f_0$  is its 3-dB cutoff frequency of the filter. For the results displayed in Fig. 6.9, the following filter parameter values were used:

1.  $N = 3$ , and  $f_0 = 0.6$  Hz for binary PAM
2.  $N = 3$ , and  $f_0 = 0.3$  Hz for 4 – PAM

<sup>6</sup>The smallest possible noise margin places an *upper bound* on the probability of symbol error due to the unavoidable presence of additive channel noise; the notion “probability of symbol error” is formally defined in Chapter 10.

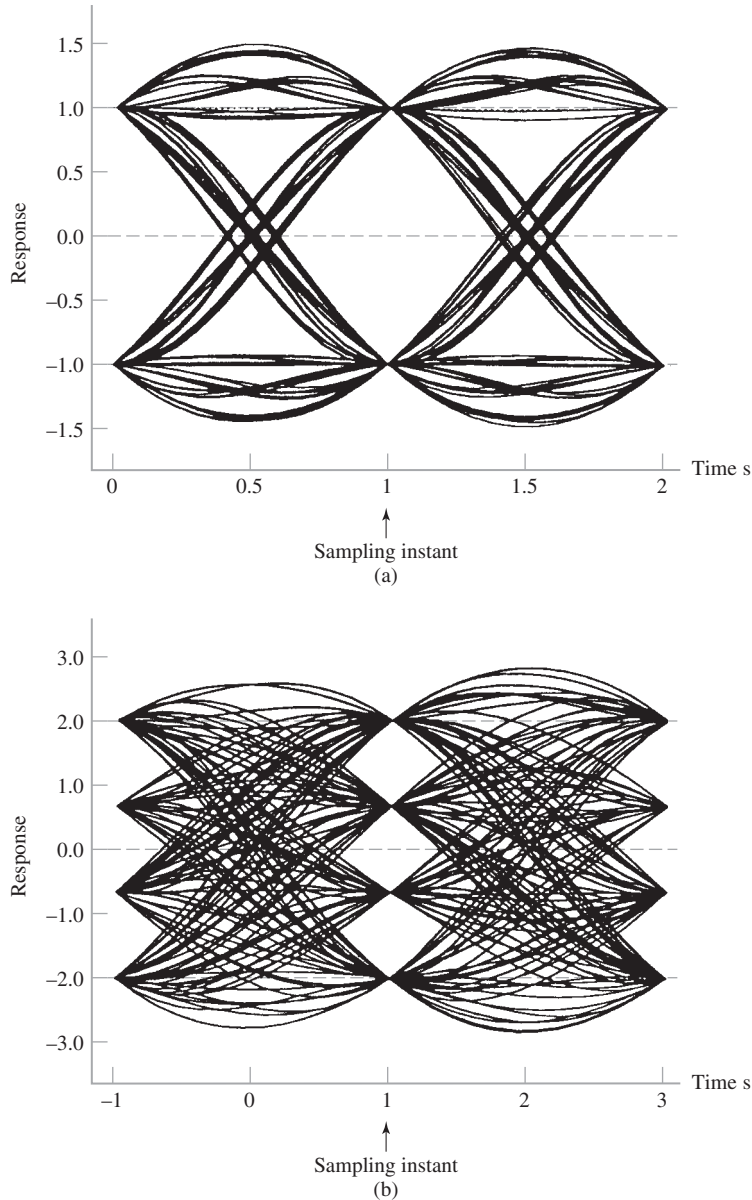


**FIGURE 6.8** Eye diagram of received signal with no bandwidth limitation. (a)  $M = 2$ . (b)  $M = 4$ .

With the roll-off factor  $\alpha = 0.5$  and Nyquist bandwidth  $B_0 = 0.5$  Hz, for binary PAM, the use of Eq. (6.21) defines the transmission bandwidth of the PAM transmission system to be

$$B_T = 0.5(1 + 0.5) = 0.75 \text{ Hz}$$

Although the channel bandwidth cutoff frequency is greater than absolutely necessary, its effect on the passband is observed in a decrease in the size of the eye opening. Instead of the distinct values at time  $t = 1$  s (as shown in Figs. 6.8(a) and 6.8(b)), now there is a blurred region. If the channel bandwidth were to be reduced further, the eye would close even more until finally no distinct eye opening would be recognizable.

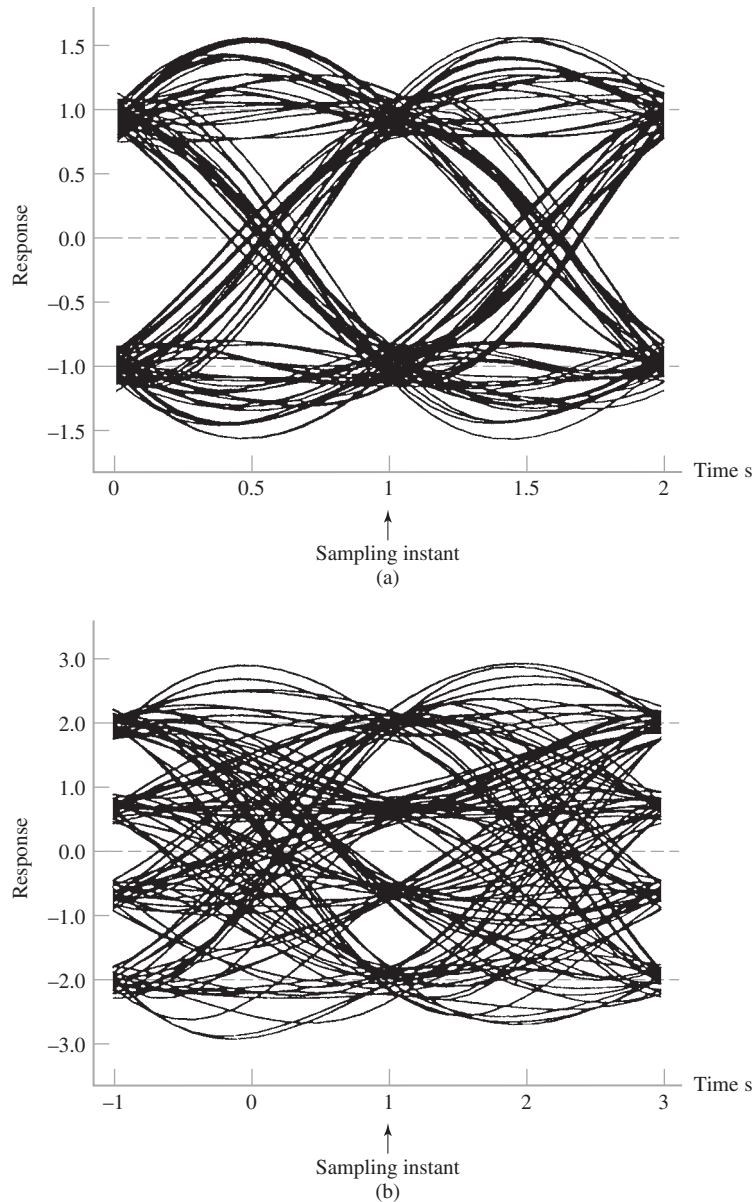


**FIGURE 6.9** Eye diagram of received signal, using a bandwidth-limited channel. (a)  $M = 2$ . (b)  $M = 4$ .

## 6.8 Theme Example: Equalization

An efficient approach to *high-speed transmission* of digital data over a linear band-limited communication channel (exemplified by telephone channels for example) is to use a combination of two signal-processing strategies:

- ▶ *Discrete pulse-amplitude modulation* (PAM), which encodes the amplitudes of successive pulses in a periodic pulse train with a discrete set of possible amplitude levels.
- ▶ *Linear modulation scheme*, which offers the virtue of bandwidth conservation to transmit the encoded pulse train over the channel.

In the receiver part of the data-transmission system, the received signal is demodulated and synchronously sampled, then finally decisions are made as to which particular symbols were transmitted. When the transmitted signal-to-noise ratio is high, we find that the number of detectable amplitude levels is essentially limited by intersymbol interference rather than additive channel noise. In principle, if the channel is known precisely, then it is virtually always possible to make the intersymbol interference at the sampling instants arbitrarily small by using a suitable pair of transmit- and receive-filters, so as to control the pulse shape in the manner described in previous sections of the chapter. Thus, insofar as the intersymbol interference problem is concerned, we may consider the task of data transmission over the channel as being at baseband.

In practice, however, we seldom have prior knowledge of the exact channel characteristics. Moreover, there is the problem of imprecision that arises in the physical implementation of the pulse-shaping filters. The net result of these practical realities is that there will always be some *residual distortion* for intersymbol interference to be a limiting factor on the data rate sustainable by the system. To compensate for the intrinsic residual distortion, we may use a process known as *equalization*. The filter used to perform this process is called an *equalizer*.

Thus, in addition to pulse shaping performed by the receive-filter, we now have a new function to perform—namely, equalization of residual distortion. Since these two functions are both linear, we propose to combine them in a single structure. Moreover, recognizing the need for a structure with *adjustable* coefficients to deal with the equalization process, we propose to use a structure known as the *transversal filter*. This filter, depicted in Fig. 6.10, consists of the following components:

- ▶ *Delay line*, whose taps are uniformly spaced  $T$  seconds apart;  $T$  is the symbol duration.
- ▶ *Adjustable weights*, which are connected to the taps of the delay line.
- ▶ *Summer*, which adds successively delayed versions of the input signal, after they have been individually weighted.

With channel equalization as the function of interest and the transversal filter with adjustable coefficients as the structure to perform it, it is apropos that we refer to this new structure as the *adjustable transversal equalizer* or simply *transversal equalizer*.

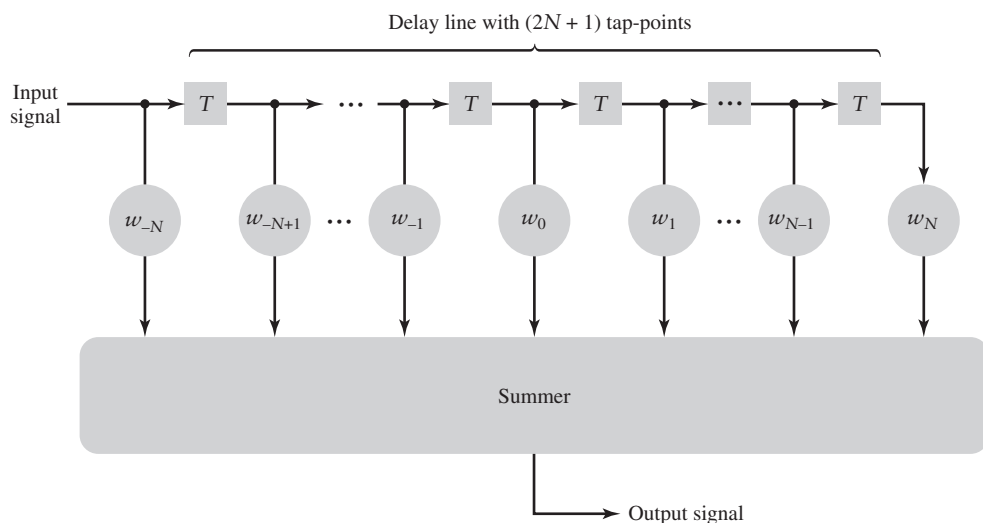


**FIGURE 6.10** Transversal filter.

### ■ ZERO-FORCING EQUALIZATION

To proceed with the solution to the equalization problem, consider then the composite system depicted in Fig. 6.11:

- ▶ The first subsystem characterized by the impulse response  $c(t)$  represents the combined action of the transmit-filter and communication channel.
- ▶ The second subsystem characterized by the impulse response  $h_{\text{eq}}(t)$  accounts for pulse shaping combined with residual-distortion equalization in the receiver.

For *structural symmetry* with respect to the midpoint of the adjustable transversal equalizer, the total number of taps is chosen to be  $(2N + 1)$ . Correspondingly, let the weights (coefficients) of the equalizer be denoted by  $w_{-N}, \dots, w_{-1}, w_0, w_1, \dots, w_N$ . On this basis, we may express the impulse response of the equalizer as

$$h_{\text{eq}}(t) = \sum_{k=-N}^N w_k \delta(t - kT) \quad (6.36)$$

where  $\delta(t)$  is the Dirac delta function and  $w_k$  is the weight connected to the  $k$ th tap of the delay line in the equalizer. According to Fig. 6.11, the transversal equalizer of impulse response  $h_{\text{eq}}(t)$  is connected in cascade with the transmit filter-channel combination of impulse response  $c(t)$ . Let  $p(t)$  denote the overall impulse response of this cascade connection. We may then express  $p(t)$  as the convolution of  $c(t)$  with  $h_{\text{eq}}(t)$ , as shown by

$$\begin{aligned} p(t) &= c(t) \star h_{\text{eq}}(t) \\ &= c(t) \star \sum_{k=-N}^N w_k \delta(t - kT) \end{aligned} \quad (6.37)$$

where the symbol  $\star$  denotes convolution. Interchanging the order of summation and convolution, which we are permitted to do because the two subsystems of Fig. 6.11 are both linear, we may write

$$\begin{aligned} p(t) &= \sum_{k=-N}^N w_k c(t) \star \delta(t - kT) \\ &= \sum_{k=-N}^N w_k c(t - kT) \end{aligned} \quad (6.38)$$

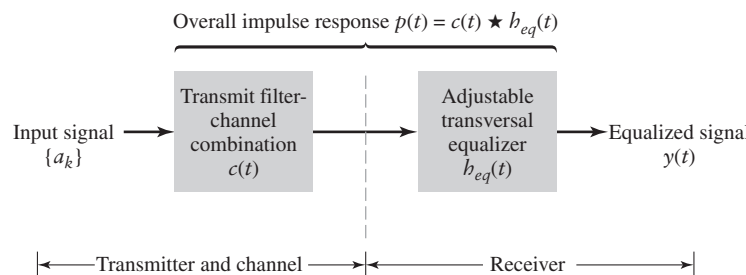


**FIGURE 6.11** Simplified depiction of the scenario for solving the channel-equalization problem.

where, in the last line, we made use of the sifting property of the delta function. Evaluating Eq. (6.38) at the sampling times  $t = iT$ , we get the *discrete convolution sum*.

$$p(iT) = \sum_{k=-N}^N w_k c((i-k)T) \quad (6.39)$$

To simplify the presentation, let  $p_i = p(iT)$  and  $c_i = c(iT)$ . We may then rewrite Eq. (6.39) in the compact form

$$p_i = \sum_{k=-N}^N w_k c_{i-k} \quad (6.40)$$

Elimination of the intersymbol interference requires that we satisfy the Nyquist criterion for distortionless transmission described in Eq. (6.11), on the basis of which we write

$$p_i = \begin{cases} \sqrt{E}, & \text{for } i = 0 \\ 0, & \text{for all } i \neq 0 \end{cases}$$

where  $E$  is the transmitted signal energy per symbol. From Eq. (6.40) we note that there are only  $(2N + 1)$  adjustable weights at our disposal. Hence, the Nyquist criterion for distortionless transmission can only be approximately satisfied (depending on  $N$ ) as follows:

$$p_i = \begin{cases} \sqrt{E}, & i = 0 \\ 0, & i = \pm 1, \pm 2, \dots, \pm N \end{cases} \quad (6.41)$$

Hence, imposing the condition of Eq. (6.39) on the discrete convolution sum of Eq. (6.40), we obtain a system of  $(2N + 1)$  simultaneous equations:

$$\sum_{k=-N}^N w_k c_{i-k} = \begin{cases} \sqrt{E}, & i = 0 \\ 0, & i = \pm 1, \pm 2, \dots, \pm N \end{cases} \quad (6.42)$$

Equivalently, in matrix form we may write

$$\begin{bmatrix} c_0 & \cdots & c_{-N+1} & c_{-N} & c_{-N-1} & \cdots & c_{-2N} \\ \vdots & \vdots & \vdots & \vdots & \vdots & \vdots & \vdots \\ c_{N-1} & \cdots & c_0 & c_{-1} & c_{-2} & \cdots & c_{-N-1} \\ c_N & \cdots & c_1 & c_0 & c_{-1} & \cdots & c_{-N} \\ c_{N+1} & \cdots & c_2 & c_1 & c_0 & \cdots & c_{-N+1} \\ \vdots & \vdots & \vdots & \vdots & \vdots & \vdots & \vdots \\ c_{2N} & \cdots & c_{N+1} & c_N & c_{N-1} & \cdots & c_0 \end{bmatrix} \begin{bmatrix} w_{-N} \\ \vdots \\ w_{-1} \\ w_0 \\ w_1 \\ \vdots \\ w_N \end{bmatrix} = \begin{bmatrix} 0 \\ \vdots \\ 0 \\ \sqrt{E} \\ 0 \\ \vdots \\ 0 \end{bmatrix} \quad (6.43)$$

A transversal equalizer described by Eq. (6.42), or equivalently Eq. (6.43), is referred to as a *zero-forcing equalizer*, so called because the equalizer forces the intersymbol interference to be zero at  $(2N + 1)$  sampling instants of the received signal. The zero-forcing equalizer is optimum in the sense that it minimizes the *peak distortion* in the absence of noise; peak distortion is defined in Eq. (6.34). Another nice feature of the zero-forcing equalizer is that it is relatively simple to implement. Moreover, in theory, the longer we make the equalizer (i.e., permit  $N$  to approach infinity), the more closely will the equalized system approach the ideal condition specified by the Nyquist criterion for distortionless transmission across

the channel. Note, however, that since the zero-forcing equalizer ignores the effect of additive channel noise, the equalized system does not always offer the best solution to the intersymbol interference problem.<sup>7</sup>

► **Drill Problem 6.6** Assume the following perfect conditions:

- The residual distortion in the data transmission system is zero.
  - The pulse shaping is partitioned equally between the transmit filter-channel combination and the receiver.
  - The transversal equalizer is infinitely long.
- (a) Find the corresponding value of the equalizer's transfer function in terms of the overall pulse spectrum  $P(f)$ .
- (b) For the roll-off factor  $\alpha = 1$ , demonstrate that a transversal equalizer of infinite length would essentially satisfy the perfect condition found in part (a) of the problem. ◀

■ **How Could the Receiver Determine the  $\{c_k\}$ ?**

Given the coefficients  $c_{-N}, \dots, c_{-1}, c_0, c_1, \dots, c_N$ , defining the sampled impulse response of the transmit filter-channel combination, we may then use the simultaneous system of equations (6.43) to solve for the corresponding  $(2N + 1)$  weights of the transversal equalizer.<sup>8</sup> This computation, however, presumes that the receiver already has knowledge of the set of coefficients  $\{c_k\}_{k=-N}^N$ . But, how can the receiver acquire this knowledge?

A commonly used method of addressing this fundamental question is to use a *pilot-assisted training* session that proceeds as follows:

1. For the binary data sequence  $\{b_k\}$  applied to the transmitter input, use a deterministic sequence of 1s and 0s that is noise-like in character, hence the reference to this sequence as a *pseudo-noise (PN) sequence*. The reason for using such a sequence as the *pilot* is to provide a measure of uniqueness.
2. The *PN* sequence is known *a priori* to the receiver. Accordingly, with the receiver synchronized to the transmitter, the receiver is enabled to know when to initiate the training session.
3. Finally, knowing the transmitted *PN* sequence and measuring the corresponding channel output, it is a straight-forward matter for the receiver to estimate the sequence  $\{c_k\}$  representing the sampled impulse response of the transmit-filter and channel combined.

---

<sup>7</sup>For an equalizer more robust than the zero-forcing equalizer, we look to a different optimization criterion—namely, the *mean-square error criterion*—which accounts for the combined effects of residual distortion and channel noise. The mean-square error (e.g., average error power) is defined as the expected value of the squared error (difference) between the “desired” response and the “actual” response of the equalizer; expectation is a statistical operator, the discussion of which is deferred to Chapter 8.

For detailed discussion of the minimum mean-square-error equalizer and its adaptive implementation, see Haykin (2001). Unlike a fixed equalizer (i.e., a transversal equalizer whose tap weights are fixed once their individual adjustments have been computed), an *adaptive equalizer* is equipped with a mechanism that continually adjusts the tap weights of the equalizer so as to compensate for the time-varying nature of telephone and wireless channels, which is another practical reality of digital communications.

<sup>8</sup>The solution of Eq. (6.43), namely, the  $(2N + 1)$  weights of the transversal equalizer, is defined by the inverse of the  $(2N + 1)$ -by- $(2N + 1)$  matrix of known coefficients on the left-hand side of the equation multiplied by the highly sparse column vector on the right-hand side. For large  $N$ , computation of the inverse matrix becomes troublesome, in which case we have to seek another approach, for details, see Haykin (2001).

## 6.9 Summary and Discussion

The subject of digital data transmission over a communication channel encompasses two different families of applications, depending on the type of channel being considered:

- (i) *Baseband data transmission*, for which the channel is of a low-pass type.
- (ii) *Band-pass data transmission*, for which the channel is of a band-pass type. (Band-pass data transmission is also referred to as passband data transmission.)

In this chapter, we studied baseband data transmission. The study of band-pass data transmission is taken up in Chapter 7.

In particular, this chapter focused on the intersymbol interference problem, which arises due to imperfections in the frequency response of the channel, assumed to be linear. With attention directed at a signal pulse of interest at the channel output, intersymbol interference (ISI) refers to the effect on that pulse due to *cross-talk* or *spillover* from all other signal pulses in the data stream applied to the channel input.

A corrective measure widely used in practice is to *shape* the overall pulse spectrum of the baseband system, starting from the source of the message signal all the way to the receiver. The optimum solution for the pulse spectrum is provided by the Nyquist channel, which guarantees zero intersymbol interference at a bit rate equal to twice the channel bandwidth. However, this optimum solution to the intersymbol interference problem is unrealizable due to its brick-wall characterization. To circumvent the issue of unrealizability, we may use the raised-cosine pulse spectrum, which provides design flexibility through the *roll-off factor* that varies between zero and unity. Note, however, that the use of a nonzero roll-off factor is a necessary but not sufficient condition for physical realizability of the solution to the zero-intersymbol interference problem. In addition, the raised-cosine pulse spectrum must be associated with a linear phase characteristic whose slope depends on the roll-off factor, as discussed in Problem 6.4. It is also noteworthy that a more sophisticated solution to the intersymbol interference problem is provided by partitioning the overall task of pulse shaping equally between the transmitter and receiver, using the root raised-cosine pulse spectrum.

In this chapter, we also studied a practical issue closely related to intersymbol interference: how to evaluate it experimentally. The eye pattern is a tool that addresses this issue in a very insightful manner. Indeed, in a single picture, the eye pattern portrays the degrading effects of timing jitter, intersymbol interference (due to system imperfections), and channel noise, all of which are of a random nature. In this context, there is a basic difference between intersymbol interference and noise. Intersymbol interference is a *signal-dependent phenomenon*; it therefore disappears when the information-bearing signal is switched off. On the other hand, noise is always there, regardless of whether there is data transmission or not.

One last comment is in order. In addition to pulse shaping, there is another corrective measure for dealing with the intersymbol interference problem—namely, channel equalization. This second corrective measure involves the use of a transversal filter with adjustable coefficients; the filter is placed in the receiver and adjusted in a principled manner so as to compensate for residual distortion resulting from imperfections in the channel's impulse response.

## ADDITIONAL PROBLEMS

---

- 6.7 Starting with Eq. (6.17) for the raised-cosine pulse spectrum  $P(f)$ , use the inverse Fourier transform to derive the corresponding time response  $p(t)$  defined in Eq. (6.19).

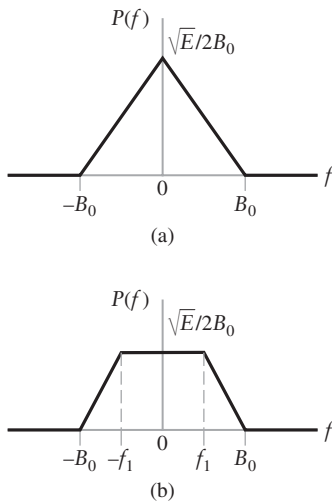
- 6.8 The raised-cosine pulse spectrum for a roll-off factor of unity is given by

$$P(f) = \begin{cases} \frac{\sqrt{E}}{2B_0} \cos^2\left(\frac{\pi f}{4B_0}\right), & 0 \leq |f| < 2B_0 \\ 0, & 2B_0 \leq |f| \end{cases}$$

which is a special case of Eq. (6.17) for  $\alpha = 1$ . Show that the time response  $p(t)$ , the inverse Fourier transform of  $P(f)$ , is

$$p(t) = \sqrt{E} \frac{\operatorname{sinc}(4B_0 t)}{1 - 16B_0^2 t^2}$$

- 6.9 A computer puts out binary data at the rate of 56 kilobits per second. The computer output is transmitted using a baseband binary PAM system that is designed to have a raised-cosine pulse spectrum. Determine the transmission bandwidth required for each of the following roll-off factors:
- (a)  $\alpha = 0.25$
  - (b)  $\alpha = 0.5$
  - (c)  $\alpha = 0.75$
  - (d)  $\alpha = 1.0$
- 6.10 A binary PAM wave is to be transmitted over a low-pass channel with bandwidth of 75 kHz. The bit duration is  $10 \mu\text{s}$ . Find a raised-cosine pulse spectrum that satisfies these requirements.
- 6.11 Consider a channel with bandwidth 3.0 kHz, which is available for data transmission using binary PAM. Plot the permissible bit (signaling) rate  $1/T_b$  versus the excess bandwidth  $f_v$ , assuming that the roll-off factor  $\alpha$  varies from zero to unity, and that the criterion for zero intersymbol interference is satisfied.
- 6.12 You are given a channel of bandwidth 3.0 kHz. The requirement is to transmit data over the channel at the rate of 4.5 kilobits/s using binary PAM.
- (a) What is the maximum roll-off factor in the raised-cosine pulse spectrum that can accommodate this data transmission?
  - (b) What is the corresponding excess bandwidth?
- 6.13 This problem follows up on the pulse-shaping criterion for zero intersymbol interference, which is embodied in Eq. (6.30). This criterion can be satisfied by an infinite number of overall pulse spectra denoted by  $P(f)$ . The brick-wall spectrum of Fig. 6.2(a) and the raised-cosine pulse spectrum of Fig. 6.4(a) are two such examples. The pulse spectra shown in parts (a) and (b) of Fig. 6.12 are two other examples that can also satisfy the pulse-shaping criterion of Eq. (6.30).
- (a) Derive the condition that the bandwidth  $B_0$  in Fig. 6.12(a) must satisfy for the requirement of zero intersymbol interference to be satisfied for binary PAM.
  - (b) Repeat the problem for the pulse spectrum of Fig. 6.12(b).
  - (c) Given the four pulse spectra, the two of Figs. 6.2(b) and 6.3(a) and those of Fig. 6.12, why then is it that the raised-cosine pulse spectrum of Fig. 6.3(a) is the preferred choice in practice? Justify your answer.

**FIGURE 6.12** Problem 6.13

- 6.14 Repeat Problem 6.12, given that each set of three successive binary digits in the computer output is coded into one of eight possible amplitude levels, and the resulting signal is transmitted by using an 8-level PAM system designed to have a raised-cosine pulse spectrum.
- 6.15 An analog signal is sampled, quantized, and encoded into a binary PCM wave. The number of representation levels used is 128. A synchronizing pulse is added at the end of each code word. The resulting PCM signal is transmitted over a channel of bandwidth 13 kHz using a *quaternary* PAM system with a raised-cosine pulse spectrum. The roll-off factor is unity.
- Find the rate (in bits per second) at which information is transmitted through the channel.
  - Find the rate at which the analog signal is sampled. What is the maximum possible value for the highest frequency component of the analog signal?
- 6.16 A binary wave using non-return-to-zero signaling is generated by representing symbol 1 by a pulse of amplitude +1 and symbol 0 by a pulse of amplitude -1; in both cases, the pulse duration equals the bit duration. This signal is applied to a low-pass RC filter with transfer function:

$$H(f) = \frac{1}{1 + jf/f_0}$$

Construct the eye pattern for the filter output for the following sequences:

- Alternating 1s and 0s.
  - A long sequence of 1s followed by a long sequence of 0s.
  - A long sequence of 1s followed by a single 0 and then a long sequence of 1s.
- Assume a bit rate of  $2B_0$  bits per second.

- 6.17 The binary sequence 011010 is transmitted through a channel having a raised-cosine pulse spectrum with a roll-off factor of unity. Assume the use of non-return-to-zero signaling, with symbols 1 and 0 represented by +1 and -1, respectively.
- Construct the received wave to scale, and indicate the best sampling times for regeneration.
  - Construct the eye pattern for this received wave and show that it is completely open.
  - Determine the zero crossings of the received wave.
- 6.18 The sampled impulse response of a data-transmission system (encompassing the transmit filter and channel) is defined by

$$c_n = \{0.0, 0.15, 0.68, -0.22, 0.08\}$$

For zero-forcing equalization of the system, it is proposed to use a three-tap transversal filter.

- (a) Calculate the adjustable weights of the equalizer.  
 (b) Using the equalizer determined in part (a), calculate the residual intersymbol interference at the equalizer output.  
 (c) Identify the magnitude of the sample making the largest contribution to the residual intersymbol interference.
- 6.19 Repeat Problem 6.18, this time using a five-tap transversal filter for zero-forcing equalization of the system. Compare the residual intersymbol interference at the output of the equalizer with that in Problem 6.18, and comment on the benefit gained by using a longer transversal filter for the equalization process.

### ADVANCED PROBLEMS

The treatment of intersymbol interference presented in much of this chapter has viewed it as an undesirable phenomenon. Nevertheless, by adding intersymbol interference to the transmitted signal in a controlled manner, it is possible to achieve a signaling rate of  $2B_0$  symbols per second in a channel of bandwidth  $B_0$  hertz. Such an approach is called *correlative coding* or *partial-response signaling*. The next four problems address issues related to correlative coding, as summarized here:

- Problems 6.20 and 6.21 pertain to duobinary signaling. In particular, Problem 6.20 addresses the duobinary conversion filter, the use of which can lead to a propagation of errors. To mitigate this problem, we use a precoder addressed in Problem 6.21.
  - Problem 6.22 pertains to a modification of the schemes described in Problems 6.20 and 6.21.
  - Finally, Problem 6.23 probes the use of modified duobinary signaling for single sideband modulation applied to data transmission.
- 6.20 Figure 6.13 depicts the duobinary signaling scheme in its simplest form. The incoming binary sequence  $\{b_k\}$  consists of uncorrelated binary symbols 1 and 0, each having duration  $T_b$ . This sequence is first applied to a pulse-amplitude modulator to produce the two-level sequence  $\{a_k\}$  consisting of pulses (short enough to be viewed as unit impulses). Specifically,

$$a_k = \begin{cases} +1, & \text{if symbol } b_k \text{ is 1} \\ -1, & \text{if symbol } b_k \text{ is 0} \end{cases}$$

The two-level sequence  $\{a_k\}$  is next applied to the duobinary conversion filter enclosed inside the dashed rectangle in Fig. 6.13, where the Nyquist channel  $H_{\text{opt}}(f)$  is defined by (see Eq. (6.15))

$$H_{\text{opt}}(f) = \begin{cases} \frac{\sqrt{E}}{2B_0}, & \text{for } -B_0 < f < B_0 \\ 0, & \text{otherwise} \end{cases}$$

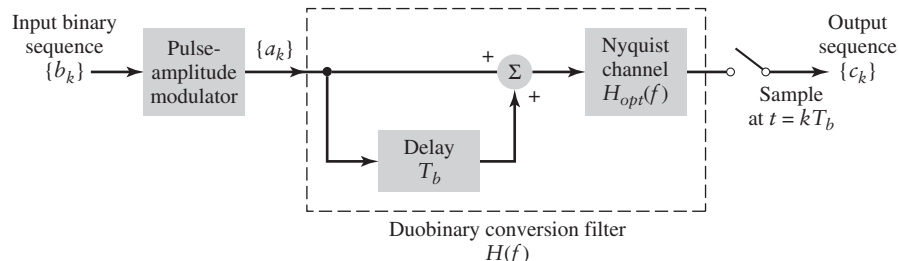


FIGURE 6.13 Problem 6.20

At the receiver, the channel output is sampled every  $T_b$  seconds in synchronism with the transmitter; the sample so produced is denoted by  $c_k$ . An estimate  $\hat{a}_k$  of the original symbol  $a_k$  is produced by using the rule

$$\hat{a}_k = c_k - \hat{a}_{k-1}$$

where  $\hat{a}_{k-1}$  is the previous estimate.

- (a) Determine the overall frequency response  $H(f)$  of the duobinary conversion filter.
  - (b) Determine the impulse response  $h(t)$  of this filter.
  - (c) The above-described rule used in the receiver is an example of *decision feedback*, which may be viewed as an inverse of the delay-line filter at the transmitter. A major drawback of this decision rule is that once errors are made, they tend to *propagate* through the output. Why? Justify your answer.
- 6.21 To mitigate the *error propagation phenomenon* discussed in part (c) of Problem 6.20, we may use a *precoder*, as depicted in Fig. 6.14. The precoding is applied to the input binary sequence  $\{b_k\}$ , producing a new binary sequence  $\{d_k\}$  defined by

$$d_k = b_k \oplus d_{k-1}$$

where the symbol  $\oplus$  denotes *modulo-two addition*. This addition is equivalent to the EXCLUSIVE-OR operation, which operates as follows. The output  $d_k$  is a symbol 1 if inputs,  $b_k$  or  $d_{k-1}$ , differ from each other; otherwise, the output  $d_k$  is symbol 0.

As shown in Figure 6.14, the precoded binary sequence  $\{d_k\}$  is applied to a pulse-amplitude modulator, followed by the duobinary conversion filter; both of these two components follow exactly the same descriptions presented in Problem 6.20. This time, however, the decision rule used by the receiver for detecting the original binary sequence  $\{b_k\}$  from the three-level sequence  $\{c_k\}$  is defined by

If  $|c_k| < 1$ , say binary symbol  $b_k$  is 1  
If  $|c_k| > 1$ , say binary symbol  $b_k$  is 0

According to this decision, the detector consists of a rectifier followed by a threshold device. Most important, if any  $c_k$  is received in error, the error is confined to that instant.

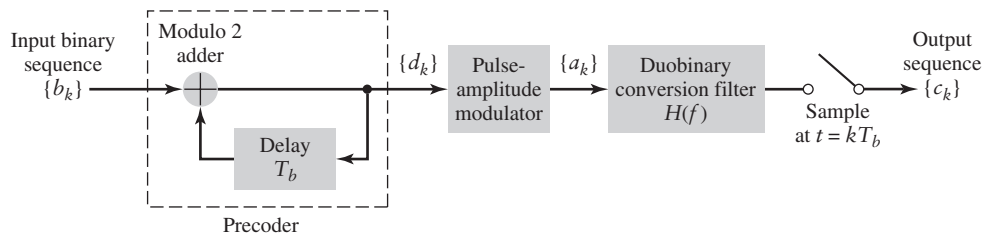


FIGURE 6.14 Problem 6.21

To illustrate the operation of the duobinary signaling scheme with precoding, consider the input data sequence

$$\{b_k\} = 0010110$$

To proceed with the precoding of this sequence, add an extra bit to the precoder output; this extra bit is chosen arbitrarily to be 1. Hence, do the following:

- (a) Determine the precoded sequence  $\{d_k\}$ , and then the two-level sequence  $\{a_k\}$  produced by the pulse-amplitude modulator.

- (b) Determine the duobinary code output  $\{c_k\}$ .  
 (c) Applying  $\{c_k\}$  to the rectifier-based detector described above, determine the resulting binary sequence. Thereby, demonstrate the correct reconstruction of the original sequence.
- 6.22 In this problem, we consider another correlative scheme known as *modified duobinary signaling*, which is depicted in Fig. 6.15. The correlative encoding strategy is now defined by

$$c_k = a_k - a_{k-2}$$

which involves a correlation span of two binary symbols.

- (a) Determine the frequency response  $H(f)$  of the modified duobinary conversion filter enclosed inside the second dashed rectangle in Fig. 6.15.  
 (b) Determine the impulse response  $h(t)$  of this filter, and show that it has three distinguishable levels at the sampling instants.  
 (c) For decoding in the receiver, demonstrate the successful use of the decision rule:

$$\hat{b}_k = \begin{cases} \text{symbol 1, } & \text{if } |c_k| > 1 \\ \text{symbol 0, } & \text{if } |c_k| < 1 \end{cases}$$

For the demonstration, again use the input sequence 0010110.

- (d) In light of your findings in parts (a) through (c), discuss the advantages of the modified duobinary encoder over the duobinary encoder discussed in Problem 6.21.

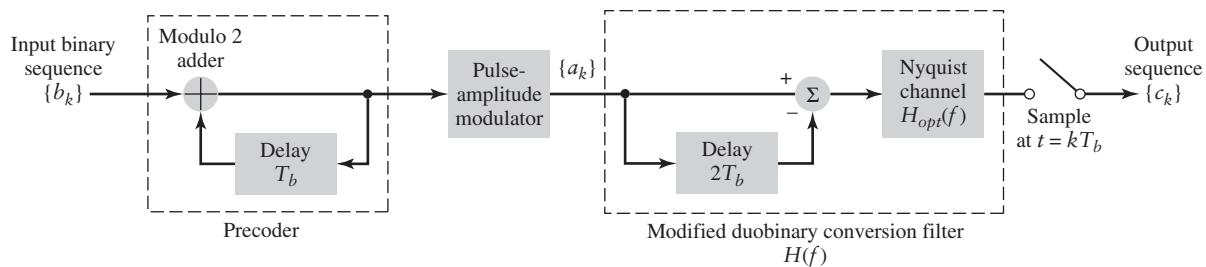


**FIGURE 6.15** Problem 6.22

- 6.23 The modified duobinary signaling scheme described in Problem 6.22 is well-suited for single sideband modulation applied to binary data transmission over a linear channel. Justify the practical reality of this statement.

## CHAPTER 7

# DIGITAL BAND-PASS MODULATION TECHNIQUES

In baseband data transmission, which we studied in Chapter 6, an incoming serial data stream is represented in the form of a discrete pulse-amplitude modulated wave that can be transmitted over a low-pass channel (e.g., a coaxial cable). What if the requirement is to transmit the data stream over a band-pass channel, exemplified by wireless and satellite channels? In applications of this kind, we usually resort to the use of a *modulation strategy configured around a sinusoidal carrier* whose amplitude, phase, or frequency is varied in accordance with the information-bearing data stream. Digital modulation techniques dealing with band-pass data transmission are studied in this chapter.

The primary aim of the chapter is to describe some important digital band-pass modulation techniques used in practice. In particular, we describe three basic modulation schemes: namely, amplitude-shift keying, phase-shift keying, and frequency-shift keying, followed by some of their variants. Another issue that will receive particular attention is that of coherent versus noncoherent detection. A digital communication system is said to be *coherent* if the receiver is synchronized to the transmitter with respect to carrier phase; otherwise, the system is said to be *noncoherent*. Naturally, a noncoherent system offers the practical advantage of reduced complexity but at the cost of degraded performance. Considerations of the issue of noise performance evaluation are deferred to Chapter 10.

This chapter will teach us three lessons:

- ▶ *Lesson 1: Each digital band-pass modulation scheme is defined by a transmitted signal with a unique phasor representation.*
- ▶ *Lesson 2: At the receiving end, digital demodulation techniques encompass different forms, depending on whether the receiver is coherent or noncoherent.*
- ▶ *Lesson 3: Two ways of classifying digital modulation schemes are (a) by the type of modulation used, and (b) whether the transmitted data stream is in binary or M-ary form.*

### 7.1 Some Preliminaries

Given a binary source that emits symbols 0 and 1, *the modulation process involves switching or keying the amplitude, phase, or frequency of a sinusoidal carrier wave between a pair of possible values in accordance with symbols 0 and 1*. To be more specific, consider the sinusoidal carrier

$$c(t) = A_c \cos(2\pi f_c t + \phi_c) \quad (7.1)$$

where  $A_c$  is the carrier amplitude,  $f_c$  is the carrier frequency, and  $\phi_c$  is the carrier phase. Given these three parameters of the carrier  $c(t)$ , we may now identify three distinct forms of *binary modulation*:

1. *Binary amplitude shift-keying* (BASK), in which the carrier frequency and carrier phase are both maintained constant, while the carrier amplitude is keyed between the two possible values used to represent symbols 0 and 1.
2. *Binary phase-shift keying* (BPSK), in which the carrier amplitude and carrier frequency are both maintained constant, while the carrier phase is keyed between the two possible values (e.g.,  $0^\circ$  and  $180^\circ$ ) used to represent symbols 0 and 1.
3. *Binary frequency-shift keying* (BFSK), in which the carrier amplitude and carrier phase are both maintained constant, while the carrier frequency is keyed between the two possible values used to represent symbols 0 and 1.

In light of these definitions, we see that BASK, BPSK, and BFSK are special cases of amplitude modulation, phase modulation, and frequency modulation, respectively. Indeed, it was with this close relationship between analog and digital modulation techniques in mind that in the “Summary and Discussion” sections of Chapter 3 on amplitude modulation and Chapter 4 on angle modulation, we briefly highlighted the connections between analog and digital modulation schemes. An important conclusion that we can draw from the close relationship between analog and digital modulation techniques is that despite their basic differences, BASK, BPSK, and BFSK share a common feature: all three of them are examples of a *band-pass process*.

In the analog communications literature, the sinusoidal carrier  $c(t)$  is commonly defined as in Eq. (7.1). On the other hand, in the digital communications literature, the usual practice is to assume that the carrier  $c(t)$  has *unit energy measured over one symbol (bit) duration*. Specifically, from Problem 3.28, we recall that the carrier amplitude

$$A_c = \sqrt{\frac{2}{T_b}} \quad (7.2)$$

where  $T_b$  is the *bit duration*. Using the terminology of Eq. (7.2), we may thus express the carrier  $c(t)$  in the equivalent form

$$c(t) = \sqrt{\frac{2}{T_b}} \cos(2\pi f_c t + \phi_c) \quad (7.3)$$

From the material presented in Chapter 2 on the Fourier representation of signals and systems, we learned that decreasing the duration of a rectangular pulse has the effect of widening the effective band of frequencies contained in the pulse. In a corresponding fashion, decreasing the bit duration  $T_b$  has the effect of increasing the transmission bandwidth requirement of a binary modulated wave.

One other lesson learned from material covered in previous chapters—namely, Chapters 3 and 4—is the fact that the transmission bandwidth requirement of an angle-modulated wave is greater than that of the corresponding amplitude-modulated wave. In light of that lesson, we may say that the transmission bandwidth requirement of BFSK is greater than that of BASK for a given binary source. However, the same does *not* hold for BPSK, as we shall see from the material presented in this chapter. This is one of many differences that distinguish digital modulation from analog modulation.

### ■ BAND-PASS ASSUMPTION

The spectrum of a digitally modulated wave, exemplified by BASK, BPSK and BFSK, is centered on the carrier frequency  $f_c$ , implicitly or explicitly. Moreover, as with analog modulation, it is normal practice to assume that the carrier frequency  $f_c$  is large compared with the “bandwidth” of the incoming binary data stream that acts as the modulating signal. This band-pass assumption has certain implications, as discussed next.

To be specific, consider a linear modulation scheme for which the modulated wave is defined by

$$s(t) = b(t)c(t) \quad (7.4)$$

where  $b(t)$  denotes an incoming binary wave. Then, setting the carrier phase  $\phi_c = 0$  for convenience of presentation, we may use Eq. (7.3) to express the modulated wave  $s(t)$  as

$$s(t) = \sqrt{\frac{2}{T_b}} b(t) \cos(2\pi f_c t) \quad (7.5)$$

Under the assumption  $f_c \gg W$ , where  $W$  is the bandwidth of the binary wave  $b(t)$ , there will be *no* spectral overlap in the generation of  $s(t)$  (i.e., the spectral content of the modulated wave for positive frequencies is essentially separated from its spectral content for negative frequencies).

Another implication of the band-pass assumption is that we may express *the transmitted signal energy per bit* as

$$\begin{aligned} E_b &= \int_0^{T_b} |s(t)|^2 dt \\ &= \frac{2}{T_b} \int_0^{T_b} |b(t)|^2 \cos^2(2\pi f_c t) dt \end{aligned} \quad (7.6)$$

Using the trigonometric identity

$$\cos^2(2\pi f_c t) = \frac{1}{2}[1 + \cos(4\pi f_c t)]$$

we may rewrite Eq. (7.6) as

$$E_b = \frac{1}{T_b} \int_0^{T_b} |b(t)|^2 dt + \frac{1}{T_b} \int_0^{T_b} |b(t)|^2 \cos(4\pi f_c t) dt \quad (7.7)$$

The band-pass assumption implies that  $|b(t)|^2$  is essentially constant over one complete cycle of the sinusoidal wave  $\cos(4\pi f_c t)$ , which, in turn, means that

$$\int_0^{T_b} |b(t)|^2 \cos(4\pi f_c t) dt \approx 0$$

Accordingly, we may approximate Eq. (7.7) as

$$E_b \approx \frac{1}{T_b} \int_0^{T_b} |b(t)|^2 dt \quad (7.8)$$

In words, for linear digital modulation schemes governed by Eq. (7.5), the transmitted signal energy (on a per bit basis) is a scaled version of the energy in the incoming binary wave responsible for modulating the sinusoidal carrier.

► **Drill Problem 7.1** Invoking the band-pass assumption, show that

$$\int_0^{T_b} \sin(2\pi f_c t) \cos(2\pi f_c t) dt \approx 0$$

regardless of how the bit duration  $T_b$  is exactly related to  $f_c$  as long as  $f_c \gg 1/T_b$ . ◀

► **Drill Problem 7.2** Show that Eq. (7.8) is *invariant* with respect to the carrier phase  $\phi_c$  (i.e., it holds for all  $\phi_c$ ). ◀

## 7.2 Binary Amplitude-Shift Keying

Binary amplitude-shift keying (BASK) is one of the earliest forms of digital modulation used in radio telegraphy at the beginning of the twentieth century. To formally describe BASK, consider a binary data stream  $b(t)$  which is of the *ON-OFF signaling* variety. That is,  $b(t)$  is defined by

$$b(t) = \begin{cases} \sqrt{E_b}, & \text{for binary symbol 1} \\ 0, & \text{for binary symbol 0} \end{cases} \quad (7.9)$$

Then, multiplying  $b(t)$  by the sinusoidal carrier wave of Eq. (7.3) with the phase  $\phi_c$  set equal to zero for convenience of presentation, we get the BASK wave

$$s(t) = \begin{cases} \sqrt{\frac{2E_b}{T_b}} \cos(2\pi f_c t), & \text{for symbol 1} \\ 0, & \text{for symbol 0} \end{cases} \quad (7.10)$$

The carrier frequency  $f_c$  may have an arbitrary value, consistent with transmitting the modulated signal anywhere in the electromagnetic radio spectrum, so long as it satisfies the band-pass assumption.

When a bit duration is occupied by symbol 1, the transmitted signal energy is  $E_b$ . When the bit duration is occupied by symbol 0, the transmitted signal energy is zero. On this basis, we may express the *average transmitted signal energy* as

$$E_{av} = \frac{E_b}{2} \quad (7.11)$$

For this formula to hold, however, the two binary symbols must be *equiprobable*. In other words, if we are given a *long* binary data stream, then symbols 1 and 0 occur in essentially equal numbers in that data stream. For this equality to hold, however, there must be *no bias* involved in the generation of the bit stream, either in favor of symbol 1 or symbol 0.

### ■ GENERATION AND DETECTION OF ASK SIGNALS

From Eqs. (7.9) and (7.10), we readily see that a BASK signal is readily generated by using a product modulator with two inputs. One input, the ON-OFF signal of Eq. (7.9), is the modulating signal. The sinusoidal carrier wave

$$c(t) = \sqrt{\frac{2}{T_b}} \cos(2\pi f_c t)$$

supplies the other input.

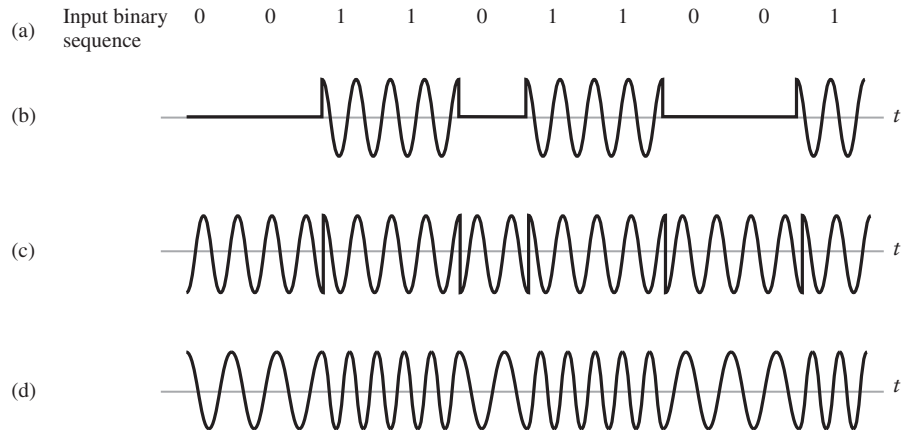


**FIGURE 7.1** The three basic forms of signaling binary information. (a) Binary data stream. (b) Amplitude-shift keying, (c) Phase-shift keying, (d) Frequency-shift keying with continuous phase.

A property of BASK that is immediately apparent from Fig. 7.1(b), which depicts the BASK waveform corresponding to the incoming binary data stream of Fig. 7.1(a), is the *non-constancy of the envelope* of the modulated wave. Accordingly, insofar as detection of the BASK wave is concerned, the simplest way is to use an envelope detector, exploiting the non-constant-envelope property of the BASK signal.

### ■ COMPUTER EXPERIMENT I: SPECTRAL ANALYSIS OF BASK

Consider a binary data stream that consists of a *square wave*, the amplitude of which alternates between the constant levels  $\sqrt{E_b}$  and zero every  $T_b$  seconds. The square wave is centered on the origin for convenience of the presentation. The objective of the experiment is twofold:

- (i) To investigate the effect of varying the carrier frequency  $f_c$  on the power spectrum of the BASK signal  $s(t)$ , assuming that the square wave is fixed. Recall that the power spectrum of a signal (expressed in decibels) is defined as 10 times the logarithm (to base 10) of the squared magnitude (amplitude) spectrum of the signal.
- (ii) To investigate the effect of varying the frequency of the square wave on the spectrum of the BASK signal, assuming that the sinusoidal carrier wave is fixed.

For the purpose of computer evaluation, we set the carrier frequency  $f_c = n/T_b$  where  $n$  is an integer. This choice of the carrier frequency  $f_c$  permits the simulation of a band-pass system on a digital computer without requiring  $f_c \gg 1/T_b$ ; the only restriction on the choice is to make sure that spectral overlap is avoided. (We follow this practice when performing computer experiments as we go forward in the study of other digital modulation schemes.)

To plot the power spectra (in decibels) of the digitally modulated waves (in this experiment and others to follow), we use the fast Fourier transform (FFT) algorithm, which was discussed in Section 2.10. The simulation parameters used in the computer experiments (this one and the subsequent experiments) are as follows:

Number of data bits (1s and 0s)	= 100
Sampling frequency, $f_s$	= 100 Hz
Number of data points (samples)	= $100 \times f_s = 10,000$ data points
Block size of the FFT, $N$	= 4096

Results of the computation are plotted in Figs. 7.2 and 7.3.

The two parts of Fig. 7.2 correspond to objective (i) of the experiment. Specifically, the two plots shown in Fig. 7.2 correspond to the following parameters:

$$\text{Bit duration, } T_b = 1 \text{ s}$$

$$\text{Carrier frequency, } f_c = \begin{cases} 4 \text{ Hz for Fig. 7.2(a)} \\ 8 \text{ Hz for Fig. 7.2(b)} \end{cases}$$

The second set of results plotted in Fig. 7.3 corresponds to objective (ii) of the experiment, using the following parameters:

$$\text{Carrier frequency, } f_c = 8 \text{ Hz}$$

$$\text{Bit duration, } T_b = \begin{cases} 1 \text{ s for Fig. 7.3(a)} \\ \frac{1}{2} \text{ s for Fig. 7.3(b)} \end{cases}$$

In each part of Figs. 7.2 and 7.3, we show two power spectral plots: one shaded, resulting from the computation, and the other, well-defined curve, obtained from theory. (We follow a similar practice in the computer experiments to follow.) Here we must recognize that the binary data streams used in the experiments are of finite length, hence the jagged appearance depicted in the figures. In contrast, theory leads to a solid curve, which closely follows the “envelope” of the computational results.

In light of the results plotted in Figs. 7.2 and 7.3, we can make the following observations for positive frequencies:

1. The spectrum of the BASK signal contains a line component at  $f = f_c$ .
2. When the square wave is fixed and the carrier frequency is doubled, the mid-band frequency of the BASK signal is likewise doubled.
3. When the carrier is fixed and the bit duration is halved, the width of the main lobe of the sinc function defining the envelope of the BASK spectrum is doubled, which, in turn, means that the transmission bandwidth of the BASK signal is doubled.
4. The transmission bandwidth of BASK, measured in terms of the width of the main lobe of its spectrum, is equal to  $2/T_b$ , where  $T_b$  is the bit duration.

These observations support the statement: the BASK signal is an example of amplitude modulation that includes the carrier wave as a component in its composition.

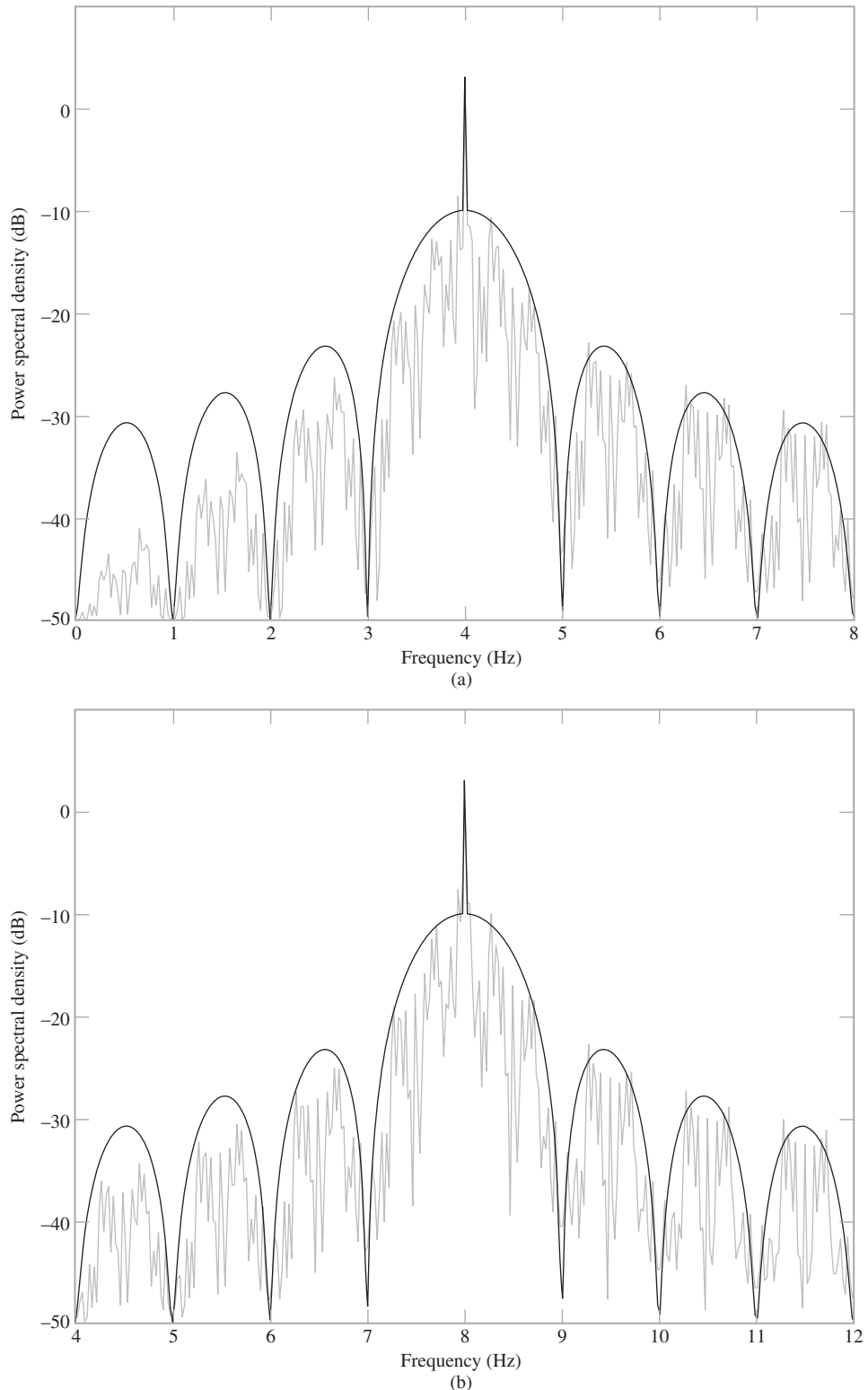


**FIGURE 7.2** Power spectra of BASK signal produced by square wave as the modulating signal for varying modulation frequency: (a)  $f_c = 4$  Hz and  $T_b = 1$  s; (b)  $f_c = 8$  Hz and  $T_b = 1$  s.

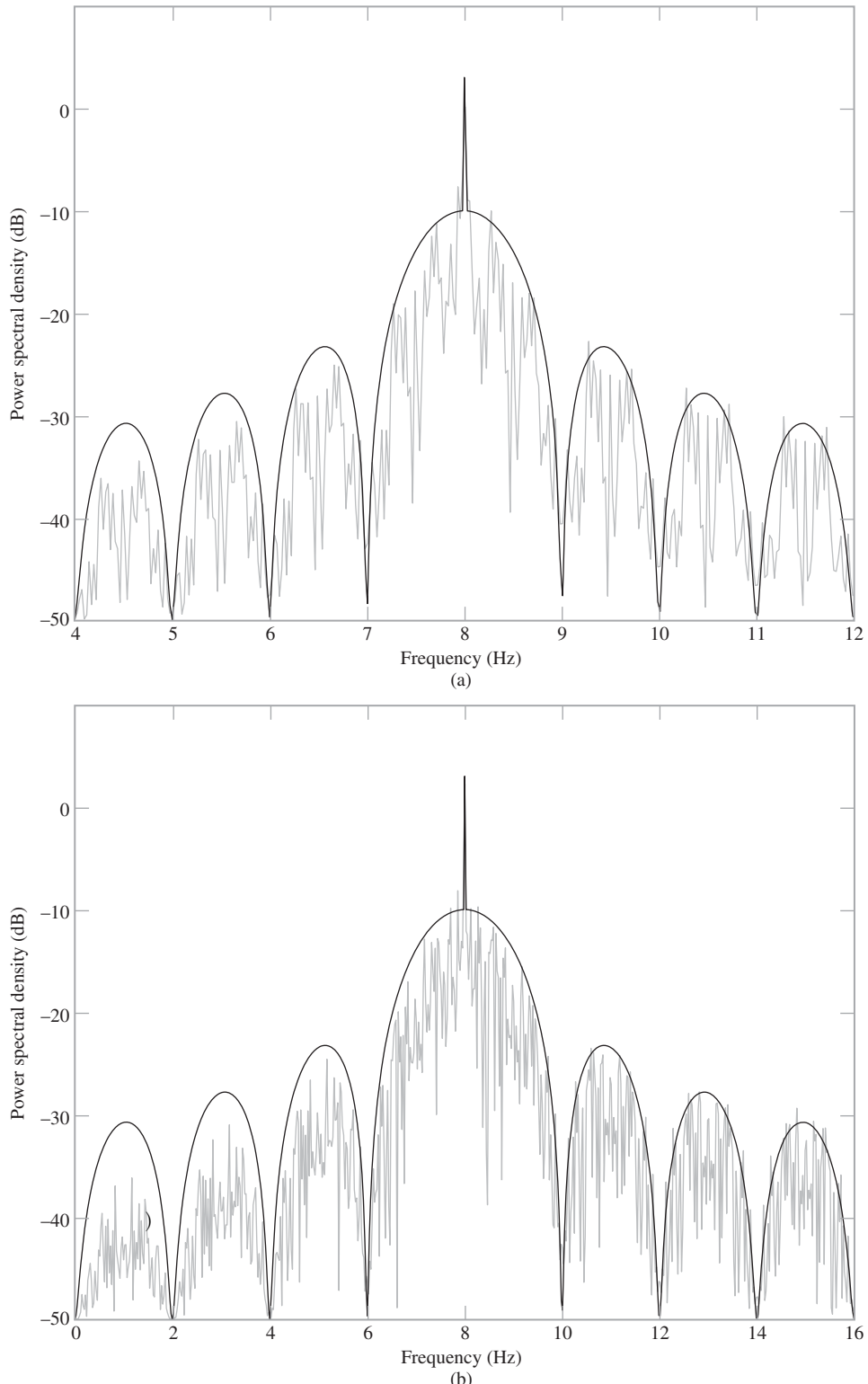


**FIGURE 7.3** Power spectra of BASK signal produced by square wave as the modulating signal for varying bit duration: (a)  $f_c = 8$  Hz and  $T_b = 1$  s; (b)  $f_c = 8$  Hz and  $T_b = 1/2$  s

## 7.3 Phase-Shift Keying

### BINARY PHASE-SHIFT KEYING (BPSK)

In the simplest form of phase-shift keying known as *binary phase-shift keying (BPSK)*, the pair of signals  $s_1(t)$  and  $s_2(t)$  used to represent symbols 1 and 0, respectively, are defined by

$$s_i(t) = \begin{cases} \sqrt{\frac{2E_b}{T_b}} \cos(2\pi f_c t), & \text{for symbol 1 corresponding to } i = 1 \\ \sqrt{\frac{2E_b}{T_b}} \cos(2\pi f_c t + \pi) = -\sqrt{\frac{2E_b}{T_b}} \cos(2\pi f_c t), & \text{for symbol 0 corresponding to } i = 2 \end{cases} \quad (7.12)$$

where  $0 \leq t \leq T_b$ , with  $T_b$  denoting the bit duration and  $E_b$  denoting the transmitted signal energy per bit; see the waveform of Fig. 7.1 (c) for a representation example of BPSK. A pair of sinusoidal waves,  $s_1(t)$  and  $s_2(t)$ , which differ only in a relative phase-shift of  $\pi$  radians as defined in Eq. (7.12), are referred to as *antipodal signals*. From the two lines of this equation, we see that BPSK is in actual fact a special case of double-sideband suppressed-carried (DSB-SC) modulation, a remark that was previously pointed out in Section 3.10.

BPSK differs from BASK in an important respect: the envelope of the modulated signal  $s(t)$  is maintained *constant* at the value  $\sqrt{2E_b/T_b}$  for all time  $t$ . This property, which follows directly from Eq. (7.12), has two important consequences:

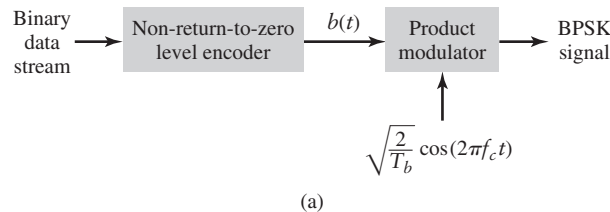
1. The transmitted energy per bit,  $E_b$  is constant; equivalently, the average transmitted power is constant.
2. Demodulation of BPSK cannot be performed using envelope detection; rather, we have to look to coherent detection as described next.

### GENERATION AND COHERENT DETECTION OF BPSK SIGNALS

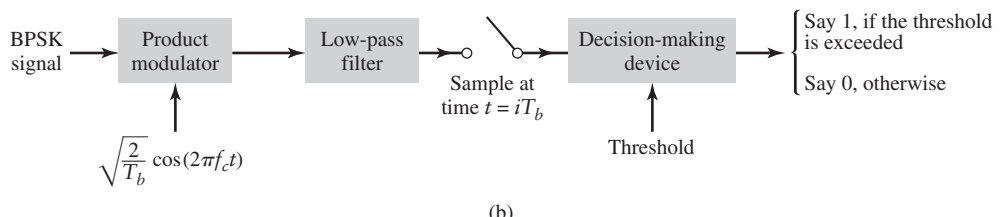
#### (i) Generation

To generate the BPSK signal, we build on the fact that the BPSK signal is a special case of DSB-SC modulation. Specifically, we use a product modulator consisting of two components (see Fig. 7.4(a)):

- (i) *Non-return-to-zero level encoder*, whereby the input binary data sequence is encoded in polar form with symbols 1 and 0 represented by the constant-amplitude levels:  $\sqrt{E_b}$  and  $-\sqrt{E_b}$ , respectively.



(a)



(b)

**FIGURE 7.4** (a) BPSK modulator. (b) Coherent detector for BPSK; for the sampler, integer  $i = 0, \pm 1, \pm 2, \dots$ .

- (ii) *Product modulator*, which multiplies the level-encoded binary wave by the sinusoidal carrier  $c(t)$  of amplitude  $\sqrt{2}/T_b$  to produce the BPSK signal.

The timing pulses used to generate the level-encoded binary wave and the sinusoidal carrier wave are usually, but not necessarily, extracted from a common master clock.

**(ii) Detection**

To detect the original binary sequence of 1s and 0s, the BPSK signal  $x(t)$  at the channel output is applied to a receiver that consists of four sections, as depicted in Fig. 7.4(b):

- (i) *Product modulator*, which is also supplied with a locally generated reference signal that is a replica of the carrier wave  $c(t)$ .
- (ii) *Low-pass filter*, designed to remove the double-frequency components of the product modulator output (i.e., the components centered on  $2f_c$ ) and pass the zero-frequency components.
- (iii) *Sampler*, which uniformly samples the output of the low-pass filter at  $t = i T_b$ , where  $i = 0, \pm 1, \pm 2, \dots$ ; the local clock governing the operation of the sampler is *synchronized* with the clock responsible for bit-timing in the transmitter.
- (iv) *Decision-making device*, which compares the sampled value of the low-pass filter's output to an externally supplied *threshold*, every  $T_b$  seconds. If the threshold is exceeded, the device decides in favor of symbol 1; otherwise, it decides in favor of symbol 0.

The BPSK receiver described in Fig. 7.4 is said to be *coherent* in the sense that the sinusoidal reference signal applied to the product modulator in the demodulator is *synchronous* in phase (and, of course, frequency) with the carrier wave used in the modulator. This requirement can be achieved by using a phase-locked loop, which was described in Section 4.8. In addition to synchrony with respect to carrier phase, the receiver also has an accurate knowledge of the interval occupied by each binary symbol.

The operation of the coherent BPSK receiver in Fig. 7.4(b) follows a procedure similar to that described for the demodulation of a double-sideband suppressed-carrier (DSB-SC) modulated wave (described in Section 3.3) with a couple of important additions: sampler and decision-making device. The rationale for this similarity builds on what we have already stated: BPSK is simply another form of DSB-SC modulation.

However, an issue that needs particular attention is how to design the low-pass filter in Fig. 7.4(b). Specifically, what should the bandwidth of the filter be? From the conclusion drawn from the graphical results presented in Fig. 2.28 on the response of an ideal low-pass filter to an input rectangular pulse for varying time-bandwidth product, we recall that a time-bandwidth product equal to or greater than unity is a necessary requirement to ensure that the waveform of the filter input is recognizable from the resulting output. For the problem at hand, we may therefore state that the bandwidth of the low-pass filter in the coherent BPSK receiver of Fig. 7.4(b) has to be equal to or greater than the reciprocal of the bit duration  $T_b$  for satisfactory operation of the receiver.

## ■ COMPUTER EXPERIMENT II: SPECTRAL ANALYSIS OF BPSK

As with the experiment on BASK, consider a binary data stream that consists of a square wave, the amplitude of which alternates between  $+\sqrt{E_b}$  and  $-\sqrt{E_b}$  every  $T_b$  seconds. The square wave is centered on the origin. The objectives of this second experiment are similar to those of Computer Experiment I on BASK:

- (i) To evaluate the effect of varying the carrier frequency  $f_c$  on the power spectrum of the BPSK signal, for a fixed square modulating wave.
- (ii) To evaluate the effect of varying modulation frequency on the power spectrum of the BPSK signal for a fixed carrier frequency.

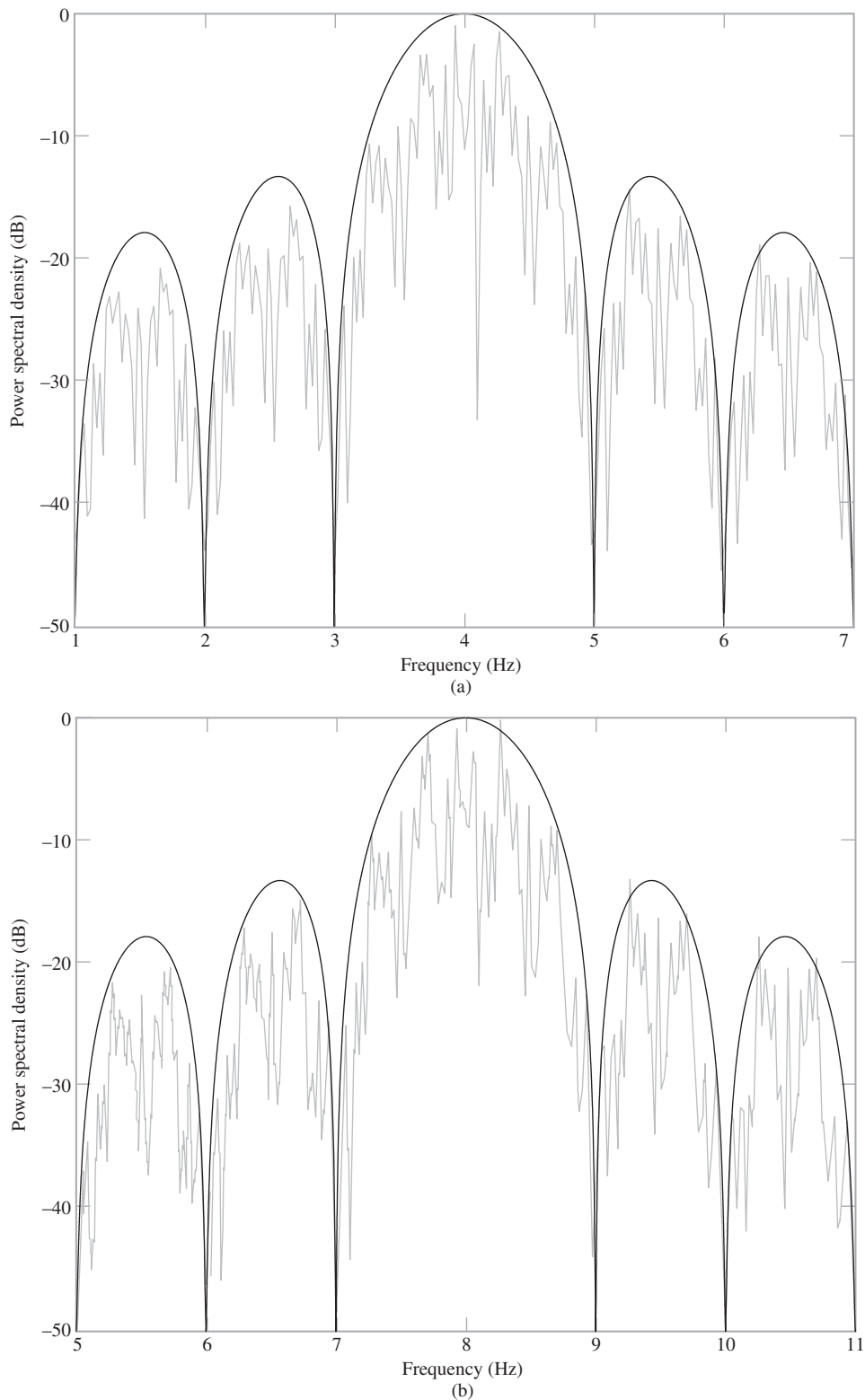


**FIGURE 7.5** Power spectra of BPSK signal produced by square wave as the modulating signal for varying modulation frequency: (a)  $f_c = 4$  Hz and  $T_b = 1$  s; (b)  $f_c = 8$  Hz and  $T_b = 1$  s.

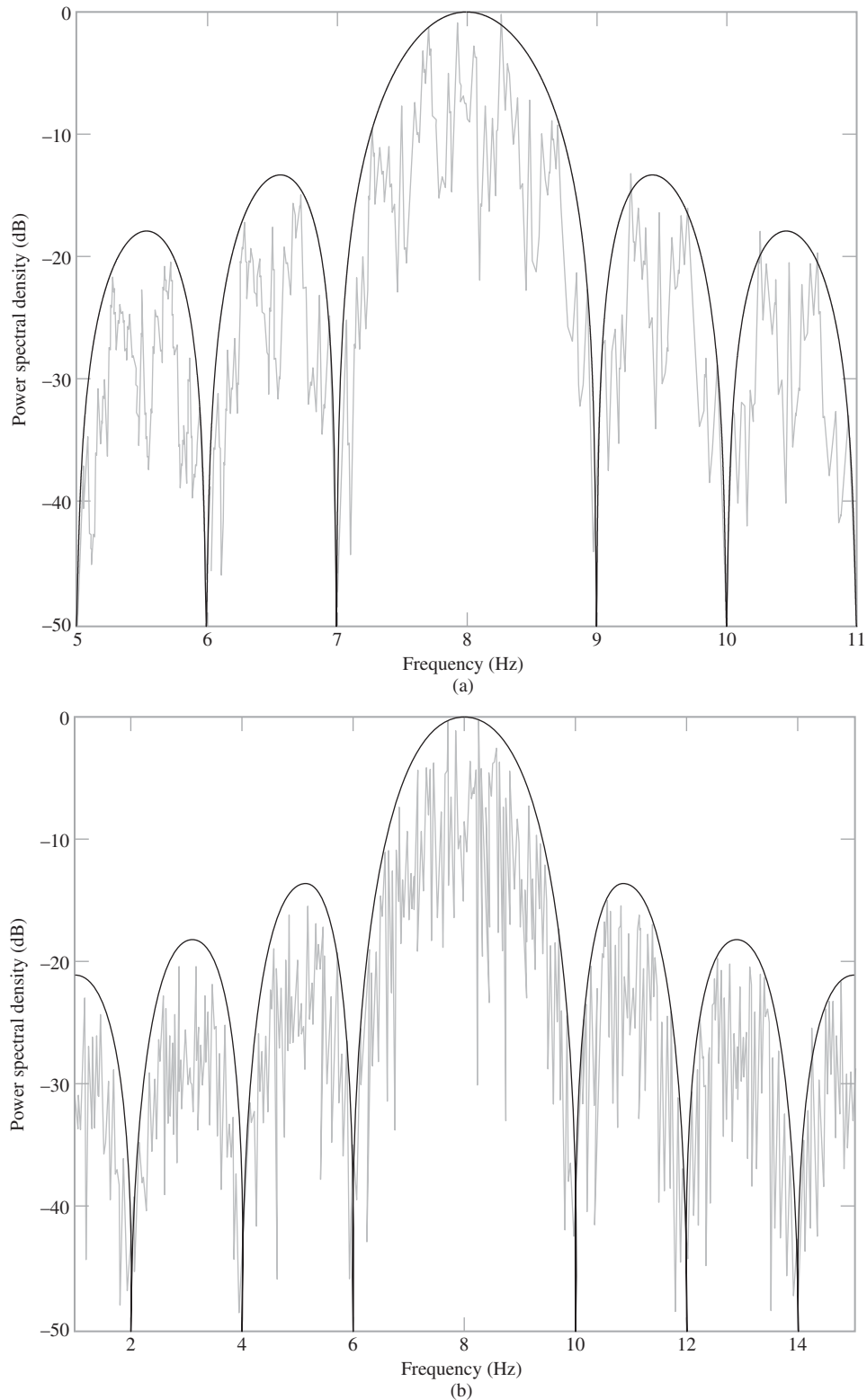


**FIGURE 7.6** Power spectra of BPSK signal produced by square wave as the modulating signal for varying bit duration: (a)  $f_c = 8$  Hz and  $T_b = 1$  s; (b)  $f_c = 8$  Hz and  $T_b = 1/2$  s.

To be consistent with Experiment I on BASK, objectives (i) and (ii) are investigated for the same sets of frequencies used in that experiment. The results of the experiment on BPSK are plotted in Figs. 7.5 and 7.6, where, as before, we show computational results alongside the corresponding theoretical ones. Comparing these two figures with Figs. 7.2 and 7.3 for BASK, respectively, we can make two important observations:

1. BASK and BPSK signals occupy the same transmission bandwidth—namely,  $2/T_b$ —which defines the width of the main lobe of the sinc-shaped power spectra.
2. The BASK spectrum includes a carrier component, whereas this component is absent from the BPSK spectrum. With this observation we are merely restating the fact that BASK is an example of amplitude modulation, whereas BPSK is an example of double sideband-suppressed carrier modulation.

This second observation has practical implications of its own:

- ▶ The presence of carrier in the BASK spectrum means that the binary data stream can be recovered by envelope detection of the BASK signal.
- ▶ On the other hand, suppression of the carrier in the BPSK spectrum mandates the use of coherent detection for recovery of the binary data stream from the BASK signal, as discussed on page 271.

### ■ QUADRIPHASE-SHIFT KEYING

An important goal of digital communication is the *efficient utilization of channel bandwidth*. This goal is attained by a bandwidth-conserving modulation scheme known as quadriphase-shift keying, which builds on the same idea as that of quadrature-carrier multiplexing that was discussed in Section 3.5.

In *quadriphase-shift keying* (QPSK), as with BPSK, information carried by the transmitted signal is contained in the phase of a sinusoidal carrier. In particular, the phase of the sinusoidal carrier takes on one of four equally spaced values, such as  $\pi/4$ ,  $3\pi/4$ ,  $5\pi/4$ , and  $7\pi/4$ . For this set of values, we define the transmitted signal as

$$s_i(t) = \begin{cases} \sqrt{\frac{2E}{T}} \cos\left[2\pi f_c t + (2i - 1)\frac{\pi}{4}\right], & 0 \leq t \leq T \\ 0, & \text{elsewhere} \end{cases} \quad (7.13)$$

where  $i = 1, 2, 3, 4$ ;  $E$  is the *transmitted signal energy per symbol* and  $T$  is the *symbol duration*. Each one of the four equally spaced phase values corresponds to a unique pair of bits called a *dibit*. For example, we may choose the foregoing set of phase values to represent the *Gray encoded* set of dibits: 10, 00, 01, and 11. In this form of encoding, we see that only a single bit is changed from one dibit to the next. Note that the *symbol duration* (i.e., the duration of each dibit) is twice the bit duration, as shown by

$$T = 2T_b \quad (7.14)$$

Using a well-known trigonometric identity, we may recast the transmitted signal in the interval  $0 \leq t \leq T$  in the expanded form

$$s_i(t) = \sqrt{\frac{2E}{T}} \cos\left[(2i - 1)\frac{\pi}{4}\right] \cos(2\pi f_c t) - \sqrt{\frac{2E}{T}} \sin\left[(2i - 1)\frac{\pi}{4}\right] \sin(2\pi f_c t) \quad (7.15)$$

where  $i = 1, 2, 3, 4$ . Based on the expanded form of Eq. (7.15), we can make some important observations:

1. In reality, the QPSK signal consists of the sum of two BPSK signals.
2. One BPSK signal, represented by the first term

$$\sqrt{2E/T} \cos[(2i - 1)\pi/4] \cos[(2\pi f_c t)],$$

defines the product of modulating a binary wave by the sinusoidal carrier  $\sqrt{2/T} \cos(2\pi f_c t)$ , which has unit energy over the symbol duration  $T$ . We also recognize that

$$\sqrt{E} \cos\left[(2i - 1)\frac{\pi}{4}\right] = \begin{cases} \sqrt{E/2} & \text{for } i = 1, 4 \\ -\sqrt{E/2} & \text{for } i = 2, 3 \end{cases} \quad (7.16)$$

We therefore see that this binary wave has an amplitude equal to  $\pm\sqrt{E/2}$ .

3. The other BPSK signal, represented by the second term

$$-\sqrt{2E/T} \sin\left[(2i - 1)\frac{\pi}{4}\right] \sin(2\pi f_c t),$$

defines the product of modulating a different binary wave by the sinusoidal carrier  $\sqrt{2/T} \sin(2\pi f_c t)$ , which also has unit energy per symbol. This time, we recognize that

$$-\sqrt{E} \sin\left[(2i - 1)\frac{\pi}{4}\right] = \begin{cases} -\sqrt{E/2} & \text{for } i = 1, 2 \\ \sqrt{E/2} & \text{for } i = 3, 4 \end{cases} \quad (7.17)$$

We therefore see that this second binary wave also has an amplitude equal to  $\pm\sqrt{E/2}$ , albeit in a different way with respect to the index  $i$ .

4. The two binary waves defined in Eqs. (7.16) and (7.17) share a common value for the symbol duration—namely,  $T$ .
5. The two sinusoidal carrier waves identified under points 2 and 3 are in phase quadrature with respect to each other. Moreover, they both have unit energy per symbol duration. We may therefore state that these two carrier waves constitute an *orthonormal pair of basis functions*.
6. For each possible value of the index  $i$ , Eqs. (7.16) and (7.17) identify the corresponding dabit, as outlined in Table 7.1. This table also includes other related entries pertaining to the phase of the QPSK signal, and the amplitudes of the two binary waves identified under points 2 and 3.

**TABLE 7.1 Relationship Between Index  $i$  And Identity of Corresponding Dabit, and Other Related Matters**

Index $i$	Phase of QPSK signal (radians)	Amplitudes of constituent binary waves			Input dabit $0 \leq t \leq T$
		Binary wave 1 $a_1(t)$	Binary wave 2 $a_2(t)$		
1	$\pi/4$	$+\sqrt{E/2}$	$-\sqrt{E/2}$		10
2	$3\pi/4$	$-\sqrt{E/2}$	$-\sqrt{E/2}$		00
3	$5\pi/4$	$-\sqrt{E/2}$	$+\sqrt{E/2}$		01
4	$7\pi/4$	$+\sqrt{E/2}$	$+\sqrt{E/2}$		11

## ■ GENERATION AND COHERENT DETECTION OF QPSK SIGNALS

In light of the six points summarized above as well as the material presented previously in this section on BPSK, we may construct the block diagrams depicted in Fig. 7.7 for the generation and coherent detection of QPSK signals, as described here:

### (i) Generation

To generate the QPSK signal, the incoming binary data stream is first converted into polar form by a *non-return-to-zero level encoder*; the encoder output is denoted by  $b(t)$ .

Symbols 1 and 0 are thereby represented by  $\sqrt{E_b}$  and  $-\sqrt{E_b}$ , where  $E_b = E/2$ . The resulting binary wave is next divided by means of a *demultiplexer* (consisting of a serial-to-parallel converter) into two separate binary waves consisting of the odd- and even-numbered input bits of  $b(t)$ . These two binary waves, referred to as the *demultiplexed components* of the input binary wave, are denoted by  $a_1(t)$  and  $a_2(t)$ . In any signaling interval, the amplitudes of  $a_1(t)$  and  $a_2(t)$  are determined in accordance with columns 3 and 4 of Table 7.1, depending on the particular dabit that is being transmitted. The demultiplexed binary waves  $a_1(t)$  and  $a_2(t)$  are used to modulate the pair of quadrature carriers—namely,  $\sqrt{2/T} \cos(2\pi f_c t)$  and  $\sqrt{2/T} \sin(2\pi f_c t)$ . Finally, the two BPSK signals are subtracted to produce the desired QPSK signals, as depicted in Fig. 7.7(a).

### (ii) Detection

The QPSK receiver consists of an *in-phase (I)-channel* and *quadrature (Q)-channel* with a common input, as depicted in Fig. 7.7(b). Each channel is itself made up of a product modulator, low-pass filter, sampler, and decision-making device. Under ideal conditions,

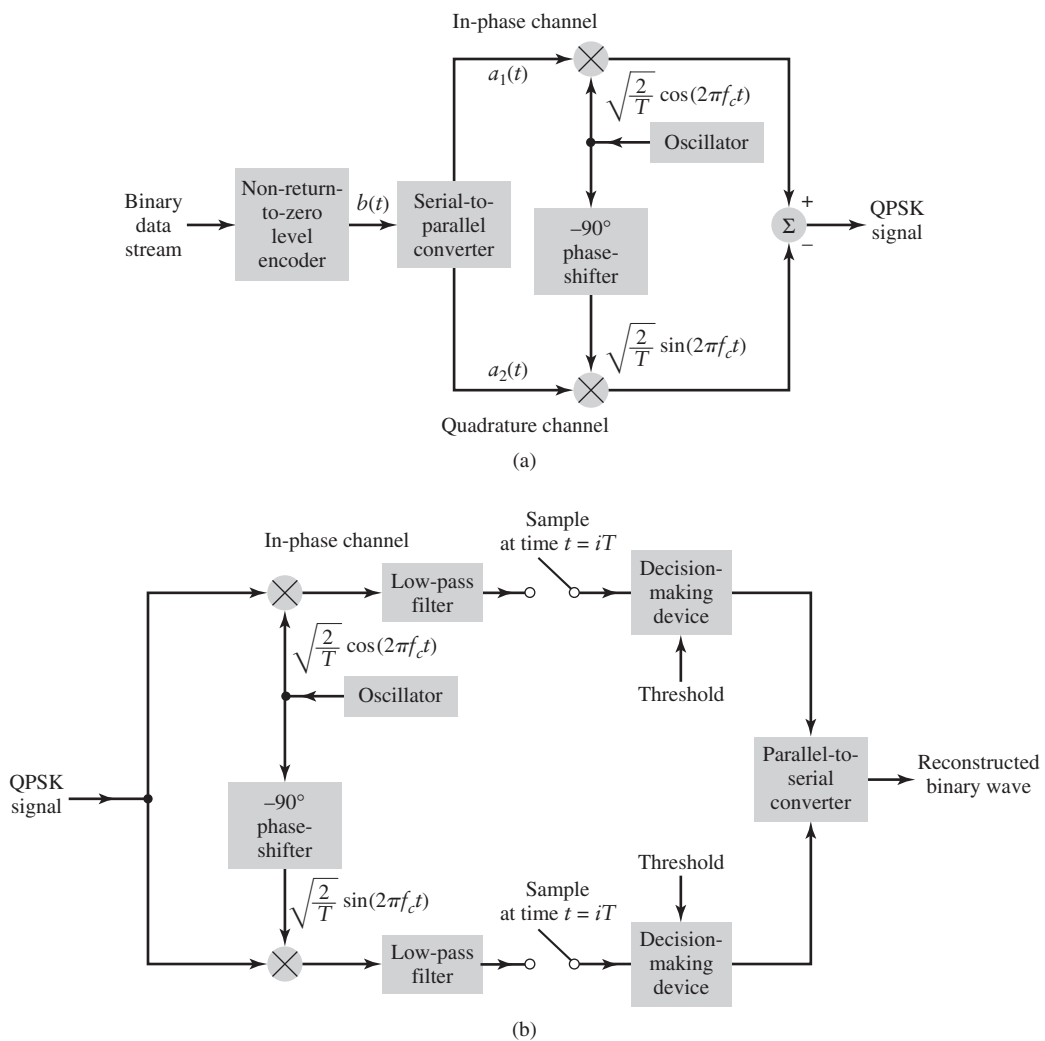


**FIGURE 7.7** Block diagrams of (a) QPSK transmitter and (b) coherent QPSK receiver; for the two synchronous samplers, integer  $i = 0, \pm 1, \pm 2, \dots$

the *I*- and *Q*-channels of the receiver, respectively, recover the demultiplexed components  $a_1(t)$  and  $a_2(t)$  responsible for modulating the orthogonal pair of carriers in the transmitter. Accordingly, by applying the outputs of these two channels to a *multiplexer* (consisting of a parallel-to-serial converter), the receiver recovers the original binary sequence. (We will return to the coherent detection of QPSK in Chapter 10.)

The design of the QPSK receiver builds on the strategy described for the coherent BPSK receiver. Specifically, each of the two low-pass filters in the coherent QPSK receiver of Fig. 7.7(b) must be assigned a bandwidth equal to or greater than the reciprocal of the symbol duration  $T$  for satisfactory operation of the receiver.

It is informative that we compare the QPSK transmitter and receiver depicted in Fig. 7.7 to the transmitter and receiver of the quadrature multiplexing system of Fig. 3.17. We see that although these two figures address different applications, one analog and the other digital, they are both covered by the same underlying principle: *bandwidth conservation*. As such, it is not surprising to see that their respective transmitters and receivers share similar structures.

### ■ OFFSET QUADRIphASE-SHIFT KEYING

In QPSK, the carrier amplitude is maintained constant. However, the carrier phase may jump by  $\pm 90^\circ$  or  $\pm 180^\circ$  every two-bit (dibit) duration. This latter property can be of particular concern when the QPSK signal is filtered during the course of transmission over a communication channel. Unfortunately, such a filtering action can cause the carrier amplitude, and therefore the envelope of the QPSK signal, to fluctuate. When the data transmission system contains nonlinear components, fluctuations of this kind are undesirable as they tend to distort the received signal; the net result is a reduced opening of the eye diagram, which was discussed in Section 6.6.

The extent of amplitude fluctuations exhibited by QPSK signals may be reduced by using a variant of quadriphase-shift keying known as the *offset quadriphase-shift keying* (OQPSK).<sup>1</sup> In OQPSK, the demultiplexed binary wave labeled  $a_2(t)$  in Fig. 7.7(a) is delayed (i.e., offset) by one bit duration with respect to the other demultiplexed binary wave labeled  $a_1(t)$  in that figure. This modification has the effect of confining the likely occurrence of phase transitions to  $0^\circ$  and  $\pm 90^\circ$ . However, the  $\pm 90^\circ$  phase transitions in OQPSK occur twice as frequently but with a reduced range of amplitude fluctuations, compared with QPSK. In addition to the  $\pm 90^\circ$  phase transitions, there are also  $\pm 180^\circ$  phase transitions in QPSK. We therefore find that amplitude fluctuations in OQPSK due to filtering have a smaller amplitude than in QPSK. The remarks made herein on phase transitions are illustrated in the next example.

#### EXAMPLE 7.1 Phase transitions

Parts (a) and (b) of Fig. 7.8 depict the waveforms of QPSK and OQPSK, both of which are produced by the binary data stream 0011011001 with the following composition over the interval  $0 \leq t \leq 10T_b$ :

- ▶ The input dabit (i.e., the pair of adjacent bits in the binary data stream) changes in going from the interval  $0 \leq t \leq 2T_b$  to the next interval  $2T_b \leq t \leq 4T_b$ .
- ▶ The dabit changes again in going from the interval  $2T_b \leq t \leq 4T_b$  to the next interval  $4T_b \leq t \leq 6T_b$ .
- ▶ The dabit changes yet again in going from the interval  $4T_b \leq t \leq 6T_b$  to the next interval  $6T_b \leq t \leq 8T_b$ .

<sup>1</sup>OQPSK is also referred to as *staggered quadriphase-shift keying* (SQPSK).

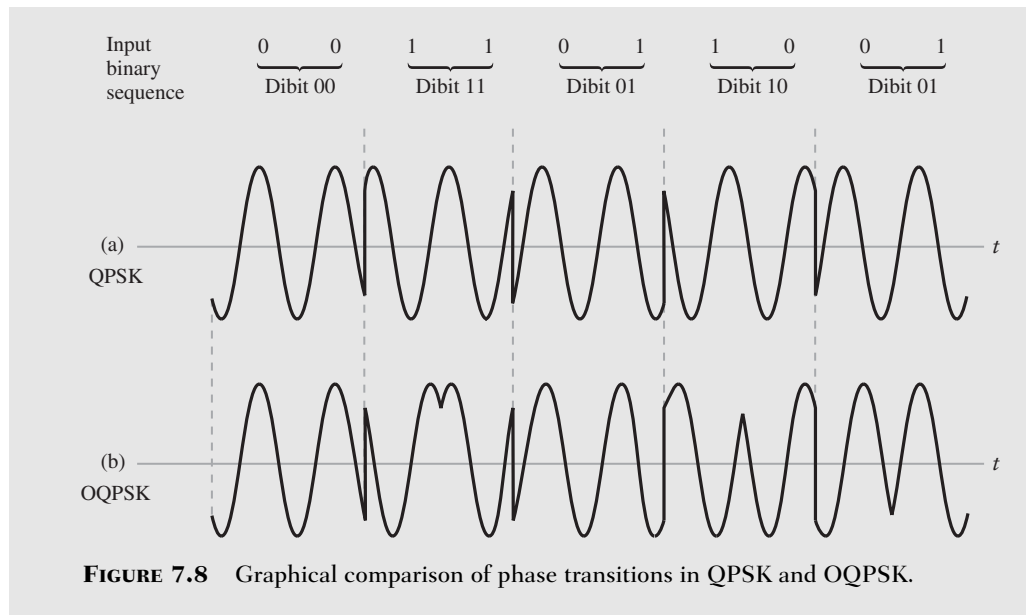


**FIGURE 7.8** Graphical comparison of phase transitions in QPSK and OQPSK.

- ▶ Finally, the dibit is changed one last time in going from the interval  $6T_b \leq t \leq 8T_b$  to the interval  $8T_b \leq t \leq 10T_b$ .

Examining the two waveforms of Fig. 7.8, we find the following:

- (i) In QPSK, the carrier phase undergoes jumps of  $0^\circ$ ,  $\pm 90^\circ$ , or  $\pm 180^\circ$  every  $2T_b$  seconds.
- (ii) In OQPSK, on the other hand, the carrier phase experiences only jumps of  $0^\circ$  or  $\pm 90^\circ$  every  $T_b$  seconds.

### ■ COMPUTER EXPERIMENT III: QPSK AND OQPSK SPECTRA

For our next experiment, we evaluate the power spectra of QPSK and OQPSK signals, assuming the use of square waves for the incoming data streams; here again the FFT algorithm is used to do the evaluation. Specifically, the evaluations are made for a fixed value of carrier frequency and two different bit durations:

- (i) *QPSK Spectra* Parts (a) and (b) of Fig. 7.9 display the power spectra (in decibels) of QPSK for the following parameters:

Carrier frequency,  $f_c = 8$  Hz

$$\text{Bit duration, } T_b = \begin{cases} 1 \text{ s for part (a) of the figure} \\ \frac{1}{2} \text{ s for part (b) of the figure} \end{cases}$$

- (ii) *OQPSK Spectra* Parts (a) and (b) of Fig. 7.10 display the corresponding power spectra of OQPSK for the same parameters used for QPSK.

As before, each part of Figs. 7.9 and 7.10 includes two spectral plots, one computational and the other theoretical, with good agreement between theory and experiment.

The important conclusion, drawn from comparing the two parts of Fig. 7.9 for QPSK with those of Fig. 7.10 for OQPSK, is summarized as follows: although these two digital methods of modulation naturally yield different waveforms, the power spectra of QPSK and OQPSK are identical for the same set of system parameters.

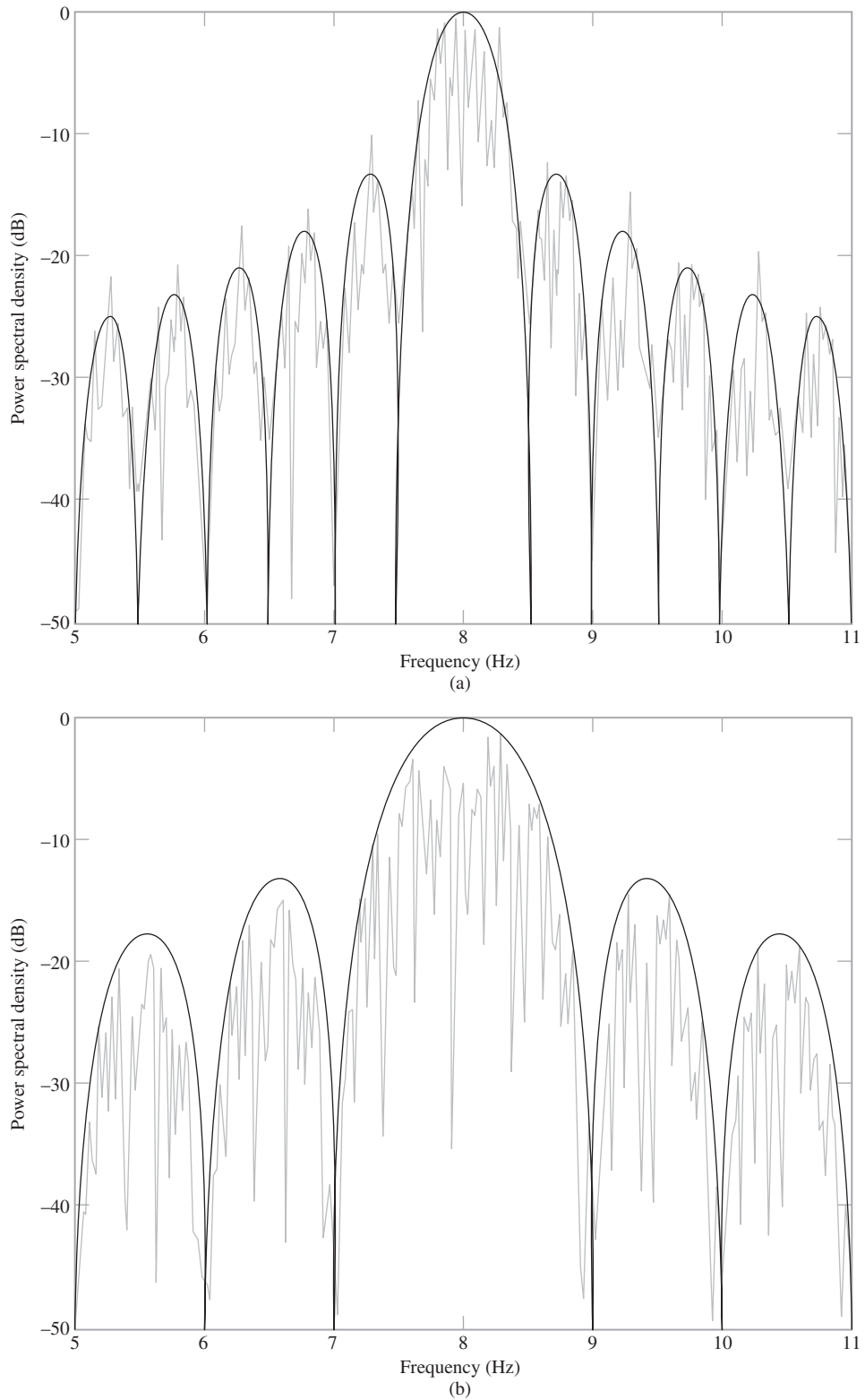


**FIGURE 7.9** Power spectra of QPSK produced by square wave as the modulating signal for fixed carrier frequency and varying bit duration: (a)  $f_c = 8$  Hz and  $T_b = 1$  s; (b)  $f_c = 8$  Hz and  $T_b = 1/2$  s.

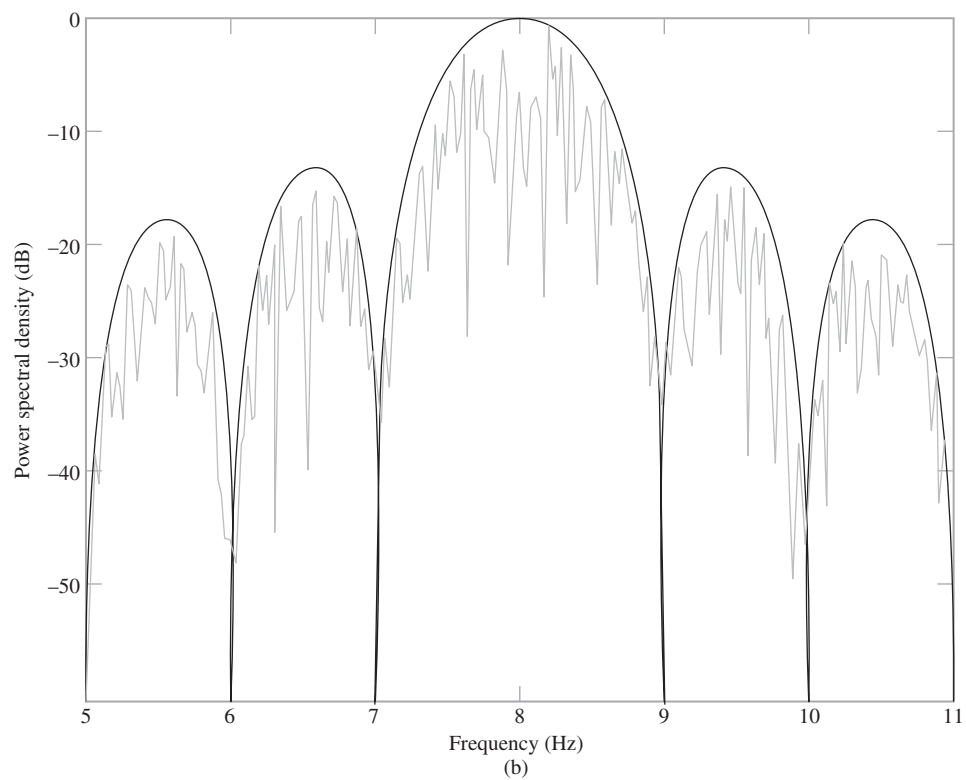
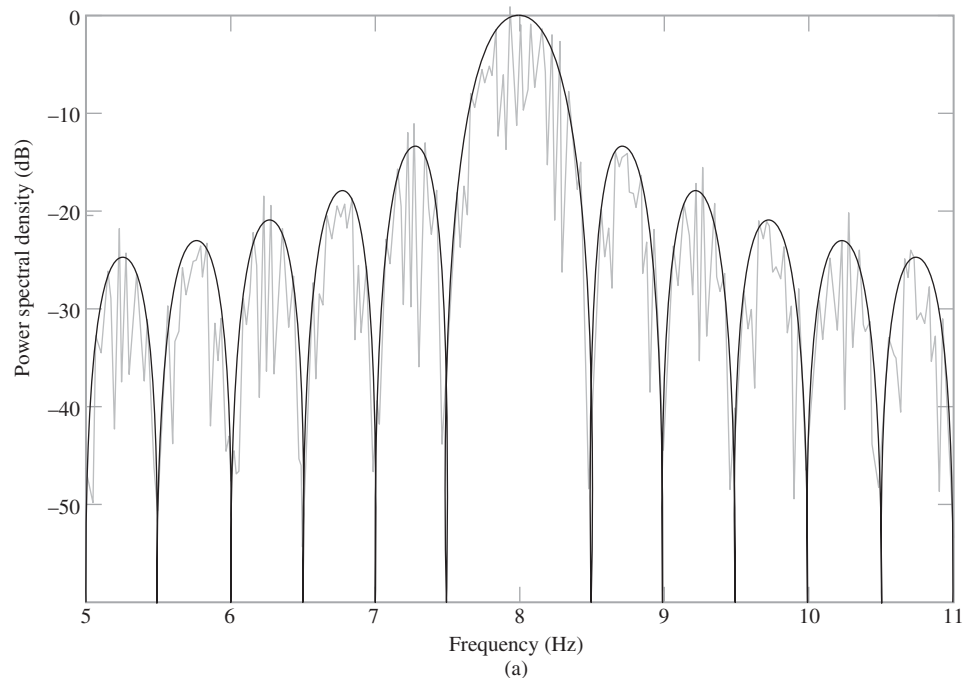


**FIGURE 7.10** Power spectra of OQPSK produced by square wave as the modulating signal for fixed carrier frequency and varying bit duration: (a)  $f_c = 8$  Hz and  $T_b = 1$  s; (b)  $f_c = 8$  Hz and  $T_b = 1/2$  s.

Moreover, comparing the power spectral plots of Fig. 7.9 for QPSK with those of Fig. 7.6 for BPSK, we observe that QPSK occupies a bandwidth equal to one half that of BPSK.

► **Drill Problem 7.3** Although QPSK and OQPSK signals have different waveforms, their magnitude spectra are identical; but their phase spectra differ by a linear phase component. Justify the validity of this two-fold statement. ◀

## 7.4 Frequency-Shift Keying

### ■ BINARY FREQUENCY-SHIFT KEYING (BFSK)

In the simplest form of frequency-shift keying known as *binary frequency-shift keying (BFSK)*, symbols 0 and 1 are distinguished from each other by transmitting one of two sinusoidal waves that differ in frequency by a fixed amount. A typical pair of sinusoidal waves is described by

$$s_i(t) = \begin{cases} \sqrt{\frac{2E_b}{T_b}} \cos(2\pi f_1 t), & \text{for symbol 1 corresponding to } i = 1 \\ \sqrt{\frac{2E_b}{T_b}} \cos(2\pi f_2 t), & \text{for symbol 0 corresponding to } i = 2 \end{cases} \quad (7.18)$$

where  $E_b$  is the transmitted signal energy per bit. When the frequencies  $f_1$  and  $f_2$  are chosen in such a way that they differ from each other by an amount equal to the reciprocal of the bit duration  $T_b$ , the BFSK signal is referred to as *Sunde's BFSK* after its originator. This modulated signal is a *continuous-phase signal* in the sense that phase continuity is always maintained, including the inter-bit switching times.

### ■ COMPUTER EXPERIMENT IV: SUNDE'S BFSK

#### (i) Waveform

Figure 7.11 plots the waveform of Sunde's BFSK produced by the input binary sequence 0011011001 for a bit duration  $T_b = 1$  s. Part (a) of the figure displays the waveform of the input sequence, and part (b) displays the corresponding waveform

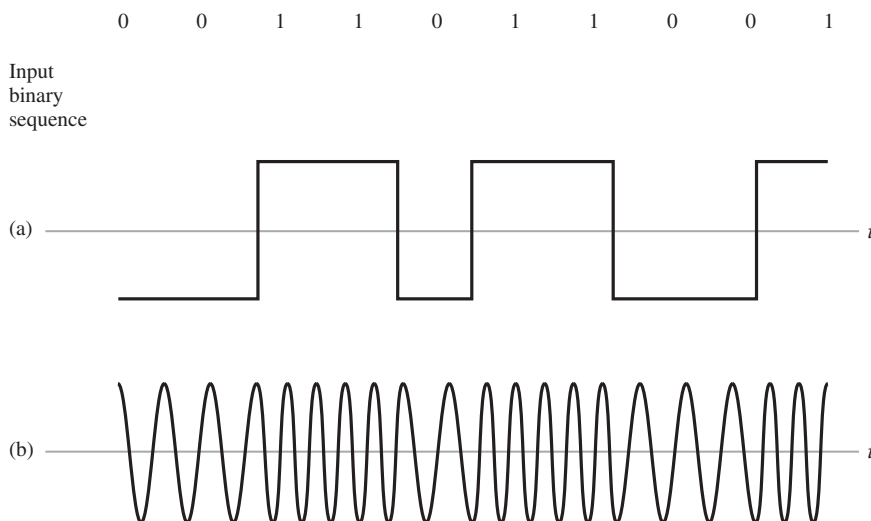


**FIGURE 7.11** (a) Binary sequence and its non-return-to-zero level-encoded waveform. (b) Sunde's BFSK signal.

of the BFSK signal. The latter part of the figure clearly displays the phase-continuous property of Sunde's BFSK.

(ii) *Spectrum*

Figure 7.12 shows two superimposed spectral plots of Sunde's BFSK for a square-wave input for positive frequencies; as before, one plot is computational and the other is theoretical. The system parameters used for the computation are as follows:

$$\begin{array}{ll} \text{Bit duration,} & T_b = 1 \text{ s} \\ \text{Carrier frequency,} & f_c = 8 \text{ Hz} \end{array}$$

Examining Fig. 7.12, we can make the following observations for positive frequencies:

- (i) The spectrum contains two line components at the frequency  $f = f_c \pm 1/(2T_b)$ ; which equal 7.5 Hz and 8.5 Hz for  $f_c = 8$  Hz and  $T_b = 1$  s.
- (ii) The main lobe occupies a band of width equal to  $(3/T_b) = 3$  Hz, centered on the carrier frequency  $f_c = 8$  Hz.
- (iii) The largest sidelobe is about 21 dB below the main lobe.

► **Drill Problem 7.4** Show that the modulation process involved in generating Sunde's BFSK is nonlinear. ◀

### ■ CONTINUOUS-PHASE FREQUENCY-SHIFT KEYING

Sunde's BFSK is the simplest form of a family of digitally modulated signals known collectively as *continuous-phase frequency-shift keying (CPFSK) signals*, which exhibit the following distinctive property:

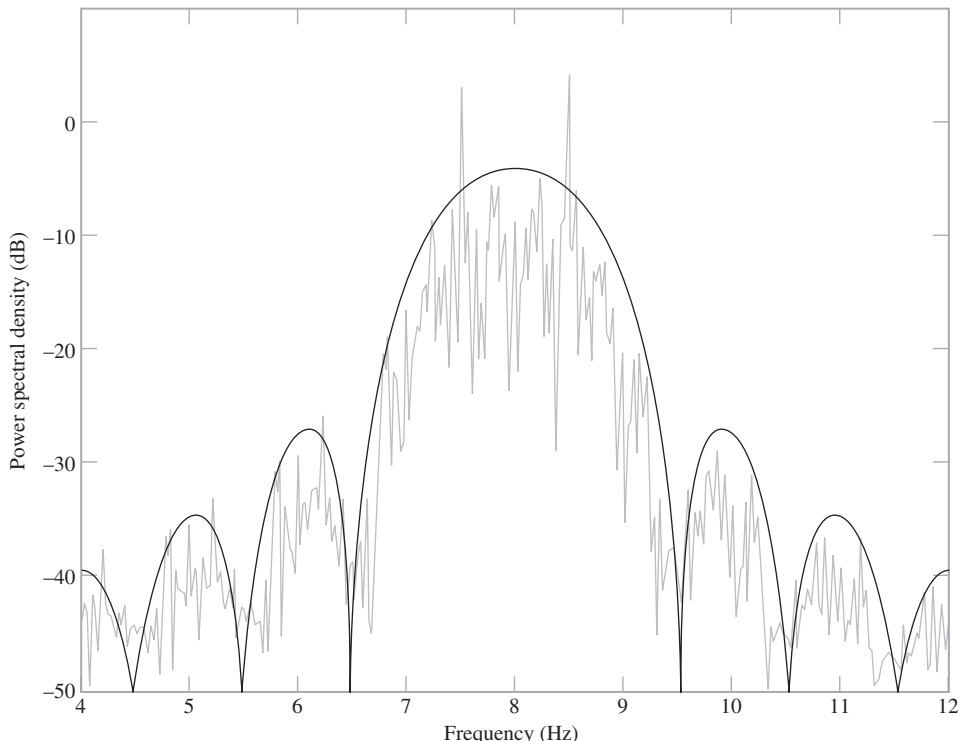


**FIGURE 7.12** Power spectrum of Sunde's BFSK produced by square wave as the modulating signal for the following parameters:  $f_c = 8$  Hz and  $T_b = 1$  s.

The modulated wave maintains phase continuity at all transition points, even though at those points in time the incoming binary data stream switches back and forth between symbols 0 and 1.

In other words, the CPFSK signal is a continuous-wave modulated wave like any other angle-modulated wave experienced in the analog world, despite the fact that the modulating wave is itself discontinuous.

In Sunde's BFSK, the overall excursion  $\delta f$  in the transmitted frequency from symbol 0 to symbol 1, or vice versa, is equal to the bit rate of the incoming data stream. In another special form of CPFSK known as *minimum shift keying* (MSK), the binary modulation process uses a different value for the frequency excursion  $\delta f$ , with the result that this new modulated wave offers superior spectral properties to Sunde's BFSK.

### ■ MINIMUM-SHIFT KEYING

In MSK, the *overall frequency excursion*  $\delta f$  from binary symbol 1 to symbol 0, or vice versa, is one half the bit rate, as shown by

$$\begin{aligned}\delta f &= f_1 - f_2 \\ &= \frac{1}{2T_b}\end{aligned}\quad (7.19)$$

The unmodulated carrier frequency is the arithmetic mean of the two transmitted frequencies  $f_1$  and  $f_2$ ; that is,

$$f_c = \frac{1}{2}(f_1 + f_2) \quad (7.20)$$

Expressing  $f_1$  and  $f_2$  in terms of the carrier frequency  $f_c$  and overall frequency excursion  $\delta f$ , we have

$$f_1 = f_c + \frac{\delta f}{2}, \quad \text{for symbol 1} \quad (7.21)$$

$$f_2 = f_c - \frac{\delta f}{2}, \quad \text{for symbol 0} \quad (7.22)$$

Accordingly, we formally define the MSK signal as the angle-modulated wave

$$s(t) = \sqrt{\frac{2E_b}{T_b}} \cos[2\pi f_c t + \theta(t)] \quad (7.23)$$

where  $\theta(t)$  is the phase of the MSK signal. In particular, when frequency  $f_1$  is transmitted, corresponding to symbol 1, we find from Eqs. (7.21) and (7.23) that the phase  $\theta(t)$  assumes the value

$$\begin{aligned}\theta(t) &= 2\pi\left(\frac{\delta f}{2}\right)t \\ &= \frac{\pi t}{2T_b}, \quad \text{for symbol 1}\end{aligned}\quad (7.24)$$

In words, this means that at time  $t = T_b$ , the transmission of symbol 1 increases the phase of the MSK signal  $s(t)$  by  $\pi/2$  radians. By the same token, when frequency  $f_2$  is transmitted, corresponding to symbol 0, we find from Eqs. (7.22) and (7.23) that the phase  $\theta(t)$  assumes the value

$$\begin{aligned}\theta(t) &= 2\pi\left(-\frac{\delta f}{2}\right)t \\ &= -\frac{\pi t}{2T_b}, \quad \text{for symbol 0}\end{aligned}\quad (7.25)$$

This means that at time  $t = T_b$ , the transmission of symbol 0 decreases the phase of  $s(t)$  by  $\pi/2$  radians.

The phase changes described in Eqs. (7.24) and (7.25) for MSK are radically different from their corresponding counterparts for Sunde's BFSK. Specifically, the phase of Sunde's BFSK signal changes by  $-\pi$  radians at the termination of the interval representing symbol 0, and  $+\pi$  radians for symbol 1. However, the changes  $-\pi$  and  $+\pi$  are *exactly the same, modulo  $2\pi$* . This observation, in effect, means that Sunde's BFSK has *no memory*; in other words, knowing which particular change occurred in the previous bit interval provides no help in the current bit interval. In contrast, we have a completely different situation in the case of MSK by virtue of the different ways in which the transmissions of symbols 1 and 0 affect the phase  $\theta(t)$ , as shown in Eqs. (7.24) and (7.25). Note also that the overall frequency excursion  $\delta f$  in MSK is the *minimum frequency spacing* between symbols 0 and 1 that allows their FSK representations to be coherently orthogonal, hence the terminology "minimum-shift keying."

#### EXAMPLE 7.2: Relationship Between OQPSK and MSK Waveforms

The purpose of this example is to illustrate the relationship that exists between OQPSK and MSK waveforms. Figures 7.13 and 7.14 bear out this fundamental relationship:

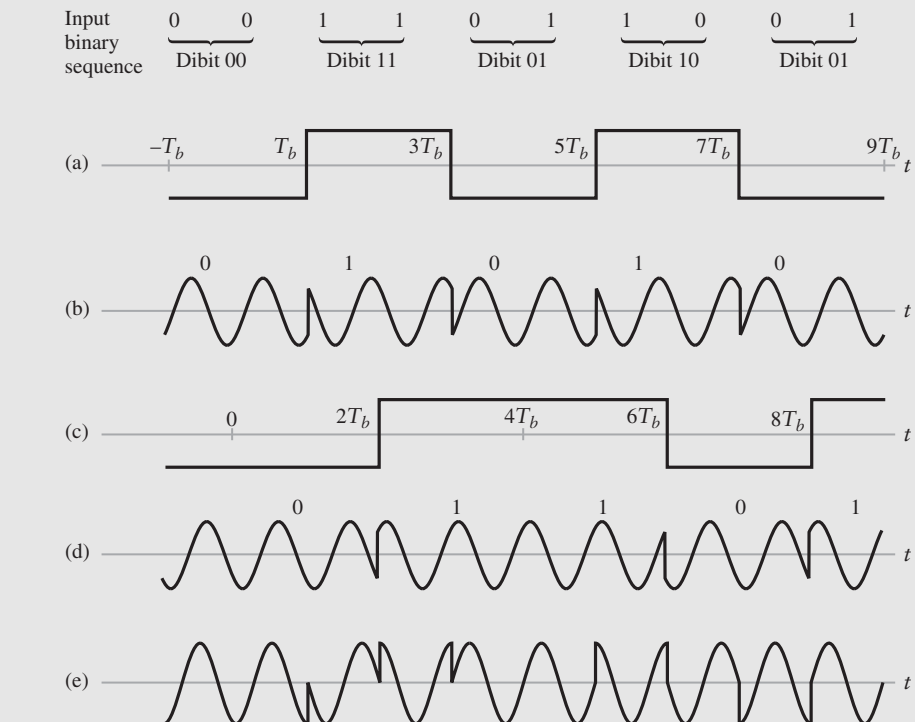


**FIGURE 7.13** OQPSK signal components: (a) Modulating signal for in-phase component. (b) Modulated waveform of in-phase component. (c) Modulating signal for quadrature component. (d) Modulated waveform of quadrature component. (e) Waveform of OQPSK signal obtained by subtracting (d) from (b).

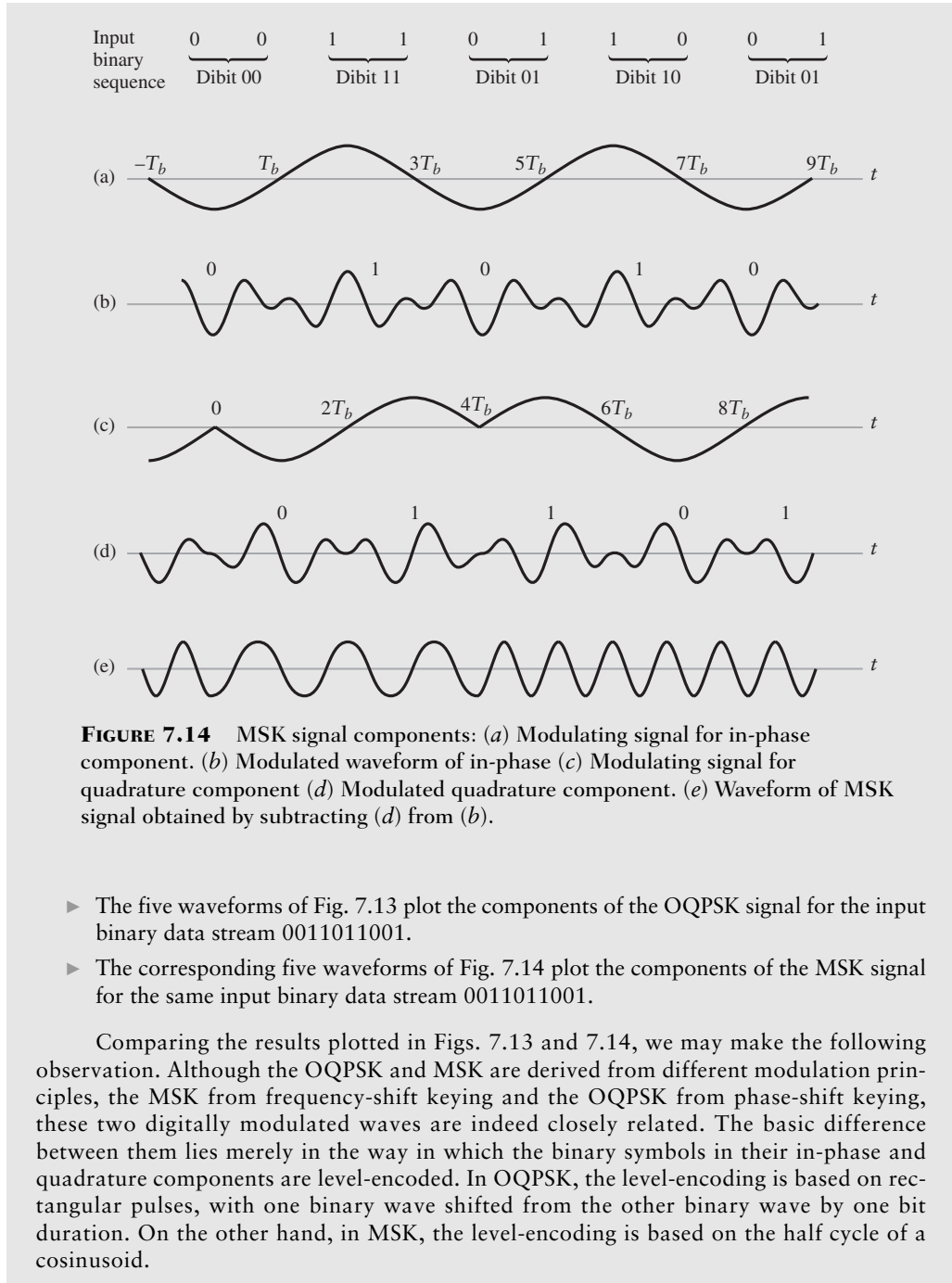


**FIGURE 7.14** MSK signal components: (a) Modulating signal for in-phase component. (b) Modulated waveform of in-phase (c) Modulating signal for quadrature component (d) Modulated quadrature component. (e) Waveform of MSK signal obtained by subtracting (d) from (b).

- ▶ The five waveforms of Fig. 7.13 plot the components of the OQPSK signal for the input binary data stream 0011011001.
- ▶ The corresponding five waveforms of Fig. 7.14 plot the components of the MSK signal for the same input binary data stream 0011011001.

Comparing the results plotted in Figs. 7.13 and 7.14, we may make the following observation. Although the OQPSK and MSK are derived from different modulation principles, the MSK from frequency-shift keying and the OQPSK from phase-shift keying, these two digitally modulated waves are indeed closely related. The basic difference between them lies merely in the way in which the binary symbols in their in-phase and quadrature components are level-encoded. In OQPSK, the level-encoding is based on rectangular pulses, with one binary wave shifted from the other binary wave by one bit duration. On the other hand, in MSK, the level-encoding is based on the half cycle of a sinusoid.

The insightful close relationship of MSK to OQPSK derived from Example 7.2 sets the stage for an analytic formulation of the MSK signal, as described next.

### ■ FORMULATION OF MINIMUM-SHIFT KEYING<sup>2</sup>

To proceed with the formulation, we refer back to Eq. (7.23), and use a well-known trigonometric identity to expand the angle-modulated wave (i.e., MSK signal)  $s(t)$  as

$$s(t) = \sqrt{\frac{2E_b}{T_b}} \cos(\theta(t)) \cos(2\pi f_c t) - \sqrt{\frac{2E_b}{T_b}} \sin(\theta(t)) \sin(2\pi f_c t) \quad (7.26)$$

In light of this equation, we make two identifications:

$$(i) \ s_I(t) = \sqrt{E_b} \cos(\theta(t)) \text{ is the in-phase (I) component associated with the carrier } \sqrt{2/T_b} \cos(2\pi f_c t). \quad (7.27)$$

$$(ii) \ s_Q(t) = \sqrt{E_b} \sin(\theta(t)) \text{ is the quadrature (Q) component associated with the } 90^\circ\text{-phase-shifted carrier.} \quad (7.28)$$

To highlight the bearing of the incoming binary data stream on the composition of  $s_I(t)$  and  $s_Q(t)$ , we reformulate them respectively as follows:

$$s_I(t) = a_1(t) \cos(2\pi f_0 t) \quad (7.29)$$

and

$$s_Q(t) = a_2(t) \sin(2\pi f_0 t) \quad (7.30)$$

The  $a_1(t)$  and  $a_2(t)$  are two binary waves that are extracted from the incoming binary data stream through demultiplexing and offsetting, in a manner similar to OQPSK. As such, they take on the value +1 or -1 in symbol (i.e., dabit) intervals of duration  $T = 2T_b$ , where  $T_b$  is the bit duration of the incoming binary data stream. The two data signals  $a_1(t)$  and  $a_2(t)$  are respectively weighted by the sinusoidal functions  $\cos(2\pi f_0 t)$  and  $\sin(2\pi f_0 t)$ , where the frequency  $f_0$  is to be determined. To define  $f_0$ , we use Eqs. (7.29) and (7.30) to reconstruct the original angle-modulated wave  $s(t)$  in terms of the data signals  $a_1(t)$  and  $a_2(t)$ . In so doing, we obtain

$$\begin{aligned} \theta(t) &= -\tan^{-1} \left[ \frac{s_Q(t)}{s_I(t)} \right] \\ &= -\tan^{-1} \left[ \frac{a_2(t)}{a_1(t)} \tan(2\pi f_0 t) \right] \end{aligned} \quad (7.31)$$

on the basis of which we recognize two possible scenarios that can arise:

1.  $a_2(t) = a_1(t)$  This scenario arises when two successive binary symbols (constituting a dabit) in the incoming data stream are the same (i.e., both are 0s or 1s); hence, Eq. (7.31) reduces to

$$\begin{aligned} \theta(t) &= -\tan^{-1} [\tan(2\pi f_0 t)] \\ &= -2\pi f_0 t \end{aligned} \quad (7.32)$$

2.  $a_2(t) = -a_1(t)$  This second scenario arises when two successive binary symbols (i.e., dibits) in the incoming data stream are different; hence, Eq. (7.31) reduces to

$$\begin{aligned} \theta(t) &= -\tan^{-1} [-\tan(2\pi f_0 t)] \\ &= 2\pi f_0 t \end{aligned} \quad (7.33)$$

---

<sup>2</sup>Analytic formulation of the MSK presented herein follows Ziemer and Tranter (2002).

Equations (7.32) and (7.33) are respectively of similar mathematical forms as Eqs. (7.25) and (7.24). Accordingly, we may now formally define

$$f_0 = \frac{1}{4T_b} \quad (7.34)$$

To sum up, given a non-return-to-zero level encoded binary wave  $b(t)$  of prescribed bit duration  $T_b$  and a sinusoidal carrier wave of frequency  $f_c$ , we may formulate the MSK signal by proceeding as follows:

1. Use the given binary wave  $b(t)$  to construct the binary demultiplexed-offset waves  $a_1(t)$  and  $a_2(t)$ .
2. Use Eq. (7.34) to determine the frequency  $f_0$ .
3. Use Eqs. (7.29) and (7.30) to determine the in-phase component  $s_I(t)$  and quadrature component  $s_Q(t)$ , respectively from which the MSK signal  $s(t)$  follows.

Indeed, it is this procedure that was used in Example 7.3 to construct the MSK signal from its related components.

► **Drill Problem 7.5** To summarize matters, we may say that MSK is an OQPSK where the symbols in the in-phase and quadrature components (on a dabit-by-dabit basis) are weighted by the basic pulse function

$$p(t) = \sin\left(\frac{\pi t}{2T_b}\right) \text{rect}\left(\frac{t}{2T_b} - \frac{1}{2}\right)$$

where  $T_b$  is the bit duration, and  $\text{rect}(t)$  is the rectangular function of unit duration and unit amplitude. Justify this summary. ◀

► **Drill Problem 7.6** The sequence 11011100 is applied to an MSK modulator. Assuming that the angle  $\theta(t)$  of the MSK signal is zero at time  $t = 0$ , plot the trellis diagram that displays the evolution of  $\theta(t)$  over the eight binary symbols of the input sequence. ◀

► **Drill Problem 7.7** The process of angle modulation involved in the generation of an MSK signal is linear. Justify this assertion. ◀

► **Drill Problem 7.8** A simple way of demodulating an MSK signal is to use a frequency discriminator, which was discussed in Chapter 4 on angle modulation. Justify this use and specify the linear input-output characteristic of the discriminator. ◀

### ■ COMPUTER EXPERIMENT V: MSK SPECTRUM

In this computer experiment, we evaluate the power spectrum of an MSK signal produced by a square wave input. The parameters of the experiment are as follows:

Bit duration,  $T_b = 1$  s

Carrier frequency,  $f_c = 8$  Hz

Figure 7.15 shows two power spectral plots of the MSK signal, one computational and the other theoretical. Comparing this figure with that of QPSK in Fig. 7.9(a) and that of Sunde's BFSK in Fig. 7.12 for the same set of parameters, we can make the following observations for positive frequencies:

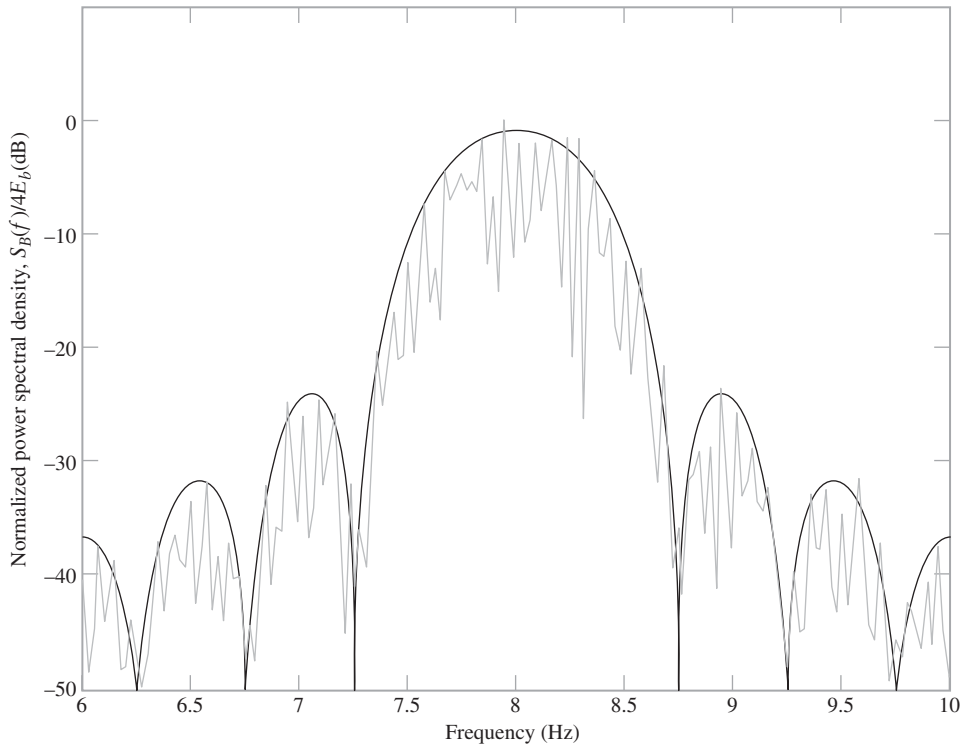


**FIGURE 7.15** Power spectrum of MSK produced by square wave as the modulating signal for the following parameters:  $f_c = 8$  Hz and  $T_b = 1$  s.

- (i) *MSK versus QPSK:* The main lobe of MSK occupies a frequency band whose width is  $1.5/T_b = 1.5$  Hz, centered on the carrier frequency  $f_c = 8$  Hz. On this basis, the transmission bandwidth of MSK is 50 percent larger than that of QPSK. However, the sidelobes of MSK are considerably smaller than those of QPSK.
- (ii) *MSK versus Sunde's BFSK:* The transmission bandwidth of MSK is one half that of Sunde's BFSK. Moreover, Sunde's BFSK exhibits two line components at  $f = f_c \pm 1/(2T_b)$ , whereas the spectrum of MSK is continuous across the whole frequency band.

Figure 7.16 plots the power spectrum of the MSK signal for the same set of parameters as those used in Fig. 7.15. In Fig. 7.16, the frequency spans the range from 0 to 50 Hz, whereas in Fig. 7.15, the frequency spans the range from 6 to 10 Hz. The motivation for including Fig. 7.16 is merely to illustrate that although the carrier frequency  $f_c$  is not high enough to completely eliminate spectral overlap, the overlap is relatively small as evidenced by

- ▶ The small value of the spectrum at zero frequency.
- ▶ The small degree of asymmetry about the carrier frequency  $f_c = 8$  Hz.

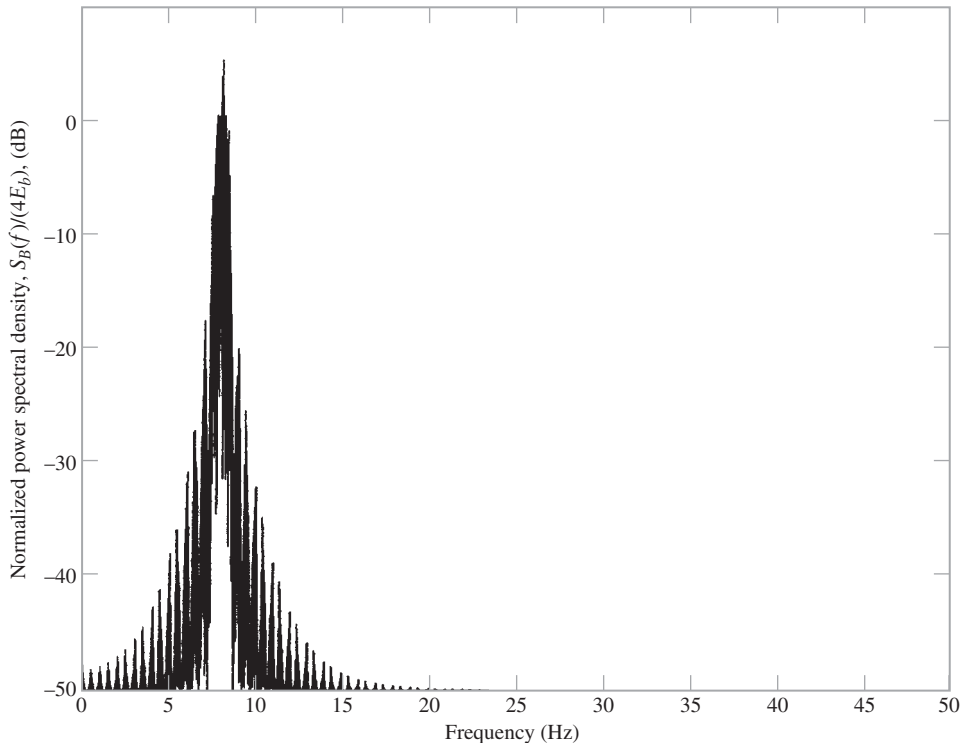


**FIGURE 7.16** Illustrative confirmation that for MSK produced by a square modulating wave, the carrier frequency  $f_c = 8 \text{ Hz}$  is high enough to produce insignificant spectral overlap for bit duration  $T_b = 1 \text{ s}$ .

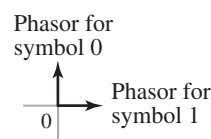
## 7.5 Summary of Three Binary Signaling Schemes

Parts (b), (c), and (d) of Fig. 7.1 illustrate the waveforms of the three basic signaling schemes, BASK, BPSK, and BFSK, which are respectively produced by the binary data stream 0011011001 in part (a) of the figure. This figure clearly illustrates the following points:

- (i) BASK, BPSK, and BFSK are the digital counterparts of amplitude modulation, phase modulation, and frequency modulation, respectively; this point further reinforces previous observations.
- (ii) Both BASK and BPSK exhibit *discontinuity*. In contrast, it is possible to configure BFSK in such a way that *phase continuity* is maintained across the entire input binary data stream. In actual fact, the BFSK waveform plotted in part (d) of the figure is an example of minimum-shift keying, which exhibits this property.

Moreover, Table 7.2 presents a summary of the three binary modulation schemes: BASK, BPSK, and BFSK. Columns 2 and 3 of the table summarize the discriminants that distinguish these three basic schemes in mathematical terms. The last column of the table portrays *phasor* representations of the three schemes, thereby picturing the discriminants that distinguish them in graphical terms.

**TABLE 7.2 Summary of Three Basic Binary Modulation Schemes**

Type of modulation scheme	Variable parameter	Definition of modulated wave $s_1(t)$ or $s_2(t)$ , for $0 \leq t \leq T_b$	Phasor representation of modulated wave
1. Binary amplitude-shift keying (BASK)	$\begin{pmatrix} \text{Carrier amplitude} \\ A_c \end{pmatrix} = \begin{cases} \sqrt{\frac{2}{T_b}} & \text{for symbol 1} \\ 0 & \text{for symbol 0} \end{cases}$	$s_1(t) = \sqrt{\frac{2E_b}{T_b}} \cos(2\pi f_c t)$ for symbol 1 $s_2(t) = 0$ for symbol 0	Zero phasor for symbol 0 
2. Binary phase-shift keying (BPSK)	$\begin{pmatrix} \text{Carrier phase} \\ \phi_c \end{pmatrix} = \begin{cases} 0 & \text{for symbol 1} \\ \pi & \text{for symbol 0} \end{cases}$	$s_1(t) = \sqrt{\frac{2E_b}{T_b}} \cos(2\pi f_c t)$ for symbol 1 $s_2(t) = \sqrt{\frac{2E_b}{T_b}} \cos(2\pi f_c t + \pi)$ for symbol 0	Phasor for symbol 0 
3. Binary frequency-shift keying (BFSK)	$\begin{pmatrix} \text{Carrier frequency} \\ f_c \end{pmatrix} = \begin{cases} f_1 & \text{for symbol 1} \\ f_2 & \text{for symbol 0} \end{cases}$	$s_1(t) = \sqrt{\frac{2E_b}{T_b}} \cos(2\pi f_1 t)$ for symbol 1 $s_2(t) = \sqrt{\frac{2E_b}{T_b}} \cos(2\pi f_2 t)$ for symbol 0	Phasor for symbol 0 

*Notations* $T_b$  = bit duration $E_b$  = transmitted signal energy per bitCarrier:  $c(t) = A_c \cos(2\pi f_c t + \phi_c)$ The carrier phase  $\phi_c$  is set equal to zero for both BASK and BFSK.

## 7.6 Noncoherent Digital Modulation Schemes

Coherent receivers, exemplified by the schemes shown in Figs. 7.4(b) and 7.7(b), require knowledge of the carrier wave's phase reference to establish synchronism with their respective transmitters. However, in some communication environments, it is either impractical or too expensive to phase-synchronize a receiver to its transmitter. In situations of this kind, we resort to the use of *noncoherent detection* by abandoning the use of phase synchronization between the receiver and its transmitter, knowing that when we do so the receiver performance is degraded in the presence of channel noise (as discussed in Chapter 10).

In discussing binary signaling techniques, we described BASK, BPSK, and BFSK, in that order. This ordering was motivated by the following considerations. Both BASK and BPSK are examples of linear modulation, with increasing complexity in going from BASK and BPSK. On the other hand, BFSK is in general an example of nonlinear modulation, hence leaving it until last. In this section, however, we change the order in which the pertinent noncoherent detection schemes are considered. Specifically, we first consider the noncoherent detection of BASK, followed by that of BFSK. The rationale for this new ordering is guided by the fact that both of them use similar techniques based on band-pass filtering, but with increasing complexity in going from BASK to BFSK. The discussion is completed by tackling the noncoherent detection of BPSK, which requires more careful considerations of its own.

### ■ NONCOHERENT DETECTION OF BASK SIGNAL

Referring to Eq. (7.10), we see that the generation of BASK signals involves the use of a single sinusoidal carrier of frequency  $f_c$  for symbol 1 and switching off the transmission for symbol 0. Now, the system designer would have knowledge of two system parameters:

- ▶ The carrier frequency  $f_c$ .
- ▶ The transmission bandwidth, which is determined by the bit duration  $T_b$ .

It is therefore natural to make use of these known parameters in designing the noncoherent receiver for BASK. Specifically, the receiver consists of a band-pass filter, followed by an envelope detector, then a sampler, and finally a decision-making device, as depicted in Fig. 7.17.

The *band-pass filter* is designed to have a mid-band frequency equal to the carrier frequency  $f_c$  and a bandwidth equal to the transmission bandwidth of the BASK signal. Moreover, it is assumed that the intersymbol interference (ISI) produced by the filter is negligible, which, in turn, requires that the rise time and decay time of the response of the filter to a rectangular pulse be short compared to the bit duration  $T_b$ . Under these conditions, we

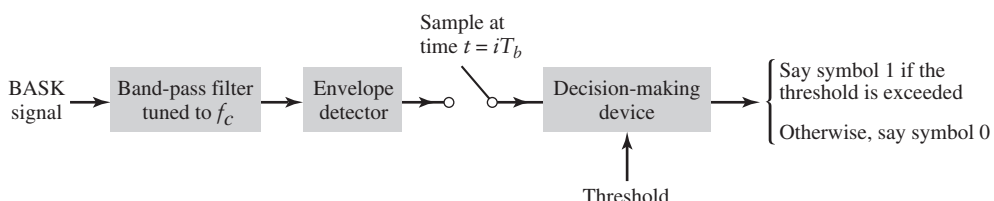


**FIGURE 7.17** Noncoherent BASK receiver; the integer  $i$  for the sampler equals  $0, \pm 1, \pm 2, \dots$

find that in response to the incoming BASK signal (assumed to be noise-free), the band-pass filter produces a pulsed sinusoid for symbol 1 and, ideally, no output for symbol 0. Next, the *envelope detector* traces the envelope of the filtered version of the BASK signal. Finally, the *decision-making device* working in conjunction with the *sampler*, regenerates the original binary data stream by comparing the sampled envelope-detector output against a pre-set *threshold* every  $T_b$  seconds; this operation assumes the availability of bit-timing in the receiver. If the threshold is exceeded at time  $t = iT_b$ ,  $i = 0, \pm 1, \pm 2, \dots$ , the receiver decides in favor of symbol 1; otherwise, it decides in favor of symbol 0. In the absence of channel noise and channel distortion, the receiver output (on a bit-by-bit basis) would be an exact replica of the original binary data stream applied to the transmitter, subject to the above-mentioned assumptions on the band-pass filter.

### ■ NONCOHERENT DETECTION OF BFSK SIGNALS

In the case of BFSK, we recall from Section 7.4 that the transmissions of symbols 1 and 0 are represented by two carrier waves of frequencies  $f_1$  and  $f_2$ , respectively, with adequate spacing between them. In light of this characterization, we may build on the noncoherent detection of BASK by formulating the noncoherent BFSK receiver of Fig. 7.18. The receiver consists of two paths, one dealing with frequency  $f_1$  (i.e., symbol 1) and the other dealing with frequency  $f_2$  (i.e., symbol 0):

- ▶ Path 1 uses a band-pass filter of mid-band frequency  $f_1$ . The filtered version of the incoming BFSK signal is envelope-detected and then sampled at time  $t = iT_b$ ,  $i = 0, \pm 1, \pm 2, \dots$ , to produce the output  $v_1$ .
- ▶ Path 2 uses a band-pass filter of mid-band frequency  $f_2$ . As with path 1, the filtered version of the BFSK signal is envelope-detected and then sampled at time  $t = iT_b$ ,  $i = 0, \pm 1, \pm 2, \dots$ , to produce a different output  $v_2$ .

The two band-pass filters have the same bandwidth, equal to the transmission bandwidth of the BFSK signal. Moreover, as pointed out in dealing with BASK, the intersymbol interference produced by the filters is assumed to be negligible.

The outputs of the two paths,  $v_1$  and  $v_2$ , are applied to a *comparator*, where decisions on the composition of the BFSK signal are repeated every  $T_b$  seconds. Here again, the availability of bit timing is assumed in the receiver. Recognizing that the upper path corresponds to symbol 1 and the lower path corresponds to symbol 0, the comparator decides in favor

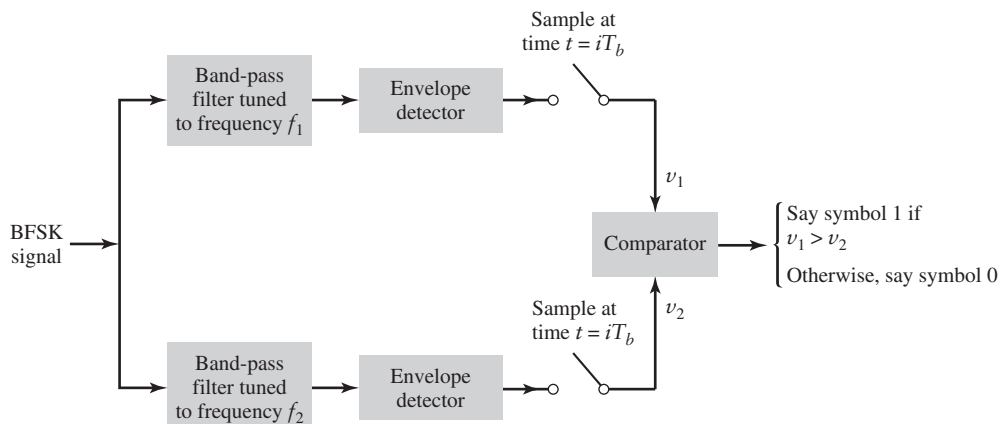


**FIGURE 7.18** Noncoherent BFSK receiver; the two samplers operate synchronously, with  $i = 0, \pm 1, \pm 2, \dots$ .

of symbol 1 if  $v_1$  is greater than  $v_2$  at the specified bit-timing instant; otherwise, the decision is made in favor of symbol 0. In a noise-free environment and no channel distortion, the receiver output (on a bit-by-bit basis) would again be a replica of the original binary data stream applied to the transmitter input.

### ■ DIFFERENTIAL PHASE-SHIFT KEYING

From the above discussion, we see that both amplitude-shift keying and frequency-shift keying lend themselves naturally to noncoherent detection whenever it is impractical to maintain carrier-phase synchronization of the receiver to the transmitter. But in the case of phase-shift keying, we cannot have noncoherent detection in the traditional sense because the term “noncoherent” means having to do without carrier-phase information. To get around this difficulty, we employ a “pseudo PSK” technique known as *differential phase-shift keying* (DPSK), which, in a loose sense, does permit the use of noncoherent detection.

DPSK eliminates the need for a coherent reference signal at the receiver by combining two basic operations at the transmitter:

- ▶ *Differential encoding* of the input binary wave (which was discussed under line codes in Section 5.9).
- ▶ *Phase-shift keying* (which was discussed in Section 7.3).

It is because of this combination that we speak of “differential phase-shift keying.” In effect, to send symbol 0, we phase advance the current signal waveform by 180 degrees, and to send symbol 1 we leave the phase of the current signal waveform unchanged. Correspondingly, the receiver is equipped with a storage capability (i.e., memory) designed to measure the *relative phase difference* between the waveforms received during two successive bit intervals. Provided the unknown phase  $\theta$  varies slowly (i.e., slow enough for it to be considered essentially constant over two bit intervals), the phase difference between waveforms received in two successive bit intervals will be essentially independent of  $\theta$ .

#### ***Generation and Detection of DPSK Signals***

##### (i) *Generation*

The differential encoding process at the transmitter input starts with an *arbitrary first bit, serving merely as reference*. Let  $\{d_k\}$  denote the differentially encoded sequence with this added reference bit. To generate this sequence, the transmitter performs the following two operations:

- ▶ If the incoming binary symbol  $b_k$  is 1, then the symbol  $d_k$  is unchanged with respect to the previous symbol  $d_{k-1}$ .
- ▶ If the incoming binary symbol  $b_k$  is 0, then the symbol  $d_k$  is changed with respect to the previous symbol  $d_{k-1}$ .

The differentially encoded sequence  $\{d_k\}$  thus generated is used to phase-shift a sinusoidal carrier wave with phase angles 0 and  $\pi$  radians, representing symbols 1 and 0, respectively.

The block diagram of the DPSK transmitter is shown in Fig. 7.19(a). It consists, in part, of a *logic network* and a *one-bit delay element* (acting as the memory unit) interconnected so as to convert the raw binary sequence  $\{b_k\}$  into a differentially encoded sequence  $\{d_k\}$ . This sequence is amplitude-level encoded and then used to modulate a carrier wave of frequency  $f_c$ , thereby producing the desired DPSK signal.

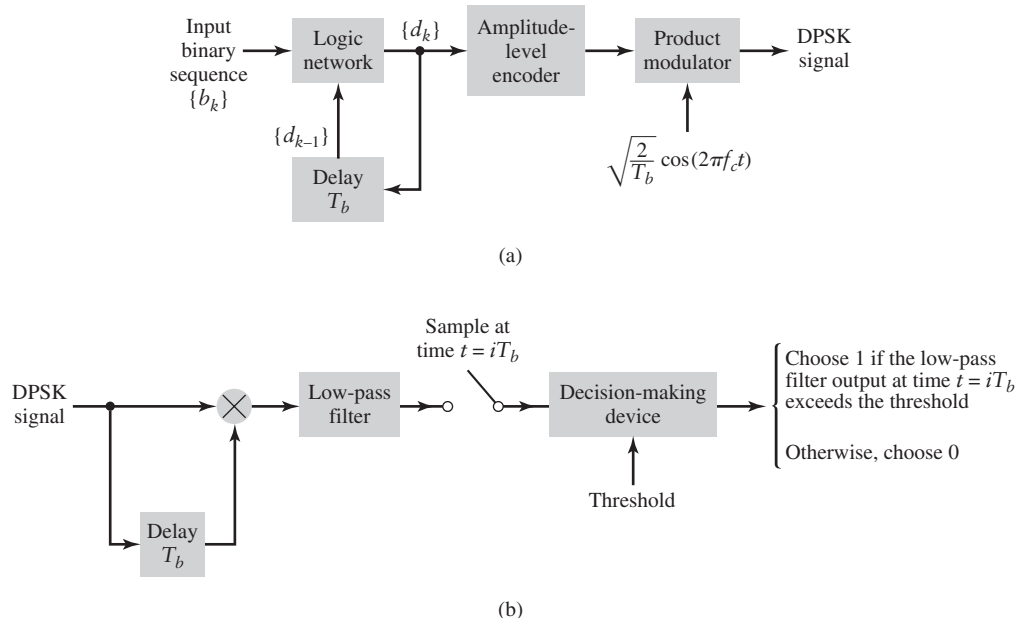


**FIGURE 7.19** Block diagrams for (a) DPSK transmitter and (b) DPSK receiver; for the sampler, integer  $i = 0, \pm 1, \pm 2, \dots$

### (ii) Detection

For the detection of DPSK signals, we take advantage of the fact that the phase-modulated pulses pertaining to two successive bits are identical except for a possible sign reversal. Hence, the incoming pulse is multiplied by the preceding pulse, which, in effect, means that the preceding pulse serves the purpose of a *locally generated reference signal*. On this basis, we may formulate the receiver of Fig. 7.19(b) for the detection of DPSK signals. Comparing the DPSK detector of Fig. 7.19(b) and the coherent BPSK detector of Fig. 7.4(b), we see that the two receiver structures are similar except for the source of the locally generated reference signal. According to Fig. 7.19(b), the DPSK signal is detectable, given knowledge of the *reference bit*, which, as mentioned previously, is inserted at the very beginning of the incoming binary data stream. In particular, applying the sampled output of the low-pass filter to a decision-making device supplied with a prescribed *threshold*, detection of the DPSK signal is accomplished. If the threshold is exceeded, the receiver decides in favor of symbol 1; otherwise, the decision is made in favor of symbol 0. Here again, it is assumed that the receiver is supplied with bit-timing information for the sampler to work properly.

#### EXAMPLE 7.3 From Binary Data Stream to DPSK Signal and Back

Starting with the binary data stream  $\{b_k\}$  given in the first row of Table 7.3 and using symbol 1 as the first reference bit, we may construct the differentially encoded stream  $\{d_k\}$  in row 3 of the table. The second row is the delayed version of  $\{d_k\}$  by one bit. Note that for each index  $k$ , the symbol  $d_k$  is the complement of the modulo-2 sum of  $b_k$  and  $d_{k-1}$ . The fourth row of Table 7.3 defines the phase (in radians) of the transmitted DPSK signal.

The last two rows of Table 7.3 pertain to the DPSK receiver. Row 5 of the table defines the polarity (positive or negative) of the low-pass filter output in the receiver of Fig. 7.19(b). The final row of the table defines the binary data stream produced at the receiver output, which is identical to the input binary data stream at the top of the table, as it should be in a noise-free environment.

**TABLE 7.3 Illustration of the Generation and Detection of DPSK Signal**

$\{b_k\}$	1	0	0	1	0	0	1	1
$\{d_{k-1}\}$	1	1	0	1	1	0	1	1
Differentially encoded sequence $\{d_k\}$	1	1	0	1	1	0	1	1
Transmitted phase (radians)	0	0	$\pi$	0	0	$\pi$	0	0
Sampler's output (polarity)	+	-	-	+	-	-	+	+
Binary symbol at decision-maker's output	1	0	0	1	0	0	1	1

Note: The symbol 1 inserted at the beginning of the differentially encoded sequence  $d_k$  is the reference bit.

## 7.7 M-ary Digital Modulation Schemes

By definition, in an *M-ary digital modulation scheme*, we send any one of  $M$  possible signals  $s_1(t), s_2(t), \dots, s_M(t)$  during each signaling (symbol) interval of duration  $T$ . In almost all applications,  $M = 2^m$  where  $m$  is an integer. Under this condition, the symbol duration  $T = mT_b$ , where  $T_b$  is the bit duration.

*M-ary* modulation schemes are preferred over binary modulation schemes for transmitting digital data over band-pass channels when the requirement is to *conserve bandwidth at the expense of both increased power and increased system complexity*. In practice, we rarely find a communication channel that has the exact bandwidth required for transmitting the output of an information-bearing source by means of binary modulation schemes. Thus, when the bandwidth of the channel is less than the required value, we resort to an *M-ary* modulation scheme for maximum bandwidth conservation.

### M-ARY PHASE-SHIFT KEYING

To illustrate the capability of *M-ary* modulation schemes for bandwidth conservation, consider first the transmission of information consisting of a binary sequence with bit duration  $T_b$ . If we were to transmit this information by means of binary PSK, for example, we would require a channel bandwidth that is inversely proportional to the bit duration  $T_b$ . However, if we take blocks of  $m$  bits to produce a symbol and use an *M-ary PSK scheme* with  $M = 2^m$  and symbol duration  $T = mT_b$ , then the bandwidth required is proportional to  $1/(mT_b)$ . This simple argument shows that the use of *M-ary* PSK provides a reduction in transmission bandwidth by a factor  $m = \log_2 M$  over binary PSK.

In *M-ary* PSK, the available phase of  $2\pi$  radians is apportioned equally and in a discrete way among the  $M$  transmitted signals, as shown by the phase-modulated signal

$$s_i(t) = \sqrt{\frac{2E}{T}} \cos\left(2\pi f_c t + \frac{2\pi}{M} i\right), \quad i = 0, 1, \dots, M-1 \quad (7.35)$$

where  $E$  is the signal energy per symbol, and  $f_c$  is the carrier frequency. Using a well-known trigonometric identity, we may expand Eq. (7.35) as

$$\begin{aligned} s_i(t) &= \left[ \sqrt{E} \cos\left(\frac{2\pi}{M} i\right) \right] \left[ \sqrt{\frac{2}{T}} \cos(2\pi f_c t) \right] \\ &\quad - \left[ \sqrt{E} \sin\left(\frac{2\pi}{M} i\right) \right] \left[ \sqrt{\frac{2}{T}} \sin(2\pi f_c t) \right], \quad i = 0, 1, \dots, M-1 \quad (7.36) \end{aligned}$$

The discrete coefficients  $\sqrt{E} \cos\left(\frac{2\pi}{M} i\right)$  and  $-\sqrt{E} \sin\left(\frac{2\pi}{M} i\right)$  are respectively referred to as the *in-phase* and *quadrature components* of the  $M$ -ary PSK signal  $s_i(t)$ . We now recognize that

$$\left\{ \left[ \sqrt{E} \cos\left(\frac{2\pi}{M} i\right) \right]^2 + \left[ \sqrt{E} \sin\left(\frac{2\pi}{M} i\right) \right]^2 \right\}^{1/2} = \sqrt{E}, \quad \text{for all } i \quad (7.37)$$

Accordingly,  $M$ -ary PSK modulation has the unique property that the in-phase and quadrature components of the modulated signal  $s_i(t)$  are *interrelated* in such a way that the discrete envelope of the signal is constrained to remain constant at the value  $\sqrt{E}$  for all  $M$ . The modulation strategy of QPSK discussed in Section 7.3 is an example of  $M$ -ary PSK with the number of phase levels  $M = 4$ .

### Signal-Space Diagram

The result described in Eq. (7.37), combined with the fact that the in-phase and quadrature components of  $M$ -ary PSK are discrete, leads to an insightful geometric portrayal of  $M$ -ary PSK. To explain, suppose we construct a two-dimensional diagram with the horizontal and vertical axes respectively defined by the following pair of *orthonormal functions*:

$$\phi_1(t) = \sqrt{\frac{2}{T}} \cos(2\pi f_c t), \quad 0 \leq t \leq T \quad (7.38)$$

and

$$\phi_2(t) = \sqrt{\frac{2}{T}} \sin(2\pi f_c t), \quad 0 \leq t \leq T \quad (7.39)$$

where the band-pass assumption implies orthogonality; the scaling factor  $\sqrt{\frac{2}{T}}$  assures unit energy over the interval  $T$  for both  $\phi_1(t)$  and  $\phi_2(t)$ . On this basis, we may represent the in-phase component  $\sqrt{E} \cos\left(\frac{2\pi}{M} i\right)$  and quadrature component  $-\sqrt{E} \sin\left(\frac{2\pi}{M} i\right)$  for  $i = 0, 1, \dots, M - 1$  as a set of points in this two-dimensional diagram, as illustrated in Fig. 7.19 for  $M = 8$ . Such a diagram is referred to as a *signal-space diagram*.

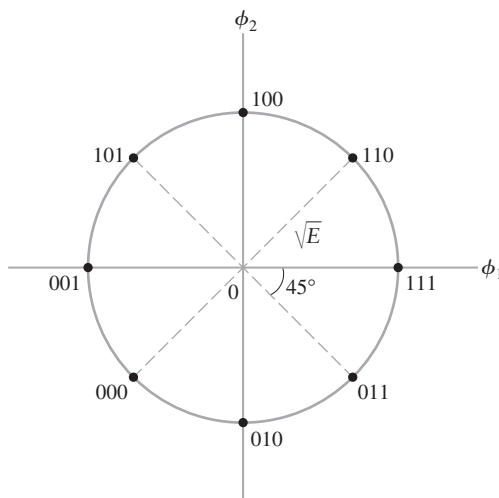


FIGURE 7.20 Signal-space diagram of 8-PSK.

Figure 7.20 leads us to make three important observations:

1. M-ary PSK is described in geometric terms by a *constellation of M signal points distributed uniformly on a circle of radius  $\sqrt{E}$* .
2. Each signal point in the figure corresponds to the signal  $s_i(t)$  of Eq. (7.35) for a particular value of the index  $i$ .
3. The squared length from the origin to each signal point is equal to the signal energy  $E$ .

In light of these observations, we may now formally state that the signal-space-diagram of Fig. 7.20 completely sums up the geometric description of M-ary PSK in an insightful manner. Note that the 3-bit sequences corresponding to the 8 signal points are *Gray-encoded*, with only a single bit changing as we move along the constellation in the figure from one signal point to an adjacent one.

### ■ M-ARY QUADRATURE AMPLITUDE MODULATION

Suppose next that the constraint of Eq. (7.37) that characterizes M-ary PSK modulation is removed. Then, the in-phase and quadrature components of the resulting M-ary modulated signal are permitted to be *independent* of each other. Specifically, the mathematical description of the new modulated signal assumes the form

$$s_i(t) = \sqrt{\frac{2E_0}{T}} a_i \cos(2\pi f_c t) - \sqrt{\frac{2E_0}{T}} b_i \sin(2\pi f_c t), \quad i = 0, 1, \dots, M-1 \quad (7.40)$$

where the level parameter  $a_i$  in the in-phase component and the level parameter  $b_i$  in the quadrature component are *independent of each other for all i*. This new modulation scheme is called *M-ary quadrature amplitude modulation* (QAM). Note also that the constant  $E_0$  is the energy of the signal pertaining to a particular value of the index  $i$  for which the amplitude of the modulated signal is the lowest.

M-ary QAM is a *hybrid* form of M-ary modulation, in the sense that it combines amplitude-shift keying and phase-shift keying. It includes two special cases:

- (i) If  $b_i = 0$  for all  $i$ , the modulated signal  $s_i(t)$  of Eq. (7.40) reduces to

$$s_i(t) = \sqrt{\frac{2E_0}{T}} a_i \cos(2\pi f_c t) \quad i = 0, 1, \dots, M-1$$

which defines *M-ary amplitude-shift keying* (*M-ary ASK*).

- (ii) If  $E_0 = E$  and the constraint

$$(Ea_i^2 + Eb_i^2)^{1/2} = \sqrt{E}, \quad \text{for all } i$$

is satisfied, then the modulated signal  $s_i(t)$  of Eq. (7.40) reduces to M-ary PSK.

### **Signal-Space Diagram**

Figure 7.21 portrays the signal-space representation of M-ary QAM for  $M = 16$ , with each signal point being defined by a pair of level parameters  $a_i$  and  $b_i$ , where  $i = 1, 2, 3, 4$ . This time, we see that the signal points are distributed uniformly on a rectangular grid. The rectangular property of the signal-space diagram is testimony to the fact that the in-phase and quadrature components of M-ary QAM are independent of each other. Moreover, we see from Fig. 7.21 that, unlike M-ary PSK, the different signal points of M-ary QAM are characterized by different energy levels, and so they should be. Note also that each signal point in the constellation corresponds to a specific *quadbit*, which is made up of 4 bits. Assuming the use of Gray encoding, only one bit is changed as we go from each signal point in the constellation horizontally or vertically to an adjacent point, as illustrated in Fig. 7.21.

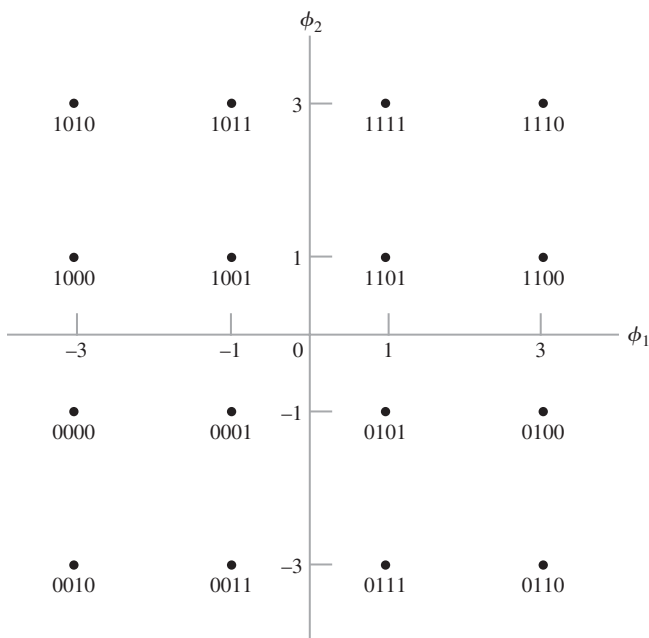


**FIGURE 7.21** Signal-space diagram of Gray-encoded  $M$ -ary QAM for  $M = 16$ .

### ■ M-ARY FREQUENCY-SHIFT KEYING

However, when we consider the  $M$ -ary version of frequency-shift keying, the picture is quite different from that described for  $M$ -ary PSK or  $M$ -ary QAM. Specifically, in one form of  $M$ -ary FSK, the transmitted signals are defined for some fixed integer  $n$  as follows:

$$s_i(t) = \sqrt{\frac{2E}{T}} \cos\left[\frac{\pi}{T}(n + i)t\right], \quad i = 0, 1, \dots, M - 1 \quad 0 \leq t \leq T \quad (7.41)$$

The  $M$  transmitted signals are all of equal duration  $T$  and equal energy  $E$ . With the individual signal frequencies separated from each other by  $1/(2T)$  hertz, the signals in Eq. (7.41) are *orthogonal*; that is, they satisfy the condition

$$\int_0^T s_i(t)s_j(t) dt = \begin{cases} E & \text{for } i = j \\ 0 & \text{for } i \neq j \end{cases} \quad (7.42)$$

Like  $M$ -ary PSK, the envelope of  $M$ -ary FSK is constant for all  $M$ , which follows directly from Eq. (7.41). Hence, both of these  $M$ -ary modulation strategies can be used over non-linear channels. On the other hand,  $M$ -ary QAM can only be used over linear channels because its discrete envelope varies with the index  $i$  (i.e., the particular signal point chosen for transmission).

### Signal-Space Diagram

To develop a geometric representation of  $M$ -ary FSK, we start with Eq. (7.41). In terms of the signals  $s_i(t)$  defined therein, we introduce a complete set of orthonormal functions:

$$\phi_i(t) = \frac{1}{\sqrt{E}} s_i(t) \quad i = 0, 1, \dots, M - 1 \quad 0 \leq t \leq T \quad (7.43)$$

Unlike  $M$ -ary PSK and  $M$ -ary QAM, we now find that  $M$ -ary FSK is described by an  *$M$ -dimensional signal-space diagram*, where the number of signal points is equal to the number of coordinates. The visualization of such a diagram is difficult beyond  $M = 3$ . Figure 7.22 illustrates the geometric representation of  $M$ -ary FSK for  $M = 3$ .

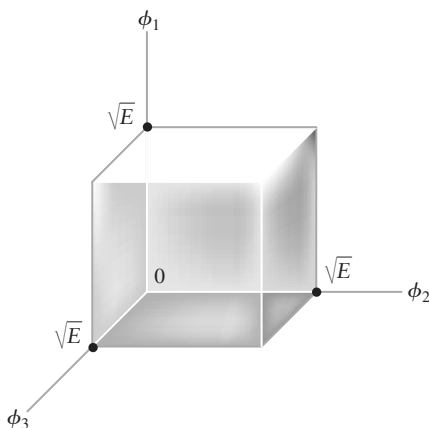


**FIGURE 7.22** Signal constellation for  $M$ -ary FSK for  $M = 3$ .

► **Drill Problem 7.9** Starting with Eq. (7.41), prove the orthogonality property of Eq. (7.42) that characterizes  $M$ -ary FSK. ◀

## 7.8 Mapping of Digitally Modulated Waveforms Onto Constellations of Signal Points

The idea of signal-space diagrams mentioned at various points in Section 7.7 is of profound importance in statistical communication theory. In particular, it provides the mathematical basis for the *geometric representation of energy signals*, exemplified by digitally modulated waveforms. For a specific method of digital modulation, the geometric representation is pictured in the form of a constellation of points in the signal-space diagram, which is unique to that method.

The purpose of this section is to do two things:

- Consolidate the idea of a signal-space diagram pictorially.
- Discuss what this idea teaches us in the analysis of noise in digital communication systems, which we treat later in the book.

With consolidation in mind, Fig. 7.23 on BPSK shows the way in which the two waveforms  $s_1(t)$  and  $s_2(t)$ , respectively representing binary symbols 1 and 0, are mapped onto the *transmitted signal points*  $s_1$  and  $s_2$ . The key question is: how is the mapping

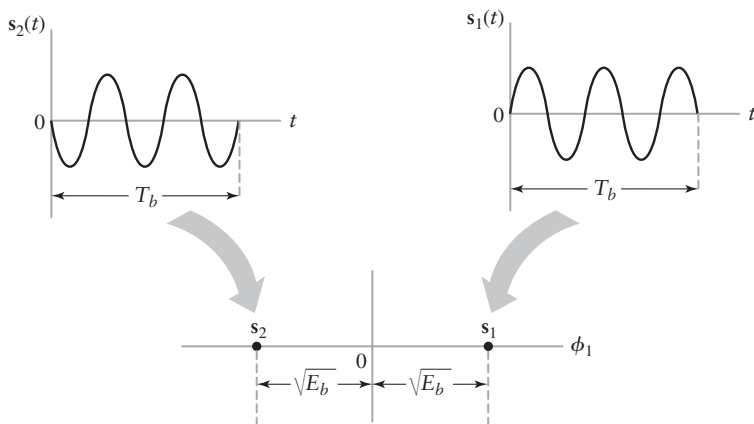


**FIGURE 7.23** Mapping of BPSK signal onto a one-dimensional signal-space diagram.

accomplished? The answer lies in the use of a *correlator*. First, we note that the signal-space representation of BPSK is simple, involving a single basis function:

$$\phi_1(t) = \sqrt{\frac{2}{T_b}} \cos(2\pi f_c t) \quad (7.44)$$

In more specific terms, each of the two signaling waveforms  $s_1(t)$  and  $s_2(t)$  is correlated with the basis function  $\phi_1(t)$ . The use of correlation provides another way of designing a receiver for the coherent detection of BPSK. For the issue at hand, we proceed in two steps as follows:

1. Correlating the signal

$$s_1(t) = \sqrt{\frac{2E_b}{T_b}} \cos(2\pi f_c t) \quad \text{for symbol 1} \quad (7.45)$$

with the basis function  $\phi_1(t)$  over the time interval  $0 \leq t \leq T_b$ , we get the signal point

$$\begin{aligned} s_1 &= \int_0^{T_b} \phi_1(t)s_1(t) dt \\ &= \int_0^{T_b} \frac{2}{T_b} \sqrt{E_b} \cos^2(2\pi f_c t) dt \end{aligned} \quad (7.46)$$

Under the band-pass assumption, Eq. (7.46) simplifies to

$$s_1 = \sqrt{E_b} \quad (7.47)$$

2. Similarly, we may show that the signal

$$s_2(t) = -\sqrt{\frac{2E_b}{T_b}} \cos(2\pi f_c t) \quad \text{for symbol 0} \quad (7.48)$$

is represented by the signal point

$$s_2 = -\sqrt{E_b} \quad (7.49)$$

These two results are indeed what is portrayed in Fig. 7.23.

► **Drill Problem 7.10** Justify Eqs. (7.47) and (7.49). ◀

Consider next the picture depicted in Fig. 7.24, pertaining to BFSK. As with BPSK, the signal-space diagram consists of two *transmitted signal points*: the point  $s_1$  representing the transmission of binary symbol 1 and the point  $s_2$  representing the transmission of binary symbol 0. Following a procedure similar to that which led to the signal-space mapping of BPSK, we may construct the signal-space mapping of Fig. 7.24 for BFSK, where the two signal points are defined by

$$s_1 = \begin{bmatrix} \sqrt{E_b} \\ 0 \end{bmatrix} \quad (7.50)$$

and

$$s_2 = \begin{bmatrix} 0 \\ \sqrt{E_b} \end{bmatrix} \quad (7.51)$$

The two signal-space diagrams of Figs. 7.23 and 7.24 differ in one important respect: *dimensionality*, which is defined by the pertinent number of basis functions. The BPSK sig-

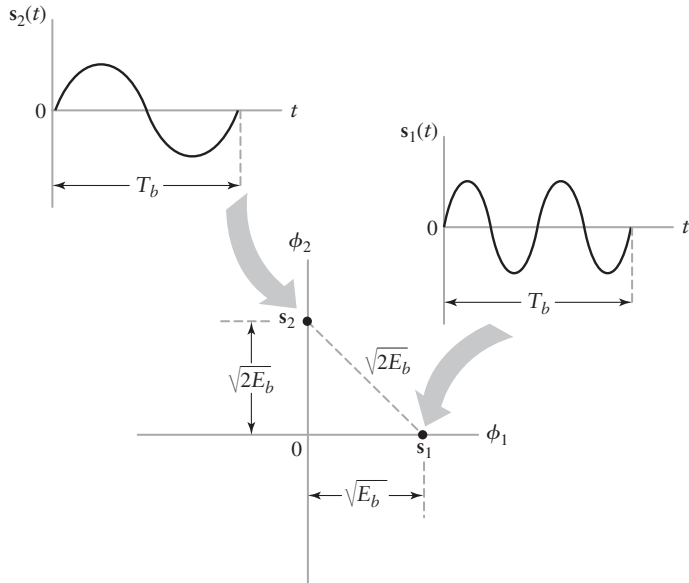


**FIGURE 7.24** Mapping of BFSK onto two-dimensional signal-space diagram.

nal-space diagram of Fig. 7.23 is one-dimensional, as it involves the single basis function  $\phi_1(t)$  of Eq. (7.44). On the other hand, the BFSK signal-space diagram of Fig. 7.24 is two-dimensional, as it involves the pair of basis functions

$$\phi_1(t) = \sqrt{\frac{2}{T_b}} \cos(2\pi f_1 t) \quad (7.52)$$

and

$$\phi_2(t) = \sqrt{\frac{2}{T_b}} \cos(2\pi f_2 t) \quad (7.53)$$

What insight can we learn from these two signal-space diagrams when considering the effect of additive channel noise on BPSK and BFSK? To answer this question, we first note that the separation between the signal points for BPSK is  $2\sqrt{E_b}$  whereas it is  $\sqrt{2E_b}$  for BFSK, assuming that the signal energy per bit,  $E_b$ , and the bit duration,  $T_b$ , are the same for both schemes. In other words, we may now make our first statement:

1. The separation between the transmitted signal points for BPSK is  $\sqrt{2}$  times that for BFSK.

As for the presence of additive channel noise, it has the effect of causing the *received signal point to wander about the transmitted signal point in a random fashion*. Accordingly, we make our second statement:

2. The received signal point lies inside a “cloud” centered on the transmitted signal point.

In light of statements 1 and 2, we are now emboldened to say that under the assumption of an identical statistical characterization of additive channel noise (and therefore an identical cloud of uncertainty) for both BPSK and BFSK schemes, noise degrades the performance of BFSK to a greater extent than BPSK. The validity of this observation is confirmed in Chapter 10, where it is put on a mathematical basis.

## 7.9 Theme Examples

### ■ ORTHOGONAL FREQUENCY-DIVISION MULTIPLEXING

In Section 2.11, we discussed the frequency response of twisted pairs used to connect homes to telephone central switching offices. We found that the frequency response for short cables is quite flat over the voice band but deteriorates as the cable length increases. For our first theme example, we consider how we might transmit high-speed data using twisted pairs to the home. This service is often referred to as *digital subscriber line* (DSL).

Consider a transmission medium that has the arbitrary frequency response shown in Fig. 7.25(a). It is clear that this medium will alter the transmitted spectrum of Fig. 7.25(b) and thereby cause significant intersymbol interference with most of the digital modulation techniques discussed in this chapter. We refer to modulation techniques that have characteristics similar to Fig. 7.25(b) as *single-carrier* systems.

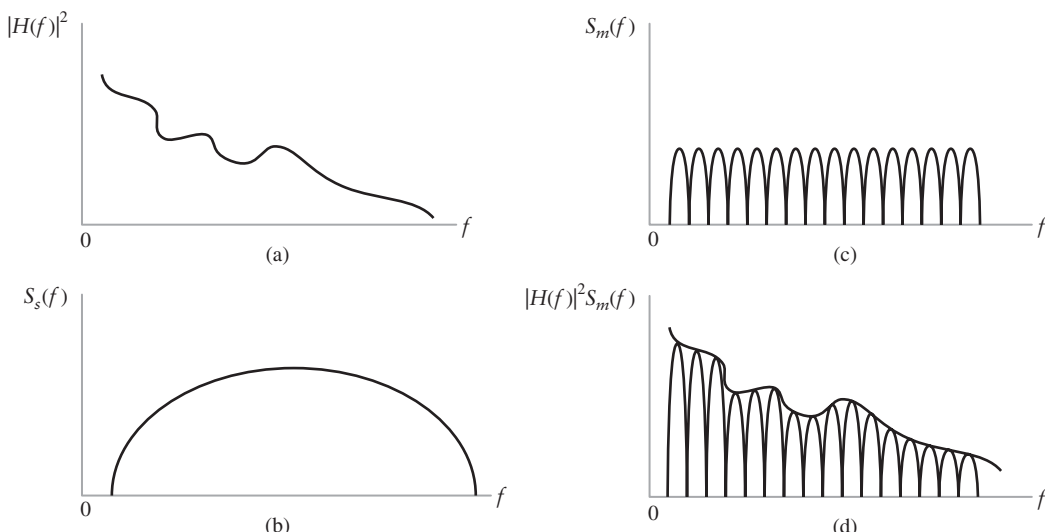


**FIGURE 7.25** (a) Frequency response squared of channel. (b) Transmit power spectral density of single-carrier modulation. (c) Transmit power spectral density of multi-carrier modulation. (d) Received power spectral density of multi-carrier modulation.

Consider next the *multi-carrier system* shown in Fig. 7.25(c) where a single transmitter employs multiple carriers, each being responsible for a fraction of the overall data rate. With multi-carrier transmission, the medium will have the same effect on the overall spectrum, but the spectrum of the individual carriers is relatively undistorted except for possible gain change and phase rotation, as shown in Fig. 7.25(d).

Now let us consider how we could implement such a multi-carrier system where the individual components are referred to as *subcarriers*. Since all of the subcarriers are generated by the same source, we assume that they can be synchronized. First, consider a single symbol period and let there be \$N\$ subcarriers with frequencies \$\{f\_n\}\$ and information-carrying bits \$\{b\_n\}\$. The \$n\$th subcarrier signal may then be represented as

$$s_n(t) = b_n \exp(j2\pi f_n t), \quad 0 \leq t \leq T \quad (7.54)$$

If \$b\_n\$ is \$\pm 1\$, then Eq.(7.54) is simply a complex baseband representation of BPSK at the subcarrier frequency \$f\_n\$. Hence, the multi-carrier signal over one symbol period can be

represented as the sum of Eq.(7.54) over all subcarriers, as shown by

$$\begin{aligned} s(t) &= \sum_{n=0}^{N-1} s_n(t) \\ &= \sum_{n=0}^{N-1} b_n \exp(j2\pi f_n t) \quad 0 \leq t \leq T \end{aligned} \quad (7.55)$$

Now we ingeniously make the following two decisions:

- We sample this multi-carrier signal at intervals of  $T_s$  where  $T_s = T/N$ .
- We choose the subcarrier frequencies to be spaced at intervals of  $f_n = n/T$ . Then Eq. (7.55), evaluated at  $t = kT_s$ , becomes

$$s(kT_s) = \sum_{n=0}^{N-1} b_k \exp\left(j2\pi \frac{kn}{N}\right) \quad (7.56)$$

Comparing what we have presented here with the material in Section 2.10, we find that the sampled multi-carrier signal is simply the inverse discrete Fourier transform (DFT) of the data stream  $\{b_n\}$ . Consequently, we can represent this data transmission system as shown in Fig. 7.26, where the transmitter includes a serial-to-parallel conversion of the data stream followed by an inverse DFT subsystem. The receiver performs the inverse processing with respect to the transmitter. If we make the additional assumption that  $N$  is an integer power of two, then the system can be implemented efficiently with the fast Fourier transform (FFT) algorithm, which was also discussed in Section 2.10.

Not only do the decisions regarding the sampling and frequency intervals facilitate a simple implementation, they also have the following practical benefits:

- The adjacent channels are spaced at intervals  $1/T_s$ ; this choice implies that there is significant spectral overlap, and hence the modulation scheme minimizes the amount of bandwidth required.
- The fact that the subcarrier frequencies are a multiple of the symbol period means that they are orthogonal<sup>3</sup> over a symbol period. Consequently, there is no interference between the subcarriers even though they overlap significantly.
- The subcarrier frequencies are continuous from one symbol interval to the next, meaning there is no distortion of the spectral properties when we transmit a continuous stream of data.

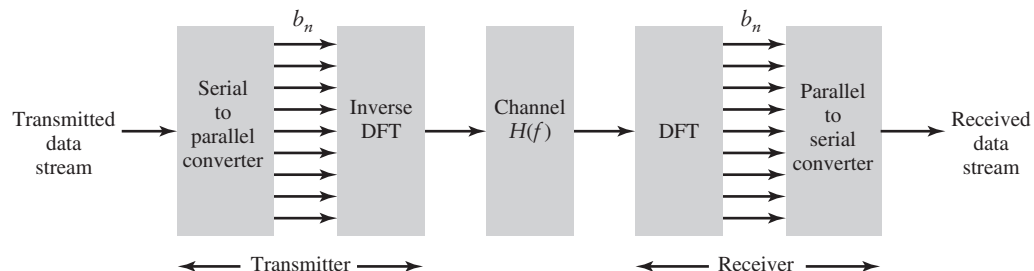


**FIGURE 7.26** Block diagram of OFDM system.

<sup>3</sup>Orthogonality means that the condition

$$\int_0^T s_n(t)s_k^*(t) dt = 0$$

holds for  $n \neq k$ .

- ▶ Symbols may be continuously extended by a simple repetition referred to as *cyclic prefix* or *postfix*; this feature can be used beneficially in channels that tend to lengthen the pulse interval.

The combination of the multiplexing subcarriers in the frequency domain and the orthogonality of these subcarriers lead to the name *orthogonal frequency division multiplex* (OFDM) for this multi-carrier modulation technique.<sup>4</sup>

### ■ GLOBAL SYSTEM FOR MOBILE (GSM) COMMUNICATION

In Chapter 4, we discussed the idea of frequency modulation, based on the definition

$$s(t) = A_c \cos\left(2\pi f_c t + 2\pi k_f \int_0^t m(\tau) d\tau\right) \quad (7.57)$$

where the message signal  $m(t)$  is an analog signal. In this second theme example, we consider angle modulation that is produced by a digital message signal defined by

$$m(t) = \sum_{n=0}^N b_n p(t - nT) \quad (7.58)$$

where  $T$  is the symbol period,  $b_n$  is the data symbol of the  $n$ th symbol period, and  $p(t)$  is the pulse shape applied at each symbol period. In the historical course of events, analog modulation was the mainstay of radio communications for many years before the advent of digital communications. Consequently, for initial digital communications, it was often most convenient to use an FM transmitter, hence the term *digital FM*. Digital FM systems have a number of advantages, not the least of which is power efficiency due to their constant envelope.

The desirable power efficiency made digital FM a strong contender for wireless applications using handheld terminals with small battery packs. In fact, a form of digital FM was chosen as a European standard in 1991 and later spread to other parts of the world under the name *GSM (Global System for Mobile Communications)*.

The actual modulation selected for GSM is called *Gaussian minimum shift keying* (GMSK), which is a special combination of Eqs. (7.57) and (7.58). In particular, we introduce three conditions:

1. The pulse shape is chosen to have the Gaussian shape

$$p(t) = c \exp\{-\pi c^2 t^2\} \quad (7.59)$$

where the scale factor  $c = B\sqrt{2\pi/\log(2)}$ , and the logarithm is the natural logarithm.

2. The factor  $B$  controls the signal bandwidth, which, for prescribed symbol period  $T$ , is chosen such that the time-bandwidth product  $BT = 0.3$ .
3. The frequency sensitivity factor  $k_f$  of the modulator is selected such that the phase change over one symbol period is  $\pi/2$  radians.

Under these three conditions, it turns out that the resulting GMSK signal has a compact spectrum and may be coherently detected with only 0.46-dB degradation relative to ideal BPSK performance in noise.

GSM communication (embodying GMSK) may therefore be viewed as a practical example of the evolution of an analog FM system to a digital system, which attempts to retain the advantages of the former.<sup>5</sup>

<sup>4</sup>For a more detailed discussion of OFDM, see Bahai and Saltzberg (1999).

<sup>5</sup>For detailed discussion of GMSK, see Steele and Hanzo (1999).

## ■ DIGITAL TELEVISION

For the third and last theme example, we consider *digital television*. There is a worldwide movement from analog to digital television with the objective of providing high-quality video and audio. In North America, the analog NTSC<sup>6</sup> television standard is being replaced by the *digital Advanced Television (ATV) standard*. For backward compatibility, the new ATV standard is designed to fit into the 6-MHz channel bandwidth used by current NTSC service. The ATV system provides two levels of service:

- (i) 19 Mb/s of throughput in a 6-MHz channel broadcast by terrestrial radio.
- (ii) 38 Mb/s of throughput in a 6 MHz channel used by cable networks.

Similar to analog television, digital television is a complex system; the block diagram of Fig. 7.27 is a hint of the complexity involved. Let us consider the different components shown in the figure.

Of primary importance are the *audio and video sources*, without which there would be no need for the remainder. Nowadays, these sources may take one of many forms, either analog or digital; thus the transmitter must support a variety of interfaces. The ancillary data include control data, and data associated with the program audio and video services, such as closed captioning.

The first operation on the source data is *source encoding*. This operation refers to signal processing applied to the video and audio data streams to eliminate *redundancy* and minimize the bit rate required for transmission; it is also referred to as *data compression*. The amount of compression possible depends both on the underlying dynamics of the video or audio signal and the amount of distortion permissible; in general, the objective is to make any distortion imperceptible to a human user. Since the system is designed to carry high-resolution video, achieving this objective using the available bandwidth requires complex video and audio compression algorithms.

The ATV system employs a number of source coding and compression algorithms. For video, the algorithm defined in the MPEG-2 standard is used. This compression algorithm is capable of coding standard definition television at bit rates from four to nine megabits per second and high definition television from 15 to 25 megabits per second.

For audio source coding, an algorithm from the Dolby AC-3 standard is used. This same algorithm is used for laser discs and DVDs. For a 5.1-channel system, this second algorithm can achieve compression ratios in the range of ten to one for high-quality audio.

The *multiplexer* of Fig. 7.27 provides three specific functions:

1. Dividing the digital data stream into “packets” of information.
2. Providing a unique identifier for each packet or packet type.
3. Multiplexing the video packets, audio packets, and ancillary data packets into a single data stream.

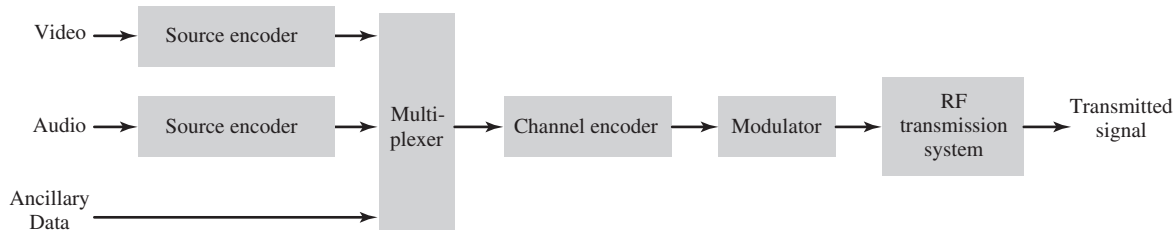


**FIGURE 7.27** Digital television broadcasting model.

<sup>6</sup>NTSC stands for National Television System Committee.

Given the bandwidth limitations, this multiplexing must be done in a highly efficient manner.

The last three blocks of Fig. 7.27 correspond to the physical layer of digital transmission systems. The channel encoder takes the data bit stream and adds additional channel encoding information that is, in turn, used by the receiver to correct errors that may occur due to transmission impairments (see Section 10.8 on error detection and correction). The modulator uses the digital data stream information to modulate the transmitted carrier. The modulation subsystem offers two transmission modes, corresponding to the two levels of service:

1. *Terrestrial broadcast mode*, referred to as 8-VSB, uses an 8-ary PAM signal with vestigial sideband modulation to transmit 19 megabits/s.
2. *High data rate mode*, intended for cable transmission and referred to as 16-VSB, uses a 16-ary PAM signal with vestigial sideband modulation to transmit 38 megabits/s.

We have seen vestigial sideband modulation (VSB) applied to analog signals in Chapter 3. This raises the question: how is VSB used to transport a digital signal?

Recall that, at complex baseband, the frequency response of the sideband sharing filter in a VSB modulator looks similar to that shown in Fig. 7.28(a); see Problem 3.32. The modulator passes most positive frequencies without distortion, and blocks most negative frequency components of the signal. In the region near zero frequency, the frequency response tapers from 1 to 0, leaving a vestige of the negative frequency component of the signal. To analyze a digital VSB modulator, we note that this frequency response may be expressed as the sum of the two frequency responses, denoted by  $H_I(f)$  and  $H_Q(f)$ , as shown in Figs. 7.28(b) and 7.28(c), respectively. The first frequency response,  $H_I(f)$ , corresponds to an all-pass filter that passes the signal without distortion; since  $H_I(f)$  is an even function of frequency, it has a purely real impulse response,  $h_I(t)$ . The second frequency response,  $H_Q(f)$ , corresponds to a filter that passes most positive frequencies without distortion but inverts the phase of the negative frequency components; since  $H_Q(f)$  is an odd function of frequency, it has a purely imaginary impulse response,  $j h_Q(t)$ .

Let the input to the VSB modulator be a real digital signal defined by

$$m(t) = \sum_{n=0}^N a_n p(t - nT) \quad (7.60)$$

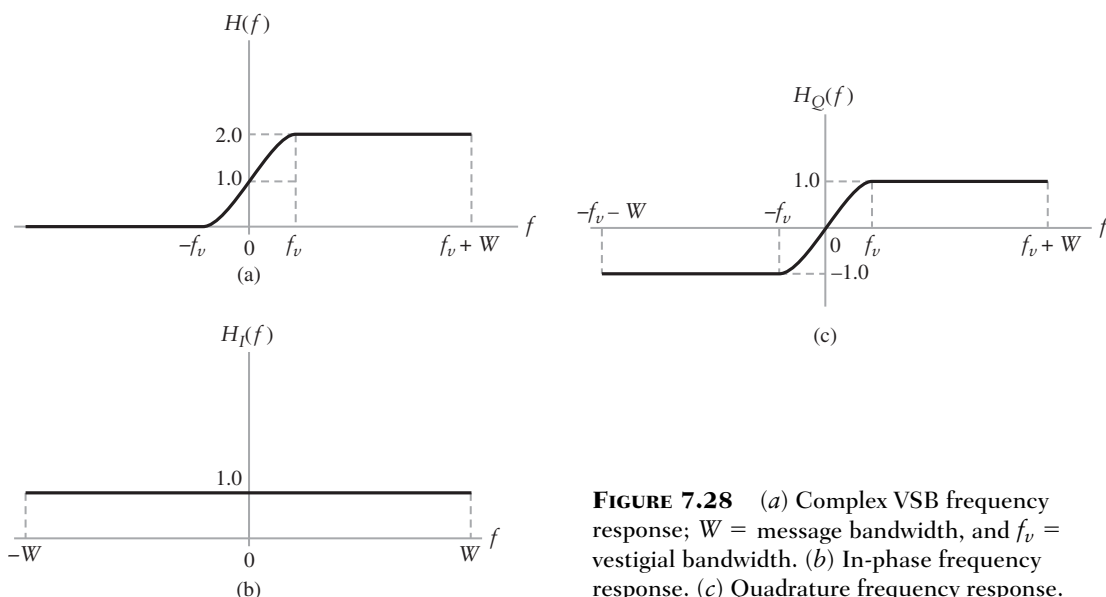


**FIGURE 7.28** (a) Complex VSB frequency response;  $W$  = message bandwidth, and  $f_v$  = vestigial bandwidth. (b) In-phase frequency response. (c) Quadrature frequency response.

where  $a_n$  is one of  $\pm 1$ ,  $\pm 3$ ,  $\pm 5$ , or  $\pm 7$  for an 8-ary PAM signal. The pulse shape  $p(t)$  corresponds to a root-raised cosine spectral shape; this form of pulse shaping was discussed in Section 6.4. The complex baseband representation at the output of the VSB modulator is therefore

$$\tilde{s}(t) = (h_I(t) + jh_Q(t)) \star m(t) \quad (7.61)$$

where  $\star$  denotes convolution. Since  $h_I(t)$  is an all-pass filter, we have  $h_I(t) \star m(t) = m(t)$ , and we let  $m_Q(t) = h_Q(t) \star m(t)$ . We may thus rewrite Eq. (7.61) as

$$\tilde{s}(t) = m(t) + jm_Q(t) \quad (7.62)$$

The band-pass transmitted signal is therefore given by

$$s(t) = \operatorname{Re}[\tilde{s}(t) \exp(j2\pi f_c t)] \quad (7.63)$$

where  $f_c$  is the carrier frequency. At the receiver, we coherently recover the signal by multiplying the  $s(t)$  of Eq. (7.63) by  $\cos(2\pi f_c t)$  (i.e., a locally generated replica of the carrier) to obtain (in the absence of channel noise)

$$\begin{aligned} x(t) &= s(t) \cos(2\pi f_c t) \\ &= \{m(t) \cos(2\pi f_c t) - m_Q(t) \sin(2\pi f_c t)\} \cos(2\pi f_c t) \end{aligned} \quad (7.64)$$

Using double-angle trigonometric identities, Eq. (7.64) reduces to

$$x(t) = \frac{1}{2}m(t)[1 + \cos(4\pi f_c t)] - \frac{1}{2}m_Q(t) \sin(4\pi f_c t) \quad (7.65)$$

which consists of a baseband term and two high-frequency terms centered at  $2f_c$ . If we low-pass filter  $x(t)$ , we are then left with  $\frac{1}{2}m(t)$ , which, except for the scaling factor 1/2, is the original message signal.<sup>8</sup>

The approach described herein can be applied to any signal and does not depend on the level of digital modulation. Thus, it can be applied equally well to 8-ary or 16-ary PAM. Furthermore, it simplifies the receiver as only a real channel has to be processed.

The ATV symbol rate ( $1/T$ ) with either 8-VSB or 16-VSB is 10.76 megasymbols per second. With 8-VSB, there are three bits per symbol and the raw channel bit rate is three times the symbol rate; overhead and redundant bits for forward error-correction reduce the user information to approximately 19 megabits per second. The bit rate is twice this value with 16-VSB. With VSB modulation, the channel bandwidth is approximately half the symbol rate or 5.38 MHz. Thus the VSB modulated signal fits nicely in a 6-MHz channel with some margin for filter tails and frequency error. It should be noted that the ATV system also includes a pilot tone (a dc level at complex baseband); this pilot tone is set at 11.3 dB below the signal level, which is used by the receiver to coherently recover the original information-bearing signal.

## 7.10 Summary and Discussion

In this chapter, we discussed some important digital band-pass modulation schemes, as summarized here:

- (i) *Amplitude-shift keying (ASK)*, with emphasis on binary signaling.

---

<sup>8</sup>It is of interest to note that we may use a root-raised cosine pulse shape for low-pass filtering of  $x(t)$  in the receiver, which is matched to the transmit pulse shape so as to provide a performance free of intersymbol interference.

- (ii) *Phase-shift keying (PSK)* with emphasis on binary and quaternary forms of signaling. (Quaternary signaling works with pairs of bits, whereas, of course, binary signaling works with single bits). Under quaternary signaling, we discussed quadriphase-shift keying (QPSK) and a variant of it called offset quadriphase-shift keying (OQPSK). The advantage of OQPSK over QPSK is that it is less sensitive to nonlinearities.
- (iii) *Frequency-shift keying (FSK)* with emphasis on binary signaling. We also discussed a modification of binary FSK known as minimum-shift keying (MSK), which is an example of continuous-phase frequency-shift keying (CPFSK). An important property of MSK is that it uses minimum frequency spacing, which, in turn, allows the two FSK signals representing symbols 0 and 1 to be coherently orthogonal so as not to interfere with one another in the process of coherent detection in the receiver. For its generation, MSK follows a procedure similar to OQPSK insofar as the extraction of the demultiplexed-offset streams from the incoming binary data stream is concerned. They differ from each other in a simple and important respect: in OQPSK, these two auxiliary binary waves are weighted by a rectangular function on a bit-by-bit basis; whereas in MSK, the weighting is performed by the positive half cycle of a cosinusoid.
- (iv) *Coherent detection*, which means that regardless of the modulation scheme of interest, the receiver must be synchronized with the transmitter in two respects: carrier phase and bit timing.
- (v) *Noncoherent detection*, which refers to a scheme in which the receiver ignores knowledge of the carrier phase between its own operation and that of the transmitter. The implementation of noncoherent detection is straightforward for both amplitude-shift keying and frequency-shift keying. However, the noncoherent form of phase-shift keying requires more detailed attention. Specifically, a pseudo-form of noncoherent detection is worked out by combining differential encoding and phase-shift keying, which results in differential phase-shift keying (DPSK). Note, however, that all noncoherent receivers, regardless of their origin, require knowledge of bit-timing information.
- (vi) *Spectral analysis*, which was demonstrated by way of experiments performed on example *band-pass* signals representative of different digital modulation strategies. The experiments were of illustrative value by virtue of the fact that the bit rate was a small fraction of the carrier frequency. In practice, however, we usually find that the bit rate is orders of magnitude smaller than the carrier frequency. In such situations, the recommended procedure is to perform the spectral analysis at *baseband*, where (without loss of essential information) the presence of the carrier wave is removed by representing the modulated signal in terms of its in-phase and quadrature components. The reader is referred to Problem 7.30 for a repeat of the spectral analysis, this time using the baseband approach.
- (vii) *M-ary signaling schemes*, whose use is preferred over binary modulation schemes for transmitting digital data over band-pass channels when the need for conserving channel bandwidth is of profound importance. In both *M-ary PSK* and *M-ary FSK* signaling schemes, the envelope of the transmitted signal is constant, thereby permitting their use over nonlinear channels. In contrast, in *M-ary QAM*, the envelope of the transmitted signal is variable, which therefore limits its use to linear band-pass channels.

For theme examples, we considered three digital systems of pervasive use in their own individual ways:

- *Orthogonal frequency-division multiplexing (OFDM)*, which provides the basis for high-speed data transmission using twisted pairs that connect homes to telephone central switching offices.

- *Global system for mobile (GSM) communication*, which embodies a modification of MSK known as Gaussian-filtered minimum shift-keying (GMSK).
- *Digital television*, the objective of which is to provide high-quality video and audio using channel parameters similar to analog television.

One last comment is in order. Throughout the discussion of receivers in this chapter, be they of the coherent or noncoherent kind, we ignored a practical reality: the unavoidable presence of additive channel noise. Inevitably, the transmitted signal is perturbed by this reality, which, in turn, has the effect of producing errors in the estimated binary data stream at the receiver output. The effect of channel noise is discussed in Chapter 10, but we have to first study the characterization of random signals and noise, which we do in the next chapter.

## ADDITIONAL PROBLEMS

- 7.11 The binary sequence 11100101 is applied to an ASK modulator. The bit duration is  $1 \mu\text{s}$ , and the sinusoidal carrier wave used to represent symbol 1 has a frequency equal to 7 MHz.
- Find the transmission bandwidth of the transmitted signal.
  - Plot the waveform of the transmitted ASK signal.  
Assume that the line encoder and the carrier-wave oscillator are controlled by a common clock.
- 7.12 Repeat Problem 7.11, assuming that the line encoder and the carrier-wave generator operate independently of each other. Comment on your results.
- 7.13 (a) Repeat Problem 7.11 for the case when the binary sequence 11100101 is applied to a PSK modulator, assuming that the line encoder and sinusoidal carrier-wave oscillator are operated from a common clock.  
(b) Repeat your calculations, assuming that the line encoder and carrier-wave oscillator operate independently.
- 7.14 The binary sequence 11100101 is applied to a QPSK modulator. The bit duration is  $1 \mu\text{s}$ . The carrier frequency is 6 MHz.
- Calculate the transmission bandwidth of the QPSK signal.
  - Plot the waveform of the QPSK signal.
- 7.15 Repeat Problem 7.14 for the signaling case of OQPSK.
- 7.16 The binary sequence 11100101 is applied to Sunde's BFSK modulator. The bit duration is  $1 \mu\text{s}$ . The carrier frequencies used to represent symbols 0 and 1 are 2.5 MHz and 3.5 MHz, respectively.
- Calculate the transmission bandwidth of the BFSK signal.
  - Plot the waveform of the BFSK signal.
- 7.17 As remarked previously, the waveform plotted in Fig. 7.1(d) is an example of MSK. Determine
- The frequency excursion  $\delta f$  of the MSK.
  - The frequency parameter  $f_0$ .
- 7.18 The binary sequence 11100101 is applied to a MSK modulator. The bit duration is  $1 \mu\text{s}$ . The carrier frequencies used to represent symbols 0 and 1 are 2.5 MHz and 3 MHz, respectively. Plot the waveform of the MSK signal.
- 7.19 Consider an MSK modulator that uses a sinusoidal carrier with frequency  $f_c = 50 \text{ MHz}$ . The bit rate of the incoming binary stream is  $20 \times 10^3 \text{ bits/s}$ .
- Calculate the instantaneous frequency of the MSK modulator for a data sequence in which symbols 0 and 1 alternate.
  - Repeat the calculation in part (a) for a data sequence that consists of all 0s. What if the sequence consists of all 1s?

- 7.20 Suppose you are given an MSK signal  $s(t)$ . How would you extract the bit-timing signal from  $s(t)$ ? Explain.
- 7.21 Consider the noncoherent receiver of Fig. 7.17 for BASK and that of Fig. 7.18 for BFSK. Roughly speaking, the noncoherent BFSK receiver is twice as complex as the noncoherent BASK receiver. What would be the advantage of the BFSK system over the BASK system, given that they operate on the same binary data stream and the same communication channel? Justify your answer.  
*Hint:* Refer to the pertinent phasor representations in Table 7.2.
- 7.22 Figure 7.29 depicts a receiver for the noncoherent detection of BFSK signals. The receiver consists of two paths; the band-pass filter in the top path is tuned to the carrier frequency  $f_1$  representing symbol 1, and the band-pass filter in the lower path is tuned to the alternative carrier frequency  $f_2$  representing symbol 0. These two filters are followed by a pair of *energy-level detectors*, whose outputs are applied to the comparator to recover the original binary data stream. Identify the conditions that the receiver of Fig. 7.29 must satisfy for it to be an alternative to the noncoherent BFSK receiver of Fig. 7.18.

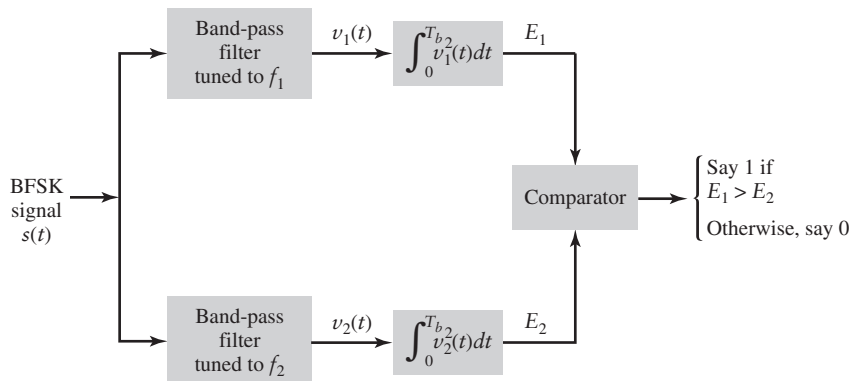


**FIGURE 7.29** Problem 7.22

- 7.23 The binary sequence 11100101 is applied to a DPSK system. The bit duration is 1  $\mu$ s. The carrier frequency is 6 MHz.
- Calculate the transmission bandwidth of the system.
  - Plot the waveform of the transmitted signal.
  - Using the transmitted sequence of part (b), plot the waveform produced by the receiver, and compare it against the original binary sequence.

### ADVANCED PROBLEMS

---

- 7.24 Consider a phase-locked loop consisting of a multiplier, loop filter, and voltage-controlled oscillator (VCO); you may refer to Section 4.8 for a description of the phase-locked loop for the demodulation of analog frequency modulation. Let the signal applied to the multiplier input be a PSK signal defined by

$$s(t) = A_c \cos[2\pi f_c t + k_p b(t)]$$

where  $k_p$  is the phase sensitivity, and the data signal  $b(t)$  takes on the value +1 for binary symbol 1 and -1 for binary symbol 0. The VCO output is

$$r(t) = A_c \sin[2\pi f_c t + \theta(t)]$$

- (a) Evaluate the loop filter output, assuming that this filter removes only modulated components with twice the carrier frequency  $f_c$ .
- (b) Show that this output is proportional to the data signal  $b(t)$  when the loop is phase locked; that is,  $\theta(t) = 0$ .
- 7.25 (a) In a coherent FSK system, the signals  $s_1(t)$  and  $s_2(t)$  representing symbols 1 and 0, respectively, are defined by

$$s_1(t) = A_c \cos\left[2\pi\left(f_c + \frac{\Delta f}{2}\right)t\right], \quad 0 \leq t \leq T_b \quad (1)$$

and

$$s_2(t) = A_c \cos\left[2\pi\left(f_c - \frac{\Delta f}{2}\right)t\right], \quad 0 \leq t \leq T_b \quad (2)$$

Assuming that  $f_c > \Delta f$ , show that the correlation coefficient of the signals  $s_1(t)$  and  $s_2(t)$ , defined by

$$\rho = \frac{\int_0^{T_b} s_1(t)s_2(t) dt}{\sqrt{\int_0^{T_b} s_1^2(t) dt}}$$

is approximately given by

$$\rho \approx \text{sinc}(2 \Delta f T_b)$$

- (b) What is the minimum value of frequency shift  $\Delta f$  for which the signals  $s_1(t)$  and  $s_2(t)$  are orthogonal?
- 7.26 A BFSK signal with discontinuous phase is generated by using the incoming binary data stream to switch between two independent sinusoidal oscillators:

$$\begin{aligned} \text{Symbol 1: } & \sqrt{\frac{2E_b}{T_b}} \cos(2\pi f_1 t + \theta_1) \\ \text{Symbol 0: } & \sqrt{\frac{2E_b}{T_b}} \cos(2\pi f_2 t + \theta_2) \end{aligned}$$

- (a) Show that this BFSK signal may be expressed as the sum of two independent BASK signals.
- (b) For  $\theta_1 = 30^\circ$  and  $\theta_2 = 45^\circ$ , plot the BFSK waveform for the binary data stream 01101001, and compare your result to that of Fig. 7.1(d) for continuous-phase BFSK.
- 7.27 Table 7.4 shows the phase transitions experienced by an MSK signal. Verify the entries listed in this table.

**TABLE 7.4 Phase Transitions in MSK**

Transmitted bit $0 \leq t \leq T_b$	Phase state (radians)	
	$\theta(0)$	$\theta(T_b)$
0	0	$-\pi/2$
1	$\pi$	$-\pi/2$
0	$\pi$	$+\pi/2$
1	0	$+\pi/2$

- 7.28 The generation and detection of QPSK can be viewed as an example of the “divide and conquer” strategy. In particular, the implementation of QPSK is achieved by
- Knowing how to generate and detect BPSK.
  - Using the idea of quadrature multiplexing.

Extend what we have learned from this example, and thereby develop the transmitter for generating 8-PSK and the receiver for detecting it.

### ■ COMPUTER EXPERIMENTS

- 7.29 In this problem, we continue Computer Experiment III on the spectral comparison of QPSK and OQPSK. Specifically, using the parameters

Carrier frequency,  $f_c = 8 \text{ Hz}$

Bit duration,  $T_b = 1\text{s}$

compute the phase spectra of these two digital modulation methods. Hence, justify the assertion made in Drill Problem 7.3 that these two methods differ by a linear phase component, and determine the slope of that component.

- 7.30 The purpose of this experiment is to demonstrate that the simulation of a digitally modulated signal on a computer can be simplified by using the idea of complex envelope that was introduced in Chapter 3. In particular, the experiment compares band-pass and baseband forms of data transmission, supported by the matlab scripts provided in Appendix 7. The scripts provided therein also cater to the generation of binary random sequences needed to perform the experiment and thereby add practical realism to the experiments.

- (a) To proceed then, generate two random binary sequences  $b_I(t)$  and  $b_Q(t)$  and use them to form the multiplexed band-pass signal

$$s(t) = b_I(t)\cos(2\pi f_c t) - b_Q(t)\sin(2\pi f_c t)$$

Hence, compute the magnitude spectrum of  $s(t)$ , using the following parameters:

Carrier frequency,  $f_c = 10 \text{ Hz}$

Symbol (bit) duration,  $T_b = 1\text{s}$

Assume that the two binary sequences are synchronized and they both use amplitude levels  $\pm 1$  to represent symbols 0 and 1.

- (b) Using complex notations, define the complex envelope

$$\tilde{b}(t) = b_I(t) + jb_Q(t)$$

on the basis of which we may reconstruct the original band-pass signal

$$s(t) = \operatorname{Re}\{\tilde{b}(t)\exp(j2\pi f_c t)\}$$

Specifically, compute the magnitude spectrum of the complex envelope  $\tilde{b}(t)$ , and compare it to the magnitude spectrum of  $s(t)$  computed in part (a). Comment on the computational significance of this comparison.

- 7.31 Repeat Problem 7.30, this time using a raised-cosine pulse shape of roll-off factor  $\alpha = 1$  to construct the binary sequences  $b_I(t)$  and  $b_Q(t)$ ; Appendix 7 provides the matlab scripts for generating the raised-cosine pulse. Compute the magnitude spectrum of the complex envelope  $\tilde{b}(t)$ , and compare it to the magnitude spectrum of the band-pass signal  $s(t)$ . Comment on your results.

## CHAPTER 8

# RANDOM SIGNALS AND NOISE

The term “random” is used to describe erratic and apparently unpredictable variations of an observed signal. Random signals in one form or another are encountered in every practical communication system. Consider voice communication, in which voice is often converted to an electrical signal by means of a microphone before processing for transmission. If this electrical signal is displayed on an oscilloscope, we might be tempted on first sight to say the signal appears to be quite random; that is, it would be difficult to predict or reproduce. Similarly, with digital communications, if we consider the stream of 0s and 1s that are transported over the Internet, they appear quite random—they are always 0 or 1, but their order and location are quite unpredictable. This randomness or unpredictability is a fundamental property of information.<sup>1</sup> If the information were predictable, there would be no need to communicate, because the other end could predict the information before receiving it.

On the other hand, noise is the bane of most communication systems. Noise limits the range and/or quality with which information-bearing signals may be transported over a channel. *Noise* may be defined as any unwanted signal interfering with or distorting the signal being communicated. Noise is another example of a random signal—if noise was predictable, we would then predict it at the receiver and remove it, negating its effect. Thus, in some ways, noise is similar to information in terms of its random nature. It is the object of the communications engineer to sift one from the other to the maximum extent possible.

Although information and noise are random signals, they still have properties that can be measured and analyzed, in some average sense. It is the purpose of this chapter to introduce the tools that are necessary to analyze information and noise and that are required to understand the signal detection techniques described in the remainder of the book.

The material in this chapter teaches us the following lessons:

- *Lesson 1: Random events and signals can be modeled as the outcomes of random experiments.*

---

<sup>1</sup>The concept of randomness in communications is expanded upon in the book by Wozencraft and Jacobs (1965) and it is one of the fundamental tenets of information theory; see Cover and Thomas (1991).

- *Lesson 2: Random variables provide a general representation for analyzing, comparing, and processing outcomes of random experiments. Statistical properties of random events can be obtained from the expectation of the various functions of these random variables; the expectation should be viewed as an operator.*
- *Lesson 3: Gaussian random variables play a key role in the analysis of random signals because of the central limit theorem and their mathematical tractability.*
- *Lesson 4: A random process may be viewed as a family of random variables, indexed by a time parameter. Then we can extend the analysis techniques for random variables to study the time-variation of random processes.*
- *Lesson 5: White noise is one of the most important random processes in the study of communication systems, both from a practical viewpoint and for the mathematical tractability of its statistical properties.*
- *Lesson 6: Narrowband noise can be analyzed in terms of its in-phase and quadrature components, in a manner similar to narrowband communication signals.*

## 8.1 Probability and Random Variables

Probability theory is rooted in situations that involve performing an experiment with an outcome that is subject to chance. That is, if the experiment is repeated, the outcome may differ due to the influence of an underlying random phenomenon. Such an experiment is referred to as a *random experiment*. For example, the experiment may be the observation of the result of the tossing of a fair coin. In this experiment, the possible outcomes of a trial are “heads” and “tails.”

We ask that a random experiment have the following properties:

1. On any trial of the experiment, the outcome is unpredictable.
2. For a large number of trials of the experiment, the outcomes exhibit *statistical regularity*. That is, a definite average pattern of outcomes is observed if the experiment is repeated a large number of times.

### ■ RELATIVE-FREQUENCY APPROACH

To elaborate on the concept of statistical regularity, let event  $A$  denote one of the possible outcomes of a random experiment. For example, in the coin-tossing experiment, event  $A$  may represent “heads.” Suppose that in  $n$  trials of the experiment, event  $A$  occurs  $n_A$  times. We may then assign the ratio  $n_A/n$  to the event  $A$ . This ratio is called the *relative frequency* of the event  $A$ . Clearly, the relative frequency is a nonnegative real number less than or equal to one. That is to say,

$$0 \leq \frac{n_A}{n} \leq 1 \quad (8.1)$$

If event  $A$  occurs in none of the trials,  $(n_A/n) = 0$ . If, on the other hand, event  $A$  occurs in all of the trials,  $(n_A/n) = 1$ .

We say that the experiment exhibits statistical regularity if, for any sequence of  $n$  trials, the relative frequency  $n_A/n$  converges to a limit as  $n$  becomes large. We define this limit

$$P[A] = \lim_{n \rightarrow \infty} \left( \frac{n_A}{n} \right) \quad (8.2)$$

as the *probability of event A*. Thus, in the coin-tossing experiment, we expect that in a million tosses of a fair coin, for example, about half of the outcomes will be heads.

The probability of an event is intended to represent the likelihood that a trial of the experiment will result in the occurrence of the event. For many engineering applications and games of chance, the use of Eq. (8.2) to define the probability of an event is acceptable. On the other hand, consider the statistical analysis of the stock market: How are we to achieve repeatability of such an experiment? A more satisfying approach is to state the properties that any measure of probability is expected to have, postulating them as *axioms*, then use the relative-frequency interpretation to justify them.

### ■ THE AXIOMS OF PROBABILITY

When we perform a random experiment, it is natural for us to be aware of the various outcomes that are likely to arise. In this context, it is convenient to think of an experiment and its possible outcomes as defining a space and its points. With each possible outcome of the experiment, we associate a point called the *sample point*, which we denote by  $s_k$ . The totality of all sample points, corresponding to the aggregate of all possible outcomes of the experiment, is called the *sample space*, which we denote by  $S$ . An *event* corresponds to either a single sample point or a set of sample points. In particular, the entire sample space  $S$  is called the *sure event*, and the null set  $\phi$  is called the *null* or *impossible event*; and a single sample point is called an *elementary event*.

Consider for example, an experiment that involves the throw of a die. In this experiment there are six possible outcomes; the showing of one, two, three, four, five, and six dots on the upper face of the die. By assigning a sample point to each of these possible outcomes, we have a sample space that consists of six sample points, as shown in Fig. 8.1.

The elementary event describing the statement “a six shows” corresponds to the sample point  $\{6\}$ . On the other hand, the event describing the statement “an even number of dots shows” corresponds to the subset  $\{2, 4, 6\}$  of the sample space. Note that the term “event” is used interchangeably to describe the subset or the statement.

We are now ready to make a formal definition of probability. A probability system consists of the triple:

1. A sample space  $S$  of elementary events (outcomes).

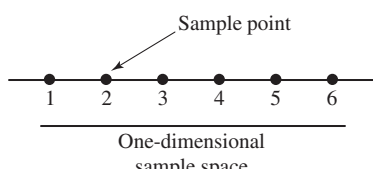


**FIGURE 8.1** Sample space of the experiment of throwing a die.

2. A class  $\mathcal{E}$  of events that are subsets of  $S$ .
3. A probability measure  $P[A]$  assigned to each event  $A$  in the class  $\mathcal{E}$ , which has the following properties:
  - (i)  $P[S] = 1$
  - (ii)  $0 \leq P[A] \leq 1$
  - (iii) If  $A \cup B$  is the union of two mutually exclusive events in the class  $\mathcal{E}$ , then

$$P[A \cup B] = P[A] + P[B] \quad (8.3)$$

Properties (i), (ii), and (iii) are known as the axioms of probability. Axiom (i) states that the probability of the sure event is one. Axiom (ii) states that the probability of an event is a nonnegative number less than or equal to unity. Axiom (iii) states that the probability of the union of two mutually exclusive events is the sum of probabilities of the individual events.

Although the axiomatic approach to probability theory is abstract in nature, all three axioms have relative frequency interpretations. Axiom (ii) corresponds to Eq. (8.1). Axiom (i) corresponds to the limiting case of Eq. (8.1) when the event  $A$  occurs in all trials. To interpret axiom (iii), we note that if event  $A$  occurs  $n_A$  times in  $n$  trials and event  $B$  occurs  $n_B$  times, then the union of event “ $A$  or  $B$ ” occurs in  $n_A + n_B$  trials (since  $A$  and  $B$  can never occur on the same trial). Hence,  $n_{A+B} = n_A + n_B$ , and so we have

$$\frac{n_{A \cup B}}{n} = \frac{n_A}{n} + \frac{n_B}{n} \quad (8.4)$$

which has the mathematical form similar to that of axiom (iii).

This abstract definition of a probability system is illustrated in Fig. 8.2. The sample space  $S$  is mapped to events via the random experiment. The events may be elementary outcomes of the sample space or larger subsets of the sample space. The probability function assigns a value between 0 and 1 to each of these events. The probability value is not unique to the event; mutually exclusive events may be assigned the same probability. However, the probability of the union of all events—that is, the sure event—is always unity.

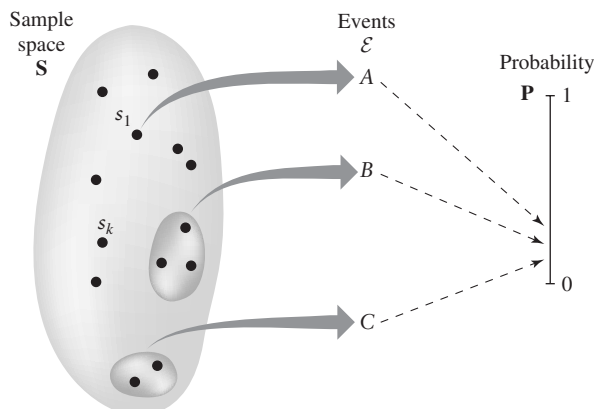


**FIGURE 8.2** Illustration of the relationship between sample space, events, and probability.

## ■ RANDOM VARIABLES

While the meaning of the outcome of a random experiment is clear, such outcomes are often not the most convenient representation for mathematical analysis. For example, heads or tails is not a convenient mathematical representation. As another example, consider a random experiment where we draw colored balls from an urn; the color is not directly amenable to mathematical analysis.

In these cases, it is often more convenient if we assign a number or a range of values to the outcomes of a random experiment. For example, a head could correspond to 1 and a tail to 0. We use the expression *random variable* to describe this process of assigning a number to the outcome of a random experiment.

In general, a function whose domain is a sample space and whose range is a set of real numbers is called a random variable of the experiment. That is, for events in  $\mathcal{E}$ , a random variable assigns a subset of the real line. Thus, if the outcome of the experiment is  $s$ , we denote the random variable as  $X(s)$  or just  $X$ . Note that  $X$  is a function, even if it is, for historical reasons, called a random variable. We denote a particular outcome of a random experiment by  $x$ ; that is,  $X(s_k) = x$ . *There may be more than one random variable associated with the same random experiment.*

The concept of a random variable is illustrated in Fig. 8.3, where we have suppressed the events but show subsets of the sample space being mapped directly to a subset of the real line. The probability function applies to this random variable in exactly the same manner that it applies to the underlying events.

The benefit of using random variables is that probability analysis can now be developed in terms of real-valued quantities regardless of the form or shape of the underlying events of the random experiment. Random variables may be *discrete* and take only a finite number of values, such as in the coin-tossing experiment. Alternatively, random variables may be *continuous* and take a range of real values. For example, the random variable that represents the amplitude of a noise voltage at a particular instant in time is a continuous random variable because, in theory, it may take on any value between plus and minus

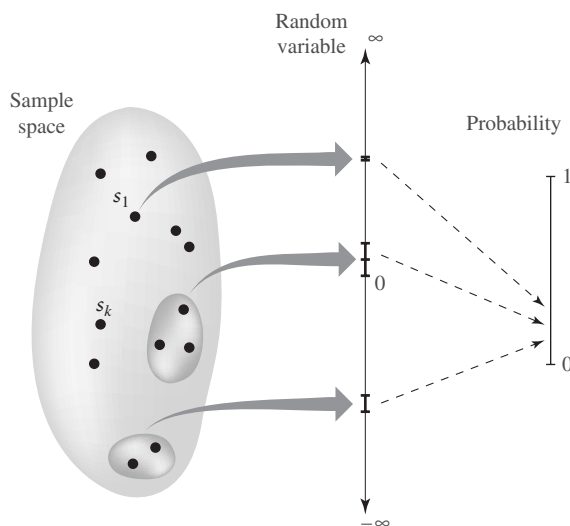


**FIGURE 8.3** Illustration of the relationship between sample space, random variables, and probability.

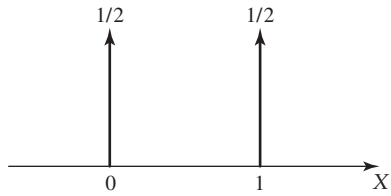


**FIGURE 8.4** Illustration of probability mass function for coin-tossing experiment.

infinity. Random variables may also be complex valued, but a complex-valued random variable may always be treated as a vector of two real-valued random variables.

For a discrete-valued random variable, the *probability mass function* describes the probability of each possible value of the random variable. For the coin-tossing experiment, if it is a fair coin, the probability mass function of the associated random variable may be written as

$$P[X = x] = \begin{cases} \frac{1}{2}, & x = 0 \\ \frac{1}{2}, & x = 1 \\ 0, & \text{otherwise} \end{cases} \quad (8.5)$$

This probability mass function is illustrated in Fig. 8.4, where delta functions of weight  $\frac{1}{2}$  are used to represent the probability mass at each of the two points, 0 and 1.

#### EXAMPLE 8.1 Bernoulli Random Variable

Consider the coin-tossing experiment in which the probability of heads is  $p$ . Let  $X$  be a random variable that takes the value 0 if the result is tails and 1 if it is heads. We say that  $X$  is a *Bernoulli random variable*. The probability mass function of a Bernoulli random variable is

$$P[X = x] = \begin{cases} 1 - p, & x = 0 \\ p, & x = 1 \\ 0, & \text{otherwise} \end{cases} \quad (8.6)$$

### DISTRIBUTION FUNCTIONS

Closely related to the probability mass function is the *probability distribution function*. This is the probability that the random variable  $X$  takes any value less than or equal to  $x$ . The distribution function is written as  $F_X(x)$ , so

$$F_X(x) = P[X \leq x] \quad (8.7)$$

The function  $F_X(x)$  is a function of  $x$ , not of the random variable  $X$ . However, it depends on the assignment of the random variable  $X$ , which accounts for the use of  $X$  as subscript. For any point  $x$ , the distribution function expresses the probability that the value of  $X$  is less than  $x$ .

The distribution function has two basic properties, which follow directly from Eq. (8.7):

1. The distribution function  $F_X(x)$  is bounded between zero and one.
2. The distribution function  $F_X(x)$  is a monotone nondecreasing function of  $x$ ; that is,

$$F_X(x_1) \leq F_X(x_2) \quad \text{if } x_1 \leq x_2$$

If  $X$  is a continuous-valued random variable and  $F_X(x)$  is differentiable with respect to  $x$ , then a third commonly used function is the *probability density function*, denoted by  $f_X(x)$ , where

$$f_X(x) = \frac{\partial}{\partial x} F_X(x) \quad (8.8)$$

A probability density function has three basic properties:

1. Since the distribution function is monotone nondecreasing, it follows that the density function is nonnegative for all values of  $x$ .
2. The distribution function may be recovered from the density function by integration, as shown by

$$F_X(x) = \int_{-\infty}^x f_X(s) ds \quad (8.9)$$

3. Property 2 implies that the total area under the curve of the density function is unity.

### EXAMPLE 8.2 Bernoulli Distribution Function

Continuing with Example 8.1, we see that the probability distribution function of the Bernoulli random variable is given by

$$F_X(x) = \begin{cases} 0, & x < 0 \\ 1 - p, & 0 \leq x < 1 \\ 1, & x \geq 1 \end{cases}$$

### EXAMPLE 8.3 Uniform Distribution

Consider a random variable  $X$  with the density function

$$f_X(x) = \begin{cases} \frac{1}{b-a}, & a \leq x \leq b \\ 0, & \text{otherwise} \end{cases} \quad (8.10)$$

This function, shown in Fig. 8.5(a), satisfies the requirements of a probability density because  $f_X(x) \geq 0$ , and the area under the curve is unity. A random variable having the probability density function of Eq. (8.10) is said to be *uniformly distributed*.

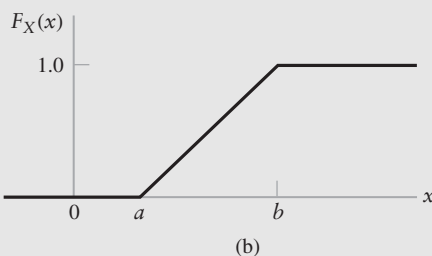
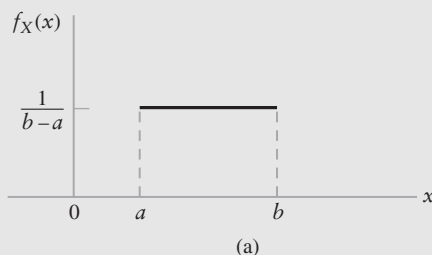


**FIGURE 8.5** The uniform distribution.  
(a) The probability density function.  
(b) The distribution function.

The corresponding distribution function of the uniformly distributed random variable  $X$  is continuous everywhere, as shown by

$$F_X(x) = \int_{-\infty}^x f_X(s) ds = \begin{cases} 0, & x < a \\ \frac{x-a}{b-a}, & a \leq x \leq b \\ 1, & x > b \end{cases}$$

This distribution function is plotted in Fig. 8.5(b).

### ■ SEVERAL RANDOM VARIABLES

Thus far we have focused attention on situations involving a single random variable. However, we find frequently that the outcome of an experiment may be described by several different random variables, and we are interested in the relationships between these random variables. In this section, we consider the case of two random variables, but the approach can be extended to any number of random variables.

Consider two random variables  $X$  and  $Y$ . We define the *joint distribution function*  $F_{X, Y}(x, y)$  as the probability that the random variable  $X$  is less than or equal to a specified value  $x$  and that the random variable  $Y$  is less than or equal to a specified value  $y$ . The joint distribution function,  $F_{X, Y}(x, y)$ , is the probability that the outcome of an experiment will result in a sample point lying inside the quadrant ( $-\infty < X \leq x, -\infty < Y \leq y$ ) of the joint sample space. That is,

$$F_{X, Y}(x, y) = P[X \leq x, Y \leq y] \quad (8.11)$$

Suppose that the joint distribution function  $F_{X, Y}(x, y)$  is continuous everywhere, and that the partial derivative

$$f_{X, Y}(x, y) = \frac{\partial^2 F_{X, Y}(x, y)}{\partial x \partial y} \quad (8.12)$$

exists and is continuous everywhere. We call the function  $f_{X, Y}(x, y)$  *the joint probability density function* of the random variables  $X$  and  $Y$ . The joint distribution function  $F_{X, Y}(x, y)$  is a monotone nondecreasing function of both  $x$  and  $y$ . Therefore, from Eq. (8.12), it follows that the joint probability density function  $f_{X, Y}(x, y)$  is always nonnegative. Also, the total volume under the graph of a joint probability density function is unity.

The probability density function for a single random variable, say  $X$ , can be obtained from its joint probability density function with a second random variable, say  $Y$ , in the following way. We first note that

$$F_X(x) = \int_{-\infty}^{\infty} \int_{-\infty}^x f_{X, Y}(\xi, \eta) d\xi d\eta \quad (8.13)$$

Differentiating both sides of Eq.(8.13) with respect to  $x$ , we get the desired relation

$$f_X(x) = \int_{-\infty}^{\infty} f_{X, Y}(x, \eta) d\eta \quad (8.14)$$

Thus the probability density function  $f_X(x)$  may be obtained from the joint probability density function  $f_{X, Y}(x, y)$  by simply integrating over all possible values of the random variable  $Y$ . The use of similar arguments in the context of the other random variable  $Y$  yields  $f_Y(y)$ . The probability density functions  $f_X(x)$  and  $f_Y(y)$  are called *marginal densities*.

Two random variables,  $X$  and  $Y$ , are *statistically independent* if the outcome of  $X$  does not affect the outcome  $Y$ . Mathematically, for independent  $X$  and  $Y$ , the joint probability,  $P[X \in A, Y \in B]$ , is the product of the individual probabilities; that is,

$$P[X \in A, Y \in B] = P[X \in A]P[Y \in B] \quad (8.15)$$

for all sets  $A$  and  $B$  in the respective ranges of  $X$  and  $Y$ . The property of Eq. (8.15) immediately extends to distribution functions by letting  $A = (-\infty, x]$  and  $B = (-\infty, y]$ ; that is,

$$F_{X, Y}(x, y) = F_X(x)F_Y(y) \quad (8.16)$$

A similar property holds for the joint density function. In general, for situations involving two or more independent random variables, the variables may be addressed separately without concern for their interaction with other random variables. To simplify notation when considering the probabilities of random variables, we will often suppress the sets involved; for instance, Eq. (8.15) is often written simply as  $P[X, Y] = P[X]P[Y]$ .

#### EXAMPLE 8.4 Binomial Random Variable

Consider a sequence of coin-tossing experiments where the probability of a head is  $p$  and let  $X_n$  be the Bernoulli random variable representing the outcome of the  $n$ th toss. Since the outcome of one coin toss is not expected to influence the outcome of subsequent coin tosses, this set is referred to as a set of *independent Bernoulli trials*.

Let  $Y$  be the number of heads that occur on  $N$  tosses of the coins. This new random variable may be expressed as

$$Y = \sum_{n=1}^N X_n \quad (8.17)$$

What is the probability mass function of  $Y$ ?

First consider the probability of obtaining  $y$  heads in a row followed by  $N - y$  tails. Using the independence of the trials, repeated application of Eq. (8.15) implies that this probability is given by

$$\begin{aligned} P[y \text{ heads followed by } N - y \text{ tails}] &= ppp \dots pp(1 - p)(1 - p) \dots (1 - p) \\ &= p^y(1 - p)^{N-y} \end{aligned}$$

By symmetry, this is the probability of any sequence of  $N$  trials that has  $y$  heads. To determine the probability of obtaining  $y$  heads anywhere in the  $N$  trials, the relative frequency definition of probability implies we simply have to count the number of possible arrangements of  $N$  tosses that have  $y$  heads and  $N - y$  tails. That is, the probability that  $Y = y$  is given by

$$P[Y = y] = \binom{N}{y} p^y(1 - p)^{N-y} \quad (8.18)$$

where

$$\binom{N}{y} = \frac{N!}{y!(N - y)!}$$

is the combinatorial function. Equation (8.18) defines the probability mass function of  $Y$  and the random variable  $Y$  is said to have a *binomial distribution*. The binomial distribution derives its name from the fact that the values of  $P[Y = y]$  are the successive terms in the expansion of the binomial expression

$$[p + (1 - p)]^N \quad (8.19)$$

where the  $(y + 1)$ st term of the expansion corresponds to  $\mathbf{P}[Y = y]$ . The binomial probability mass function for  $N = 20$  and  $p = \frac{1}{2}$  is illustrated in Fig. 8.6.

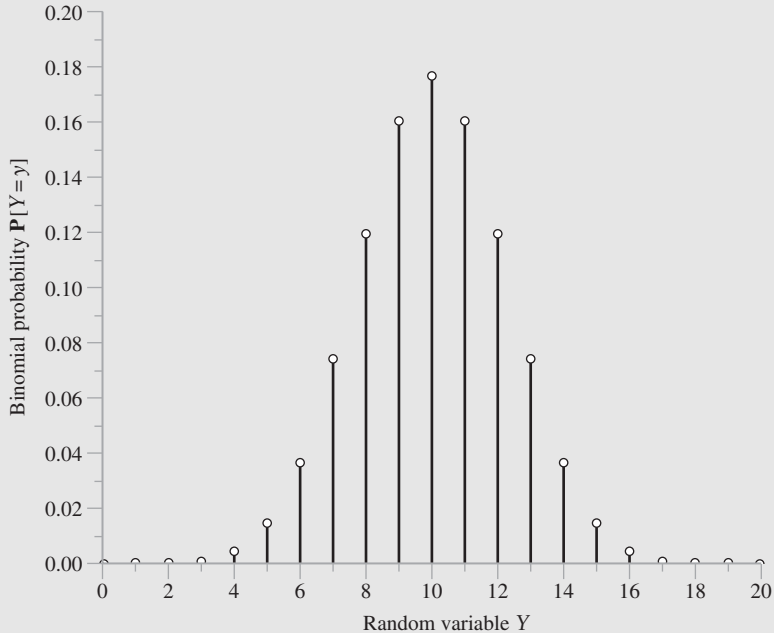


**FIGURE 8.6** The binomial probability mass function for  $N = 20$  and  $p = \frac{1}{2}$ .

### EXAMPLE 8.5 Binomial Distribution Function

This example addresses the probability distribution function of a binomial random variable.

By the definition of Eq. (8.7), the distribution function is given by  $F_Y(y) = \mathbf{P}[Y \leq y]$ , thus for a binomial random variable we have

$$\begin{aligned} F_Y(y) &= \mathbf{P}[Y \leq y] \\ &= \sum_{k=0}^y \mathbf{P}[Y = k] \\ &= \sum_{k=0}^y \binom{N}{k} p^k (1-p)^{N-k} \end{aligned} \quad (8.20)$$

This distribution function of  $Y$  is illustrated in Fig. 8.7 for  $N = 20$  and  $p = \frac{1}{2}$ . We can use the observation of Eq. (8.19) to show that

$$\begin{aligned} F_Y(N) &= \sum_{k=0}^N \binom{N}{k} p^k (1-p)^{N-k} \\ &= [p + (1-p)]^N \\ &= 1 \end{aligned} \quad (8.21)$$

as it should for a distribution function.

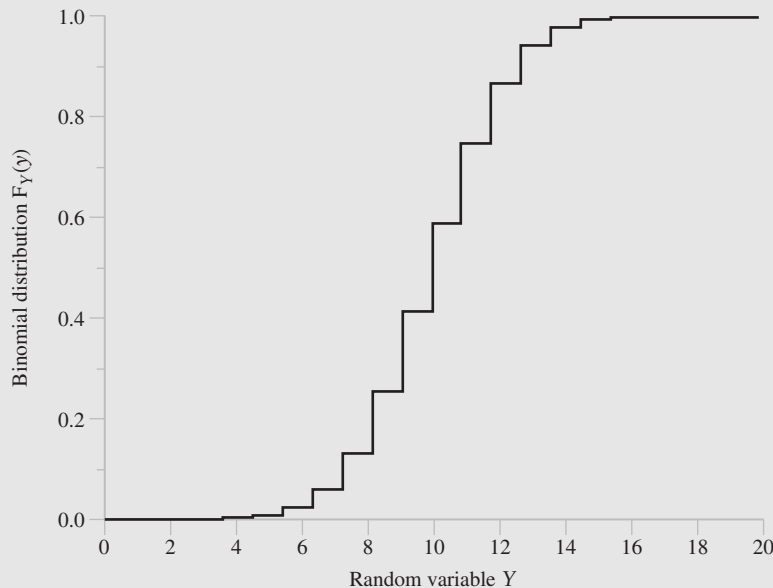


**FIGURE 8.7** The binomial distribution function for  $N = 20$  and  $p = \frac{1}{2}$ .

► **Drill Problem 8.1** An information packet contains 200 bits. This packet is transmitted over a communications channel where the probability of error for each bit is  $10^{-3}$ . What is the probability that the packet is received error-free? ◀

► **Drill Problem 8.2** Suppose the packet of Problem 8.1 includes an error-correcting code that can correct up to three errors located anywhere in the packet. What is the probability that a particular packet is received in error in this case? ◀

### ■ CONDITIONAL PROBABILITY

Suppose we are studying a random experiment or signal that has been characterized by two random variables,  $X$  and  $Y$ , which are not independent. Then we would expect that knowing the value of one random variable, say  $X$ , would influence the values observed for the other random variable. For example, consider tossing two dice. Suppose  $X$  represents the number showing on the first die and  $Y$  represents the sum of the two dice. Knowing  $X = 3$  will clearly influence the value that we would expect to see for  $Y$ .

We let  $P[Y|X]$  denote the probability mass function of  $Y$  given that  $X$  has occurred. The probability  $P[Y|X]$  is called the *conditional probability* of  $Y$  given  $X$ . Assuming  $X$  has nonzero probability, the conditional probability is defined as

$$P[Y|X] = \frac{P[X, Y]}{P[X]} \quad (8.22)$$

where  $P[X, Y]$  is the joint probability of the two random variables. This definition may be justified using a relative frequency interpretation.

We may rewrite Eq. (8.22) as

$$P[X, Y] = P[Y|X] P[X] \quad (8.23)$$

If we consider the conditional probability of  $X$  given  $Y$ , we may also write

$$P[X, Y] = P[X|Y] P[Y] \quad (8.24)$$

Equations (8.23) and (8.24) state that the joint probability of two events may be expressed as the product of the conditional probability of one event given the other, and the elementary probability of the other. Note that the conditional probabilities  $P[Y|X]$  and  $P[X|Y]$  have the same properties as the various probabilities previously defined.

Situations may exist where the conditional probability  $P[X|Y]$  and the probabilities  $P[X]$  and  $P[Y]$  are easily determined directly, but the conditional probability  $P[Y|X]$  is desired. From Eqs. (8.23) and (8.24), it follows that, provided  $P[X] \neq 0$ , we may determine  $P[Y|X]$  by using the relation

$$P[Y|X] = \frac{P[X|Y] P[Y]}{P[X]} \quad (8.25)$$

This relation is a special form of *Bayes' rule*.

Suppose that the conditional probability  $P[Y|X]$  is simply equal to the probability of occurrence of  $Y$ ; that is,

$$P[Y|X] = P[Y] \quad (8.26)$$

Under this condition, the joint probability of  $X$  and  $Y$  is equal to the product of the individual probabilities:

$$P[X, Y] = P[X] P[Y] \quad (8.27)$$

It then follows from Eq. (8.24) that  $P[X|Y] = P[X]$ . In this case, knowledge of the outcome of a random variable tells us no more about probability of the outcome of the other random variable than we knew without that knowledge. Random variables  $X$  and  $Y$  that satisfy this condition are said to be *statistically independent*.

#### EXAMPLE 8.6 Binary Symmetric Channel

Consider a *discrete memoryless channel* used to transmit binary data. The channel is said to be *discrete* in that it is designed to handle discrete messages. It is *memoryless* in the sense that the channel output at any time depends only on the channel input at that time. Due to the unavoidable presence of *noise* on the channel, errors are made in the received binary data stream. Specifically, when symbol 1 is sent, *occasionally* an error is made and symbol 0 is received, and vice versa. The channel is assumed to be *symmetric*, which means that the probability of receiving symbol 1 when 0 is sent is the same as the probability of receiving symbol 0 when symbol 1 is sent.

To describe the probabilistic nature of this channel fully, we need two sets of probabilities:

1. The *a priori* probability of sending binary symbols 0 and 1 is given by

$$P[X = x] = \begin{cases} p_0 & x = 0 \\ p_1 & x = 1 \end{cases}$$

where  $X$  is the random variable representing the transmitted symbol. Note that  $p_0 + p_1 = 1$ , so  $X$  is a Bernoulli random variable.

2. The conditional probability of error is given by

$$P[Y = 1|X = 0] = P[Y = 0|X = 1] = p$$

where  $Y$  is the random variable representing the received symbol. The conditional probability  $P[Y = 0|X = 1]$  is the probability that symbol 0 is received given that symbol 1 was sent.

The requirement is to determine the *a posteriori* probabilities  $P[X = 0|Y = 0]$  and  $P[X = 1|Y = 1]$ . The conditional probability  $P[X = 0|Y = 0]$  is the probability that symbol 0 was sent if symbol 0 was received, and similarly for  $P[X = 1|Y = 1]$ . Both these conditional probabilities refer to events that are observed “after the fact”; hence the name “*a posteriori*” probabilities.

Since the events  $Y = 0$  and  $Y = 1$  are mutually exclusive, and the probability of receiving symbol 0 or symbol 1 is unity, we have from axiom (iii):

$$P[Y = 0|X = 0] + P[Y = 1|X = 0] = 1$$

That is to say,

$$P[Y = 0|X = 0] = 1 - p$$

Similarly, we may write

$$P[Y = 1|X = 1] = 1 - p$$

Accordingly, we may use the transition probability diagram shown in Fig. 8.8 to represent the binary communication channel specified in this example; the term “transition probability” refers to the conditional probability of error. Figure 8.8 clearly depicts the (assumed) symmetric nature of the channel; hence the name “binary symmetric channel.”

From Figure 8.8 we deduce the following results:

1. The probability of receiving symbol 0 is given by

$$\begin{aligned} P[Y = 0] &= P[Y = 0|X = 0]P[X = 0] + P[Y = 0|X = 1]P[X = 1] \\ &= (1 - p)p_0 + pp_1 \end{aligned} \quad (8.28)$$

2. The probability of receiving symbol 1 is given by

$$\begin{aligned} P[Y = 1] &= P[Y = 1|X = 0]P[X = 0] + P[Y = 1|X = 1]P[X = 1] \\ &= pp_0 + (1 - p)p_1 \end{aligned} \quad (8.29)$$

Therefore, applying Bayes’ rule, we obtain

$$\begin{aligned} P[X = 0|Y = 0] &= \frac{P[Y = 0|X = 0]P[X = 0]}{P[Y = 0]} \\ &= \frac{(1 - p)p_0}{(1 - p)p_0 + pp_1} \end{aligned} \quad (8.30)$$

and

$$\begin{aligned} P[X = 1|Y = 1] &= \frac{P[Y = 1|X = 1]P[X = 1]}{P[Y = 1]} \\ &= \frac{(1 - p)p_1}{pp_0 + (1 - p)p_1} \end{aligned} \quad (8.31)$$

These are the desired results.

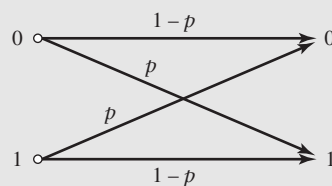


**FIGURE 8.8** Transition probability diagram of binary symmetric channel.

► **Drill Problem 8.3** Continuing with Example 8.6, find the following conditional probabilities:  $P[X = 0|Y = 1]$  and  $P[X = 1|Y = 0]$ . ◀

► **Drill Problem 8.4** Consider a binary symmetric channel for which the conditional probability of error  $p = 10^{-4}$ , and symbols 0 and 1 occur with equal probability. Calculate the following probabilities:

- The probability of receiving symbol 0.
- The probability of receiving symbol 1.
- The probability that symbol 0 was sent given that symbol 0 is received.
- The probability that symbol 1 was sent given that symbol 0 is received.

## 8.2 Expectation

The probability distribution function, while it provides a complete description of the random variable, may include more detail than is necessary in some instances. We may wish to use simple statistical averages, such as the mean and variance, to describe the random variable.

### ■ MEAN

These statistical averages or *expectations* are denoted by, for example,  $E[g(X)]$  for the expected value of a function  $g(\cdot)$  of the random variable  $X$ . For the case of the expected value of  $X$ , we denote the mean using the shorthand  $\mu_X$ . For a discrete random variable  $X$ , the *mean*,  $\mu_X$ , is the weighted sum of the possible outcomes

$$\begin{aligned}\mu_X &= E[X] \\ &= \sum_X x P[X = x]\end{aligned}\quad (8.32)$$

where the sum is over all possible outcomes of the random variable  $X$ . For a continuous random variable with a density function  $f_X(x)$ , the analogous definition of the expected value is

$$E[X] = \int_{-\infty}^{\infty} x f_X(x) dx \quad (8.33)$$

Often the mean value of a random variable is estimated from  $N$  observations of the random variable  $\{x_1, x_2, \dots, x_N\}$ , using the *estimator*

$$\hat{\mu}_X = \frac{1}{N} \sum_{n=1}^N x_n \quad (8.34)$$

That is, we estimate the mean of the distribution by averaging over a number of observations of the random variable. This estimator is based on the relative frequency definition of probability. For example, if the possible outcomes of a random variable  $Z$  are  $1, 2, 3, \dots, M$ , then the estimator becomes

$$\hat{\mu}_Z = \frac{1 \cdot n_1 + 2 \cdot n_2 + \dots + M \cdot n_M}{N}$$

where  $n_i$  is the number of times that the observation  $Z = i$  occurs. We may rewrite this equation as

$$\begin{aligned}\hat{\mu}_Z &= \sum_{i=1}^M i \frac{n_i}{N} \\ &\approx \sum_{i=1}^M i \mathbf{P}[Z = i]\end{aligned}$$

That is, we expect the more probable outcomes to occur more frequently when a number of observations are made.

Returning to the general case, if we consider  $X$  as a random variable representing observations of the voltage of a random signal, then the mean value of  $X$  represents the average voltage or *dc offset* of the signal.

### ■ VARIANCE

The variance of a random variable is an estimate of the spread of the probability distribution about the mean. For discrete random variables, the variance,  $\sigma_X^2$ , is given by the expectation of the squared distance of each outcome from the mean value of the distribution.

$$\begin{aligned}\sigma_X^2 &= \text{Var}(X) \\ &= \mathbf{E}[(X - \mu_X)^2] \\ &= \sum_X (x - \mu_X)^2 \mathbf{P}[X = x]\end{aligned}\tag{8.35}$$

For a continuous random variable with density function  $f_X(x)$ , the analogous definition of variance is given by

$$\sigma_X^2 = \int_{-\infty}^{\infty} (x - \mu_X)^2 f_X(x) dx\tag{8.36}$$

As is the case for the mean, we may estimate the variance of a random variable from  $N$  independent observations using the formula

$$\hat{\sigma}_X^2 = \frac{1}{N-1} \sum_{n=1}^N (x_n - \hat{\mu}_X)^2\tag{8.37}$$

We may justify this estimator using the relative frequency interpretation of probability. For example, if we use the random variable  $Z$  defined previously, we have

$$\begin{aligned}\hat{\sigma}_Z^2 &= \frac{(1 - \hat{\mu}_Z)^2 \cdot n_1 + (2 - \hat{\mu}_Z)^2 \cdot n_2 + \cdots + (M - \hat{\mu}_Z)^2 \cdot n_M}{N-1} \\ &= \frac{N}{N-1} \sum_{n_i=1}^M (i - \hat{\mu}_Z)^2 \frac{n_i}{N} \\ &\approx \frac{N}{N-1} \sum_{i=1}^M (i - \hat{\mu}_Z)^2 \mathbf{P}[Z = i]\end{aligned}\tag{8.38}$$

The factor  $N/(N-1)$  appearing on the right-hand side of Eq. (8.38) is due to the assumption that the same  $N$  observations are used to estimate the mean  $\hat{\mu}$ . With this factor, the expected value of the right-hand side is  $\sigma_Z^2$  and, consequently, Eq. (8.37) is an *unbiased estimator* of the variance. We say  $\hat{g}$  is an unbiased estimator of  $g$  if  $\mathbf{E}[\hat{g}] = \mathbf{E}[g]$ .

If we consider  $X$  as a random variable representing observations of the voltage of a random signal, then the variance represents the *ac power* of the signal. The second moment of  $X$ ,  $E[X^2]$ , is also called the *mean-square value* of the random signal and it physically represents the *total power of the signal*.

#### EXAMPLE 8.7 Mean and Variance of a Bernoulli Random Variable

If  $X$  is a Bernoulli random variable with parameter  $p$ , then the expected value of  $X$  is

$$\begin{aligned} E[X] &= \sum_{k=0}^1 kP[X = k] \\ &= 0 \cdot (1 - p) + 1 \cdot p \\ &= p \end{aligned}$$

With  $\mu_X = E[X]$ , the variance of  $X$  is given by

$$\begin{aligned} \sigma_X^2 &= \sum_{k=0}^1 (k - \mu_X)^2 P[X = k] \\ &= (0 - p)^2(1 - p) + (1 - p)^2p \\ &= (p^2 - p^3) + (p - 2p^2 + p^3) \\ &= p(1 - p) \end{aligned}$$

### ■ COVARIANCE

Also of importance in the analysis of communication systems are the statistical averages between two random variables. The *covariance* of two random variables,  $X$  and  $Y$ , is given by the expected value of the product of the two random variables,

$$\text{Cov}(X, Y) = E[(X - \mu_X)(Y - \mu_Y)] \quad (8.39)$$

We may expand this equation to obtain<sup>2</sup> (see Problem 8.23)

$$\text{Cov}(X, Y) = E[XY] - \mu_X\mu_Y \quad (8.40)$$

If the two random variables are continuous with joint density,  $f_{X, Y}(x, y)$ , then the expectation term of Eq. (8.40) is given by

$$E[XY] = \int_{-\infty}^{\infty} \int_{-\infty}^{\infty} xy f_{X, Y}(x, y) dx dy \quad (8.41)$$

If the two random variables happen to be independent, then

$$\begin{aligned} E[XY] &= \int_{-\infty}^{\infty} \int_{-\infty}^{\infty} xy f_X(x) f_Y(y) dx dy \\ &= \int_{-\infty}^{\infty} xf_X(x) dx \int_{-\infty}^{\infty} yf_Y(y) dy \\ &= E[X]E[Y] \end{aligned} \quad (8.42)$$

as we might intuitively expect. Substituting this result into Eq. (8.40), we find that the covariance of independent random variables is zero. It should be noted however that

<sup>2</sup>If the random variables are complex valued, then this expression is modified to  $\text{Cov}(X, Y) = E[XY^*] - \mu_X\mu_Y^*$ , where the asterisk denotes complex conjugation. In such a situation,  $\text{Cov}(X, Y)$  and  $\text{Cov}(Y, X)$  are unequal.

the opposite is not always true: zero covariance does not, in general, imply independence.

► **Drill Problem 8.5** Determine the mean and variance of a random variable that is uniformly distributed between  $a$  and  $b$ . ◀

## 8.3 Transformation of Random Variables

In communication systems, random signals may be processed by several devices, linear or nonlinear, before the final output. If we represent a random signal as a random variable and know its distribution function before processing, it is logical to ask: what is the new distribution function of the random variable after processing? In this section, we provide some answers to this question when the transformation is *one-to-one*.<sup>3</sup> For example, assume that a random variable  $X$  with distribution  $F_X(x)$  is transformed to  $Y = aX + b$ . What is the distribution function of  $Y$ ?

We answer this question by returning to probability fundamentals. Consider the probability that  $X$  belongs to the set  $A$  where  $A$  is a subset the real line. If  $X \in A$ , then it follows that  $Y \in B$  where  $B$  is defined by  $B = aA + b$ ; hence, we have

$$\mathbf{P}[X \in A] = \mathbf{P}[Y \in B] \quad (8.43)$$

Suppose the set  $B$  is the real line from  $-\infty$  to  $y$ , which we write as  $(-\infty, y]$ . Then the set  $A$  is given by  $A = (B - b)/a = (-\infty, (y - b)/a]$ . So, we may write

$$\begin{aligned} F_Y(y) &= \mathbf{P}[Y \in (-\infty, y)] \\ &= \mathbf{P}[X \in (-\infty, (y - b)/a)] \\ &= F_X\left(\frac{y - b}{a}\right) \end{aligned} \quad (8.44)$$

which defines the relationship between distribution functions of the original random variable  $X$  and that of the transformed random variable  $Y$ . In general, if  $Y = g(X)$  is a one-to-one transformation of the random variable  $X$  to the random variable  $Y$ , then the distribution function of  $Y$  is given by

$$F_Y(y) = F_X(g^{-1}(y)) \quad (8.45)$$

where the symbol  $g^{-1}(y)$  denotes the *functional inverse* of  $g(y)$ . It can be shown that if  $X$

has a density  $f(x)$ , then the density of  $Y$  is  $f_X(g^{-1}(y)) \left| \frac{dg^{-1}(y)}{dy} \right|$ , provided that the transformation is differentiable.

### EXAMPLE 8.8 The Cosine Transformation

Let  $X$  be a random variable that is uniformly distributed on  $[0, 2\pi]$ . Let  $Y$  be the transformed variable,  $Y = \cos(X)$ . We wish to find the distribution function of  $Y$ .

We first observe that the transformation  $Y = \cos(X)$  is not one-to-one, so we cannot use the above theory directly. However, we note that we can split the range of  $X$  into two intervals  $[0, \pi]$  and  $[\pi, 2\pi]$  where, in each interval, the transformation is one-to-one. Consequently, if  $Y$  belongs to the set  $B$ , then  $X$  belongs to the set  $A_1 = \cos^{-1}(B) \cap [0, \pi]$  or  $X$  belongs to the set  $A_2 = \cos^{-1}(B) \cap [\pi, 2\pi]$ . Since the two sets  $A_1$  and  $A_2$  are disjoint, we may use the axioms of probability to write

$$\mathbf{P}[Y \in B] = \mathbf{P}[X \in A_1] + \mathbf{P}[X \in A_2] \quad (8.46)$$

<sup>3</sup>For further examples of functions of random variables, see pages 119–126 of Leon-Garcia (1994) and pages 179–190 of Bertsekas and Tsitsiklis (2002).

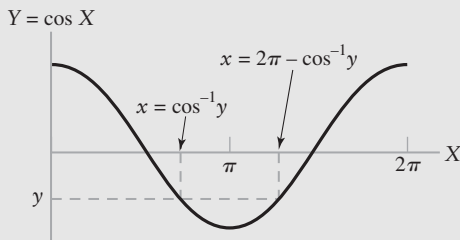


**FIGURE 8.9** Illustration of cosine transformation.

When  $B = (-\infty, y]$ , we then have from Fig. 8.9

$$A_1 = \begin{cases} \phi, & y < -1 \\ [\cos^{-1}(y), \pi], & |y| \leq 1 \\ [0, \pi], & y > 1 \end{cases} \quad \text{and} \quad A_2 = \begin{cases} \phi, & y < -1 \\ [\pi, 2\pi - \cos^{-1}(y)], & |y| \leq 1 \\ [\pi, 2\pi], & y > 1 \end{cases}$$

where  $\cos^{-1}(y)$  refers to the principal value; that is,  $\cos^{-1}(y)$  is always in  $[0, \pi]$ . Evaluating Eq. (8.46) we have

$$\begin{aligned} F_Y(y) &= \begin{cases} P[\phi] + P[\phi], & y < -1 \\ P[A], & |y| \leq 1 \\ P[0, \pi] + P[\pi, 2\pi], & y > 1 \end{cases} \\ &= \begin{cases} 0, & y < -1 \\ P[A], & |y| \leq 1 \\ 1, & y > 1 \end{cases} \end{aligned} \quad (8.47)$$

where  $A = [\cos^{-1}(y), 2\pi - \cos^{-1}(y)]$ . Since  $X$  is uniformly distributed with density  $1/2\pi$ , this probability is proportional to the length of interval  $A$ ; that is,

$$P[X \in A] = \frac{2\pi - 2\cos^{-1}(y)}{2\pi}$$

Substituting this result into Eq. (8.47) defines the distribution of  $Y$ .

► **Drill Problem 8.6** Let  $X$  be a random variable and let  $Y = (X - \mu_X)/\sigma_X$ . What are the mean and variance of the random variable  $Y$ ? ◀

► **Drill Problem 8.7** What is the probability density function of the random variable  $Y$  of Example 8.8? Sketch this density function. ◀

## 8.4 Gaussian Random Variables<sup>4</sup>

The *Gaussian random variable*<sup>5</sup> plays an important role in many applications and is by far the most commonly encountered random variable in the statistical analysis of communica-

<sup>4</sup>The Gaussian distribution is named after the great mathematician C. G. Gauss. At age 18, Gauss invented the method of least squares for finding the best estimate of a quantity based on a sequence of measurements. Gauss later used the method of least squares for estimating orbits of planets with noisy measurements, a procedure that was published in 1809 in his book *Theory of Motion of Heavenly Bodies*. In connection with the error of observation, he developed the Gaussian distribution.

<sup>5</sup>Gaussian random variables are also called *normal random variables*. Engineers and physicists tend to use the term “Gaussian” while mathematicians tend to use the term “normal.”

cation systems. A Gaussian random variable is a continuous random variable with a density function given by

$$f_X(x) = \frac{1}{\sqrt{2\pi}\sigma_X} \exp\left\{-\frac{(x - \mu_X)^2}{2\sigma_X^2}\right\} \quad (8.48)$$

where the Gaussian random variable  $X$  has mean  $\mu_X$  and variance  $\sigma_X^2$ . This density function extends from  $-\infty$  to  $\infty$  and is symmetric about the mean  $\mu_X$ . A Gaussian random variable has a number of properties that we will state without proof<sup>6</sup>:

1. A Gaussian random variable is completely characterized by its mean and variance.
2. A Gaussian random variable plus a constant is another Gaussian random variable with the mean adjusted by the constant.
3. A Gaussian random variable multiplied by a constant is another Gaussian random variable where both the mean and variance are affected by the constant.
4. The sum of two independent Gaussian random variables is also a Gaussian random variable.
5. The weighted sum of  $N$  independent Gaussian random variables is a Gaussian random variable.
6. If two Gaussian random variables have zero covariance (uncorrelated), they are also independent.

Except for properties 2 and 3, these properties do not hold, in general, for other types of random variables.

For the special case of a Gaussian random variable with a mean of zero,  $\mu_X = 0$ , and a variance of unity,  $\sigma_X^2 = 1$ , the density function is given by

$$f_X(x) = \frac{1}{\sqrt{2\pi}} \exp(-x^2/2), \quad -\infty < x < \infty \quad (8.49)$$

which has the familiar bell-shaped curve depicted in Fig. 8.10(a).

The distribution function of this *normalized Gaussian random variable* is given by the integral of this function

$$\begin{aligned} F_X(x) &= \int_{-\infty}^x f_X(s) ds \\ &= \frac{1}{\sqrt{2\pi}} \int_{-\infty}^x \exp(-s^2/2) ds \end{aligned} \quad (8.50)$$

and illustrated in Fig. 8.10(b). There is no closed-form solution for this integral but, due to frequent appearance of integrals of this type, numerous related functions have been defined and tabulated. The related function, often used in the communications context, is the *Q-function*, defined as<sup>7</sup>

$$\begin{aligned} Q(x) &= \frac{1}{\sqrt{2\pi}} \int_x^\infty \exp(-s^2/2) ds \\ &= 1 - F_X(x) \end{aligned} \quad (8.51)$$

---

<sup>6</sup>A proof of these properties may be found in Chapter 4 of Leon-Garcia (1994) and Chapter 3 of Bertsekas and Tsitsiklis (2002).

<sup>7</sup>Appendix 4 presents tabulated values of the *Q-function*  $Q(x)$ .

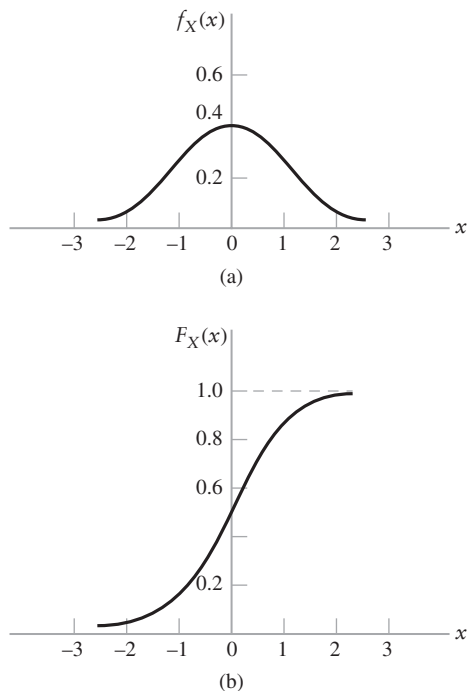


**FIGURE 8.10** The normalized Gaussian distribution. (a) The probability density function. (b) The distribution function.

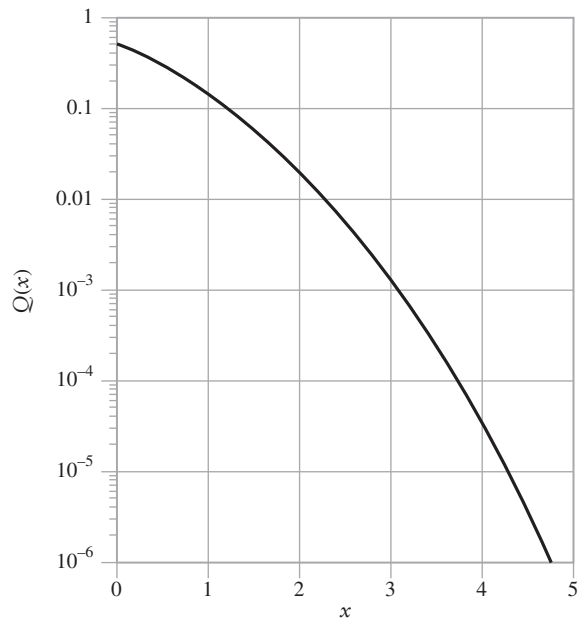


**FIGURE 8.11** The  $Q$ -function.

The last line of Eq. (8.51) indicates that the *Q-function is the complement of the normalized Gaussian distribution function*. The  $Q$ -function is plotted in Fig. 8.11.

To reiterate: with Gaussian random variables, the mean and variance have particular importance because they completely characterize the distribution function.

#### EXAMPLE 8.9 Probability of Bit Error with PAM

In a pulse-amplitude modulation (PAM) transmission scheme, binary data are represented with voltage levels of  $+A$  for a 1 and  $-A$  for a 0. Suppose that a 1 is transmitted and received in the presence of Gaussian noise having a mean of zero and a variance of  $\sigma^2$ . We wish to find the probability that the bit is incorrectly detected.

The received data can be represented by the random variable  $Y$ , defined as

$$Y = A + N \quad (8.52)$$

where  $N$  is a Gaussian random variable with zero mean and variance  $\sigma^2$ . It follows from the properties of random variables that  $Y$  is also a Gaussian random variable but with a mean of  $A$  and a variance of  $\sigma^2$ , as illustrated in Fig. 8.12.

The probability that an error occurs is the probability that  $Y$  has a value less than zero. This probability corresponds to the shaded area under the curve of Fig. 8.12. Mathematically, this probability is given by

$$P[Y < 0] = \int_{-\infty}^0 \frac{1}{\sqrt{2\pi}\sigma} \exp\{-(y-A)^2/2\sigma^2\} dy \quad (8.53)$$

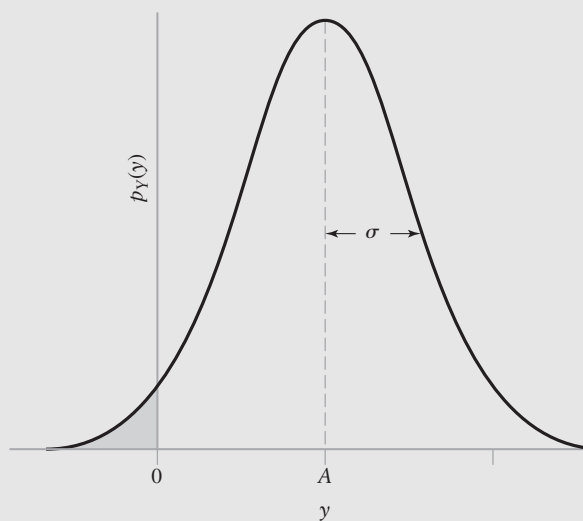


**FIGURE 8.12** Density function of noisy PAM signal  $Y$ .

If we make the change of variable by setting

$$s = -\frac{y - A}{\sigma} \quad (8.54)$$

then Eq. (8.53) becomes

$$\begin{aligned} \mathbf{P}[Y < 0] &= \frac{1}{\sqrt{2\pi}} \int_{A/\sigma}^{\infty} \exp\{-s^2/2\} \, ds \\ &= Q\left(\frac{A}{\sigma}\right) \end{aligned} \quad (8.55)$$

where we have used the definition of the  $Q$ -function in Eq. (8.51). We will return to this example in Chapter 10.

► **Drill Problem 8.8** Show that the mean and variance of a Gaussian random variable  $X$  with the density function given by Eq. (8.48) are  $\mu_X$  and  $\sigma_X^2$ , respectively. ◀

► **Drill Problem 8.9** Show that for a Gaussian random variable  $X$  with mean  $\mu_X$  and variance  $\sigma_X^2$ , the transformation  $Y = (X - \mu_X)/\sigma_X$  converts  $X$  to a normalized Gaussian random variable with zero mean and with variance. ◀

## 8.5 The Central Limit Theorem

An important result in probability theory that is closely related to the Gaussian distribution is the *central limit theorem*. Let  $X_1, X_2, \dots, X_n$  be a set of random variables with the following properties:

1. The  $X_k$  with  $k = 1, 2, 3, \dots, n$  are statistically independent.
2. The  $X_k$  all have the same probability density function.
3. Both the mean and the variance exist for each  $X_k$ .

We do not assume that the density function of the  $X_k$  is Gaussian. Let  $Y$  be a new random variable defined as

$$Y = \sum_{k=1}^n X_k \quad (8.56)$$

Then, according to the central limit theorem, the normalized random variable

$$Z = \frac{Y - E[Y]}{\sigma_Y} \quad (8.57)$$

approaches a Gaussian random variable with zero mean and unit variance as the number of the random variables  $X_1, X_2, \dots, X_n$  increases without limit. That is, as  $n$  becomes large, the distribution of  $Z$  approaches that of a zero-mean Gaussian random variable with unit variance, as shown by

$$F_Z(z) \rightarrow \int_{-\infty}^z \frac{1}{\sqrt{2\pi}} \exp\left\{-\frac{s^2}{2}\right\} ds \quad (8.58)$$

This is a mathematical statement of the central limit theorem. In words, *the normalized distribution of the sum of independent, identically distributed random variables approaches a Gaussian distribution as the number of random variables increases, regardless of the individual distributions.* Thus, Gaussian random variables are common because they characterize the asymptotic properties of many other types of random variables.

When  $n$  is finite, the Gaussian approximation of Eq. (8.58) is most accurate in the central portion of the density function (hence the central limit) and less accurate in the “tails” of the density function.

### ■ COMPUTER EXPERIMENT: SUMS OF RANDOM VARIABLES

In Problem 8.55 toward the end of this chapter, we describe a computer experiment to demonstrate the central limit theorem. In this experiment, we consider the random variable

$$Z = \sum_{i=1}^N X_i$$

where the  $X_i$  are independent, uniformly distributed random variables on the interval from  $-1$  to  $+1$ . In the computer experiment, we compute 20,000 samples of  $Z$  for  $N = 5$ , and estimate the corresponding density function by forming a histogram of the results. In Fig. 8.13, we compare this histogram (scaled for unit area) to the Gaussian density function having the same mean and variance. As the graph indicates, it does not take many random contributions to approach an overall Gaussian distribution.

The results of this experiment indicate how powerful the central limit theorem is and explain why Gaussian models are ubiquitous in the analysis of random signals in communications and elsewhere. An added bonus is the mathematical tractability of Gaussian random variables and the fact that the distribution type is unchanged after linear processing but, of course, the mean and variance of the Gaussian distribution are subjected to change.

**► Drill Problem 8.10** Determine the mean and variance of the sum of five independent uniformly distributed random variables on the interval from  $-1$  to  $+1$ . ◀

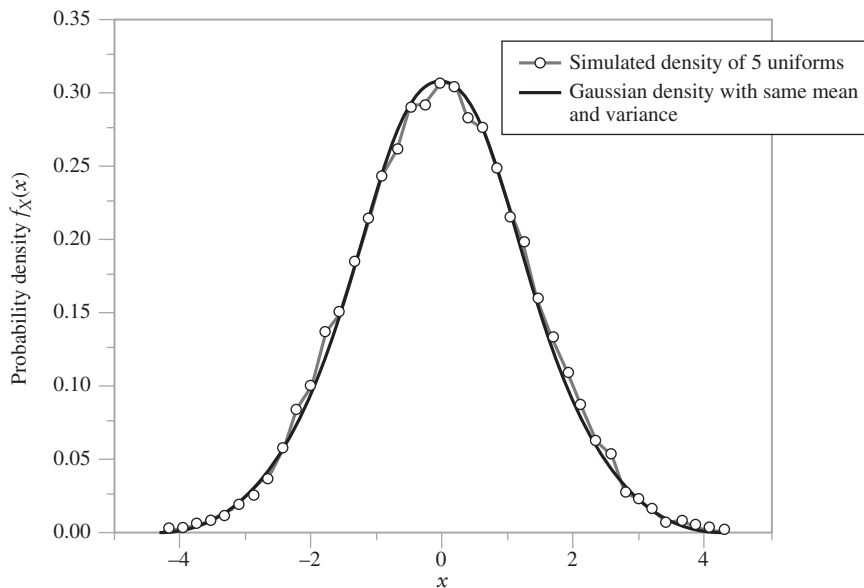


**FIGURE 8.13** Comparison of the empirical density of sum of five uniform variables with a Gaussian density having the same mean and variance.

## 8.6 Random Processes

In a radio communication system, the received signal usually consists of an information-bearing signal component, a random interference component, and channel noise. The information-bearing signal may represent, for example, a voice signal that, typically, consists of randomly spaced bursts of energy of random duration. The interference component may represent spurious electromagnetic waves produced by other communication systems operating in the vicinity of the radio receiver. A major source of channel noise is thermal noise, which is caused by the random motion of the electrons in conductors and devices at the front end of the receiver. We thus find that the received time-varying signal is random in nature. In this section, we combine the concepts of time variation and random variables to introduce the concept of *random processes*. Although it is not possible to predict the exact value of the random signal or process in advance, it is possible to describe the signal in terms of the statistical parameters such as average power and power spectral density, as will be shown in this chapter.

Random processes represent the formal mathematical model of these random signals. From the above discussion, random processes have the following properties:

1. Random processes are functions of time.
2. Random processes are random in the sense that it is not possible to predict exactly what waveform will be observed in the future.

Analogous to random variables, when discussing an experiment involving random processes it is convenient to think in terms of a sample space. Specifically, each outcome of the experiment is associated with a sample point. However, in this case each sample point represents a time-varying function. The aggregate of all possible outcomes of the experiment is referred

to as the sample space, ensemble, or random process. Reiterating, each point in the sample space or *ensemble* is a function of time. As an integral part of the definition of a random process, we assume the existence of a probability distribution over appropriate sets in the sample space, so we may speak of the probability of various events.

Consider a random experiment specified by the outcomes  $s$  from a sample space  $S$ , and the probabilities of these events. Suppose that we assign to each sample point  $s$  a function of time with the label

$$X(t, s), \quad -T < t < T \quad (8.59)$$

where  $2T$  is the total observation period. For a fixed sample point  $s_j$ , the function of  $X(t, s_j)$  is called a *realization* or a *sample function* of the random process. To simplify notation, we denote this sample function as

$$x_j(t) = X(t, s_j) \quad (8.60)$$

Figure 8.14 illustrates a set of sample functions  $\{x_j(t): j = 1, 2, \dots\}$ . From this figure, we note that at a fixed  $t_k$  inside the observation window, the set of numbers

$$\{x_1(t_k), x_2(t_k), \dots, x_n(t_k)\} = \{X(t_k, s_1), X(t_k, s_2), \dots, X(t_k, s_n)\}$$

is a random variable. Thus, we have an indexed ensemble (family) of random variables  $\{X(t, s)\}$ , which is called a random process. To simplify notation, it is convenient to suppress the  $s$  and use  $X(t)$  to denote the random process.

To compare:

- With a random variable, the outcome of random experiment is mapped to a real number.
- With a random process, the outcome of random experiment is mapped into a waveform that is a function of time.

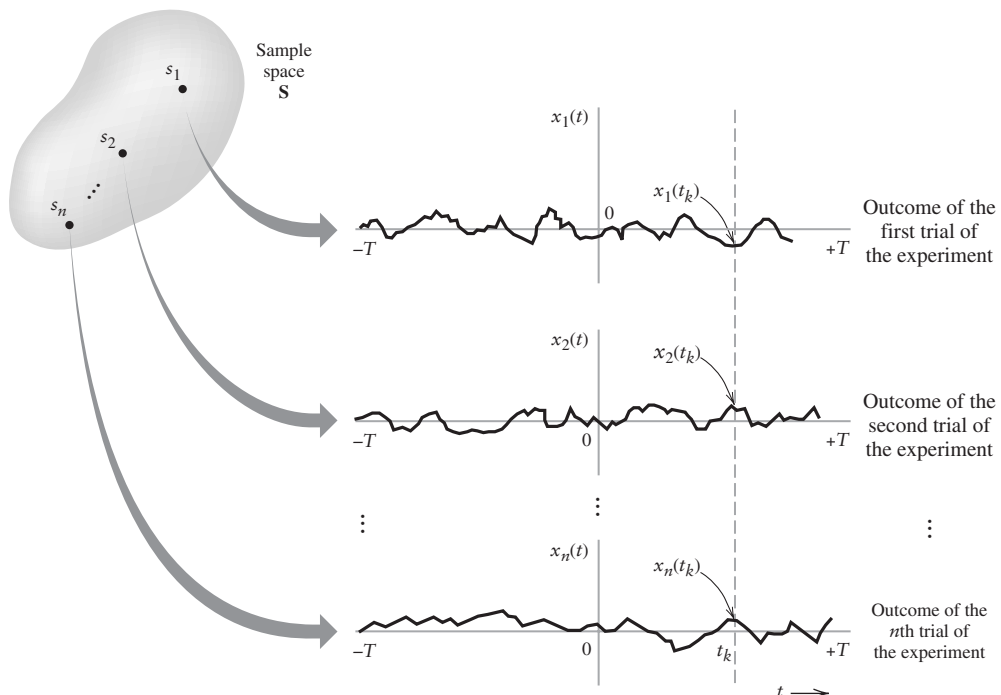


**FIGURE 8.14** Illustration of the relationship between sample space and the ensemble of sample functions.

At any point in the observation window,  $t_k$ , the possible outcomes of a random process can be represented as a random variable. *The family of all such random variables, indexed by the time variable  $t$ , forms the random process.*

The range of possible random processes is quite large. To restrict this range to random processes that are both: (i) typical of real-world situations, and (ii) mathematically tractable, we need two technical conditions, *stationarity* and *ergodicity*, which we discuss in what follows.

## ■ STATIONARY RANDOM PROCESSES

With real-world random processes, we often find that the statistical characterization of a process is independent of the time at which the observations occur. That is, if a random process is divided into a number of time intervals, the various sections of the process exhibit essentially the same statistical properties. Such a process is said to be *stationary*. Otherwise, it is said to be *nonstationary*.

This characterization is loosely analogous to linear systems theory, where we define time-invariant systems as those whose impulse response does not vary with time. This is to be contrasted with time-varying systems, whose impulse response varies with time. As with time-invariant systems, stationary random processes are often more mathematically tractable and simpler to analyze.

To be more precise, let  $X(t)$  be a random process that is observed at time  $t_1$ . Let  $F_{X(t_1)}(x)$  be the probability distribution function associated with observations of the different sample functions of the random process at time  $t_1$ . Suppose the same random process is observed at time  $t_1 + \tau$ , and the corresponding distribution function is  $F_{X(t_1+\tau)}(x)$ . Then if

$$F_{X(t_1+\tau)}(x) = F_{X(t_1)}(x) \quad (8.61)$$

for all  $t_1$  and all  $\tau$ , we say the process is *stationary to the first order*. A *first-order stationary random process has a distribution function that is independent of time*. As a consequence, statistical parameters such as the mean and variance are also independent of time for such a process. For example, suppose  $F_{X(t_1)}(x)$  has the density  $f_{X(t_1)}(x)$ . Then the mean value

$$\mu_X = \int_{-\infty}^{\infty} sf_{X(t_1)}(s) ds = \int_{-\infty}^{\infty} sf_{X(t_1+\tau)}(s) ds \quad (8.62)$$

does not change with time because the distribution function (and hence the density) are time invariant.

Next, consider sampling the random process  $X(t)$  at two points in time  $t_1$  and  $t_2$ , with the corresponding joint distribution function  $F_{X(t_1), X(t_2)}(x_1, x_2)$ . Suppose a second set of observations are made at times  $t_1 + \tau$  and  $t_2 + \tau$ , and the corresponding joint distribution is  $F_{X(t_1+\tau), X(t_2+\tau)}(x_1, x_2)$ . Then if, for all  $t_1, t_2$ , and  $\tau$ , we find that

$$F_{X(t_1+\tau), X(t_2+\tau)}(x_1, x_2) = F_{X(t_1), X(t_2)}(x_1, x_2) \quad (8.63)$$

we say the process is *stationary to the second order*. Stationarity to the second order implies that statistical quantities such as covariance and correlation, which we will discuss in the following, do not depend upon absolute time.

The definition of a  $k$ th-order stationary random process follows in a similar manner. If the equivalence between distribution functions holds for all time shifts  $\tau$ , all  $k$ , and all possible observation times  $t_1, t_2, \dots, t_k$ , then we say the process is *strictly stationary*. In other words, a random process  $X(t)$  is strictly stationary if the joint distribution of any set of random variables obtained by observing the random process  $X(t)$  is invariant with respect to the location of the origin  $t = 0$ .

► **Drill Problem 8.11** A random process is defined by the function

$$X(t, \theta) = A \cos(2\pi ft + \theta)$$

where  $A$  and  $f$  are constants, and  $\theta$  is uniformly distributed over the interval 0 to  $2\pi$ . Is  $X$  stationary to the first order? ◀

► **Drill Problem 8.12** Show that a random process that is stationary to the second order is also stationary to the first order. ◀

## 8.7 Correlation of Random Processes

While random processes are, by definition, unpredictable, we often observe that samples of the process at different times may be correlated. For example, if  $X(t_1)$  is large, then we might also expect  $X(t_1 + \tau)$  to be large, if  $\tau$  is small. To quantify this relationship, consider the covariance of two random variables, defined in Section 8.2, applied to samples of the random process  $X(t)$  at times  $t_1$  and  $t_2$ . That is, the covariance of the two random variables  $X(t_1)$  and  $X(t_2)$  is given by

$$\text{Cov}(X(t_1), X(t_2)) = \mathbb{E}[X(t_1)X(t_2)] - \mu_{X(t_1)}\mu_{X(t_2)} \quad (8.64)$$

We define the first term on the right-hand side of Eq. (8.64) as the *autocorrelation* of the random process and use the generic notation

$$R_X(t, s) = \mathbb{E}[X(t)X^*(s)] \quad (8.65)$$

where we have used the asterisk to denote conjugation for the case when  $X(t)$  may be complex valued. If  $X(t)$  is stationary to the second order or higher, then Eq. (8.64) may be written as

$$\begin{aligned} R_X(t, s) &= \mathbb{E}[X(t)X^*(s)] \\ &= R_X(t - s) \end{aligned} \quad (8.66)$$

Stationarity in the second order also implies the mean of the random process is constant. If this mean is zero, then the autocorrelation and covariance functions of a random process are equivalent. The following will show the importance of the autocorrelation function as a descriptor of random processes.

For many applications we do not require a random process to have all of the properties necessary to be stationary in the second order. In particular, we often only require:

1. The mean of the random process is a constant independent of time:  $\mathbb{E}[X(t)] = \mu_X$  for all  $t$ .
2. The autocorrelation of the random process only depends upon the time difference:  $\mathbb{E}[X(t)X^*(t - \tau)] = R_X(\tau)$ , for all  $t$  and  $\tau$ .

If a random process has these two properties, then we say it is *wide-sense stationary* or *weakly stationary*. Note that wide-sense stationarity does not imply stationarity to the second order. Neither does stationarity to the second order imply wide-sense stationary, as the first and second moments may not exist. In the rest of the book, we shall assume that all processes of interest are wide-sense stationary.

## ■ PROPERTIES OF THE AUTOCORRELATION FUNCTION

The autocorrelation function of a wide-sense stationary random process has the following properties for a real-valued process:

**PROPERTY 1 Power of a Wide-Sense Stationary Process** *The second moment or mean-square value of a real-valued random process is given by*

$$\begin{aligned} R_X(0) &= \mathbb{E}[X(t)X(t)] \\ &= \mathbb{E}[X^2(t)] \end{aligned} \quad (8.67)$$

The mean-square value is therefore equivalent to the average power of the process.

**PROPERTY 2 Symmetry** *The autocorrelation of a real-valued wide-sense stationary process has even symmetry.*

To show this, consider

$$\begin{aligned} R_X(-\tau) &= \mathbb{E}[X(t)X(t + \tau)] \\ &= \mathbb{E}[X(t + \tau)X(t)] \\ &= R_X(\tau) \end{aligned} \quad (8.68)$$

**PROPERTY 3 Maximum Value** *The autocorrelation function of a wide-sense stationary random process is a maximum at the origin.*

To show this property for a real-valued process, form the nonnegative quantity

$$\begin{aligned} 0 &\leq \mathbb{E}[(X(t) \pm X(t - \tau))^2] \\ &\leq \mathbb{E}[X^2(t)] + \mathbb{E}[X^2(t - \tau)] \pm 2\mathbb{E}[X(t)X(t - \tau)] \\ &\leq 2R_X(0) \pm 2R_X(\tau) \end{aligned} \quad (8.69)$$

Rearranging the last relationship, we have  $R_X(0) \geq |R_X(\tau)|$ .

The physical significance of the autocorrelation function  $R_X(\tau)$  is that it provides a means of describing the interdependence of two random variables obtained by observing a random process  $X(t)$  at times  $\tau$  seconds apart. It is therefore apparent that the more rapidly the random process  $X(t)$  changes with time, the more rapidly will the autocorrelation function  $R_X(\tau)$  decrease from its maximum  $R_X(0)$  as  $\tau$  increases, as illustrated in Fig. 8.15. This decrease may be characterized by the *decorrelation time*  $\tau_0$ ; specifically, for  $\tau > \tau_0$ , the magnitude of the correlation  $R_X(\tau)$  remains below some prescribed value. We may thus define the decorrelation time  $\tau_0$  of a stationary process  $X(t)$  of zero mean as the time for the magnitude of the autocorrelation function  $R_X(\tau)$  to decrease to, say, 1 percent of its maximum value  $R_X(0)$ .

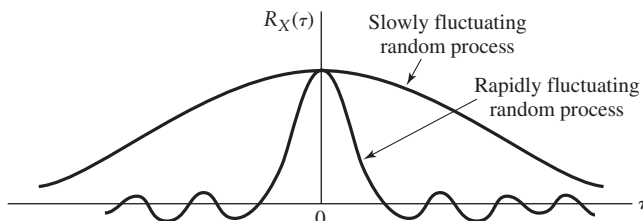


**FIGURE 8.15** Illustration of autocorrelation functions of slowly and rapidly fluctuating random processes.

**EXAMPLE 8.10** Autocorrelation of a Random Cosine Process

Let  $X(t)$  be a random process defined by

$$X(t) = A \cos(2\pi ft + \theta)$$

where the amplitude  $A$  and frequency  $f$  are known, but  $\theta$  is uniformly distributed on the interval between 0 and  $2\pi$ . This is a special type of random process where a single parameter  $\theta$  defines the sample function for all time. The requirement is to find the autocorrelation of  $X(t)$ .

The autocorrelation is given by

$$\begin{aligned} R_X(t, t - \tau) &= E[X(t)X(t - \tau)] \\ &= A^2 E[\cos(2\pi ft + \theta) \cos(2\pi f(t - \tau) + \theta)] \end{aligned}$$

Applying the trigonometric identity  $2 \cos A \cos B = \cos(A - B) + \cos(A + B)$  to this relation, we obtain

$$R_X(t, t - \tau) = \frac{A^2}{2} \cos(2\pi f\tau) + \frac{A^2}{2} E[\cos(4\pi ft - 2\pi f\tau + 2\theta)]$$

Since  $\theta$  is uniformly distributed between 0 and  $2\pi$ , we have

$$\begin{aligned} E[\cos(4\pi ft - 2\pi f\tau + 2\theta)] &= \frac{1}{2\pi} \int_0^{2\pi} \cos(4\pi ft - 2\pi f\tau + 2\theta) d\theta \\ &= \frac{1}{4\pi} \sin(4\pi ft - 2\pi f\tau + 2\theta) \Big|_0^{2\pi} \\ &= 0 \end{aligned}$$

Consequently, the expression for the autocorrelation reduces to

$$R_X(t, t - \tau) = \frac{A^2}{2} \cos(2\pi f\tau)$$

The autocorrelation clearly only depends upon the time difference  $\tau$  in this example, and the process can be shown to be wide-sense stationary.

► **Drill Problem 8.13** Let  $X(t)$  be a random process defined by

$$X(t) = A \cos(2\pi ft)$$

where  $A$  is uniformly distributed between 0 and 1, and  $f$  is constant. Determine the autocorrelation function of  $X$ . Is  $X$  wide-sense stationary? ◀

■ **ERGODICITY**

To determine the statistical properties of random processes, we usually have to compute expectations. The expectation of a random process at a particular point in time requires separate independent realizations of the random process. For example, for a random process,  $X(t)$  with  $N$  equiprobable realizations  $\{x_j(t): j = 1, 2, \dots, N\}$ , the expected value and second moment of the random process at time  $t = t_k$  are respectively given by the *ensemble averages*

$$E[X(t_k)] = \frac{1}{N} \sum_{j=1}^N x_j(t_k) \quad (8.70)$$

and

$$E[X^2(t_k)] = \frac{1}{N} \sum_{j=1}^N x_j^2(t_k) \quad (8.71)$$

If the process is wide-sense stationary, then the mean value and second moment computed by these two equations do not depend upon the time  $t_k$ .

In practical problems involving random processes, what will generally be available to the user is not the random process, but one of its sample functions,  $x(t)$ . In such cases, the most easily measurable parameters are time averages. For example, the *time average* of a continuous sample function drawn from a real-valued process is given by

$$\mathcal{E}[x] = \lim_{T \rightarrow \infty} \frac{1}{2T} \int_{-T}^T x(t) dt \quad (8.72)$$

and the *time-autocorrelation of the sample function* is given by

$$\mathcal{R}_x(\tau) = \lim_{T \rightarrow \infty} \frac{1}{2T} \int_{-T}^T x(t)x(t - \tau) dt \quad (8.73)$$

So the question is: *When are the time averages of a sample function equal to the ensemble averages of the corresponding random process?* Intuitively, if the statistics of the random process  $X(t)$  do not change with time, then we might expect the time averages and ensemble averages to be equivalent.

Depending upon the stationary properties of a random process, various time averages of the sample functions may be used to approximate the corresponding ensemble averages or expectations. Random processes for which this equivalence holds are said to be *ergodic*. In most physical applications, *wide-sense stationary processes are assumed to be ergodic*, in which case *time averages and expectations can be used interchangeably*.

The alert reader will note that, just as with stationarity, there are varying degrees of ergodicity. The equivalences of Eqs. (8.70) and (8.72) on the one hand and the corresponding Eqs. (8.66) and (8.73) on the other hand are analogous to a form of first-order and second-order ergodicity.

Furthermore, if we assume that the real-valued random process is ergodic, then we can express the autocorrelation function as

$$\begin{aligned} R_X(\tau) &= \mathbb{E}[X(t)X(t - \tau)] \\ &= \lim_{T \rightarrow \infty} \frac{1}{2T} \int_{-T}^T x(t)x(t - \tau) dt \end{aligned} \quad (8.74)$$

where  $x(t)$  is a sample function of the random process  $X(t)$ . This definition of autocorrelation is identical to the definition of correlation for deterministic power signals as described in Chapter 2. As a consequence, the autocorrelation of an ergodic random process has many of the same properties as the autocorrelation of deterministic signals.

The concept of ergodicity also naturally leads to the idea of estimators for the autocorrelation function. In particular, if  $x(t)$  is a sample function of a wide-sense stationary ergodic process  $X(t)$ , then an *estimate of the autocorrelation* of a real-valued process for lag  $\tau = \tau_0$  is (see Fig. 2.29)

$$\hat{R}_X(\tau_0) = \frac{1}{N} \sum_{n=1}^N x(t_n)x(t_n - \tau_0) \quad (8.75)$$

where  $\{t_n\}$  is a convenient set of sampling times, uniformly spaced or otherwise. Similar to the estimators of the mean and variance of a random variable, this estimate of the autocorrelation is motivated by the relative frequency definition of probability.

#### EXAMPLE 8.11 Discrete-Time Autocorrelation

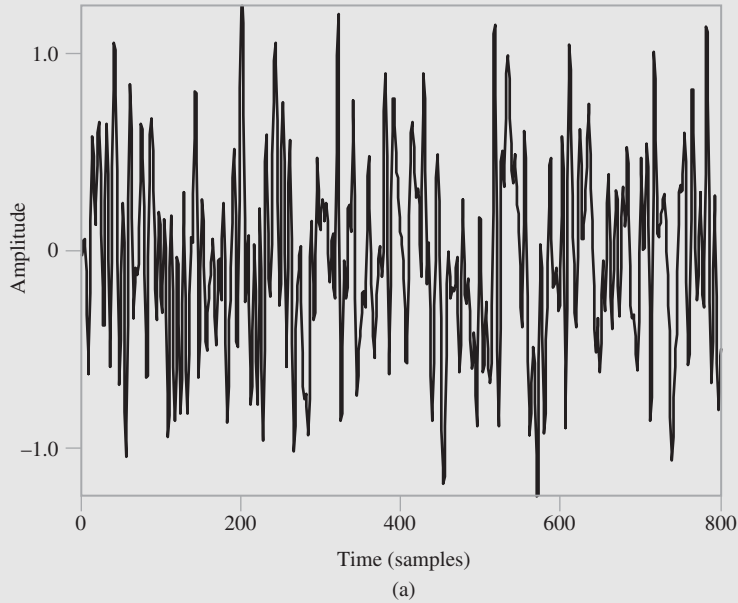
In a digital communication system, we often sample a continuous signal at discrete times  $t_n = nT_s$  where  $T_s$  is the sampling interval. This sampled signal  $\{X(t_1), X(t_2), \dots\}$  is a discrete-time random process for which we can define the discrete-time autocorrelation function

$$R_X(kT_s) = \mathbb{E}[X(nT_s)X((n - k)T_s)] \quad (8.76)$$

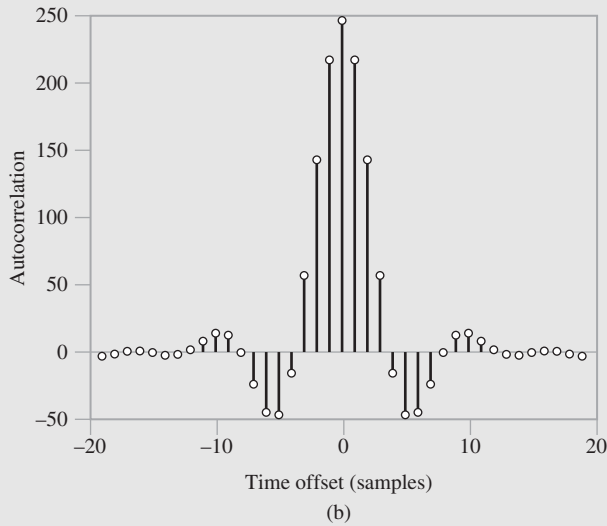
where the expectation is the usual ensemble average. As suggested in this section, we may wish to estimate this autocorrelation by performing a time average over a particular sample function. This time average, over  $N$  samples of the sample function  $x(t)$ , is defined as

$$\mathcal{R}_x(kT_s) = \frac{1}{N} \sum_{n=1}^N x(nT_s)x((n-k)T_s) \quad (8.77)$$

In Fig. 8.16(a), we plot a random signal as a function of time. For this signal, the time-averaged autocorrelation of the random signal is shown in Fig. 8.16(b). The horizontal axis represents the time lag  $\tau$  in sample periods. Although the signal is quite random in the time domain, it has a smooth autocorrelation function as shown in Fig. 8.16(b).



(a)



(b)

**FIGURE 8.16** Illustration of (a) a random signal, and (b) its autocorrelation.

► **Drill Problem 8.14** A discrete-time random process  $\{Y_n: n = \dots, -1, 0, 1, 2, \dots\}$  is defined by

$$Y_n = \alpha_0 Z_n + \alpha_1 Z_{n-1}$$

where  $\{Z_n\}$  is a random process with autocorrelation function  $R_Z(n) = \sigma^2 \delta(n)$ , where  $\delta(n)$  is the delta function. What is the autocorrelation function  $R_Y(n, m) = E[Y_n Y_m]$ ? Is the process  $\{Y_n\}$  wide-sense stationary? ◀

## 8.8 Spectra of Random Signals

As described above, a random signal may be viewed as belonging to an ensemble of signals, generated by some probabilistic mechanism. Hence, no two signals exhibit the same variation in time. Let  $x(t)$  denote a sample function of a random process  $X(t)$ . Figure 8.17 shows a plot of the waveform of  $x_T(t)$  on the interval  $-T < t < T$ . We may define the Fourier transform of the sample function  $x_T(t)$  as

$$\xi_T(f) = \int_{-\infty}^{\infty} x_T(t) \exp(-j2\pi ft) dt \quad (8.78)$$

This transform converts the sample function  $x_T(t)$  to a new sample function  $\xi_T(f)$ .<sup>8</sup> We define the collection (ensemble) of all such new sample functions as the new random process  $\Xi_T(f)$ . Effectively, the Fourier transform has converted a family of random variables  $X(t)$  indexed by parameter  $t$  to a new family of random variables  $\Xi_T(f)$  indexed by parameter  $f$ .

From the discussion of Chapter 2, we recall that the power spectral density of the sample function  $x(t)$  over the interval  $-T < t < T$  is  $|\xi_T(f)|^2/2T$  where  $\xi_T(f)$  is the Fourier transform of  $x_T(t)$ . This power spectral density will depend on the particular sample function  $x(t)$  drawn from the ensemble. Accordingly, to obtain the power spectral density of the random process, we must perform an ensemble-averaging operation and then take the limit as  $T$  approaches infinity.

The ensemble-averaging operation requires using the probability distribution of the ensemble. The value of  $f$  is held fixed while averaging over the ensemble. For the present discussion, it is sufficient to acknowledge the ensemble-averaging operation by using the expectation operator  $E$ . We thus write the ensemble-averaged value of the

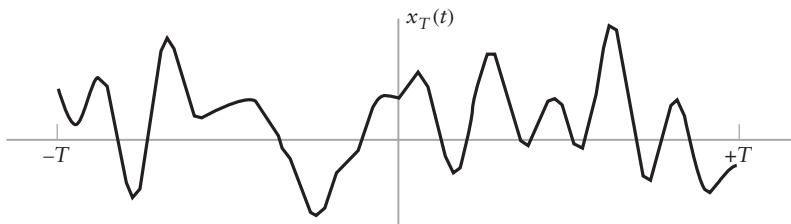


**FIGURE 8.17** Sample function of a random process.

<sup>8</sup>We previously have used the notation  $x(t) \rightleftharpoons X(f)$  to denote a Fourier-transform pair. However, the use of  $X(t)$  to represent the random process introduces a possible ambiguity in notation. Hence, in this section we use  $x(t) \rightleftharpoons \xi(f)$  as a Fourier-transform pair of sample functions, and  $X(t) \rightleftharpoons \Xi(f)$  as a Fourier-transform pair of random processes.

new random process  $|\Xi_T(f)|^2$  as  $\mathbf{E}[|\Xi_T(f)|^2]$  and the corresponding power spectral density of the random process  $X(t)$  as

$$S_X(f) = \lim_{T \rightarrow \infty} \frac{1}{2T} \mathbf{E}[|\Xi_T(f)|^2] \quad (8.79)$$

It is important to note that in Eq. (8.79), the ensemble averaging must be performed before the limit is taken. Also critical to this definition is that the process be wide-sense stationary.

This approach of determining the power spectral density through an ensemble average may be used to motivate an estimator of the power spectral density given a sample function of an ergodic stationary process. In Section 2.10, we saw how the discrete Fourier transform (DFT) may be used to numerically approximate the Fourier transform. In particular, if  $\{x_n: n = 0, 1, \dots, N - 1\}$  are uniformly spaced samples of a function  $x(t)$  at  $t = nT_s$ , then the discrete Fourier transform is defined as

$$\xi_k = \sum_{n=0}^{N-1} x_n W^{kn} \quad (8.80)$$

where  $W = \exp(-j2\pi/N)$  and  $\{\xi_k\}$  are samples of the frequency-domain response at  $f = k/NT_s$ . Consequently, we may estimate the power spectral density of a random process by the following three steps:

1. Partition the sample function  $x(t)$  into  $M$  sections of length  $NT_s$  and sample at intervals  $T_s$ .
2. Perform a DFT on each section of length  $NT_s$ . Let  $\{\xi_{k+mN}\}$  where  $m = 0, \dots, M - 1$  represent the  $M$  DFT outputs, one set for each section.
3. Average the magnitude squared of each DFT, and then the power spectral density estimate is given by

$$\begin{aligned} \hat{S}_X\left(\frac{k}{NT_s}\right) &= \frac{1}{M} \sum_{m=0}^{M-1} |\xi_{k+mN}|^2 \\ &= \frac{1}{M} \sum_{m=0}^{M-1} \left| \sum_{n=0}^{N-1} x_{n+mN} W^{kn} \right|^2, \quad k = 0, \dots, M - 1 \end{aligned} \quad (8.81)$$

This result clearly relies on the process being ergodic.

### ■ PROPERTIES OF THE POWER SPECTRAL DENSITY

The power spectral density  $S_X(f)$  and the autocorrelation function  $R_X(\tau)$  of a wide-sense stationary random process form a Fourier-transform pair in the variables  $f$  and  $\tau$ . In particular, the same Weiner-Khintchine relations that apply to deterministic processes also relate the power spectral density and autocorrelation function of a random process, as shown by

$$S_X(f) = \int_{-\infty}^{\infty} R_X(\tau) \exp(-j2\pi f\tau) d\tau \quad (8.82)$$

and

$$R_X(\tau) = \int_{-\infty}^{\infty} S_X(f) \exp(j2\pi f\tau) df \quad (8.83)$$

Equations (8.82) and (8.83) are the basic relations of the spectral analysis theory of random processes. The Weiner–Khintchine relations show that if either the autocorrelation or the power spectral density of the random process is known, the other may be found exactly.

We can use this pair of relations to derive some general properties of the power spectral density of a wide-sense stationary process.

**PROPERTY 1 Mean-Square Value** *The mean-square value of a stationary process equals the total area under the graph of the power spectral density; that is,*

$$\mathbf{E}[|X(t)|^2] = \int_{-\infty}^{\infty} S_X(f) df \quad (8.84)$$

This property follows directly from Eq. (8.83) by putting  $\tau = 0$  and noting that

$$R_X(0) = \mathbf{E}[|X(t)|^2]$$

**PROPERTY 2 Nonnegativity** *The power spectral density of a stationary random process is always nonnegative; that is,*

$$S_X(f) \geq 0, \quad \text{for all } f \quad (8.85)$$

This follows from the definition of the power spectral density given in Eq. (8.79).

**PROPERTY 3 Symmetry** *The power spectral density of a real random process is an even function of frequency; that is,*

$$S_X(-f) = S_X(f) \quad (8.86)$$

This property is readily obtained by first substituting  $-f$  for  $f$  in Eq. (8.82).

$$S_X(-f) = \int_{-\infty}^{\infty} R_X(\tau) \exp(j2\pi f\tau) d\tau$$

Next, substituting  $-\tau$  for  $\tau$ , and recognizing that  $R_X(-\tau) = R_X(\tau)$  for a real process, we obtain

$$S_X(-f) = \int_{-\infty}^{\infty} R_X(\tau) \exp(-j2\pi f\tau) d\tau = S_X(f)$$

which is the desired result.

**PROPERTY 4 Filtered Random Processes** *If a stationary random process  $X(t)$  with spectrum  $S_X(f)$  is passed through a linear filter with frequency response  $H(f)$ , the spectrum of the stationary output random process  $Y(t)$  is given by*

$$S_Y(f) = |H(f)|^2 S_X(f) \quad (8.87)$$

This result is analogous to that obtained for deterministic signals.<sup>9</sup>

---

<sup>9</sup>The proof of this result for deterministic signals follows from the convolution theorem of Section 2.2. The proof for random processes may be found in Chapter 1 of Haykin (2001).

**EXAMPLE 8.12** Filtering a Random Sinusoid

A random signal  $X(t)$  with autocorrelation function

$$R_X(\tau) = \frac{A^2}{2} \cos(2\pi f_c \tau)$$

is processed by a causal filter with impulse response  $h(t)$  that is zero for negative time to produce the new random process

$$Y(t) = \int_0^t h(t-s)X(s) ds$$

If the filter has an impulse response corresponding to the frequency response

$$H(f) = \frac{1}{1 + j2\pi RCf} \quad (8.88)$$

what is the autocorrelation function of  $Y(t)$ ?

From Property 4 of power spectral densities of random processes, we have that the spectral density of  $Y(t)$  is given by

$$S_Y(f) = |H(f)|^2 S_X(f)$$

We may use the Fourier-transform pair

$$\cos(2\pi f_c \tau) \Longleftrightarrow \frac{1}{2} [\delta(f - f_c) + \delta(f + f_c)] \quad (8.89)$$

to obtain the spectral density  $S_X(f)$ . Hence,

$$\begin{aligned} S_Y(f) &= \frac{1}{2} |H(f)|^2 [\delta(f - f_c) + \delta(f + f_c)] \\ &= \frac{1}{2} |H(f_c)|^2 [\delta(f - f_c) + \delta(f + f_c)] \end{aligned}$$

where the last line anticipates the sifting property of the Dirac delta function. Using the inverse Fourier transform of  $S_Y(f)$  and evaluating  $H(f)$  of Eq. (8.88) at  $f = f_c$ , we get

$$R_Y(\tau) = \frac{1}{1 + (2\pi RCf_c)^2} \cos(2\pi f_c \tau)$$

We thus see that, similar to deterministic sinusoids, linear filtering does not affect the frequency of a random sinusoid.

► **Drill Problem 8.15** For the discrete-time process of Problem 8.14, use the discrete Fourier transform to approximate the corresponding spectrum. That is, compute and sketch

$$S_Y(k) = \sum_{n=0}^{N-1} R_Y(n) W^{kn}$$

If the sampling in the time domain is at  $n/T_s$  where  $n = 0, 1, 2, \dots, N - 1$ , what frequency does the integer  $k$  correspond to? ◀

## 8.9 Gaussian Processes

Up to this point in our discussion, we have presented the theory of random processes in general terms. In the remainder of this chapter, we consider this theory in the context of some important random processes that are commonly encountered in the study of communication systems.

We have seen how Gaussian random variables play a fundamental role in communication systems because (i) many physical processes that generate noise in communication systems can be considered approximately Gaussian distributed; and (ii) the Gaussian random variable is mathematically tractable and therefore convenient to deal with.

Similarly, a Gaussian process plays an important role in the study of random processes for two reasons. First, the Gaussian process has many properties that make analytic results possible. Second, the random processes produced by physical phenomena are often such that a Gaussian model is appropriate.

Before we define a Gaussian process, we must provide some background regarding the joint distribution of multiple Gaussian random variables. The joint distribution of  $N$  Gaussian random variables may be written as<sup>10</sup>

$$f_{\mathbf{X}}(\mathbf{x}) = \frac{1}{(2\pi)^{N/2}|\Lambda|^{1/2}} \exp\left\{-\frac{1}{2}(\mathbf{x} - \boldsymbol{\mu})^T \Lambda^{-1} (\mathbf{x} - \boldsymbol{\mu})\right\} \quad (8.90)$$

which is called the *multi-variate Gaussian distribution*. In Eq. (8.90), the respective quantities are:

$\mathbf{X} = (X_1, X_2, \dots, X_N)$  represents an  $N$ -dimensional vector of Gaussian random variables

$\mathbf{x} = (x_1, x_2, \dots, x_N)$  is the corresponding vector of indeterminates

$\boldsymbol{\mu} = (\mathbb{E}[X_1], \mathbb{E}[X_2], \dots, \mathbb{E}[X_N])$  is the  $N$ -dimensional vector of means

$\Lambda$  is the  $N$ -by- $N$  covariance matrix with individual elements given by  $\Lambda_{ij} = \text{Cov}(X_i, X_j)$

The notation  $|\Lambda|$  denotes the determinant of matrix  $\Lambda$ . With this definition of the multi-variate Gaussian distribution we have a basis for defining a Gaussian random process.

A random process  $X(t)$ , with  $t$  taking values in the set  $T$ , is said to be a *Gaussian process* if, for any integer  $k$  and any subset  $\{t_1, t_2, \dots, t_k\}$  of  $T$ , the  $k$  random variables  $\{X(t_1), X(t_2), \dots, X(t_k)\}$  is jointly Gaussian distributed. That is, for any  $k$ ,  $f_{X(t_1), \dots, X(t_k)}(x_1, \dots, x_k)$  has a density equivalent to Eq. (8.90).

A Gaussian process has the following properties:

1. If a Gaussian process is wide-sense stationary, then it is also stationary in the strict sense.
2. If a Gaussian process is applied to a stable linear filter, then the random process  $Y(t)$  produced at the output of the filter is also Gaussian.
3. If integration is defined in the mean-square sense, then we may interchange the order of the operations of integration and expectation with a Gaussian random process.<sup>11</sup>

This first property comes from observing that if a Gaussian process is wide-sense stationary, then (i) its mean does not vary with time, and (ii) the elements  $\Lambda_{ij}$  of the covariance matrix only depend on the time difference  $t_i - t_j$ , and not on the absolute  $t$ . Since the  $N$ -dimensional joint distribution of samples of a Gaussian process only depends on the mean and covariance through Eq. (8.90), a wide-sense stationary Gaussian process is also strictly stationary.

<sup>10</sup>See Chapter 4 of Leon-Garcia (1994).

<sup>11</sup>See Chapter 6 of Leon-Garcia (1994). The mean-square convergence of  $\{Y_n\}$  to  $Y$  implies that

$$\lim_{n \rightarrow \infty} \mathbb{E}[(Y - Y_n)^2] = 0$$

The second property comes from observing that the filtering operation can be written as

$$Y(t) = \int_0^t h(t-s)X(s) ds \quad (8.91)$$

if we use the following three facts:

1. The integral of Eq. (8.91) is defined as the mean-square limit of the sums

$$Y(t) = \lim_{\Delta s \rightarrow 0} \sum_i b(t - i \Delta s) x(i \Delta s) \Delta s$$

Hence, we observe that the right-hand side is a weighted sum of the Gaussian random variables  $X(i \Delta s)$ .

2. Recall from the properties of Gaussian random variables that a weighted sum of Gaussian random variables is another Gaussian random variable.
3. If a sequence of Gaussian random variables converges in the mean-square sense, then the result is a Gaussian random variable.

Together these three facts<sup>12</sup> can be used to prove that  $Y(t)$  is also a Gaussian random process.

The third property of Gaussian processes implies that if  $Y(t)$  is given by Eq. (8.91) then the mean of the output is given by

$$\begin{aligned} E[Y(t)] &= E\left[\int_0^t b(t-s)X(s) ds\right] \\ &= \int_0^t b(t-s)E[X(s)] ds \\ &= \mu_Y(t) \end{aligned}$$

These results are very useful in communication systems, where linear filtering of random processes occurs quite often.

► **Drill Problem 8.16** Is the discrete-time process  $\{Y_n: n = 0, 1, 2, \dots\}$  defined by  $Y_0 = 0$  and

$$Y_{n+1} = \alpha Y_n + W_n$$

a Gaussian process, if  $W_n$  is Gaussian? Assume that  $|\alpha| < 1$ . Justify your answer. ◀

## 8.10 White Noise

The noise analysis of communication systems is often based on an idealized noise process called white noise. *The power spectral density of white noise is independent of frequency.* White noise is analogous to the term “white light” in the sense that all frequency components are present in equal amounts. We denote the power spectral density of a white noise process  $W(t)$  as

$$S_W(f) = \frac{N_0}{2} \quad (8.92)$$

where the factor  $\frac{1}{2}$  has been included to indicate that half the power is associated with positive frequencies and half with negative frequencies, as illustrated in Fig. 8.18(a). The dimensions

<sup>12</sup>The invariance of the Gaussian distribution type after filtering is shown in Chapter 11 of Thomas (1971).

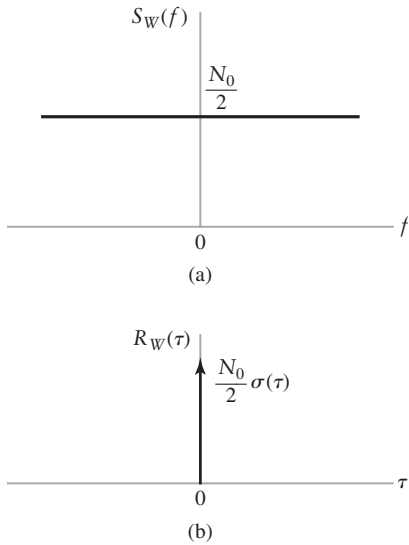


**FIGURE 8.18** Characteristics of white noise.  
(a) Power spectral density. (b) Autocorrelation function.

of  $N_0$  are watts per hertz. The parameter  $N_0$  is usually measured at the input stage of a communications receiver. Since there is no delta function at the origin in the power spectral density of Fig. 8.18(a), white noise has no dc power. That is, its mean or average value is zero.

Since the autocorrelation function is the inverse Fourier transform of the power spectral density, it follows from Eq. (8.92) that the autocorrelation of white noise is given by

$$R_W(\tau) = \frac{N_0}{2} \delta(\tau) \quad (8.93)$$

The autocorrelation function of white noise consists of a delta function weighted by the factor  $N_0/2$  located at  $\tau = 0$ , as in Fig. 8.18(b). We note that  $R_W(\tau)$  is zero for  $\tau \neq 0$ . Consequently, any two different samples of white noise, no matter how close together in time they are taken, are uncorrelated.

Strictly speaking, white noise has infinite average power and, as such, it is not physically realizable. Nevertheless, white noise has convenient mathematical properties and is therefore useful in system analysis. Utility of the white noise process is parallel to that of an impulse function or delta function in the analysis of linear systems. The effect of the impulse is observed only after it has passed through a system with finite bandwidth. Likewise, the effect of white noise is observed only after passing through a system of finite bandwidth. We may therefore state that as long as the bandwidth of a noise process at the input of a system is appreciably larger than that of the system itself, we may model the noise process as white noise. This is usually the case in practical communication systems.

#### EXAMPLE 8.13 Ideal Low-Pass Filtered White Noise

Suppose that a white noise process  $W(t)$  of zero mean and power spectral density  $N_0/2$  is applied to an ideal low-pass filter of bandwidth  $B$  with a unity gain passband amplitude response. The power spectral density of the noise process  $N(t)$  appearing at the filter output is therefore (see Fig. 8.19(a))

$$S_N(f) = \begin{cases} \frac{N_0}{2}, & |f| < B \\ 0, & |f| > B \end{cases} \quad (8.94)$$

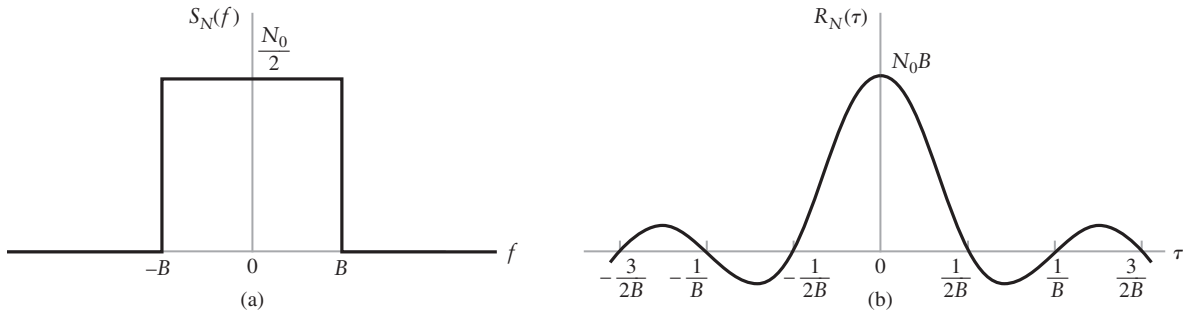


**FIGURE 8.19** Characteristics of low-pass filtered white noise. (a) Power spectral density. (b) Autocorrelation function.

The autocorrelation function of  $N(t)$  is the inverse Fourier transform of the power spectral density shown in Fig. 8.19(a).

$$\begin{aligned} R_N(\tau) &= \int_{-B}^B \frac{N_0}{2} \exp(j2\pi f_c \tau) df \\ &= N_0 B \operatorname{sinc}(2B\tau) \end{aligned} \quad (8.95)$$

This autocorrelation function is plotted in Fig. 8.19(b). We see that  $R_N(\tau)$  has its maximum value of  $N_0 B$  at the origin, is symmetric in  $\tau$ , and passes through zero at  $\tau = \pm n/2B$  where  $n = 1, 2, 3, \dots$ .

#### EXAMPLE 8.14 RC Low-Pass Filtered White Noise

Consider a white noise process  $W(t)$  of zero mean and power spectral density  $N_0/2$  applied to the low-pass RC filter, as in Fig. 8.20(a). The transfer function of the filter is

$$H(f) = \frac{1}{1 + j2\pi f RC} \quad (8.96)$$

From Eq. (8.87), we find that the power spectral density of the noise  $N(t)$  appearing at the low-pass RC filter output is therefore (see Fig. 8.20(b))

$$S_N(f) = \frac{N_0/2}{1 + (2\pi f RC)^2}$$

From Eq. (2.16) of Chapter 2, we have the Fourier-transform pair

$$\exp(-a|\tau|) \iff \frac{2a}{a^2 + (2\pi f)^2}$$

Therefore, using the dilation property of the Fourier-transform (see Section 2.2), we find that the autocorrelation of the filtered noise process  $N(t)$  is

$$R_N(\tau) = \frac{N_0}{4RC} \exp\left(-\frac{|\tau|}{RC}\right)$$

which is plotted in Fig. 8.20(c).

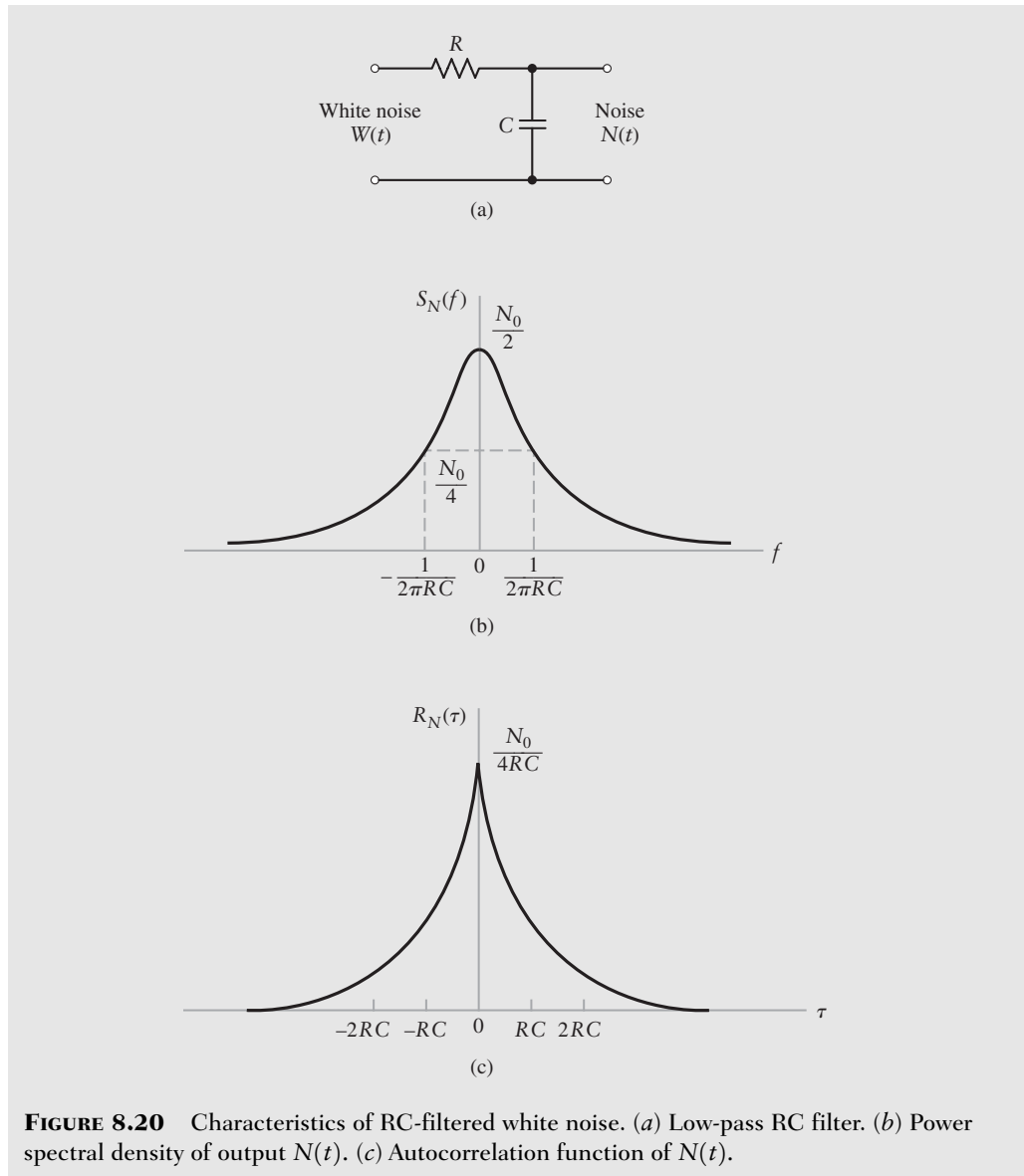


**FIGURE 8.20** Characteristics of RC-filtered white noise. (a) Low-pass RC filter. (b) Power spectral density of output  $N(t)$ . (c) Autocorrelation function of  $N(t)$ .

► **Drill Problem 8.17** A discrete-time white noise process  $\{W_n\}$  has an autocorrelation function given by  $R_W(n) = N_0\delta(n)$ .

- Using the discrete Fourier transform, determine the power spectral density of  $\{W_n\}$ .
- The white noise process is passed through a discrete-time filter having a discrete-frequency response

$$H(k) = \frac{1 - (\alpha W^k)^N}{1 - \alpha W^k}$$

where, for a  $N$ -point discrete Fourier transform,  $W = \exp\{-j2\pi/N\}$ . What is the power spectral density of the filter output? ◀

## 8.11 Narrowband Noise

A communication receiver includes multiple signal-processing stages. A common signal-processing stage for passband systems is a narrowband filter whose bandwidth is just large enough to pass the modulated component of the received signal essentially undistorted, but not so large as to admit excessive noise into the receiver. The noise process appearing at the output of such a filter is called *narrowband noise*. If the narrowband noise has a spectrum centered at the mid-band frequencies  $\pm f_c$  as illustrated in Fig. 8.21(a), we find that a sample function of the narrowband noise process is somewhat similar to a sine wave of frequency  $f_c$  that varies slowly in amplitude and phase, as illustrated in Fig. 8.21(b).

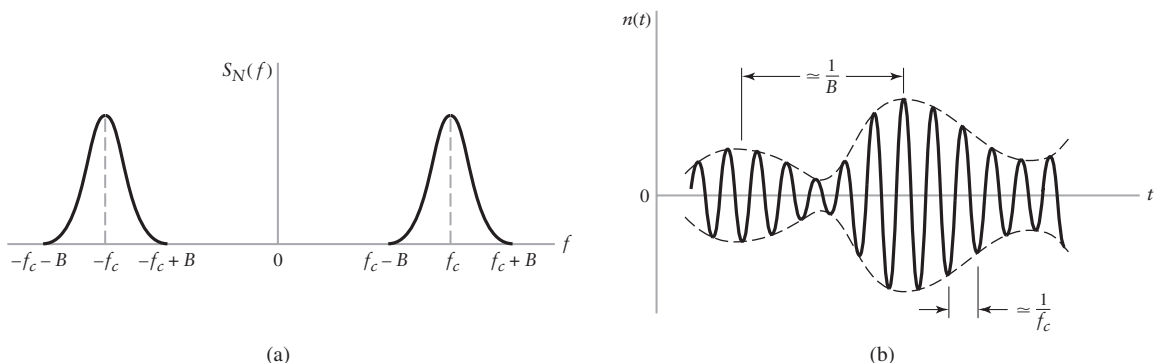


**FIGURE 8.21** (a) Power spectral density of narrowband noise. (b) Sample function of narrowband noise.

Narrowband noise can be represented mathematically using *in-phase* and *quadrature components*, just as we used them to represent narrowband signals in Chapter 2 and subsequent chapters. For the narrowband noise process  $N(t)$  of bandwidth  $2B$  and centered on frequency  $f_c$  of Fig. 8.21, we may represent  $N(t)$  in the form

$$N(t) = N_I(t) \cos(2\pi f_c t) - N_Q(t) \sin(2\pi f_c t) \quad (8.97)$$

where  $N_I(t)$  is called the *in-phase component* of  $N(t)$  and  $N_Q(t)$  is the *quadrature component*. Both  $N_I(t)$  and  $N_Q(t)$  are low-pass random processes; that is, their spectra are confined to  $0 < |f| < B$ . Knowledge of the in-phase and quadrature components, as well as the center frequency  $f_c$ , fully characterizes the narrowband noise.

Given the narrowband noise sample function  $n(t)$ , the in-phase and quadrature components may be extracted using the scheme shown in Fig. 8.22(a). The two low-pass filters are assumed to be ideal with bandwidth equal to  $B$ . This scheme follows directly from the representation of narrowband noise given in Eq. (8.97). Alternatively, if we are given the in-phase and quadrature components, we may generate the narrowband noise  $n(t)$  using Fig. 8.22(b).

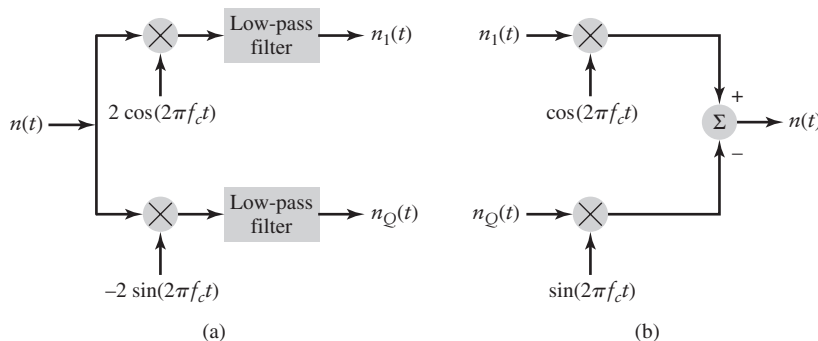


**FIGURE 8.22** (a) Extraction of in-phase and quadrature components of narrowband noise process. (b) Generation of narrowband noise process from its in-phase and quadrature components.

The in-phase and quadrature components of narrowband noise have the following important properties:<sup>13</sup>

1. The in-phase component  $N_I(t)$  and quadrature component  $N_Q(t)$  of narrowband noise  $N(t)$  have zero mean.
2. If the narrowband noise  $N(t)$  is Gaussian, then its in-phase and quadrature components are Gaussian.
3. If the narrowband noise  $N(t)$  is stationary, then its in-phase and quadrature components are stationary.
4. Both the in-phase component  $N_I(t)$  and  $N_Q(t)$  have the same power spectral density. This power spectral density is related to the power spectral density of the narrowband density  $S_N(f)$  by

$$S_{N_I}(f) = S_{N_Q}(f) = \begin{cases} S_N(f - f_c) + S_N(f + f_c), & -B \leq f \leq B \\ 0, & \text{otherwise} \end{cases} \quad (8.98)$$

5. The in-phase component  $N_I(t)$  and quadrature component  $N_Q(t)$  have the same variance as the narrowband noise  $N(t)$ .

As an illustration of these properties, consider narrowband noise having the power spectral density shown in Fig. 8.23(a). According to Property 4 above, the spectrum of the in-phase component of the narrowband noise is given by

$$S_{N_I}(f) = \begin{cases} N_0, & -B \leq f \leq B \\ 0, & \text{otherwise} \end{cases}$$

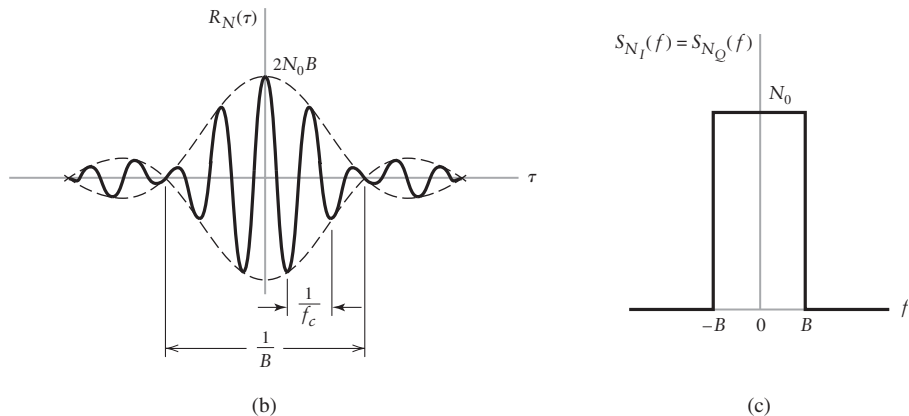
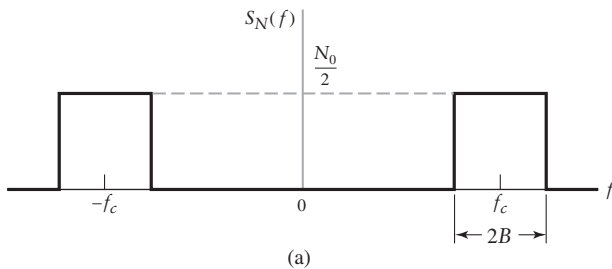


**FIGURE 8.23** Characteristics of ideal band-pass filtered white noise. (a) Power spectral density. (b) Autocorrelation function. (c) Power spectral density of in-phase and quadrature components.

<sup>13</sup>The justification of these properties is discussed in Chapter 1 of Haykin (2001).

and the quadrature component has a similar spectrum. Thus the spectral density of the in-phase component is twice that of narrowband noise. However, since the narrowband noise has nonzero spectral density in two bands of width  $2B$  centered at  $\pm f_c$ , we have that

$$\int_{-\infty}^{\infty} S_N(f) df = \int_{-\infty}^{\infty} S_{N_I}(f) df = 2N_0B$$

which confirms Property 5 that the in-phase component has the same variance (power) as the narrowband noise.

#### EXAMPLE 8.15 Ideal Band-Pass Filtered White Noise

Consider white Gaussian noise of zero mean and power spectral density  $N_0/2$ , which is passed through an ideal band-pass filter with center frequency  $f_c$ , bandwidth  $2B$ , and passband magnitude response of unity. The power spectral density of the filtered white noise is then

$$S_N(f) = \begin{cases} N_0/2, & |f - f_c| < B \\ N_0/2, & |f + f_c| < B \\ 0, & \text{otherwise} \end{cases} \quad (8.99)$$

as illustrated in Fig. 8.23(a). The problem is to determine the autocorrelation functions of  $N(t)$  and its in-phase and quadrature components.

The autocorrelation function of  $n(t)$  is the inverse Fourier transform of the power spectral density characteristic of Eq. (8.99), as shown by

$$\begin{aligned} R_N(\tau) &= \int_{-f_c-B}^{-f_c+B} \frac{N_0}{2} \exp(j2\pi f_c \tau) df + \int_{f_c-B}^{f_c+B} \frac{N_0}{2} \exp(j2\pi f_c \tau) df \\ &= N_0B \operatorname{sinc}(2B\tau)[\exp(-j2\pi f_c \tau) + \exp(2\pi f_c \tau)] \\ &= 2N_0B \operatorname{sinc}(2B\tau) \cos(2\pi f_c \tau) \end{aligned} \quad (8.100)$$

This autocorrelation function of the ideal narrowband noise is plotted in Fig. 8.23(b).

From Property 4 of narrowband noise, the in-phase and quadrature components have an identical spectral density as shown in Fig. 8.23(c). The autocorrelation function of  $N_I(t)$  or  $N_Q(t)$  is therefore (see Example 8.13)

$$R_{N_I}(\tau) = R_{N_Q}(\tau) = 2N_0B \operatorname{sinc}(2B\tau) \quad (8.101)$$

#### ■ NOISE-EQUIVALENT BANDWIDTH

In Example 8.13, we observed that when a source of white noise of zero mean and power spectral density  $N_0/2$  is connected across the input of an ideal low-pass filter of bandwidth  $B$  and unity band-pass gain, the average output power (or equivalently  $R_N(0)$ ) is  $N_0B$ . In Example 8.14, we observed that when a similar source is connected to a low-pass  $RC$  filter, the corresponding average output power is  $N_0/(4RC)$ . For this filter, the 3-dB bandwidth is equal to  $1/(2\pi RC)$ . We may therefore make two important observations. First, the filtered white noise has finite average power. Second, the average power is proportional to bandwidth. We may generalize these observations to include all kinds of low-pass filters by defining the *noise-equivalent bandwidth* as follows.

Suppose a white noise source with spectrum  $S_W(f) = N_0/2$  is connected to the input of an arbitrary filter of transfer function  $H(f)$ . From Properties 1 and 4 of power spectral densities, the average output noise power is

$$\begin{aligned}
 P_N &= \int_{-\infty}^{\infty} |H(f)|^2 S_W(f) df \\
 &= \int_{-\infty}^{\infty} |H(f)|^2 \frac{N_0}{2} df \\
 &= N_0 \int_0^{\infty} |H(f)|^2 df
 \end{aligned} \tag{8.102}$$

where, in the last line, we have made use of the fact that the amplitude response  $|H(f)|$  is an even function of frequency. Now consider the same noise source connected to the input of an ideal low-pass filter of zero-frequency response  $H(0)$  and bandwidth  $B_N$  as illustrated in Fig. 8.24. In this case the average output noise power is

$$P_N = N_0 B_N |H(0)|^2 \tag{8.103}$$

By equating Eqs. (8.102) and (8.103), we determine the bandwidth  $B_N$  of the ideal filter that produces the same noise power as the arbitrary filter. Doing this, we obtain

$$B_N = \frac{\int_0^{\infty} |H(f)|^2 df}{|H(0)|^2} \tag{8.104}$$

The bandwidth  $B_N$  is called the *noise-equivalent bandwidth* for a low-pass filter. Thus, the procedure for calculating the noise-equivalent bandwidth consists of replacing the arbitrary low-pass filter of transfer function  $H(f)$  with an equivalent ideal low-pass filter of zero-frequency response  $H(0)$  and bandwidth  $B_N$ , as illustrated in Fig. 8.24.

In a similar way, we may define the *noise-equivalent bandwidth for a band-pass filter*, as illustrated in Fig. 8.25. This figure depicts the square amplitude response of the filter for positive frequencies only. Thus, the noise-equivalent bandwidth for a band-pass filter may be defined as

$$B_N = \frac{\int_0^{\infty} |H(f)|^2 df}{|H(f_c)|^2} \tag{8.105}$$

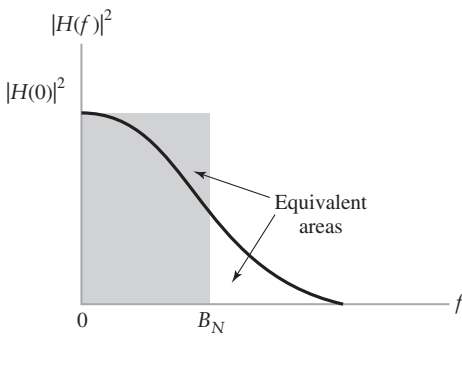


**FIGURE 8.24** Illustration of arbitrary low-pass filter  $H(f)$  and ideal low-pass filter of bandwidth  $B_N$ .

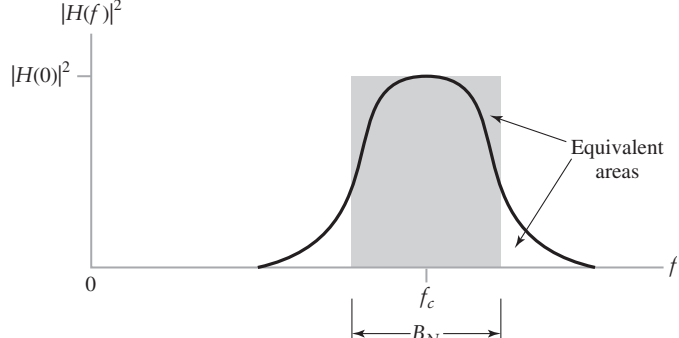


**FIGURE 8.25** Illustration of arbitrary bandpass filter  $H(f)$  and ideal bandpass filter of bandwidth  $B_N$ .

where  $|H(f_c)|^2$  is the center-frequency amplitude response of the filter. In fact, we recognize that Eq. (8.105) may be used to represent both cases by setting  $f_c = 0$  for low-pass filters. Then we have the general result

$$P_N = N_0 |H(f_c)|^2 B_N \quad (8.106)$$

and the effect of passing white noise through a filter may be separated into two parts:

- ▶ The center-frequency power gain  $|H(f_c)|^2$ .
- ▶ The noise equivalent bandwidth  $B_N$ , representing the *frequency selectivity* of the filter.

This separation applies whether the filter is low-pass or band-pass. Hence, as a general rule we may say that effect of noise in the system is reduced by narrowing the system bandwidth.

#### EXAMPLE 8.16 Noise Equivalent Bandwidth of RC Filter

Consider the single-pole low-pass filter of Example 8.14. The transfer function of this filter is

$$H(f) = \frac{1}{1 + j2\pi fRC}$$

We wish to find the noise equivalent bandwidth of this filter.

The noise equivalent bandwidth of this filter is

$$\begin{aligned} B_N &= \frac{1}{|H(0)|^2} \int_0^\infty |H(f)|^2 df \\ &= 1 \times \int_0^\infty \frac{df}{1 + (2\pi fRC)^2} \end{aligned}$$

Recognizing the integrand as the scaled derivative of  $\tan^{-1}(f)$ , we obtain

$$\begin{aligned} B_N &= \frac{1}{2\pi RC} \tan^{-1}(2\pi fRC) \Big|_0^\infty \\ &= \frac{1}{2\pi RC} \left( \frac{\pi}{2} - 0 \right) \\ &= \frac{1}{4RC} \end{aligned}$$

Due to the slow roll-off of the single-pole filter, the noise bandwidth is slightly larger than its 3-dB bandwidth,  $B_{3dB} = 1/(2\pi RC)$ .

## 8.12 Summary and Discussion

We began this chapter by indicating that information and noise are both random signals; indeed, it is this randomness or unpredictability that is a key property of communication systems. However, even random signals have statistical characteristics that may be measured. We subsequently presented several important tools for characterizing random signals.

We introduced a random experiment as a model for unpredictable phenomena; and the relative frequency definition of probability as a means of assigning a likelihood to the outcome of a random experiment. This led to the three basic axioms of probability theory.

Random variables were introduced as a function whose domain is the sample space of the random experiment and whose range is the real numbers. Random variables provide a method to unify the treatment of a wide variety of random experiments. Probability distribution and density functions were shown as fundamental methods of characterizing a random variable.

The study of functions of random variables led naturally to the concept of expectation and the statistical moments and covariance of random variables.

Gaussian random variables were introduced as a particular important type of random variable in the study of communication systems.

Considering time as parameter in random signals led to the study of random processes. A random process was defined as a family of random variables indexed by time as a parameter. Stationary, ergodic, and wide-sense stationary random processes were introduced as models of most physical processes exhibiting random behavior. It was shown that wide-sense stationary random processes have many of the properties of deterministic power signals, including the fact that the Weiner–Khintchine formulas relate the spectrum of the random process to its autocorrelation.

Gaussian processes and white noise were introduced as important random processes in the analysis of communication systems.

Finally, it was shown that, similar to deterministic signals, we may consider bandpass or narrowband versions of noise. This narrowband noise has in-phase and quadrature components, similar to deterministic signals.

This chapter has been a brief and certainly not complete introduction to the random signals and noise that are commonly found in communication systems, but the treatment presented herein is adequate for an introductory treatment of statistical communication theory. The two subsequent chapters will illustrate the importance of the material presented in this chapter in designing receivers and evaluating communication system performance.

## ADDITIONAL PROBLEMS

- 8.18 Consider a deck of 52 cards, divided into four different suits, with 13 cards in each suit ranging from the two up through the ace. Assume that all the cards are equally likely to be drawn.
  - (a) Suppose that a single card is drawn from a full deck. What is the probability that this card is the ace of diamonds? What is the probability that the single card drawn is an ace of any one of the four suits?
  - (b) Suppose that two cards are drawn from the full deck. What is the probability that the cards drawn are an ace and a king, not necessarily the same suit? What if they are of the same suit?
- 8.19 Suppose a player has one red die and one white die. How many outcomes are possible in the random experiment of tossing the two dice? Suppose the dice are indistinguishable, how many outcomes are possible?
- 8.20 Refer to Problem 8.19.
  - (a) What is the probability of throwing a red 5 and a white 2?
  - (b) If the dice are indistinguishable, what is the probability of throwing a sum of 7? If they are distinguishable, what is this probability?
- 8.21 Consider a random variable  $X$  that is uniformly distributed between the values of 0 and 1 with probability  $\frac{1}{4}$ , takes on the value 1 with probability  $\frac{1}{4}$ , and is uniformly distributed between values 1 and 2 with probability  $\frac{1}{2}$ . Determine the distribution function of the random variable  $X$ .

- 8.22 Consider a random variable  $X$  defined by the double-exponential density

$$f_X(x) = a \exp(-b|x|), \quad -\infty < x < \infty$$

where  $a$  and  $b$  are constants.

- (a) Determine the relationship between  $a$  and  $b$  so that  $f_X(x)$  is a probability density function.
- (b) Determine the corresponding distribution function  $F_X(x)$ .
- (c) Find the probability that the random variable  $X$  lies between 1 and 2.

- 8.23 Show that the expression for the variance of a random variable can be expressed in terms of the first and second moments as

$$\text{Var}(X) = E[X^2] - E[X]^2$$

- 8.24 A random variable  $R$  is Rayleigh distributed with its probability density function given by

$$f_R(r) = \begin{cases} \frac{r}{b} \exp\left(-\frac{r^2}{2b}\right), & 0 < r < \infty \\ 0, & \text{otherwise} \end{cases}$$

- (a) Determine the corresponding distribution function  $F_R(r)$ .
- (b) Show that the mean of  $R$  is equal to  $\sqrt{b\pi/2}$ .
- (c) What is the mean-square value of  $R$ ?
- (d) What is the variance of  $R$ ?

- 8.25 Consider a uniformly distributed random variable  $Z$ , defined by

$$f_Z(z) = \begin{cases} \frac{1}{2\pi}, & 0 \leq z \leq 2\pi \\ 0, & \text{otherwise} \end{cases}$$

The two random variables  $X$  and  $Y$  are related to  $Z$  by  $X = \sin(Z)$  and  $Y = \cos(Z)$ .

- (a) Determine the probability density functions of  $X$  and  $Y$ .
- (b) Show that  $X$  and  $Y$  are uncorrelated random variables.
- (c) Are  $X$  and  $Y$  statistically independent? Why?

- 8.26 A Gaussian random variable has zero mean and a standard deviation of 10 V. A constant voltage of 5 V is added to this random variable.

- (a) Determine the probability that a measurement of this composite signal yields a positive value.
- (b) Determine the probability that the arithmetic mean of two independent measurements of this signal is positive.

- 8.27 Consider a random process  $X(t)$  defined by

$$X(t) = \sin(2\pi Wt)$$

in which the frequency  $W$  is a random variable with the probability density function

$$f_W(w) = \begin{cases} \frac{1}{B}, & 0 \leq w \leq B \\ 0, & \text{otherwise} \end{cases}$$

Show that  $X(t)$  is nonstationary.

- 8.28 Consider the sinusoidal process

$$X(t) = A \cos(2\pi f_c t)$$

where the frequency  $f_c$  is constant and the amplitude  $A$  is uniformly distributed:

$$f_A(a) = \begin{cases} 1, & 0 \leq a \leq 1 \\ 0, & \text{otherwise} \end{cases}$$

Determine whether or not this process is stationary in the strict sense.

- 8.29 A random process  $X(t)$  is defined by

$$X(t) = A \cos(2\pi f_c t)$$

where  $A$  is a Gaussian random variable of zero mean and variance  $\sigma_A^2$ . This random process is applied to an ideal integrator, producing an output  $Y(t)$  defined by

$$Y(t) = \int_0^t X(\tau) d\tau$$

- (a) Determine the probability density function of the output  $Y(t)$  at a particular time  $t_k$ .
- (b) Determine whether or not  $Y(t)$  is stationary.

- 8.30 Prove the following two properties of the autocorrelation function  $R_X(\tau)$  of a random process  $X(t)$ :

- (a) If  $X(t)$  contains a dc component equal to  $A$ , then  $R_X(\tau)$  contains a constant component equal to  $A^2$ .
- (b) If  $X(t)$  contains a sinusoidal component, then  $R_X(\tau)$  also contains a sinusoidal component of the same frequency.

- 8.31 A discrete-time random process  $\{Y_n\}$  is defined by

$$Y_n = \alpha Y_{n-1} + W_n, \quad n = \dots, -1, 0, +1, \dots$$

where the zero-mean random process  $\{W_n\}$  is stationary with autocorrelation function  $R_W(k) = \sigma^2 \delta(k)$ . What is the autocorrelation function  $R_Y(k)$  of  $Y_n$ ? Is  $Y_n$  a wide-sense stationary process? Justify your answer.

- 8.32 Find the power spectral density of the process that has the autocorrelation function

$$R_X(\tau) = \begin{cases} \sigma^2(1 - |\tau|), & \text{for } |\tau| \leq 1 \\ 0, & \text{for } |\tau| > 1 \end{cases}$$

- 8.33 A random pulse has amplitude  $A$  and duration  $T$  but starts at an arbitrary time  $t_0$ . That is, the random process is defined as

$$X(t) = A \operatorname{rect}(t + t_0)$$

where  $\operatorname{rect}(t)$  is defined in Section 2.9. The random variable  $t_0$  is assumed to be uniformly distributed over  $[0, T]$  with density

$$f_{t_0}(s) = \begin{cases} \frac{1}{T}, & 0 \leq s \leq T \\ 0, & \text{otherwise} \end{cases}$$

- (a) What is the autocorrelation function of the random process  $X(t)$ ?
- (b) What is the spectrum of the random process  $X(t)$ ?

- 8.34 Given that a stationary random process  $X(t)$  has an autocorrelation function  $R_X(\tau)$  and a power spectral density  $S_X(f)$ , show that:

- (a) The autocorrelation function of  $dx(t)/dt$ , the first derivative of  $X(t)$ , is equal to the negative of the second derivative of  $R_X(\tau)$ .
- (b) The power spectral density of  $dx(t)/dt$ , is equal to  $4\pi^2 f^2 S_X(f)$ .

*Hint:* See the solution to problem 2.24

- 8.35 Consider a wide-sense stationary process  $X(t)$  having the power spectral density  $S_X(f)$  shown in Fig. 8.26. Find the autocorrelation function  $R_X(\tau)$  of the process  $X(t)$ .

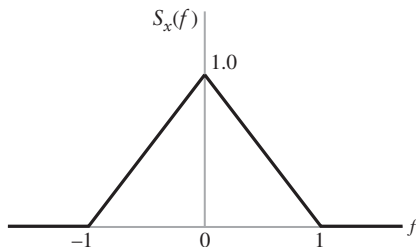


FIGURE 8.26 Problem 8.35.

- 8.36 The power spectral density of a random process  $X(t)$  is shown in Fig. 8.27.
- Determine and sketch the autocorrelation function  $R_X(\tau)$  of  $X(t)$ .
  - What is the dc power contained in  $X(t)$ ?
  - What is the ac power contained in  $X(t)$ ?
  - What sampling rates will give uncorrelated samples of  $X(t)$ ? Are the samples statistically independent?

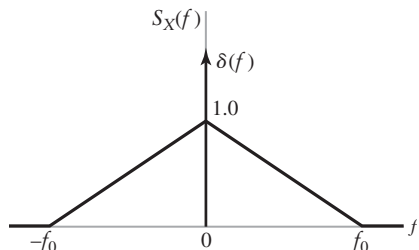


FIGURE 8.27 Problem 8.36.

- 8.37 Consider the two linear filters shown in cascade as in Fig. 8.28. Let  $X(t)$  be a stationary process with autocorrelation function  $R_X(\tau)$ . The random process appearing at the first filter output is  $V(t)$  and that at the second filter output is  $Y(t)$ .
- Find the autocorrelation function of  $V(t)$ .
  - Find the autocorrelation function of  $Y(t)$ .

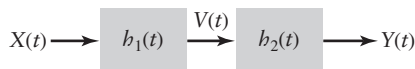


FIGURE 8.28 Problem 8.37.

- 8.38 The power spectral density of a narrowband random process  $X(t)$  is as shown in Fig. 8.29. Find the power spectral densities of the in-phase and quadrature components of  $X(t)$ , assuming  $f_c = 5$  Hz.

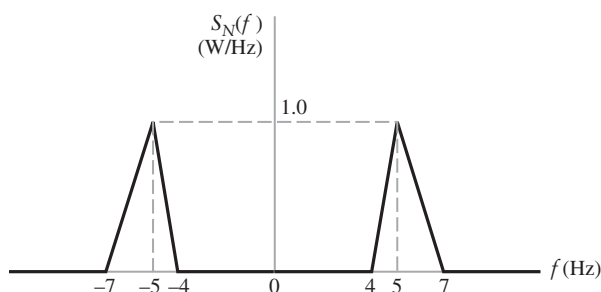


FIGURE 8.29 Problem 8.38.

- 8.39 Assume the narrowband process  $X(t)$  described in Problem 8.38 is Gaussian with zero mean and variance  $\sigma_X^2$ .
- Calculate  $\sigma_X^2$ .
  - Determine the joint probability density function of the random variables  $Y$  and  $Z$  obtained by observing the in-phase and quadrature components of  $X(t)$  at some fixed time.

### ADVANCED PROBLEMS

---

- 8.40 Find the probability that the last two digits of the cube of a natural number (1, 2, 3, ...) will be 01.
- 8.41 Consider the random experiment of selecting a number uniformly distributed over the range  $\{1, 2, 3, \dots, 120\}$ . Let  $A$ ,  $B$ , and  $C$  be the events that the selected number is a multiple of 3, 4, and 6, respectively.
- What is the probability of event  $A$ —that is,  $P[A]$ ?
  - What is  $P[B]??$
  - What is  $P[A \cap B]$ ?
  - What is  $P[A \cup B]$ ?
  - What is  $P[A \cap C]$ ?
- 8.42 A message consists of ten 0s and 1s.
- How many such messages are there?
  - How many such messages are there that contain exactly four 1s?
  - Suppose the 10th bit is not independent of the others but is chosen such that the modulo-2 sum of all the bits is zero. This is referred to as an even-parity sequence. How many such even-parity sequences are there?
  - If this ten-bit even-parity sequence is transmitted over a channel that has a probability of error  $p$  for each bit. What is the probability that the received sequence contains an undetected error?
- 8.43 The probability that an event occurs at least once in four independent trials is equal to 0.59. What is the probability of occurrence of the event in one trial, if the probabilities are equal in all trials?
- 8.44 The arrival times of two signals at a receiver are uniformly distributed over the interval  $[0, T]$ . The receiver will be jammed if the time difference in the arrivals is less than  $\tau$ . Find the probability that the receiver will be jammed.
- 8.45 A telegraph system (an early version of digital communications) transmits either a dot or dash signal. Assume the transmission properties are such that  $2/5$  of the dots and  $1/3$  of the dashes are received incorrectly. Suppose the ratio of transmitted dots to transmitted dashes is 5 to 3. What is the probability that a received signal is as transmitted if:
- The received signal is a dot?
  - The received signal is a dash?
- 8.46 Four radio signals are emitted successively. The probability of reception for each of them is independent of the reception of the others and equal, respectively, 0.1, 0.2, 0.3, and 0.4. Find the probability that  $k$  signals will be received where  $k = 1, 2, 3, 4$ .
- 8.47 In a computer-communication network, the arrival time  $\tau$  between messages is modeled with an exponential distribution function having the density

$$f_T(\tau) = \begin{cases} \frac{1}{\lambda} e^{-\lambda\tau}, & \tau \geq 0 \\ 0, & \text{otherwise} \end{cases}$$

- (a) What is the mean time between messages with this distribution?  
 (b) What is the variance in this time between messages?
- 8.48 If  $X$  has a density  $f_X(x)$ , find the density of the random variable  $Y$  defined as follows:
- $Y = aX + b$  for constants  $a$  and  $b$ .
  - $Y = X^2$ .
  - $Y = \sqrt{X}$ , assuming  $X$  is a nonnegative random variable.
- 8.49 Let  $X$  and  $Y$  be two independent random variables with density functions  $f_X(x)$  and  $f_Y(y)$ , respectively. Show that the random variable  $Z = X + Y$  has a density function given by

$$f_Z(z) = \int_{-\infty}^0 f_Y(z-s) f_X(s) ds$$

*Hint:  $\mathbf{P}[Z \leq z] = P[X \leq z, Y \leq z - X]$*

- 8.50 Find the spectral density  $S_Z(f)$  if

$$Z(t) = X(t) + Y(t)$$

where  $X(t)$  and  $Y(t)$  are independent zero-mean random processes with

$$R_X(\tau) = a_1 e^{-\alpha_1 |\tau|}, \quad \text{and} \quad R_Y(\tau) = a_2 e^{-\alpha_2 |\tau|}.$$

- 8.51 Consider a random process  $X(t)$  defined by

$$X(t) = \sin(2\pi f_c t)$$

where the frequency  $f_c$  is a random variable uniformly distributed over the interval  $[0, W]$ . Show that  $X(t)$  is nonstationary. *Hint: Examine specific sample functions of the random process  $X(t)$  for, say, the frequencies  $W/4$ ,  $W/2$ , and  $W$ .*

- 8.52 The oscillators used in communication systems are not ideal but often suffer from a distortion known as *phase noise*. Such an oscillator may be modeled by the random process

$$Y(t) = A \cos(2\pi f_c t + \phi(t))$$

where  $\phi(t)$  is a slowly varying random process. Describe and justify the conditions on the random process  $\phi(t)$  such that  $Y(t)$  is wide-sense stationary.

- 8.53 A baseband signal is disturbed by an additive noise process  $N(t)$  as shown by

$$X(t) = A \sin(0.3\pi t) + N(t)$$

where  $N(t)$  is a stationary Gaussian process of zero mean and variance  $\sigma^2$ .

- (a) Determine the density functions of the random variables  $X_1$  and  $X_2$  where

$$X_1 = X(t)|_{t=1}$$

$$X_2 = X(t)|_{t=2}$$

- (b) The noise process  $N(t)$  has an autocorrelation function given by

$$R_N(\tau) = \sigma^2 \exp(-|\tau|)$$

Determine the joint density function of  $X_1$  and  $X_2$ , that is,  $f_{X_1, X_2}(x_1, x_2)$ .

**■ COMPUTER EXPERIMENTS**

- 8.54 For this die-tossing experiment, a MATLAB script is included in Appendix 7. The MATLAB script simulates the tossing of a biased die 1000 times. The steps to the script are:

- ▶ Roll the die  $N$  times and save the results in  $X$ .
- ▶ Compute a histogram on  $X$  to obtain the probabilities of the different faces.

Repeat the experiment for  $N = 10, 100, 1000$ , and 10,000. Comment on the relative frequency definition of probability as a function of  $N$ , the number of throws.

- 8.55 To demonstrate the central limit theorem, we compute 20,000 samples of  $Z$  for  $N = 5$ , and estimate the corresponding probability density function by forming a histogram of the results. A MATLAB script for performing this is included in Appendix 7. Compare this histogram (scaled for unit area) to the Gaussian density function having the same mean and variance.

- 8.56 Revise the script for Problem 8.55 to find the distribution of a sum of Bernoulli random variables. Compare it to the Gaussian distribution as  $N$  becomes large.

- 8.57 Revise the script for Problem 8.55 so the mean values are not identical but have a random distribution as well, but with the same overall mean. Compute the distribution of the sum.

- 8.58 In this computer experiment, we will simulate a Gaussian random process digitally. A MATLAB script in Appendix 7 generates a discrete-time white Gaussian process and filters it with a discrete-time root-raised cosine filter (as discussed in Chapter 6). In the script, we perform the following steps:

- Generate a discrete-time white Gaussian process.
- Filter this Gaussian process with a root-raised cosine filter having 25 percent excess bandwidth.
- Compute the spectrum of the resulting discrete-time process.
- Compute the autocorrelation of the resulting discrete-time process.

- (a) Determine the autocorrelation of the filtered sequence.  
(b) Determine the spectrum of the filtered sequence.

Comment on the results.

## CHAPTER 9

# NOISE IN ANALOG COMMUNICATIONS

In this chapter, we revisit the analog modulation methods of Chapters 3 and 4 in light of the noise-related concepts introduced in Chapter 8. In practice, we find that modulated signals, regardless of their kind, are perturbed by noise and by the imperfect characteristics of the channel during transmission. Noise can broadly be defined as any unknown signal that affects the recovery of the desired signal. There may be many sources of noise in a communication system, but often the major sources are the communication devices themselves or interference encountered during the course of transmission. There are several ways that noise can affect the desired signal, but one of the most common ways is as an additive distortion. That is, the received signal is modeled as<sup>1</sup>

$$r(t) = s(t) + w(t) \quad (9.1)$$

where  $s(t)$  is the transmitted signal and  $w(t)$  is the additive noise. If we knew the noise exactly, then we could subtract it from  $r(t)$  and recover the transmitted signal exactly. Unfortunately, this is rarely the case. Much of communication system design is related to processing the received signal  $r(t)$  in a manner that minimizes the effect of additive noise.

This chapter will focus on the detection of analog signals in the presence of additive noise. The material in this chapter teaches us the following lessons.

- *Lesson 1: Minimizing the effects of noise is a prime concern in analog communications, and consequently the ratio of signal power to noise power is an important metric for assessing analog communication quality.*
- *Lesson 2: Amplitude modulation may be detected either coherently requiring the use of a synchronized oscillator or non-coherently by means of a simple envelope detector. However, there is a performance penalty to be paid for non-coherent detection.*
- *Lesson 3: Frequency modulation is nonlinear and the output noise spectrum is parabolic when the input noise spectrum is flat. Frequency modulation has the advantage that it allows us to trade bandwidth for improved performance.*
- *Lesson 4: Pre- and de-emphasis filtering is a method of reducing the output noise of an FM demodulator without distorting the signal. This technique may be used to significantly improve the performance of frequency modulation systems.*

---

<sup>1</sup>In this chapter and the following, we use lowercase letters for random signals with the understanding that they represent sample functions of the underlying random processes.

## 9.1 Noise in Communication Systems

Before we look at techniques for minimizing the effects of noise, we will review some of the properties of noise. In Chapter 8, we identified noise as a random process but, even though a noise process is unpredictable, there are still methods of characterizing its behavior. In particular, we may use statistical parameters such as:

- ▶ *The mean of the random process.* For noise, the mean value corresponds to the *dc offset*. In most communication systems, dc offsets are removed by design since they require power and carry little information. Consequently, both noise and signal are generally assumed to have zero mean.
- ▶ *The autocorrelation of the random process.* In Chapter 11, we will describe physical models for receiver noise and means of characterizing it. As it turns out, *white noise*, as described in Chapter 8, is often a good mathematical model for receiver noise, and we will use this model extensively in Chapters 9 and 10. With white noise, samples at one instant in time are uncorrelated with those at another instant in time regardless of the separation; that is, the autocorrelation of white noise is described by

$$R_w(\tau) = \frac{N_0}{2} \delta(\tau) \quad (9.2)$$

where  $\delta(\tau)$  is the Dirac delta function and  $N_0/2$  is the two-sided power spectral density.

- ▶ *The spectrum of the random process.* For additive white Gaussian noise the spectrum is flat and defined as

$$S_w(f) = \frac{N_0}{2} \quad (9.3)$$

The Weiner–Khintchine relations state that the spectrum of Eq. (9.3) is the Fourier transform of the autocorrelation function of Eq. (9.2).

Given the characteristics of the noise, we must determine how it affects the received signal. To compute noise power, we must measure the noise over a specified bandwidth. We have seen that the noise power at the output of a filter of equivalent-noise bandwidth  $B_T$  is

$$N = N_0 B_T \quad (9.4)$$

where, for convenience of presentation, we have assumed that  $|H(f_c)| = 1$ . Clearly, the smaller the bandwidth  $B_T$ , the smaller the noise power  $N$  will be. Relating this back to the detection of the received signal  $r(t) = s(t) + w(t)$  of Eq. (9.1), it seems intuitive that we should make  $B_T$  as small as possible to minimize the noise but it should be no smaller than the bandwidth of  $s(t)$ , otherwise we will distort the desired signal.

This situation is illustrated in Fig. 9.1, where the transmitted signal is distorted by additive white noise and the combination is passed through a filter of bandwidth  $B_T$ . If the

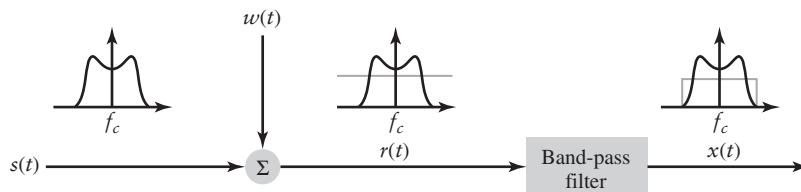


**FIGURE 9.1** Block diagram of signal plus noise before and after filtering, showing spectra at each point.

filter bandwidth is greater than the signal bandwidth, then we retain all of the desired signal energy. However, if the filter is no larger than required to pass the signal undistorted, then it will minimize the amount of noise passed. Consequently, the bandwidth  $B_T$  is referred to as the transmission bandwidth of the signal. The matching of the receiver filter to the bandwidth of the transmitted signal is the basis of many optimum detection schemes.

In the following, we shall represent the signal after initial filtering as  $x(t) = s(t) + n(t)$  where  $n(t)$  is narrowband noise, as contrasted to  $w(t)$ , which is assumed to be white.

## 9.2 Signal-To-Noise Ratios

Given that communication deals with random signals—with randomness being a quality of both the information being transmitted and the noise hampering the transmission—how do we quantify the performance of a particular communication system? In this chapter, we will focus on *signal-to-noise ratio* (SNR) as the measure of quality for analog systems; this statistical parameter has importance in digital systems as well, as we shall see in Chapter 10.

As described above and repeated below for convenience, the received signal in many communication systems can be modeled as the sum of the desired signal,  $s(t)$ , and a narrowband noise signal,  $n(t)$ , as shown by

$$x(t) = s(t) + n(t) \quad (9.5)$$

Both of the terms on the right-hand side of Eq. (9.5) are random. The signal is random due to the unpredictability of its information content, and the noise is random for reasons described in Section 9.1. In Chapter 8, we saw that the two simplest parameters for partially describing a random variable are the mean and variance. For reasons described previously, dc offsets are assumed to be zero. Consequently, for zero-mean processes, a simple measure of the signal quality is the ratio of the variances of the desired and undesired signals. On this basis, the signal-to-noise ratio is formally defined by

$$\text{SNR} = \frac{\mathbf{E}[s^2(t)]}{\mathbf{E}[n^2(t)]} \quad (9.6)$$

where  $\mathbf{E}$  is the expectation operator. For a communication signal, a squared signal level is usually proportional to power. Consequently, the signal-to-noise ratio is often considered to be a ratio of the average signal power to the average noise power. Equivalently, it can be considered to be a ratio of the average signal energy per unit time to the average noise energy per unit time; this latter interpretation is more common in digital communication systems. If we happen to be using a complex representation of the signals and noise, then instead of squared values, Eq. (9.6) would use magnitude-squared values.

### EXAMPLE 9.1 Sinusoidal Signal-to-Noise Ratio

Consider the case where the transmitted signal in Eq. (9.5) is

$$s(t) = A_c \cos(2\pi f_c t + \theta)$$

where the phase  $\theta$  is unknown at the receiver. The signal is received in the presence of additive noise as shown in Fig. 9.2. The noise is white and Gaussian with power spectral density  $N_0/2$ .

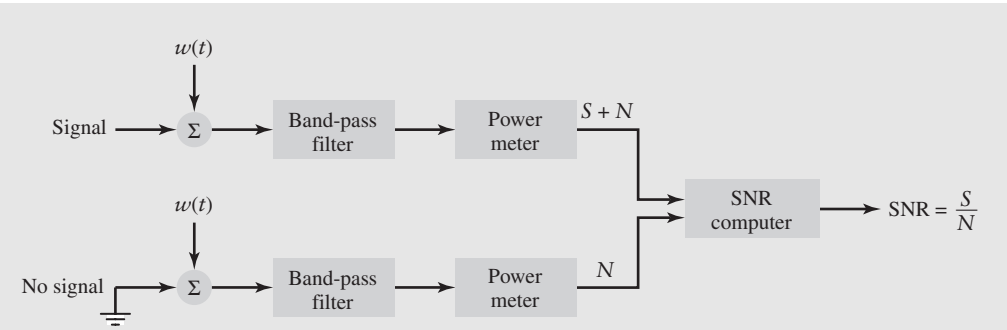


**FIGURE 9.2** SNR measurement scheme for Example 9.1.

In this case, although the signal is random, it is also periodic. Consequently, we can estimate its average power by integrating over one cycle (i.e., equating an ensemble average with a time average).

$$\begin{aligned}
 E[s^2(t)] &= \frac{1}{T} \int_0^T (A_c \cos(2\pi f_c t + \theta))^2 dt \\
 &= \frac{A_c^2}{2T} \int_0^T (1 + \cos(4\pi f_c t + 2\theta)) dt \\
 &= \frac{A_c^2}{2T} \left[ t + \frac{\sin(4\pi f_c t + 2\theta)}{4\pi f_c} \right]_0^T \\
 &= \frac{A_c^2}{2}
 \end{aligned} \tag{9.7}$$

Theoretically, the white noise extends to infinite frequency. The narrowband noise process,  $n(t)$ , is the result of passing the white noise process through a band-pass filter with noise-equivalent bandwidth  $B_T$ . Under this assumption, we compute the noise power

$$\begin{aligned}
 E[n^2(t)] &= N \\
 &= N_0 B_T
 \end{aligned} \tag{9.8}$$

Substituting the results of Eqs. (9.7) and (9.8) into (9.6), the signal-to-noise ratio becomes

$$\text{SNR} = \frac{A_c^2}{2N_0 B_T} \tag{9.9}$$

Since the bandwidth of the signal is arbitrarily narrow in this example, the choice of the bandwidth  $B_T$  is somewhat arbitrary. Consequently, in practice, the related *carrier-to-noise density ratio* is defined by

$$\frac{C}{N_0} = \frac{A_c^2}{2N_0} \tag{9.10}$$

which is not dimensionless like the SNR, but it is independent of the choice of bandwidth. The  $C/N_0$  ratio has units of hertz where  $N_0$  is measured in watts per hertz and the carrier power  $C = A_c^2/2$  is measured in watts.

The signal-to-noise ratio is clearly measured at the receiver, but there are several points in the receiver where the measurement may be carried out. In fact, measurements

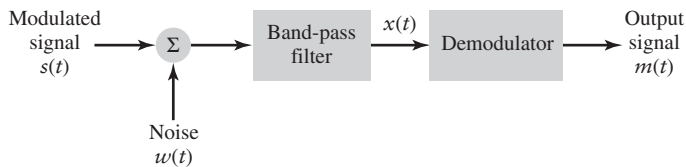


**FIGURE 9.3** High-level block diagram of a communications receiver.

at particular points in the receiver have their own particular importance and value. For instance:

- ▶ If the signal-to-noise ratio is measured at the front-end of the receiver, then it is usually a measure of the quality of the transmission link and the receiver front-end.
- ▶ If the signal-to-noise ratio is measured at the output of the receiver, it is a measure of the quality of the recovered information-bearing signal whether it be audio, video, or otherwise.

To illustrate these two points, consider the block diagram of a typical analog communication receiver presented in Fig. 9.3. The signal plus white Gaussian noise is passed through a band-pass filter to produce the band-pass signal,  $x(t)$ . The signal  $x(t)$  is processed by the demodulator to recover the original message signal  $m(t)$ . The SNR measured at the input to the demodulator is referred to as the *pre-detection signal-to-noise ratio*.

Of equal or greater importance is the signal-to-noise ratio of the recovered message at the output of the demodulator. This metric defines the quality of the signal that is delivered to the end user. We refer to this output SNR as the *post-detection signal-to-noise ratio*. It should be noted that the signal and noise characteristics may differ significantly between the pre-detection and post-detection calculations.

The calculation of the post-detection signal-to-noise ratio involves the use of an idealized receiver model, the details of which naturally depend on the channel noise and the type of demodulation used in the receiver. We will have more to say on these issues in subsequent sections of the chapter. In order to compare different analog modulation-demodulation schemes, we introduce the idea of a *reference transmission model* as depicted in Fig. 9.4. This reference model is equivalent to transmitting the message at baseband. In this model, two assumptions are made:

1. The message power is the same as the modulated signal power of the modulation scheme under study.
  2. The baseband low-pass filter passes the message signal and rejects out-of-band noise.
- Accordingly, we may define the *reference signal-to-noise ratio*,  $\text{SNR}_{\text{ref}}$ , as

$$\text{SNR}_{\text{ref}} = \frac{\text{average power of the modulated message signal}}{\text{average power of noise measured in the message bandwidth}} \quad (9.11)$$

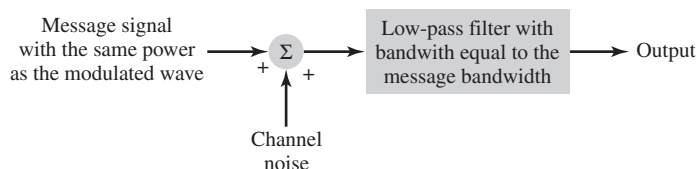


**FIGURE 9.4** Reference transmission model for analog communications.

The reference signal-to-noise ratio of Eq. (9.11) may be used to compare different modulation–demodulation schemes by using it to normalize the post-detection signal-to-noise ratios. That is, we may define a *figure of merit* for a particular modulation–demodulation scheme as follows:

$$\text{Figure of merit} = \frac{\text{post-detection SNR}}{\text{reference SNR}}$$

Clearly, the higher the value that the figure of merit has, the better the noise performance of the receiver will be.

To summarize our consideration of signal-to-noise ratios:

- The pre-detection SNR is measured before the signal is demodulated.
- The post-detection SNR is measured after the signal is demodulated.
- The reference SNR is defined on the basis of a baseband transmission model.
- The figure of merit is a dimensionless metric for comparing different analog modulation–demodulation schemes and is defined as the ratio of the post-detection and reference SNRs.

- **Drill Problem 9.1** In practice, we often cannot measure the signal by itself but must measure the signal plus noise. Explain how the SNR would be calculated in this case. ◀

## 9.3 Band-Pass Receiver Structures

In a band-pass communication system, the information is transmitted on some carrier frequency, typically using an arrangement similar to the left-hand side of Fig. 9.5. The transmitter includes a modulator that produces an output at a standard intermediate frequency (IF) and a local mixer-translates (up-converts) this output to a “channel” or radio frequency (RF).

The right-hand side of Fig. 9.5 shows an example of a *superheterodyne receiver* that was discussed in Section 3.9. At the receiver, a tunable local oscillator frequency-translates (down-converts) this channel frequency to a standard intermediate frequency (IF) for demodulation. Common examples are AM radio transmissions, where the RF channels’ frequencies lie in the range between 510 and 1600 kHz, and a common IF is 455 kHz; another example is FM radio, where the RF channels are in the range from 88 to 108 MHz and the IF is typically 10.7 MHz.

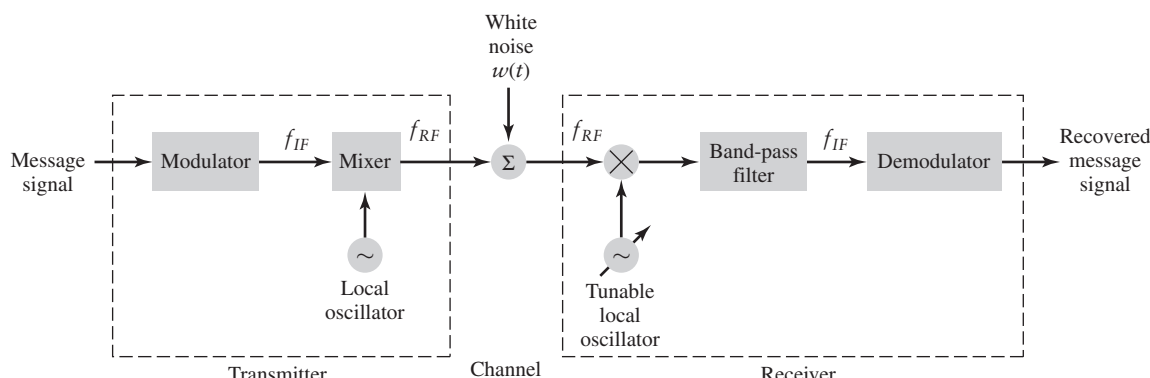


**FIGURE 9.5** Block diagram of band-pass transmission showing a superheterodyne receiver.

In Chapter 3, we saw how to represent band-pass signals using the in-phase and quadrature representation with

$$s(t) = s_I(t) \cos(2\pi f_c t) - s_Q(t) \sin(2\pi f_c t) \quad (9.12)$$

where  $s_I(t)$  is the in-phase component of  $s(t)$ , and  $s_Q(t)$  is its quadrature component. Most receivers immediately limit the white noise power by processing the received signal with a band-pass filter as shown in Fig. 9.5. Typically, there is a band-pass filter before and after the local oscillator. The filter preceding the local oscillator is centered at a higher RF frequency and is usually much wider, wide enough to encompass all RF channels that the receiver is intended to handle. For example, with an FM receiver the band-pass filter preceding the local oscillator would pass the frequencies from 88 to 108 MHz. The band-pass filter following the oscillator passes the signal of a single RF channel relatively undistorted but limits the noise to those components within the passband of the filter. With the same FM receiver, the band-pass filter after the local oscillator would be approximately 200 kHz wide; it is the effects of this narrower filter that are of most interest to us.

## 9.4 Noise in Linear Receivers Using Coherent Detection

In Chapter 3, we looked at the generation and detection of amplitude-modulated signals. A variety of amplitude-modulated signals were considered therein, with their demodulation depending upon whether the carrier was present in the transmitter signal or not. In the case of double-sideband suppressed-carrier (DSB-SC) modulation, the modulated signal is represented as

$$s(t) = A_c m(t) \cos(2\pi f_c t + \theta) \quad (9.13)$$

where  $f_c$  is the carrier frequency, and  $m(t)$  is the message signal; the carrier phase  $\theta$  is a random variable, but not varying during the course of transmission. For suppressed-carrier signals, linear coherent detection was identified as the proper demodulation strategy. In particular, a linear receiver for this signal could be implemented as shown in Fig. 9.6.

In Fig. 9.6, the received RF signal is the sum of the modulated signal and white Gaussian noise  $w(t)$ . The received signal is down-converted to an IF by multiplication with a sinusoid of frequency  $f_c - f_{RF}$ . This down-conversion is performed by the product modulator shown as mixer 1 in Fig. 9.6. After band-pass filtering, the resulting signal is

$$x(t) = s(t) + n(t) \quad (9.14)$$

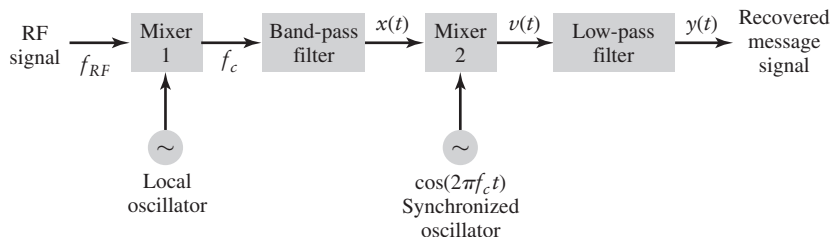


**FIGURE 9.6** A linear DSB-SC receiver using coherent demodulation.

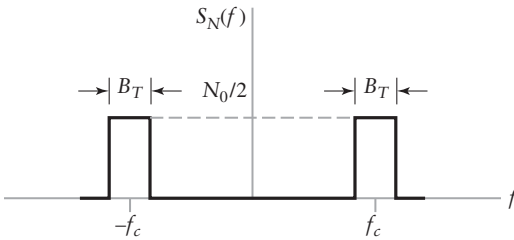


**FIGURE 9.7** Power spectral density of band-pass noise.

where  $s(t)$  is the undistorted modulated signal and  $n(t)$  is the band-pass noise at the output of the filter. The assumed power spectral density of the band-pass noise is illustrated in Fig. 9.7. Equation 9.14 assumes that the band-pass filter has a sufficiently wide and flat passband that does not cause any significant distortion to the modulated signal. This equation also assumes that the gain of the filter is unity. In practice, the filter gain will often differ from unity but will affect the signal and noise equally, so there is no loss of generality by assuming that the gain is unity.

### ■ PRE-DETECTION SNR

For analog signals, our measure of quality is the signal-to-noise ratio. For the signal  $s(t)$  of Eq. (9.13), the average power of the signal component is given by expected value of the squared magnitude. Since the carrier and modulating signal are independent, this can be broken down into two components as follows:

$$\mathbf{E}[s^2(t)] = \mathbf{E}[(A_c \cos(2\pi f_c t + \theta))^2] \mathbf{E}[m^2(t)] \quad (9.15)$$

If we let

$$P = \mathbf{E}[m^2(t)] \quad (9.16)$$

be the average signal (message) power and using the result of Example 9.1 for the first factor of Eq. (9.15), we have

$$\mathbf{E}[s^2(t)] = \frac{A_c^2 P}{2} \quad (9.17)$$

That is, the average received signal power due to the modulated component is  $A_c^2 P / 2$ . The signal  $s(t)$  is the output of a product modulator that has its inputs  $A_c \cos(2\pi f_c t + \theta)$  and  $m(t)$ , both of which have units of volts. Due to internal scaling, the output of this product modulator has units of volts, not volts-squared. Consequently, the expression for  $\mathbf{E}[s^2(t)]$  has units of power not power-squared.

If the band-pass filter has a noise bandwidth  $B_T$ , then the noise power passed by this filter is by definition  $N_0 B_T$ . Consequently, the signal-to-noise ratio of the signal is

$$\text{SNR}_{\text{pre}}^{\text{DSB}} = \frac{A_c^2 P}{2N_0 B_T} \quad (9.18)$$

This is the *pre-detection signal-to-noise ratio* of the DSB-SC system because it is measured at a point in the system before the message signal  $m(t)$  is demodulated.

### ■ POST-DETECTION SNR

Next, we wish to determine the post-detection or output SNR of the DSB-SC system. The post-detection signal-to-noise ratio is the ratio of the message signal power to the noise power after demodulation/detection. The post-detection SNR depends on both the modulation and demodulation techniques.

Using the narrowband representation of the band-pass noise, the signal at the input to the coherent detector of Fig. 9.6 may be represented as

$$x(t) = s(t) + n_I(t) \cos(2\pi f_c t) - n_Q(t) \sin(2\pi f_c t) \quad (9.19)$$

where  $n_I(t)$  and  $n_Q(t)$  are the in-phase and quadrature components of  $n(t)$  with respect to the carrier. The output of mixer 2 in Fig. 9.6 is given by

$$\begin{aligned} v(t) &= x(t) \cos(2\pi f_c t) \\ &= \frac{1}{2}(A_c m(t) + n_I(t)) \\ &\quad + \frac{1}{2}(A_c m(t) + n_I(t)) \cos(4\pi f_c t) - \frac{1}{2}n_Q(t) \sin(4\pi f_c t) \end{aligned} \quad (9.20)$$

where we have used the double-angle formulas

$$\cos A \cos A = \frac{1 + \cos 2A}{2} \quad \text{and} \quad \sin A \cos A = \frac{\sin 2A}{2}$$

Note that the second line of Eq. (9.20) has two parts: the first part represents the baseband signal and in-phase component of the noise, while the second part represents quadrature component of its noise centered at the much higher frequency of  $2f_c$ . These high-frequency components are removed with a low-pass filter as shown in Fig. 9.6, and the result is

$$y(t) = \frac{1}{2}(A_c m(t) + n_I(t)) \quad (9.21)$$

In Eqs. (9.20) and (9.21) we assume the gains of the second mixer and the low-pass filter are unity, without loss of generality. Two observations can be made:

- ▶ The message signal  $m(t)$  and the in-phase component of the filtered noise  $n_I(t)$  appear additively in the output.
- ▶ The quadrature component of the noise is completely rejected by the demodulator.

From Eq. (9.21), we may compute the output or post-detection signal to noise ratio by noting the following:

- ▶ The message component is  $\frac{1}{2}A_c m(t)$ , so analogous to the computation of the pre-detection signal power, the post-detection signal power is  $\frac{1}{4}A_c^2 P$  where  $P$  is the average message power as defined in Eq. (9.16).
- ▶ The noise component is  $\frac{1}{2}n_I(t)$  after low-pass filtering. As described in Section 8.11, the in-phase component has a noise spectral density of  $N_0$  over the bandwidth from  $-B_T/2$  to  $B_T/2$ . If the low-pass filter has a noise bandwidth  $W$ , corresponding to the message bandwidth, which is less than or equal to  $B_T/2$ , then the output noise power is

$$\begin{aligned} \mathbf{E}[n_I^2(t)] &= \int_{-W}^{W} N_0 df \\ &= 2N_0 W \end{aligned} \quad (9.22)$$

Thus the power in  $n_I(t)$  is  $2N_0 W$ .

Combining these observations, we obtain the post-detection SNR of

$$\begin{aligned}\text{SNR}_{\text{post}}^{\text{DSB}} &= \frac{\frac{1}{4}(A_c^2)P}{\frac{1}{4}(2N_0 W)} \\ &= \frac{A_c^2 P}{2N_0 W}\end{aligned}\quad (9.23)$$

Consequently, if  $W \approx B_T/2$ , the post-detection SNR is twice the pre-detection SNR. This is due to the fact that the quadrature component of the noise has been discarded by the synchronous demodulator.

### ■ FIGURE OF MERIT

It should be clear that for the reference transmission model defined in Section 9.2, the average noise power for a message of bandwidth  $W$  is  $N_0 W$ . For DSB-SC modulation the average modulated message power is given by Eq. (9.17), and consequently the reference SNR for this transmission scheme is  $\text{SNR}_{\text{ref}} = A_c^2 P / (2N_0 W)$ . The corresponding figure of merit for this receiver is

$$\text{Figure of merit} = \frac{\text{SNR}_{\text{post}}^{\text{DSB}}}{\text{SNR}_{\text{ref}}} = 1$$

This illustrates that we lose nothing in performance by using a band-pass modulation scheme compared to the baseband modulation scheme, even though the bandwidth of the former is twice as wide. Consequently, DSB-SC modulation provides a baseline against which we may compare other amplitude modulation detection schemes.

► **Drill Problem 9.2** A DSC-SC modulated signal is transmitted over a noisy channel, having a noise spectral density  $N_0/2$  of  $2 \times 10^{-17}$  watts per hertz. The message bandwidth is 4 kHz and the carrier frequency is 200 kHz. Assume that the average received power of the signal is  $-80$  dBm. Determine the post-detection signal-to-noise ratio of the receiver. ◀

## 9.5 Noise In AM Receivers Using Envelope Detection

In Section 3.1, we discussed envelope detection of amplitude modulation with a non-suppressed carrier. Envelope detection results in a simpler receiver than the coherent approach as it does not require the circuitry to produce a synchronized carrier for demodulation. Recall from Section 3.1 that the envelope-modulated signal is represented by

$$s(t) = A_c(1 + k_a m(t)) \cos(2\pi f_c t) \quad (9.24)$$

where  $A_c \cos(2\pi f_c t)$  is the carrier wave,  $m(t)$  is the message signal, and  $k_a$  is the amplitude sensitivity of the modulator. For envelope detection, the receiver model is depicted in Fig. 9.8. The front end of this receiver is identical to that of the coherent receiver. That is, the received signal, including additive noise, is passed through a band-pass filter.

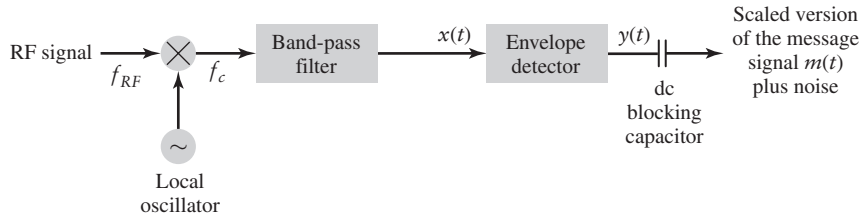


**FIGURE 9.8** Model of AM receiver using envelope detection.

### ■ PRE-DETECTION SNR

Before discussing the remainder of the circuit, let us consider the (pre-detection) SNR of this band-pass signal. In Eq. (9.24), the average power of the carrier component is  $A_c^2/2$  due to the sinusoidal nature of the carrier. The power in the modulated part of the signal is

$$\begin{aligned} \mathbf{E}[(1 + k_a m(t))^2] &= \mathbf{E}[1 + 2k_a m(t) + k_a^2 m^2(t)] \\ &= 1 + 2k_a \mathbf{E}[m(t)] + k_a^2 \mathbf{E}[m^2(t)] \\ &= 1 + k_a^2 P \end{aligned} \quad (9.25)$$

where we assume the message signal has zero mean,  $\mathbf{E}[m(t)] = 0$ , and the message power  $P$  is defined as in Eq. (9.16). Consequently, the received signal power is  $A_c^2(1 + k_a^2 P)/2$ . As with the linear receiver, we assume without loss of generality that the gain of the band-pass filter is unity, so the pre-detection signal-to-noise ratio is given by

$$\text{SNR}_{\text{pre}}^{\text{AM}} = \frac{A_c^2(1 + k_a^2 P)}{2N_0 B_T} \quad (9.26)$$

where  $B_T$  is the noise bandwidth of the band-pass filter.

### ■ POST-DETECTION SNR

To determine the post-detection signal-to-noise ratio, we must analyze the effects of the remainder of the circuit of Fig. 9.8—in particular, the envelope detector, which can be modeled as shown in Fig. 9.9, and whose operation was described in Section 3.1. As with the linear receiver of Section 9.4, we can represent the noise in terms of its in-phase and quadrature components, and consequently model the input to the envelope detector as

$$\begin{aligned} x(t) &= s(t) + n(t) \\ &= [A_c + A_c k_a m(t) + n_I(t)] \cos(2\pi f_c t) - n_Q(t) \sin(2\pi f_c t) \end{aligned} \quad (9.27)$$

The object of the envelope detector is to recover the low-frequency amplitude variations of the high-frequency signal depicted in Fig. 9.10. Conceptually, this can be represented in a phasor diagram as shown in Fig. 9.11, where the signal component of the phasor is  $A_c(1 + k_a m(t))$ , and the noise has two orthogonal phasor components,  $n_I(t)$  and  $n_Q(t)$ .

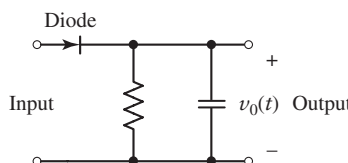


**FIGURE 9.9** Circuit diagram of envelope detector.

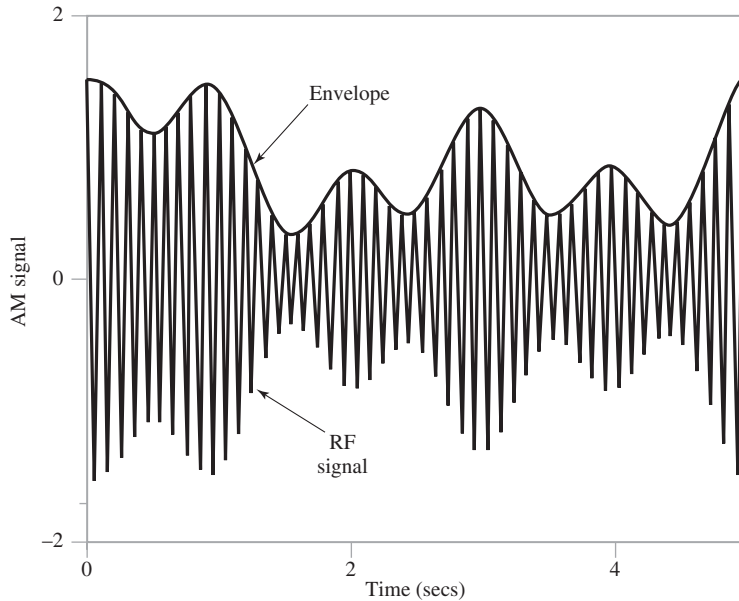


**FIGURE 9.10** Illustration of envelope on high-frequency carrier.

From Fig. 9.11, the output of the envelope detector is the amplitude of the phasor representing  $x(t)$  and it is given by

$$\begin{aligned} y(t) &= \text{envelope of } x(t) \\ &= \{[A_c(1 + k_a m(t)) + n_I(t)]^2 + n_Q^2(t)\}^{1/2} \end{aligned} \quad (9.28)$$

The above expression is the output of an ideal envelope detector. Note that the phase of  $x(t)$  does not appear in this expression; it has been eliminated because it is of no interest to us. This expression for  $y(t)$  is somewhat complex but can be simplified to provide some insightful results. If we assume that the signal is much larger than the noise, then using the approximation  $\sqrt{A^2 + B^2} \approx A$  when  $A \gg B$ , we may write

$$y(t) \approx A_c + A_c k_a m(t) + n_I(t) \quad (9.29)$$

under high SNR conditions. This new expression for the demodulated signal has three components: dc component, signal component, and noise component. The dc term can be removed with a capacitor, as shown in Fig. 9.8, leaving just the signal and noise terms; the result so obtained is similar to what was observed with the linear receiver.

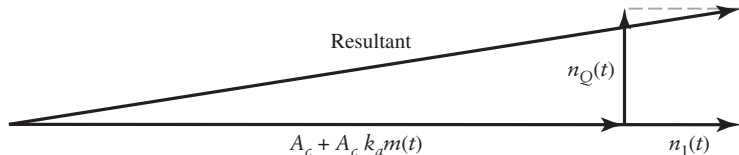


**FIGURE 9.11** Phasor diagram for AM wave plus narrowband noise.

Accordingly, the post-detection SNR for the envelope detection of AM, using a message bandwidth  $W$ , is given by

$$\text{SNR}_{\text{post}}^{\text{AM}} = \frac{A_c^2 k_a^2 P}{2N_0 W} \quad (9.30)$$

where the numerator represents the average power of the message  $A_c k_a m(t)$ , and the denominator represents the average power of  $n_I(t)$  from Eq. (9.22).

This evaluation of the output SNR is only valid under two conditions:

- ▶ The SNR is high.
- ▶  $k_a$  is adjusted for 100% modulation or less, so there is no distortion of the signal envelope.

As with suppressed-carrier amplitude modulation, the message bandwidth  $W$  is approximately one-half of the transmission bandwidth  $B_T$ .

### ■ FIGURE OF MERIT

For AM modulation, the average transmitted power is given by the product of Eq. (9.25) and the carrier power  $A_c^2/2$ ; consequently the reference SNR is  $A_c^2(1 + k_a^2 P)/(2N_0 W)$ . Combining this result with Eq. (9.30), the figure of merit for this AM modulation-demodulation scheme is

$$\text{Figure of merit} = \frac{\text{SNR}_{\text{post}}^{\text{AM}}}{\text{SNR}_{\text{ref}}} = \frac{k_a^2 P}{1 + k_a^2 P} \quad (9.31)$$

Since the product  $k_a^2 P$  is always less than unity (otherwise the signal would be over modulated), the figure of merit for this system is always less than 0.5. Hence, the noise performance of an envelope-detector receiver is always inferior to a DSB-SC receiver, the reason is that at least half of the power is wasted transmitting the carrier as a component of the modulated (transmitted) signal.

This completes the noise analysis of envelope modulation, but we note that a mathematical analysis can also be performed when the signal-to-noise ratio is low.<sup>2</sup> From Eq. (9.30), we see that the post-detection SNR has an inverse linear dependence on the noise spectral density. With low signal-to-noise conditions, nonlinear effects appear. Synchronous detection does not have this nonlinear behavior, but the quality of the voice is still poor at low post-detection SNRs.

### ■ COMPUTER EXPERIMENT: ENVELOPE DETECTION

In Problem 9.26, we describe a computer experiment that simulates envelope detection using the phasor notation given above. In the experiment, the message is a sinusoidal wave  $m(t) = A \sin(2\pi f_m t)$ , for which we create a time-varying phasor and add a corresponding noise phasor. In this experiment, we compute the pre-detection and post-detection SNRs for samples of its signal. These two measures are plotted against one another in Fig. 9.12 for  $k_a = 0.3$ . Also shown in this plot is the theoretical performance of these two measures as given by Eqs. (9.26) and (9.30).

---

<sup>2</sup>See Chapter 2 of Haykin (2001).

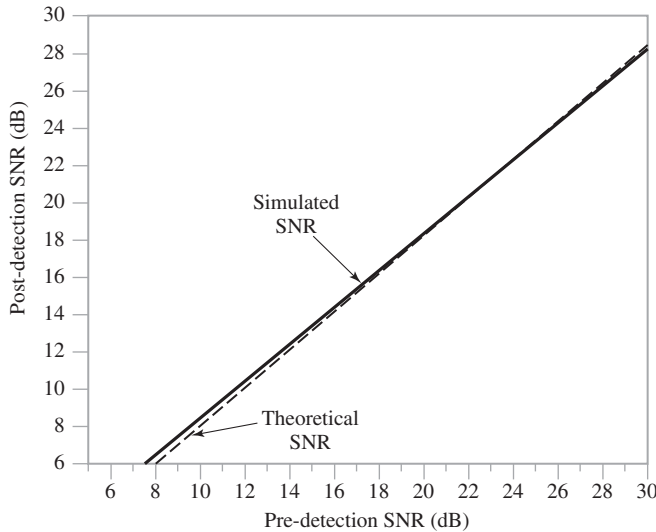


**FIGURE 9.12** Comparison of pre-detection and post-detection SNRs with simulated envelope detection of AM.

The post-detection SNR is computed as follows:

- The output signal power is determined by passing a noiseless signal through the envelope detector and measuring the output power.
- The output noise power is computed by passing signal plus noise through the envelope detector and subtracting the output obtained from the clean signal only. With this approach, any distortion due to the product of noise and signal components is included as noise contribution.

The ratio of the two quantities is used as an estimate of the output SNR.

As we can see from Fig. 9.12, there is close agreement between theory and experiment at high SNR values, which is to be expected. There are some minor discrepancies, but these can be attributed to the limitations of the discrete time simulation. At lower SNR there is some variation from theory as might also be expected.

► **Drill Problem 9.3** For the same received signal power, compare the post-detection SNRs of DSB-SC with coherent detection and envelope detection with  $k_a = 0.2$  and  $0.4$ . Assume that the average message power is  $P = 1$ . ◀

► **Drill Problem 9.4** In practice, there is an arbitrary phase  $\theta$  in Eq. (9.24). How will this affect the results of Section 9.5. ◀

## 9.6 Noise in SSB Receivers

We now consider the case of a coherent receiver with an incoming SSB wave. Using the definitions of Section 3.6, we assume that only the lower sideband is transmitted, so that we may express the modulated wave as

$$s(t) = \frac{A_c}{2}m(t)\cos(2\pi f_c t) + \frac{A_c}{2}\hat{m}(t)\sin(2\pi f_c t) \quad (9.32)$$

where  $\hat{m}(t)$  is the Hilbert transform of the message signal  $m(t)$ . We may make the following observations concerning the in-phase and quadrature components of  $s(t)$  in Eq. (9.32):

1. The two components  $m(t)$  and  $\hat{m}(t)$  are uncorrelated with each other. Therefore, their power spectral densities are additive.
2. The Hilbert transform  $\hat{m}(t)$  is obtained by passing  $m(t)$  through a linear filter with transfer function  $-j \operatorname{sgn}(f)$ . The squared magnitude of this transfer function is equal to one for all  $f$ . Accordingly,  $m(t)$  and  $\hat{m}(t)$  have the same average power  $P$ .

Thus, proceeding in a manner similar to that for the DSB-SC receiver, we find that the in-phase and quadrature components of the SSB modulated wave  $s(t)$  contribute an average power of  $A_c^2 P/8$  each. The average power of  $s(t)$  is therefore  $A_c^2 P/4$ . This result is half that of the DSB-SC case, which is intuitively satisfying.

### ■ PRE-DETECTION SNR

For the SSB signal, the transmission bandwidth  $B_T$  is approximately equal to the message bandwidth  $W$ . Consequently, using the signal power calculation of the previous section, the pre-detection signal-to-noise ratio of a coherent receiver with SSB modulation is

$$\text{SNR}_{\text{pre}}^{\text{SSB}} = \frac{A_c^2 P}{4N_0 W} \quad (9.33)$$

### ■ POST-DETECTION SNR

Using the same superheterodyne receiver of Figure 9.6, the band-pass signal after multiplication with the synchronous oscillator output  $\cos(2\pi f_c t)$  is

$$\begin{aligned} v(t) &= x(t) \cos(2\pi f_c t) \\ &= \frac{1}{2} \left( \frac{A_c}{2} m(t) + n_I(t) \right) \\ &\quad + \frac{1}{2} \left( \frac{A_c}{2} m(t) + n_I(t) \right) \cos(4\pi f_c t) - \frac{1}{2} \left( \frac{A_c}{2} \hat{m}(t) + n_Q(t) \right) \sin(4\pi f_c t) \end{aligned} \quad (9.34)$$

After low-pass filtering the  $v(t)$ , we are left with

$$y(t) = \frac{1}{2} \left( \frac{A_c}{2} m(t) + n_I(t) \right) \quad (9.35)$$

As expected, we see that the quadrature component  $\hat{m}(t)$  of the message signal has been eliminated from the detector output. With a band-pass filter tailor-made for the SSB signal, the band-pass noise  $n(t)$  will also be of single sideband nature. However, as noted in Eq. (8.98), the spectrum of the in-phase component of the noise  $n_I(t)$  is given by

$$S_{N_I}(f) = \begin{cases} S_N(f - f_c) + S_N(f + f_c), & -B \leq f \leq B \\ 0, & \text{otherwise} \end{cases} \quad (9.36)$$

For the single sideband case,  $S_N(f)$  is  $N_0/2$  for  $f_c < f < f_c + W$  and for  $-f_c - W < f < -f_c$ . Consequently,

$$S_{N_I}(f) = \begin{cases} \frac{N_0}{2}, & -W \leq f \leq W \\ 0, & \text{otherwise} \end{cases} \quad (9.37)$$

In other words, the spectral density of  $n_I(t)$  is double-sided, as in the DSB-SC case, but with half of the power. In a practical application, the SSB filter will attenuate the low-frequency components of the signal plus noise. Hence, in practice, the spectrum of  $n_I(t)$  will often have a notch at dc.

From Eq. (9.35), the message component in the receiver output is  $A_c m(t)/4$  so that the average power of the recovered message is  $A_c^2 P/16$ . The corresponding noise power from Eqs. (9.35) and (9.37) is  $\frac{1}{4} N_0 W$ . Accordingly, the post-detection signal-to-noise ratio of a system using SSB modulation in the transmitter and coherent detection in the receiver is the ratio of these two powers; namely,

$$\text{SNR}_{\text{post}}^{\text{SSB}} = \frac{A_c^2 P}{4N_o W} \quad (9.38)$$

### ■ FIGURE OF MERIT

The average signal power for the SSB system, as discussed above, is  $A_c^2 P/4$ . Consequently, the reference SNR is  $A_c^2 P/(4N_0 W)$ . The figure of merit for the SSB system is the ratio of Eq. (9.38) to the latter; that is,

$$\text{Figure of merit} = \frac{\text{SNR}_{\text{post}}^{\text{SSB}}}{\text{SNR}_{\text{ref}}} = 1 \quad (9.39)$$

Consequently, SSB transmission has the same figure of merit as DSB-SC. The performance of vestigial sideband with coherent detection is similar to that of SSB.

Comparing the results for the different amplitude modulation schemes, we find that there are a number of design tradeoffs. Double-sideband suppressed carrier modulation provides the same SNR performance as the baseband reference model but requires synchronization circuitry to perform coherent detection. Non-suppressed-carrier AM simplifies the receiver design significantly as it is implemented with an envelope detector. However, non-suppressed-carrier AM requires significantly more transmitter power to obtain the same SNR performance as the baseband reference model. Single-sideband modulation achieves the same SNR performance as the baseband reference model but only requires half the transmission bandwidth of the DSB-SC system. On the other hand, SSB requires more transmitter processing. *These observations are our first indication that communication system design involves a tradeoff between power, bandwidth, and processing complexity.*

► **Drill Problem 9.5** The message signal of Problem 9.2 having a bandwidth  $W$  of 4 kHz is transmitted over the same noisy channel having a noise spectral density  $N_0/2$  of  $2 \times 10^{-17}$  watts per hertz using single-sideband modulation. If the average received power of the signal is  $-80$  dBm, what is the post-detection signal-to-noise ratio of the receiver? Compare the transmission bandwidth of the SSB receiver to that of the DSB-SC receiver. ◀

## 9.7 Detection of Frequency Modulation (FM)

We now turn to the detection of a frequency-modulated carrier in noise. Recall from Section 4.1 that the frequency-modulated signal is given by

$$s(t) = A_c \cos \left[ 2\pi f_c t + 2\pi k_f \int_0^t m(\tau) d\tau \right] \quad (9.40)$$

where  $A_c$  is the carrier amplitude,  $f_c$  is the carrier frequency,  $k_f$  is the frequency sensitivity factor of the modulator, and  $m(t)$  is the message signal. The received FM signal  $s(t)$  has a carrier frequency  $f_c$  and a transmission bandwidth  $B_T$ , such that a negligible amount of power lies outside the frequency band  $f_c \pm B_T/2$  for positive frequencies, and similarly for negative frequencies.

### ■ PRE-DETECTION SNR

For FM detection, we assume a receiver model as shown in Fig. 9.13. As before, we assume that the noise  $w(t)$  is a white zero-mean Gaussian process with power spectral density  $N_0/2$ . The FM detector consists of a band-pass filter, a limiter, a discriminator, and a low-pass filter. The band-pass filter has a center frequency  $f_c$  and bandwidth  $B_T$  so that it passes the FM signal without distortion. Ordinarily,  $B_T$  is small compared with the center frequency  $f_c$ , so that we may use the narrowband representation for  $n(t)$ , the filtered version of the channel noise  $w(t)$ . The pre-detection SNR in this case is simply the carrier power  $A_c^2/2$  divided by the noise passed by the bandpass filter,  $N_0 B_T$ ; namely,

$$\text{SNR}_{\text{pre}}^{\text{FM}} = \frac{A_c^2}{2N_0 B_T}$$

In an FM system, the message signal is embedded in the variations of the instantaneous frequency of the carrier. The amplitude of the carrier is constant. Therefore any variations of the carrier amplitude at the receiver input must result from noise or interference. The amplitude *limiter*, following the band-pass filter in the receiver model of Fig. 9.13, is used to remove amplitude variations by clipping the modulated wave. The resulting wave is almost rectangular. This wave is rounded by another band-pass filter that is an integral part of the limiter, thereby suppressing harmonics of the carrier frequency that are caused by the clipping.

The discriminator in the model of Fig. 9.13 consists of two components (see Chapter 4):

1. A *slope network* or *differentiator* with a purely imaginary frequency response that varies linearly with frequency. It produces a hybrid-modulated wave in which both amplitude and frequency vary in accordance with the message signal.

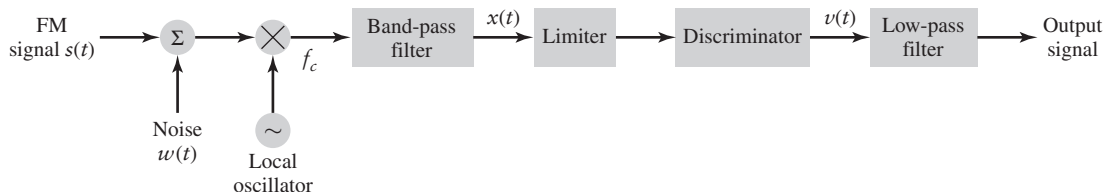


**FIGURE 9.13** Model of an FM receiver.

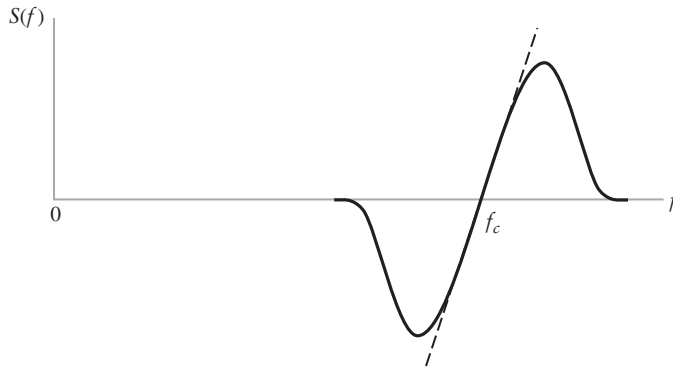


**FIGURE 9.14** Amplitude response of slope network used in FM discriminator.

2. An *envelope detector* that recovers the amplitude variation and reproduces the message signal.

The slope network and envelope detector are usually implemented as integral parts of the single physical unit. An example of the amplitude response of the composite slope network is shown in Fig. 9.14. The envelope detector was discussed in the previous section; see also Chapter 3. The combined use of the slope network and envelope detector as an FM demodulator was discussed in Section 4.8.

The post-detection filter, labeled “low-pass filter” in Fig. 9.13, has a bandwidth that is just large enough to pass the highest frequency component of the message signal. This filter removes the out-of-band components of the noise at the discriminator output and thereby keeps the effect of the output noise to a minimum.

### ■ POST-DETECTION SNR

The noisy FM signal after band-pass filtering may be represented as

$$x(t) = s(t) + n(t) \quad (9.41)$$

where  $s(t)$  is given by Eq. (9.40). In previous developments, we have expressed the filtered noise  $n(t)$  at the band-pass filter output in Fig. 9.13 in terms of its in-phase and quadrature components

$$n(t) = n_I(t) \cos(2\pi f_c t) - n_Q(t) \sin(2\pi f_c t) \quad (9.42)$$

We may equivalently express  $n(t)$  in terms of its envelope and phase as (see Problem 4.3.)

$$n(t) = r(t) \cos[2\pi f_c t + \phi_n(t)] \quad (9.43)$$

where the envelope is

$$r(t) = [n_I^2(t) + n_Q^2(t)]^{1/2} \quad (9.44)$$

and the phase is

$$\phi_n(t) = \tan^{-1} \left( \frac{n_Q(t)}{n_I(t)} \right) \quad (9.45)$$

One of the properties of this polar representation is that the phase  $\phi_n(t)$  is uniformly distributed between 0 and  $2\pi$  radians.

To proceed, we note that the phase of  $s(t)$  is

$$\phi(t) = 2\pi k_f \int_0^t m(\tau) d\tau \quad (9.46)$$

Combining Eqs. (9.40), (9.43), and (9.46), the noisy signal at the output of the band-pass filter may be expressed as

$$\begin{aligned} x(t) &= s(t) + n(t) \\ &= A_c \cos[2\pi f_c t + \phi(t)] + r(t) \cos[2\pi f_c t + \psi_n(t)] \end{aligned} \quad (9.47)$$

It is informative to represent  $x(t)$  by means of a phasor diagram, as in Fig. 9.15 where we have used the signal term  $s(t)$  as the reference. In Fig. 9.15, the amplitude of the noise is  $r(t)$  and the phase difference  $\psi_n(t) = \phi_n(t) - \phi(t)$  is the angle between the noise phasor and the signal phasor. The phase  $\theta(t)$  of the resultant is given by

$$\theta(t) = \phi(t) + \tan^{-1} \left\{ \frac{r(t) \sin(\psi_n(t))}{A_c + r(t) \cos(\psi_n(t))} \right\} \quad (9.48)$$

The envelope of  $x(t)$  is of no interest to us, because the envelope variations at the band-pass filter output are removed by the limiter.

To obtain useful results, we make some approximations regarding  $\theta(t)$ . First, we assume that the carrier-to-noise ratio measured at the discriminator input is large. If  $R$  denotes observations of the sample function  $r(t)$  of the noise envelope, then most of the time the random variable  $R$  is small compared to the carrier amplitude  $A_c$ . Under this condition, and noting that  $\tan^{-1} \xi \approx \xi$  since  $\xi \ll 1$ , the expression for the phase simplifies to

$$\theta(t) = \phi(t) + \frac{r(t)}{A_c} \sin[\psi_n(t)] \quad (9.49)$$

We simplify this expression even further by ignoring the modulation component in the second term of Eq. (9.49), and replacing  $\psi_n(t) = \phi_n(t) - \phi(t)$  with  $\phi_n(t)$ . This is justified because the phase  $\phi_n(t)$  is uniformly distributed between 0 and  $2\pi$  radians and, since  $\phi(t)$  is independent of  $\phi_n(t)$ , it is reasonable to assume that the phase difference  $\phi_n(t) - \phi(t)$  is also uniformly distributed over  $2\pi$  radians. Theoretical considerations show that this assumption is justified provided that the carrier-to-noise ratio is high.<sup>3</sup> Then noting that the quadrature component of the noise is  $n_Q(t) = r(t) \sin[\phi_n(t)]$ , we may simplify Eq. (9.49) to

$$\theta(t) = \phi(t) + \frac{n_Q(t)}{A_c} \quad (9.50)$$

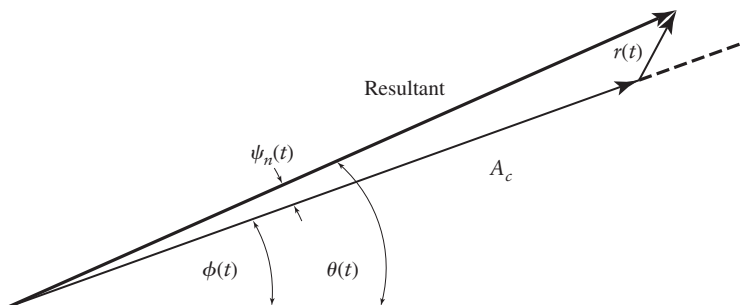


**FIGURE 9.15** Phasor diagram for FM signal plus narrowband noise assuming high carrier-to-noise ratio.

<sup>3</sup>See Chapter 5 of Downing (1964).

Using the expression for  $\phi(t)$  given by Eq. (9.46), Eq. (9.50) can be expressed as

$$\theta(t) \approx 2\pi k_f \int_0^t m(\tau) d\tau + \frac{n_Q(t)}{A_c} \quad (9.51)$$

Our objective is to determine the error in the instantaneous frequency of the carrier wave caused by the presence of the filtered noise  $n(t)$ . With an ideal discriminator, its output is proportional to the derivative  $d\theta(t)/dt$ . Using the expression for  $\theta(t)$  in Eq. (9.51), the ideal discriminator output, scaled by  $2\pi$ , is therefore

$$\begin{aligned} v(t) &= \frac{1}{2\pi} \frac{d\theta(t)}{dt} \\ &= k_f m(t) + n_d(t) \end{aligned} \quad (9.52)$$

where the noise term  $n_d(t)$  is defined by

$$n_d(t) = \frac{1}{2\pi A_c} \frac{dn_Q(t)}{dt} \quad (9.53)$$

We now see that, provided the carrier-to-noise ratio is high, the discriminator output  $v(t)$  consists of the original message signal  $m(t)$  multiplied by the constant factor  $k_f$ , plus an additive noise component  $n_d(t)$ . *The additive noise at the discriminator output is determined essentially by the quadrature component  $n_Q(t)$  of the narrowband noise  $n(t)$ .*

Accordingly, we may use the *post-detection signal-to-noise ratio*, as previously defined, to assess the output quality of the FM receiver. The post-detection signal-to-noise ratio is defined as the ratio of the average output signal power to the average output noise power. From Eq. (9.52) we see that the message component of the discriminator output, and therefore the low-pass filter output, is  $k_f m(t)$ . Hence, the average output signal power is equal to  $k_f^2 P$  where  $P$  is the average power of the message signal  $m(t)$ .

To determine the average output noise power, we note that the noise  $n_d(t)$  at the discriminator output is proportional to the time derivative of the quadrature noise component  $n_Q(t)$ . Since the differentiation of a function with respect to time corresponds to multiplication of its Fourier transform by  $j2\pi f$ , it follows that we may obtain the noise process  $n_d(t)$  by passing  $n_Q(t)$  through a linear filter with a frequency response equal to

$$G(f) = \frac{j2\pi f}{2\pi A_c} = \frac{jf}{A_c} \quad (9.54)$$

This means that the power spectral density  $S_{N_d}(f)$  of the noise  $n_d(t)$  is related to the power spectral density  $S_{N_Q}(f)$  of the quadrature noise component  $n_Q(t)$  as follows:

$$\begin{aligned} S_{N_d}(f) &= |G(f)|^2 S_{N_Q}(f) \\ &= \frac{f^2}{A_c^2} S_{N_Q}(f) \end{aligned} \quad (9.55)$$

With the band-pass filter in the receiver model of Fig. 9.13 having an ideal frequency response characterized by bandwidth  $B_T$  and midband frequency  $f_c$ , it follows that the narrowband noise  $n(t)$  will have a power spectral density characteristic that is similarly shaped. If the input noise is white then, from the properties of the in-phase and quadrature components of narrowband noise described in Section 8.11, the power spectral density of  $n_Q(t)$  will be the low-pass equivalent of the sum of the positive and negative frequency responses of the band-pass filter. This means that the quadrature component  $n_Q(t)$  of the narrowband

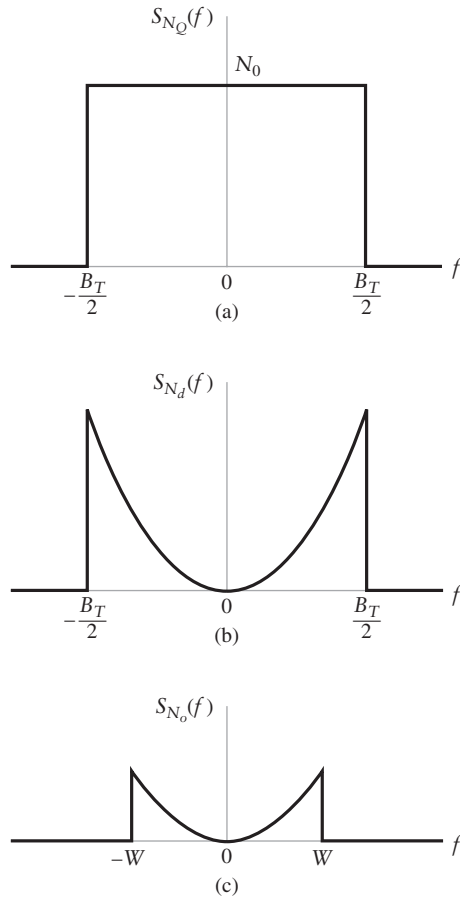


**FIGURE 9.16** Noise analysis of FM receiver. (a) Power spectral density of quadrature component  $n_Q(t)$  of narrowband noise  $n(t)$ . (b) Power spectral density  $n_d(t)$  at discriminator output. (c) Power spectral density of noise  $n_o(t)$  at receiver output.

noise will have the ideal low-pass characteristic shown in Fig. 9.16 (a). The corresponding power spectral density of the noise  $n_d(t)$  is shown in Fig. 9.16 (b); that is,

$$S_{N_d}(f) = \begin{cases} \frac{N_0 f^2}{A_c^2}, & |f| < \frac{B_T}{2} \\ 0, & \text{otherwise} \end{cases} \quad (9.56)$$

In the receiver model of Fig. 9.13, the discriminator output is followed by a low-pass filter with a bandwidth equal to the message bandwidth  $W$ . For wideband FM, we usually find that  $W$  is smaller than  $B_T/2$  where  $B_T$  is the transmission bandwidth of the FM signal. This means that the out-of-band components of noise  $n_d(t)$  will be rejected. Therefore, the power spectral density  $S_{N_o}(f)$  of the noise  $n_o(t)$  appearing at the receiver output is defined by

$$S_{N_o}(f) = \begin{cases} \frac{N_0 f^2}{A_c^2}, & |f| < W \\ 0, & \text{otherwise} \end{cases} \quad (9.57)$$

as shown in Fig. 9.16(c). The average output noise power is determined by integrating the power spectral density  $S_{N_o}(f)$  from  $-W$  to  $W$ . Doing so, we obtain the following result:

$$\begin{aligned}\text{Average post-detection noise power} &= \frac{N_0}{A_c^2} \int_{-W}^W f^2 df \\ &= \frac{2N_0 W^3}{3A_c^2}\end{aligned}\quad (9.58)$$

From Eqs. (9.52) and (9.16) the average output signal power is  $k_f^2 P$ . As mentioned earlier, provided the carrier-to-noise ratio is high, the post-detection signal-to-noise ratio is equal to the ratio of  $k_f^2 P$  to the right-hand side of Eq. (9.58), thereby yielding

$$\text{SNR}_{\text{post}}^{\text{FM}} = \frac{3A_c^2 k_f^2 P}{2N_0 W^3}\quad (9.59)$$

Hence, the post-detection SNR of an FM demodulator has a nonlinear dependence on both the frequency sensitivity and the message bandwidth.

### ■ FIGURE OF MERIT

With FM modulation, the modulated signal power is simply  $A_c^2/2$ , hence the reference SNR is  $A_c^2/(2N_0 W)$ . Consequently, the figure of merit for this system is given by

$$\begin{aligned}\text{Figure of merit} &= \frac{\text{SNR}_{\text{post}}^{\text{FM}}}{\text{SNR}_{\text{ref}}} = \frac{\frac{3A_c^2 k_f^2 P}{2N_0 W^3}}{\frac{A_c^2}{2N_0 W}} \\ &= 3 \left( \frac{k_f^2 P}{W^2} \right) \\ &= 3D^2\end{aligned}\quad (9.60)$$

where, in the last line, we have introduced the definition  $D = k_f P^{1/2}/W$  as the deviation ratio for the FM system in light of the material presented in Section 4.6. Recall from that section that the generalized Carson rule yields the transmission bandwidth  $B_T = 2(k_f P^{1/2} + W) \approx 2k_f P^{1/2}$  for an FM signal. So, substituting  $B_T/2$  for  $k_f P^{1/2}$  in the definition of  $D$ , the figure of merit for an FM system is approximately given by

$$\text{Figure of merit} \approx \frac{3}{4} \left( \frac{B_T}{W} \right)^2\quad (9.61)$$

Consequently, an increase in the transmission bandwidth  $B_T$  provides a corresponding quadratic increase in the output signal-to-noise ratio with an FM system compared to the reference system. Thus, when the carrier to noise level is high, unlike an amplitude modulation system an FM system allows us to *trade bandwidth for improved performance* in accordance with a square law.

#### EXAMPLE 9.2 Noise in FM Multiplexed Channels

In the FM stereo multiplexing strategy described in Section 4.9, we wish to determine the post-detection SNR of the stereo difference signal  $m_l(t) - m_r(t)$ , assuming that the transmission bandwidth is 200 kHz, the baseband bandwidth is 19 kHz, and the pre-detection SNR is 12 dB.

From the material presented previously in this section, the pre-detection SNR is

$$\text{SNR}_{\text{pre}} = \frac{A_c^2}{2N_0B_T}$$

Ignoring the pilot component, the average post-detection noise power in the upper channel of the FM multiplex is

$$\begin{aligned} N &= \frac{N_0}{A_c^2} \times 2 \int_W^{3W} f^2 df \\ &= \frac{52W^3N_0}{3A_c^2} \end{aligned}$$

The post-detection SNR on the upper channel is

$$\begin{aligned} \text{SNR}_{\text{post}} &= \frac{3A_c^2k_f^2(P/2)}{52N_0W^3} \\ &= \frac{A_c^2}{2N_0B_T} \frac{3}{52} \frac{k_f^2PB_T}{W^3} \\ &\approx \frac{A_c^2}{2N_0B_T} \frac{3/4}{52} \left( \frac{B_T}{W} \right)^3 \\ &= 266.6 \\ &\approx 24.3 \text{ dB} \end{aligned}$$

where we have used the approximation to Carson's rule that  $B_T \approx 2k_fP^{1/2}$  and have assumed that half of the power is in the upper channel.

### ■ THRESHOLD EFFECT

The formula of Eq. (9.59), defining the post-detection SNR ratio of an FM receiver, is valid only if the pre-detection SNR, measured at the discriminator input, is high compared to unity. If the pre-detection SNR is lowered, the FM receiver breaks down. At first, individual clicks are heard in the receiver output, and as the pre-detection SNR decreases further, the clicks merge to a crackling or sputtering sound. At and below this breakdown point, Eq. (9.59) fails to accurately predict the post-detection SNR. This phenomenon is known as the *threshold effect*; its evaluation is however beyond the scope of this book.

### ■ COMPUTER EXPERIMENT: THRESHOLD EFFECT WITH FM

In Problem 9.27, we describe a computer experiment for simulating the detection of an FM signal in noise. The signal and noise are both generated using complex phasor notation, but they are subsequently up-converted to an IF, creating a band-pass signal, to apply discriminator detection.

The complex phasor of the FM signal is given by

$$s(t) = A_c \exp \left\{ -j2\pi k_f \int_0^t m(\tau) d\tau \right\}$$

where (for the results that follow) we have  $m(t) = \sin(2\pi t)$  and  $k_f = 20$  hertz per unit amplitude. This signal was transmitted with a band-pass transmission bandwidth of  $B_T = 62.5$  Hz and a baseband detection bandwidth of  $W = 5.5$  Hz.

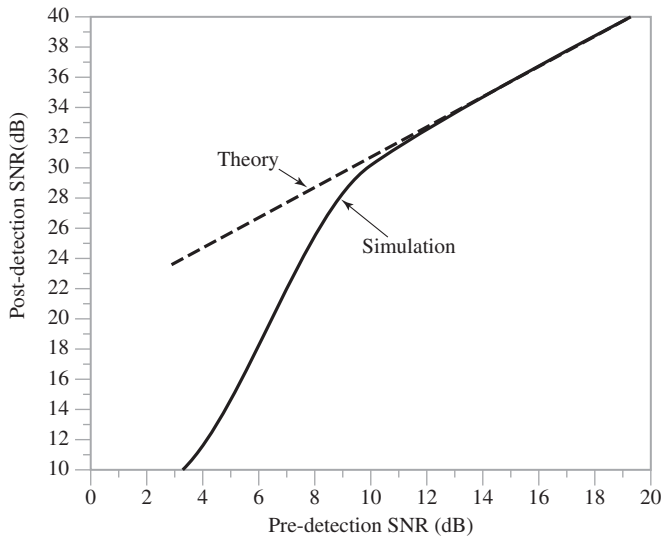


**FIGURE 9.17** Comparison of pre-detection and post-detection SNRs for a simulated FM receiver. ( $f_m = 1$  Hz,  $k_f = 20$  Hz,  $B_T = 62.5$  Hz,  $W = 5.5$  Hz,  $A_c = 1$ )

Similar to the AM computer experiment, we measure the pre-detection and post-detection SNRs of the signal and compare the results to the theory developed in this section. These results are shown in Fig. 9.17 for the above set of parameters. The results show that the theory clearly matches the measured performance at high SNR. At low SNR we have a threshold effect as mentioned, where the post-detection SNR degrades very rapidly as the pre-detection SNR is decreased past a value of 10 dBs.

► **Drill Problem 9.6** The signal  $m(t) = \cos(2000\pi t)$  is transmitted by means of frequency modulation. If the frequency sensitivity  $k_f$  is 2 kHz per volt, what is the Carson's rule bandwidth of the FM signal? If the pre-detection SNR is 17 dB, calculate the post-detection SNR. Assume that the FM demodulator includes an ideal low-pass filter with bandwidth 3.1 kHz. ◀

► **Drill Problem 9.7** Compute the post-detection SNR in the lower channel for Example 9.2 and compare it to the upper channel. ◀

## 9.8 FM Pre-emphasis and De-emphasis

From the square-law nature of the output noise spectrum of an FM receiver, the noise is most severe at large values of  $|f|$ . This becomes a significant issue in FM stereo transmission where the upper channel,  $(m_l(t) - m_r(t))$ , suffers significantly more noise than the lower channel,  $(m_l(t) + m_r(t))$ .

Suppose the demodulator includes a low-pass filter which gradually increases attenuation as  $|f|$  approaches  $W$  rather than being approximately flat for  $|f| < W$  and cutting off sharply at  $W$ . Such a filter with transfer function  $H_{de}(f)$  is presented in Fig. 9.18(b). This filter will *de-emphasize* the effects of noise at high frequency as illustrated in the figure.

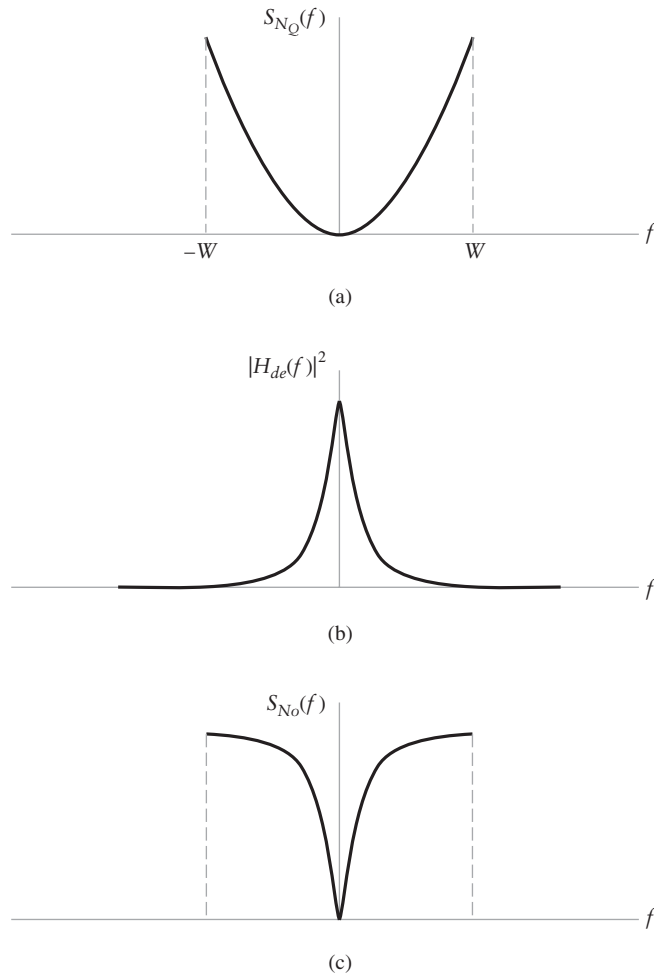


**FIGURE 9.18** Use of pre-emphasis and de-emphasis in an FM system. (a) Output noise spectrum before de-emphasis. (b) Frequency response of de-emphasis filter. (c) Noise spectrum after de-emphasis.

As well as reducing the noise, the de-emphasis filter will distort the received signal. To compensate this distortion, we appropriately pre-distort or *pre-emphasize* the baseband signal at the transmitter, prior to FM modulation, using a filter with the frequency response

$$H_{\text{pre}}(f) = \frac{1}{H_{\text{de}}(f)} \quad |f| < W \quad (9.62)$$

With a matching combination of pre-emphasis and de-emphasis as described by Eqs. (9.61) and (9.62), the signal is recovered undistorted and, most important, with reduced noise levels.

The *de-emphasis filter* is often a simple resistance-capacitance (RC) circuit with

$$H_{\text{de}}(f) = \frac{1}{1 + j \frac{f}{f_{3\text{dB}}}} \quad (9.63)$$

This filter is approximately flat for  $|f| < f_{3dB}$ , the 3-dB bandwidth of the filter. With this choice, the noise spectrum for  $|f| > f_{3dB}$  becomes flat over most of the message bandwidth as shown in Figure 9.18(c).

At the transmitting end, the pre-emphasis filter is

$$H_{\text{pre}}(f) = 1 + j \frac{f}{f_{3dB}} \quad (9.64)$$

This second filter has little effect at low frequencies where  $|f| < f_{3dB}$ . At frequencies  $|f| > f_{3dB}$  (recall that the transfer function of a differentiator is  $j2\pi f$ ), the filter of Eq. (9.64) is approximately equivalent to a differentiator. Thus the pre-emphasized signal is the sum of the original signal plus its derivative. Consequently, the modulated signal is approximately

$$\begin{aligned} s(t) &= A_c \cos \left( 2\pi f_c t + 2\pi k_f \int_0^t \left( m(s) + \alpha \frac{dm(s)}{ds} \right) ds \right) \\ &= A_c \cos \left( 2\pi f_c t + 2\pi k_f \int_0^t m(s) ds + 2\pi k_f \alpha m(t) \right) \end{aligned}$$

where  $\alpha = 1/f_{3dB}$ . Thus, pre-emphasized FM is really a combination of frequency modulation and phase modulation.

Pre-emphasis is used in many applications other than FM stereo broadcasting. Pre-emphasis can be used to advantage whenever portions of the message band are degraded relative to others. That is, portions of the message band that are most sensitive to noise are amplified (emphasized) before transmission. At the receiver, the signal is de-emphasized to reverse the distortion introduced by the transmitter; at the same time the de-emphasis reduces the noise that falls in the most sensitive part of the message band. For example, the Dolby system for tape recording pre-emphasizes high frequencies for sound recording so that high-frequency surface noise can be de-emphasized during playback.

### EXAMPLE 9.3 Pre-emphasis Improvement

In this example, we address the improvement in the post-detection signal-to-noise ratio of an FM receiver with the pre-and de-emphasis networks of Eqs. (9.64) and (9.63).

From Eq. (9.58), the noise power without de-emphasis is given by

$$N = \frac{2}{3} \frac{N_0 W^3}{A_c^2}$$

The corresponding noise power with de-emphasis is given by

$$\begin{aligned} N_{\text{de}} &= \int_{-W}^W \frac{N_0 f^2 / A_c^2}{1 + (f/f_{3dB})^2} df \\ &= 2 \frac{N_0}{A_c^2} \left[ (W/f_{3dB}) - \tan^{-1}(W/f_{3dB}) \right] (f_{3dB})^3 \end{aligned}$$

The improvement provided by de-emphasis is the ratio of these last two expressions,

$$I = \frac{N}{N_{\text{de}}} = \frac{(W/f_{3dB})^3}{3[(W/f_{3dB}) - \tan^{-1}(W/f_{3dB})]}$$

In commercial FM broadcasting, we typically have  $f_{3dB} = 2.1$  kHz, and we may reasonably assume  $W = 15$  kHz. This set of values yields  $I = 22$ , which corresponds to an improvement of 13 dB in the post-detection signal-to-noise ratio of the receiver. This example illustrates that a significant improvement in the noise performance of an FM system may be achieved by using pre-emphasis and de-emphasis filters made up of simple RC circuits.

► **Drill Problem 9.8** An FM system has a pre-detection SNR of 15 dB. If the transmission bandwidth is 30 MHz and the message bandwidth is 6 MHz, what is the post-detection SNR? Suppose the system includes pre-emphasis and de-emphasis filters as described by Eqs. (9.63) and (9.64). What is the post-detection SNR if the  $f_{3dB}$  of the de-emphasis filter is 800 kHz? ◀

## 9.9 Summary and Discussion

In this chapter, we looked at the detection of various analog modulated signals in the presence of additive noise. We began by reviewing the characteristics of Gaussian noise, the most common impairment in communication systems. We next introduced the concepts of pre-detection and post-detection signal-to-noise ratio (SNR) and established the ratio of the post-detection SNR to the SNR of a baseband reference model as the figure of merit for comparing analog communication systems.

Subsequently, we analyzed the noise performance of a number of different amplitude modulation schemes and found:

- (i) The detection of DSB-SC with a linear coherent receiver has the same SNR performance as the baseband reference model but requires synchronization circuitry to recover the coherent carrier for demodulation.
- (ii) Non-suppressed carrier AM systems allow simple receiver design including the use of envelope detection, but they result in significant wastage of transmitter power compared to coherent systems.
- (iii) Analog SSB modulation provides the same SNR performance as DSB-SC while requiring only half the transmission bandwidth.

The analysis of the noise performance of FM signals indicates that the output noise spectrum has a parabolic shape quite unlike what was observed with AM detection. This behavior results in the ability of FM to trade off signal bandwidth for improved noise performance in accordance with a square law. Pre- and de-emphasis spectral weighting may be used to significantly improve the post-detection signal-to-noise ratios of FM systems. We also observed that discriminator detection of FM exhibits a threshold phenomenon where performance rapidly degrades below a certain pre-detection SNR.

In this chapter, we have shown the importance of noise analysis based on signal-to-noise ratio in the evaluation of the performance of analog communication systems. This type of noise analysis is fundamental to the understanding and design of any communication system, be it analog or digital.

**ADDITIONAL PROBLEMS****9.9 A sample function**

$$x(t) = A_c \cos(2\pi f_c t) + w(t)$$

is applied to a low-pass RC filter. The amplitude  $A_c$  and frequency  $f_c$  of the sinusoidal component are constants, and  $w(t)$  is white noise of zero mean and power spectral density  $N_0/2$ . Find an expression for the output signal-to-noise ratio with the sinusoidal component of  $x(t)$  regarded as the signal of interest.

- 9.10** A DSC-SC modulated signal is transmitted over a noisy channel, with the power spectral density of the noise as shown in Fig. 9.19. The message bandwidth is 4 kHz and the carrier frequency is 200 kHz. Assume that the average received power of the signal is  $-80$  dBm, and determine the output signal-to-noise ratio of the receiver.

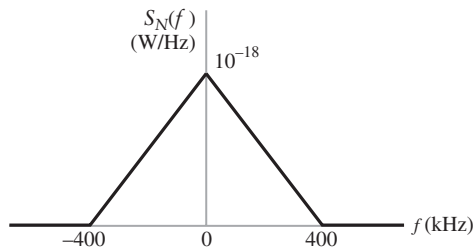


**FIGURE 9.19** Problem 9.10.

- 9.11** Derive an expression for the post-detection signal-to-noise ratio of the coherent receiver of Fig. 9.6, assuming that the modulated signal  $s(t)$  is produced by sinusoidal modulating wave

$$m(t) = A_m \cos(2\pi f_m t)$$

Perform your calculation for the following two receiver types:

- (a) Coherent DSB-SC receiver
- (b) Coherent SSB receiver

Assume the message bandwidth is  $f_m$ . Evaluate these expressions for a received signal strength of 100 picowatts, noise spectral density of  $10^{-15}$  watts per hertz, and  $f_m$  of 3 kHz.

- 9.12** Evaluate the autocorrelation function of the in-phase and quadrature components of narrow-band noise at the coherent detector input for the DSB-SC system. Assume the band-pass noise spectral density is  $S_N(f) = N_0/2$  for  $|f - f_c| < B_T$ .
- 9.13** Assume a message signal  $m(t)$  has the power spectral density

$$S_M(f) = \begin{cases} a \frac{|f|}{W}, & |f| \leq W \\ 0, & \text{otherwise} \end{cases}$$

where  $a$  and  $W$  are constants. Find the expression for post-detection SNR of the receiver when

- (a) The signal is transmitted by DSB-SC.
- (b) The signal is transmitted by amplitude modulation with amplitude sensitivity  $k_a = 0.3$ .
- (c) The signal is transmitted using frequency modulation with frequency sensitivity  $k_f = 500$  hertz per volt.

Assume that white Gaussian noise of zero mean and power spectral density  $N_0/2$  is added to the signal at the receiver input.

- 9.14** A 10 kilowatt transmitter amplitude modulates a carrier with a tone  $m(t) = \sin(2000\pi t)$ , using 50 percent modulation. Propagation losses between the transmitter and the receiver attenuate the signal by 90 dB. The receiver has a front-end noise with spectral density  $N_0 = -113$  watts/Hz and includes a bandpass filter with bandwidth  $B_T = 2W = 10$  kHz. What is the post-detection signal-to-noise ratio, assuming that the receiver uses an envelope detector?
- 9.15** The average noise power per unit bandwidth measured at the front end of an AM receiver is  $10^{-6}$  watts per Hz. The modulating signal is sinusoidal, with a carrier power of 80 watts and a sideband power of 10 watts per sideband. The message bandwidth is 4 kHz. Assuming the use of an envelope detector in the receiver, determine the output signal-to-noise ratio of the system. By how many decibels is this system inferior to a DSB-SC modulation system?
- 9.16** An AM receiver, operating with a sinusoidal modulating wave and 80 percent modulation, has a post-detection signal-to-noise ratio of 30 dB. What is the corresponding pre-detection signal-to-noise ratio?
- 9.17** The signal  $m(t) = \cos(400\pi t)$  is transmitted via FM. There is an ideal band-pass filter passing  $100 \leq |f| \leq 300$  at the discriminator output. Calculate the post-detection SNR given that  $k_f = 1$  kHz per volt, and the pre-detection SNR is 500. Use Carson's rule to estimate the pre-detection bandwidth.
- 9.18** Suppose that the spectrum of a modulating signal occupies the frequency band  $f_1 \leq |f| \leq f_2$ . To accommodate this signal, the receiver of an FM system (without pre-emphasis) uses an ideal band-pass filter connected to the output of the frequency discriminator; the filter passes frequencies in the interval  $f_1 \leq |f| \leq f_2$ . Determine the output signal-to-noise ratio and figure of merit of the system in the presence of additive white noise at the receiver input.
- 9.19** An FM system, operating at a pre-detection SNR of 14 dB, requires a post-detection SNR of 30 dB, and has a message power of 1 watt and bandwidth of 50 kHz. Using Carson's rule, estimate what the transmission bandwidth of the system must be. Suppose this system includes pre-emphasis and de-emphasis network with  $f_{3dB}$  of 10 kHz. What transmission bandwidth is required in this case?

### ADVANCED PROBLEMS

---

- 9.20** Assume that the narrowband noise  $n(t)$  is Gaussian and its power spectral density  $S_N(f)$  is symmetric about the midband frequency  $f_c$ . Show that the in-phase and quadrature components of  $n(t)$  are statistically independent.
- 9.21** Suppose that the receiver bandpass-filter magnitude response  $|H_{BP}(f)|$  has symmetry about  $\pm f_c$  and noise bandwidth  $B_T$ . From the properties of narrowband noise described in Section 8.11, what is the spectral density  $S_N(f)$  of the in-phase and quadrature components of the narrowband noise  $n(t)$  at the output of the filter? Show that the autocorrelation of  $n(t)$  is
- $$R_N(\tau) = \rho(\tau) \cos(2\pi f_c \tau)$$
- where  $\rho(\tau) = F^{-1}[S_N(f)]$ ; justify the approximation  $\rho(\tau) \approx 1$  for  $|\tau| \ll 1/B_T$ .
- 9.22** Assume that, in the DSB-SC demodulator of Fig. 9.6, there is a phase error  $\phi$  in the synchronized oscillator such that its output is  $\cos(2\pi f_c t + \phi)$ . Find an expression for the coherent detector output and show that the post-detection SNR is reduced by the factor  $\cos^2 \phi$ .
- 9.23** In a receiver using coherent detection, the sinusoidal wave generated by the local oscillator suffers from a phase error  $\theta(t)$  with respect to the carrier wave  $\cos(2\pi f_c t)$ . Assuming that  $\theta(t)$  is a zero-mean Gaussian process of variance  $\sigma_\theta^2$  and that most of the time the maximum value of  $\theta(t)$  is small compared to unity, find the mean-square error of the receiver output for DSB-SC modulation. The mean-square error is defined as the expected value of the squared difference between the receiver output and message signal component of a synchronous receiver output.

- 9.24** Equation (9.59) is the FM post-detection noise for an ideal low-pass filter. Find the post-detection noise for an FM signal when the post-detection filter is a second-order low-pass filter with magnitude resonance

$$|H(f)| = \frac{1}{(1 + (f/W)^4)^{1/2}}$$

Assume  $|H_{BP}(f + f_c)|^2 \approx 1$  for  $|f| < B_T/2$  and  $B_T \gg 2W$ .

- 9.25** Consider a communication system with a transmission loss of 100 dB and a noise spectral density of  $10^{-14}$  W/Hz at the receiver input. If the average message power is  $P = 1$  watt and the bandwidth is 10 kHz, find the average transmitter power (in kilowatts) required for a post-detection SNR of 40 dB or better when the modulation is:

- (a) AM with  $k_a = 1$ ; repeat the calculation for  $k_a = 0.1$ .
- (b) FM with  $k_f = 10, 50$ , and  $100$  kHz per volt.

In the FM case, check for threshold limitations by confirming that the pre-detection SNR is greater than 12 dB.

## ■ COMPUTER EXPERIMENTS

- 9.26** In this experiment, we investigate the performance of amplitude modulation in noise. The MATLAB script for AM experiment is provided in Appendix 7, it simulates envelope modulation by a sine wave with a modulation index of 0.3, adds noise, and then envelope-detects the message. Using this script:
- (a) Plot the envelope modulated signal.
  - (b) Using the supporting function “spectra,” plot its spectrum.
  - (c) Plot the envelope-detected signal before low-pass filtering.
  - (d) Compare the post-detection SNR to theory.
- 9.27** In this second computer experiment, we investigate the performance of a FM in noise. Using the MATLAB script for the FM experiment provided in Appendix 7:
- (a) Plot the spectrum of the baseband FM signal.
  - (b) Plot the spectrum of the band-pass FM plus noise.
  - (c) Plot the spectrum of the detected signal prior to low-pass filtering.
  - (d) Plot the spectrum of the detected signal after low-pass filtering.
  - (e) Compare pre-detection and post-detection SNRs for the FM receiver.

## CHAPTER 10

# NOISE IN DIGITAL COMMUNICATIONS

In the last twenty years, digital communication has been replacing existing analog communication in almost every instance. New communication services typically only consider digital communication. There are a number of reasons for this evolution in communication methods. Two technical reasons are the greater noise tolerance provided by digital communication, and the almost exact reproducibility of digital sequences at the receiver. Two strong external reasons for the increased dominance of digital communications are the rapid growth of machine-to-machine communications, such as on the Internet, and the spectacular evolution of digital electronics. In addition, the ability to further improve the robustness of digital communications through the use of error-correction codes is an important advantage over analog. Because digital communications have a greater noise tolerance than analog, digital communications are applied in situations where analog communications would never be. In these demanding situations, noise can still have a significant effect on digital communications, and this is what we will investigate in the chapter.

Broadly speaking, the purpose of detection is to establish the presence or absence of an information-bearing signal in noise. For this reason, we begin our analysis of the effects of noise on digital communications by considering the transmission of a single pulse. The characteristics of noise in digital systems are similar to those in analog systems; specifically, the received signal may be modeled as

$$r(t) = s(t) + w(t) \quad (10.1)$$

where  $s(t)$  is the transmitted signal and  $w(t)$  is the additive noise. As observed in previous chapters, there are numerous similarities between analog and digital modulation techniques. We will presently find that there are also similarities between analog and digital receiver structures.

The material in this chapter teaches us the following lessons.

- *Lesson 1: The bit error rate is the primary measure of performance quality of digital communication systems, and it is typically a nonlinear function of the signal-to-noise ratio.*
- *Lesson 2: Analysis of single-pulse detection permits a simple derivation of the principle of matched filtering. Matched filtering may be applied to the optimum detection of many linear digital modulation schemes.*
- *Lesson 3: The bit error rate performance of binary pulse-amplitude modulation (PAM) improves exponentially with the signal-to-noise ratio in additive white Gaussian noise.*

- *Lesson 4: Receivers for binary and quaternary band-pass linear modulation schemes are straightforward to develop from matched-filter principles and their performance is similar to binary PAM.*
- *Lesson 5: Non-coherent detection of digital signals results in a simpler receiver structure but at the expense of a degradation in bit error rate performance.*
- *Lesson 6: The provision of redundancy in the transmitted signal through the addition of parity-check bits may be used for forward-error correction. Forward-error correction provides a powerful method to improve the performance of digital modulation schemes.*

## 10.1 Bit Error Rate

With digital systems, it is the output quality of the information that is the primary concern. Since the information is digital and usually has a binary representation, this quality is measured in terms of the *average bit error rate* (BER). A bit error occurs whenever the transmitted bit and the corresponding received bit do not agree; this is a random event. Let  $n$  denote the number of bit errors observed in a sequence of bits of length  $N$ ; then the relative frequency definition of BER is

$$\text{BER} = \lim_{N \rightarrow \infty} \left( \frac{n}{N} \right) \quad (10.2)$$

In some digital systems, other measures of quality, closely related to the bit error rate, are often used. For example, many digital systems transfer information in *packets* and, regardless of whether there is one error in the packet or a hundred, the whole packet must be discarded. In these systems, the measure of quality is often the *packet error rate* (PER). This can be directly related to the BER if the bit errors are statistically independent.

Naturally, the required bit error rate of a digital system depends upon the application. For example:

- For vocoded speech,<sup>1</sup> a BER of  $10^{-2}$  to  $10^{-3}$  is often considered sufficient.
- For data transmission over wireless channels, a bit error rate of  $10^{-5}$  to  $10^{-6}$  is often the objective.
- For video transmission, a BER of  $10^{-7}$  to  $10^{-12}$  is often the objective, depending upon the quality desired and the encoding method.
- For financial data, a BER of  $10^{-11}$  or better is often the requirement.

Given the availability of different digital modulation–demodulation strategies, we need to compare their performance. Conceptually, we would like a figure of merit such as we used with analog modulation–demodulation systems that we could assign to each digital transmission scheme. Unfortunately, that is not as easy to do with digital systems because quality is usually not a linear function of the signal-to-noise ratio.

---

<sup>1</sup>Speech vocoders analyze the characteristics of short segments of speech, and parameters describing these characteristics are transmitted rather than actual samples of the speech. The length of the speech segments is typically 20 milliseconds. The advantage of vocoded speech over the PCM techniques described in Chapter 5 is the significant reduction in the bit rate required for an accurate representation. There are a wide variety of speech coding algorithms, and further details may be found in Gold and Morgan (1999).

However, we may define the equivalent of a reference SNR for digital systems. In particular, for digital systems, the reference SNR is the ratio of the *modulated energy per information bit* to the *one-sided noise spectral density*; namely,

$$\begin{aligned}\text{SNR}_{\text{ref}}^{\text{digital}} &= \frac{\text{Modulated energy per bit}}{\text{Noise spectral density}} \\ &= \frac{E_b}{N_0}\end{aligned}$$

This definition differs from the analog definition of reference SNR in three respects.

1. The analog definition was a ratio of powers. The digital definition is a ratio of energies, since the units of noise spectral density are watts/Hz, which is equivalent to energy. Consequently, the digital definition is dimensionless, as is the analog definition.
2. The definition uses the one-sided noise spectral density; that is, it assumes all of the noise occurs on positive frequencies. This assumption is simply a matter of convenience.
3. The reference SNR is independent of transmission rate. Since it is a ratio of energies, it has essentially been normalized by the bit rate.

To compare digital modulation–demodulation strategies, the objective is to determine the bit error rate performance as a function of the reference SNR, denoted by  $E_b/N_0$ . This *digital reference model* provides a frame of reference for a fair comparison of the different schemes.

#### EXAMPLE 10.1 Computing Packet Error Rate

A transmission system is designed to transfer data with a BER of  $10^{-5}$  or better. If this system is used to transmit packets of 1000 bits, what is the expected packet error rate? Assume the bit errors are statistically independent.

Under the assumption of independent bit errors, the bits in a packet form the equivalent of a Bernoulli sequence. Consequently, the number of bit errors has a binomial distribution as described in Example 8.5. The probability of a packet error is simply one minus the probability that the packet has no errors; that is, they are complementary events. Consequently, if  $n$  is the number of bit errors, the packet error rate is given by

$$\begin{aligned}\text{PER} &= 1 - P_{\text{binomial}}(n = 0) \\ &= 1 - \binom{1000}{0}(1 - 10^{-5})^{1000}(10^{-5})^0 \\ &= 9.95 \times 10^{-3}\end{aligned}$$

► **Drill Problem 10.1** Let  $H_0$  be the event that a 0 is transmitted and let  $R_0$  be the event that a 0 is received. Define  $H_1$  and  $R_1$ , similarly for a 1. Express the BER in terms of the probability of these events when:

- (a) The probability of a 1 error is the same as the probability as a 0 error.
- (b) The probability of a 1 being transmitted is not the same as the probability of a 0 being transmitted.

## 10.2 Detection of a Single Pulse in Noise

With the analog schemes, we saw that it was desirable to make filter bandwidths as small as possible to minimize the noise, yet not so small that they would distort the desired signal. In a loose sense, we may say that the filters are matched to the signal in a frequency-

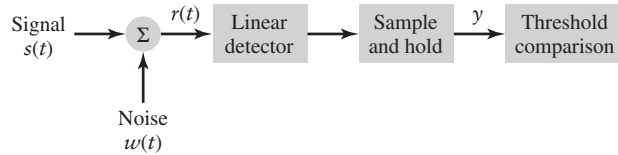


**FIGURE 10.1** Processing of a single pulse.

domain context. With digital schemes there is a more precise definition of matched filtering, as we shall see in what follows.

We begin with the situation shown in Fig. 10.1 for the detection of a single pulse transmitted at baseband. The received signal is first processed by a linear detector; the output of the detector is sampled and compared to a threshold. This threshold comparison is used to determine which of the following two situations has occurred:

1. The received signal  $r(t)$  consists solely of white Gaussian noise  $w(t)$ .
2. The received signal  $r(t)$  consists of  $w(t)$  plus a signal  $s(t)$  of known form.

The noise is assumed to have zero mean and spectral density  $N_0/2$ . At the receiver, we wish to determine which of these two situations is true by processing the signal  $r(t)$  in such a way that, if the signal  $s(t)$  is present, the receiver output at some arbitrary time  $t = T$  will be considerably greater than if  $s(t)$  is absent.

A practical example of the situation described above is binary pulse-amplitude modulation (PAM) using on-off signaling. A pulse  $s(t)$  may represent symbol 1, whereas the absence of the pulse may represent symbol 0. The objective is to maximize the receiver output when the pulse is present and to minimize its output when only noise is present.

For the single-pulse transmission scheme just described, our present objective is to *maximize the signal-to-noise ratio* at the output of the receiver. Mathematically, there are two possible forms for the received signal:

$$r(t) = \begin{cases} s(t) + w(t), & \text{pulse present} \\ w(t), & \text{pulse absent} \end{cases} \quad (10.3)$$

For this development, we assume that  $s(t)$  is a baseband pulse, and is nonzero only in the interval  $0 \leq t \leq T$ . Our detection strategy is to filter the received signal and sample the filter output at time  $T$ . The filter, described by impulse response  $g(t)$ , is assumed to be linear and time-invariant. Hence, the random variable for determining whether the pulse is present is defined by a form of the convolution integral:

$$Y = \int_0^T g(T-t)r(t) dt \quad (10.4)$$

The objective is to determine the filter  $g(t)$  that maximizes the signal-to-noise ratio of the output  $Y$ . To analyze Eq. (10.4) we use the first line of Eq. (10.3) to expand it as follows:

$$Y = \int_0^T g(T-t)s(t) dt + \int_0^T g(T-t)w(t) dt \quad (10.5)$$

The first integral on the right-hand side of Eq. (10.5) is the signal term, which will be zero if the pulse is absent, and the second integral is the noise term which is always there. We begin by analyzing the noise term. Let the noise contribution be denoted by

$$N = \int_0^T g(T-t)w(t) dt \quad (10.6)$$

This sampling of the filter output converts the random process  $w(t)$  to a random variable  $N$ . If the noise process  $w(t)$  has units of volts, then Eq. (10.6) can be thought of as a weighted summation of the noise over time, in which case  $N$  has units of volt-seconds. The expected value of  $N$ , defined by

$$\begin{aligned} \mathbb{E}[N] &= \int_0^T g(T-t)\mathbb{E}[w(t)] dt \\ &= 0 \end{aligned} \quad (10.7)$$

is therefore zero. This result follows from the interchange of expectation and integration discussed in Section 8.9, and the fact that additive white Gaussian noise  $w(t)$  is assumed to have zero mean. The variance of the output noise is given by

$$\begin{aligned} \text{Var}(N) &= \mathbb{E}[N^2] \\ &= \mathbb{E}\left[\int_0^T g(T-t)w(t) dt \int_0^T g(T-\tau)w(\tau) d\tau\right] \\ &= \int_0^T \int_0^T g(T-t)g(T-\tau)\mathbb{E}[w(t)w(\tau)] dt d\tau \end{aligned} \quad (10.8)$$

where, once again, we have changed the order of integration and expectation; we are permitted to do this because both of these operations are linear. We assume that the noise process is white such that  $\mathbb{E}[w(t)w(\tau)] = N_0/2 \delta(t - \tau)$ , where  $\delta(t)$  is the Dirac delta function. Then we may rewrite Eq. (10.8) as

$$\begin{aligned} \mathbb{E}[N^2] &= \int_0^T \int_0^T g(T-t)g(T-\tau) \frac{N_0}{2} \delta(t - \tau) dt d\tau \\ &= \frac{N_0}{2} \int_0^T |g(T-\tau)|^2 d\tau \\ &= \frac{N_0 T}{2} \end{aligned} \quad (10.9)$$

The second line of Eq. (10.9) follows from the first due to the sifting property of the delta function. The third line follows from the assumption that the receive filter,  $g(t)$ , has been normalized; that is,

$$\int_0^T |g(t)|^2 dt = T \quad (10.10)$$

The units of power spectral density are watts per hertz or watt-seconds. Thus,  $N_0 T$  in Eq. (10.9) has units of watt-(seconds)<sup>2</sup>; if we assume that measurement is performed with a one-ohm resistor, then this is equivalent to (volt-seconds)<sup>2</sup>. This observation shows that the units of  $\mathbb{E}[N^2]$  are consistent with those of  $N$ . To summarize, the noise sample at the output of the linear receiver has

- ▶ A mean of zero.
- ▶ A variance of  $N_0 T/2$ .
- ▶ A Gaussian distribution, since a filtered Gaussian process is also Gaussian (see Section 8.9).

It should also be noted that other than the normalization constraint of Eq. (10.10), this analysis of the noise component has placed no additional constraints on the choice of the filter impulse response  $g(t)$ .

Next we consider the signal component of Eq. (10.5) given by

$$S = \int_0^T g(T - \tau)s(\tau) d\tau \quad (10.11)$$

To maximize the signal-to-noise ratio, we choose  $g(t)$  to maximize Eq. (10.11) subject to the constraint of Eq. (10.10). To solve this maximization problem we use the Schwarz inequality for integrals (see Appendix 5). The *Schwarz inequality* for integrals is described by

$$\left| \int_{-\infty}^{\infty} g(T - t)s(t) dt \right|^2 \leq \int_{-\infty}^{\infty} |g(T - t)|^2 dt \int_{-\infty}^{\infty} |s(t)|^2 dt \quad (10.12)$$

which holds with equality if

$$g(T - t) = cs(t) \quad (10.13)$$

for some scalar  $c$ . Consequently, the signal of Eq. (10.11) and the signal-to-noise ratio are maximized if Eq. (10.13) is satisfied and the scalar  $c$  is chosen such that the constraint Eq. (10.10) is satisfied.

Equation (10.13) implies that the receive filter is matched to the transmit-pulse shape. This is the *principle of matched filter detection* that was alluded to in previous sections. That is, with single-pulse transmission, *processing the received signal with a filter matched to the transmitted signal maximizes the signal-to-noise ratio*.

If we substitute Eq. (10.13) into the detector of Eq. (10.4), we obtain

$$Y = c \int_0^T s(t)r(t) dt$$

In the general case, where the timing of the received pulse is not known exactly, we could compute a number of outputs at different time offsets  $\tau$  as follows:

$$Y(\tau) = c \int_{-\infty}^{\infty} s(t)r(t - \tau) dt$$

Recall from Chapter 8 that this expression is the equivalent to the cross-correlation of two ergodic signals  $s(t)$  and  $r(t)$ . Consequently, the receiver structure of Eq. (10.4) with  $g(T - t) = cs(t)$  is also referred to as a *correlation receiver*. With  $r(t)$  defined by Eq. (10.1), the signal component of this correlation is maximized at  $\tau = 0$ . This emphasizes the importance of synchronization when performing optimum detection.

► **Drill Problem 10.2** Suppose that in Eq. (10.4),  $r(t)$  represents a complex baseband signal instead of a real signal. What would be the ideal choice for  $g(t)$  in this case? Justify your answer.◀

## 10.3 Optimum Detection of Binary PAM in Noise

Single-pulse transmission, while convenient for analysis, has limited communication potential. We now extend the results of the previous section to the case where pulses are sent in consecutive intervals. In particular, consider binary PAM transmission with on-off signaling as shown in Fig. 10.2. This form of signaling may be represented as

$$s(t) = A \sum_{k=0}^{\infty} b_k h(t - kT) \quad (10.14)$$

where  $b_k$  is zero if the  $k$ th bit is a 0,  $b_k$  is one if the  $k$ th bit is a 1, and  $h(t)$  is a rectangular pulse of length  $T$  but centered at  $t = T/2$ . With transmitted pulse shape  $h(t) = \text{rect}[(t - T/2)/T]$ , the matched filter for this pulse shape is  $g(T - t) = h(t)$ . (See Problem 10.3.)



**FIGURE 10.2** Example of binary PAM transmission with on–off signaling;  $T$  denotes symbol interval.

The advantage of rectangular pulses is that the  $k$ th pulse is contained within the interval  $(k - 1)T < t < kT$ , and does not interfere with pulses in the adjacent intervals. Consequently, the matched filter for a pulse in the interval  $(k - 1)T < t < kT$  is the matched filter for a single pulse time-shifted to this interval. That is, in the  $k$ th symbol interval, the matched filter is  $g_k(T - t) = h(t - kT)$ . The output of the matched filter receiver at the end of the  $k$ th symbol interval is

$$\begin{aligned} Y_k &= \int_{-\infty}^{kT} g_k(T - t)r(t) dt \\ &= \int_{(k-1)T}^{kT} h(t - kT)r(t) dt \end{aligned} \quad (10.15)$$

where  $r(t) = s(t) + w(t)$  with  $s(t)$  given by Eq. (10.14). The second line of Eq. (10.15) follows from the fact that  $h(t - kT)$  is only nonzero over the interval  $(k - 1)T < t < kT$ .

Since the matched filter  $h(t) = 1$  wherever it is nonzero, we have

$$\begin{aligned} Y_k &= \int_{(k-1)T}^{kT} \text{rect}\left(\frac{t - (k + 1/2)T}{T}\right)r(t) dt \\ &= \int_{(k-1)T}^{kT} r(t) dt \end{aligned} \quad (10.16)$$

Equation (10.16) is the mathematical description of a physical device known as an *integrate-and-dump detector*. This device simply integrates the received signal over the symbol interval, samples the output, and then starts fresh for the next interval as shown in Fig. 10.3. This simple detector is optimum for rectangular signaling, which follows from Eq. (10.16).

► **Drill Problem 10.3** If  $g(t) = c \text{ rect}\left[\frac{\alpha(t - T/2)}{T}\right]$ , determine  $c$  such that  $g(t)$  satisfies Eq. (10.10) where  $\alpha > 1$ . ◀

### ■ BER PERFORMANCE

While the matched filter is optimum in terms of maximizing the signal-to-noise ratio, we would like to estimate the performance provided by such a scheme. As described in Section 10.2, the figure of merit for digital systems is typically the bit error rate (BER)—that is, the average fraction of received bits that are erroneously detected.

With the on–off transmission scheme described above, the receiver must make a decision between two hypotheses:

$$\begin{aligned} H_0: b_k &= 0 \text{ was transmitted} \\ H_1: b_k &= 1 \text{ was transmitted} \end{aligned} \quad (10.17)$$

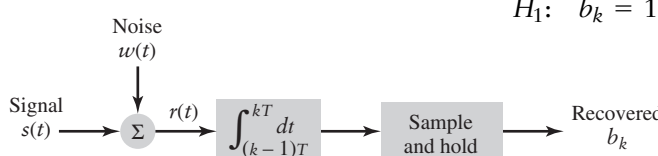


**FIGURE 10.3** The integrate-and-dump detector.

based on the received signal  $Y_k$  during the  $k$ th symbol interval. Since we have shown that, with rectangular pulse shapes, detection is independent from one symbol interval to the next, we are justified to drop the subscript  $k$  in what follows.

A reasonable criterion for choosing between these two hypotheses is to choose *the most likely hypothesis based on the observation*. That is, we compare the two conditional probabilities (where  $y$  is the value of the random variable  $Y$ ):

- $P(H_0|y)$  is the probability that a 0 was transmitted if  $y$  is received.
- $P(H_1|y)$  is the probability that a 1 was transmitted if  $y$  is received.

The largest of these two probabilities provides the decision for the bit under scrutiny. This situation is quite unlike analog communications, where we attempt to minimize the distortion on the received signal due to the noise. In digital communications, if reliable decisions are possible, then the transmitted message is recovered with no distortion.

Practically, we would like a simple decision rule for deciding between the two hypotheses,  $H_0$  and  $H_1$ . An example of such a decision rule is to choose  $H_0$ ; that is, choose 0 if  $y$  is less than some threshold  $\gamma$  and choose 1 if not. Intuitively, if  $b_k$  is either 0 or 1, then we would set the threshold  $\gamma$  at  $\frac{1}{2}$  and compare  $y$  to this threshold. If  $y$  is greater than  $\gamma$  then the decision is  $H_1$ ; otherwise, the decision is  $H_0$ . This intuitive decision rule is optimum in many situations, but let us show why.

Consider the probability of making an error with this decision rule based on conditional probabilities. If a 1 is transmitted, the probability of an error is

$$P[0 \text{ decided } | H_1] = P[Y < \gamma | H_1] \quad (10.18)$$

where  $Y$  is the random variable associated with the observation  $y$ . We refer to this error as a *Type I error*. To compute this probability recall, from the discussion in Section 10.2, that the random variable at the output of the matched filter upon which we base our decision—namely,

$$Y = S + N \quad (10.19)$$

has two components. From Eqs. (10.7) and (10.9),  $N$  is a zero-mean Gaussian random variable with variance  $\sigma^2 = N_0 T/2$ . From Eq. (10.14), the signal component of  $Y$  has a deterministic part, which is the pulse shape, and a random component, which is the modulation bit,  $b_k$ . However, for a particular symbol interval, modulation bit is fixed and  $S$  is obtained by substituting Eq. (10.14) into Eq. (10.11); specifically, for nominal  $k = 0$ , we have

$$\begin{aligned} S &= Ab \int_0^T h(t)h(t) dt \\ &= ATb \end{aligned} \quad (10.20)$$

where the second line follows from the normalized property of the matched filter (see Eq. [10.10]) and  $b = 0$  or 1 depending upon whether a 0 or 1 is being transmitted. Note that  $S$  has units of volt-seconds, consistent with previous developments.

From Eq. (10.20) we find that  $S$  has a mean  $\mu = AT$  when  $b = 1$  is being transmitted. Correspondingly,  $Y$  has a Gaussian distribution with mean  $\mu = AT$ , and its density function is given by

$$f_Y(y) = \frac{1}{\sqrt{2\pi}\sigma} \exp\{-(y - \mu)/2\sigma^2\} \quad (10.21)$$

which is depicted in Fig. 10.4.

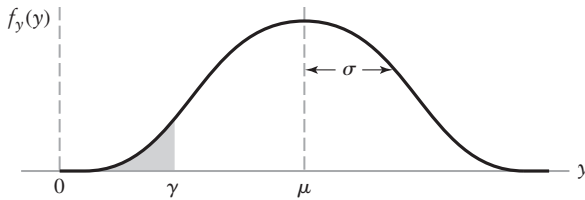


**FIGURE 10.4** The Gaussian density function for detecting a 1 with on–off signaling.

The probability of a Type I error, as specified by Eq. (10.18), is the probability that the output  $Y$  falls in the shaded area, below  $\gamma$  in Fig. 10.4. Mathematically, this probability is the integral of the shaded area of the Gaussian density function

$$\begin{aligned} \mathbf{P}[Y < \gamma | H_1] &= \frac{1}{\sqrt{2\pi}\sigma} \int_{-\infty}^{\gamma} \exp(-(y - \mu)^2/2\sigma^2) dy \\ &= Q\left(\frac{\mu - \gamma}{\sigma}\right) \end{aligned} \quad (10.22)$$

where the  $Q$ -function was defined in Section 8.4.

Equation (10.22) is not the only contributor to the bit errors. An error can also occur if a 0 is transmitted and a 1 is detected. We refer to this error as a *Type II error*. It can be shown that the probability of a Type II error is (see Problem 10.4)

$$\mathbf{P}[Y > \gamma | H_0] = Q\left(\frac{\gamma}{\sigma}\right) \quad (10.23)$$

The probability regions associated with Type I and Type II errors are illustrated in Fig. 10.5. The combined probability of error is given by Bayes' rule (see Section 8.1)

$$P_e = \mathbf{P}[Y < \gamma | H_1] \cdot \mathbf{P}[H_1] + \mathbf{P}[Y > \gamma | H_0] \cdot \mathbf{P}[H_0] \quad (10.24)$$

where  $\mathbf{P}[H_i]$  is the *a priori* probability that 0 or 1 is transmitted. Typically, the transmitted bits are equiprobable, which means that

$$\mathbf{P}[H_1] = \mathbf{P}[H_0] = \frac{1}{2} \quad (10.25)$$

Consequently, the average probability of error is given by

$$P_e = \frac{1}{2} Q\left(\frac{\mu - \gamma}{\sigma}\right) + \frac{1}{2} Q\left(\frac{\gamma}{\sigma}\right) \quad (10.26)$$

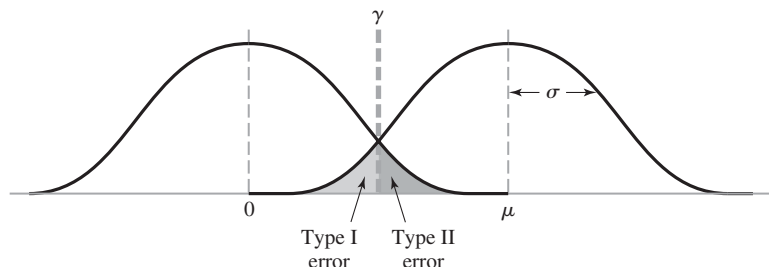


**FIGURE 10.5** Illustration of decision errors for 0 and 1 with on–off signaling.

Often we would like the probabilities of the two types of errors,  $P[\text{Type I error}]$  and  $P[\text{Type II error}]$ , to be equal; so we choose  $\gamma = \mu/2$ . It can be shown that this choice of  $\gamma$  minimizes the probability of error described by Eq. (10.26) (see Problem 10.22). Consequently, we have that the average probability of error is given by

$$P_e = Q\left(\frac{\mu}{2\sigma}\right) \quad (10.27)$$

That is, the probability of a bit error depends upon the ratio of the signal mean  $\mu$  when 1 is transmitted to the noise standard deviation  $\sigma$  through the nonlinear function  $Q$ .

Our next step is to express this probability of bit error in terms of the digital reference model. This evaluation may be broken down into two components:

- To express the variance in terms of the noise spectral density, we have, from Eq. (10.9), that  $\sigma^2 = N_0 T/2$ .
- To express the signal amplitude  $A$  in terms of the energy per bit  $E_b$ , we assume that 0 and 1 are equally likely to be transmitted. Then the average energy per bit at the receiver input is

$$\begin{aligned} E_b &= \mathbf{E}\left[\int_0^T |s(t)|^2 dt\right] \\ &= A^2 \mathbf{E}[b^2] \int_0^T |h(t)|^2 dt \\ &= A^2 \left\{ \frac{1}{2} \cdot 0 + \frac{1}{2} \cdot 1 \right\} T \\ &= \frac{A^2 T}{2} \end{aligned} \quad (10.28)$$

where, in the second line, we have separated the deterministic and random parts of the signal and the third line follows from the fact that  $h(t) = \text{rect}[(t - T/2)/T]$ . Consequently, we have that  $A = \sqrt{2E_b/T}$  for the case of on-off PAM signaling.

By substituting these values for  $\sigma$  and  $\mu = AT$  into Eq. (10.27), the result obtained is

$$P_e^{\text{on-off}} = Q\left(\sqrt{\frac{E_b}{N_0}}\right) \quad (10.29)$$

It is interesting to note that if, instead of on-off keying with levels of 0 and  $A$ , we used bipolar levels of  $-A/2$  and  $+A/2$ , then the above analysis would be unchanged except that the threshold would now be  $\gamma = 0$ . However, with the bipolar scheme the energy per bit is  $E_b = A^2 T/4$ , and the bit error rate in terms of the digital reference model is

$$P_e^{\text{bipolar}} = Q\left(\sqrt{\frac{2E_b}{N_0}}\right) \quad (10.30)$$

Since the  $Q$ -function is a monotone decreasing function of its argument, Eq. (10.30) implies that a smaller  $E_b/N_0$  ratio will produce the same error rate as the on-off scheme characterized by Eq. (10.29). Thus, we find that bipolar signaling is a more power-efficient method of achieving the same bit error rate performance than the on-off signaling scheme.

- **Drill Problem 10.4** Show that with on-off signaling, the probability of a Type II error in Eq. (10.23) is given by

$$\mathbf{P}[Y > \gamma | H_0] = Q\left(\frac{\gamma}{\sigma}\right)$$

### ■ NONRECTANGULAR PULSE SHAPES

We saw in Chapter 6 that due to spectral limitations and channel effects, the received signal may not have a rectangular pulse shape. If we combine this observation with noise, the received signal may be represented as

$$r(t) = A \sum_{k=0}^{\infty} b_k p(t - kT) + w(t) \quad (10.31)$$

where  $p(t)$  is the pulse shape. Since this pulse shape is not necessarily confined to an interval of length  $T$ , one might expect that intersymbol interference would be an issue in a continuous transmission scheme.

In particular, we consider the case where  $p(t)$  is a *normalized root-raised cosine pulse shape* described in Section 6.4. For a single pulse having a root-raised cosine spectral shape, the matched-filter theory of Section 10.2 still applies. In addition, this pulse shape has the following orthogonality property when  $E = 1$  (see Problems 10.5 and 10.12):

$$\int_{-\infty}^{\infty} p(kT - t)p(t - lT) dt = \delta(k - l) \quad (10.32)$$

where  $\delta(t)$  is the Dirac delta function. Applying the matched filter for the  $k$ th symbol of  $r(t)$  to Eq. (10.31), we get

$$\begin{aligned} Y_k &= \int_{-\infty}^{\infty} p(kT - t)r(t) dt \\ &= Ab_k \int_{-\infty}^{\infty} p(kT - t)p(t - kT) dt + N_k + \sum_{l \neq k} Ab_l \int_{-\infty}^{\infty} p(kT - t)p(t - lT) dt \end{aligned} \quad (10.33)$$

where  $k$ th noise term is

$$N_k = \int_{-\infty}^{\infty} p(kT - t)w(t) dt \quad (10.34)$$

The first two terms of Eq. (10.33) represent the usual signal-plus-noise term associated with single pulse detection. The third term represents the interference due to adjacent symbols. However, if we substitute Eq. (10.32) into Eq. (10.33), we see that the detector output reduces to that of single-pulse detection. That is, there is no intersymbol interference with the proper choice of pulse shaping. Under these conditions,  $Y_k = Ab_k + N_k$ , and the BER performance is the same as with rectangular pulse shaping, which is a remarkable result. The implementation of such a scheme is shown in Fig. 10.6, which involves the use of root-raised cosine pulse shaping.

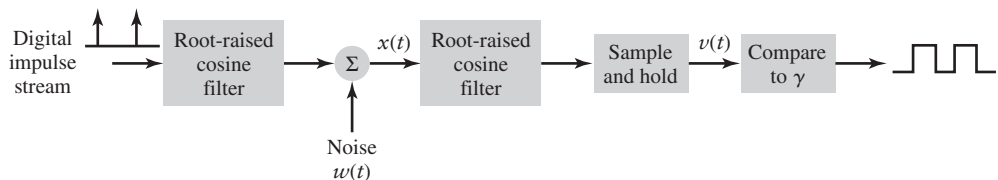


**FIGURE 10.6** Implementation of PAM with root-raised cosine filtering.  
(Root-raised cosine pulse shaping was discussed in Section 6.4.)

► **Drill Problem 10.5** Prove the property of root-raised cosine pulse shape  $p(t)$  given by Eq. (10.32), using the following steps:

- If  $R(f)$  is the Fourier transform representation of  $p(t)$ , what is the Fourier transform representation of  $p(t - IT)$ ?
- What is the Fourier transform of  $q(\tau) = \int_{-\infty}^{\infty} p(\tau - t)p(t - IT) dt$ ? What spectral shape does it have?
- What is  $q(\tau)$ ? What is  $q(kT)$ ?

Use these results to show that Eq. (10.32) holds. ◀

## 10.4 Optimum Detection of BPSK

As described in Chapter 7, one of the simplest forms of digital band-pass communications is binary phase-shift keying. With BPSK, the transmitted signal is

$$s(t) = \begin{cases} A_c \cos(2\pi f_c t), & 0 \leq t \leq T \text{ if a 1 is sent} \\ A_c \cos(2\pi f_c t + \pi), & 0 \leq t \leq T \text{ if a 0 is sent} \end{cases}$$

That is, opposing phases of the same carrier are transmitted to represent the binary symbols. The detection of BPSK is simplified by noting that since  $\cos(2\pi f_c t + \pi) = -\cos(2\pi f_c t)$ , the transmitted signal may be equally represented as

$$s(t) = \begin{cases} A_c \cos(2\pi f_c t), & 0 \leq t \leq T \text{ if a 1 is sent} \\ -A_c \cos(2\pi f_c t), & 0 \leq t \leq T \text{ if a 0 is sent} \end{cases} \quad (10.35)$$

Hence, in general, we may write

$$s(t) = A_c m(t) \cos(2\pi f_c t) \quad (10.36)$$

where, for single pulse transmission,  $m(t) = +1$  for a 1 and  $m(t) = -1$  for a 0 with  $0 \leq t \leq T$ . In the more general case, when transmitting multiple bits, we have

$$m(t) = \sum_{k=0}^{N-1} b_k h(t - kT) \quad (10.37)$$

where  $h(t)$  is the rectangular pulse  $\text{rect}\left(\frac{t - T/2}{T}\right)$ . Thus, BPSK has a form very similar to double-sideband suppressed-carrier (DSB-SC) modulation that is used for analog communications, a point which was made previously in Chapter 3. Consequently, to recover the message, we may use a receiver structure analogous to the coherent receiver structure used with DSB-SC. A typical receiver structure for BPSK is shown in Fig. 10.7, where the RF signal plus white Gaussian noise,  $s(t) + w(t)$ , is frequency-translated to an IF where it is band-pass filtered. The band-pass signal,  $x(t)$ , is the input to the coherent BPSK detector.

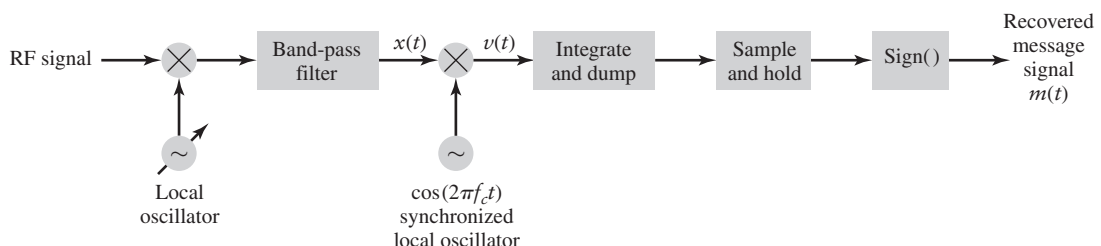


**FIGURE 10.7** Typical BPSK receiver structure.

### ■ DETECTION OF BPSK IN NOISE

Following the development for DSB-SC demodulation of Section 9.4, the signal plus band-pass noise at the input to the coherent BPSK detector of Fig. 10.7 may be represented as

$$x(t) = s(t) + n_I(t) \cos(2\pi f_c t) - n_Q(t) \sin(2\pi f_c t) \quad (10.38)$$

where  $n_I(t)$  and  $n_Q(t)$  are the in-phase and quadrature components of the band-pass noise  $n(t)$ , respectively. The output of the product modulator in Fig. 10.7 is given by

$$\begin{aligned} v(t) &= x(t) \cos(2\pi f_c t) \\ &= \frac{1}{2} [A_c m(t) + n_I(t)] + \left[ \frac{1}{2} (A_c m(t) + n_I(t)) \cos(4\pi f_c t) - \frac{1}{2} n_Q(t) \sin(4\pi f_c t) \right] \end{aligned} \quad (10.39)$$

where we have used the double angle formulas:  $\cos A \cos B = \frac{1}{2}\{\cos(A - B) + \cos(A + B)\}$  and  $\sin A \cos B = \frac{1}{2}\{\sin(A - B) + \sin(A + B)\}$ . Let us consider the two parts of the second line of Eq. (10.39). The first part represents the baseband signal plus a baseband component of the noise, while the second part represents signal and noise centered at the much higher frequency of  $2f_c$ .

With the analog DSB-SC signal, we used a low-pass filter to remove the high-frequency noise components and recover the desired signal. With digital signals, we know that a matched filter is the optimum method to recover the data. We could combine the matched filter with a low-pass filter to achieve the desired results, as long as the low-pass filter does not distort the desired signal. However, if we recognize that the matched filter

$$\begin{aligned} g(T - t) &= h(t) \\ &= \text{rect}\left(\frac{t - T/2}{T}\right) \end{aligned}$$

is already a low-pass filter, then there is no need for the second filter.

The observant reader will note that in the derivation of the matched filter, we assume that the noise is white. The in-phase component  $n_I(t)$  is narrowband noise and hence not white. However, it can be shown that as long as the bandpass filter has a wider bandwidth than that of the signal and the noise spectral density is approximately flat over the bandwidth of the signal, the matched-filter principle still applies.

In the case where  $m(t)$  consists of rectangular pulses, the optimum detector after downconversion is the integrate-and-dump filter, as was shown for the case of pulse-amplitude modulation (PAM). The output of the integrate-and-dump detector in this case is therefore

$$\begin{aligned} Y_k &\approx \frac{1}{2} \int_{(k-1)T}^{kT} [A_c m(t) + n_I(t)] dt \\ &= \frac{A_c T}{2} b_k + N_k \end{aligned} \quad (10.40)$$

Equation (10.40) assumes that the high-frequency terms have negligible impact on the detector output. The noise term in Eq. (10.40) is given by

$$N_k \approx \frac{1}{2} \int_{(k-1)T}^{kT} n_I(t) dt \quad (10.41)$$

Recall from Section 8.11 that if the power spectral density of the narrowband noise  $n(t)$  is  $N_0/2$ , then the power spectral density of the in-phase component of the noise  $n_I(t)$  is  $N_0$ , over their respective frequency bands. Accordingly, we may write

$$\begin{aligned}
\mathbf{E}[N_k^2] &= \frac{1}{4} \mathbf{E} \left[ \int_{(k-1)T}^{kT} \int_{(k-1)T}^{kT} n_I(t) n_I(s) dt ds \right] \\
&= \frac{1}{4} \left[ \int_{(k-1)T}^{kT} \int_{(k-1)T}^{kT} N_0 \delta(t-s) dt ds \right] \\
&= \frac{1}{4} \int_{(k-1)T}^{kT} N_0 ds \\
&= \frac{N_0 T}{4}
\end{aligned}$$

Thus, the variance  $\sigma^2$  of  $N_k$  in Eq. (10.41) is  $\frac{1}{4} N_0 T$ .

In Fig. 7.4(b), we show a BPSK demodulator quite similar to that shown in Fig. 10.7. The main difference between the two demodulators is that the low-pass filter of the former is replaced by the integrator of the latter. In the noiseless case of Chapter 7, the purpose of the low-pass filter is to remove the high-frequency components, while retaining the desired baseband signal. The integrator of Fig. 10.7 also acts as a low-pass filter removing the high-frequency components but, due to its matched property, it additionally removes as much noise as possible from the signal, and thereby maximizes the signal-to-noise ratio at the demodulator output. Note that in digital communications, the objective is to recover the information, 0s and 1s, as reliably as possible. Unlike analog communications, there is no requirement that the transmitted waveform should be recovered with minimum distortion.

## ■ PERFORMANCE ANALYSIS

The bit error rate analysis with BPSK is similar to the analysis of bipolar signaling in Section 10.3. The threshold for deciding between a 0 and a 1 at the output of the matched filter is set at zero. A threshold of zero has the practical advantage that it does not have to be calibrated if the transmission path has an unknown gain.

From Eq. (10.40), the mean signal value is  $A_c T/2$  or  $-A_c T/2$ , depending upon whether  $b_k$  is +1 or -1, respectively. If we assume a 1 was transmitted and let  $\mu = A_c T/2$ , then the probability of error is

$$\begin{aligned}
P_e &= P[Y < 0] \\
&= \frac{1}{\sqrt{2\pi}\sigma} \int_{-\infty}^0 \exp\left\{-\frac{(y-\mu)^2}{2\sigma^2}\right\} dy
\end{aligned} \tag{10.42}$$

Consequently, analogous to Eq. (10.22) with  $\gamma = 0$ , the bit error rate is given by

$$P_e = Q\left(\frac{\mu}{\sigma}\right) \tag{10.43}$$

By symmetry, this result holds when either a +1 or -1 is transmitted. In terms of the digital reference model, we note that the energy per bit with BPSK, assuming the energy of the pulses in  $m(t)$  is normalized, is simply  $E_b = A_c^2 T/2$ . Using this result in the definition of  $\mu$ , with  $b_k = +1$ , we have

$$\mu = \frac{A_c T}{2} = \sqrt{\frac{2E_b}{T}} \frac{T}{2} = \sqrt{\frac{E_b T}{2}}$$

Substituting the value of  $\mu$  so obtained and  $\sigma = \frac{1}{2}\sqrt{N_0 T}$  into Eq. (10.43), we obtain the result

$$P_e^{\text{BPSK}} = Q\left(\sqrt{\frac{2E_b}{N_0}}\right) \quad (10.44)$$

This BER performance is exactly the same as that of the baseband bipolar scheme as given in Eq. (10.30). That is, there is no difference in BER performance between the low-pass bipolar PAM signaling and bandpass BPSK modulation. Thus, just as in the analog case, there is no change in the figure of merit when we go from a baseband system to an equivalent coherent band-pass system.

The analysis of BPSK can be extended to nonrectangular pulse shaping in a manner similar to what occurred at baseband. For nonrectangular pulse shaping, we represent the transmitted signal as

$$s(t) = A_c \sum_{k=-\infty}^{\infty} b_k p(t - kT) \cos(2\pi f_c t) \quad (10.45)$$

where  $p(t)$  is the pulse shape and  $b_k = \pm 1$  represents the data. This combination of pulse shaping and BPSK modulation forms an important method of communicating binary information and controlling the bandwidth required for the transmission. In particular, BPSK modulation allows multiple users to use the same transmission medium by choosing carrier frequencies  $f_c$ ; and the pulse shaping limits the transmitted signal bandwidth and thus reduces or eliminates the interference between communication links using different  $f_c$ .

► **Drill Problem 10.6** Compare the transmission bandwidth required for binary PAM and BPSK modulation, if both signals have a data rate of 9600 bps and use root-raised cosine pulse spectrum with a roll-off factor of 0.5. ◀

► **Drill Problem 10.7** Sketch a block diagram of a transmission system including both transmitter and receiver for BPSK modulation with root-raised cosine pulse shaping. ◀

## 10.5 Detection of QPSK and QAM in Noise

With an understanding of binary data detection in noise for both the baseband (PAM) and passband (BPSK) at our disposal, we now extend these results to more complex modulation schemes such as quadri-phase-shift keying (QPSK) and quadrature amplitude modulation (QAM).

### ■ DETECTION OF QPSK IN NOISE

We saw in Section 7.3 that QPSK-modulated signal  $s(t)$  could be represented in the form

$$s(t) = A_c \cos(2\pi f_c t + \phi(t)) \quad (10.46)$$

for  $0 \leq t \leq T$ . The carrier is transmitted in one of four phases with each phase representing a two-bit pair (i.e., dabit), as given by

$$\phi(t) = \begin{cases} \frac{3\pi}{4}, & \text{dibit 00} \\ \frac{\pi}{4}, & \text{dibit 10} \\ -\frac{\pi}{4}, & \text{dibit 11} \\ -\frac{3\pi}{4}, & \text{dibit 01} \end{cases} \quad (10.47)$$

It was also shown that Eq. (10.46) could be represented in a quadrature form by expanding the cosine term to obtain

$$\begin{aligned} s(t) &= A_c \cos[\phi(t)] \cos(2\pi f_c t) - A_c \sin[\phi(t)] \sin(2\pi f_c t) \\ &= A_c m_I(t) \cos(2\pi f_c t) - A_c m_Q(t) \sin(2\pi f_c t) \end{aligned} \quad (10.48)$$

In Eq. (10.48), we have identified  $\cos[\phi(t)]$  as the in-phase component  $m_I(t)$  of the message signal, and  $\sin[\phi(t)]$  as its quadrature component  $m_Q(t)$ . The similarity of Eq. (10.48) to quadrature-carrier multiplexing discussed in Section 3.5 for analog signals leads to the quadrature receiver shown in Fig. 10.8. Using in-phase and quadrature representation for the band-pass noise, we find that the QPSK input to the coherent detector of Fig. 10.8 is described by

$$\begin{aligned} x(t) &= s(t) + n(t) \\ &= (A_c m_I(t) + n_I(t)) \cos(2\pi f_c t) - (A_c m_Q(t) + n_Q(t)) \sin(2\pi f_c t) \end{aligned} \quad (10.49)$$

Analogous to the results obtained with the detection of BPSK, the intermediate output of the upper branch of Fig. 10.8 is

$$\begin{aligned} v_I(t) &= \frac{1}{2}(A_c m_I(t) + n_I(t)) \\ &\quad + \frac{1}{2}(A_c m_I(t) + n_I(t)) \cos(4\pi f_c t) - \frac{1}{2}(A_c m_Q(t) + n_Q(t)) \sin(4\pi f_c t) \end{aligned} \quad (10.50)$$

where the right-hand term on the first line is a low-pass signal; and the terms on the second line are high-frequency signals. As with BPSK using rectangular pulse shaping, since  $m_I(t)$  is constant over the duration of pulse, a matched filter with a rectangular shape (integrate-and-dump) can be used to recover  $m_I(t)$  to maximize the signal-to-noise ratio of the output. As previously mentioned, such a filter will also reject the high-frequency terms.

The comments made in Section 10.4 also apply to Fig. 10.8 when comparing it to Fig. 7.7(b). In Figure 7.7(b), the low-pass filter removes high-frequency components. In Fig. 10.8, the integrator serves this purpose as well as maximizing the signal-to-noise ratio.

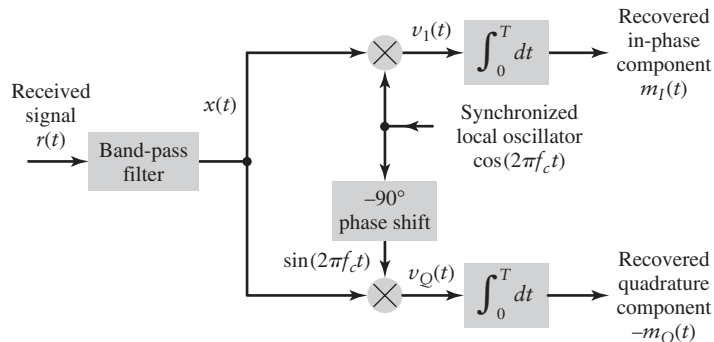


**FIGURE 10.8** Quadrature receiver for QPSK.

Similarly, the output of the lower branch of the quadrature detector is

$$\begin{aligned} v_Q(t) &= -\frac{1}{2}(A_c m_Q(t) + n_Q(t)) \\ &\quad + \frac{1}{2}(A_c m_Q(t) + n_Q(t)) \cos(4\pi f_c t) + \frac{1}{2}(A_c m_I(t) + n_I(t)) \sin(4\pi f_c t) \end{aligned} \quad (10.51)$$

The baseband signal  $m_Q(t)$  can be recovered in a manner similar to  $m_I(t)$ .

For the in-phase component, if the first bit of the dabit is a 0, then the mean output is

$$\mu = \frac{A_c T}{2} \cos\left(\frac{\pm 3\pi}{4}\right) = -\frac{A_c T}{2\sqrt{2}}$$

If on the other hand, the first bit of the dabit is a 1 then

$$\mu = \frac{A_c T}{2} \cos\left(\frac{\pm \pi}{4}\right) = \frac{A_c T}{2\sqrt{2}}$$

After low-pass filtering, the form of Eq. (10.50) is the same as we found with BPSK in Eq. (10.40). Consequently, the probability of error on the in-phase branch of the QPSK signal is

$$P_e = Q\left(\frac{|\mu|}{\sigma}\right) \quad (10.52)$$

where  $\sigma$  is the square root of the noise variance (i.e. the standard deviation). The  $|\mu|$  indicates the symmetry between the 0 bit and the 1 bit. The same result holds for the quadrature component. To express this result in terms of the digital reference model we note that, with QPSK modulation, two bits are transmitted in one symbol interval of length  $T$ . Consequently, the average energy by bit may be determined from

$$\begin{aligned} 2E_b &= E\left[\int_0^T s^2(t) dt\right] \\ &= A_c^2 \int_0^T \cos^2(2\pi f_c t + \phi(t)) dt \\ &= A_c^2 \int_0^T \frac{1 + \cos(4\pi f_c t + 2\phi(t))}{2} dt \\ &\approx \frac{A_c^2 T}{2} \end{aligned} \quad (10.53)$$

where, under the bandpass assumption, the integral of the high-frequency term is approximately zero. We also note that the noise variance at each branch output is unchanged from BPSK with  $\sigma^2 = \frac{1}{4}N_0 T$ . With this difference, the bit error rate with  $v_I(t)$  after matched filtering is given by

$$\begin{aligned} P_e^{\text{QPSK}} &= Q\left(\frac{|\mu|}{\sigma}\right) \\ &= Q\left(\frac{A_c T / 2\sqrt{2}}{\sqrt{1/4 N_0 T}}\right) \\ &= Q\left(\sqrt{\frac{2E_b}{N_0}}\right) \end{aligned} \quad (10.54)$$

where we have made the substitution  $A_c = \sqrt{4E_b/T}$  from Eq. (10.53). A similar result follows for  $v_Q(t)$  by symmetry.

Consequently, in terms of energy per bit, the QPSK performance is exactly the same as BPSK, even though we are *transmitting twice as many bits through the same channel*. This important result is due to the inherent orthogonal nature of the in-phase and quadrature components. Once again we may draw an analogy with analog communications, where comparing double-sideband and single-sideband transmission, we found that we could obtain the same quality of performance but with half of the transmission bandwidth. With QPSK modulation, we use the same transmission bandwidth as BPSK but transmit twice as many bits with the same reliability.

As described in Section 7.3, offset-QPSK or OQPSK is a variant of QPSK modulation wherein the quadrature component is delayed by one-half of symbol period relative to the in-phase component. Under the bandpass assumption, delaying the quadrature component does not change its orthogonality with the in-phase component. Consequently, we may use the same quadrature detector for recovering an OQPSK as is used for QPSK. The only difference is that the sampling of the integrate-and-dump detector of the quadrature component occurs one-half symbol latter than that for the in-phase component.

As a result of this similarity between the OQPSK and QPSK, the bit error rate performance of both schemes is identical if the transmission path does not distort the signal. As mentioned in Chapter 7, one advantage of OQPSK is its reduced phase variations and potentially less distortion if the transmission path includes nonlinear components such as an amplifier operating near or at saturation. Under such nonlinear conditions, OQPSK may perform better than QPSK.

► **Drill Problem 10.8** Show that the integral of the high-frequency term in Eq. (10.53) is approximately zero. ◀

### ■ DETECTION OF QAM IN NOISE

Quadrature amplitude modulation (QAM), discussed in Section 7.7, is also a band-pass modulation strategy due to its use of the in-phase and quadrature components of the carrier. QAM can be viewed as a hybrid of multi-level PAM and QPSK. In particular, QAM uses in-phase and quadrature components for transmission just as QPSK does. However, in each of the in-phase and quadrature components in QAM, the modulator uses multiple levels—that is, more than the two levels of  $\pm\cos\phi$  or  $\pm\sin\phi$  used in QPSK.

First, let us consider multi-level PAM. Let the baseband modulated signal be represented by

$$s(t) = A \sum_{k=0}^{\infty} c_k h(t - kT) \quad (10.55)$$

where the  $c_k$  represent different modulation levels. For example, with four-level PAM, the scalar  $c_k$  could be selected from the set  $\{-3, -1, +1, +3\}$ . The eye diagram for such a multi-level signal could look like Fig. 10.9.

If we review the analysis of the optimum procedure that led to the matched filter detector, we find that it did not depend on the signal amplitude. Consequently, the detector design for the multi-level PAM receiver is identical to that for on-off PAM. The only difference between binary PAM and multi-level PAM is the threshold comparisons used to determine which of the levels were transmitted, as depicted in Fig. 10.10.

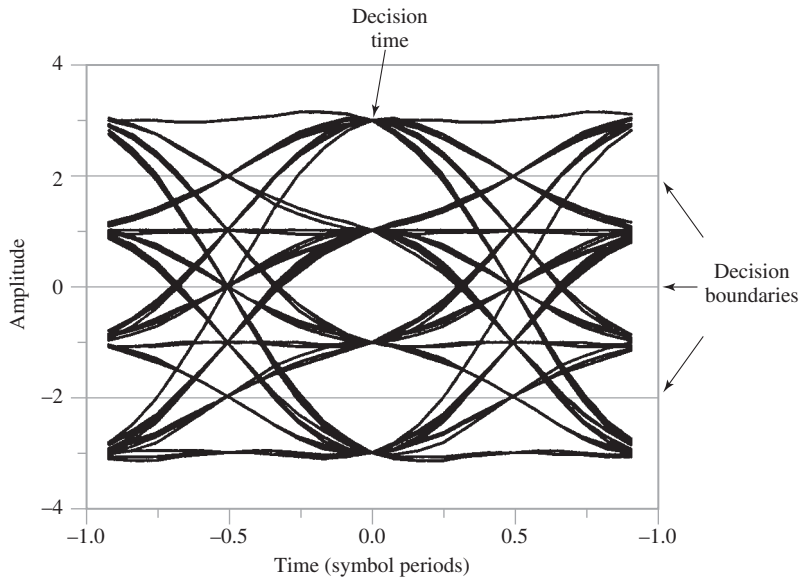


**FIGURE 10.9** Eye diagram for four-level PAM.

For each symbol value  $y$  at the output of the detector, the probability of error is intuitively minimized by choosing the closest modulation level—for example, from  $\{-3, -1, +1, +3\}$ . We do this by comparing the output  $y$  to a series of thresholds before making the decision. For the four-level eye diagram shown in Fig. 10.9, the thresholds are at the values 0 and  $\pm 2$ . Such a threshold tree is shown in Fig. 10.11. Then, for example, if  $0 < y < 2$ , we estimate  $c_k = +1$ ; if  $-2 < y < 0$ , we estimate  $c_k = -1$ .

We will now discuss the performance of such a detector, but for simplicity we shall assume the symbol period  $T$  is one. For most scenarios, errors will be made with the nearest neighbor. For example, for the symbol  $+1$  the most likely erroneous decisions are the nearest neighbor symbols of  $+3$  and  $-1$ . If, in general, we assume the transmitted signal level is  $\mu$  and the separation between nearest neighbors is  $2A$ , then, for those symbols that have two nearest neighbors, the probability of error for these symbols is

$$\begin{aligned} P_e &= \mathbf{P}[y < \mu - A \text{ or } y > \mu + A] \\ &= \frac{1}{\sqrt{2\pi}\sigma} \int_{-\infty}^{\mu-A} \exp\left\{-\frac{(y-\mu)^2}{2\sigma^2}\right\} dy + \frac{1}{\sqrt{2\pi}\sigma} \int_{\mu+A}^{\infty} \exp\left\{-\frac{(y-\mu)^2}{2\sigma^2}\right\} dy \\ &= 2Q\left(\frac{A}{\sigma}\right) \end{aligned} \quad (10.56)$$

where  $\sigma$  is the noise standard deviation. This result applies for all those symbols that have two nearest neighbors. For the outer symbols, which have only one neighbor, the probability of error is half of the value defined in Eq. (10.56). Combining these two cases, it can

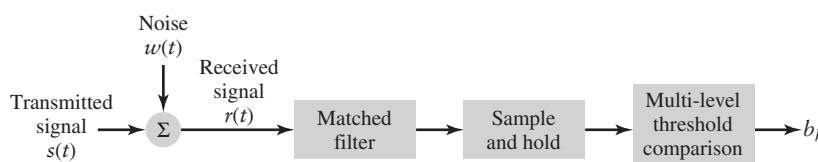


**FIGURE 10.10** Multi-level PAM detector.

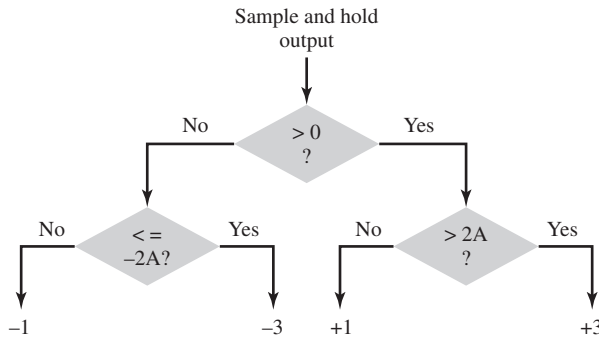


**FIGURE 10.11** Illustration of decision rules with four level PAM.

be shown (see Problem 10.23) that the probability of error for  $M$ -ary PAM is, with the modulation levels separated by a distance  $2A$ ,

$$P_e^{\text{PAM}} = 2 \left( \frac{M-1}{M} \right) Q \left( \frac{A}{\sigma} \right) \quad (10.57)$$

Although this expression appears similar to that obtained with binary transmission, there are two important differences that should be noted:

1. Equation (10.57) represents a *symbol error rate*. Each symbol represents more than one bit. Consequently, each symbol error may correspond to more than one bit error, although the symbols are usually arranged, that is, Gray encoded, so that it does not.
2. With binary transmission with levels of  $+A$  and  $-A$ , the average transmitted power is  $A^2$ . With the  $M$ -ary PAM strategy, assuming all levels are equally likely and separated by  $2A$ , we can show that the average transmitted power is  $(M^2 - 1)A^2/3$  (see Problem 10.23); consequently, the extra throughput provided by multi-level PAM requires significantly more power to achieve the same performance.

Assuming baseband transmission, we can relate the performance of multi-level PAM to the digital reference model as follows:

- If we assume that the number of levels  $M$  is a power of 2—that is,  $M = 2^\beta$ —then each symbol represents  $\beta$  bits.
- The average received energy per bit is  $E_b = \frac{(M^2 - 1)A^2 T}{3\beta}$ .
- The noise variance at the output of the matched filter is  $\sigma^2 = N_0 T / 2 = N_0 / 2$  under the assumption  $T = 1$ . This is unchanged from the binary PAM case of Eq. (10.9).

Substituting these results in Eq. (10.57), the probability of symbol error in terms of the digital reference SNR is

$$P_e^{\text{PAM}} = 2 \left( \frac{M-1}{M} \right) Q \left( \sqrt{\frac{6\beta}{M^2 - 1}} \sqrt{\frac{E_b}{N_0}} \right) \quad (10.58)$$

The advantage of the  $M$ -ary modulation scheme is the increased number of bits,  $\beta = \log_2 M$ , transmitted across the channel with each modulated symbol. However, the disadvantage of PAM is the performance penalty to be paid when increasing the number of modulation levels. If we let  $\rho = \sqrt{6\beta/(M^2 - 1)}$  in Eq. (10.58), then for  $M = 2$  we have  $\rho = \sqrt{2}$ , which is the standard result for bipolar PAM, BPSK, and QPSK. For  $M = 4$ ,  $\rho = \sqrt{4/5}$ , which implies significantly more energy per bit must be transmitted to obtain the same error rate. For  $M = 8$ ,  $\rho = \sqrt{2/7}$ , which implies even more energy per bit is required to obtain the same error rate.

With this very brief introduction to the performance of multi-level PAM in noise, we repeat that many forms of quadrature amplitude modulation (QAM) consist of multi-level PAM signals for both the in-phase and quadrature components,  $m_I(t)$  and  $m_Q(t)$ , of a band-pass signal and therefore make the following observations:

- ▶ We may use independent PAM schemes on the in-phase and quadrature components. That is to say, one PAM signal  $m_I(t)$  modulates the in-phase carrier  $\cos(2\pi f_c t)$  and the second PAM signal  $m_Q(t)$  modulates the quadrature carrier  $\sin(2\pi f_c t)$ .
- ▶ Due to the orthogonality of the in-phase and quadrature components, the error rate is the same on both; and the same as the baseband PAM system.

With a QAM scheme, twice as much data may be transmitted in the same bandwidth as the baseband PAM scheme with the same power efficiency. This property is a simple extension of the comparison that was made between BPSK and QPSK modulation.

## 10.6 Optimum Detection of Binary FSK

From Chapter 7, another simple form of digital band-pass modulation is frequency-shift keying (FSK). The previous modulation schemes and receiver structures considered in this chapter are in many ways analogous with amplitude modulation even though some are referred to as phase-shift keying. Frequency-shift keying, however, is more closely related to frequency modulation. With FSK, different frequencies are used to represent the data bits and the transmitted signal for  $0 \leq t \leq T$  is

$$s(t) = \begin{cases} A_c \cos(2\pi f_1 t), & 0 \leq t \leq T \text{ if a 1 is sent} \\ A_c \cos(2\pi f_2 t), & 0 \leq t \leq T \text{ if a 0 is sent} \end{cases} \quad (10.59)$$

In previous sections where the waveform was amplitude modulated, we observed that the signal could be detected optimally with a single matched filter. With the FSK transmission system of Eq. (10.59), we actually have two different sinusoidal waveforms with unequal  $f_1$  and  $f_2$ . It seems logical then to design matched filters for each of these two waveforms and select the one that produces the largest output as shown in Fig. 10.12. In particular, the two matched filters are

$$g_1(t) = \sqrt{2} \cos(2\pi f_1 t)$$

and

$$g_2(t) = \sqrt{2} \cos(2\pi f_2 t) \quad (10.60)$$

corresponding to a 1 and a 0, respectively.

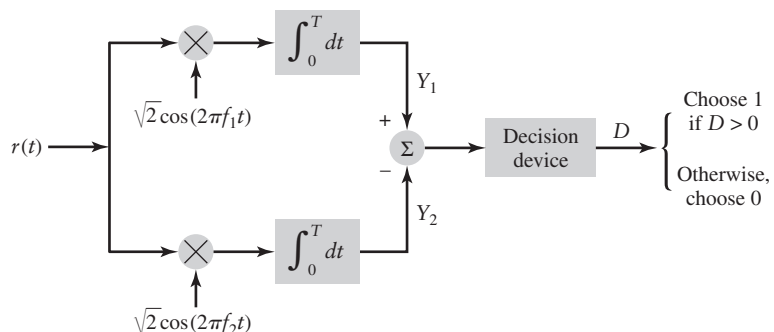


**FIGURE 10.12** Coherent detection of binary FSK.

To analyze the performance of the FSK detector of Fig. 10.12, we make the simplifying assumption that the frequencies  $f_1$  and  $f_2$  have been selected such that the corresponding waveforms are orthogonal; that is,

$$\int_0^T \cos(2\pi f_1 t) \cos(2\pi f_2 t) dt = 0 \quad (10.61)$$

Technically, this implies that  $(f_1 - f_2)T$  is an integer under the bandpass assumption (see Problem 10.16). This assumption is not necessary in practice, but violation of this assumption does result in degraded performance (see Problem 10.24). Let the received signal be

$$r(t) = s(t) + w(t) \quad (10.62)$$

Suppose a 1 is transmitted. Then the output of the matched filter corresponding to a 0 is

$$\begin{aligned} Y_2 &= \int_0^T r(t) \sqrt{2} \cos(2\pi f_2 t) dt \\ &= \int_0^T (A_c \cos(2\pi f_1 t) + w(t)) \sqrt{2} \cos(2\pi f_2 t) dt \\ &= 0 + N_2 \end{aligned} \quad (10.63)$$

where, from Eq. (10.61), the first part of the integral is zero due to the orthogonality of the two pulse shapes. The noise component at the output of the matched filter for a 0 is

$$N_2 = \int_0^T w(t) \sqrt{2} \cos(2\pi f_2 t) dt \quad (10.64)$$

Consequently, when a 1 is transmitted, the output of the filter matched to a 0 has a mean of zero and a variance corresponding to that of  $N_2$ . On the other hand, the output of the filter matched to a 1 is

$$\begin{aligned} Y_1 &= \int_0^T r(t) \sqrt{2} \cos(2\pi f_1 t) dt \\ &= \int_0^T (A_c \cos(2\pi f_1 t) + w(t)) \sqrt{2} \cos(2\pi f_1 t) dt \\ &\approx \frac{A_c T}{\sqrt{2}} + N_1 \end{aligned} \quad (10.65)$$

The step from the second to the third line of Eq. (10.65) uses the double angle formula  $2 \cos^2 A = 1 + \cos 2A$ . The approximation in Eq. (10.65) is the bandpass assumption that the integral of a high-frequency component is approximately zero over the interval from 0 to  $T$ . The noise component of Eq. (10.65) is defined as

$$N_1 = \int_0^T w(t) \sqrt{2} \cos(2\pi f_1 t) dt \quad (10.66)$$

When a 1 is transmitted, the output of the filter matched to a 1 has the mean  $\mu = A_c T / \sqrt{2}$  and a variance corresponding to that of  $N_1$ . A symmetric result is obtained when a 0 is transmitted.

To determine which bit was transmitted, we compare the output of our two matched filters. The simplest comparison is to form the difference between the outputs,  $D = Y_1 - Y_2$ . If a 1 is transmitted, then the mean value of  $D$  is  $\mu = A_c T / \sqrt{2}$ . If a 0 is transmitted, then

the mean value of  $D$  is  $\mu = -A_c T / \sqrt{2}$ . The obvious decision rule in this case is to choose 1 if  $D$  is greater than zero, and 0 otherwise.

The random variable  $D$  contains the difference of  $N_1$  and  $N_2$ . We claim that these two noise terms are independent Gaussian random variables (see Problem 10.9). Since  $D$  is the difference of two independent Gaussian random variables, it has a variance  $\sigma^2 = \text{Var}(N_1) + \text{Var}(N_2) = 2 \text{Var}(N_1)$ . By analogy with bipolar PAM in Section 10.3, the probability of error for binary FSK is

$$P_e = Q\left(\frac{|\mu|}{\sigma}\right) \quad (10.67)$$

Putting this in terms of the digital reference SNR, we find that from inspection of Eq. (10.59), the energy per bit is  $E_b = A_c^2 T / 2$  for FSK. The noise variance of the combination of the two terms  $N_1$  and  $N_2$  is  $\sigma^2 = 2(N_0 T / 2) = N_0 T$  (see Problem 10.9). Accordingly, the BER in terms of the digital reference model is

$$P_e^{\text{FSK}} = Q\left(\sqrt{\frac{E_b}{N_0}}\right) \quad (10.68)$$

This bit error rate performance is similar to that of on-off signaling that we saw in Section 10.3. Both on-off PAM and FSK are forms of *orthogonal signaling*, whereas modulation techniques such as bipolar PAM and BPSK are referred to as *antipodal signaling*. In general, we see that antipodal signaling provides a  $10 \log_{10} 2 = 3$  dB advantage over orthogonal signaling in bit error rate performance.

► **Drill Problem 10.9** Use Eqs. (10.61), (10.64), and (10.66) to show that  $N_1$  and  $N_2$  are uncorrelated and therefore independent Gaussian random variables. Compute the variance of  $N_1 - N_2$ . ◀

## 10.7 Differential Detection in Noise

In Chapter 7, we introduced differential detection of BPSK as a simple method of recovering the data without the complexity of coherent detection. A typical receiver structure for the differential detection of BPSK in the presence of noise is shown in Fig. 10.13. The received RF signal is first down-converted to the IF frequency  $f_c$  and then band-pass filtered. The band-pass signal at the output of this filter may be represented by

$$x(t) = A_c d_k \cos(2\pi f_c t + \theta) + n(t), \quad (k-1)T < t \leq kT \quad (10.69)$$

where  $T$  is the bit period and  $\theta$  is the unknown carrier phase. The differentially encoded bit  $d_k$  is defined by the equation  $d_k = b_k d_{k-1}$  where  $b_k$  is the  $k$ th information bit.<sup>2</sup> With

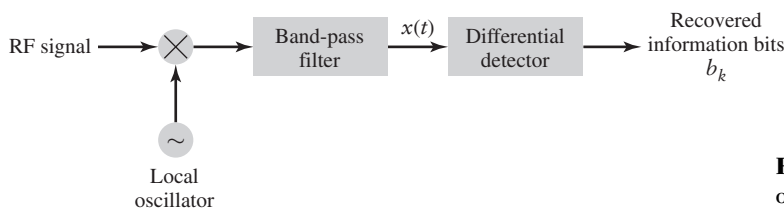


**FIGURE 10.13** Band-pass processing of differential detector.

<sup>2</sup>In the discussion of differential encoding in Section 7.6,  $b_k$  was assumed to take the logical values 0 and 1. The differentially encoded symbols were given by  $d_k = b_k \oplus d_{k-1}$  which were then modulated. In this section, we assume  $b_k$  takes the real values of +1 and -1, and  $d_k = d_{k-1} b_k$  provides the PAM levels directly. These two representations are equivalent.

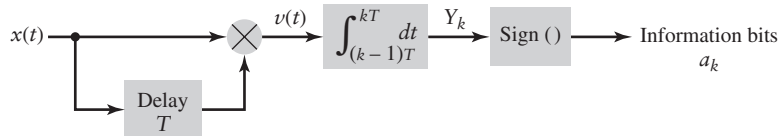


FIGURE 10.14 Differential detector.

coherent detection, synchronization circuits must estimate the phase  $\theta$  to produce a coherent reference for down-conversion to baseband. With differential detection, we use the *delay-and-multiply* circuit shown in Fig. 10.14. The output of the delay-and-multiply circuit is

$$\begin{aligned} v(t) &= x(t)x(t - T) \\ &= A_c^2 d_k d_{k-1} \cos(2\pi f_c t + \theta) \cos(2\pi f_c(t - T) + \theta) + \omega(t) \end{aligned} \quad (10.70)$$

where

$$\omega(t) = A_c d_k \cos(2\pi f_c t + \theta) n(t - T) + A_c d_{k-1} \cos(2\pi f_c(t - T) + \theta) n(t) + n(t)n(t - T) \quad (10.71)$$

is the sum of signal-cross-noise and noise-cross-noise terms. We have implicitly assumed that the unknown phase  $\theta$  remains essentially constant over two-bit intervals. By using the trigonometric identity  $\cos A \cos B = \frac{1}{2}[\cos(A - B) + \cos(A + B)]$ , we may expand Eq. (10.70) to obtain

$$v(t) = \frac{A_c^2}{2} d_k d_{k-1} \{\cos(2\pi f_c T) + \cos(4\pi f_c t - 2\pi f_c T + 2\theta)\} + \omega(t) \quad (10.72)$$

The integrate-and-dump detector depicted in Fig. 10.14 removes the high-frequency components of Eq. (10.72), and we are left with

$$\begin{aligned} Y_k &= \int_{(k-1)T}^{kT} v(t) dt \\ &= \frac{A_c^2 T}{2} d_k d_{k-1} \cos(2\pi f_c T) + N_k \end{aligned} \quad (10.73)$$

where the additive random variable  $N_k$  is due to  $\omega(t)$  of Eq. (10.71). If the frequency  $f_c$  is chosen such that  $f_c T$  is approximately an integer, then  $\cos(2\pi f_c T) \approx 1$  and

$$\begin{aligned} Y_k &= \frac{A_c^2 T}{2} d_k d_{k-1} + N_k \\ &= \frac{A_c^2 T}{2} b_k + N_k \end{aligned} \quad (10.74)$$

where we have used the fact that the data information  $b_k$  has been differentially encoded so that  $b_k = d_k d_{k-1}$ .

Consequently, in terms of noise performance, the major difference between a DPSK system and a coherent binary PSK is not in the differential encoding, which can be used in either case, but rather lies in the way in which the reference signal is derived for the phase detection of the received signal. Specifically, in a DPSK receiver the reference is contaminated by additive noise to the same extent as the information pulse; that is, they have the

same signal-to-noise ratio. This is evident in the presence of both the noise-cross-signal and the noise-cross-noise terms in the expression for  $\omega(t)$  in Eq. (10.71). This makes the statistical characterization of the random variable  $N_k$  and therefore determination of the overall probability of error in DPSK receivers somewhat complicated, and beyond the scope of this book. However, the formula is<sup>3</sup>

$$P_e^{\text{DPSK}} = 0.5 \exp\left(-\frac{E_b}{N_0}\right) \quad (10.75)$$

It is of interest to note that, since in a DPSK receiver decisions are made on the basis of the signal received in two successive bit intervals, there is a tendency for bit errors to occur in pairs. The main requirement that  $f_c T$  is approximately an integer in a differential receiver may be alleviated in many cases if the IF is chosen to be approximately zero; that is,  $f_c \approx 0$  Hz.

## 10.8 Summary of Digital Performance

### ■ GRAY ENCODING

In this section, we summarize the performance of the different digital modulation-demodulation strategies. However, before we do this, we must elaborate upon a comment made regarding PAM. In particular, with  $M$ -ary PAM we calculated the probability of a symbol error. Since, for  $M > 2$ , a symbol is comprised of more than one bit, a symbol error may imply more than one bit error. However, by clever assignment of bits to symbols, the likelihood of this occurring can be made small. Specifically, we refer to *Gray encoding* of symbols where there is only a one-bit difference between adjacent symbols. In Fig. 10.15, we show Gray-encoding strategies for 8-ary PAM and for 8-PSK. Observe that the most common error with both constellations is to select a nearest neighbor. However, there is only a one-bit difference between all nearest neighbors. Hence, for this encoding, the symbol error rate and bit error rate are almost identical. The exception to this equality occurs in very noisy channels where the probability of selecting a symbol that is not a nearest neighbor becomes more likely.

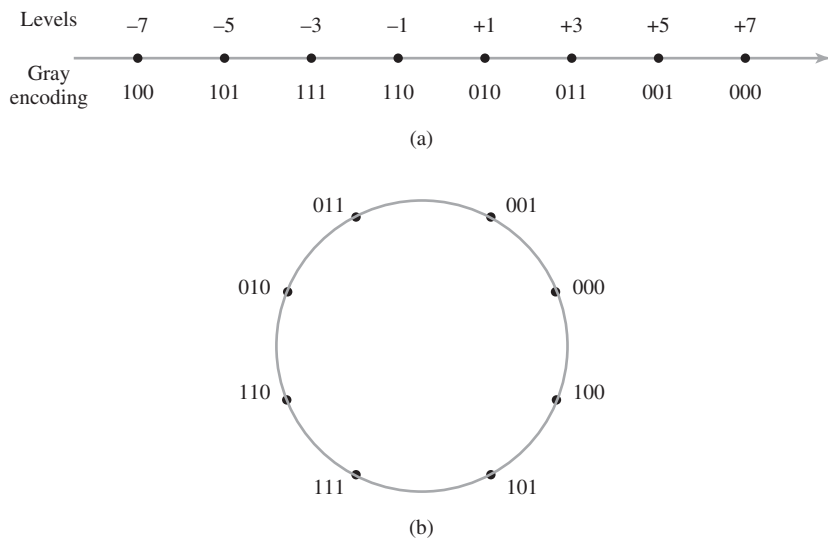


**FIGURE 10.15** Gray-encoding of (a) 8-ary PAM and (b) 8-PSK.

<sup>3</sup>For derivation of the formula given in Eq. (10.75), see Haykin (2001), pp. 407–417.

## ■ PERFORMANCE COMPARISON

Under the assumption that the symbol error rate is the same as bit error rate, we may formulate the performance comparison of the different modulation–demodulation strategies shown in Table 10.1. We have split the table between baseband and bandpass counterparts where they exist. Although  $M$ -ary PAM does have a bandpass equivalent, it is rarely used; QAM is typically used instead. In Table 10.1, we have extrapolated the results for  $M$ -ary PAM to  $M$ -ary QAM as discussed in the text, based on the analogy between baseband bipolar signaling and QPSK modulation.

**TABLE 10.1 Comparison of BER Performance for Various Modulation–Demodulation Strategies. Detection is Coherent Unless Otherwise Indicated. (The Parameter  $\beta$  is the Number of Bits per Symbol in the in-Phase or Quadrature Dimension.)**

Modulation–Demodulation		Bit Error Rate
Baseband	Bandpass	
On-off PAM	ASK	$Q\left(\sqrt{\frac{E_b}{N_0}}\right)$
Bipolar PAM	BPSK	$Q\left(\sqrt{\frac{2E_b}{N_0}}\right)$
$M$ -ary PAM		$2 \frac{M-1}{M} Q\left(\sqrt{\frac{6\beta}{M^2-1}} \sqrt{\frac{E_b}{N_0}}\right)$
	QPSK	$Q\left(\sqrt{\frac{2E_b}{N_0}}\right)$
$M$ -ary QAM		$2 \frac{\sqrt{M}-1}{\sqrt{M}} Q\left(\sqrt{\frac{6\beta}{M-1}} \sqrt{\frac{E_b}{N_0}}\right)$
Binary FSK		$Q\left(\sqrt{\frac{E_b}{N_0}}\right)$
Differential BPSK		$\frac{1}{2} \exp\left(-\frac{E_b}{N_0}\right)$

For the  $M$ -ary signaling results in Table 10.1 we have assumed that:

- ▶ For  $M > 2$ , the signal-to-noise ratio is sufficient for the symbol error rate to be approximately equal to the bit error rate with Gray encoding.
- ▶ The modulation order  $M$  is a power of 2; that is,  $M = 2^\beta$  for integer  $\beta$ . For  $M$ -ary QAM, there is an implicit assumption that  $\beta$  is even.
- ▶ The  $M$ -ary QAM strategy uses a  $M$ -ary PAM strategy in each of the in-phase and quadrature components.

In Fig. 10.16, we graphically compare the BER performance of several different digital transmission strategies. Note that the reference signal-to-noise ratio  $E_b/N_0$  is measured in decibels.

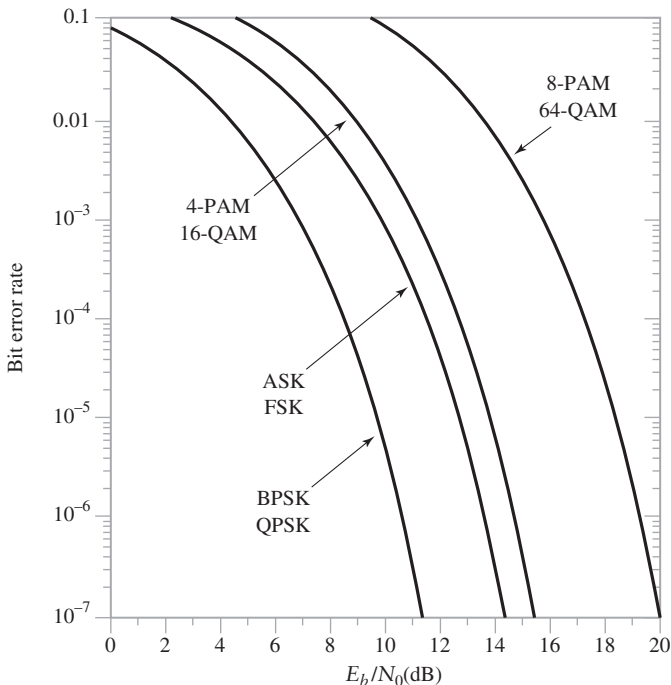


**FIGURE 10.16** Comparison of BER versus  $E_b/N_0$  for several digital transmission strategies.

If we compare the performance of a digital transmission system with that of an analog transmission system, we may make the following observations:

- ▶ With analog systems, we typically need post-detection signal-to-noise ratios of 20 to 30 dB for acceptable voice transmission. With AM modulation, the channel bandwidth is typically 3 to 5 kHz. With FM transmission, the channel bandwidth is typically 25 to 30 kHz.
- ▶ With the PCM encoding of voice, the signal is usually sampled at 8 kHz with 8 bits of resolution (256 levels). The resulting data rate is 64 kilobits per second. If this data stream is sent over a channel with a quadrature modulation scheme such as QPSK with 32 kbps for each of the in-phase and quadrature components, the nominal digital signal bandwidth is 32 kHz. If the tolerable error rate on this data is  $10^{-5}$ , then from Fig. 10.16, the post-detection  $E_b/N_0$  must be 9.6 dB or larger.
- ▶ With advanced voice coding techniques (vocoders), human speech can be represented with reasonable quality with as little as 4 kbps. This requires a transmission bandwidth of approximately 2 kHz. These vocoders can operate with bit error rates as high as  $10^{-2}$  with little degradation in quality, thus reducing the  $E_b/N_0$  required to be as low as 4 dB.

The conclusion is that with the progression from analog to digital techniques, we are improving the robustness of transmission; by robustness we mean relative insensitivity to noise. With progress in signal processing, we are reducing the bandwidth requirements as well.

- ▶ **Drill Problem 10.10** Plot the BER performance of differential BPSK and compare the results to Fig. 10.16. ◀

### ■ NOISE IN SIGNAL-SPACE MODELS

In Chapter 7, we saw how different coherent modulation strategies could be represented in terms of their signal-space diagrams. With the signal space diagram or constellation, each symbol is represented as a signal point with the appropriate choice of basis functions. For example, QPSK may be represented as

$$s(t) = \pm \sqrt{E_b} \phi_1(t) \pm \sqrt{E_b} \phi_2(t) \quad (10.76)$$

where the choice of signs indicates the bit polarity. The basis functions are

$$\phi_1(t) = \sqrt{\frac{2}{T}} \cos(2\pi f_c t), \quad 0 \leq t \leq T \quad (10.77)$$

and

$$\phi_2(t) = \sqrt{\frac{2}{T}} \sin(2\pi f_c t), \quad 0 \leq t \leq T \quad (10.78)$$

which are orthonormal under the band-pass assumption. A noisy signal-space diagram for QPSK is shown in Fig. 10.17, where the four points of the constellation are  $(+\sqrt{E_b}, +\sqrt{E_b})$ ,  $(+\sqrt{E_b}, -\sqrt{E_b})$ ,  $(-\sqrt{E_b}, -\sqrt{E_b})$ , and  $(-\sqrt{E_b}, +\sqrt{E_b})$ . When there is channel noise present, the received signal point is located randomly about the transmitted signal point. In Fig. 10.17, the noisy received signal point lies inside the “noise cloud” centered on the transmitted signal point of  $(+\sqrt{E_b}, +\sqrt{E_b})$ .

If the channel noise is Gaussian, then the cloud of Fig. 10.17 represents a two-dimensional Gaussian distribution with mean  $(+\sqrt{E_b}, +\sqrt{E_b})$ . The variance of this distribution,  $\sigma^2$ , depends upon the signal-to-noise ratio of the channel. Now consider the probability of an error when detecting this signal point. There are two types of errors that may occur; the channel noise can cause the received signal point to be on the opposite side of the  $\phi_1(t)$  axis. This would cause an error in the second bit of the pair. Alternatively, if the channel noise causes the received signal point to fall to the left of the  $\phi_2(t)$  axis, then an error will occur in the first bit. In the less likely event that the received signal point falls in the third quadrant when  $(+\sqrt{E_b}, +\sqrt{E_b})$  is transmitted,

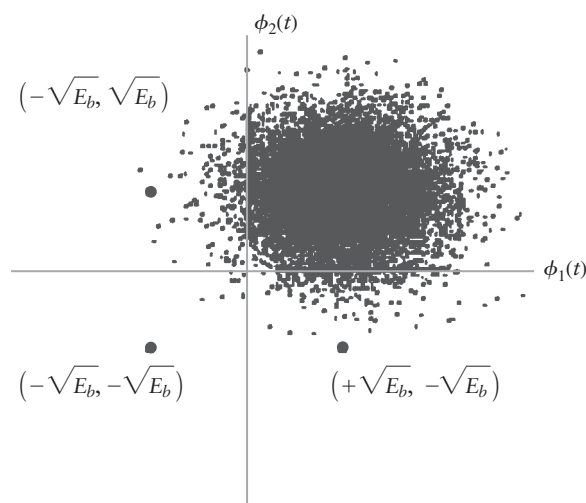


**FIGURE 10.17** Signal space representation of noisy constellation.

then an error will occur in both bits. Clearly, the probability of either type of error is related to the ratio of  $\sqrt{E_b}$  to the noise standard deviation  $\sigma$ . Although not obvious from the diagram, the probability of either type of error is independent of the other.

For this constellation, there is a circle of radius  $\sqrt{E_b}$  around each signal point in which no error can occur. That is,  $\sqrt{E_b}$  is the maximum error distance over which we can always guarantee perfect detection. This signal space can be easily extended to multiple dimensions. For example, if the signal points are  $(\pm\sqrt{E_b}, \pm\sqrt{E_b}, \pm\sqrt{E_b})$ , then around each signal point, there is a sphere of radius  $\sqrt{E_b}$  in which noise is guaranteed not to cause an error.

How would we generate such higher dimensional signals in practice? Consider the signal

$$s(t) = s_1\phi_1(t) + s_2\phi_2(t) + s_3\phi_3(t) + s_4\phi_4(t)$$

where  $\phi_1(t)$  and  $\phi_2(t)$  are as defined in Eqs. (10.77) and (10.78) but extended such they are zero on the interval  $T < t \leq 2T$ . The remaining two orthonormal functions are given by

$$\phi_3(t) = \begin{cases} 0, & 0 < t \leq T \\ \sqrt{\frac{2}{T}} \cos(2\pi f_c t), & T < t \leq 2T \end{cases} \quad (10.79)$$

and

$$\phi_4(t) = \begin{cases} 0, & 0 < t \leq T \\ \sqrt{\frac{2}{T}} \sin(2\pi f_c t), & T < t \leq 2T \end{cases} \quad (10.80)$$

Under the band-pass assumption, the functions  $\phi_3(t)$  and  $\phi_4(t)$  are clearly orthogonal with each other and, since they are zero whenever  $\phi_1(t)$  and  $\phi_2(t)$  are nonzero, they are also orthogonal to these functions. The resulting signal point is defined by the four-dimensional vector  $(s_1, s_2, s_3, s_4)$  where  $s_i$  is  $\pm\sqrt{E_b}$ . While this four-dimensional space may seem to have a somewhat artificial construction, its usefulness will become more evident once we discuss error-correcting codes in the next section.

## 10.9 Error Detection and Correction

A fundamental characteristic of communication systems is that the receiver has no prior knowledge of the information that is being transmitted across the channel. Consequently, in a digital transmission scheme, when the channel produces errors in the detected bits, it degrades the quality of communications. In this section, we look at some elementary ways of detecting and correcting errors that occur in transmission.<sup>4</sup>

In previous sections, we have shown that bit error rate performance of a digital system depends on the post-detection SNR. If the only channel impairment is additive white Gaussian noise, then this BER often has an exponential dependence on the SNR, as exemplified by the  $Q$ -function. As a result, the BER quickly becomes very small as the SNR improves—usually providing much better transmission quality than can be achieved by

<sup>4</sup>The field of error correction and detection was essentially born in the late 1940s with the classic papers of R. Hamming and C. Shannon. Since then an enormous amount of research has been performed in this area. Some introductory books in the field include Clark and Cain (1981), Lin and Costello (2004) and Blahut (1983). The material in this section is adapted from Arazi (1988).

analog methods. In some instances, this digital performance is still insufficient and we wish to improve it further. Some examples are:

- ▶ In radio (wireless) channels, the received signal strength may vary with time due to fading. So, even though the average signal strength would imply good performance in a nonfading channel, the system experiences much poorer performance when the signal is faded.
- ▶ In satellite applications, the satellite has limited transmitter power. In such cases, we may wish to obtain similar BER performance with less transmitted energy.
- ▶ In some cable transmission systems, cables may be bundled together so closely that there may be crosstalk between the wires. That is, one communication link occasionally causes interference into another. In such circumstances, it may be useful to have redundancy in the system to correct errors introduced by occasional interference.

We can achieve the goal of improved bit error rate performance by adding some *redundancy* into the transmitted sequence. The purpose of this redundancy is to allow the receiver to detect and/or correct errors that are introduced during transmission. This kind of operation is referred to as *forward-error correction* (FEC), and its position in the digital transmission system is shown in Fig. 10.18:

- ▶ The incoming digital message (*information bits*) are *encoded* to produce the *channel bits*. The channel bits include the information bits, possibly in a modified form, plus additional bits that are used for error correction.
- ▶ The channel bits are *modulated* and transmitted over the channel.
- ▶ The received signal plus noise is *demodulated* to produce the estimated channel bits.
- ▶ The estimated channel bits are then *decoded* to provide an estimate of the original digital message.

By error detection, we mean the ability of the receiver to detect when one or more errors have occurred during the transmission of the data. This does not imply that the receiver can correct the detected errors. Nor does it imply that the receiver will be able to detect all situations in which errors occur.

Consider the transmission of a block of data containing  $k$  information bits. As stated above, the receiver knows nothing about the  $k$  information bits and yet the block needs properties that will help the receiver to detect when an error occurs. Let us assume that each block contains  $n > k$  bits. The extra  $(n - k)$  bits are *redundant*; that is, they carry no new information. However, the receiver uses these bits to determine when an error occurs.

To explain how this may be done, we introduce the following concepts:

- ▶ Let bits be represented by 0 and 1 values.
- ▶ Let  $\oplus$  represent *modulo-2 addition*. When this operation is applied to pairs of bits we obtain the results:  $0 \oplus 0 = 1 \oplus 1 = 0$  and  $0 \oplus 1 = 1 \oplus 0 = 1$ .
- ▶ The  $\oplus$  operator may also be applied to blocks of bits, where it means the modulo-2 sum of the respective elements of the blocks. For example,  $[1001] \oplus [0101] = [1100]$ .

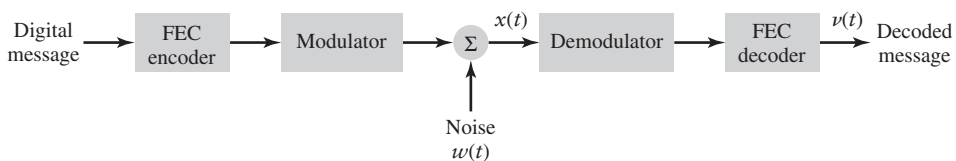


**FIGURE 10.18** Block diagram of system including coding and decoding.

Now for a block of  $k$  information bits  $[x_1 x_2 \dots x_k]$ , suppose we add the *parity-check bit*  $p$  such that

$$x_1 \oplus x_2 \oplus \dots \oplus x_k \oplus p = 0 \quad (10.81)$$

and transmit the  $n = k + 1$  bits  $[x_1 x_2 \dots x_k, p]$ . Since this extended block satisfies Eq. (10.81), we say the block of bits has *even parity*.

At the receiver, we perform the modulo-2 sum of the block of  $n$  received bits. If the result is 1 (that is, it has odd parity), then we state that there was an error in the transmission. From this statement, it should be clear that a single parity bit would detect whether 1, 3, 5, ..., that is, an odd number of errors, occurred during transmission. If an even number 2, 4, 6, ... of errors occurs, the modulo-2 sum (the parity checksum) would be zero and the errors will not be detected. This reinforces the earlier statement that error-detection procedures cannot detect all errors. Thus, the error detection scheme consists of two components. The *encoder*, which processes the information bits, computes the parity bits based on the information, and formats the combination of the information and parity for transmission. The *decoder* computes the parity *checksums* of the received bits and declares whether an error has been detected. With this background, we define *the error detection capability of a code as the maximum number of errors that the receiver can always detect in the transmitted code word*.

### ■ ERROR DETECTION WITH BLOCK CODES

A *block code* is a collection of binary blocks called *code words*, all of the same length. For example, in Table 10.2, we show all binary blocks of length four with even parity. A code word of length  $n$  includes  $(n - k)$  parity bits that are calculated from the information bits. Consequently, the number of code words in an  $(n, k)$  block code is  $2^k$ .

**TABLE 10.2 All Code Words of Length 4 with Even Parity.**

Code words	
0000	1001
0011	1010
0101	1100
0110	1111

Let  $\mathbf{A}$  and  $\mathbf{B}$  represent any two code words of length  $n$  belonging to a block code. We say a block code is *linear* if the sum of the two code words  $\mathbf{A} \oplus \mathbf{B} = \mathbf{C}$  is also a code word. Note that a linear code always contains the all-zero code word since  $\mathbf{A} \oplus \mathbf{A} = \mathbf{0}$ .

To analyze the error detection and error correction capabilities of block codes, we need several definitions. We define the *Hamming weight* of a binary block as the number of 1s in the block. For a binary block  $\mathbf{A}$ , we will represent the Hamming weight of  $\mathbf{A}$  as  $w_H(\mathbf{A})$ . For example, the Hamming weight of  $[1\ 0\ 0\ 1]$  is two.

The *Hamming distance* between any two binary blocks is the number of places in which they differ. Since the expression  $\mathbf{A} \oplus \mathbf{B}$ , has 1s in every location that  $\mathbf{A}$  and  $\mathbf{B}$  differ and zeros elsewhere, the Hamming distance  $d_H(\mathbf{A}, \mathbf{B})$  may be expressed as

$$d_H(\mathbf{A}, \mathbf{B}) = w_H(\mathbf{A} \oplus \mathbf{B}) \quad (10.82)$$

The *minimum Hamming distance of a code* is the minimum value obtained by measuring the distance between all possible pairs of code words. Mathematically, the minimum Hamming distance  $d_{\min}$  is given by

$$d_{\min} = \min_{A, B} d_H(A, B) \quad (10.83)$$

This assumes that  $A$  and  $B$  are not equal. Since a linear code always contains the all zeros code word, it follows by setting  $B = 0$  in Eq. (10.83) that  $d_{\min}$  is the minimum number of 1s in any nonzero code word.

Let  $A$  be the transmitted code word and  $C$  be the received binary block. We claim that the binary block  $C$  will always be detected as erroneous unless it is another code word. To show this, let  $E$  be the error vector—that is, the binary block with 1s indicating the location of errors. Then we may write

$$C = A \oplus E \quad (10.84)$$

since adding a 1 modulo-2 to a bit will always alter that bit. By adding  $A$  to both sides, Eq. (10.84) may also be written as

$$A \oplus C = E \quad (10.85)$$

*With a linear code, if  $C$  is a code word, then so is  $E$ .* This is an important property of linear block codes. Consequently, for us to guarantee that the error can be detected, the number of error bits must be less than  $d_{\min}$ :

$$\max w_H(E) < d_{\min} \quad (10.86)$$

That is, the maximum weight error that can always be detected is  $d_{\min} - 1$ . A  $(k, k)$  block code that has no parity bits has a minimum Hamming distance of 1; thus the receiver cannot detect any errors in the received binary block. A single parity check  $(k + 1, k)$  code has a minimum Hamming distance of 2. Thus, the single parity check code can always detect a single bit error in the received binary block.

### EXAMPLE 10.2 Properties of Linear Block Codes

For the length 4 code of Table 10.2, we show by example that:

- (a) The sum of two code words is a code word:

$$[0011] \oplus [1100] = [1111]$$

- (b) The sum of a code word with itself is the zero code word:

$$[1010] \oplus [1010] = [0000]$$

- (c) The sum of any code word and an error vector corresponding to one error is not a code word:

$$[1001] \oplus [0001] = [1000]$$

- (d) At least some error vectors of weight 2 are not detectable:

$$[1010] \oplus [0011] = [1001]$$

## ■ ERROR CORRECTION

Correcting errors requires both detecting errors and determining the location of those errors. We define the *error correction capability* of a code as the maximum number of errors that the receiver will *always* be able to correct in the received binary block.

Let  $\mathbf{A}$  and  $\mathbf{B}$  be two code words separated by  $d_{\min}$ . Assume that code word  $\mathbf{A}$  is transmitted and the binary block  $\mathbf{C}$  is received. Suppose the received binary block  $\mathbf{C}$  is an equal distance from each of the code words  $\mathbf{A}$  and  $\mathbf{B}$ ; that is, it has the property that

$$d_H(\mathbf{A}, \mathbf{C}) = d_H(\mathbf{B}, \mathbf{C}) = d_{\min}/2 \quad (10.87)$$

Hence,  $\mathbf{C}$  lies halfway between  $\mathbf{A}$  and  $\mathbf{B}$ . In this case, even though  $\mathbf{A}$  was transmitted, the receiver has no justification for choosing  $\mathbf{A}$  over  $\mathbf{B}$  as the correct code word since the distance of both to the received block is the same. Let  $\mathbf{C} = \mathbf{A} \oplus \mathbf{E}$  where  $\mathbf{E}$  is the error vector. Then for  $\mathbf{C}$  to be correctable—that is, to recover  $\mathbf{A}$  from  $\mathbf{C}$ —the discussion surrounding Eq. (10.87) implies that

$$\max w_H(\mathbf{E}) < d_{\min}/2 \quad (10.88)$$

We may therefore state that error correction is possible if the number of errors is less than half of the minimum Hamming distance of the code.

Clearly, then, *the objective when designing a forward error-correction code is to add parity bits to increase the minimum Hamming distance*, as this improves both the error detection and error-correction capabilities of the code.

### EXAMPLE 10.3 Three Parity Bits

In this example, we construct a  $(7, 4)$  code. That is, the code words are of length 7 bits and each code word contains four information bits. Let  $\mathbf{X} = [x_1, x_2, x_3, x_4]$  be the four information bits and construct the three parity bits as follows:

$$\begin{aligned} p_1 &= x_1 \oplus x_2 \oplus x_3 \oplus x_4 \\ p_2 &= x_1 \oplus x_2 \\ p_3 &= x_3 \oplus x_4 \end{aligned}$$

The code words of this code are shown in Table 10.3.

**TABLE 10.3 The Sixteen Code Words for Example 10.3.**

$[x_1, x_2, x_3, x_4, p_1, p_2, p_3]$	
0000000	1000101
0001110	1001011
0010110	1010011
0011010	1011101
0100101	1100000
0101011	1101110
0110011	1110110
0111101	1111000

This code contains the code word  $[1100000]$ , which has Hamming weight 2. Thus the minimum distance of this code is 2. We therefore conclude that adding three parity bits is not always sufficient to obtain  $d_{\min} = 3$ . In the next section, we will consider a better  $(7, 4)$  code.

### ■ HAMMING CODES

In this section, we consider some simple but efficient codes known as Hamming codes, which were among the first error-correcting codes to be devised. Hamming codes are a family of codes with block lengths  $n = 2^m - 1$  for  $m = 3, 4, 5, \dots$ . For a specific block

length  $n$ , there are  $m$  parity bits and  $2^m - 1 - m$  information bits. Example Hamming codes are the  $(7, 4)$ ,  $(15, 11)$ , and  $(31, 26)$  codes. All of these codes have a minimum Hamming distance  $d_{\min} = 3$  and thus can correct all single bit errors.

As previously described, there are two steps to the coding process. The first step is the *encoding* that occurs at the transmitter; this requires the calculation of the parity bits based on the information bits. The second step is the *decoding* that occurs at the receiver; this requires the evaluation of the parity checksums to determine if, and where, the parity equations have been violated.

We will first consider the Hamming  $(7, 4)$  code and let  $\mathbf{X} = [x_1, x_2, x_3, x_4]$  represent the four information bits. To encode these bits we define the  $k$ -by- $n$  *generator matrix* of the Hamming  $(7, 4)$  code as

$$\mathbf{G} = \left[ \begin{array}{cccc|ccc} 1 & 0 & 0 & 0 & 1 & 0 & 1 \\ 0 & 1 & 0 & 0 & 1 & 1 & 1 \\ 0 & 0 & 1 & 0 & 1 & 1 & 0 \\ 0 & 0 & 0 & 1 & 0 & 1 & 1 \end{array} \right] \quad (10.89)$$

Using this generator matrix, the seven-element code word  $\mathbf{C} = [c_1, c_2, c_3, c_4, c_5, c_6, c_7]$  to be transmitted is given by

$$\mathbf{C} = \mathbf{X} \cdot \mathbf{G} \quad (10.90)$$

where the dot  $\cdot$  implies the vector-matrix multiply but using modulo-2 arithmetic; that is, the elements  $c_k$  of  $\mathbf{C}$  are given by

$$c_k = \bigoplus_{j=1}^4 x_j G_{jk}$$

If we expand Eq. (10.90), then we find that the elements of the code word are

$$\begin{aligned} c_1 &= x_1 \\ c_2 &= x_2 \\ c_3 &= x_3 \\ c_4 &= x_4 \\ c_5 &= x_1 \oplus x_2 \oplus x_3 \\ c_6 &= x_2 \oplus x_3 \oplus x_4 \\ c_7 &= x_1 \oplus x_2 \oplus x_4 \end{aligned} \quad (10.91)$$

Comparing Eqs. (10.89) and (10.91), we observe that the first four columns of  $\mathbf{G}$  are the identity matrix and map the information bits to themselves. The last three columns of  $\mathbf{G}$  form the parity check equations of the code. Each block code has its own unique generator matrix; although different generator matrices may produce codes with equivalent properties. For example, if we exchange any two columns of  $\mathbf{G}$  we will get a different block code, but it will have the same error-correcting properties as the above code.

Let  $\mathbf{R} = [r_1, r_2, r_3, r_4, r_5, r_6, r_7]$  represent the seven received, and possibly wrong, bits of the  $(7, 4)$  Hamming code. How do we decode these bits? One possible decoding strategy is a *list decoder*. With this strategy, we make a list of all  $2^7$  possible received blocks and compute the closest code word, in terms of Hamming distance, beforehand. Then, for any received block, we look it up on this list and determine the nearest code word. This list decoder will work conceptually for any code. However, as  $n$  becomes large, the list becomes too long to be of practical value.

A *computational decoding strategy* is therefore a preferable alternative to the list decoder. To this end, for the  $(7, 4)$  Hamming code we may define the  $(n - k)$ -by- $n$  parity check matrix  $\mathbf{H}$  as

$$\mathbf{H} = \begin{bmatrix} 1 & 0 & 1 \\ 1 & 1 & 1 \\ 1 & 1 & 0 \\ 0 & 1 & 1 \\ \hline 1 & 0 & 0 \\ 0 & 1 & 0 \\ 0 & 0 & 1 \end{bmatrix} \quad (10.92)$$

Note that the lower 3-by-3 portion of  $\mathbf{H}$  forms a unit matrix, and the part above the unit matrix is the transpose of the part of the generating matrix to left of the unit matrix in Eq. (10.89). Hence, the columns of the parity matrix  $\mathbf{H}$  form the coefficients of the parity equations that the code words of the Hamming code should satisfy. For a  $(n, k)$  linear code, the columns of matrix  $\mathbf{H}$  describe the  $(n - k)$  independent equations upon which the  $(n - k)$  parity bits are computed.

Suppose the received binary block is  $\mathbf{R} = \mathbf{C} \oplus \mathbf{E}$  where  $\mathbf{C}$  is the transmitted code word and  $\mathbf{E}$  is the error vector. We compute the product of the received vector and the parity-check matrix

$$\begin{aligned} \mathbf{S} &= \mathbf{R} \cdot \mathbf{H} \\ &= (\mathbf{C} + \mathbf{E}) \cdot \mathbf{H} \\ &= \mathbf{C} \cdot \mathbf{H} + \mathbf{E} \cdot \mathbf{H} \end{aligned} \quad (10.93)$$

Since  $\mathbf{C}$  is a code word, it satisfies the parity-check equations and  $\mathbf{C} \cdot \mathbf{H} = 0$ . Therefore

$$\mathbf{S} = \mathbf{E} \cdot \mathbf{H} \quad (10.94)$$

The  $(n - k)$ -dimensional vector  $\mathbf{S}$  is called the *error syndrome*. Suppose  $\mathbf{E}$  corresponds to a single-bit error in the  $m$ th bit of the code word. The syndrome  $\mathbf{S}$  will then correspond to the  $m$ th row of the parity check matrix  $\mathbf{H}$ . Note that the rows of  $\mathbf{H}$  are unique. Thus we can use the syndrome to determine the position of any single-bit error. This mapping is shown in Table 10.4. A syndrome of  $[0, 0, 0]$  implies that no error occurred.

**TABLE 10.4 Syndrome Decoding for Hamming  $(7, 4)$  Code.**

Error ( $\mathbf{E}$ )	Syndrome ( $\mathbf{S}$ )	Decimal Rep.
0000000	000	0
1000000	101	5
0100000	111	7
0010000	110	6
0001000	011	3
0000100	100	4
0000010	010	2
0000001	001	1

Thus, we have shown that the Hamming  $(7, 4)$  code can correct any single-bit error. Can it correct more than one error? If  $\mathbf{E}$  contains two errors, then the syndrome will consist of the modulo-2 sum of two rows of  $\mathbf{H}$ . This sum will produce a third row in  $\mathbf{H}$ , and may thus

be indistinguishable from the single-bit error that also produces this row. Consequently, the Hamming (7, 4) code can correct all single-bit errors but not two-bit errors. In other words, the  $d_{\min}$  of the code must be 3.

On the error-detection side, we again note that any two-bit error will produce a third row of  $\mathbf{H}$ . Since this third row is nonzero, this means we can detect (but not correct) all two-bit errors with the Hamming (7, 4) code. Note, however, that if the three-bit error  $\mathbf{E} = [1011000]$  occurs, then the syndrome  $\mathbf{S} = 0$ . Therefore, the code cannot detect all three-bit errors. This provides further confirmation that  $d_{\min}$  is 3 for this code.

#### EXAMPLE 10.4 Error Correction with a Hamming Code

Four information bits are encoded with a Hamming (7, 4) code whose generator matrix is given by Eq. (10.89). The received bit sequence is  $\mathbf{R} = [1101110]$ . What sequence was transmitted if one error occurred during the transmission?

Multiplying  $\mathbf{R}$  by the parity check matrix, we obtain the error syndrome

$$\begin{aligned}\mathbf{S} &= \mathbf{R} \cdot \mathbf{H} \\ &= [111]\end{aligned}$$

Since the error syndrome is nonzero, we know that one or more errors occurred. From Table 10.4, a single error in the second bit from the left would cause this sequence, so we conclude that the transmitted sequence is [1001110] and the information bits are [1001].

#### EXAMPLE 10.5 Probability of Block Error

Suppose a BPSK transmission strategy is encoded with a (7, 4) Hamming block code. Compare the block error rate with and without decoding.

From Section 10.4 the probability of a bit error with BPSK is  $P_e = Q(\sqrt{2E_b/N_0})$ . A block of uncoded seven bits is received correctly if it contains no errors. The probability of a block error—that is, one or more bit errors—is the complement of this; namely,

$$P_b^{\text{uncoded}} = 1 - (1 - P_e)^7 \quad (10.95)$$

With the (7, 4) Hamming code, the probability of a block error is the probability of two or more errors over a seven-bit block. This probability is given by

$$P_b^{\text{coded}} = 1 - (1 - P'_e)^7 - \binom{7}{1}(1 - P'_e)^6 P'_e \quad (10.96)$$

where  $P'_e$  is the probability of a bit error with a Hamming code. If  $P'_e = P_e$ , then the probability of a block error is clearly reduced with the Hamming code. However, there is a nuance that must be considered. This is why we have used  $P'_e$  in the Eq. (10.96) as opposed to  $P_e$ . In particular, in the digital reference model,  $E_b$  refers to the *energy per information bit*. With the Hamming (7, 4) code, we are transmitting four information bits and three parity bits, for a total of seven *channel bits* per block. Letting  $E_c$  represent the energy per channel bit, we find that the energy of seven channel bits corresponds to the energy of four information bits:

$$E_c = \frac{4}{7} E_b \quad (10.97)$$

Furthermore, the probability of error  $P'_e$  in Eq. (10.96) represents the probability of a channel-bit error, so using the probability of error for BPSK and Eq. (10.97), we have

$$\begin{aligned}P'_e &= Q\left(\sqrt{\frac{2E_c}{N_0}}\right) \\ &= Q\left(\sqrt{\frac{8E_b}{7N_0}}\right) \quad (10.98)\end{aligned}$$

In this way, we may make a fair comparison between the uncoded and coded transmission strategies. The block error rates of these two strategies are shown in Figure 10.19. The coding provides approximately 1 dB improvement in the block error rate performance.

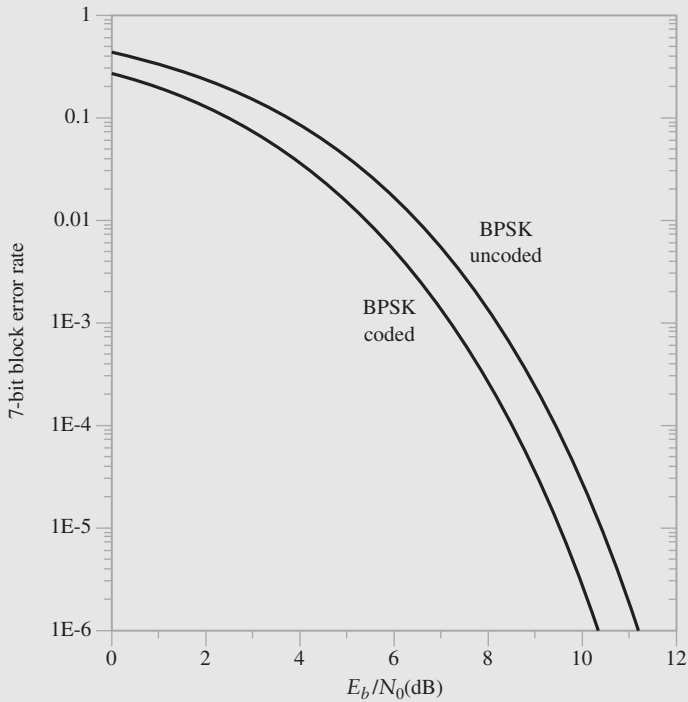


**FIGURE 10.19** Comparison of 7-bit block error rate of uncoded BPSK and Hamming (7, 4) coded BPSK.

### ■ MORE POWERFUL CODES

While Hamming codes are simple to explain and are very efficient codes, they are by no means the only forward-error-correction codes. Other FEC codes include:

- ▶ *Reed–Solomon and Bose–Chaudhuri–Hocquenghem (BCH) block codes.* Like the Hamming codes, these are  $(n, k)$  codes where there are  $k$  information bits and a total of  $n$  bits including  $n - k$  parity bits.<sup>5</sup> The values of  $n$  and  $k$  are not as restricted as with Hamming codes, which provides greater flexibility.
- ▶ *Convolutional codes.* As the name suggests, these codes are the result of the convolution of one or more parity-check equations with the information bits. For example, if the information bits are  $x_1, x_2, x_3, \dots$ , then we generate the sequence of parity bits using the relation

$$p_k = x_k \oplus x_{k-2} \oplus x_{k-3} \oplus x_{k-5} \quad (10.99)$$

Thus, every input bit  $x_k$  results in two bits  $x_k$  and  $p_k$  being transmitted over the channel. Transmitting  $x_k$  and  $p_k$  for each information bit is an example of a rate  $\frac{1}{2}$ ; that is, there are two channel bits for each information bit. This is an example of *systematic convolutional code* where the information bit  $x_k$  is explicitly transmitted. In *non-*

<sup>5</sup>With Reed–Solomon codes, the  $n$  and  $k$  in  $(n, k)$  often refer to total symbols and information symbols in a code word where a symbol corresponds to  $m$  bits.

*systematic convolutional codes* there may be two parity equations such as Eq. (10.99), and the two parity bits produced for each information bit  $x_k$  are transmitted but the information bit  $x_k$  is not. The error-correcting capabilities of a convolutional code are usually determined by the span (in bits) of the parity-check equation, which is referred to as the *memory* of the code. Unfortunately, the decoding complexity increases exponentially with the memory of the code, so practical codes are usually limited to memory of less than ten bits.

- *Turbo codes.* Turbo codes are block codes but use a continuous encoding strategy similar to convolutional codes. For example, with a rate  $\frac{1}{3}$  Turbo code, the three transmitted bits for each information bit  $x_k$  could be

$$\begin{aligned} x_k \\ p_k &= p_{k-1} \oplus x_k \oplus x_{k-2} \oplus x_{k-4} \\ q_k &= q_{k-1} \oplus x_k^i \oplus x_{k-2}^i \oplus x_{k-4}^i \end{aligned} \quad (10.100)$$

With Turbo codes, the parity is determined by a recursive equation; that is, the  $k$ th parity bit depends upon the  $(k - 1)^{\text{th}}$  parity bit as well as the input bits. Note that in Eq. (10.100) the formula for the  $p$  and  $q$  parity bits are the same; the difference is that the  $q$ -formula uses  $x_k^i$ , which refers to the same information bits but in an interleaved order. Interleaving means shuffling the order of the bits in a pseudo-random fashion.

For both block codes and convolutional codes, the general principle is to add parity bits in such a way as to maximize the minimum distance  $d_{\min}$ . However, maximizing the minimum distance is subject to two important constraints:

1. The *code rate*; that is, the ratio of the number of information bits to the total number of bits in a code word must be reasonable. This ensures that the communication system has a significant information throughput.
2. The code must permit a practical decoding strategy. It is relatively easy to construct codes with large minimum distances, but the corresponding decoding strategies are often too complex to be of practical use.

Even with practical decoding strategies and large minimum distances, there are limits to how reliable data can be transmitted. The theoretical limits fall in the area of Shannon channel capacity theory. Shannon theory<sup>6</sup> tells us that *if the transmission rate is below the channel capacity, then there exist forward error-correcting codes that permit error-free transmission*. Enormous strides in approaching these theoretical limits have been made in recent years with the discovery of Turbo codes. Turbo codes draw features from both convolutional and block codes. Although  $d_{\min}$  is important in the design of Turbo codes, other distinct features of these codes improve performance at low signal-to-noise ratios.

## ■ SIGNAL-SPACE INTERPRETATION OF FORWARD-ERROR-CORRECTION CODES

In Section 10.8 we saw how we could construct a four-dimensional vector with a signal-space representation of

$$\begin{aligned} \mathbf{s} &= [\pm\sqrt{E_b}, \pm\sqrt{E_b}, \pm\sqrt{E_b}, \pm\sqrt{E_b}] \\ &= \sqrt{E_b}[\pm 1, \pm 1, \pm 1, \pm 1] \end{aligned} \quad (10.101)$$

where there are sixteen points in the constellation defined by  $\mathbf{s}$ . To be specific, we consider the construction of an  $N$ -dimensional signal vector in the context of error-correcting codes.

For a linear code, we defined a code word  $\mathbf{c}$  of length  $N$  comprised of informa-

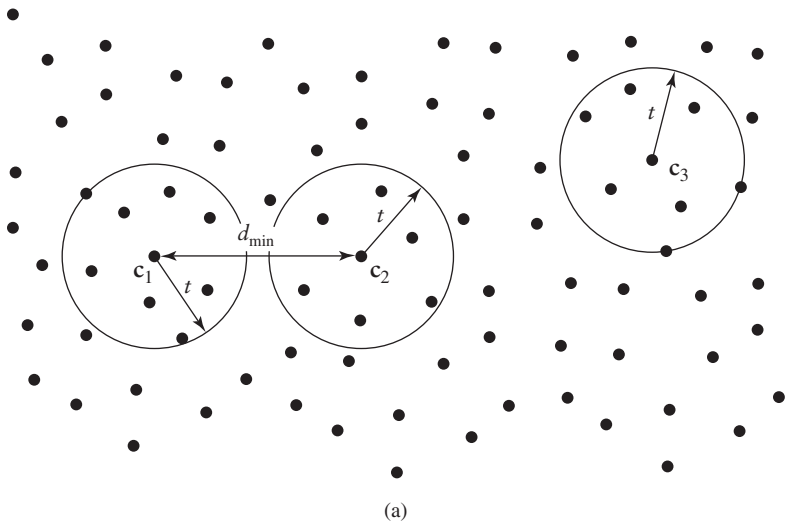
---

<sup>6</sup>For a discussion of the Shannon theory and its implications, see the book by Cover and Thomas (1991).

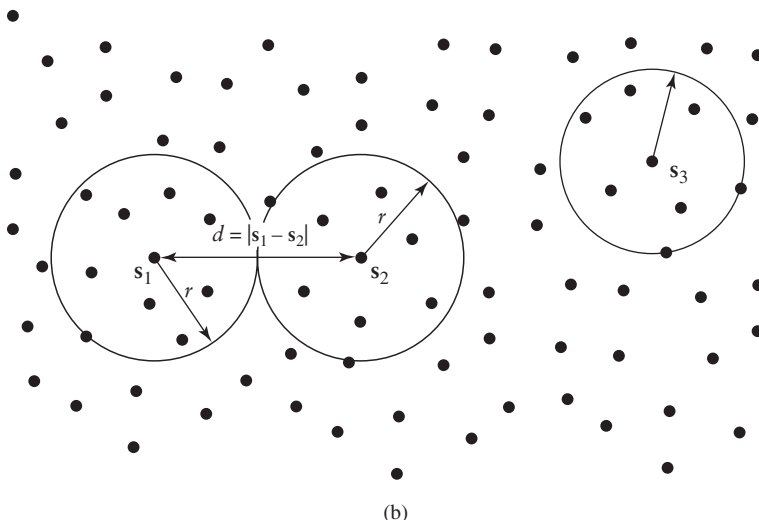
tion bits and parity bits. In general, for a binary vector of length  $N$ , there were always  $2^N$  possible values. However, with a code word, the special relationship of the information bits and the parity bits implies that there are only  $2^k$  possible values for  $\mathbf{c}$  where  $k$  is the number of information bits and  $N - k$  is the number of parity bits.

For transmission, we must assign real values to each code word. Let  $\mathbf{s} = [s_1, s_2, s_3 \dots, s_N]$  be a *real-valued code word* where we assume that  $s_i$  takes a value of either  $+\sqrt{E_b}$  or  $-\sqrt{E_b}$  depending upon whether the data symbol is 0 or 1. We may consider  $\mathbf{s}$  as a signal-space vector. Analogous to the code word  $\mathbf{c}$ , there are only  $2^k$  possible values for the signal space vector in a space of dimension  $N$ .

With this new definition of the signal space, we can explain some of the concepts of coding theory geometrically as shown in Fig. 10.20. In particular, for a linear code we defined the minimum Hamming distance as the number of locations where the binary code words differ. In geometric terms, if  $\mathbf{c}_1$  and  $\mathbf{c}_2$  are two code words with minimum Hamming distance  $d_{\min}$ , then they may be illustrated, in a two-dimensional sense, as shown in Fig. 10.20(a). The circles of radius  $t = \lfloor (d_{\min} - 1)/2 \rfloor$ , denoting the smallest integer less than  $d_{\min}/2$ , enclose the binary vectors that can be correctly decoded to the code words at their



(a)



(b)

**FIGURE 10.20** Illustration of minimum distance in:  
 (a) code word space with  
 $t = \lfloor (d_{\min} - 1)/2 \rfloor$ ;  
 and (b) signal space with  
 $d = 2\sqrt{d_{\min}E_b}$  and  $r = \sqrt{d_{\min}E_b}$ .

respective centers. In reality, these circles represent  $N$ -dimensional spheres.

In signal space, the squared geometric (Euclidean) distance between two neighboring signal space vectors is defined by the squared *Euclidean distance*

$$\begin{aligned} d^2 &= \|\mathbf{s}_1 - \mathbf{s}_2\|^2 \\ &= \sum_{i=1}^N (s_{1i} - s_{2i})^2 \\ &= d_{\min}(2\sqrt{E_b})^2 \\ &= 4d_{\min}E_b \end{aligned} \quad (10.102)$$

where we have used the fact that neighboring signal-space vectors,  $\mathbf{s}_1$  and  $\mathbf{s}_2$ , differ in  $d_{\min}$  elements if they represent code words. Thus, the Hamming distance between code words and the geometric distance between their corresponding signal-space vectors are directly related. In code space, we may select two code words of minimum separation and draw spheres of radius  $t$  around them. Since the code has minimum distance  $d_{\min}$ , this implies there are no other code words within this sphere; any point within this sphere will be closer to its center than to any other code word. Similarly, in signal space, we may draw spheres of radius  $r = \sqrt{d_{\min}E_b}$  around each signal space vector representing a code word, as shown in Fig. 10.20(b), and there are no other signal space vectors representing code words within this sphere.

This resonates with our definition of the error correction capability of a code: Any received signal that lies within a distance  $d_{\min}/2$  of the transmitted code can be uniquely corrected to that code word. Received signals that are beyond this distance may be erroneously corrected if they fall in other spheres or they may be properly corrected if they fall in the gaps between spheres and are closer to the transmitted code word than any other. The error detection capability means the received signal does not fall directly on another code word.

The Hamming (7, 4) code is an example that has  $2^4$  code word (points) in a seven-dimensional signal space and the minimum distance between any two code words is three. Similarly, the Hamming (15, 11) codes is an example that has  $2^{11}$  code words (points) in a 15-dimensional space and again the minimum distance is three.

## 10.10 Summary and Discussion

In this chapter, we investigated the detection of digitally modulated signals in noise. We began by establishing bit error rate (BER) as the figure of merit for comparing digital communication systems and observed that BER is typically not a linear function of the signal-to-noise ratio. Next, we addressed the detection of various digital modulation schemes in the presence of noise and made the following observations:

- (i) Analysis of the detection of a single pulse in noise shows the optimality of matched filtering. The matched-filter principle is a mainstay for the subsequent digital detection techniques. We showed that the bit error rate performance using matched filtering was closely related to the  $Q$ -function that was defined in Chapter 8.
- (ii) We showed how the principle of matched filtering may be extended to the detection of pulse-amplitude modulation, and that bit error rate performance may be determined in a manner similar to single-pulse detection.
- (iii) We discussed how the receiver structure for the coherent detection of band-pass modulation strategies such as BPSK, QPSK, and QAM was similar to coherent detection of corresponding analog signals. After down-conversion to baseband, the principle of matched filtering also applies to these modulation strategies, and BER performance equivalent to the corresponding baseband systems is thereby obtained.

- (iv) We showed how quadrature modulation schemes such as QPSK and QAM provide the same performance as their one-dimensional counterparts of BPSK and PAM, due to the orthogonality of the in-phase and quadrature components of the modulated signals. In particular, we showed how QPSK modulation provides the same BER as BPSK for the same  $E_b/N_0$  but provides double the throughput.
- (v) We also showed that antipodal strategies such as BPSK are more power efficient than orthogonal transmission strategies such as on-off signaling and FSK.
- (vi) We introduced the concept of non-coherent detection when we illustrated that BPSK could be detected using a new approach where the transmitted bits are differentially encoded. The simplicity of this detection technique results in a small BER performance penalty.

The signal-space concepts introduced in Chapter 7 provide an intuitive geometrical interpretation of the relative performance of the different coherent digital modulation strategies in noise. Finally, we closed the chapter with a brief introduction of forward error correction coding, which can be combined with any of the above digital modulation strategies to reduce the power required to achieve the same bit error rate performance—however, there is usually a power and bandwidth tradeoff that must be made when using forward-error-correction coding in the design of digital communication systems.

### ADDITIONAL PROBLEMS

---

- 10.11** A communications system that transmits single isolated pulses is subject to multipath such that, if the transmitted pulse is  $p(t)$  of length  $T$ , the received signal is

$$s(t) = p(t) + \alpha p(t - \tau)$$

Assuming that  $\alpha$  and  $\tau$  are known, determine the optimum receiver filter for signal in the presence of white Gaussian noise of power spectral density  $N_0/2$ . What is the post-detection SNR at the output of this filter?

- 10.12** The impulse response corresponding to a root-raised cosine spectrum, normalized to satisfy Eq. (10.10), is given by

$$g(t) = \left(\frac{4\alpha}{\pi}\right) \frac{\cos\left[\frac{(1+\alpha)\pi t}{T}\right] + \frac{T}{4\alpha t} \sin\left[\frac{(1-\alpha)\pi t}{T}\right]}{1 - \left(\frac{4\alpha t}{T}\right)^2}$$

where  $T = 1/(2B_0)$  is the symbol period and  $\alpha$  is the roll-off factor. Obtain a discrete-time representation of this impulse response by sampling it at  $t = 0.1nT$  for integer  $n$  such that  $-3T < t < 3T$ . Numerically approximate matched filtering (e.g. with MatLab) by performing the discrete-time convolution

$$q_k = 0.1 \sum_{n=-60}^{60} g_n g_{k-n}$$

where  $g_n = g(0.1nT)$ . What is the value of  $q_k = q(0.1kT)$  for  $k = \pm 20, \pm 10$ , and 0?

- 10.13** Determine the discrete-time autocorrelation function of the noise sequence  $\{N_k\}$  defined by Eq. (10.34)

$$N_k = \int_{-\infty}^{\infty} p(kT - t)w(t)dt$$

where  $w(t)$  is a white Gaussian noise process and the pulse  $p(t)$  corresponds to a root-raised cosine spectrum. How are the noise samples corresponding to adjacent bit intervals related?

- 10.14** Draw the Gray-encoded constellation (signal-space diagram) for 16-QAM and for 64-QAM. Can you suggest a constellation for 32-QAM?

- 10.15 Write the defining equation for a QAM-modulated signal. Based on the discussion of QPSK and multi-level PAM, draw the block diagram for a coherent QAM receiver.
- 10.16 Show that if  $T$  is a multiple of the period of  $f_c$ , then the terms  $\sin(2\pi f_c t)$  and  $\cos(2\pi f_c t)$  are orthogonal over the interval  $[t_0, T + t_0]$ .
- 10.17 For a rectangular pulse shape, by how much does the null-to-null transmission bandwidth increase, if the transmission rate is increased by a factor of three?
- 10.18 Under the bandpass assumptions, determine the conditions under which the two signals  $\cos(2\pi f_0 t)$  and  $\cos(2\pi f_1 t)$  are orthogonal over the interval from 0 to  $T$ .
- 10.19 Encode the sequence 1101 with a Hamming (7, 4) block code.
- 10.20 The Hamming (7, 4) encoded sequence 1001000 was received. If the number of transmission errors is less than two, what was the transmitted sequence?
- 10.21 A Hamming (15, 11) block code is applied to a BPSK transmission scheme. Compare the block error rate performance of the uncoded and coded systems. Explain how this would differ if the modulation strategy was QPSK.

## ADVANCED PROBLEMS

---

- 10.22 Show that the choice  $\gamma = \mu/2$  minimizes the probability of error given by Eq. (10.26).  
*Hint:* The  $Q$ -function is continuously differentiable.

- 10.23 For  $M$ -ary PAM,

- (a) Show that the formula for probability of error, namely,

$$P_e = 2\left(\frac{M-1}{M}\right)Q\left(\frac{A}{\sigma}\right)$$

holds for  $M = 2, 3$ , and  $4$ . By mathematical induction, show that it holds for all  $M$ .

- (b) Show the formula for average power, namely,

$$P = \frac{(M^2 - 1)A^2}{3}$$

holds for  $M = 2$ , and  $3$ . Show it holds for all  $M$ .

- 10.24 Consider binary FSK transmission where  $(f_1 - f_2)T$  is not an integer.

- (a) What is the mean output of the upper correlator of Fig. 10.12, if a 1 is transmitted? What is the mean output of the lower correlator?  
(b) Are the random variables  $N_1$  and  $N_2$  independent under these conditions? What is the variance of  $N_1 - N_2$ ?  
(c) Describe the properties of the random variable  $D$  of Fig. 10.12 in this case.

- 10.25 Show that the noise variance of the in-phase component  $n_I(t)$  of the band-pass noise is the same as the band-pass noise  $n(t)$  variance; that is, for a band-pass noise of bandwidth  $B_N$ , we have

$$\mathbb{E}[n_I^2(t)] = N_0 B_N$$

- 10.26 In this problem, we investigate the effects when transmit and receive filters do not combine to form an ISI-free pulse shape. To be specific, data are transmitted at baseband using binary PAM with an exponential pulse shape  $g(t) = \exp(t/T)u(t)$  where  $T$  is the symbol period (see Example 2.2). The receiver detects the data using an integrate-and-dump detector.

- (a) With data symbols represented as  $\pm 1$ , what is magnitude of the signal component at the output of the detector?  
(b) What is the worst case magnitude of the intersymbol interference at the output of the detector. (Assume the data stream has infinite length.) Using the value obtained in part (a) as a reference, by what percentage is the eye opening reduced by this interference.

- (c) What is the rms magnitude of the intersymbol interference at the output of the detector? If this interference is treated as equivalent to noise, what is the equivalent signal-to-noise ratio at the output of the detector? Comment on how this would affect bit error rate performance of this system when there is also receiver noise present.
- 10.27 A BPSK signal is applied to a matched-filter receiver that lacks perfect phase synchronization with the transmitter. Specifically, it is supplied with a local carrier whose phase differs from that of the carrier used in the transmitter by  $\phi$  radians.
- Determine the effect of the phase error  $\phi$  on the average probability of error of this receiver.
  - As a check on the formula derived in part (a), show that when the phase error is zero the formula reduces to the same form as in Eq. (10.44).
- 10.28 A binary FSK system transmits data at the rate of 2.5 times megabits per second. During the course of transmission, white Gaussian noise of zero mean and power spectral density  $10^{-20}$  watts per hertz is added to the signal. In the absence of noise, the amplitude of the received signal is  $1 \mu\text{V}$  across 50 ohm impedance. Determine the average probability of error assuming coherent detection of the binary FSK signal.
- 10.29 One of the simplest forms of forward error correction code is the repetition code. With an  $N$ -repetition code, the same bit is sent  $N$  times, and the decoder decides in favor of the bit that is detected on the majority of trials (assuming  $N$  is odd). For a BPSK transmission scheme, determine the BER performance of a 3-repetition code.

### ■ COMPUTER EXPERIMENTS

- 10.30 In this experiment, we simulate the performance of bipolar signaling in additive white Gaussian noise. The MATLAB script included in Appendix 7 for this experiment does the following:
- It generates a random sequence with rectangular pulse shaping.
  - It adds Gaussian noise.
  - It detects the data with a simulated integrate-and-dump detector.
- With this MATLAB script:
- Compute the spectrum of the transmitted signal and compare to the theoretical.
  - Explain the computation of the noise variance given an  $E_b/N_0$  ratio.
  - Confirm the theoretically predicted bit error rate for  $E_b/N_0$  from 0 to 10 dB.
- 10.31 In this experiment, we simulate the performance of bipolar signaling in additive white Gaussian noise but with root-raised-cosine pulse shaping. A MATLAB script is included in Appendix 7 for doing this simulation. Hence, do the following:
- Compute the spectrum of the transmitted signal and compare to the theoretical. Also compare to the transmit spectrum with rectangular pulse shaping.
  - Plot the eye diagram of the received signal under no noise conditions. Explain the relationship of the eye opening to the bit error rate performance.
  - Confirm the theoretically predicted bit error rate for  $E_b/N_0$  from 0 to 10 dB.
- 10.32 In this experiment, we simulate the effect of various mismatches in the communication system and their effects on performance. In particular, modify the MATLAB scripts of the two preceding problems to do the following:
- Simulate the performance of a system using rectangular pulse-shaping at the transmitter and raised cosine pulse shaping at the receiver. Comment on the performance degradation.
  - In the case of matched root-raised cosine filtering, include a complex phase rotation  $\exp(j\theta)$  in the channel. Plot the resulting eye diagram for  $\theta$  being the equivalent of  $5^\circ$ ,  $10^\circ$ ,  $20^\circ$ , and  $45^\circ$ . compare to the case of  $\theta = 0^\circ$ . Do likewise for the BER performance. What modification to the theoretical BER formula would accurately model this behavior?

## CHAPTER 11

# SYSTEM AND NOISE CALCULATIONS

The inevitable presence of noise undermines the reliable transmission of signals through a communication system. In previous chapters, we have modeled noise as white, Gaussian, and additive. This model was mathematically tractable and allowed us to obtain numerous analytical results about the performance of analog and digital communications in noise. In those previous chapters, we claimed that white Gaussian model was a reasonable model of reality. Now we consider in greater detail the potential sources of noise and how they arise. The sources of noise may be external to the system (e.g., atmospheric noise, galactic noise, manmade noise) or internal to the system. The second category includes an important type of noise that arises due to spontaneous fluctuations of current or voltage in electrical circuits. This type of noise, in one way or another, is present in every communication system and represents a fundamental limitation on the transmission and detection of signals.

In this chapter, we briefly discuss the physical sources of noise in electrical circuits and develop quantitative models for measuring and predicting the presence of noise in a communication system. We then consider the effect propagation has on the received power level. In particular, we consider free-space propagation of radio waves and the propagation of radio waves in a terrestrial mobile environment. When the two concepts of received signal level and system noise level are combined, we have the signal-to-noise ratio, which represents the fundamental figure of merit for the quality of transmission across a communication channel.

This chapter teaches us the following lessons:

- *Lesson 1: Noise in communication systems may be generated by a number of sources, but often the sources are the communication devices themselves. Thermal noise and shot noise are examples of white noise processes generated by electrical circuits.*
- *Lesson 2: In a free-space environment, the received signal strength is attenuated proportional to square of the transmission distance. However, signal strength can be enhanced by directional antennas at both the transmitting and receiving sites.*
- *Lesson 3: In a terrestrial environment, radio communication may occur over many paths. The constructive and destructive interference between the different paths leads, in general, to the so-called multipath phenomenon, which causes much greater propagation losses than predicted by the free-space model. In addition, movement of either the transmitting or receiving terminals results in further variation of the received signal strength.*

## 11.1 Electrical Noise

In an electrical circuit, noise is generated by various physical phenomena.<sup>1</sup> We have thermal noise produced by the random motion of electrons in conducting media, and shot noise produced by random fluctuations of current flow in electronic devices. These two are the most common examples of spontaneous fluctuation noise encountered in electrical circuits.

Besides thermal noise and shot noise, transistors exhibit a low-frequency noise phenomenon known as *flicker noise*. The mean-square value of flicker noise is inversely proportional to frequency; hence it is also referred to as “one-over- $f$ ” noise. Yet another type of noise encountered in semiconductor devices is burst noise, whose mean-square value falls off as  $1/f^2$ .

Flicker noise and burst noise are both non-white, with their degrading effects being observed at low frequencies. Ordinarily, they can be ignored above a few kilohertz. On the other hand, thermal noise and shot noise are both white for all practical purposes; hence their degrading influence on the operation of a communication system extends right across the complete frequency band of interest. A brief discussion of thermal noise and shot noise is therefore in order.

### ■ THERMAL NOISE

Thermal noise is a ubiquitous source of noise that arises from thermally induced motion of electrons in conducting media. In a conductor, there are a large number of “free” electrons and an equally large number of ions bound by strong molecular forces. The ions vibrate randomly about their normal positions. The free electrons move along randomly oriented paths, due to continuous collisions with the vibrating ions. The net effect of the random motion is an electric current that is likewise random. The mean value of the current is zero since, on average, there are as many electrons moving in one direction as there are in another.

A thorough analysis of thermal noise requires the use of thermodynamic and quantum mechanical considerations that are beyond the scope of this book. For the purpose of the discussion presented here, it suffices to say that the power spectral density of thermal noise produced by a resistor is given by<sup>2</sup>

$$S_{TN}(f) = \frac{2h|f|}{\exp(h|f|/kT) - 1} \quad (11.1)$$

where  $T$  is the *absolute temperature* in Kelvin,  $k$  is *Boltzmann’s constant*, and  $h$  is Planck’s constant. Note that the power spectral density  $S_{TN}(f)$  is measured in watts per hertz. For “low” frequencies defined by

$$f \ll \frac{kT}{h} \quad (11.2)$$

we may use the approximation

$$\exp\left(\frac{h|f|}{kT}\right) \approx 1 + \frac{h|f|}{kT} \quad (11.3)$$

<sup>1</sup>For a detailed treatment of electrical noise, see Bell (1985), Van Der Ziel (1970), and Robinson (1974).

<sup>2</sup>For a discussion of the physical issues involved in the formulation of Eq. (11.1), and for a historical account of the pertinent literature, see Bell (1985).

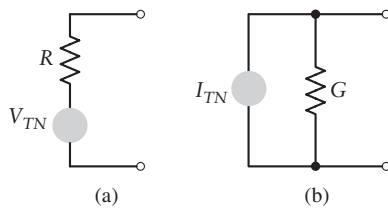


**FIGURE 11.1** Models of a noisy resistor: (a) Thévenin equivalent circuit and (b) Norton equivalent circuit.

Substituting this approximate formula into Eq. (11.1) we arrive at the corresponding approximate formula for the power spectral density of thermal noise:

$$S_{TN}(f) \approx 2kT \quad (11.4)$$

By substituting the values for Boltzmann's constant,  $k = 1.38 \times 10^{-23}$  watts/Hz/K, Planck's constant,  $h = 6.63 \times 10^{-34}$  watt-second<sup>2</sup>, we find that, at a nominal temperature of  $T = T_0 = 290$  K (17 °C),

$$\frac{kT}{h} = 6 \times 10^{12} \text{ Hz} \quad (11.5)$$

This upper frequency limit lies in the infrared region of the electromagnetic spectrum that is well above the frequencies encountered in conventional electrical communication systems. Therefore, for all practical purposes the use of the formula of Eq. (11.4) is justified.

Thus given a resistor of  $R$  ohms, we find from Eq. (11.4) that the mean-square value of the thermal noise voltage measured across the terminals of the resistor equals

$$\begin{aligned} E[V_{TN}^2] &= 2RB_N S_{TN}(f) \\ &= 4kT R B_N \text{ volts}^2 \end{aligned} \quad (11.6)$$

where  $B_N$  is the bandwidth (in hertz) over which the noise voltage is measured. The factor 2 in the first line of Eq. (11.6) comes from the fact that the spectral density has both positive and negative frequencies. We may thus model a noisy resistor by the *Thévenin equivalent circuit* consisting of a noise voltage generator with a mean square value of  $E[V_{TN}^2]$  in series with a noiseless resistor, as in Fig. 11.1(a). Alternatively, we may use the *Norton equivalent circuit* consisting of a noise current generator in parallel with a noiseless conductance  $G = 1/R$ , as in Fig. 11.1(b). The mean-square value of the noise current generator is

$$\begin{aligned} E[I_{TN}^2] &= \frac{1}{R^2} E[V_{TN}^2] \\ &= 4kT G B_N \text{ amps}^2 \end{aligned} \quad (11.7)$$

Since the number of electrons in a resistor is very large and their random motions inside the resistor are statistically independent of each other, the central limit theorem indicates that thermal noise is Gaussian distributed. Accordingly, for the band of frequencies encountered in electrical communication systems, we may model thermal noise as *white Gaussian noise* of zero mean.

#### EXAMPLE 11.1 Noise Voltage in AM Radio

The front-end filter of a radio passes the broadcast AM band from 535 kHz to 1605 kHz. The radio input has an effective resistance of 300 ohms. What is the root-mean-square noise voltage that we would expect to observe due to this resistance?

From Eq. (11.6), the mean-square thermal noise voltage at room temperature is

$$\begin{aligned} \text{E}[V_{TN}^2] &= 4kTB_N \\ &= 4 \times (1.38 \times 10^{-23}) \times 290 \times 300 \times (1070 \times 10^3) \\ &= 5.14 \times 10^{-12} \text{ volts}^2 \end{aligned}$$

Hence, the root-mean-square thermal noise voltage is 2.3 microvolts.

### ■ AVAILABLE NOISE POWER

Noise calculations involve the transfer of power from a source to a load, so we find that the use of the *maximum-power transfer theorem* is applicable. This theorem states that the maximum possible power is transferred from a source of internal resistance  $R$  to a load of resistance  $R_L$  when  $R_L = R$ . Under this matched condition, the power produced by the source is divided equally between the internal resistance of the source and the load resistance. The power delivered to the load is referred to as the *available power*. Applying the maximum-power transfer theorem to the Thévenin equivalent circuit of Fig. 11.1(a) or the Norton equivalent circuit of Fig. 11.1(b), we readily find that a noisy resistor produces an *available power* equal to  $kTB_N$  watts.

#### EXAMPLE 11.2 Noise Power

What is the available noise power produced by a 10 kilo-ohm resistor over the bandwidth from 0 to 10 MHz?

The available noise power at room temperature is

$$\begin{aligned} P_N &= kTB_N \\ &= (1.38 \times 10^{-23}) \times 290 \times 10^7 \\ &= 4.0 \times 10^{-14} \text{ watts} \end{aligned}$$

The root-mean-square (rms) voltage this power produces across a matched load of 10 kilo-ohms is

$$\begin{aligned} V_{\text{rms}} &= \sqrt{P_N R} \\ &= 20.0 \text{ microvolts} \end{aligned}$$

► **Drill Problem 11.1** What is the root-mean-square voltage across a 10 mega-ohm resistor at room temperature if it is measured over a 1 GHz bandwidth? What is the available noise power? ◀

### ■ SHOT NOISE

Shot noise arises in electronic devices due to the discrete nature of current flow in the device. The process assumes the existence of an average current flow that manifests itself in the form of electrons flowing from the cathode to the plate in vacuum tubes; holes and electrons flowing in semi-conductor devices; and photons emitted in photodiodes. Although the average number of particles moving across the device per unit time is assumed to be constant, the process of current flow through the device exhibits fluctuations about the average value. The manner in which these fluctuations arise varies from one device to another. In a vacuum-tube device, the fluctuations are produced by the random emission of electrons from the cathode. In a semiconductor device, the cause is the random diffusion of electrons or the

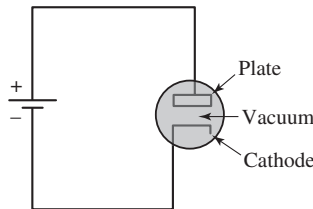


**FIGURE 11.2** A temperature-limited vacuum diode.

random recombination of electrons with holes. In a photodiode, it is the random emission of photons. In all these devices, the physical mechanism that controls current flow through the device has built-in statistical fluctuations about some average value. The shot noise produced by these fluctuations is thus dependent on the average value of the current.

Consider, for example, a temperature-limited vacuum diode, shown in Fig. 11.2. The diode consists of two electrodes enclosed in a vacuum: a cathode, which is heated so that it emits electrons; and an anode or plate, which is maintained at a positive potential with respect to the cathode so that it gathers the electrons. We assume that the cathode–plate potential difference is large enough to cause the electrons emitted thermionically by the heated cathode to be pulled to the plate with such high velocities that the space-charge effects are negligible. The plate current is then determined effectively by the rate at which electrons are emitted from the cathode. By considering the plate current as the sum of a succession of current pulses, with each pulse caused by the transit of one electron through the cathode–plate space, we find that the mean-square value of the randomly fluctuating component of the current is given by

$$\mathbb{E}[I_{\text{shot}}^2] = 2qIB_N \text{ amps}^2 \quad (11.8)$$

where  $q$  is the electron charge equal to  $1.60 \times 10^{-19}$  coulombs,  $I$  is the mean value of the current in amperes, and  $B_N$  is the bandwidth of the measuring instrument in hertz. Equation (11.8) is called the *Schottky formula*. The typical transit time of an electron from cathode to plate is on the order of  $10^{-9}$  seconds. The Schottky formula holds provided that the operating frequency is small compared with the reciprocal of the transmit time, so that we may neglect transit time effects.

Another important characteristic of shot noise is that it is Gaussian distributed with zero mean. This characteristic follows from the fact that the number of electrons contributing to the shot noise current is very large, and their random emissions from the cathode are, for practical purposes, statistically independent of each other. Hence, the central limit theorem predicts a Gaussian distribution for shot noise.

The Schottky formula also holds for a semiconductor junction diode. In this case, the mean value of the current is given by the *diode equation*

$$I = I_s \exp\left(\frac{qV}{kT}\right) - I_s \quad (11.9)$$

where  $V$  is the voltage applied across the diode and  $I_s$  is the saturation current; the other constants are as defined previously. The two components of the current  $I$  produce statistically independent shot-noise contributions of their own, as shown by

$$\begin{aligned} \mathbb{E}[I_{\text{shot}}^2] &= 2qI_s \exp\left(\frac{qV}{kT}\right)B_N + 2qI_s B_N \\ &= 2q(I + 2I_s)B_N \end{aligned} \quad (11.10)$$

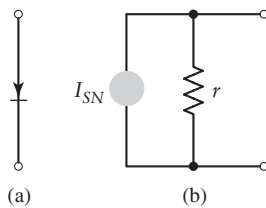


**FIGURE 11.3** (a) Junction diode.  
(b) Shot noise model.

Figure 11.3 shows the shot noise model of the junction diode.<sup>3</sup> The model includes the dynamic resistance of the diode, defined by

$$r = \frac{\delta V}{\delta I} = \frac{kT}{q(I + I_s)}$$

Note, however, unlike ordinary resistor the dynamic resistance  $r$  is noiseless since it does not involve power dissipation.

In a bipolar junction transistor, shot noise is generated at both the emitter and collector junctions. On the other hand, in junction field-effect transistors, the use of an insulated gate structure avoids junction shot noise; nevertheless, shot noise is produced by the flow of gate current. Of course, in both devices, thermal noise arises from the internal ohmic resistance: *base resistance* in a bipolar transistor and *channel resistance* in a field effect transistor.

► **Drill Problem 11.2** What is the available noise power over 1 MHz due to shot noise from a junction diode that has a voltage differential of 0.7 volts and carries an average current of 0.1 milliamperes? Assume that the current source of the Norton equivalent circuit of Fig. 11.3(b) has a resistance of 250 ohms. ◀

## 11.2 Noise Figure

A convenient measure of the noise performance of a linear two-port device is furnished by the so-called *noise figure*. Consider a linear two-port device connected to a signal source of internal impedance  $Z(f) = R(f) + jX(f)$ , as in Fig. 11.4. The noise voltage  $w(t)$  represents the thermal noise associated with the internal resistance  $R(f)$  of the source. The output noise of the two-port device is made up of two contributions, one due to the signal source and the other due to the device itself. We define the available output noise power in a band of width  $\Delta f$  centered at frequency  $f$  as the maximum average noise power in this band obtainable at the output of the device. The maximum noise power that the two-port device can deliver to an external load is obtained when the load impedance is the complex conjugate of the output impedance of the device—that is, when the resistance is matched

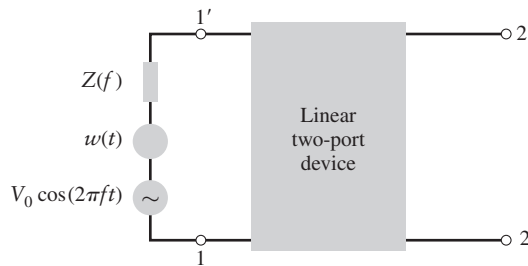


**FIGURE 11.4** Linear two-port device.

<sup>3</sup>For details of noise models for semiconductor devices and transistors, see Robinson (1974), pp. 93–116.

and the reactance is tuned out. We define the *noise figure of the two-port device as the ratio of the total available output noise power (due to the device and the source) per unit bandwidth to the portion thereof due to the source.*

Let the spectral density of the total available noise power of the device output be  $S_{NO}(f)$  and the spectral density of the available noise power due to the source at the device input be  $S_{NS}(f)$ . Also let  $G(f)$  denote the available power gain of the two-port device, defined as the ratio of the available signal power at the output of the device to the available signal power of the source when the signal is a sinusoidal wave of frequency  $f$ . Then we may express the noise figure  $F$  of the device as

$$F(f) = \frac{S_{NO}(f)}{G(f)S_{NS}(f)} \quad (11.11)$$

If the device were noise-free,  $S_{NO}(f) = G(f)S_{NS}(f)$  and the noise figure would then be unity. In a physical device, however,  $S_{NO}(f)$  is larger than  $G(f)S_{NS}(f)$ , so that the noise figure is always larger than unity. The noise figure is commonly expressed in decibels—that is, as  $10 \log_{10}(F)$ .

The noise figure  $F$  of Eq. (11.11) is a function of the operating frequency  $f$ ; it is therefore referred to as the *spot noise figure*. In contrast, we may define the *average noise figure*  $F_0$  of a two-port device as the ratio of the total noise power at the device output to the output noise power due solely to the source. That is,

$$F_0 = \frac{\int_{-\infty}^{\infty} S_{NO}(f) df}{\int_{-\infty}^{\infty} G(f)S_{NS}(f) df} \quad (11.12)$$

It is apparent that, in the case where thermal noise in the input circuit corresponds to a constant resistance  $R(f)$ , and the device has a constant gain throughout a fixed band with zero gain at other frequencies, the spot noise figure  $F$  and the average noise figure  $F_0$  are identical.

#### EXAMPLE 11.3 Noise Figure Calculation

The input of a two-port network with a gain of 10 dB and a constant noise figure of 8 dB is connected to a resistor that generates a power spectral density  $S_{NS}(f) = kT_0$  where  $T_0$  is the nominal temperature. What is the noise spectral density at the output of the two-port network?

From Eq. (11.11) applied at arbitrary frequency  $f$ , we find that the output noise spectral density is

$$S_{NO}(f) = F(f)G(f)S_{NS}(f)$$

Expressed in decibels, we have

$$\begin{aligned} S_{NO} &= F_{dB} + G_{dB} + (kT_0)_{dBm/Hz} \\ &= 10 + 8 + (-174) \\ &= -156 \text{ dBm/Hz} \end{aligned}$$

where we have used the fact that  $kT_0 = 1.38 \times 10^{-23} \times 290 \text{ watts/Hz} \approx -174 \text{ dBm/Hz}$ .

## 11.3 Equivalent Noise Temperature

A disadvantage of the noise figure  $F$  is that, when it is used to compare low-noise devices, the values are all close to unity, which makes the comparison difficult. In such cases, it is preferable to use the *equivalent noise temperature*. Consider a linear two-port device whose input

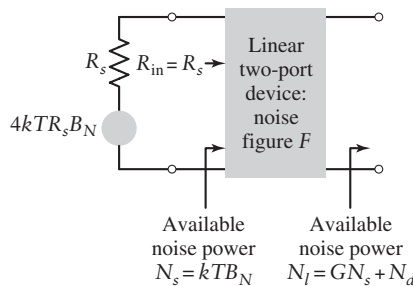


**FIGURE 11.5** Linear two-port device matched to the internal resistance of a source connected to the input.

resistance is matched to the internal resistance of the source as shown in Fig. 11.5. In this diagram, we also include the noise voltage generator associated with the internal resistance  $R_s$  of the source. From Eq. (11.3) the mean-square value of this noise voltage is  $4kTR_sB_N$  where  $k$  is Boltzmann's constant. Hence, the available noise power at the device input is

$$N_s = kTB_N \quad (11.13)$$

Let  $N_d$  denote the noise power contributed by the two-port device to the total available output noise power  $N_l$ . We define  $N_d$  as

$$N_d = GkT_eB_N \quad (11.14)$$

where  $G$  is the available power gain of the device and  $T_e$  is the equivalent noise temperature of the device. Then it follows that the total output noise power is

$$\begin{aligned} N_l &= GN_s + N_d \\ &= Gk(T + T_e)B_N \end{aligned} \quad (11.15)$$

The noise figure of the device is therefore

$$F = \frac{N_l}{GN_s} = \frac{T + T_e}{T} \quad (11.16)$$

Solving Eq. (11.16) for the equivalent noise temperature, we obtain

$$T_e = T(F - 1) \quad (11.17)$$

where the noise figure is measured under matched input conditions, and the noise source is set at temperature  $T$ . Equation (11.17) provides the relationship between the noise figure and equivalent noise temperature of a two-port network.

► **Drill Problem 11.3** An electronic device has a noise figure of 10 dB. What is the equivalent noise temperature? ◀

► **Drill Problem 11.4** The device of Problem 11.3 has a gain of 17dB and is connected to a spectrum analyzer. If the input to the device has an equivalent temperature of 290 K and the spectrum analyzer is noiseless, express the measured power spectral density in dBm/Hz. If the spectrum analyzer has a noise figure of 25 dB, what is the measured power spectral density in this case? ◀

### ■ NOISE SPECTRAL DENSITY

A two-port network with equivalent noise temperature  $T_e$  (referred to the input) produces the available noise power

$$N_{av} = kT_eB_N \quad (11.18)$$

Recognizing that  $N_{av} = N_0B_N$ , we find that the noise may be modeled as additive white Gaussian noise with zero mean and power spectral density  $N_0/2$ , where

$$N_0 = kT_e \quad (11.19)$$

The power spectral density of the noise so modeled depends only on Boltzmann's constant and the equivalent noise temperature  $T_e$ . It is the simplicity of this model that makes the equivalent noise temperature of a composite network such a useful concept.

## 11.4 Cascade Connection of Two-Port Networks

It is often necessary to evaluate the noise figure of a cascade connection of two-port networks whose individual noise figures are known. Consider Fig. 11.6, consisting of a pair of two-port networks of noise figures  $F_1$  and  $F_2$  and power gains  $G_1$  and  $G_2$ , connected in cascade. It is assumed that the devices are matched, and that the noise figure  $F_2$  of the second network is defined assuming an input noise power  $N_1$ .

At the input of the first network, we have a noise power  $N_1$  contributed by the source, plus an equivalent noise power  $(F_1 - 1)N_1$  contributed by the network itself. The output noise power from the first network is therefore  $F_1N_1G_1$ . Added to this noise power at the input of the second network, we have the equivalent extra power  $(F_2 - 1)N_1$  contributed by the second network itself. The output noise power from this second network is therefore equal to  $F_1G_1N_1G_2 + (F_2 - 1)N_1G_2$ . We may consider the noise figure  $F$  as the ratio of the actual output noise power to the output noise power if the networks are noiseless. We may therefore express the overall noise figure of the cascade connection of Fig. 11.6 as

$$\begin{aligned} F &= \frac{F_1G_1N_1G_2 + (F_2 - 1)N_1G_2}{N_1G_1G_2} \\ &= F_1 + \frac{F_2 - 1}{G_1} \end{aligned} \quad (11.20)$$

The result may be readily extended to the cascade connection of any number of two-port networks, as shown by

$$F = F_1 + \frac{F_2 - 1}{G_1} + \frac{F_3 - 1}{G_1G_2} + \frac{F_4 - 1}{G_1G_2G_3} + \dots \quad (11.21)$$

where  $F_1, F_2, F_3, \dots$ , are the individual noise figures and  $G_1, G_2, G_3, \dots$ , are the available power gains, respectively. Equation (11.21) shows that if the first stage of the cascade connection in Fig. 11.6 has a high gain, the overall noise figure  $F$  is dominated by the noise figure of the first stage.

Correspondingly, we may express the overall equivalent noise temperature of the cascade connection of any number of noisy two-port networks as follows:

$$T_e = T_1 + \frac{T_2}{G_1} + \frac{T_3}{G_1G_2} + \frac{T_4}{G_1G_2G_3} + \dots \quad (11.22)$$

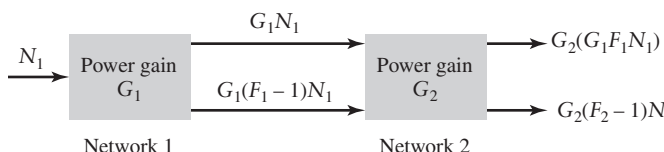


**FIGURE 11.6** A cascade of two noisy networks.

where  $T_1, T_2, T_3, \dots$ , are the equivalent noise temperatures of the individual networks. From Eq. (11.22) we also see that if the first stage of a cascade connection of noisy two-port networks has a large power gain, then the overall value of the equivalent noise temperature  $T_e$  is practically the same as that of the first stage. For this reason, in a low-noise receiver, extra care is taken in the design of the pre-amplifier or low-noise amplifier at the very front end of the receiver.

#### EXAMPLE 11.4 System Noise Temperature of a Satellite Receiver

A satellite receiver consists of an antenna that has a noise temperature of 50 K. This is followed by a low-noise amplifier with 30 dB of gain and noise temperature of 70 K. The low-noise amplifier, in turn, is followed by a second stage amplifier with a gain of 40 dB and noise temperature of 1500 K. What is the system noise temperature?

For this three-stage system, Eq. (11.22) shows that the system noise temperature is given by

$$T_e = T_1 + \frac{T_2}{G_1} + \frac{T_3}{G_1 G_2}$$

where  $T_1, T_2$ , and  $T_3$  are the noise temperatures of the antenna, low-noise amplifier, and second stage amplifier, respectively. Since the antenna does not provide any electrical gain to the received signal,  $G_1 = 1$ . Consequently, the effective noise temperature is

$$\begin{aligned} T_e &= 50 + \frac{70}{1} + \frac{1500}{1 \times 1000} \\ &= 121.5 \text{ K} \end{aligned}$$

► **Drill Problem 11.5** A broadcast television receiver consists of an antenna with a noise temperature of 290 K and a pre-amplifier with an available power gain of 20 dB and a noise figure of 9 dB. A second-stage amplifier in the receiver provides another 20 dB of gain and has a noise figure of 20 dB. What is the noise figure of the overall system? ◀

## 11.5 Free-Space Link Calculations

In this section, we move on to the issue of signal and noise power calculations for radio links that rely on line-of-sight propagation through space. Such calculations are encountered in satellite communications,<sup>4</sup> for example. In a satellite system, the message signal is transmitted from a ground station via the uplink to a geosynchronous satellite, amplified in a transponder therein, and then retransmitted from the satellite via the downlink to another ground Earth station. The satellite is positioned in a geostationary orbit (around the Earth) so that it is always visible to different ground stations located inside the satellite antenna's coverage zone on the Earth's surface. The satellite, in effect, acts as a repeater in the sky. Another application with line-of-sight propagation characteristics is deep-space communication<sup>5</sup> of information between a spacecraft and a ground station. In this second application, the system includes a tracking capability such that the spacecraft is always visible to one of multiple ground stations. For the analysis presented here, we will consider the satellite link as illustrative of space applications.

<sup>4</sup>For a detailed treatment of link calculations for satellite communications, see Chapter 4 of Pratt and Bostian (1986).

<sup>5</sup>For a detailed treatment of link calculations for deep-space communications, see Chapter 3 of Yuen (1983).

## ■ CALCULATION OF RECEIVED SIGNAL POWER

Figure 11.7 illustrates a down-link between a spacecraft and a ground Earth station. The link includes a transmitting source (on the spacecraft) with its output radiated through the spacecraft's antenna. At the ground station, a receiving antenna is used to collect signal power from the incoming electromagnetic wave and feed it to the low-noise receiver through a waveguide.

Let the transmitting source radiate a total power  $P_T$ . If this power is radiated *isotropically* (i.e., uniformly in all directions), the power flux density at a distance  $r$  from the source is  $P_T/(4\pi r^2)$ , where  $4\pi r^2$  is the surface area of a sphere of radius  $r$ . In practice, we use a highly directional antenna so that the transmitted power is radiated primarily along a particular direction of interest. The antenna has a gain that is defined as the ratio of power radiated per unit solid angle in a given direction to the average power radiated per solid angle. Let  $G_T$  denote the gain of the transmitting antenna in the direction in which the maximum power is radiated; this direction is called the *boresight* of the antenna. The gain  $G_T$  is a measure of the increase in power radiated by the antenna over that radiated by an isotropic source. Thus for a transmitter of total power  $P_T$  driving a lossless antenna with gain  $G_T$ , the power flux density at distance  $r$  in the direction of the antenna boresight is given by

$$\Phi = \frac{P_T G_T}{4\pi r^2} \quad (11.23)$$

Let  $A_{\text{eff}}$  denote the *effective aperture area* of the receiving antenna. This area is related to the physical aperture area  $A$  of the antenna by the formula

$$A_{\text{eff}} = \eta A \quad (11.24)$$

where  $\eta$  is the *aperture efficiency*. Typically  $\eta$  is in the range of 40 to 90 percent, depending on the type of antenna employed. The gain of the receiving antenna  $G_R$  is defined in terms of the effective aperture  $A_{\text{eff}}$  by

$$G_R = \frac{4\pi A_{\text{eff}}}{\lambda^2} \quad (11.25)$$

where  $\lambda$  is the wavelength of the transmitted electromagnetic wave;  $\lambda$  is equal to  $c/f$  where  $c$  is the speed of propagation (which is the same as the speed of light), and  $f$  is the transmission frequency. Equivalently, we have

$$A_{\text{eff}} = \frac{G_R \lambda^2}{4\pi} \quad (11.26)$$

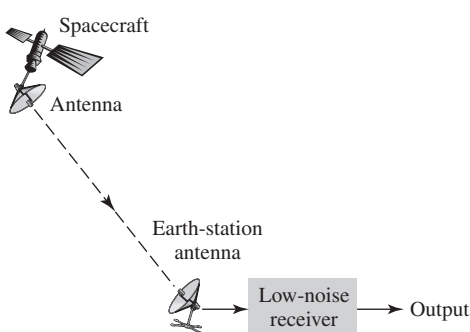


**FIGURE 11.7** Space communication down-link.

Hence, given the power flux density  $\Phi$  at the receiving antenna with an effective aperture area  $A_{\text{eff}}$ , the received power is

$$P_R = A_{\text{eff}}\Phi \quad (11.27)$$

Thus, substituting Eqs. (11.23) and (11.26) into (11.27), we obtain the result

$$P_R = P_T G_T G_R \left( \frac{\lambda}{4\pi r} \right)^2 \quad (11.28)$$

Equation (11.28) is known as the *Friis transmission formula*, which relates the received power to the transmitted power. The product  $P_T G_T$  in this equation is called the *effective isotropic radiated power* (EIRP). It describes the combination of the transmitting source and antenna in terms of an effective isotropic source with power  $P_T G_T$  radiated uniformly in all directions. The term  $(4\pi r/\lambda)^2$  is called the *path loss* or *free-space loss*; it may be viewed as the ratio of transmitted power to received power between two antennas that are separated by a distance  $r$ .

From Eq. (11.28) we see that for given values of wavelength  $\lambda$  and distance  $r$ , the received power may be increased by three methods:

1. *The spacecraft-transmitted power  $P_T$  is increased.* The transmitted power  $P_T$  may be 20 watts or less. Even though this transmitted power may appear low, the input power required for its generation represents a substantial fraction of the total power available on the spacecraft. Hence, there is a physical limit on how large a value we can assign to the transmitted power  $P_T$ .
2. *The gain  $G_T$  of the transmitting antenna is increased.* This will help concentrate the transmitted power rather intensely in the direction of the receiving antenna. However, a large value of  $G_T$  requires the use of a large antenna. The choice of  $G_T$  is therefore limited by size and weight constraints of the spacecraft.
3. *The gain  $G_R$  of the receiving antenna is increased.* This will enable the receiver to collect as much of the radiated signal power as possible. Here again, size and weight constraints place a physical limit on the size of the ground-station antenna, although these constraints are far less demanding than those on the spacecraft antenna; we typically<sup>6</sup> have  $G_R \gg G_T$ .

Let the receiving antenna gain and space loss be expressed in decibels (dB). Likewise, let the effective radiated power and the received power be expressed in *decibels relative to one watt* (dBW). Then we may restate the Friis transmission formula in the form

$$P_R = \text{EIRP} + G_R - L_p \quad (11.29)$$

where

$$\text{EIRP} = 10 \log_{10}(P_T G_T) \quad (11.30)$$

$$G_R = 10 \log_{10} \left( \frac{4\pi A_{\text{eff}}}{\lambda^2} \right) \quad (11.31)$$

$$L_p = 20 \log_{10} \left( \frac{4\pi r}{\lambda} \right) \quad (11.32)$$

In Eq. (11.25),  $G_R$  is represented as a power ratio, whereas in Eq. (11.31) it is expressed in decibels. Equation (11.29) is idealized in that it does not account for all losses

<sup>6</sup>There are exceptions to this rule, most notably satellite-to-mobile terminal communications and direct-to-home satellite television broadcasts.

in the link. To correct for this, it is customary to include a term that represents the combined effect of losses in the atmosphere due to rain attenuation, losses in the transmitting and receiving antennas, and possible loss of gain due to mispointing of the antennas. Let  $L_0$  denote the overall value of this loss expressed in decibels; this term is sometimes called the *system margin*. Then we may modify the expression for the received signal power as

$$P_R = \text{EIRP} + G_R - L_p - L_0 \quad (11.33)$$

Equation (11.33) represents the *link (power) budget* in that it allows the system designer of a telecommunication link to adjust controllable parameters such as EIRP or the receiving antenna gain  $G_R$  and make quick calculations of the received power.

The received power  $P_R$  is commonly called the *carrier power*. This nomenclature is derived from early satellite systems where phase or frequency modulation was commonly employed. Since these modulation strategies maintain the envelope of the sinusoidal carrier constant, the carrier power is typically equal to the received power.

#### EXAMPLE 11.5 Satellite Link Budget

A geostationary satellite is located at a distance of 40,000 km from an Earth station. At the satellite a source at a frequency of 4 GHz radiates a power of 10 watts through an antenna with a gain of 20 dB. Assume that the effective aperture area of the receiving antenna is  $10 \text{ m}^2$ . Calculate the received signal power, ignoring nonideal losses in the links.

The effective radiated power with  $P_T = 10 \text{ W}$  and  $G_T = 20 \text{ dB}$  is

$$\begin{aligned} \text{EIRP} &= 10 \log_{10}(P_T G_T) \\ &= 10 \log_{10} P_T + 10 \log_{10} G_T \\ &= 10 \log_{10} 10 + 20 \\ &= 30 \text{ dBW} \end{aligned}$$

The speed of propagation equals the speed of light:  $c = 3 \times 10^8 \text{ m/s}$ . The wavelength of the transmitted 4 GHz electromagnetic wave is therefore

$$\begin{aligned} \lambda &= \frac{c}{f} \\ &= \frac{3 \times 10^8}{4 \times 10^9} \\ &= 0.075 \text{ m} \end{aligned}$$

Hence, the path loss equals

$$\begin{aligned} L_p &= 20 \log_{10}\left(\frac{4\pi r}{\lambda}\right) \\ &= 20 \log_{10}\left(\frac{4\pi \times 4 \times 10^7}{0.075}\right) \\ &= 196.5 \text{ dB} \end{aligned}$$

The gain of the receiving antenna with  $A_{\text{eff}} = 10 \text{ m}^2$  is

$$\begin{aligned} G_R &= 10 \log_{10}\left(\frac{4\pi A_{\text{eff}}}{\lambda^2}\right) \\ &= 10 \log_{10}\left(\frac{4\pi \times 10}{0.075^2}\right) \\ &= 43.5 \text{ dB} \end{aligned}$$

Thus, using Eq. (11.29) and ignoring the system margin  $L_0$ , we find that the received signal power equals

$$\begin{aligned} P_R &= 30 + 43.5 - 196.5 \\ &= -123 \text{ dBW} \end{aligned}$$

Equivalently, the received power may be written as  $P_R = 5 \times 10^{-13}$  watts. The low value of  $P_R$  indicates that the received signal at the Earth station is extremely weak. Other losses on the link (accounted for in the system margin) at the Earth station will make the received signal even weaker.

► **Drill Problem 11.6** A satellite antenna has a diameter of 4.6 meters and operates at 12 GHz. What is the antenna gain if the aperture efficiency is 60 percent? If the same antenna was used at 4 GHz, what would be the corresponding gain? ◀

► **Drill Problem 11.7** A satellite at a distance of 40,000 kilometers transmits a signal at 12 GHz with an EIRP of 10 watts toward a 4.6 meter antenna that has an aperture efficiency of 60 percent. What is the received signal level at the antenna output? ◀

### ■ CARRIER-TO-NOISE RATIO

The *carrier-to-noise ratio* (CNR) is defined as the ratio of carrier power to the available noise power, with both measured at the receiver input. As mentioned previously, the carrier power is the same as the received signal power  $P_R$ . The formula for  $P_R$  is described by the Friis transmission equation (11.28). To calculate the available noise power at the receiver input, we use the expression  $kT_sB_N$ , where  $k$  is Boltzmann's constant,  $T_s$  is the system noise temperature, and  $B_N$  is the noise bandwidth. We therefore have

$$\text{CNR} = \frac{P_R}{kT_sB_N} \quad (11.34)$$

Here again, the simplicity of this formula stems from the use of noise temperature as the measure of how noisy the system is. *The carrier-to-noise ratio is often the same as the pre-detection SNR discussed in Chapter 9.*

#### EXAMPLE 11.6 Calculation of CNR

Consider an Earth station receiver with a cryogenically cooled amplifier. The equivalent noise temperature of the receiver is 20K. The Earth station uses a large antenna operating at a frequency of 4 GHz and an elevation of 15 degrees; the antenna noise temperature is estimated to be 50K. Calculate the system noise temperature, assuming no loss in the antenna feed and waveguide. Then calculate the carrier-to-noise ratio, assuming a carrier power of  $-123$  dBW (as in Example 11.5) and a noise bandwidth of 36 MHz.

From Eq. (11.22), we see that with  $G_1 = 1$  the system noise temperature equals

$$\begin{aligned} T_s &= T_a + T_e \\ &= 50 + 20 \\ &= 70 \text{ K} \end{aligned}$$

The available noise power in the 36 MHz bandwidth is therefore

$$\begin{aligned} kT_sB_N &= 1.38 \times 10^{-23} \times 70 \times (36 \times 10^6) \\ &= 3.48 \times 10^{-14} \text{ W} \\ &= -134.6 \text{ dBW} \end{aligned}$$

Thus the use of Eq. (11.34) yields the following value for the carrier-to-noise ratio expressed in decibels:

$$\begin{aligned}10 \log_{10}(\text{CNR}) &= -123 + 134.6 \\&= 11.6 \text{ dB}\end{aligned}$$

Recall from our discussion of analog receivers in Chapter 9 that this CNR would just be sufficient to operate an FM system at threshold. In contrast, this CNR would provide a satisfactory bit error rate for many digital systems.

► **Drill Problem 11.8** The antenna of Problem 11.7 has a noise temperature of 70 K and is directly connected to a receiver with an equivalent noise temperature of 50 K and a gain of 60 dB. What is the system noise temperature? If the transmitted signal has a bandwidth of 100 kHz, what is the carrier-to-noise ratio? If the digital signal has a bit rate of 150 kbps, what is  $E_b/N_0$ ? ◀

## 11.6 Terrestrial Mobile Radio

Free-space propagation is often a good model for satellite communications where there is a clear line-of-sight between the transmitter and the receiver. It also provides insight because there is a simple theoretical explanation for propagation losses.

With terrestrial communications, on the other hand, both antennas are usually relatively close to the ground. Consequently, buildings, terrain, and vegetation may obstruct the line-of-sight path. Terrestrial radio communication often relies on the *reflection* of electromagnetic waves from various surfaces or *diffraction* of these waves around various objects. With these additional modes of propagation, there are a multitude of possible propagation paths between the transmitter and receiver, and the receiver often receives a significant signal from more than one path. This phenomenon is referred to as *multipath* propagation. With multiple waves arriving at the same location, propagation properties may differ significantly from free-space propagation.

There are three basic propagation modes that apply to terrestrial propagation: free-space, reflection, and diffraction.<sup>7</sup>

1. *Free-space propagation* depends upon a line-of-sight path between the transmitter and the receiver and a certain clearance around that path. The required clearance, illustrated in Fig. 11.8, is related to the separation of the two, and the wavelength of transmission. A rule of thumb is that a volume known as the *first Fresnel zone* must be kept clear of objects for approximate free-space propagation. The Fresnel zone defines an ellipsoid of revolution. Objects within the first Fresnel zone will affect transmission and cause deviation from the free-space propagation model. The radius of the first Fresnel zone varies with the position between the transmitting and receiving antenna; it is given by

$$b = \sqrt{\frac{\lambda d_1 d_2}{d_1 + d_2}} \quad (11.35)$$

where  $\lambda$  is the wavelength of transmission,  $d_1$  is the distance to the transmitter, and  $d_2$  is the distance to the receiver, for the particular point along the path.

<sup>7</sup>See Chapter 2 of Haykin and Moher (2004) for further details.

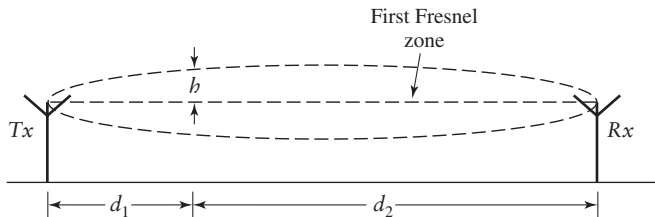


FIGURE 11.8 The first Fresnel zone for free-space propagation.

2. *Reflection* refers to the bouncing of electromagnetic waves from surrounding objects such as buildings, mountains, and passing vehicles. In terrestrial wireless communications, there is often no direct line-of-sight path between the transmitter and receiver, and communications rely on reflection and the following mode of diffraction. Reflection often further attenuates the signal and may affect the phase as well.
3. *Diffraction* refers to the bending of electromagnetic waves around objects such as buildings or terrain such as hills, and through objects such as trees and other forms of vegetation.

In terrestrial propagation, the received signal is often the combination of many of these modes of propagation. That is, the transmitted signal may arrive at the receiver over many paths, as illustrated in Fig. 11.9. The signals on these different paths can constructively, or destructively, interfere with each other. Thus multipath transmission may have quite different properties from free-space propagation. Measurements indicate that terrestrial propagation can be broken down into several components. In the following, we describe two of these components: the median path loss and fast fading.

#### EXAMPLE 11.7 Ghosting

Before the advent of cable and direct satellite transmission, television signals were mainly received *over the air* via terrestrial links. A phenomenon, sometimes referred to as *ghosting*, would sometimes be observed with weaker (i.e., more distant) television stations. With ghosting, we would observe the image and a replica of the image in a slightly offset position. This ghost is a visual instance of multipath; it is a copy of the original signal being received at a slightly delayed time.

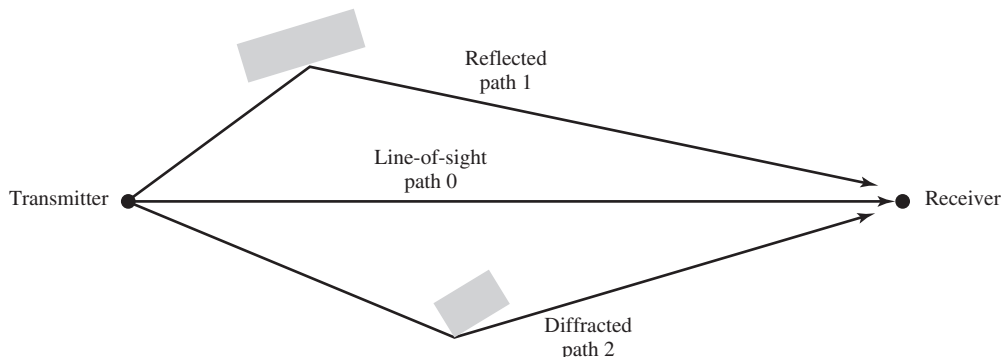


FIGURE 11.9 Illustration of multiple transmission paths between transmitter and receiver.

► **Drill Problem 11.9** The transmitting and receiving antennas for a 4-GHz signal are located on top of 20-meter towers separated by two kilometers. For free-space propagation, what is the maximum height permitted for an object located midway between the two towers? ◀

### ■ MEDIAN PATH LOSS<sup>8</sup>

With free-space path propagation, there is a relatively simple theoretical model for predicting the propagation loss as a function of distance. With other modes of propagation—reflection and diffraction—the calculation is not as simple, especially when there are multiple reflections and/or diffractions. For simple scenarios, we can develop tractable mathematical models for the propagation losses due to reflection and diffraction. With more practical scenarios, we may still construct a physical model of the environment including terrain, buildings, and vegetation, and, using computer analysis, estimate propagation losses of particular paths.

Alternatively, we may use a *statistical approach* where the propagation characteristics are empirically approximated on the basis of measurements in certain general types of environments, such as urban, suburban, and rural. The statistical approach is broken down into two components: an estimate of the *median path loss* and a random component that depends upon the physical features of the local terrain.

The measurement of the field strength in various environments as a function of the distance  $r$ , from the transmitter to the receiver motivates a simple propagation model for median path loss having the form

$$\frac{P_R}{P_T} = \frac{\beta}{r^n} \quad (11.36)$$

where, typically, the *path-loss exponent*  $n$  ranges from 2 to 5 depending on the propagation environment. The parameter  $\beta$  represents a gain that is related to frequency and antenna gains, and may also be related to antenna heights and other factors. The right-hand side of Eq. (11.36) is sometimes written in the equivalent form

$$\frac{P_R}{P_T} = \frac{\beta_o}{(r/r_o)^n} \quad (11.37)$$

In this representation,  $\beta_o$  represents the measured path gain at the reference distance  $r_o$ . In the absence of other information,  $\beta_o$  may be taken as the free-space path gain at a distance of one meter. (The reference path loss is the inverse of  $\beta_o$ ).

Numerous propagation studies have been carried out trying to closely identify the different environmental effects. The conclusion drawn from these studies is that most of these effects are locally dependent and difficult, if not impossible, to characterize in general. Some example values for the exponent  $n$  in the model of Eq. (11.36) are given in Table 11.1.

While this table indicates general trends, there are exceptions. For example, if the propagation path is along a straight street with skyscrapers on either side, there may be a ducting (waveguide) effect and propagation losses may be similar to free space or even less.

This model for median path loss is quite flexible and is intended for analytical study of problems, as it allows us to parameterize performance of various system-related factors. For commercial applications in a terrestrial environment, either a field measurement campaign or detail modeling of the environment is preferred.

---

<sup>8</sup>In this section, we present a relatively simple model for median path loss. This simple model is adequate for understanding the factors affecting path loss. For practical applications, more sophisticated models have been developed that depend on the application. An example is the Okumura–Hata model for land-mobile radio propagation of frequencies between 150 MHz and 1 GHz. See Chapter 2 of Haykin and Moher (2004) for more details.

**TABLE 11.1** Example Path-Loss exponents.

Environment	<i>n</i>
Free space	2
Flat rural	3
Rolling rural	3.5
Suburban, low rise	4
Dense urban, skyscrapers	4.5

**EXAMPLE 11.8** Terrestrial Link Budget

A propagation measurement campaign indicates that in an urban area, the median path loss can be modeled as

$$L_p = 41 + 31 \log_{10}(r)$$

where the path loss is in decibels and  $r$  is in meters. In addition to the median path loss, the system must include 12 dB of margin to compensate for signal strength variations. If the transmitter EIRP is five watts, find the minimum signal strength expected at a distance of five kilometers.

We solve this problem by appealing to the Friis transmission formula in the decibel format; namely,

$$P_R = \text{EIRP} - L_p - L_0 + G_R$$

The problem statement provides all of the quantities on the right-hand side except  $G_R$ . We make the assumption that the receiver is mobile and the antenna gain is approximately unity; that is,  $G_R = 0$  dB. Then, at a range of 5 km,

$$\begin{aligned} P_R &= 10 \log_{10} 5 - 41 - 31 \log_{10} 5000 - 12 + 0 \\ &= -160.7 \text{ dBW} \\ &= -130.7 \text{ dBm} \end{aligned}$$

► **Drill Problem 11.10** A measurement campaign indicates that the median path loss at 900 MHz in a suburban area may be modeled with a path-loss exponent of 2.9. What is the median path loss at a distance of three kilometers using this model? How does this loss compare to the free-space loss at the same distance? ◀

**■ RANDOM PATH LOSSES**

The median path loss is simply that: the median attenuation as a function of distance; 50 percent of locations will have greater loss and 50 percent will have less. The actual loss will depend upon the exact terrain, buildings, and vegetation along the path. One of the several contributors to these variations about the median value is movement of the transmitting or receiving terminal. For example, the received power level at a moving terminal that is at a relatively constant distance from the transmitter may be as shown in Fig. 11.10. For this figure, the median received signal strength is about  $-95$  dBm, but variations as much as 7 dB above and 35 dB below may be observed.

These fast variations of the signal strength are due to reflections from local objects that rapidly change the carrier phase over small distances. Changing the phase of the reflections causes them to sometimes add constructively and sometimes destructively. This fast fading is often called *Rayleigh fading*, so named after the probability distribution function that is used to model the amplitude variations. If  $R$  is the signal amplitude, with a root-mean-

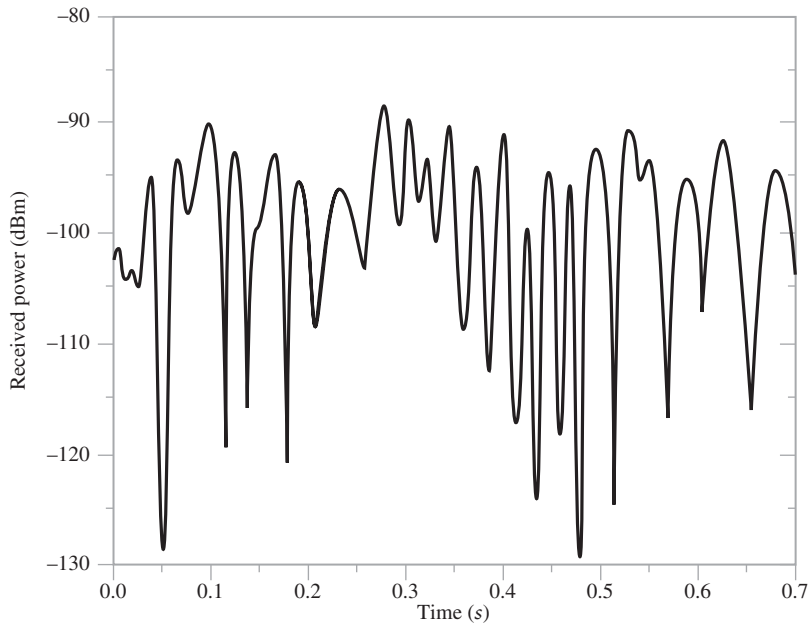


**FIGURE 11.10** Illustration of received signal power variations in Rayleigh fading.

square level of  $R_{\text{rms}}$ , then the probability that the amplitude is below a given level  $r$  is given by the *Rayleigh distribution function*

$$P[R < r] = 1 - \exp\left(-\frac{r^2}{R_{\text{rms}}^2}\right) \quad (11.38)$$

The Rayleigh distribution is plotted in Fig. 11.11. The median of the distribution is approximately  $R_{\text{rms}}$ . This implies that for 50 percent of locations there is constructive interference ( $R > R_{\text{rms}}$ ) and for 50 percent of locations there is destructive interference ( $R < R_{\text{rms}}$ ).

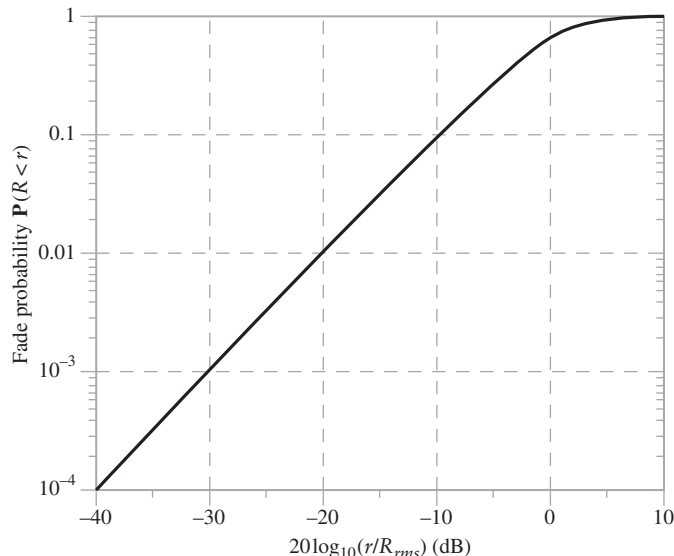


**FIGURE 11.11** Normalized Rayleigh amplitude distribution ( $r/R_{\text{rms}}$ ).

Deep fades of 20 dB ( $R < 0.1R_{\text{rms}}$ ) or more occur only rarely (with a probability of 1 percent). However, Fig. 11.11 indicates that there can be a wide variation in received signal strength due to local reflections.

### EXAMPLE 11.9 Margin for Rayleigh Fading

Suppose a mobile radio has a receiver sensitivity of  $-90 \text{ dBm}$ . That is,  $-90 \text{ dBm}$  is the minimum signal level that the receiver can reliably demodulate. The system operates at 900 MHz and the intended range is 2 kilometers. Find the transmitter power required to serve this receiver if the propagation environment has a path-loss exponent  $n = 2.9$  and the receiver must tolerate 90 percent of the fades.

If the receiver must tolerate 90 percent of the fades, then the Rayleigh distribution function of Fig. 11.11 indicates that the system should include 10 dB of margin. Consequently, the median signal level should be 10 dB above the receiver sensitivity at the edge of coverage—that is,  $-80 \text{ dBm}$ . Then using Eq. (11.37), we have

$$P_T = \frac{P_R}{\frac{\beta_0}{(r/r_o)^{2.9}}}$$

We assume  $\beta_0$  is the free-space path gain at one meter, so

$$\begin{aligned}\beta_0 (\text{dB}) &= -L_p (1\text{m}) = -20 \log_{10} \left( \frac{4\pi}{\lambda} \right) \\ &= -31.5 \text{ dB}\end{aligned}$$

at 900 MHz. Expressing the above equation for  $P_T$  in decibel format, we obtain

$$\begin{aligned}P_T &= P_R - \beta_0 + 29 \log_{10} \left( \frac{2000}{1} \right) \\ &= -80 + 31.5 + 95.7 \\ &= +47 \text{ dBm}\end{aligned}$$

This corresponds to approximately a 50-watt transmitter.

► **Drill Problem 11.11** Express the true median of the Rayleigh distribution as a fraction of the  $R_{\text{rms}}$  value? What is the decibel error in the approximation  $R_{\text{median}} \approx R_{\text{rms}}$ ? ◀

## 11.7 Summary and Discussion

In this chapter, we have characterized specific sources of noise and signal attenuation in practical communication systems. These are the inputs required to calculate the signal-to-noise ratios used to characterize receiver performance in previous chapters. In particular:

- (i) Several sources of thermal noise were identified, and we characterized their power spectral densities through the simple relation  $N_0 = kT$ , where  $k$  is Boltzmann's constant and  $T$  is the absolute temperature in Kelvin.
- (ii) The related concepts of noise figure and equivalent noise temperature were defined and used to characterize the contributions that various electronic devices or noise sources make to the overall noise. We then showed how the overall noise is calculated in a cascaded two-port system.

- (iii) The Friis equation was developed to mathematically model the relationship between transmitted and received signal strengths as a function of transmitting and receiving antenna gains and path loss.
- (iv) Propagation losses ranging from free-space conditions, typical of satellite channels, to those typical of terrestrial mobile applications were described. Variations about median path loss were identified as an important consideration in terrestrial propagation.

This chapter has provided a brief introduction to two communication channels—satellite and terrestrial—and the effects that propagation and noise have on communication performance. The propagation loss of the channel is a key component in determining the signal power at the receiver. The physical noise sources are the contributors to the noise power at the receiver. The combination of these two quantities—that is, the ratio of the signal power to the noise power—forms the primary method of assessing the quality of a communication link.

## ADDITIONAL PROBLEMS

---

- 11.12 Compute the noise spectral density in watts per hertz of:
  - (a) An ideal resistor at nominal temperature of 290 K.
  - (b) An amplifier with an equivalent noise temperature of 22,000 K.
- 11.13 For the two cases of Problem 11.12, compute the pre-detection SNR when the received signal power is:
  - (a)  $-60$  dBm and the receive bandwidth is 1 MHz.
  - (b)  $-90$  dBm and the receive bandwidth is 30 kHz.Express the answers in both absolute terms and decibels.
- 11.14 A wireless local area network transmits a signal that has a noise bandwidth of approximately 6 MHz. If the signal strength at the receiver input terminals is  $-90$  dBm and the receiver noise figure is 8 dB, what is the pre-detection signal-to-noise ratio?
- 11.15 A communications receiver includes a whip antenna whose noise temperature is approximately that of the Earth—that is, 290 K. The receiver pre-amplifier has a noise figure of 4 dB and a gain of 25 dB. Calculate (a) the equivalent noise temperature of the antenna and the pre-amplifier, and (b) the combined noise figure.
- 11.16 A parabolic antenna with a diameter of 0.75 meters is used to receive a 12 GHz satellite signal. Calculate the gain in decibels of this antenna. Assume that the antenna efficiency is 60 percent.
- 11.17 If the system noise temperature of a satellite receiver is 300 K, what is the required received signal strength to produce a  $C/N_0$  of 80 dB?
- 11.18 If a satellite is 40,000 km from the antenna of Problem 11.16, what satellite EIRP will produce a signal strength of  $-110$  dBm at the antenna terminals? Assume that the transmission frequency is 12 GHz.
- 11.19 Antennas are placed on two 35-meter office towers that are separated by 10 kilometers. Find the minimum height of a building between the two towers that would disturb the assumption of free-space propagation.
- 11.20 If a receiver has a sensitivity of  $-90$  dBm and a 12-dB noise figure, what is minimum pre-detection signal-to-noise ratio of an 8-kHz signal?

## ADVANCED PROBLEMS

---

- 11.21** A satellite antenna is installed on the tail of an aircraft and has a noise temperature of 100 K. The antenna is connected by a coaxial cable to a low-noise amplifier in the equipment bay at the front of the aircraft. The cable causes 2-dB attenuation of the signal. The low-noise amplifier has a gain of 60 dB and a noise temperature of 120 K. What is the system noise temperature? Where would a better place for the low-noise amplifier be?
- 11.22** A wireless local area network transmitter radiates 200 milliwatts. Experimentation indicates that the path loss is accurately described by

$$L_p = 31 + 33 \log_{10}(r)$$

where the path loss is in decibels and  $r$  is the range in meters. If the minimum receiver sensitivity is  $-85$  dBm, what is the range of the transmitter?

- 11.23** A mobile radio transmits 30 watts and the median path loss may be approximated by

$$L_p = 69 + 31 \log_{10}(r)$$

where the path loss is in decibels and  $r$  is the range in kilometers. The receiver sensitivity is  $-110$  dBm and 12 dB of margin must be included to compensate for variations about the median path loss. Determine the range of the transmitter.

- 11.24** A cellular telephone transmits 600 milliwatts of power.
- (a) The receiver sensitivity is  $-90$  dBm, what would the range of the telephone be under free-space propagation? Assume that the transmitting and receiving antennas have unity gain and the transmission is at 900 MHz.
  - (b) If propagation conditions actually show a path-loss exponent of 3.1 with a fixed gain  $\beta = -36$  dB, what would the range in this case be?
- 11.25** A line-of-sight 10-kilometer radio link is required to transmit data at a rate of 1 megabit per second at a center frequency of 4 GHz. The transmitter uses an antenna with 10 dB gain and QPSK modulation with a root-raised cosine pulse spectrum having a roll-off factor of 0.5. The receiver also has an antenna with 10 dB gain and has a system noise temperature of 900 K. What is the minimum transmit power required to achieve a bit error rate of  $10^{-5}$ ?
- 11.26** A land-mobile radio transmits 128 kbps at a frequency of 700 MHz. The transmitter uses an omni-directional antenna and 16-QAM modulation with a root-raised cosine pulse spectrum having a roll-off of 0.5. The receiver also uses an omni-directional antenna and has noise figure of 6 dB. If the path loss between the transmitter and receiver is given by

$$L_p(r) = 30 + 28 \log_{10}(r) \text{ dB}$$

where  $r$  is in meters, calculate the maximum range at which a bit error rate of  $10^{-4}$  may be achieved.

## APPENDIX 1

# POWER RATIOS AND DECIBEL

In system calculations and measurements involving the use of power ratios, it is customary practice to use a unit called the *decibel*. The decibel, commonly abbreviated as dB, is one tenth of a larger unit, the *bel*.<sup>1</sup> In practice, however, we find that for most applications the bel is too large a unit, hence, the wide use of dB as the unit for expressing power ratios. The dB is particularly appropriate for sound measurements because the ear responds to sound in an approximately logarithmic fashion. Thus, equal dB increments are perceived by the ear as equal increments in sound.

Let  $P$  denote the power at some point of interest in a system. Let  $P_0$  denote the *reference* power level with respect to which the power  $P$  is compared. The number of decibels in the power ratio  $P/P_0$  is defined as  $10 \log_{10}(P/P_0)$ . For example, a power ratio of 2 approximately corresponds to 3 dB, and a power ratio of 10 exactly corresponds to 10 dB.

We may also express the signal power  $P$  itself in dB if we divide  $P$  by one watt or one milliwatt. In the first case, we express the signal power  $P$  in dBW as  $10 \log_{10}(P/1W)$ , where W is the abbreviation for watt. In the second case, we express the signal power  $P$  in dBm as  $10 \log_{10}(P/1mW)$ , where mW is the abbreviation for milliwatt.

<sup>1</sup>The unit, bel, is named in honor of Alexander Graham Bell. In addition to inventing the telephone, Bell was the first to use logarithmic power measurements in sound and hearing research.

## APPENDIX 2

# FOURIER SERIES

In this appendix, we review the formulation of the Fourier series and develop the Fourier transform as a generalization of the Fourier series.

Let  $g_{T_0}(t)$  denote a *periodic signal* with period  $T_0$ . By using a *Fourier series expansion* of this signal, we are able to resolve it into an infinite sum of sine and cosine terms. The expansion may be expressed in the trigonometric form:

$$g_{T_0}(t) = a_0 + 2 \sum_{n=1}^{\infty} [a_n \cos(2\pi n f_0 t) + b_n \sin(2\pi n f_0 t)] \quad (\text{A2.1})$$

where  $f_0$  is the *fundamental frequency*:

$$f_0 = \frac{1}{T_0} \quad (\text{A2.2})$$

The coefficients  $a_n$  and  $b_n$  represent the amplitudes of the cosine and sine terms, respectively. The quantity  $n f_0$  represents the  $n$ th harmonic of the fundamental frequency  $f_0$ . Each of the terms  $\cos(2\pi n f_0 t)$  and  $\sin(2\pi n f_0 t)$  is called a *basis function*. These basis functions form an *orthogonal* set over the interval  $T_0$  in that they satisfy the following set of relations:

$$\int_{-T_0/2}^{T_0/2} \cos(2\pi m f_0 t) \cos(2\pi n f_0 t) dt = \begin{cases} T_0/2, & m = n \\ 0, & m \neq n \end{cases} \quad (\text{A2.3})$$

$$\int_{-T_0/2}^{T_0/2} \cos(2\pi m f_0 t) \sin(2\pi n f_0 t) dt = 0, \quad \text{for all } m \text{ and } n \quad (\text{A2.4})$$

$$\int_{-T_0/2}^{T_0/2} \sin(2\pi m f_0 t) \sin(2\pi n f_0 t) dt = \begin{cases} T_0/2, & m = n \\ 0, & m \neq n \end{cases} \quad (\text{A2.5})$$

To determine the coefficient  $a_0$ , we integrate both sides of Eq. (A2.1) over a complete period. We thus find that  $a_0$  is the *mean value* of the periodic signal  $g_{T_0}(t)$  over one period, as shown by the *time average*

$$a_0 = \frac{1}{T_0} \int_{-T_0/2}^{T_0/2} g_{T_0}(t) dt \quad (\text{A2.6})$$

To determine the coefficient  $a_n$ , we multiply both sides of Eq. (A2.1) by  $\cos(2\pi n f_0 t)$  and integrate over the interval  $-T_0/2$  to  $T_0/2$ . Then, using Eqs. (A2.3) and (A2.4) we find that

$$a_n = \frac{1}{T_0} \int_{-T_0/2}^{T_0/2} g_{T_0}(t) \cos(2\pi n f_0 t) dt, \quad n = 1, 2, \dots \quad (\text{A2.7})$$

Similarly, we find that

$$b_n = \frac{1}{T_0} \int_{-T_0/2}^{T_0/2} g_{T_0}(t) \sin(2\pi n f_0 t) dt, \quad n = 1, 2, \dots \quad (\text{A2.8})$$

A basic question that arises at this point is the following: Given a periodic signal  $g_{T_0}(t)$  of period  $T_0$ , how do we know that the Fourier series expansion of Eq. (A2.1) is

*convergent* in that the infinite sum of terms in this expansion is exactly equal to  $g_{T_0}(t)$ ? To resolve this issue, we have to show that for the coefficients  $a_0$ ,  $a_n$ , and  $b_n$  calculated in accordance with Eqs. (A2.6) to (A2.8), this series will indeed converge to  $g_{T_0}(t)$ . In general, for a periodic signal  $g_{T_0}(t)$  of arbitrary waveform, there is no guarantee that the series of Eq. (A2.1) will converge to  $g_{T_0}(t)$  or that the coefficients  $a_0$ ,  $a_n$ , and  $b_n$  will even exist. A rigorous proof of convergence of the Fourier series is beyond the scope of this book. Here we simply state that a periodic signal  $g_{T_0}(t)$  can be expanded in a Fourier series if the signal  $g_{T_0}(t)$  satisfies the *Dirichlet conditions*.

1. The function  $g_{T_0}(t)$  is single-valued within the interval  $T_0$ .
2. The function  $g_{T_0}(t)$  has at most a finite number of discontinuities in the interval  $T_0$ .
3. The function  $g_{T_0}(t)$  has a finite number of maxima and minima in the interval  $T_0$ .
4. The function  $g_{T_0}(t)$  is absolutely integrable; that is,

$$\int_{-T_0/2}^{T_0/2} |g_{T_0}(t)| dt < \infty$$

The Dirichlet conditions are satisfied by the periodic signals usually encountered in communication systems. At a point of discontinuity, the Fourier series converges to the average value just to the left of the point and the value just to the right of the point.

### ■ COMPLEX EXPONENTIAL FOURIER SERIES

The Fourier series of Eq. (A2.1) can be put into a much simpler and more elegant form with the use of complex exponentials. We do this by substituting in Eq. (A2.1) the exponential forms for the cosine and sine, namely:

$$\cos(2\pi n f_0 t) = \frac{1}{2} [\exp(j2\pi n f_0 t) + \exp(-j2\pi n f_0 t)]$$

$$\sin(2\pi n f_0 t) = \frac{1}{2j} [\exp(j2\pi n f_0 t) - \exp(-j2\pi n f_0 t)]$$

We thus obtain

$$\begin{aligned} g_{T_0}(t) = a_0 + \sum_{n=1}^{\infty} [(a_n - jb_n) \exp(j2\pi n f_0 t) \\ + (a_n + jb_n) \exp(-j2\pi n f_0 t)] \end{aligned} \quad (\text{A2.9})$$

Let  $c_n$  denote a complex coefficient related to  $a_n$  and  $b_n$  by

$$c_n = \begin{cases} a_n - jb_n, & n > 0 \\ a_0, & n = 0 \\ a_n + jb_n, & n < 0 \end{cases} \quad (\text{A2.10})$$

Then, we may simplify Eq. (A2.9) as follows:

$$g_{T_0}(t) = \sum_{n=-\infty}^{\infty} c_n \exp(j2\pi n f_0 t) \quad (\text{A2.11})$$

where

$$c_n = \frac{1}{T_0} \int_{-T_0/2}^{T_0/2} g_{T_0}(t) \exp(-j2\pi n f_0 t) dt, \quad n = 0, \pm 1, \pm 2, \dots \quad (\text{A2.12})$$

The series expansion of Eq. (A2.11) is referred to as the *complex exponential Fourier series*. The  $c_n$  are called the *complex Fourier coefficients*. Equation (A2.12) states that, given a periodic signal  $g_{T_0}(t)$ , we may determine the complete set of complex Fourier coefficients. On the other hand, Eq. (A2.11) states that, given this set of coefficients, we may reconstruct the original periodic signal  $g_{T_0}(t)$  exactly. From the mathematics of real and complex analysis, Eq. (A2.12) is an *inner product* of the signal with the *basis functions*  $\exp(j2\pi n f_0 t)$ , by whose linear combination all square-integrable periodic functions can be expressed using Eq. (A2.11).

According to this representation, a periodic signal contains all frequencies (both positive and negative) that are harmonically related to the fundamental. The presence of negative frequencies is simply a result of the fact that the mathematical model of the signal as described by Eq. (A2.11) requires the use of negative frequencies. Indeed, this representation also requires the use of complex-valued basis functions—namely,  $\exp(j2\pi n f_0 t)$ —which have no physical meaning either. The reason for using complex-valued basis functions and negative frequency components is merely to provide a compact mathematical description of a periodic signal, which is well-suited for both theoretical and practical work.

### ■ DISCRETE SPECTRUM

The representation of a periodic signal by a Fourier series is equivalent to resolution of the signal into its various harmonic components. Thus, using the complex exponential Fourier series, we find that a periodic signal  $g_{T_0}(t)$  with period  $T_0$  has components at frequencies  $0, \pm f_0, \pm 2f_0, \pm 3f_0, \dots$ , and so forth, where  $f_0 = 1/T_0$  is the fundamental frequency. That is, while the signal  $g_{T_0}(t)$  exists in the time domain, we may say that its frequency-domain description consists of components at frequencies  $0, \pm f_0, \pm 2f_0, \dots$ , called the *spectrum*. If we specify the periodic signal  $g_{T_0}(t)$ , we can determine its spectrum; conversely, if we specify the spectrum, we can determine the corresponding signal. This means that a periodic signal  $g_{T_0}(t)$  can be specified in two equivalent ways:

1. A *time-domain representation*, where  $g_{T_0}(t)$  is defined as a function of time.
2. A *frequency-domain representation*, where the signal is defined in terms of its spectrum.

Although these two descriptions are separate aspects of a given phenomenon, they are not independent of each other, but are related, as Fourier theory shows.

In general, the Fourier coefficient  $c_n$  is a complex number, and so we may express it in the form:

$$c_n = |c_n| \exp[j \arg(c_n)] \quad (\text{A2.13})$$

The  $|c_n|$  defines the amplitude of the  $n$ th harmonic component of the periodic signal  $g_{T_0}(t)$ , so that a plot of  $|c_n|$  versus frequency yields the *discrete amplitude spectrum* of the signal. A plot of  $\arg(c_n)$  versus frequency yields the *discrete phase spectrum* of the signal. We refer to the spectrum as a *discrete spectrum* because both the amplitude and phase of  $c_n$  have nonzero values only for discrete frequencies that are integer (both positive and negative) multiples of the fundamental frequency.

For a real-valued periodic function  $g_{T_0}(t)$ , we find, from the definition of the Fourier coefficient  $c_n$  given by Eq. (A2.12), that

$$c_{-n} = c_n^* \quad (\text{A2.14})$$

where  $c_n^*$  is the complex conjugate of  $c_n$ . We therefore have

$$|c_{-n}| = |c_n| \quad (\text{A2.15})$$

and

$$\arg(c_{-n}) = -\arg(c_n) \quad (\text{A2.16})$$

That is, the amplitude spectrum of a real-valued periodic signal is symmetric (an even function of  $n$ ), and the phase spectrum is odd-isymmetric (an odd function of  $n$ ) about the vertical axis passing through the origin.

**EXAMPLE** Periodic Pulse Train

Consider a periodic train of rectangular pulses of duration  $T$  and period  $T_0$ , as shown in Fig. A2.1. For convenience of analysis, the origin has been chosen to coincide with the center of the pulse. This signal may be described analytically over one period, as follows:

$$g_{T_0}(t) = \begin{cases} A, & -\frac{T}{2} \leq t \leq \frac{T}{2} \\ 0, & \text{for the remainder of the period} \end{cases} \quad (\text{A2.17})$$

Using Eq. (A2.12) to evaluate the complex Fourier coefficient  $c_n$ , we get

$$\begin{aligned} c_n &= \frac{1}{T_0} \int_{-T/2}^{T/2} A \exp(-j2\pi n f_0 t) dt \\ &= \frac{A}{n\pi} \sin\left(\frac{n\pi T}{T_0}\right), \quad n = 0, \pm 1, \pm 2, \dots \end{aligned} \quad (\text{A2.18})$$

where  $T/T_0$  is termed the *duty cycle*.

We may simplify notation by using the *sinc function*:

$$\text{sinc}(\lambda) = \frac{\sin(\pi\lambda)}{\pi\lambda} \quad (\text{A2.19})$$

Thus, we may rewrite Eq. (A2.18) as follows:

$$c_n = \frac{TA}{T_0} \text{sinc}\left(\frac{nT}{T_0}\right) = \frac{TA}{T_0} \text{sinc}(f_n T) \quad (\text{A2.20})$$

In Fig. A2.2, we have plotted the amplitude spectrum  $|c_n|$  and phase spectrum  $\arg(c_n)$  versus the discrete frequency  $f_n = n/T_0$  for a duty cycle  $T/T_0$  equal to 0.2. Based on this figure, we may note the following:

1. The line spacing in the amplitude spectrum in Fig. A2.2(a) is determined by the period  $T_0$ .
2. The envelope of the amplitude spectrum is determined by the pulse amplitude  $A$ , pulse duration  $T$ , and duty cycle  $T/T_0$ .

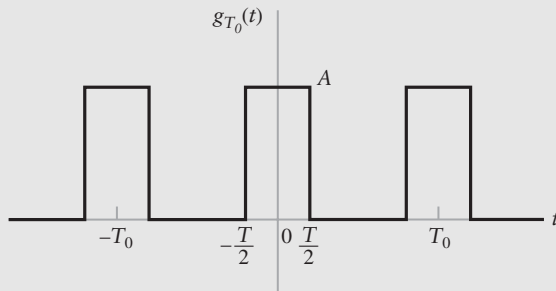


**FIGURE A2.1** Periodic train of rectangular pulses of amplitude  $A$ , duration  $T$ , and period  $T_0$ .

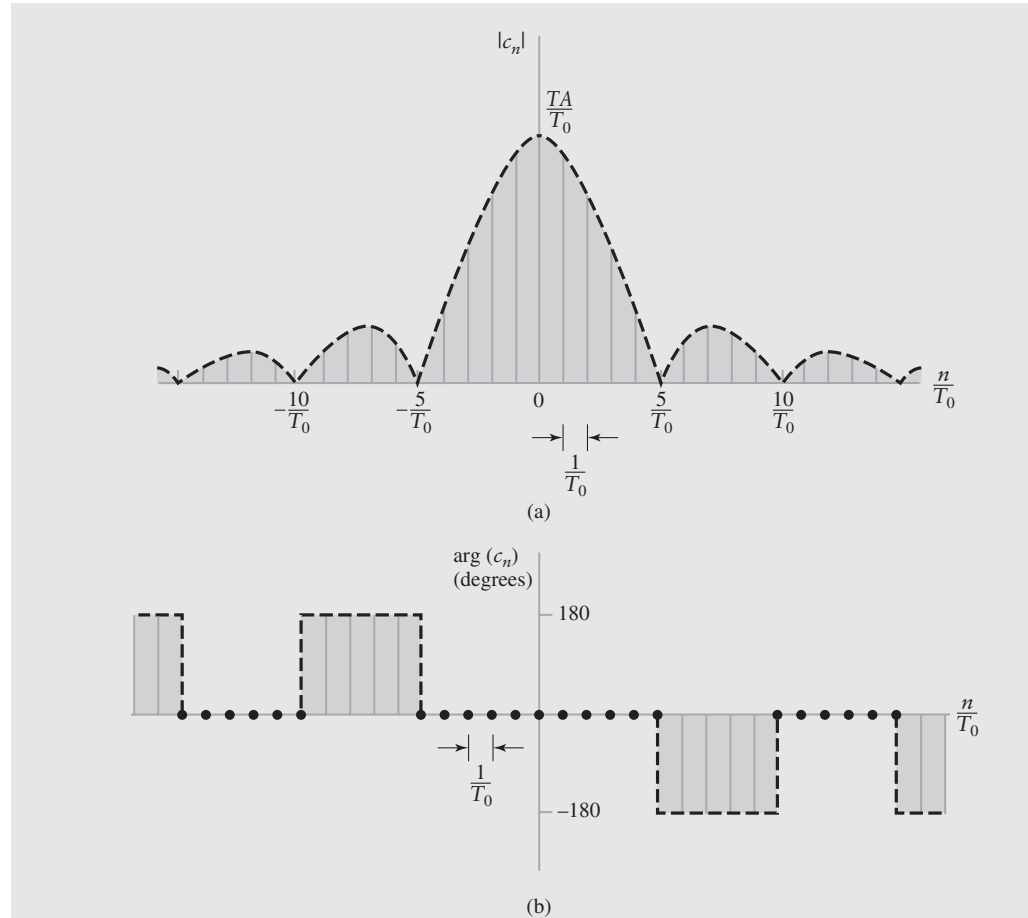


**FIGURE A2.2** Discrete spectrum of a periodic train of rectangular pulses for a duty cycle  $T/T_0 = 0.2$ . (a) Amplitude spectrum. (b) Phase spectrum.

3. Zero-crossings occur in the envelope of the amplitude spectrum at frequencies that are integer multiples of  $1/T$ .
4. The phase spectrum takes on the values 0 degrees and  $\pm 180$  degrees, depending on the polarity of  $\text{sinc}(nT/T_0)$ ; in Fig. A2.2(b) we have used both 180 degrees and  $-180$  degrees to preserve odd-symmetry.

## A2.1 Fourier Transform

In the previous section, we used the Fourier series to represent a periodic signal. We now wish to develop a similar representation for a signal  $g(t)$  that is nonperiodic in terms of complex exponential signals. In order to do this, we first construct a periodic function  $g_{T_0}(t)$  of period  $T_0$  in such a way that  $g(t)$  defines one cycle of this periodic function, as illustrated in Fig. A2.3. In the limit, we let the period  $T_0$  become infinitely large, so that we may write

$$g(t) = \lim_{T_0 \rightarrow \infty} g_{T_0}(t) \quad (\text{A2.21})$$

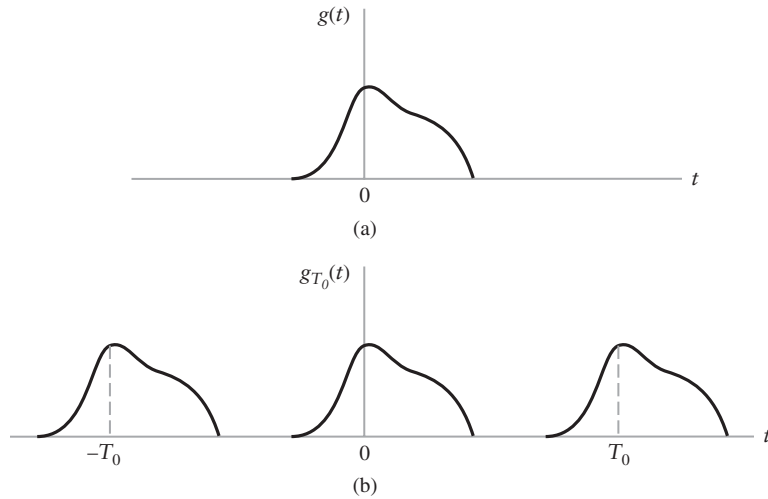


**FIGURE A2.3** Illustration of the use of an arbitrarily defined function of time to construct a periodic waveform. (a) Arbitrarily defined function of time  $g(t)$ . (b) Periodic waveform  $g_{T_0}(t)$  based on  $g(t)$ .

Representing the periodic function  $g_{T_0}(t)$  in terms of the complex exponential form of the Fourier series, we have

$$g_{T_0}(t) = \sum_{n=-\infty}^{\infty} c_n \exp\left(\frac{j2\pi nt}{T_0}\right) \quad (\text{A2.22})$$

where

$$c_n = \frac{1}{T_0} \int_{-T_0/2}^{T_0/2} g_{T_0}(t) \exp\left(-\frac{j2\pi nt}{T_0}\right) dt \quad (\text{A2.23})$$

We have purposely written the exponents as shown in Eqs. (A2.22) and (A2.23) because we wish to let  $T_0$  approach infinity in accordance with Eq. (A2.21). Define

$$\Delta f = \frac{1}{T_0} \quad (\text{A2.24})$$

$$f_n = \frac{n}{T_0} \quad (\text{A2.25})$$

and

$$G(f_n) = c_n T_0 \quad (\text{A2.26})$$

Thus, making this change of notation in the Fourier series representation of  $g_{T_0}(t)$  given in Eqs. (A2.22) and (A2.23), we get the following relations for the interval  $-T_0/2 \leq t \leq T_0/2$ :

$$g_{T_0}(t) = \sum_{n=-\infty}^{\infty} G(f_n) \exp(j2\pi f_n t) \Delta f \quad (\text{A2.27})$$

where

$$G(f_n) = \int_{-T_0/2}^{T_0/2} g_{T_0}(t) \exp(-j2\pi f_n t) dt \quad (\text{A2.28})$$

Now let the period  $T_0$  approach infinity or, equivalently, its reciprocal  $\Delta f$  approach zero. Then we find that, in the limit, the discrete frequency  $f_n$  approaches the continuous frequency variable  $f$ , and the discrete sum in Eq. (A2.27) becomes an integral defining the area under a continuous function of frequency  $f$ —namely,  $G(f) \exp(j2\pi ft)$ . Also, as  $T_0$  approaches infinity, the function  $g_{T_0}(t)$  approaches  $g(t)$ . Therefore, in the limit, Eqs. (A2.27) and (A2.28) become, respectively,

$$g(t) = \int_{-\infty}^{\infty} G(f) \exp(j2\pi ft) df \quad (A2.29)$$

where

$$G(f) = \int_{-\infty}^{\infty} g(t) \exp(-j2\pi ft) dt \quad (A2.30)$$

We have thus achieved our aim of representing an arbitrarily defined signal  $g(t)$  in terms of exponential functions over the entire interval ( $-\infty < t < \infty$ ). Given the function  $g(t)$ , Eq. (A2.30) defines the Fourier transform  $G(f)$ . Conversely, Eq. (A2.29) defines the inverse Fourier transform of  $G(f)$ .

## APPENDIX 3

# BESSEL FUNCTIONS

### A3.1 Series Solution of Bessel's Equation

In its most basic form, *Bessel's equation of order n* is written as

$$x^2 \frac{d^2y}{dx^2} + x \frac{dy}{dx} + (x^2 - n^2)y = 0 \quad (\text{A3.1})$$

which is one of the most important of all variable-coefficient differential equations. For each order  $n$ , a solution of this equation is defined by the power series

$$J_n(x) = \sum_{m=0}^{\infty} \frac{(-1)^m \left(\frac{1}{2}x\right)^{n+2m}}{m!(n+m)!} \quad (\text{A3.2})$$

The function  $J_n(x)$  is called a *Bessel function of the first kind of order n*. Equation (A3.1) has two coefficient functions—namely,  $1/x$  and  $(1 - n^2/x^2)$ . Hence, it has no finite singular points except the origin. It follows therefore that the series expansion of Eq. (A3.2) converges for all  $x > 0$ . Equation (A3.2) may thus be used to numerically calculate  $J_n(x)$  for  $n = 0, 1, 2, \dots$ . Table A3.1 presents values of  $J_n(x)$  for different orders  $n$  and varying  $x$ . It is of interest to note that the graphs of  $J_0(x)$  and  $J_1(x)$  resemble the graphs of  $\cos x$  and  $\sin x$ , respectively; see the graphs of Fig. 4.6 in Chapter 4.

**TABLE A3.1 Table of Bessel Functions<sup>a</sup>**

$n \setminus x$	$J_n(x)$									
	0.5	1	2	3	4	6	8	10	12	
0	0.9385	0.7652	0.2239	-0.2601	-0.3971	0.1506	0.1717	-0.2459	0.0477	
1	0.2423	0.4401	0.5767	0.3391	-0.0660	-0.2767	0.2346	0.0435	-0.2234	
2	0.0306	0.1149	0.3528	0.4861	0.3641	-0.2429	-0.1130	0.2546	-0.0849	
3	0.0026	0.0196	0.1289	0.3091	0.4302	0.1148	-0.2911	0.0584	0.1951	
4	0.0002	0.0025	0.0340	0.1320	0.2811	0.3576	-0.1054	-0.2196	0.1825	
5	—	0.0002	0.0070	0.0430	0.1321	0.3621	0.1858	-0.2341	-0.0735	
6		—	0.0012	0.0114	0.0491	0.2458	0.3376	-0.0145	-0.2437	
7			0.0002	0.0025	0.0152	0.1296	0.3206	0.2167	-0.1703	
8				0.0005	0.0040	0.0565	0.2235	0.3179	0.0451	
9					0.0001	0.0009	0.0212	0.1263	0.2919	0.2304
10					—	0.0002	0.0070	0.0608	0.2075	0.3005
11						—	0.0020	0.0256	0.1231	0.2704
12							0.0005	0.0096	0.0634	0.1953
13								0.0001	0.0033	0.0290
14									—	0.0120
										0.0650

<sup>a</sup>For more extensive tables of Bessel functions, see Abramowitz and Stegun (1965, pp. 358–406).

The function  $J_n(x)$  may also be expressed in the form of an integral as

$$J_n(x) = \frac{1}{\pi} \int_0^\pi \cos(x \sin \theta - n\theta) d\theta \quad (\text{A3.3})$$

or, equivalently, using complex notation, as

$$J_n(x) = \frac{1}{2\pi} \int_{-\pi}^{\pi} \exp(jx \sin \theta - jn\theta) d\theta \quad (\text{A3.4})$$

## A3.2 Properties of the Bessel Function

The Bessel function  $J_n(x)$  has certain properties:

**PROPERTY 1**

$$J_n(x) = (-1)^n J_{-n}(x) \quad (\text{A3.5})$$

To prove this relation, we replace  $\theta$  by  $(\pi - \theta)$  in Eq. (A3.3). Then, noting that  $\sin(\pi - \theta) = \sin \theta$ , we get

$$\begin{aligned} J_n(x) &= \frac{1}{\pi} \int_0^\pi \cos(x \sin \theta + n\theta - n\pi) d\theta \\ &= \frac{1}{\pi} \int_0^\pi [\cos(n\pi) \cos(x \sin \theta + n\theta) + \sin(n\pi) \sin(x \sin \theta + n\theta)] d\theta \end{aligned}$$

For integer values of  $n$ , we have

$$\begin{aligned} \cos(n\pi) &= (-1)^n \\ \sin(n\pi) &= 0 \end{aligned}$$

Therefore,

$$J_n(x) = \frac{(-1)^n}{\pi} \int_0^\pi \cos(x \sin \theta + n\theta) d\theta \quad (\text{A3.6})$$

From Eq. (A3.3), we also find that by replacing  $n$  with  $-n$ :

$$J_{-n}(x) = \frac{1}{\pi} \int_0^\pi \cos(x \sin \theta + n\theta) d\theta \quad (\text{A3.7})$$

The desired result follows immediately from Eq. (A3.6) and (A3.7).

**PROPERTY 2**

$$J_n(x) = (-1)^n J_n(-x) \quad (\text{A3.8})$$

This relation is obtained by replacing  $x$  with  $-x$  in Eq. (A3.3), and then using Eq. (A3.6).

**PROPERTY 3** *For small values of  $x$ , we have*

$$J_n(x) \simeq \frac{x^n}{2^n n!} \quad (\text{A3.9})$$

This relation is obtained simply by retaining the first term in the power series of Eq. (A3.2) and ignoring the higher order terms. Thus, when  $x$  is small, we have

$$\begin{aligned} J_0(x) &\simeq 1 \\ J_1(x) &\simeq \frac{x}{2} \end{aligned} \quad (\text{A3.10})$$

$$J_n(x) \simeq 0 \quad \text{for } n > 1$$

**PROPERTY 4**  $\sum_{n=-\infty}^{\infty} J_n^2(x) = 1 \quad \text{for all } x \quad (\text{A3.11})$

To prove this property, we proceed as follows. We observe that  $J_n(x)$  is real. Hence, multiplying Eq. (A3.4) by its own complex conjugate and summing over all possible values of  $n$ , we get

$$\sum_{n=-\infty}^{\infty} J_n^2(x) = \frac{1}{(2\pi)^2} \sum_{n=-\infty}^{\infty} \int_{-\pi}^{\pi} \int_{-\pi}^{\pi} \exp(jx \sin \theta - jn\theta - jx \sin \phi + jn\phi) d\theta d\phi$$

Interchanging the order of double integration and summation:

$$\sum_{n=-\infty}^{\infty} J_n^2(x) = \frac{1}{(2\pi)^2} \int_{-\pi}^{\pi} \int_{-\pi}^{\pi} d\theta d\phi \exp[jx(\sin \theta - \sin \phi)] \sum_{n=-\infty}^{\infty} \exp[jn(\phi - \theta)] \quad (\text{A3.12})$$

Using the following relation from Fourier transform theory for the delta function (see Chapter 2)

$$\delta(\phi) = \frac{1}{2\pi} \sum_{n=-\infty}^{\infty} \exp(jn\phi) \quad (\text{A3.13})$$

in Eq. (A3.12) and then applying the sifting property of the delta function, we finally get

$$\sum_{n=-\infty}^{\infty} J_n^2(x) = \frac{1}{2\pi} \int_{-\pi}^{\pi} d\theta = 1$$

which is the desired result.

The Bessel function  $J_n(x)$  has several other properties. However, insofar as the scope of this book is concerned, properties 1 through 4 discussed above are all that we need.

## APPENDIX 4

# THE $Q$ -FUNCTION AND ITS RELATIONSHIP TO THE ERROR FUNCTION

### A4.1 *The Q-function*

Consider a *normalized Gaussian* random variable  $u$  of zero mean and unit variance. The probability that an observed value of  $u$  is greater than  $x$  defines the *Q-function*

$$Q(x) = \frac{1}{\sqrt{2\pi}} \int_x^\infty \exp\left(-\frac{u^2}{2}\right) du, \quad x \geq 0 \quad (\text{A4.1})$$

In words, *the Q-function equals the area under the positive tail of the zero-mean, unit-variance Gaussian density function.*

From the defining equation (A4.1), the following properties of the  $Q$ -function follow:

**PROPERTY 1** For  $x = 0$ , we have the exact value

$$Q(0) = \frac{1}{2} \quad (\text{A4.2})$$

**PROPERTY 2** For  $x < 0$ , the corresponding value of the  $Q$ -function is given by the relationship

$$Q(x) = 1 - Q(|x|) \quad (\text{A4.3})$$

**PROPERTY 3** A useful bound on the  $Q$ -function is given by

$$Q(x) \leq \frac{1}{2} \exp\left(-\frac{1}{2}x^2\right), \quad x \geq 0 \quad (\text{A4.4})$$

Table A4.1 gives a short tabulation of the values of  $Q(x)$  for  $0 \leq x \leq 5$ . The properties described in Eqs. (A4.2) through (A4.4) are confirmed by examining the entries of this table.

The values of the  $Q$ -function listed in this table for  $0 \leq x \leq 3.7$  have been rounded to 5 significant decimal places; for  $3.8 \leq x \leq 5$ , we have done the rounding to 7 decimal places.

**TABLE A4.1** Table of the values of  $Q$ -function<sup>a</sup>

$x$	$Q(x)$	$x$	$Q(x)$
0.0	0.50000	2.2	0.01390
0.1	0.46017	2.3	0.01072
0.2	0.42074	2.4	0.00820
0.3	0.38209	2.5	0.00621
0.4	0.34458	2.6	0.00466
0.5	0.30854	2.7	0.00347
0.6	0.27425	2.8	0.00256
0.7	0.24196	2.9	0.00187
0.8	0.21186	3.0	0.00135
0.9	0.18406	3.1	0.00097
1.0	0.15866	3.2	0.00069
1.1	0.13567	3.3	0.00048
1.2	0.11507	3.4	0.00034
1.3	0.09680	3.5	0.00023
1.4	0.08076	3.6	0.00016
1.5	0.06681	3.7	0.00011
1.6	0.05480	3.8	$7.24 \times 10^{-5}$
1.7	0.04457	3.9	$4.81 \times 10^{-5}$
1.8	0.03593	4.0	$3.17 \times 10^{-5}$
1.9	0.02872	4.30	$0.85 \times 10^{-5}$
2.0	0.02275	4.65	$0.17 \times 10^{-5}$
2.1	0.01786	5.00	$0.03 \times 10^{-5}$

<sup>a</sup>Table A4.1 is adapted from Abramowitz and Stegun (1964), pp. 966–972. This handbook tabulates the Gaussian (normal) probability density function

## A4.2 Relationship of the $Q$ -function to the Complementary Error Function

The  $Q$ -function was introduced in Chapter 8 of the book and its use in evaluating the effect of noise in digital communications was discussed in Chapter 10. In the literature, we often find that this effect is formulated in terms of another function — namely, the complementary error function.

In this context, we first define the *error function* as

$$\text{erf}(x) = \frac{2}{\sqrt{\pi}} \int_0^x \exp(-u^2) du \quad (\text{A4.5})$$

The error function has two useful properties

$$\text{PROPERTY 1} \quad \text{erf}(-x) = -\text{erf}(x) \quad (\text{A4.6})$$

This property is known as the *symmetry relation*.

$$\text{PROPERTY 2} \quad \frac{2}{\sqrt{\pi}} \int_0^\infty \exp(-u^2) du = 1 \quad (\text{A4.7})$$

A related function, called the *complementary error function*, is defined by

$$\begin{aligned}\operatorname{erfc}(x) &= \frac{2}{\sqrt{\pi}} \int_x^{\infty} \exp(-u^2) du \\ &= 1 - \operatorname{erf}(x)\end{aligned}\quad (\text{A4.8})$$

Examining Eqs. (A4.1) and first line of Eq. (A4.8), we readily find that the  $Q$ -function and complementary error function as related as follows:

$$Q(x) = \frac{1}{2} \operatorname{erfc}\left(\frac{x}{\sqrt{2}}\right) \quad (\text{A4.9})$$

The inverse of this relationship is given by

$$\operatorname{erfc}(x) = 2Q(\sqrt{2}x) \quad (\text{A4.10})$$

Hence, given the  $Q$ -function, we may use Eq. (A 4.10) to calculate the corresponding value of the complementary error function for prescribed  $x$ . Conversely, given the complementary error function, we may calculate the corresponding  $Q$ -function using Eq. (A4.9).

## APPENDIX 5

# SCHWARZ'S INEQUALITY

Let  $g_1(t)$  and  $g_2(t)$  be functions of the real variable  $t$  in the interval  $a \leq t \leq b$ . We assume that  $g_1(t)$  and  $g_2(t)$  satisfy the conditions

$$\int_a^b |g_1(t)|^2 dt < \infty \quad (\text{A5.1})$$

$$\int_a^b |g_2(t)|^2 dt < \infty \quad (\text{A5.2})$$

Then, according to *Schwarz's inequality*, we have

$$\left| \int_a^b g_1(t)g_2(t) dt \right|^2 \leq \int_a^b |g_1(t)|^2 dt \int_a^b |g_2(t)|^2 dt \quad (\text{A5.3})$$

To prove this inequality, we first form the integral

$$\int_a^b [\lambda g_1^*(t) + g_2^*(t)][\lambda g_1(t) + g_2(t)] dt = \lambda^2 A + \lambda(B + B^*) + C \quad (\text{A5.4})$$

where  $\lambda$  is a real variable, the asterisk signifies complex conjugation, and

$$A = \int_a^b |g_1(t)|^2 dt \geq 0 \quad (\text{A5.5})$$

$$B = \int_a^b g_1^*(t)g_2(t) dt \quad (\text{A5.6})$$

$$C = \int_a^b |g_2(t)|^2 dt \geq 0 \quad (\text{A5.7})$$

The integral of Eq. (A5.4) exists, is real, and is a nonnegative function of  $\lambda$ , say  $f(\lambda)$ . Since  $f(\lambda)$  is nonnegative, it must have no real roots except possibly a double root. From the quadratic formula, we must then have

$$(B + B^*)^2 \leq 4AC \quad (\text{A5.8})$$

Note that  $(B + B^*)/2$  is equal to the real part of  $B$ . On substituting Eqs. (A5.5) to (A5.7) into (A5.8), we get

$$\left\{ \int_a^b [g_1^*(t)g_2(t) + g_1(t)g_2^*(t)] dt \right\}^2 \leq 4 \int_a^b |g_1(t)|^2 dt \int_a^b |g_2(t)|^2 dt \quad (\text{A5.9})$$

This is the most general form of Schwarz's inequality that is appropriate for complex functions  $g_1(t)$  and  $g_2(t)$ . For the case when both  $g_1(t)$  and  $g_2(t)$  are real, we have

$$g_1^*(t)g_2(t) + g_1(t)g_2^*(t) = 2g_1(t)g_2(t) \quad (\text{A5.10})$$

and Eq. (A5.3) follows immediately.

Note that equality is obtained [aside from the trivial case where both  $g_1(t)$  and  $g_2(t)$  are zero] when the double root exists in Eq. (A5.4); that is, when

$$\lambda g_1(t) + g_2(t) = \lambda g_1^*(t) + g_2^*(t) = 0 \quad (\text{A5.11})$$

Since  $\lambda$  is real,  $g_1(t)$  and  $g_2(t)$  are linearly related. Looking at the problem from a slightly different viewpoint, we see that there is a real value of  $\lambda$  for which Eq. (A5.4) is zero and for which its first derivative with respect to  $\lambda$  vanishes; that is,

$$2\lambda A + (B + B^*) = 0 \quad (\text{A5.12})$$

or

$$\lambda = -\frac{B + B^*}{2A} = -\frac{\int_a^b [g_1^*(t)g_2(t) + g_1(t)g_2^*(t)] dt}{2 \int_a^b |g_1(t)|^2 dt} \quad (\text{A5.13})$$

This relation holds if, and only if,

$$g_2(t) = -\lambda g_1(t) \quad (\text{A5.14})$$

This last relationship is equivalent to Eq. (A5.11).

## APPENDIX 6

# MATHEMATICAL TABLES

This appendix presents tabulations of (1) Fourier-transform theorems, (2) Fourier-transform pairs, (3) Hilbert-transform pairs, (4) trigonometric identities, (5) series expansions, (6) indefinite and definite integrals, (7) summations, (8) useful constants, and (9) recommended unit prefixes.

**TABLE A6.1 Fourier-Transform Theorems**

Property	Mathematical Description
1. Linearity	$ag_1(t) + bg_2(t) \rightleftharpoons aG_1(f) + bG_2(f)$ where $a$ and $b$ are constants
2. Dilation (time scaling)	$g(at) \rightleftharpoons \frac{1}{ a } G\left(\frac{f}{a}\right)$ where $a$ is a constant
3. Duality	If $\quad g(t) \rightleftharpoons G(f),$ then $\quad G(t) \rightleftharpoons g(-f)$
4. Time shifting	$g(t - t_0) \rightleftharpoons G(f) \exp(-j2\pi f t_0)$
5. Frequency shifting	$\exp(j2\pi f_c t)g(t) \rightleftharpoons G(f - f_c)$
6. Area under $g(t)$	$\int_{-\infty}^{\infty} g(t) dt = G(0)$
7. Area under $G(f)$	$g(0) = \int_{-\infty}^{\infty} G(f) df$
8. Differentiation in the time domain	$\frac{d}{dt}g(t) \rightleftharpoons j2\pi f G(f)$
9. Integration in the time domain	$\int_{-\infty}^t g(\tau) d\tau \rightleftharpoons \frac{1}{j2\pi f} G(f) + \frac{G(0)}{2} \delta(f)$
10. Conjugate functions	If $\quad g(t) \rightleftharpoons G(f),$ then $\quad g^*(t) \rightleftharpoons G^*(-f),$
11. Multiplication in the time domain	$g_1(t)g_2(t) \rightleftharpoons \int_{-\infty}^{\infty} G_1(\lambda)G_2(f - \lambda) d\lambda$
12. Convolution in the time domain	$\int_{-\infty}^{\infty} g_1(\tau)g_2(t - \tau) d\tau \rightleftharpoons G_1(f)G_2(f)$
13. Correlation theorem	$\int_{-\infty}^{\infty} g_1(t)g_2^*(t - \tau) dt \rightleftharpoons G_1(f)G_2^*(f)$
14. Rayleigh's energy theorem	$\int_{-\infty}^{\infty}  g(t) ^2 dt = \int_{-\infty}^{\infty}  G(f) ^2 df$

**TABLE A6.2 Fourier-Transform Pairs**

Time Function	Fourier Transform
$\text{rect}\left(\frac{t}{T}\right)$	$T \text{sinc}(fT)$
$\text{sinc}(2Wt)$	$\frac{1}{2W} \text{rect}\left(\frac{f}{2W}\right)$
$\exp(-at)u(t), \quad a > 0$	$\frac{1}{a + j2\pi f}$
$\exp(-a t ), \quad a > 0$	$\frac{2a}{a^2 + (2\pi f)^2}$
$\exp(-\pi t^2)$	$\exp(-\pi f^2)$
$\begin{cases} 1 - \frac{ t }{T}, &  t  < T \\ 0, &  t  \geq T \end{cases}$	$T \text{sinc}^2(fT)$
$\delta(t)$	1
1	$\delta(f)$
$\delta(t - t_0)$	$\exp(-j2\pi f t_0)$
$\exp(j2\pi f_c t)$	$\delta(f - f_c)$
$\cos(2\pi f_c t)$	$\frac{1}{2}[\delta(f - f_c) + \delta(f + f_c)]$
$\sin(2\pi f_c t)$	$\frac{1}{2j}[\delta(f - f_c) - \delta(f + f_c)]$
$\text{sgn}(t)$	$\frac{1}{j\pi f}$
$\frac{1}{\pi t}$	$-j \text{sgn}(f)$
$u(t)$	$\frac{1}{2}\delta(f) + \frac{1}{j2\pi f}$
$\sum_{i=-\infty}^{\infty} \delta(t - iT_0)$	$\frac{1}{T_0} \sum_{n=-\infty}^{\infty} \delta\left(f - \frac{n}{T_0}\right)$

Notes:  $u(t)$  = unit step function

$\delta(t)$  = Dirac delta function

$\text{rect}(t)$  = rectangular function

$\text{sgn}(t)$  = signum function

$\text{sinc}(t)$  = sinc function

**TABLE A6.3 Hilbert-Transform Pairs<sup>a</sup>**

Time Function	Hilbert Transform
$m(t) \cos(2\pi f_c t)$	$m(t) \sin(2\pi f_c t)$
$m(t) \sin(2\pi f_c t)$	$-m(t) \cos(2\pi f_c t)$
$\cos(2\pi f_c t)$	$\sin(2\pi f_c t)$
$\sin(2\pi f_c t)$	$-\cos(2\pi f_c t)$
$\delta(t)$	$\frac{1}{\pi t}$
$\frac{1}{t}$	$-\pi\delta(t)$

<sup>a</sup>In the first two pairs, it is assumed that  $m(t)$  is band limited to the interval  $-W \leq f \leq W$ , where  $W < f_c$ .

**TABLE A6.4 Trigonometric Identities**


---

$\exp(\pm j\theta) = \cos \theta \pm j \sin \theta$
$\cos \theta = \frac{1}{2}[\exp(j\theta) + \exp(-j\theta)]$
$\sin \theta = \frac{1}{2j}[\exp(j\theta) - \exp(-j\theta)]$
$\sin^2 \theta + \cos^2 \theta = 1$
$\cos^2 \theta - \sin^2 \theta = \cos(2\theta)$
$\cos^2 \theta = \frac{1}{2}[1 + \cos(2\theta)]$
$\sin^2 \theta = \frac{1}{2}[1 - \cos(2\theta)]$
$2 \sin \theta \cos \theta = \sin(2\theta)$
$\sin(\alpha \pm \beta) = \sin \alpha \cos \beta \pm \cos \alpha \sin \beta$
$\cos(\alpha \pm \beta) = \cos \alpha \cos \beta \mp \sin \alpha \sin \beta$
$\tan(\alpha \pm \beta) = \frac{\tan \alpha \pm \tan \beta}{1 \mp \tan \alpha \tan \beta}$
$\sin \alpha \sin \beta = \frac{1}{2}[\cos(\alpha - \beta) - \cos(\alpha + \beta)]$
$\cos \alpha \cos \beta = \frac{1}{2}[\cos(\alpha - \beta) + \cos(\alpha + \beta)]$
$\sin \alpha \cos \beta = \frac{1}{2}[\sin(\alpha - \beta) + \sin(\alpha + \beta)]$

---

**TABLE A6.5 Series Expansions**


---

Taylor series	$f(x) = f(a) + \frac{f'(a)}{1!}(x - a) + \frac{f''(a)}{2!}(x - a)^2 + \cdots + \frac{f^{(n)}(a)}{n!}(x - a)^n + \cdots$
where	$f^{(n)}(a) = \frac{d^n f(x)}{dx^n} \Big _{x=a}$
MacLaurin series	$f(x) = f(0) + \frac{f'(0)}{1!}x + \frac{f''(0)}{2!}x^2 + \cdots + \frac{f^{(n)}(0)}{n!}x^n + \cdots$
where	$f^{(n)}(0) = \frac{d^n f(x)}{dx^n} \Big _{x=0}$
Binomial series	$(1 + x)^n = 1 + nx + \frac{n(n-1)}{2!}x^2 + \cdots, \quad  nx  < 1$
Exponential series	$\exp x = 1 + x + \frac{1}{2!}x^2 + \cdots$
Logarithmic series	$\ln(1 + x) = x - \frac{1}{2}x^2 + \frac{1}{3}x^3 - \cdots$
Trigonometric series	$\sin x = x - \frac{1}{3!}x^3 + \frac{1}{5!}x^5 - \cdots$ $\cos x = 1 - \frac{1}{2!}x^2 + \frac{1}{4!}x^4 - \cdots$ $\tan x = x + \frac{1}{3}x^3 + \frac{2}{15}x^5 + \cdots$ $\sin^{-1} x = x + \frac{1}{6}x^3 + \frac{3}{40}x^5 + \cdots$ $\tan^{-1} x = x - \frac{1}{3}x^3 + \frac{1}{5}x^5 - \cdots, \quad  x  < 1$ $\text{sinc } x = 1 - \frac{1}{3!}(\pi x)^2 + \frac{1}{5!}(\pi x)^4 - \cdots$

---

**TABLE A6.6 Integrals***Indefinite integrals*

$\int x \sin(ax) dx = \frac{1}{a^2} [\sin(ax) - ax \cos(ax)]$
$\int x \cos(ax) dx = \frac{1}{a^2} [\cos(ax) + ax \sin(ax)]$
$\int x \exp(ax) dx = \frac{1}{a^2} \exp(ax)(ax - 1)$
$\int x \exp(ax^2) dx = \frac{1}{2a} \exp(ax^2)$
$\int \exp(ax) \sin(bx) dx = \frac{1}{a^2 + b^2} \exp(ax)[a \sin(bx) - b \cos(bx)]$
$\int \exp(ax) \cos(bx) dx = \frac{1}{a^2 + b^2} \exp(ax)[a \cos(bx) + b \sin(bx)]$
$\int \frac{dx}{a^2 + b^2 x^2} = \frac{1}{ab} \tan^{-1}\left(\frac{bx}{a}\right)$
$\int \frac{x^2 dx}{a^2 + b^2 x^2} = \frac{x}{b^2} - \frac{a}{b^3} \tan^{-1}\left(\frac{bx}{a}\right)$

*Definite integrals*

$\int_0^\infty \frac{x \sin(ax)}{b^2 + x^2} dx = \frac{\pi}{2} \exp(-ab), \quad a > 0, b > 0$
$\int_0^\infty \frac{\cos(ax)}{b^2 + x^2} dx = \frac{\pi}{2b} \exp(-ab), \quad a > 0, b > 0$
$\int_0^\infty \frac{\cos(ax)}{(b^2 - x^2)^2} dx = \frac{\pi}{4b^3} [\sin(ab) - ab \cos(ab)], \quad a > 0, b > 0$
$\int_0^\infty \text{sinc } x dx = \int_0^\infty \text{sinc}^2 x dx = \frac{1}{2}$
$\int_0^\infty \exp(-ax^2) dx = \frac{1}{2} \sqrt{\frac{\pi}{a}}, \quad a > 0$
$\int_0^\infty x^2 \exp(-ax^2) dx = \frac{1}{4a} \sqrt{\frac{\pi}{a}}, \quad a > 0$

**TABLE A6.7 Summations**

$\sum_{k=1}^K k = \frac{K(K + 1)}{2}$
$\sum_{k=1}^K k^2 = \frac{K(K + 1)(2K + 1)}{6}$
$\sum_{k=1}^K k^3 = \frac{K^2(K + 1)^2}{4}$
$\sum_{k=0}^{K-1} x^k = \frac{(x^K - 1)}{x - 1}$

**TABLE A6.8 Useful Constants***Physical Constants*

Boltzmann's constant	$k = 1.38 \times 10^{-23}$ joule/Kelvin
Planck's constant	$h = 6.626 \times 10^{-34}$ joule-second
Electron (fundamental) charge	$q = 1.602 \times 10^{-19}$ coulomb
Speed of light in vacuum	$c = 2.998 \times 10^8$ meters/second
Standard (absolute) temperature	$T_0 = 273$ Kelvin
Thermal voltage	$V_T = 0.026$ volt at room temperature
Thermal energy $kT$ at standard temperature	$kT_0 = 3.77 \times 10^{-21}$ joule
One hertz (Hz) = 1 cycle/second; 1 cycle = $2\pi$ radians	
One watt (W) = 1 joule/second	

*Mathematical Constants*

Base of natural logarithm	$e = 2.7182818$
Logarithm of $e$ to base 2	$\log_2 e = 1.442695$
Logarithm of 2 to base $e$	$\ln 2 = \log_e 2 = 0.693147$
Logarithm of 2 to base 10	$\log_{10} 2 = 0.30103$
Pi	$\pi = 3.1415927$

**TABLE A6.9 Recommended Unit Prefixes**

Multiples and Submultiples	Prefixes	Symbols
$10^{12}$	tera	T
$10^9$	giga	G
$10^6$	mega	M
$10^3$	kilo	K (k)
$10^{-3}$	milli	m
$10^{-6}$	micro	$\mu$
$10^{-9}$	nano	n
$10^{-12}$	pico	p

## APPENDIX 7

# MATLAB SCRIPTS FOR COMPUTER EXPERIMENTS TO PROBLEMS IN CHAPTERS 7–10

### **Problem 7.30**

```
%-----
% Script for Problem 7.30(a).
% Modify this script for 7.30(b)
%-----
Fs      = 32;      % (Hz) Sample rate (samples per symbol)
fc      = 10;      % (Hz) Carrier frequency
Nbits   = 5000;    % Number of bits in sequence
PulseShape = ones(1,Fs); % rectangular pulse shape

%--- Generate two random sequences -----
bI      = sign(rand(1,Nbits)-0.5);
bQ      = sign(rand(1,Nbits)-0.5);

%--- Create impulse train -----
bI_t    = [1 zeros(1,Fs-1)]' * bI;
bI_t    = bI_t(:);
bQ_t    = [1 zeros(1,Fs-1)]' * bQ;
bQ_t    = bQ_t(:);

%--- Pulse shape and create bandpass signal -----
bIp     = filter(PulseShape, 1, bI_t);
bQp     = filter(PulseShape, 1, bI_t);

t = [1:length(bIp)]' / Fs; % time scale for bandpass signal
s = bIp .* cos(2*pi*fc*t) - bQp .* sin(2*pi*fc*t);

%---- Display results -----
subplot(2,1,1), plot(t,s);      % time display
ylabel('Amplitude'). xlabel('Time (s)'). axis([0, 50, -2, 2])

nFFT = 2*256;          %frequency display
[spcc,freq] = spectrum(s,nFFT,nFFT/4,nFFT/2,Fs);
subplot(2,1,2). plot(freq, 10*log10(spec(:,l)/sqrt(nFFT)) )
ylabel('Spectrum (dB)'), xlabel('Frequency (Hz)'), axis([0, 16, -40, 10])
```

**Problem 7.31**

```
%-----  
% Modify the script for Problem 7.30 to use the following  
% raised cosine pulse shape  
% Uses offset time scale to avoid divide by zero  
%-----  
B0      = 0.5;                      % (Hz)  
t       = [-2.001: 1/Fs : + 2.001]    % offset time scale for pulse shape  
rcos    = sinc(4*B0*t) ./ (1-16*B0^2*t.^2); %from Eq.(6.20)  
PulseShape = rcos;
```

**Problem 8.54**

```
%-----  
% Probability distribution with loaded die  
%-----  
function a=Problem8_54;  
N = 1000  
  
for i=1:N  
    X(i) = LoadedDie;  
end  
[F,X] = hist(X,[1:6]);  % plot histogram of results  
stem(X,F);  
  
function b = LoadedDie  
% generate non-uniform distribution over 1..6  
b = floor(6*rand(1,1)^3) + 1;
```

**Problem 8.55**

```
%-----
% Probability distribution of five uniform variates
%-----

N      = 5;          % number of uniform r.v.s to sum
nSmpls = 20000;      % number of samples to generate

%---- Generate samples of uniform random variable -----
Y      = 2*rand(N,nSmpls)- 1;    % uniform r.v. over [-1,+1]
cSmpls = sum(Y);

%---- Compute histogram and plot -----
[N1,X] = hist(cSmpls,40); % histogram with 40 bins
Delta   = X(2)- X(1);
plot(X, N1/nSmpls/Delta); % normalize plot

%---- compare to theory -----
hold on
x      = [-5:0.01:5]
sigma2 = N*(1/3);      % variance of one uniform is 1/3
Gauss  = exp(-x.^2/2/sigma2) / sqrt(2*pi*sigma2);
plot(x,Gauss,'r');
hold off
```

**Problem 8.58**

```
N = 100000;      %---- number of samples
x = randn(1,N); %---- generate Gaussian sequence

%---- approximation to pulse shape of root raised cosine filter pulse
%   with 50% rolloff (cutoff at 1/8 of sampling rate)
rrc = [ 0.0015 -0.0082 -0.0075  0.0077  0.0212  0.0077 ...
        -0.0375 -0.0784 -0.0531  0.0784  0.2894  0.4873 ...
        0.5684  0.4873  0.2894  0.0784 -0.0531 -0.0784 ...
        -0.0375  0.0077  0.0212  0.0077 -0.0075 -0.0082...
        0.0015];
z = filter(rrc,1,x);      %---- filter random process
[P,F] = spectrum(z,256,0,Hanning(256),Fs); % compute spectrum and plot
plot(F,P(:,1));
figure(2);
Az = xcorr(z,25);         %---- compute the autocorrelation for 25 lags
plot(Az/max(abs(Az)));   %---- plot the normalized autocorrelation
grid
```

**Problem 9.26**

```

Fs = 1000 ; % sampling rate
fc = 100; % carrier frequency
%-----
% Bandpass filter - 6th order Chebychev 1
% Passband from 50 to 150 Hz
%-----
Bt = 100; % Bandpass bandwidth
b = [ 1 0 -3 0 3 0 -1];
a = [ 1.0000 -4.3705 8.6828 -10.0000 7.0486 -2.8825 0.5398];
G = 0.0115;
%-----
SNRdB = 30;
ka = 0.3;
t = [0:1/Fs:2];
A = sqrt(2); % for unity power carrier.
sigma2 = (1+ka^2*0.5) * 10^(-SNRdB/10) * (Fs/2)/Bt;
sigma = sqrt(sigma2);
m = sin(2*pi*2*t);

%---- Modulator -----
c = cos(2*pi*fc*t);
AM = A*(1+ka*m).*c;

%---- Add noise -----
AMn = AM + sigma * randn(size(AM));

%---- Bandpass filter -----
RxAMn = G*filter(b,a,AMn);
RxAM = G*filter(b,a,AM); % noise free

%---- Pre-detection SNR -----
C_N = 10*log10(sum(RxAM.^2)/sum((RxAMn-RxAM).^2))

%---- Envelope detector -----
BB_sig = EnvelopeDetector(RxAM); % clean baseband signal
BB_sign = EnvelopeDetector(RxAMn); % noisy baseband signal

%---- Compute post-detection SNR -----
error = sum((BB_sig - BB_sign).^2);
C = sum(BB_sig.^2);
SNRdBpost = 10*log10(C/error)

%---- plot output -----
figure(1);
plot(t, BB_sig); xlabel('Time (s)'), ylabel('Amplitude')
hold on, plot(t, BB_sign,'g'), hold off

% see Miscellaneous for description of Envelope Detector

```

## Problem 9.27

```

CNdB = [3:1:22]; % pre-detection SNR
Fs = 500; % sampling rate (Hz)
t = [0: (1/Fs) : 500-1/Fs]; % sample times for signal

%---- FM Modulator -----
A = 1;
kf = 20.0; % FM sensitivity
fm = 1; % frequency of modulating tone (Hz)
m = sin(2*pi*fm*t); % message signal
Int_m = cos(2*pi*fm*t) /2/pi; % integrated message
FM = A*exp(j*2*pi*kf*Int_m); % phasor representation

for i=1:length(CNdB)
    %---- Generate bandlimited baseband noise ----
    Noise = LowPassNoise(CNdB(i), length(FM));

    %---- Generate carrier -----
    fc = Fs/10; % carrier frequency for demodulation
    Carrier = exp(j*2*pi*fc * [1:length(FM)]/Fs );

    %---- Upconvert and demodulate -----
    Noisy_message = FMdiscriminator( (FM+Noise) .* Carrier, Fs);
    Clean_message = FMdiscriminator( (FM) .* Carrier, Fs);

    PreSNR(i) = 20*log10(std(FM)/std(Noise));
    %---- Compute Post-detection SNR -----
    Noise_power = sum((Noisy_message - Clean_message).^2);
    Signal_power = sum(Clean_message.^2);
    SNRdB(i) = 10*log10(Signal_power/Noise_power);

    W = 5.5; % noise bandwidth of lowpass filter used in discriminator
    Bt = Fs/8; % transmission bandwidth
    Theory(i) = 10*log10( 3*A^2*kf^2*0.5 / (2*(std(Noise)^2/Bt)*W^3));

    [CNdB(i) SNRdB(i) Theory(i)]
end

%---- plot results -----
plot(PreSNR, SNRdB)
hold on, plot(PreSNR, Theory,'g'), hold off
grid on, xlabel ('C/N (dB)'), ylabel ('Post-detection SNR (dB)')

% see Miscellaneous for description of FMdiscriminator

```

**Problem 10.30**

```

Eb_N0 = 2;
Nbts = 10000; % number of bits, increase for higher Eb/N0
Fs = 4; % number of samples per bit
b = sign(randn(1,Nbts)); % random data
pulse = ones(1,Fs);
Eb = sum(pulse.^2);
N0 = Eb / Eb_N0;
%---- perform rectangular pulse shaping ----
S = pulse' * b;
S = S(:);
plot(S(1:100));
[P,F] = spectrum(S,256,0,Hanning(256),Fs);
plot(F,P(:,1));
%---- add Gaussian noise ----
Noise = sqrt(N0/2)*randn(size(S));
R = S + Noise;

%---- integrate and dump ----
D = sum(reshape(R,Fs,Nbts));
D = sign(D); % make bit decision
%---- count errors -----
Nerrs = (Nbts - sum(D.*b))/2;
BER = Nerrs/Nbts

```

**Problem 10.31**

```

Eb_N0 = 2;
Nbts = 10000; % number of bits to simulate
Fs = 4; % number of samples per bit
b = sign(randn(1,Nbts)); % random data

%---- root raised cosine pulse shape: 100% rolloff ----
pulse = [ 0.0064 0.0000 -0.0101 0.0000 0.0182 -0.0000 -0.0424 ...
          0.0000 0.2122 0.5000 0.6367 0.5000 0.2122 -0.0000 ...
          -0.0424 0.0000 0.0182 -0.0000 -0.0101 0.0000 0.0064 ];
Delay = length(pulse);
Eb = sum(pulse.^2);
N0 = Eb / Eb_N0;

%---- perform root raised cosine pulse shaping ----
b_delta = [1 zeros(1,Fs-1)]' * b; % make b into a stream of delta functions
b_delta = b_delta(:)';
S = filter(pulse,1,[b_delta zeros(1,Delay)]); % add zeros for delay of filter

%---- add Gaussian noise ----
Noise = sqrt(N0/2)*randn(size(S));
R = S + Noise;

```

```
%---- match filter detection -----
De = filter(pulse,1,R);
D = sign(De(Delay:Fs:end)); % sample output at proper instant
D = D(1:Nbits)';
%---- count errors -----
Nerrs = (Nbts - sum(D.*b))/2;
BER = Nerrs/Nbts

%---- plot eye diagram -----
ploteye(De(Delay:end), Fs)
```

## Miscellaneous

```
function BB_sig = EnvelopeDetector(AM_sig);
%
% Lowpass filter - 4th order Butterworth cutoff freq. = 50 Hz with 1 kHz sampling rate
%
bLP = [1 4 6 4 1];
aLP = [ 1.0000 -3.1806 3.8612 -2.1122 0.4383];
GLP = 4.1660e-004;

%---- Envelope detector model -----
AM_env(1) = AM_sig(1);
decay = 0.01; % signal decay over one sample period

for i= 2:length(AM_sig);
    AM_env(i) = max(AM_sig(i), AM_env(i-1) - decay);
end
AM_rec = AM_env - mean(AM_env);

%---- low pass filter -----
BB_sig = GLP * filter(bLP, aLP, AM_rec);

function Message = FMdiscriminator(FM,Fsample);

%---- Lowpass Filter: Finite Impulse Response
%---- (36 taps Fsample = 125 Hz, Fpass=5Hz Fstop= 10Hz, 40dB )
FIR_LP = [ -0.0009 -0.0109 -0.0102 -0.0140 -0.0167 -0.0180 -0.0171 ...
           -0.0133 -0.0064 0.0038 0.0172 0.0329 0.0502 0.0676 ...
           0.0839 0.0975 0.1074 0.1126 0.1126 0.1074 0.0975 ...
           0.0839 0.0676 0.0502 0.0329 0.0172 0.0038 -0.0064 ...
           -0.0133 -0.0171 -0.0180 -0.0167 -0.0140 -0.0102 -0.0109 ...
           -0.0009];

%figure(2),spectrum(FM,512,0,Hanning(512),Fsample);
```

```
%---- FM discriminator detection -----
FMc = FM ./ abs(FM); % limiter
FMdis = (FMc(2:end)- FMc(1:end-1)) * Fsamp; % differentiator
FMenv = abs(FMdis); % envelope detector
FMIp = FMenv - mean(FMenv); % remove d.c. offset
BBdec = decimate(FMIp,2); % reduce sampling rate
BBdec = decimate(BBdec,2);
Message = filter(FIR_LP, 1, BBdec); % low pass filter

%plot(Message);

function Noise = LowPassNoise (SNRdB, Nsmpls)
%-----
% Generates lowpass noise by interpolating white
% noise with three interpolate-by-2 stages
%
sigma2 = 10^(-SNRdB/10);
sigma = sqrt(sigma2/2);

%---- Generate bandlimited baseband noise ----
Noise = sigma * (randn(1,Nsmpls/8) + j*randn(1,Nsmpls/8)); % white noise
Noise = interp(Noise,2); % upsample by two
Noise = interp(Noise,2);
Noise = interp(Noise,2);

function [T,EyeSig] = ploteye(s,ups,offset);
%-----
% Function to plot eye diagram of s
%
% Inputs
%   s - real signal
%   ups - oversample rate
%
if (nargin [less] 3), offset = 0; end
s = interp(s,4);
ups = ups*4;
f = mod(length(s),ups);
s = real(s(f+1+offset:end-(ups-offset)));

%
EyeSigRef = reshape(real(s),ups,length(s)/ups);
EyeSigm1 = EyeSigRef(ups/2+2:ups,1:end-2);
EyeSig0 = EyeSigRef(:,2:end-1);
EyeSig1 = EyeSigRef(1:ups/2,3:end);
EyeSig = [EyeSig1; EyeSig0; EyeSig1];

T = [-1+1/(ups) : 1/(ups) : +1-1/(ups)];
plot(T, EyeSig)
xlabel('Symbol periods')
ylabel('Amplitude')
```

## APPENDIX 8

# ANSWERS TO DRILL PROBLEMS

### Notes:

1. Chapter 1 has no Drill Problems and therefore no answers.
2. Many of the Drill Problems in Chapters 2 through 11 have the answers embodied in the problem statements; hence, these problems are not addressed here.

### Chapter 2

$$2.1 \quad G(f) = \frac{2\pi f_c}{1 + 4\pi^2(f - f_c)^2}$$

$$2.2 \quad g(t) = \frac{1}{\pi t} (e^{-j2\pi Wt} - 1)$$

2.3 The imaginary part of  $G(0)$  must be zero.

2.4 The imaginary part of  $G(f)$  must be an odd function of  $f$ .

$$2.11 \quad 1 + T \sum_{m=1}^{\infty} \cos(2\pi m f_0 t) = T_0 \sum_{n=-\infty}^{\infty} \delta(f - n f_0), \quad f_0 = 1/T_0$$

2.12 (a) It is possible for a system to be causal but unstable.

(b) By the same token, it is possible for the system to be stable but noncausal.

$$2.13 \quad H(f) = \sqrt{2\pi\tau} \exp(-2\pi^2\tau^2f^2)$$

$$2.14 \quad (a) \quad |H(f)| = w_{\frac{N-1}{2}} + 2 \sum_{n=0}^{\frac{1}{2}(N-1)-1} w_n \cos(2\pi n f \Delta\tau)$$

$$(b) \quad \arg(H(f)) = \exp\left(-j2\pi\left(\frac{N-1}{2}\right)f\Delta\tau\right)$$

The implication of this result is a constant delay in signal transmission across the filter, hence no phase distortion.

(c) The time delay is equal to  $(N - 1)\Delta\tau/2$ .

$$2.15 \quad R_{yx}^*(-\tau) = R_{xy}(\tau)$$

$$2.16 \quad E_g(f) = \frac{1}{a^2 + 4\pi^2 f^2}, \quad -\infty < f < \infty$$

$$2.17 \quad E_g(f) = \frac{4a^2}{(a^2 + 4\pi^2 f^2)^2}, \quad -\infty < f < \infty$$

## Chapter 3

**3.1** The envelope of the AM signal can assume zero value, if  $k_a m(t) = -1$  for some  $t$ , where  $k_a$  is the amplitude sensitivity factor and  $m(t)$  is the message signal.

- 3.2** (a) 98%
- (b) 1%

**3.3**  $f_c > W$ , where  $f_c$  is the carrier frequency and  $W$  is the message bandwidth.

**3.4** (a) The spectral context of the output  $v_2(t)$  consists of two parts:

AM part:

$$F[(a_1 + 2a_2m(t))\cos(2\pi f_c t)] = \frac{1}{2}a_1(\delta(f - f_c) + \delta(f + f_c)) + a_2(M(f - f_c) + M(f + f_c))$$

Undesirable part:

$$F[a_1m(t) + a_2A_c^2 \cos^2(2\pi f_c t) + a_2m^2(t)]$$

- (b) The required band-pass filter must have bandwidth  $2W$  centered on  $f_c$ ; that is, the cutoff frequencies of the filter are  $f_c - W$  and  $f_c + W$ .
- (c) To extract the AM wave, we require  $f_c > 3W$ .

**3.5** The average power in the lower or upper side-frequency, expressed as a percentage of the average power in the DSB-SC modulated wave, is 50%.

$$\begin{aligned} \text{(a)} \quad v(t) &= \frac{1}{4}A_c A_m [\cos(2\pi(2f_c + f_m)t) + \cos(2\pi f_m t)] \\ &\quad + \frac{1}{4}A_c A_m [\cos(2\pi(2f_c - f_m)t) + \cos(2\pi f_m t)] \end{aligned}$$

- (b) The two sinusoidal terms inside the first set of square brackets are produced by the upper side-frequency at  $f_c + f_m$ . The other two sinusoidal terms inside the second set of square brackets are produced by the side-frequency at  $f_c - f_m$ .

**3.7** Spectral overlap occurs when  $f_c < W$ . When this happens, part of the lower sideband moves into the negative frequency region, and the corresponding part of the image of that sideband moves into the positive frequency region, causing spectral overlap. The coherent detection then breaks down because the detector is unable to resolve part of the spectrum where overlap occurs.

**3.12** For the coherent detector to recover the original message signal (except for scaling), we require that  $f_c > W$ .

## Chapter 4

**4.2** The phase sensitivity factor  $k_p$  is measured in radians/volt. The frequency sensitivity factor  $k_f$  is measured in hertz/volt. Therefore, the dimensionality of product term  $2\pi k_f T$  is

$$\begin{aligned} (\text{hertz/volt}) \times (\text{second}) &= \left( \frac{\text{cycles}}{\text{second}} \frac{1}{\text{volt}} \right) \times (\text{second}) \\ &= \text{radians/volt} \end{aligned}$$

which is the same as the dimensionality of  $k_p$ .

- 4.4** (a) The envelope is

$$\begin{aligned} a(t) &= A_c \sqrt{1 + \beta^2 \sin^2(2\pi f_m t)} \\ &\approx A_c \left( 1 + \frac{1}{2} \beta^2 \sin^2(2\pi f_m t) \right) \quad \text{for small } \beta. \\ &= A_c \left( 1 + \frac{1}{4} \beta^2 - \frac{\beta^2}{4} \sin(4\pi f_m t) \right) \end{aligned}$$

Maximum envelope occurs when  $\sin(2\pi f_m t) = \pm 1$ , thereby attaining the value  $A_c \left( 1 + \frac{1}{2} \beta^2 \right)$ .

Minimum envelope occurs when  $\sin(2\pi f_m t) = 0$ , thereby attaining the value  $A_c$ . Therefore,

$$\frac{(\text{Envelope})_{\max}}{(\text{Envelope})_{\min}} = 1 + \frac{1}{2} \beta^2$$

$$(b) \frac{\text{Average power of narrow-band FM}}{\text{Average power of unmodulated carrier}} = \left( 1 + \frac{1}{2} \beta^2 \right)$$

$$(c) \text{The harmonic distortion is produced by the term } \frac{\beta^3}{3} \sin^3(2\pi f_m t). \text{ For } \beta = 0.3 \text{ radian, the distortion is } 9 \times 10^{-3} \approx 1\%, \text{ which is small enough to be ignored.}$$

## Chapter 5

- 5.5** (a) Nyquist rate = 200 Hz; Nyquist interval = 5 ms.  
 (b) Nyquist rate = 400 Hz; Nyquist interval = 2.5 ms.  
 (c) Nyquist rate and Nyquist interval are the same as in part (b).

- 5.6** (a) For  $T_s = 0.25\text{s}$ ,

$$g_\delta(t) = \sum_{n=-\infty}^{\infty} \cos\left(\frac{n\pi}{4}\right) \delta(t - 0.25n).$$

- (b) For  $T_s = 1\text{s}$ ,

$$g_\delta(t) = \sum_{n=-\infty}^{\infty} (-1)^n \delta(t - n).$$

- (c) For  $T_s = 1.5\text{s}$ ,

$$g_\delta(t) = \sum_{n=-\infty}^{\infty} \cos(1.5n\pi) \delta(t - 1.5n).$$

- 5.7** The Nyquist rate must exceed 1 Hz; correspondingly, the Nyquist interval must be less than 1 s.

## **Chapter 6**

- 6.1** For the input 001101001, the waveform at the receiver output consists of  $\text{sinc}(t/T_b)$  whenever symbol 1 is transmitted and  $-\text{sinc}(t/T_b)$  whenever symbol 0 is transmitted. There will be no intersymbol interference because the sinc pulse goes through zero whenever another symbol is transmitted.
- 6.4 (b)** The value assigned to the delay  $\tau$  should decrease with increasing  $\alpha$ :
- (i)  $\tau \approx 5\text{s}$  for  $\alpha = 0$
  - (ii)  $\tau \approx 3\text{s}$  for  $\alpha = 1/2$
  - (iii)  $\tau \approx 2.5\text{s}$  for  $\alpha = 1$

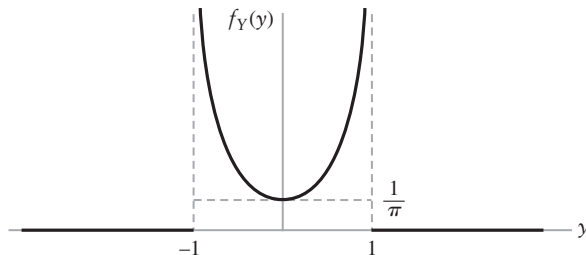
## **Chapter 7**

- 7.6** Starting at zero, the trellis increases linearly reaching  $\pi$  radians on the transmission of 11, then decreases linearly to  $\pi/2$  on the transmission of 0, increases to  $\pi$  on the transmission of 1; the level  $\pi$  is equal to  $-\pi$  modulo  $2\pi$ . It then increases linearly from  $-\pi$  to  $\pi/2$  on the transmission of 111. Finally, it decreases linearly to  $-\pi/2$  on the transmission of 00.
- 7.8** The linear input-output characteristic of the frequency discriminator has the following specifications:
- It occupies the frequency range  $f_c - \frac{1}{4}T_b < f < f_c + \frac{1}{4}T_b$ .
  - It goes through zero at  $f = f_c$ .

## **Chapter 8**

- 8.1** 0.82
- 8.2**  $5.5 \times 10^{-5}$
- 8.3**  $\frac{pp_0}{pp_0 + (1-p)p_1}$  and  $\frac{pp_1}{pp_1 + (1-p)p_0}$
- 8.4** (a) 0.5  
 (b) 0.5  
 (c) 0.9999  
 (d) 0.0001
- 8.5**  $(b+a)/2$  and  $(b-a)^2/12$
- 8.6** 0 and 1

$$8.7 \quad f_Y(y) = \begin{cases} 0, & y < -1 \\ \frac{1}{\pi\sqrt{1-y^2}}, & |y| < 1 \\ 0, & y > 1 \end{cases}$$



8.10 0 and 5/3.

8.11 Yes

8.13  $R_X(t_1, t_2) = \frac{1}{6} [\cos(2\pi f(t_1 - t_2)) + \cos(2\pi f(t_1 + t_2))]$ ; No.

8.14  $R_Y(n) = (\alpha_0^2 + \alpha_1^2)\sigma^2\delta(n) + \alpha_0\alpha_1\sigma^2(\delta(n-1) + \delta(n+1))$ ; Yes

8.15  $S_Y(k) = \beta_0 + 2\beta_1 \cos\left(\frac{2\pi k}{N}\right)$  and  $S_Y(k)$  corresponds to frequency  $\frac{kf_s}{N}$  where  $f_s$  is the sampling rate, where  $\beta_0 = (\alpha_0^2 + \alpha_1^2)\sigma^2$  and  $\beta_1 = \alpha_0\alpha_1\sigma^2$ .

8.16 Yes

8.17 (a)  $N_0$

$$(b) \quad S_Y(k) = N_0 \left| \frac{1 - (\alpha W^k)^N}{1 - \alpha W^k} \right|^2$$

## **Chapter 9**

9.1  $\text{SNR} = \frac{(S+N) - (N)}{(N)}$  where ( ) indicates independent power measurements.

9.2 18 dB

9.3  $\text{SNR}_{\text{POST}}^{\text{AM}}/\text{SNR}_{\text{POST}}^{\text{DSB}}$  is 0.04 and 0.14.

9.4 Envelope detection is insensitive to a phase offset.

9.5 18 dB and the SSB transmission bandwidth is half that of DSB-SC.

9.6 8 kHz and 20.1 dB

9.7 Upper channel is worse by 17.1 dBs

9.8 34.7 dB and 48.3 dB

## Chapter 10

10.1 (a)  $P(R_1|H_0)$

(b)  $P[R_0|H_1]P[H_1] + P[R_1|H_0]P[H_0]$

10.2  $cs^*(t)$

10.3  $\sqrt{\alpha/2}$

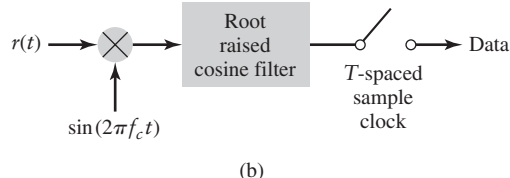
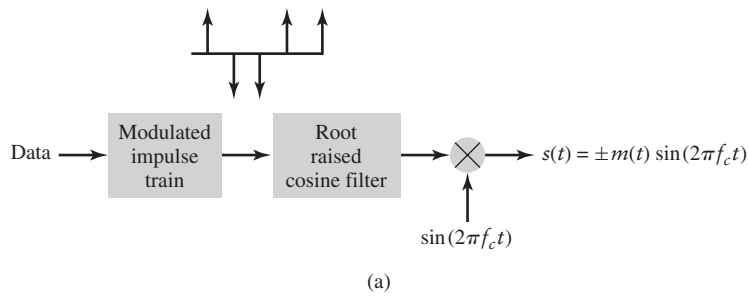
10.5 (a)  $R(f) \exp(-j2\pi fT)$

(b)  $R^2(f) \exp(-j2\pi fT)$

(c)  $q(\tau) = m(\tau - lT)$  where  $m(\tau)$  is the raised cosine pulse shape,  
 $q(kT) = m((k - l)T) = \delta(k - l)$ .

10.6 PAM bandwidth is 7.2 kHz. BPSK bandwidth is 14.4 kHz

10.7



10.9 (a)  $E[N_1 N_2] = 0$

(b)  $\text{Var}(N_1 - N_2) = N_0 T$

## ***Chapter 11***

**11.1**  $4 \times 10^{-12}$  watts and 6.3 millivolts

**11.2**  $8 \times 10^{-15}$  watts

**11.3** 2610°K

**11.4** –147 dBm/Hz and –122 dBm/Hz

**11.5** 9.97 dB

**11.6** 53.0 dB and 43.5 dB

**11.7** –143 dBW

**11.8** 120°K, 14.7 dB, and 13 dB

**11.9** 13.9 m

**11.10** 132 dB and 101 dB

**11.11**  $R_{\text{median}} = 0.83R_{\text{rms}}$

# GLOSSARY

## *Functions*

---

1. Rectangular functions

$$\text{rect}(t) = \begin{cases} 1, & -\frac{1}{2} < t < \frac{1}{2} \\ 0, & |t| > \frac{1}{2} \end{cases}$$

2. Unit step function

$$u(t) = \begin{cases} 1, & t > 0 \\ 0, & t < 0 \end{cases}$$

3. Signum function

$$\text{sgn}(t) = \begin{cases} 1, & t > 0 \\ 0, & t = 0 \\ -1, & t < 0 \end{cases}$$

4. (Dirac) delta function

$$\delta(t) = 0, \quad t \neq 0$$

$$\int_{-\infty}^{\infty} \delta(t) dt = 1$$

or, equivalently,

$$\int_{-\infty}^{\infty} g(t)\delta(t - t_0) dt = g(t_0)$$

5. Sinc function

$$\text{sinc}(x) = \frac{\sin(\pi x)}{\pi x}$$

6. Sine integral

$$\text{Si}(x) = \int_0^x \frac{\sin u}{u} du$$

7. Q-function

$$Q(x) = \frac{1}{\sqrt{2\pi}} \int_x^{\infty} \exp\left(-\frac{u^2}{2}\right) du$$

8. Binomial coefficient

$$\binom{n}{k} = \frac{n!}{(n-k)!k!}$$

9. Bessel function of the first

kind of order  $n$

$$J_n(x) = \frac{1}{2\pi} \int_{-\pi}^{\pi} \exp(jx \sin \theta - jn\theta) d\theta$$


---

## *Abbreviations*

A	ampere
ac	alternating current
ADC	analog-to-digital converter
AM	amplitude modulation
ASK	amplitude-shift keying
b/s	bits/second
BER	bit error rate
BFSK	binary frequency-shift keying
BPF	band-pass filter
BPSK	binary phase-shift keying

BSC	binary symmetric channel
codec	coder/decoder
CW	continuous wave
DAC	digital-to-analog converter
dB	decibel
dBW	decibel referenced to 1 watt
dBmW	decibel reference to 1 milliwatt
dc	direct current
DFT	discrete Fourier transform
DM	delta modulation
DPCM	differential pulse-code modulation
DPSK	differential phase-shift keying
DSB-SC	double sideband-suppressed carrier
exp	exponential
FDM	frequency-division multiplexing
FFT	fast Fourier transform
FSK	frequency-shift keying
FM	frequency modulation
GMSK	Gaussian filtered MSK
GSM	global system for mobile communications
HDTV	high-definition television
Hz	hertz
IDFT	inverse discrete Fourier transform
IF	intermediate frequency
IP	internet protocol
ISI	intersymbol interference
ISO	International Organization for Standardization
LDM	linear delta modulation
log	logarithm
LPF	low-pass filter
modem	modulator-demodulator
ms	millisecond
$\mu s$	microsecond
MSK	minimum shift keying
NRZ	nonreturn-to-zero
NTSC	National Television Systems Committee
OFDM	orthogonal frequency-division multiplexing
OOK	on-off keying
OQPSK	offset quadrature-phase-shift keying
OSI	open systems interconnection
PAM	pulse-amplitude modulation
PCM	pulse-code modulation
PDM	pulse-duration modulation

PLL	phase-locked loop
PM	phase modulation
PPM	pulse-position modulation
PSK	phase-shift keying
PWM	pulse-width modulation
QAM	quadrature amplitude modulation
QPSK	quadriphase-shift keying
RF	radio frequency
RZ	return-to-zero
s	second
SNR	signal-to-noise ratio
TDM	time-division multiplexing
TV	television
UWB	ultra wideband
V	volt
VLSI	very-large-scale integration
W	watt

## BIBLIOGRAPHY

- Abbate, J., *Inventing the Internet*, Cambridge, MA: The MIT Press, 1999.
- Anderson, J. B., *Digital Transmission Engineering*, IEEE Press, 1999.
- Abramowitz, M., and I. A. Stegun, *Handbook of Mathematical Functions with Formulas, Graphs, and Mathematical Tables*, New York: Dover, 1965.
- Arazi, B., *A Commonsense Approach to the Theory of Error Correcting Codes*, Cambridge, MA; The MIT Press, 1988.
- Bahai, A. R. S., and B. R. Saltzberg, *Multi-carrier Digital Communications: Theory and Applications of OFDM*, Kluwer, 1999.
- Baran, P., "Packet switching," in J. C. McDonald, editor, *Fundamentals of Digital Switching*, 2nd ed., pp. 193–235, New York: Plenum, 1990.
- Bell, D. A., *Noise and Solid State*, Plymouth, Eng.: Pentech Press, 1985.
- Bennett, W. R., *Introduction to Signal Transmission*, New York: McGraw-Hill, 1970.
- Bertsekas, D. M., and J. N. Tsitsiklis, *Introduction to Probability*, Athena Scientific, 2002.
- Blackman, N. M., *Noise and Its Effect on Communication*, New York: McGraw-Hill, 1966.
- Black, H. S., *Modulation Theory*, Princeton, NJ: Van Nostrand, 1953.
- Blahut, R. E., *Theory and Practice of Error Control Codes*, Reading, MA: Addison-Wesley, 1983.
- Bracewell, R. N., *The Fourier Transform and Its Applications*, 2nd ed., New York: McGraw-Hill, 1986.
- Carlson, A. B., *Communications Systems*, 2nd ed., New York: McGraw-Hill, 1975.
- Cassoli, D., M. Z. Win, and A. F. Molisch, "The ultra-wide bandwidth indoor channel: from statistical model to simulations," *IEEE Journal Selected Areas in Communications*, vol. 20, pp. 1247–1257, 2002.
- Chung, K. L., *Elementary Probability Theory with Stochastic Processes*, New York: Springer-Verlag, 1979.
- Clark, G. C. Jr., and J. B. Cain, *Error Correction Coding for Digital Communications*, New York: Plenum, 1981.
- Cooley, J. W., "How the FFT gained acceptance," *IEEE Signal Processing Magazine*, vol. 9, no. 1, pp. 10–13, January 1992.
- Catternole, K. W., *Principles of Pulse-code Modulation* (New York: American Elsevier, 1969).
- Cover, T., and J. Thomas, *Elements of Information Theory*, New York: Wiley, 1991.
- Downing, J. J., *Modulation Systems and Noise*, Englewood Cliffs, NJ: Prentice Hall, 1964.
- Erickson, G., "A fundamental introduction to the compact disc player," <http://www.tc.umn.edu/~erick205/Papers/paper.html#strengths>.
- Gitlin, R. A., J. F. Hayes, and S. B. Weinstein, *Data Communication Principles*, New York: Plenum, 1992.
- Gold, B. and N. Morgan, *Speech and Audio Signal Processing*, New York: Wiley, 1999.
- Guttman, I., S. S. Wilks, and J. S. Hunter, *Introductory Engineering Statistics*, 2nd ed., New York: Wiley, 1971.
- Haykin, S., *Adaptive Filter Theory*, 4th ed., Upper Saddle River, NJ: Prentice-Hall, 2002.
- Haykin, S., *Communications Systems*, 4th ed., New York: Wiley, 2001.
- Haykin, S., *Communication Systems*, 3rd ed., New York: Wiley, 1994.

- Haykin, S., and M. Moher, *Modern Wireless Communications*, New Jersey: Prentice Hall, 2005.
- James, J. H., B. Chen, and L. Garrison, "Implementing VoIP: a voice transmission performance progress report," *IEEE Communications Magazine*, vol. 42, no. 7, pp. 36–41, July 2004.
- Jayant, N. S., and P. Noll, *Digital Coding of Waveforms: Principles and Applications in Speech and Video*, Englewood Cliffs, NJ: Prentice-Hall, 1984.
- Jeruchim, M. C., P. Balaban, and K. S. Shanmugan, *Simulation of Communication Systems*, 2nd ed., New York: Plenum, 2000.
- Kammler, D. W., *A First Course in Fourier Analysis*, Upper Saddle River, NJ: Prentice-Hall, 2000.
- Kaneko, H. "A unified formulation of segment companding laws and synthesis of codes and digital companders", *Bell System Tech. J.*, vol. 49, pp. 1555–1588, 1970.
- Karlin, S. and H. M. Taylor, *A First Course in Stochastic Processes*, 2nd ed., New York: Academic Press, 1975.
- Lathi, B. P., *Modern Digital and Analog Communication Systems*, 3rd ed., Oxford: Oxford University Press, 1998.
- Leon-Garcia, A., *Probability and Random Processes for Electrical Engineering*, 2nd ed., Reading, MA: Addison-Wesley, 1994.
- Lin, S., and D. J. Costello, *Error Control Coding*, 2nd ed., Upper Saddle River, NJ: Prentice-Hall, 2004.
- Lucky, R. W., J. Salz, and E. J. Weldon, *Principles of Data Communication*, New York: McGraw-Hill, 1968.
- Madisetti, V. K., and D. B. Williams, editors, *The Digital Signal Processing Handbook*, CRC Press, 1998.
- McDonald, J. C. ed. *Fundamentals of Digital Switching*, 2nd edition New York: Plenum, 1990.
- McEliece, R. J., *The Theory of Information and Coding*, Reading, MA: Addison-Wesley, 1977.
- Middleton, D., *An Introduction to Statistical Communication Theory*, New York: McGraw-Hill, 1960.
- Papoulis, A., *Probability, Random Variables, and Stochastic Processes*, 2nd ed., New York: McGraw-Hill, 1984.
- Pratt, T., and C. W. Bostian, *Satellite Communications*, New York: Wiley, 1986.
- Proakis, J. G., *Digital Communications*, 3rd ed., New York: McGraw-Hill, 1999.
- Robinson, F. N., *Noise and Fluctuations in Electronic Devices and Circuits*, Oxford: Clarendon Press, 1974.
- Shannon, C. E., "A mathematical theory of communication," *Bell System Technical Journal*, vol. 27, pp. 379–423, 623–256, July, October, 1948.
- Smith, B. "Instantaneous companding of quantized signals", *Bell System Tech. J.*, vol. 36, pp. 653–709, 1957.
- Special Issue, "The Internet: past, present, and future," *IEEE Communications Magazine*, vol. 40, no. 7, pp. 42–76, July 2002.
- Steele, R. E., and L. Hanzo, *Mobile Radio Communications*, 2nd ed., New York: Wiley, 1999.
- Sveshnikov, A. A. (ed.), *Problems in Probability Theory, Mathematical Statistics and Theory of Random Functions*, New York: Dover Publications, 1968.
- Takahashi, A., and H. Yoshino, "Perceptual QoS assessment of technologies for VoIP," *IEEE Communications Magazine*, vol. 42, no. 7, pp. 28–34, July 2004.

- Tannenbaum, A. S., *Computer Networks*, 3rd ed., Englewood Cliffs, NJ: Prentice-Hall, 1996.
- Thomas, J. B., *An Introduction to Applied Probability and Random Processes*, New York: Wiley, 1971.
- Van Der Ziel, A., *Noise: Sources, Characterization, Measurement*, Englewood Cliffs, NJ: Prentice Hall, 1970.
- Willner, A. E., "Mining the optical bandwidth for a terabit per second," *IEEE Spectrum*, vol. 34, pp. 32–41, April 1997.
- Win, M. Z., and R. A. Scholtz, "Impulse radio: how it works," *IEEE Comm. Letters*, vol. 2, pp. 36–38, 1998.
- Wozencraft, J. M. and I. M. Jacobs, *Principles of Communication Engineering*, New York: Wiley, 1965. Reprinted by Waveland Press, Prospect Heights: Illinois, 1990.
- Wylie, C. R. and L. C. Barrett, *Advanced Engineering Mathematics*, 5th edition (New York: McGraw-Hill, 1982).
- Yuen, J. H. (ed.), *Deep Space Telecommunications Systems Engineering*, New York: Plenum, 1983.
- Zeimer, R. E., and W. H. Tranter, *Principles of Communications: Systems, Modulation and Noise*, 5th ed., New York: Wiley, 2002.

## INDEX

### A

Adaptive equalization, 3, 255*n.7*  
Adjustable transversal equalizer, 252  
Advanced Research Projects Agency Network (ARPANET), 3  
Advanced Television (ATV)  
standard, 305  
Aliasing, 196–198  
AM, *see* Amplitude modulation  
Amplitude distortion, 162  
Amplitude modulation (AM), 101–114  
and carrier waves, 147  
computer experiment, 106–110, 113  
envelope detection, 111–113  
overcoming limitations of, 113–114  
theory underlying, 101–106  
Amplitude modulation family, 100–148  
amplitude modulation, 101–114  
double sideband-suppressed carrier,  
114–121  
linear modulation strategies in, 100  
quadrature-carrier multiplexing, 121–123  
single-sideband modulation, 123–130  
vestigial sideband modulation, 130–137  
Amplitude response, 57, 58, 60  
AM radio, 5  
AM waves, *see* Amplitude-modulated waves  
Analog communications:  
noise in, 364–390  
signal-detection problem in, 15  
Analog filters, 70  
Analog pulse modulation, 190  
Analysis equation, 19  
Analyzer, 140  
Angle modulation, 152–185  
frequency demodulation, 174–182  
frequency discriminator, 174–178  
and phase-locked loop, 178–182  
frequency-modulated waves:  
generation of, 172–174  
PM relationship to, 159–160  
transmission bandwidth of, 170–172

frequency modulation:  
narrow-band, 160–164  
wide-band, 164–169  
and PM-FM wave relationship,  
159–160  
properties of angle-modulated waves,  
154–159  
tradeoff with, 152  
Anti-alias filter, 197  
Antipodal signals/signaling, 270, 416  
Aperture effect, 201  
Aperture efficiency, 447  
Area:  
under  $G(f)$ , 32  
under  $g(t)$ , 32  
Armstrong, Edwin H., 1  
Armstrong wide-band frequency modulator, 173  
ARPANET, 3  
ARQ (automatic repeat-request), 3  
ATV (Advanced Television)  
standard, 305  
Autocorrelation function, 70–71  
Automatic repeat-request (ARQ), 3  
Available power (noise), 440  
Average bit error rate, 395  
Average noise figure, 443  
Average power, 79

### B

Balanced frequency discriminator, 178  
Band-limited channels, 13  
Band-pass assumption, 264–265  
Band-pass data transmission, 256  
Band-pass filters, 60, 140–141  
Band-pass limiter, 188  
Band-pass receivers, noise with,  
369–370  
Band-pass signals, 40  
Band-pass to low-pass (baseband)  
transformation, 141  
Band-stop filters, 60

- Bandwidth, 39–40  
     and amplitude response, 58  
     channel, 13  
     definitions of, 40  
     and inverse relationship between time  
         and frequency, 40–41  
     and time-bandwidth product, 41  
 Bandwidth-conservation system, 121  
 Bandwidth-duration product, 41  
 Baran, P., 7n.2  
 Bardeen, John, 2  
 Baseband, 137  
 Baseband data transmission, 231–256  
     computer experiment, 249–251  
     eye pattern in, 246–251  
     intersymbol interference problem in,  
         233–234  
     of M-ary data, 245  
     and Nyquist channel, 235–237  
     and raised-cosine pulse spectrum,  
         238–245  
     roll-off portion of spectrum, 241–243  
     root raised-cosine pulse spectrum,  
         244–245  
     transmission-bandwidth requirement,  
         240–241  
 Baseband representation:  
     of band-pass filters, 140–141  
     of modulated waves, 137–140  
 Base resistance, thermal noise from, 442  
 Base station (satellite  
     communications), 6  
 Basic group (multiplexing), 146–147  
 BASK, *see* Binary amplitude-shift keying  
 BBC (British Broadcasting Corporation), 2  
 Beat (signal), 149  
 Bel, 459  
 Bell, Alexander Graham, 2, 459n.1  
 Bell Laboratories, 2, 4  
 BER, *see* Bit error rate  
 Berners-Lee, Tim, 3  
 Bernoulli distribution function, 319  
 Bernoulli random variable, 318, 328  
 Bessel functions, 165, 467–469  
 Best effort service (Internet), 10, 11  
 BFSK, *see* Binary frequency-shift keying  
 BIBO, *see* Bounded input-bounded output  
     stability criterion  
 Binary amplitude-shift keying (BASK), 263,  
     265–269  
     generation/detection of signals, 265–266  
     spectral analysis of, 266–269, 399–404  
 Binary frequency-shift keying (BFSK), 263,  
     281–282  
     detection of, 414–415  
 Binary phase-shift keying (BPSK), 263,  
     270–274  
     generation/coherent detection  
         of signals, 270–271  
         optimum detection of, 405–408  
         spectral analysis of, 271–274  
 Binomial distribution, 321  
 Bipolar chopper, 228  
 Bipolar return-to-zero (BRZ)  
     signaling, 219  
 Bit duration, 263  
 Bit error rate (BER), 395–396, 419–420  
 Bit reversal, 88  
 Block codes, 424–426, 430–431  
 Boresight, 447  
 Bose—Chaudhuri—Horcquenghem block  
     codes, 430  
 Bounded input-bounded output (BIBO)  
     stability criterion, 55–56  
 BPSK, *see* Binary phase-shift keying  
 Branches (signal-flow graph), 85–87  
 Brattain, Walter H., 2  
 British Broadcasting Corporation (BBC), 2  
 Broadcasting, 4  
 BRZ (bipolar return-to-zero)  
     signaling, 219  
 Burst noise, 438  
 Butterworth filters, 70, 249

## C

- Carrier-frequency tuning, 142  
 Carrier power (satellite systems), 449  
 Carrier-to-noise ratio (CNR), 450–451  
 Carrier wave, 14  
 Carson's rule, 170  
 Cartesian representation, 162  
 Causal systems, 55

- CDs (compact discs), 12  
Central limit theorem, 333–335  
Channels:  
    band-limited, 13  
    defined, 53  
    power-limited, 13  
Channel bandwidth, 13, 14  
Channel bits, 423, 429  
Channel noise, 13  
Chebyshev filters, 70  
Circuit switching, 7  
Clark, Arthur C., 4  
Closed-loop feedback system, 178  
Closed-loop gain, 180*n*.3  
CNR, *see* Carrier-to-noise ratio  
Code rate, 431  
Coherent detection, 116, 134  
    binary phase-shift keying, 270–271  
    double sideband-suppressed carrier  
        modulation, 116–118  
    of the DSB-SC modulated wave, 184  
    noise in linear receivers using,  
        370–373  
    with single-sideband modulation,  
        127–128  
    with vestigial sideband modulation,  
        134–135  
Communication network, 6–8  
Communication systems:  
    basic types of, 4–5  
    communication networks, 6–8  
    composition of, 5  
    data networks, 8–9  
    data storage, 12  
    design parameters for, 14  
    historical background of, 1–4  
    integration of telephone and Internet,  
        11–12  
    Internet, 9–11  
    noise in, 365–366  
    operational requirements for, 13–14  
    performance improvement for, 14  
    primary resources in, 13  
    radio, 5–6  
    theories underlying, 14–16  
Compact discs (CDs), 12  
Complementary error function, Q-function  
    and, 471–472  
Complex carrier wave, 138  
Complex envelope:  
    of the FM waves, 165  
    of the modulated wave, 138  
Complex exponential Fourier series, 50,  
    461–462  
Complex exponential function, application  
    of delta function to, 45–46  
Complex Fourier coefficient, 50  
Complex low-pass filter, 141  
Computer networks, 3–4, 6–8  
Comte, Auguste, 1  
Conditional probability, 323–326  
Conjugation rule (Fourier transforms),  
    28–29  
Connection delay (Internet), 11  
Constants, 479  
Continuous amplitude spectrum, 21  
Continuous Fourier transform, *see* Fourier  
    transform (FT)  
Continuous-phase frequency-shift keying  
    (CPFSK), 282–283  
Continuous-phase signal, 281  
Continuous phase spectrum, 21  
Continuous spectrum, 51  
Continuous-wave (CW) modulation, 100  
    amplitude modulation, 100–148  
    angle modulation, 152–185  
    families of, 100  
        pulse modulation vs., 190  
Convolutional codes, 430–431  
Convolution integral, 37, 54  
Convolution theorem (Fourier transforms),  
    37  
Correlation, 38  
Correlation receiver, 399  
Correlation theorem (Fourier transforms),  
    37–38  
Correlative coding, 259  
Costas receiver, 120–121  
Covariance, 328–329  
CPFSK, *see* Continuous-phase frequency-  
    shift keying  
Cross-correlation function, 77–78  
Cross-spectral density, 78

CW modulation, *see* Continuous-wave modulation

## D

Datagrams, 10  
 Data networks, 8–9  
 Data storage, 12  
 dBs, *see* Decibels  
 dc signal, application of delta function to, 45  
 Decibels (dBs), 13, 459  
 Decimation-in-frequency algorithm, 88  
 Decimation-in-time algorithm, 88  
 Decision thresholds/levels, 205  
 Decoder, 424  
 De-emphasis filter, 388–389  
 Deep-space links, 13  
 De Forest, Lee, 2  
 Delta function, *see* Dirac delta function  
 Delta modulation (DM), 211–216  
     delta-sigma modulation, 215–216  
     quantization errors, 214–215  
 Demultiplexed components, 276  
 Demultiplexing system, 184  
 Detection theory, 15  
 Deviation ratio, 171  
 DFT, *see* Discrete Fourier transform  
 Dabit, 274  
 Difference-frequency term, 179  
 Differential encoding, 219  
 Differential pulse-code modulation (DPCM), 216–219  
 Differentiation in the time domain (Fourier transforms), 32–34  
 Diffraction, in terrestrial mobile radio, 451, 452  
 Digital Advanced Television (ATV) standard, 305  
 Digital band-pass modulation techniques, 262–309  
     band-pass assumption in, 264–265  
     binary amplitude-shift keying, 265–269  
     frequency-shift keying, 281–289  
     mapping of waveforms onto constellations of signal points, 299–301

M-ary digital modulation schemes, 295–299  
 noncoherent detection schemes, 291–295  
     BASK signals, 291–292  
     BFSK signals, 292–293  
     differential phase-shift keying, 293–294  
     phase-shift keying, 270–281  
 Digital communication:  
     history of, 2–3  
     noise in, 394–434  
     signal-detection problem in, 15  
 Digital filters, 70  
 Digital pulse modulation, 190, 204  
 Digital radio, 5  
 Digital subscriber line (DSL), 11, 302  
 Digital switching, 7  
 Digital television, 6, 305–307  
 Digital versatile discs (DVDs), 12  
 Dilation property (Fourier transforms), 28  
 Diode equation, 441  
 Dirac comb, 51–52  
 Dirac delta function, 42–50  
     applications of, 45–50  
     and extension of Fourier transform, 42  
     in the frequency domain, 103  
     as limiting form of Gaussian pulse, 43–45  
     replication property of, 43  
     sifting property of, 42  
 Direct method (FM wave generation), 172–173  
 Dirichlet conditions, 20, 42  
 Discrete Fourier transform (DFT), 18, 81  
     and FFT, 83–84  
     interpretation of, 82–83  
 Discrete memoryless channel, 324  
 Discrete spectrum, 51, 462–464  
 Discrete-time filter, 217  
 Discrete-time Fourier transform, 194–196  
 Discrete-time signal processing, 204  
 Distribution functions, 318–320  
 DM, *see* Delta modulation  
 Double exponential pulse, 26–27  
 Double-frequency term, 179

Double sideband-suppressed carrier  
(DSB-SC) modulation, 113–121  
coherent detection, 116–118, 370–373  
computer experiment, 118–120  
Costas receiver for detection of, 120–121  
theory underlying, 114–116  
Doublet pulse, 34  
Downlink (communications), 6  
DPCM, *see* Differential pulse-code  
modulation  
DSB-SC modulation, *see* Double sideband-  
suppressed carrier modulation  
DSL, *see* Digital subscriber line  
Duty cycle, 463  
DVDs (digital versatile discs), 12

## E

Earth-orbiting satellite, 4  
Eckert, J. Presper, Jr., 3  
Effective aperture area, 447  
Effective isotropic radiated power (EIRP),  
448  
Electrical noise:  
available noise power, 440  
shot noise, 440–442  
thermal, 438–440  
Electromagnetic theory of light, 1  
Electronics, history of, 2  
Elementary event, 315  
E-mail messages, 11  
Encoder, 424  
Energy gap (in SSB modulation), 114  
Energy signals, 70–78  
autocorrelation function of, 70–71  
cross-correlation of, 77–78  
defined, 20  
energy spectral density of, 71–77  
Fourier transformability of, 20  
Wiener—Khitchine relations  
for, 71–72  
Energy spectral density, 71–77  
defined, 71  
effect of filtering on, 72–75  
of energy signals, 71–77  
interpretation of, 75–77  
and use of filters, 72–75

ENIAC, 3  
Ensembles, signal, 16  
Envelope detectors/detection, 103  
amplitude modulation, 111–113  
for AM wave demodulation, 111  
noise in AM receivers using, 373–377  
for sinusoidal AM, 113  
of VSB plus carrier, 136  
Envelope distortion, 102–103  
Equalization, 251–255  
adaptive, 3, 255*n.7*  
in pulse-amplitude modulation,  
200–202  
zero-forcing, 253–255  
Equivalent noise temperature,  
443–445  
Error correction capability, 425  
Error detection and correction  
(digital systems noise), 422–433  
block codes, 424–426, 430–431  
Bose—Chaudhuri—Horcquenghem  
block codes, 430  
convolutional codes, 430–431  
Hamming codes, 426–430  
Reed—Solomon block codes, 430  
signal-space interpretation of codes,  
431–433  
turbo codes, 431  
Error propagation phenomenon, 260  
Error syndrome, 428  
Euler’s formula, 31, 46  
Excess bandwidth, 241  
Excitation, 52  
Expectation, statistical averages of,  
326–329  
Exponential pulse(s), 23–25  
double, 26–27  
truncated decaying, 23–24  
truncated rising, 24–25  
External noise, 437  
Eye patterns, 246–251  
for M-ary transmission, 249  
peak distortion for intersymbol  
interference, 247–249  
timing features for, 247

**F**

Farnsworth, Philo T., 2  
Fast Fourier transform (FFT), 15, 83–88  
FDM, *see* Frequency-division multiplexing  
Feed-back, 173  
Fessenden, Reginald, 1  
FFT, *see* Fast Fourier transform  
Figure of merit, 373, 376, 379, 385  
Filters, 60  
  analog, 70  
  Butterworth, 70  
  Chebyshev, 70  
  defined, 53, 60  
  digital, 70  
    and energy spectral density, 72–75  
    ideal low-pass filters, 60–70  
    for superheterodyne receivers, 142  
    noise equivalent bandwidth, 354–356  
First detector, 143  
First order phase-locked loop, 182  
Fleming, John Ambrose, 2  
Flicker noise, 438  
FM, *see* Frequency modulation  
FM radio, 1, 5  
FM waves, *see* Frequency-modulated waves  
Forward-error-correction codes, 431–433  
Fourier, Joseph, 19*n*.1  
Fourier analysis, 15  
Fourier series, 19*n*.1, 460–464  
  complex exponential, 50, 461–462  
  and discrete spectrum, 462–464  
Fourier transform(s), 18–52, 464–466.  
  *See also specific headings, e.g.:*  
    Fast Fourier transform  
  and area under  $G(f)$ , 32  
  and area under  $g(t)$ , 32  
  and conjugation rule, 28–29  
  and convolution theorem, 37  
  and correlation theorem, 37–38  
  defined, 15, 19  
  and differentiation in the time domain, 32–34  
  dilation property of, 28  
  and Dirac delta function, 42–50

duality of, 29–30  
frequency-shifting property of, 30–32  
and integration in the time domain, 34–36  
inverse, 19  
and inverse relationship between time and frequency, 39–41  
linearity of, 25–28  
and modulation theorem, 36–37  
notations in, 20–21  
numerical computation of, 81–89  
DFT and IDFT, interpretation of, 82–83  
FFT algorithms, 83–88  
IDFT, computation of, 88–89  
of periodic signals, 50–52  
properties of, 475  
and pulse signal as continuous sum of exponential functions, 21–25  
and Rayleigh's energy theorem, 38–39  
theorems, 475  
time-shifting property of, 30  
Fourier-transform pairs, 19, 21, 476  
Free-space link calculations, 446–451  
  carrier-to-noise ratio, 450–451  
  received signal power, 447–450  
Free-space loss, 448  
Free-space propagation, 451  
Frequency:  
  fundamental, 50  
  inverse relationship between time and, 39–41  
Frequency content (of a signal), 18  
Frequency demodulation, 174–182  
  frequency discriminator, 174–178  
  and phase-locked loop, 178–182  
Frequency deviation, 161  
Frequency discrimination method, 125–127  
Frequency discriminator, 175  
Frequency-division multiplexing (FDM), 145–146  
  modulation steps for, 146–147  
  orthogonal, 302–304  
  stereo multiplexing, 182–184

Frequency-modulated radar, 185  
 Frequency-modulated (FM) waves,  
   154–159  
   generation of, 172–174  
   PM relationship to, 159–160  
   transmission bandwidth of, 170–172  
 Frequency modulation (FM), 154  
   detection of, 380–387  
   narrow-band, 160–164  
   origin of concept, 1  
   wide-band, 164–169  
 Frequency multiplier, 173  
 Frequency resolution, 81  
 Frequency response (in linear systems),  
   56–58  
 Frequency-sensitivity factor, 154  
 Frequency-shifting property  
   (Fourier transforms), 30–32  
 Frequency-shift keying, 281–289  
   binary, 281–282  
   continuous-phase, 282–283  
   detection of, 414–416  
   minimun-shift keying, 283–289  
 Friis transmission formula, 448, 454  
 Fundamental frequency, 50

**G**

Gauss, C. G., 330*n.4*  
 Gaussian monocycle, 223  
 Gaussian processes, 347–348  
 Gaussian pulse:  
   defined, 33  
   delta function as limiting form  
   of, 43–44  
   as unit pulse, 34  
 Gaussian random variables, 330–333  
 Generalized functions (generalized  
   distributions), 43  
 Generating functions, 50  
 Geostationary orbit, 6, 446  
 Ghosting, 452  
 Global System for Mobile (GSM)  
   Communications, 304  
 Gray encoding, 418  
 GSM (Global System for Mobile  
   Communications), 304

**H**

Hamming, R., 422*n.3*  
 Hamming codes, 426–430  
 Hamming distance, 424–425  
 Hamming weight, 424  
 Hand-held devices (for Internet  
   access), 11  
 Harmonic distortion, 162  
 HDTV, 6  
 Heat flow, 19*n.1*  
 Hertz, Heinrich, 1  
 High-definition television (HDTV), 6  
 High-pass filters, 60  
 Hilbert transform, 98–99, 139*n.4(i)*  
 Hilbert-transform pairs, 476  
 Hockham, G. A., 4  
 Hold-in frequency range, 182  
 Hosts, 7, 10  
 HTML, 3  
 HTTP, 3  
 Hybrid modulated wave, 177  
 Hypertext markup language (HTML), 3  
 Hypertext transfer protocol (HTTP), 3  
 Hypothesis testing, 15

**I**

IC (integrated circuit), 2  
 I-channel, 120–121  
 Ideal low-pass filters, 60–70  
   approximation of, 69–70  
   pulse response of, 61–69  
 Ideal sampling function (Dirac comb),  
   51–52  
 IDFT, *see* Inverse discrete Fourier  
   transform  
 Image interference (in superhet  
   receivers), 143  
 Image signals:  
   suppressing, 143  
   as two-dimensional function  
     of time, 5  
 Impossible event, 315  
 Impulse radio, 223–224  
 Impulse response, 53  
 Independent Bernoulli trials, 321

Indirect method (FM wave generation), 173  
 Information-bearing (message) signal, 101  
 Information bits, 423  
 Initial-echo control (in VoIP), 12  
 Inphase coherent detector (I-channel), 120–121  
 In-phase path (SSB modulators), 127  
 In-place computation, 88  
 Instantaneous sampling, 191–193  
 Integrals, 478  
 Integrate-and-dump detector, 400  
 Integrated circuit (IC), 2  
 Integration in the time domain (Fourier transforms), 34–36, 49–50  
 Interfaces (OSI model), 8  
 Internal noise, 437  
 Internet, 9–12  
 Internet protocol (IP), 10  
 Interpolation formula, 195, 235  
 Intersymbol interference problem, 233–234  
 Inverse discrete Fourier transform (IDFT), 82  
     computation of, 88–89  
     interpretation of, 82–83  
 Inverse Fourier transform, 19  
 Inverse Hilbert transform, 98  
 IP (Internet protocol), 10

**J**

Joint probability density function, 320

**K**

Kao, K. C., 4  
 $k$ -by- $n$  generator matrix, 427

**L**

Laser, 4  
 Layered architecture, 8  
 Linear delta modulators, 214  
 Linearity of Fourier transforms, 25–28  
 Linear receivers, noise in, 370–373  
 Linear system, 52  
 Linear time-invariant (LTI) systems, 18, 54–55

Line codes (pulse modulation), 219–220  
 Line-of-sight radio propagation, 6  
 Link budget, 449–450  
 List decoder, 427  
 Lodge, Oliver, 1  
 Logic network, 293  
 Loop filter, 178  
 Loop-gain parameter, 180  
 Lower sideband, for positive frequencies, 103  
 Low-pass filters, 60. *See also* Ideal low-pass filters  
 Low-pass signals, 40–41, 98  
 Low-pass transfer function, 131–133  
 LTI systems, *see* Linear time-invariant systems  
 Lucky, Robert, 3

**M**

Main lobe, 40  
 Manchester code, 219  
 Mapping process, 6  
 Marconi, Guglielmo, 1  
 Marginal densities, 320  
 M-ary amplitude shift keying (M-ary ASK), 297  
 M-ary data transmission, 249  
     baseband, 245  
     eye patterns for, 249, 411–412  
 M-ary digital modulation schemes:  
     frequency-shift keying, 298–299  
     phase-shift keying, 295–297  
     quadrature amplitude modulation, 297–298, 411–414  
 Mastergroups (multiplexing), 147  
 Matched filter, 3, 396–397  
 Mathematical constants, 479  
 Mathematical tables, 475–479  
 MATLAB scripts (computer experiments), 480–487  
 Mauchly, John W., 3  
 Maximum-power transfer theorem, 440  
 Maxwell, James Clerk, 1  
 Mean-square error criterion, 255*n*.7  
 Mean-square value, 345  
 Median path loss, 453–454

- Message bandwidth, 103, 130  
Message signal, 101  
Message spectrum, 103  
Microprocessors, 2  
Middleton, D., 3  
Minimum-shift keying (MSK),  
    283–289  
    formulation of, 286–287  
    power spectrum evaluation, 287–289  
Mobile radio, terrestrial, 451–452  
Modulated waves, baseband representation  
    of, 137–140  
Modulation. *See also specific types, e.g.:*  
    Pulse modulation  
    defined, 14, 100  
    primary motivation for, 100  
Modulation factor, 104  
Modulation index, 161  
Modulation theorem (Fourier transforms),  
    30, 36–37  
Modulation theory, 14  
Modulo-two addition, 260  
Morse, Samuel, 1  
Morse Code, 1  
MSK, *see* Minimum-shift keying  
Multi-carrier system, 302  
Multipath phenomenon (wireless  
    communications), 6, 451–456  
Multiplexing, 145  
Multiplier (phase-locked loops), 178
- N**
- Narrowband, 111  
Narrow-band frequency modulation,  
    160–164  
Narrowband noise, 352–356  
Natural sampling, 228  
Near-phase-lock, 179  
Negative feedback amplifier, 180*n*.3  
Nodes (signal-flow graph), 85–87  
Noise, 437–457  
    in analog communication, 364–390  
    in AM receivers using envelope  
        detection, 373–377  
    with band-pass receiver structures,  
        369–370  
detection of frequency modulation,  
    380–387  
FM pre-emphasis/de-emphasis,  
    387–390  
in linear receivers using coherent  
    detection, 370–373  
signal-to-noise ratios, 366–369  
in SSB receivers, 377–379  
cascade connection of two-port networks,  
    445–446  
in communications systems, 365–366  
defined, 13, 313, 364  
in digital communication, 394–434  
    bit error rate, 395–396  
    detection of QAM, 411–414  
    detection of QPSK, 408–411  
    detection of single pulse, 396–399  
    differential detection, 416–418  
    error detection and correction, 422–433  
    Gray encoding, 418  
    optimum detection of binary PAM,  
        399–405  
    optimum detection of BPSK, 405–408  
    optimum detection of FSK, 414–416  
    performance comparison of strategies,  
        419–420  
    in signal-space models, 421–422  
electrical, 438–442  
equivalent noise temperature, 443–445  
external vs. internal, 437  
free-space link calculations, 446–451  
narrowband, 352–356  
noise figure, 442–443  
sources of, 437  
with terrestrial mobile radio, 451–456  
white, 348–351  
Noise-equivalent bandwidth, 354–356  
Noise figure, 442–443  
Noise spectral density, 444–445  
Noncoherent detection, 291–295  
    BASK signals, 291–292  
    BFSK signals, 292–293  
    differential phase-shift keying, 293–294,  
        416–418  
Non-return-to-zero level encoder, 270,  
    275–276

Nonreturn-to-zero (NRZ) signaling, 219  
 Nonuniform quantizer, 207  
 Normalized root-raised cosine pulse shape, 404  
 Normal random variables, 330*n.5*  
 North, D. O., 3  
 Norton equivalent circuit, 439  
 Noyce, Robert, 2  
 NRZ (nonreturn-to-zero) signaling, 219  
*n*th order Bessel function, 165–166  
 Nulls, 40  
 Null event, 315  
 Null-to-null bandwidth, 40  
 Nyquist, Harry, 2, 243*n.3*  
 Nyquist channel, 235–237

**O**

Odd-symmetric time function, 27  
 Okumura—Hata model, 453*n.8*  
 One-bit delay element, 293  
 “One-over-*f*” noise, 438  
 On-off signaling, 219  
 Open-loop gain, 180*n.3*  
 Open system interconnection (OSI)  
     reference model, 8, 9  
 Optical communications, history of, 4  
 Optimum pulse shape, 235  
 Orthogonal frequency-division multiplexing, 302–304  
 Orthogonal signaling, 416  
 OSI model, *see* Open system interconnection reference model

**P**

Packets, 8, 10  
 Packet loss ratio, 11  
 Packet-switched networks, 8  
 Packet switching, 3, 7–8  
 Paley-Wiener criterion, 58  
 PAM, *see* Pulse-amplitude modulation  
 Partial-response signaling, 259  
 Passband, 60  
 Path loss, 448, 453–454  
 PBXs (private branch exchanges), 12  
 PCM, *see* Pulse-code modulation

PCs (personal computers), 3  
 PDM, *see* Pulse-duration modulation  
 Peer processes, 8, 9  
 Percentage modulation, 103, 104  
 Periodicity, 51, 84  
 Periodic signals, 124  
     Fourier transforms of, 50–52  
     in linear systems, 52–59  
 Periodogram, 80  
 Personal computer (PCs), 3  
 Phase discrimination method (SSB generation), 127  
 Phase discriminator (I- and Q-channels), 121  
 Phase error, 179  
 Phase-lock, 179  
 Phase-locked loop, 178–182  
 Phase-modulated (PM) waves, 154–159  
 Phase modulation (PM), 153  
 Phase noise, 362  
 Phase response, 57, 60  
 Phase sensitivity factor, 153  
 Phase-shift keying, 270–281  
     binary, 270–274  
     quadriphase, 274–281  
 Physical constants, 479  
 Physical layer, 9  
 Pierce, John R., 4  
 Pilot, for VSB modulated wave detection, 136*n.3*  
 Pilot-assisted training, 255, 307  
 Pixels, 5  
 PM (phase modulation), 153  
 PM waves, *see* Phase-modulated waves  
 Point-to-point communications, 4–5, 147  
 Poisson’s sum formula, 51  
 Polar representation, 162  
 Post-detection signal-to-noise ratio, 368  
     in AM receivers using envelope detection, 374–376  
     in FM modulation, 381–385  
     in linear receivers, 372–373  
     in SSB receivers, 378–379  
 Power, transmitted, 13  
 Power budget, 449  
 Power-limited channels, 13

- Power ratios, 459  
Power spectral density, 79–81, 344–346  
PPM (pulse-position modulation), 203  
Pre-detection signal-to-noise ratio, 368  
  in AM receivers using envelope detection, 374  
  in FM modulation, 380–381  
  in linear receivers, 371  
  in SSB receivers, 378  
Prediction, 217  
Private branch exchanges (PBXs), 12  
Probability theory, 16, 314–335  
  axioms of probability, 315–316  
  central limit theorem, 333–335  
  conditional probability, 323–326  
  distribution functions, 318–320  
  Gaussian random variables, 330–333  
  random variables, 317–318  
  relative-frequency approach, 314–315  
  several random variables, 320–323  
  and statistical averages of expectation, 326–329  
  and transformation of random variables, 329–330  
Product modulator, 114  
Protocol (data networks), 8  
Pulse-amplitude modulation (PAM), 198–202  
  aperture effect and equalization, 200–202  
  binary, optimum detection of, 399–405  
  performance of, 419–420  
  sample-and-hold filter, 199–200  
Pulse-code modulation (PCM), 206–211  
  invention of, 2  
  receiver operations, 211  
  regeneration along transmission path, 209–210  
  transmitter operations, 206–209  
Pulse-duration modulation (PDM), 202–203  
Pulse modulation, 190–226  
  analog, 190  
  continuous-wave modulation vs., 190  
  delta modulation, 211–216  
differential pulse-code modulation, 216–219  
digital, 190  
families of, 190  
line codes in, 219–220  
pulse-amplitude modulation, 198–202  
pulse-code modulation, 206–211  
pulse-duration modulation, 202–203  
pulse-position modulation, 203  
quantization process in, 205–206  
sampling process for:  
  and aliasing phenomenon, 196–198  
  instantaneous sampling, 191–193  
  sampling theorem, 193–196  
Pulse-position modulation (PPM), 203  
Pulse response (ideal low-pass filters), 61–69
- ## Q
- QAM, *see* quadrature-amplitude modulation  
Q-factor, 178*n*.2  
Q-function, 331, 402, 470–472  
QoS (quality of service), 11  
QPSK, *see* Quadriphase-shift keying  
Quadrature-amplitude modulation (QAM), 121–123, 414  
  detection of, in noise, 411–414  
  performance of, 419–420  
Quadrature-carrier multiplexing, 121–123  
Quadrature null effect, 117  
Quadrature path (SSB modulators), 127  
Quadrature-phase coherent detector (Q-channel), 121  
Quadriphase-shift keying (QPSK), 274–281  
  detection of, in noise, 408–411  
  generation/detection of signals, 275–277  
  offset, 277–281  
  performance of, 419–420  
  power spectra of signals, 278–281  
Quality factor (Q-factor), 178*n*.2  
Quality of service (QoS), 11  
Quantization process:  
  in delta modulation, 214–215  
  in pulse modulation, 205–206  
Quantizer characteristics, 205  
Quantum, 205

**R**

Radio, 5–6  
 digital, 5  
 history of, 1  
 impulse, 223–224  
 terrestrial mobile radio, 451–452  
 Radio frequency (RF) pulse, 31–32  
 Radio receivers, superheterodyne, 1  
 Raised-cosine pulse spectrum, 238–245  
 properties of, 241–244  
 roll-off portion of spectrum, 241–243  
 root raised-cosine pulse spectrum,  
 244–245  
 transmission-bandwidth requirement,  
 240–241  
 Random experiment, 314  
 Random processes, 16, 335–343, 365  
 correlation of, 338–343  
 stationary, 337–338  
 Random signals, 313–348  
 defined, 16, 313  
 and Gaussian processes, 347–348  
 and probability theory, 314–335  
 and random processes, 335–343  
 correlation of, 338–343  
 stationary, 337–338  
 spectra of, 343–346  
 Random variables, 317–318, 329–330  
 experiments with several, 320–323  
 Gaussian, 330–333  
 transformation of, 329–330  
 Rayleigh distribution function, 455  
 Rayleigh fading, 454–456  
 Rayleigh’s energy theorem, 38–39  
 Real-time spectrum analyzer, 187  
 Received signal power, 447–450  
 Reconstruction levels, 205  
 Rectangular pulse, 22–23  
 Reed–Solomon block codes, 430  
 Reeves, Alex, 2  
 Reference power level, 459  
 Reference signal-to-noise ratio, 368  
 Reference transmission model, 368  
 Reflection (terrestrial mobile radio),  
 451, 452  
 Reflection property (Fourier transforms), 28

Representation levels, 205  
 Response, defined, 52  
 Return-to-zero (RZ) signaling, 219  
 RF pulse, *see* Radio frequency pulse  
 rms bandwidth, *see* Root mean-square  
 bandwidth  
 Rms duration, 98  
 Roll-off factor, 238, 256  
 Root mean-square (rms) bandwidth,  
 40–41, 98  
 Root mean-square (rms) duration, 98  
 Root raised-cosine pulse spectrum,  
 244–245, 404–405  
 Routers, 7, 10  
 RZ signaling, 219

**S**

Sample point, 315  
 Sampling theorem, 193–196, 235  
 Satellite channels, 13  
 Satellite communications:  
 components of, 6  
 free-space link calculations  
 for, 446–451  
 history of, 4  
 as point-to-point system, 6  
 system noise temperature  
 of receivers, 446  
 Scanning, 5  
 Scanning variable, 70  
 Scatter diagram, 246n.4  
 Schottky formula, 441  
 Schwarz’s inequality, 473–474  
 Search engines, 11  
 Searching variable, 70  
 Second detector, 143  
 Series expansions, 477  
 Shannon, Claude, 3, 422n.3  
 Shockley, William, 2  
 Shot noise, 438, 440–442  
 Side-frequencies, 123  
 Sifting property (of Dirac delta function),  
 42–43  
 Signals. *See also* specific types, e.g.:  
 Periodic signals  
 and bandwidth, 40

- frequency content of, 18  
real-valued, conjugate symmetry  
of spectra of, 22
- Signal-dependent phenomenon, 256
- Signal detection:  
binary amplitude-shift keying, 265–266  
of binary PAM in noise, 399–405  
of BPSK, 405–408  
coherent:  
binary phase-shift keying, 270–271  
double sideband-suppressed carrier  
modulation, 116–118, 370–373  
linear receivers, 370–373  
detection theory, 15  
differential, 416–418  
with frequency modulation, 380–387  
of FSK, 414–416  
noncoherent, 291–295  
BASK signals, 291–292  
BFSK signals, 292–293  
differential phase-shift keying,  
293–294  
of QAM, 411–414  
of QPSK, 408–411  
quadriphase-shift keying, 275–277  
signal-detection problem in, 15
- Signal-detection problem, 15
- Signal-flow graph, 85–87
- Signal-space diagram, 296
- Signal-space interpretation of codes,  
431–433
- Signal-space models, noise in,  
421–422
- Signal-to-noise ratio (SNR), 13  
in analog communication, 366–369  
post-detection, 368, 372–376, 378–379,  
381–385  
as system design parameter, 14
- Signum function, 27, 47–48
- Similarity property (Fourier  
transforms), 28
- Sinc function, 22–23
- Sinc pulse, 29–30, 38–39
- Single-sideband (SSB) modulation,  
113–114, 123–130  
and amplitude modulation, 147
- coherent detection of, 127–128, 337–379  
frequency translation, 128–130  
modulators for, 125–127  
theory underlying, 123–125
- Single-sideband receivers, noise in, 377–379
- Sinusoidal carrier waves, 14, 100. *See also*  
Continuous-wave modulation
- Sinusoidal DSB-SC spectrum, 116
- Sinusoidal functions, application of delta  
function to, 46–47
- Sinusoidal modulating wave, SSB  
modulation and, 123
- Sinusoidal VSB wave modulation, 133
- Slope circuit, 175
- Slope network, 380
- SNR, *see* Signal-to-noise ratio
- Spectral density:  
cross-spectral density, 78  
energy, 71–77  
noise, 444–445  
power, 79–81
- Spectral distortion, avoiding, 110
- Spectral overlap, 110
- Speech signals, digital encoding of, 2
- Speech vecoders, 395*n.1*
- Split-phase (Manchester code), 219
- Spot noise figure, 443
- Square law, 110
- Square-law modulator, 110, 111
- Square wave, 266
- SSB modulation, *see* Single-sideband  
modulation
- Stable systems, 55–56
- Stationary random processes, 337–338
- Step-by-step switch, 2
- Step-size, 205
- Stereo multiplexing, 182–184
- Stochastic processes, 16. *See also*  
Random processes
- Stopband, 60
- Stored-program system (telephone), 2
- Strowger, A. B., 2
- Strowger switch, 2
- Subnets, Internet, 10
- Summations, 478
- Sunde's BFSK, 281–282

- Supergroup (multiplexing), 147  
 Superheterodyne receivers (superhets), 1, 142–143, 369  
 Superposition, principle of, 52  
 Superposition of Fourier transforms, 25–28  
 Sure event, 315  
 Switching, 7  
   circuit, 7  
   packet, 7–8  
 Symbol error rate, 413  
 Synchronous demodulation, 116  
 Synthesis equation, 19  
 Synthesis filter, 195, 197  
 Synthesizer, 140  
 System, defined, 52  
 Systematic convolutional code, 430–431  
 System margin, 449  
 System performance, 15
- T**
- Tapped-delay-line filter, 54–55, 217  
 TDM, *see* Time-division multiplexing  
 Telegraph, 1  
 Telephone channels, 13  
 Telephone systems:  
   first commercial service, 2  
   history of, 2  
   integration of Internet and, 11–12  
   twisted pairs, 89–90  
 Television:  
   digital, 305–307  
   high-definition, 6  
   history of, 2  
   transmissions for, 5  
 Television channels, 13  
 Television signals, VSB modulation of, 143–145  
 Terrestrial mobile radio, 451–452  
 Thermal noise, 438–440  
 Thévenin equivalent circuit, 439  
 3-dB bandwidth, 40  
 Threshold effect, 386–387  
 Time, inverse relationship between frequency and, 39–41  
 Time-bandwidth product, 41, 69  
 Time-division multiplexing (TDM), 145, 220–223  
 Time function:  
   differentiation of a, 32–33  
   integration of a, 34–36  
   odd-symmetric, 27  
   real and imaginary parts of a, 35–36  
 Time response, transmission of signals through linear systems and, 53–55  
 Time-shifting property (Fourier transforms), 30  
 T-1 carrier system, 2, 222–223, 241  
 Transistor, invention of, 2  
 Transmission bandwidth (AM waves), 104  
 Transmission lines, 89  
 Transmission losses, 4  
 Transmitted power, 13  
 Transmitters, 5  
 Transversal filter, 252  
 Triangular pulse, 34–35  
 Trigonometric identities, 477  
 Truncated decaying exponential pulse, 23–24  
 Truncated rising exponential pulse, 24–25  
 Turbo codes, 431  
 Twiddle factor, 85  
 Twisted pairs, 11, 89–90  
 Two-port devices:  
   average noise figure of, 443  
   equivalent noise temperature of, 443–445  
 Two-port networks, cascade connection of, 445–446  
 Type 1 error, 401
- U**
- Ultra-wideband (UWB) radio transmission, 223  
 Ungerboeck, G., 3  
 Unit impulse, 42  
 Unit prefixes, 479  
 Unit pulse, 34  
 Unit step function, 48–49  
 Unity peak distortion, 248  
 Uplink (communications), 6

Upper sideband, 103  
UWB (ultra-wideband) radio transmission,  
223

**V**

Vacuum-tube diode, 2  
Vacuum-tube triode, 2  
Van Duuren, H. C. A., 3  
Van Vleck, J. H., 3  
VCO, *see* Voltage-controlled oscillator  
Very large groups (multiplexing), 147  
Very-large-scale integrated (VLSI) circuits, 2  
Vestigial sideband modulation, 149  
Vestige bandwidth, 130  
Vestigial sideband (VSB) modulation,  
114, 130–137  
coherent detection of, 134–135,  
306–307  
motivation for using, 130  
sideband shaping filter for, 131–134  
SSB vs., 130  
of television signals, 143–145  
Video signal, generation of, 6  
Virtual circuits, 10  
Virtual communication, 9  
VLSI circuits, 2  
Voice over Internet Protocol  
(VoIP), 11–12  
Voice signals, 5  
VoIP, *see* Voice over Internet Protocol

Voltage-controlled oscillator (VCO):  
and the Costas receiver, 121  
and phase-locked loops, 178  
Von Neumann, John, 3  
VSB filter, 144  
VSB modulation, *see* Vestigial sideband  
modulation  
VSB-plus carrier signal, 136

**W**

Waveform distortion, 145  
Weaver, Warren, 3  
White Gaussian noise, 439  
White noise, 348–351, 438  
Wide-band frequency modulation, 164–169  
Wideband modems, 11  
Wide-band phase-shifter, 127  
Wideband signals, transmission of, 130  
Wide-sense stationary, 338  
Wiener—Khitchine relations, 71–72, 244  
Wireless channels, 13  
Wireless communications, 6  
World Wide Web, 3

**Z**

Zero-crossings, 156–157  
Zero-forcing equalization, 253–255  
Zero peak distortion, 248  
Zworykin, Vladimir K., 2